TECHNISCHE UNIVERSITÄT MÜNCHEN

Lehrstuhl für Analytische Lebensmittelchemie

Ultra-High Resolution Mass Spectrometry in Characterizing the Impact of Whole Grain Diet on Human Gut Meta-Metabolome

Kirill Smirnov

Vollständiger Abdruck der von der Fakultät Wissenschaftszentrum Weihenstephan für Ernährung, Landnutzung und Umwelt der Technischen Universität München zur Erlangung des akademischen Grades eines

Doktors der Naturwissenschaften

genehmigte Dissertation.

Vorsitzender: Univ. Prof. Dr. E. Grill

Prüfer der Dissertation:

1. apl. Prof. Dr. Ph. Schmitt-Kopplin
2. Univ. Prof. Dr. M. Rychlik
3. Univ. Prof. Dr. P. Falter-Braun

Die Dissertation wurde am 30.11.2017 bei der Technischen Universität München eingereicht und durch die Fakultät Wissenschaftszentrum Weihenstephan für Ernährung, Landnutzung und Umwelt am 26.03.2018 angenommen

« Ich bin so jung und die Welt ist so alt »

Georg Büchner

Посвящается Мыше и Софи,

Summary

Diet represents one of the major factors affecting the health of a living organism. Ingested food components can be left in their intact form or modified/processed by host and commensal bacteria followed by the absorption of the corresponding products in the gastrointestinal tract. Their further metabolic fate as well as significance for health can be very individualized, thereby representing a challenging task in deciphering involved biological processes. Along with other large-scale disciplines, such as genomics and proteomics, metabolomics has been proven to be of crucial importance in describing the subtle nature of the interplay between nutrition and host physiological status because it directly reflects the dynamics of the biological system.

Numerous analytical platforms used in metabolomics research are based on mass spectrometric measurements. Non-targeted profiling is of particular importance in discovery oriented studies and involves measuring thousands of signals simultaneously. Therefore, sophisticated pre- and post-processing as well as data analysis methods are required to unravel the complexity of such tremendous amount of information. Compared to its targeted counterpart, non-targeted metabolomics enables to provide novel hints into the scientific question of interest, thereby potentially expanding knowledge on biological systems.

The present work is concentrated on deciphering human physiological responses to whole grain diet by means of non-targeted metabolomics profiling of stool and plasma samples using direct infusion Fourier transform ion cyclotron resonance mass spectrometry. Because of the necessity to retrieve as much of meaningful information from the bulk of raw data as possible, several spectral processing methods are presented. Using multivariate statistical analysis together with network approaches, the metabolites, potentially related to diet responses, are selected and described. Moreover, their connection to clinical markers as well as gut microbiota composition is depicted in order to investigate the association of the chosen metabolites with inflammatory responses as well as the involvement of the commensal bacteria metabolism during the course of treatment. The obtained results indicate that the whole grain diet influences host stool and plasma metabolome as well as the aforementioned interaction patterns, providing a rich source for further research and development.

Zusammenfassung

Ernährung hat einen maßgeblichen Einfluss auf den Gesundheitsstatus eines Organismus. Bestimmte Nahrungsbestandteile können nach ihrer Aufnahme intakt bleiben oder durch den Wirtsorganismus und seine kommensale Bakterienflora modifiziert/prozessiert werden. Dabei entstehen Produkte die im Darm aufgenommen und weiterverwertet werden können und diese können immensen Einfluss auf die Gesundheit des Wirtes haben. Die Entschlüsselung der metabolischen Prozesse als Funktion von Nährstoffen ist eine Herausforderung, da sie sehr invididuell vorfallen können. Neben anderen «large-data-scale» Disziplinen wie Genomik und Proteomik etablierte sich die Metabolomik als eine der Kerndisziplinen, um das Zusammenspiel zwischen Ernährung, Mikrobiom und der Wirts-physiologie zu beschreiben. Diese Technik ist in der Lage die Dynamik von Metaboliten und Nährstoffen in biologischen Systemen zu reflektieren.

In der Metabolomik wird eine Vielzahl von analytischen Methoden mit dem Fokus auf die Massenspektrometrie angewandt. Hierbei spielt das «non-targeted Profiling» eine zentrale Rolle für explorative Studien, da diese Technik mehrere tausend Substanzen auf einmal detektieren kann. Die Komplexität dieser enormen Datenmenge muss deswegen durch besondere und passende Vor- and Nachbearbeitung der Daten adressiert werden. Im Vergleich zum «targeted Profiling», eröffnet die «non-targeted» Metabolomik neue Einblicke in wissenschaftlich interessante Fragestellungen zu bekommen und ermöglicht somit das Wissen über die Funktionalität biologischer Systeme zu erweitern.

Die vorliegende Arbeit beschäftigt sich mit der Untersuchung der Wirkung einer Vollkorndiät auf den menschlichen und mikrobiellen Stoffwechsel, repräsentiert durch Blut und Stuhlproben. Für die Durchführung der «non-targeted» Metabolomik wurde Direktinfusion an der hochauflösenden Fouriertransformation-Ionenzyklotronresonanz-Massenspektrometrie angewandt. Um ein Maximum an sinnvoller Information zu erhalten, werden Methoden zur spektralen Prozessierung der vielfältigen Rohdaten entwickelt. Multivariate Statistik im Zusammenspiel mit netzwerkanalytischen Methoden werden verwendet um Metabolite, deren Dynamik hauptsächlich von den untersuchten Diäten abhängt, zu selektieren und zu beschreiben. Des Weiteren wird der Zusammenhang der gewählten Metabolite mit klinischen Markern und der Komposition intestinaler Mikroorganismen betrachtet, um inflammatorische Ereignisse und den Einfluss kommensaler Bakterien als Funktion der durchgeführten Diäten

zu erforschen. Die erhaltenen Resultate weisen darauf hin, dass Vollkorndiät das Stuhl- und Plasmametabolom des Wirtes sowie deren Interaktionen mit klinischen Markern und intestinaler Mikroflora beeinflusst. Somit wurde eine wichtige Datengrundlage für eine gezieltere Erforschung der untersuchten Zusammenhänge geschaffen.

Table of Contents

List of figures

List of abbreviations

AC	**A**cyl**C**arnitine
ADON	**A**cetyl**D**e**O**xy**N**ivalenol
AGlu	**A**cetyl**Glu**tamate
AGlu-sA	**A**cetyl**Glu**tamate **s**emi**A**ldehyde
ANOVA	**AN**alysis **O**f **Va**riance
AOS	**A**cet**O**xy**S**cirpenol
API	**A**tmospheric **P**ressure **I**onization
BCAA	**B**ranched-**C**hain **A**mino **A**cid
BCFA	**B**ranched-**C**hain **F**atty **A**cid
BMA	**B**ody **M**ass **I**ndex
CAF	**C**ycloartanyl **F**erulate
CE	**C**apillary **E**lectrophoresis
CRP	**C**-**R**eactive **P**rotein
CSF	**C**ampe**S**teryl **F**erulate
deACAL	**deA**cetyl**CAL**onectrin
DHEA	**D**ocosa**H**exanoenoyl **E**thanol**A**mide
DI	**D**irect **I**nfusion
DMA	**D**i**M**ethyl**A**mine
DON	**D**e**O**xy**N**ivalenol
DPEA	**D**ocosa**P**entaenoyl **E**thanol**A**mide
DTEA	**D**ocosa**T**etraenoyl **E**thanol**A**mide
ESI	**E**lectro**S**pray **I**onization
FCS	**F**unctional **C**lass **S**coring
FGlu	**F**asting **Glu**cose
FID	**F**ree **I**nduction **D**ecay
FIns	**F**asting **Ins**ulin
FooDB	**Foo**d **D**ata**B**ase
FT-ICR	**F**ourier **T**ransform **I**on **C**yclotron **R**esonance
FusX	**Fus**arenone **X**
FWHM	**F**ull **W**idth at **H**alf **M**aximum
GC	**G**as **C**hromatography
GIT	**G**astro**I**ntestinal **T**ract
Glu	**Glu**tamate
GUI	**G**raphical **U**ser **I**nterface
HCA	**H**ierarchical **C**luster **A**nalysis
HDL	**H**igh-**D**ensity **L**ipoprotein
HMCCate	**H**ydroxy**M**ethyl**C**holetene **C**arboxyl**ate**
HMCCyde	**H**ydroxy**M**ethyl**C**holetene **C**arbaldeh**yde**
HMDB	**H**uman **M**etabolome **D**ata**B**ase
HODE	**H**ydr**O**xy**O**cta**DE**cadienoic acid
HOMA-IR	**HO**meostatic **M**odel **A**ssessment of **I**nsulin **R**esistance
HPLC	**H**igh **P**ressure **L**iquid **C**hromatography
HPODE	**H**ydro**P**eroxy**O**cta**DE**cadienoic acid
HRMS	**H**igh **R**esolution **M**ass **S**pectrometry
IGI	**I**nsulino**G**enic **I**ndex
IL-6	**I**nter**L**eukin 6
IT	**I**on **T**rap
ITDmol	**I**so**T**richo**D**er**mol**

ITDmin	**I**so**T**richo**D**er**min**
IUPAC	**I**nternational **U**nion of **P**ure and **A**pplied **C**hemistry
KEGG	**K**yoto **E**ncyclopedia of **G**enes and **G**enomes
LA	**L**inoleic **A**cid
LBP	**L**ipopolysaccharide-**B**inding **P**rotein
LC	**L**iquid **C**hromatography
LCFA	**L**ong **C**hain **F**atty **A**cid
LDL	**L**ow-**D**ensity **L**ipoprotein
LIPID MAPS	**LIPID M**etabolites **A**nd **P**athways **S**trategy
m/z	mass-to-charge
MANOVA	**M**ultivariate **An**alysis **O**f **Va**riance
MDiN	**M**ass-**Di**fference **N**etwork
METLIN	**METabolite LIN**k
MI	**M**atsuda **I**ndex
ML-SCA	**M**ulti**L**evel **S**imultaneous **C**omponent **A**nalysis
ML-PLS-DA	**M**ulti**L**evel **P**artial **L**east **S**quares **D**iscriminant **A**nalysis
MS	**M**ass **S**pectrometry
MS/MS	Tandem **M**ass **S**pectrometry
NAPE	**N**-**A**cyl**P**hosphatodyl**E**thanolamine
NEA	**N**-acyl**E**thanol**A**mine
NMR	**N**uclear **M**agnetic **R**esonance
ORA	**O**ver-**R**epresentation **A**nalysis
OEA	**O**leoyl **E**thanol**A**mide
OTU	**O**perational **T**axonomic **U**nit
OxoODE	**OxoO**cta**DE**cadienoic acid
PCA	**P**rincipal **C**omponent **A**nalysis
PEA	**P**almitoyl **E**thanol**A**mide
PEG	**P**oly**E**thylene **G**lycol
PLS	**P**artial **L**east **S**quares
ppm	**p**arts-**p**er-**b**illion
PUFA	**P**oly**U**nsaturated **F**atty **A**cid
Q	**Q**uadrupole
RMSE	**R**oot **M**ean **S**quared **E**rror
SCFA	**S**hort **C**hain **F**atty **A**cid
SEA	**S**teraoyl **E**thanol**A**mide
SHCA	**S**parse **H**ierarchical **C**luster **A**nalysis
SOM	**S**elf-**O**rganizing **M**ap
SPE	**S**olid **P**hase **E**xtraction
SSF	**S**ito**S**terol **F**erulate
TChol	**T**otal **Chol**esterol
TMA	**T**ri**M**ethyl**A**mine
TMAO	**T**ri**M**ethyl**A**mine N-**O**xide
ToF	**T**ime-**o**f-**F**light
UPLC	**U**ltrahigh **P**ressure **L**iquid **C**hromatography

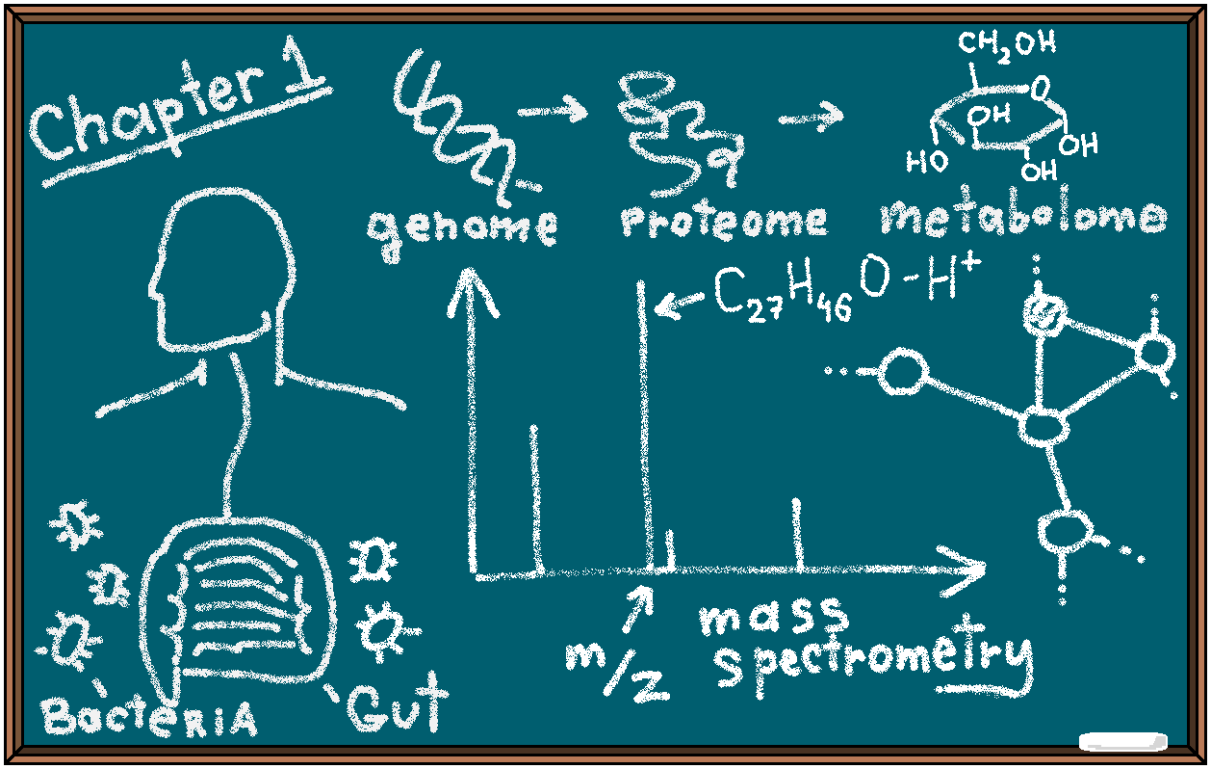
Chapter 1
genome
Proteome
metabolome
CH_2OH
HO
OH
OH
OH
$C_{27}H_{46}O-H^+$
m/z
mass spectrometry
Bacteria
Gut

Chapter I

1. Introduction

1.1. Rise of systems biology and «omics» fields

Complexity is an inseverable attribute of biological systems (Van Regenmortel, 2004). Despite of the self-evidence of this statement, nowadays this concept is acquiring special consideration. The reason lies in the emerged possibility to generate an enormous amount of informative biological data together with the progress in computer technologies capable to solve complex mathematical problems (Kitano, 2002). The term «Systems biology» was coined describing a cross-disciplinary field with a strategy to study organisms as integrated dynamical systems assembled out of interrelated genetic, protein, metabolic, and cellular components (Kesic, 2016). This discipline does not have well defined boundaries and encompasses many post-genomic fields, *e.g.* synthetic biology, systems microbiology, systems biotechnology, integrative biology, systems biomedicine, and metagenomics (Likic et al., 2010).

The genesis of modern systems biology has been caused by the intersection of relatively distinct historical routes (Kesic, 2016; Westerhoff and Palsson, 2004). Discovery of the structure and function of genetic material together with associated methods for gene manipulation (*i.e.* genetic engineering) stay at the root of the first route. Consequently, molecular biology underwent scientific revolution that opened gates for a series of breathtaking findings. Towards the end of the 20th century it is possible to observe scaling-up in fundamental experimental approaches of molecular biology with genome-scale sequencing reached in the mid-1990s when the term «genomics» was coined. The beginning of the 21st century was marked by completing the Human Genome Project, thus validating the new discipline of genomics. The success of the project induced an incredible amount of effort to sequence the genomes of other organisms including plants, animals, and microorganisms (Likic et al., 2010). After further studies, mainly focused on mapping and gene identification, it became evident that the collected sequences show enormous complexity, thus raising the necessity to shift the field into the search for relationships between sequence and function. These steps served as a critical point in the transformation of molecular biology into systems molecular biology. Further developments in automation, miniaturization, and multiplexing led to the concomitant emergence of other «omics» data types and technologies, namely transcriptomics, proteomics, and metabolomics (Kesic, 2016; Likic et al., 2010). The systems-

based approaches to analyse a tremendous amount of such high-throughput data gained importance. Their development represents the second route in the evolution of systems biology that existed in parallel with the aforementioned path and led to the formation of systems mathematical biology. The first steps can be marked by the application of general systems theory to biology in late 1960s with an attempt to study an organism in its entirety. Early works were concentrated on modelling newly discovered regulatory circuits in cells with one of the major focus on self-regulating systems (*i.e.* systems containing feedback mechanisms) naturally occurring in all the living organisms. Further advances in technologies scaled-up these efforts giving an opportunity to simulate complex dynamics of large metabolic networks. The concepts of nonlinear dynamics started to be utilized in the mathematical models, *e.g.* stochasticity, nonstationarity, chaotic behaviour, sensitivity to initial conditions. All these features undoubtedly can be attributed to biological processes that are inherently complex and nonlinear. The moment, when general systems theory and nonlinear dynamics were introduced for gene, protein, and metabolic network analyses, can be considered as a convergence of molecular and mathematical systems biology routes providing the way towards the development of modern systems biology that endeavors to integrate all existing biological, mathematical, computational, and medical knowledge.

The «Systems» view on biology usually is opposed to the reductionist position stating that an entirety can be studied by breaking it down into manageable pieces, analyzing them separately, and then predicting the behaviour of the whole from the discovered behaviour of the components (Trewavas, 2006; Van Regenmortel, 2004). Although the latter approach has proven to be useful, it is clear that certain properties of a system might not be derived solely from its constituent parts and, thereby, are considered emergent. Organization represents a crucial characteristic of living systems expressed in a hierarchical structure held together by numerous linkages. Cellular molecules followed by cells, then tissues *etc.* can depict the aforementioned hierarchy. Each level above is an emergent property resulting from complex interactions between constituents of the lower level, while, on the other side, these interactions follow the rules controlled by the higher levels. Thus, it is possible to observe mutual constraints in both upward and downward directions. The sequence of nucleotides represents a good example of this concept. Although components (single nucleotides) can be arranged together in any order in terms of physics and chemistry, only specific sequences are meaningful in the context of gene expression inside a cell. On the other side, the cell

orchestrates the sequence of events involved in DNA biosynthesis where, at each step of the process, only particular building blocks are required.

Biological systems can be characterized by their resilience, an emergent property to adapt to changes in the environment (Trewavas, 2006; Van Regenmortel, 2004). Therefore, they possess an entire set of control mechanisms responsible for their stability or an immediate response. One of the most important elements is a negative feedback that is necessary for stabilizing the output enabling a biological system to act with resilience. Feed-forward mechanisms operate in the opposite manner promoting a change rather than preserving constant behaviour. Some components of biological systems are often redundant which indicates the existence of backup mechanisms in case if one component fails. Besides, biological systems can be characterized by their modularity, *i.e.* the presence of subsystems that are physically and functionally isolated, whereas no restrictions in communication are imposed. Such an organization implies that if a failure occurs in one of the modules, remaining ones may show low or no susceptibility. Thereby, it is possible to observe many layers involved in the robustness of a system. This characteristic would be difficult to study from a reductionist perspective since there is a constant interaction between internal and external components leading to a conglomeration of complex pathways.

It is worth pointing out that the meaning of «system», representing the core of systems biology, depends on the task and objectives of a particular study together with the choices on the type and complexity of mathematical models (Likic et al., 2010). As a consequence, there is a big diversity in scope and scale between various implementations. Limitations in the current knowledge and the capability to observe experimentally the phenomena of interest create additional boundaries in building mathematical models aiming at a certain level of description. Among different approaches to build the link between the components of a system and its emergent properties, so-called «top-down» and «bottom-up» strategies are frequently utilized (Ballereau et al., 2013; Wang et al., 2015). The general «bottom-up» workflow starts with representing the relationships between different parts of the system (graphically or mathematically) moving up the specified hierarchy. Further steps include setting model parameters followed by verification of observed properties via comparison with a real system. In other words, the functions of a system are deduced from the known or assumed characteristics of the components. Although this approach may be successful for relatively small systems, it encounters difficulties when dealing with larger systems. In

contrast, «top-down» workflow first defines how certain systemic function varies due to the factor of interest by inspecting experimental data for the presence of meaningful patterns. Afterwards, hypotheses are constructed about possible mechanisms in the lower levels of organization responsible for this behaviour. However, such an approach is sensitive to perturbations and requires well-defined phenotypes for building accurate models. The solution for aforementioned challenges may be provided by using the «middle-out» strategy. In this approach a system is not necessary modeled from the bottom level in the specified hierarchy but at the level that is sufficiently well described by experimental data. Afterwards, «top-down» and «bottom-up» strategies are utilized in combination in order to extend the model to lower and higher levels in the systemic hierarchy.

Nowadays vast amounts of biological data can be produced by advanced high-throughput technologies allowing not only identification and quantification of individual components of a system (*e.g.* genes, proteins, or metabolites) but generation of large networks describing potential interactions between these components (Wang et al., 2015). Due to such an immense availability of «omics» datasets, the systems way of thinking has been becoming an achievable goal (Likic et al., 2010). However, any single type of such high-throughput data, representing only one dimension of complex biological systems, is unable to uncover solely the variety of the emergent functions. Different «omics» levels provide mutually complementary information on the corresponding mechanisms. Therefore, the full picture can only be constructed by studying the crosstalk between genes, transcripts, proteins, and metabolites, thereby enhancing the importance of integration of heterogeneous and large «omics» data. Such an approach can reveal complex and often unexpected behaviour even for systems that were missconceptually thought to be simple. For example, the majority of components (*e.g.* metabolic reactions, enzymes, and genes) of a model organism *E. coli* are well described. However, the mechanisms ensuring the stability of the system (*i.e.* homeostasis) can be strikingly different with respect to external and internal perturbations. The era of «omics» meets the challenge to mine biological knowledge and generate novel insights and reliable hypotheses from the plethora of available data. The future progress will not only depend on the development of high-throughput temporal and spatial analytical techniques, capable for high-resolution analysis, but significantly on computational tools and power (Ballereau et al., 2013). In turn, mathematical models are more than just instruments for integration or *in silico* simulations. They serve as the representation of the current status of our knowledge about particular biochemical system (Likic et al., 2010).

Going beyond basic biological research, systems biology is able to provide new insights in understanding human diseases and developing corresponding treatments through drug discovery and optimization (Wang et al., 2015). Thereby, systems biology gives a necessary impulse for the emergence of systems medicine, a discipline that will utilize new approaches for the treatment of major disorders effectively and with personalized precision. This new field will integrate «omics» and clinical data, environmental factors, and computational modelling in order to make it possible to simulate and predict disease-linked events (*i.e.* pathophenome). Observing the success of systems biology approaches, there is no doubt that systems thinking will become even more prevailing in the future (Likic et al., 2010).

1.2. Metabolomics

1.2.1. Metabolomics as the part of systems biology

Metabolites are small molecules having a broad range of activities in host metabolism (Johnson et al., 2016). Essentially, they are substrates and products of biochemical reactions responsible for many cellular functions, *e.g.* energy production and storage, signal transduction, or transportation of macromolecules. Moreover, a living organism is not limited to its set of own metabolites and receives many more from diet, activity of commensal microorganisms, and other exogenous sources. In order to study the intrinsic functions of metabolites as well as their physiological roles and the pathways associated with particular phenotypes, metabolomics approaches can be utilized. Metabolomics (the term has been introduced in 1998) can be defined as the global metabolite profiling of a system (*e.g.* cell, tissue, or biofluid) under a specific set of conditions (Junot et al., 2014; Rochfort, 2005). The similar term namely «metabonomics» sometimes is used instead describing the measurement of dynamic metabolic responses of living systems to biological stimuli or genetic modification (Nicholson and Lindon, 2008). First reports on more or less comprehensive metabolite profiling for understanding complex biological systems dates back to 1950s, albeit the term «metabolomics» was not coined yet (Kell and Oliver, 2016; Rochfort, 2005). Despite these early works, this discipline grew slowly, likely due to alleged incapability of metabolites to fit into the «DNA makes RNA makes protein» doctrine that gave rise to «natural omics» fields. Interestingly, a mathematical framework namely metabolic control analysis already back then predicted that the changes in individual genes and transcripts have little effects on metabolic fluxes but necessarily have strong influence on metabolite concentrations. In other

words, in order to maintain the constant rates in different parts of metabolic network, the constituent metabolites have to vary their concentrations over a wide range. Thus, a theory demonstrated that metabolic profiles can be connected to various disturbances assuring the significance of measuring metabolome in different biological systems. Today metabolomics is a scientific discipline of great importance, joining genomics, transcriptomics, and proteomics in the path towards global understanding of biological mechanisms.

In metabolomics research, there are two major ways to analyze a sample, namely the non-targeted and targeted approach (Johnson et al., 2016). Non-targeted research focuses on detecting the maximum amount of metabolites, possible to recover from a biological sample. There is no *a priori* knowledge on the extracted compounds, thus making this approach useful for identifying novel or unanticipated mechanisms involved in studied phenomena. By contrast, targeted metabolomics focuses on measuring a predefined set of metabolites and differs by higher sensitivity and selectivity due the method optimization towards *a priori* known compounds. The two approaches do not follow independent routes in research but often complement each other. For example, compounds found to be significant by non-targeted metabolomics are usually validated in a targeted manner. In addition to the aforementioned approaches, the so-called *in situ* metabolomics currently gains much consideration (Astarita and Langridge, 2013). It concerns providing the detailed spatial distribution of a certain metabolites on a tissue, *e.g.* by means of mass spectrometry imaging. Essential progress in instrumentation, experimental design, and sample preparation has greatly facilitated metabolomics research with anticipation of many more novel metabolites to be discovered (Kell and Oliver, 2016). In turn, constantly developing computational and bioinformatics tools effectively support the processing and analysis of massive data generated by the advanced analytical platforms. Metabolomics can be considered as an application-driven science that has rapidly embraced across the biological research community (Kell and Oliver, 2016; Rochfort, 2005). Early analyses on single metabolites naturally have grown into the global metabolome measurements for identification of disease biomarkers. On the other side, drug response profiles can be studied by evaluating the efficacy of the treatment (Kell, 2006). Consequently, metabolite profiling of different biofluids has become one of the major focus of research with a promise of establishing concepts for individualized therapy. Metabolomics has been extensively utilized in the studies on plants because of the presence of an enormous amount of compounds involved in plant ecology and stress mechanisms. In fact, some higher plants own one of the largest and most complex metabolomes in the living world.

Nowadays, nutritional sciences extensively use metabolomics approaches in order to study the effects of diet onto biological systems with an ultimate goal of establishing individualized food regimes. Such integration has the potential to optimize the health of individuals by informing them about the diets that would be beneficial for the organism homeostasis.

Despite of its obvious importance, metabolomics meets several challenges in terms of technology, experimental design, data analysis, and data integration (Rochfort, 2005). An ideal metabolomics experiment addresses measuring all metabolites in a biological sample. However, compounds making up the metabolome span substantial concentration and structural ranges (van der Greef et al., 2003). Even a single class can include compounds ranging from mg/mL to pg/mL (*e.g.* lipids), whereas different classes can comprehend a wide range of polarities. Therefore, any single method or technology cannot cover all heterogeneity and diversity hidden in metabolome. Additionally, minimization of sample preparation steps is often required in order to ensure no loss of individual components. In any biomarker discovery oriented metabolomics experiment, metabolite identification and biomarker validation represent the two biggest hurdles (Johnson et al., 2016). Frequently, only a small subset of all considerable compounds can be positively identified due to the limitation associated with *in silico* tools, databases, or *de novo* synthesis of analytical standards. From the other side, the necessity to deal with very subtle differences in metabolite concentrations is one of the common problems during the validation step. Moreover, this additional step has to be designed very carefully in order to exclude possible inter-individual metabolite variation arising from the differences in genetic factors and environmental exposures. Due to the complexity of metabolomics experiments, much of the work done has been qualitative in nature. Beyond metabolite identification, it is required to relate the identified metabolites to their biological roles. Although being challenging, the ultimate goal addresses connecting changes in metabolite concentrations to the perturbations in individual biochemical pathways leading to different phenotypic outcomes. In turn, this task raises the importance of multi-layered integrative approaches with a strategy to use metabolomics and other «omic» information for investigating metabolic pathways in a more system-wise way. Thereby, although the importance of the unique information provided by metabolomics alone is drastic, the future prospects lie in its integration into systems biology.

1.2.2. Analytical platforms

Scientific knowledge undoubtedly is driven by the advances in technologies (Zhang et al., 2012). The improvements in detection and identification of small molecules, including amino acids, peptides, lipids, carbohydrates *etc*. greatly depends on the development of the corresponding methods and tools. It is not possible to find a superior platform because every analytical technique commonly used in metabolomics research has its own advantages and drawbacks. However, they all can be characterized by lacking an ability to measure all metabolites in a sample. Therefore, the combination of analytical approaches is a necessary step towards studying a global metabolome. Analytical platforms for conducting metabolomics experiments are expensive. However, this reality is normally compensated by the low per sample costs, mainly due to the relatively high-throughput nature of metabolic profiling. Metabolomics experiments can be conducted on many biofluid and tissue types via application of different technology platforms. Nuclear magnetic resonance (NMR) spectroscopy and mass spectrometry (MS) represent the workhorses of metabolomics research allowing metabolite identification and quantification.

NMR spectroscopy is one of the most common analytical techniques for metabolome analysis, capable of simultaneous identification and quantification of organic compounds in the range of μM (Zhang et al., 2012). The measurements done via NMR spectroscopy are non-selective, thereby opening an opportunity to detect all low molecular weight compounds in a single run. However, the access to such a «holistic» perspective is greatly limited by the relatively low sensitivity of the instrument making it inappropriate for detecting many low-abundant metabolites (Shulaev, 2006; Zhang et al., 2012). In addition, the analysis of spectra obtained by one-dimensional NMR spectroscopy is often hampered by the overlap of signals from different metabolites, which can be addressed by performing two-dimensional experiments (Smirnov et al., 2016). NMR spectroscopy is very useful in analyzing biological fluids because, in addition to providing rich structural information, the technique is non-destructive, lacks intermetabolite suppression effects, and the material undergoes minimal invasion (Smirnov et al., 2016; Zhang et al., 2012). Therefore, different matrices can be analyzed, providing quantitative spectral data (Smirnov et al., 2016). Blood, urine, cerebrospinal fluid, cell culture media are among the most frequently utilized samples for metabolic profiling. The examples of the usage of NMR spectroscopy in metabolomics

research include studies on Alzheimer's disease, prostate cancer, characterization of structural transformations, metabolic flux analysis *etc*. (Shulaev, 2006; Zhang et al., 2012).

Besides NMR spectroscopy, MS has gained a central role in metabolomics research (Zhang et al., 2012). MS platforms are characterized by high sensitivity and resolution, thereby enabling to measure thousands of metabolites in a sample. As a result, very massive and complex datasets are generated. The analysis of biological matrices can be conducted via direct injection (DI) or following chromatographic separation. The former approach gives an opportunity to screen a large amount of metabolites simultaneously in a very short time, thus it is widely utilized for metabolic profiling and non-targeted analysis, especially when MS has a relatively high resolving power (Shulaev, 2006; Zhang et al., 2012). However, signal co-suppression, dealing with isobars and isomers, and differing ionization efficiencies are common drawbacks for DI MS (Forcisi et al., 2013; Zhang et al., 2012). Prior separation of metabolites according to their inherent physico-chemical properties can help to overcome such problems by decreasing the complexity of the mixture injected into MS. Therefore, coupling to the corresponding techniques is a common scenario in metabolome analysis (Shulaev, 2006; Zhang et al., 2012). Gas chromatography (GC) is one of the methods, widely utilized in combination with MS for metabolomics research due to the intrinsic efficacy and reproducibility. The technology allows simultaneous measurement of many chemically diverse metabolites including organic acids, amino acids, sugars, amines, fatty acids *etc*. However, GC-MS is limited only to volatile compounds and often a derivatization step is required to make the non-volatile metabolites amenable to this type of analysis. Although the improvements associated with chemical derivatization are significant in the context of GC-MS measurements, this process may induce an emergence of side products and artifacts. Coupling of MS to capillary electrophoresis (CE) represents another promising hyphenated separation platform. In CE-MS metabolites are separated according to their charge and size followed by their selective detection over a wide range of m/z values. Big advantages associated with this approach lie in a very high resolving power, short analysis times and the tiny sample amounts required, normally ranging from 1 to 20 nL. The method has been used to analyze many metabolites including organic acids, amino acids, nucleotides, carbohydrates, peptides *etc.* The ability of the CE to separate cations, anions, and uncharged molecules in a single run enables to measure many different metabolites spanning a wide range of physico-chemical properties. The advancements in liquid chromatography (LC) have greatly contributed to the analysis of metabolome. LC-MS is often used for characterization of

endogenous and exogenous metabolites present in complex biological samples. LC techniques are highly sensitive, do not require derivatization of compounds and are suitable for the analysis of metabolites comprising a wide range of structural and chemical properties. Moreover, LC-MS provides an opportunity to elucidate the structures of compounds considered unknown. High-pressure LC (HPLC) and ultrahigh-pressure LC (UPLC) represent the current flagships of the LC-MS based metabolomics with packing material size of 3-5 μm and up to 2 μm, respectively. HPLC can be utilized, due to the combination of high resolution and analytical flexibility, for the analysis of unique metabolites or metabolite classes as well as of a broad range of compound classes. The separation power of UPLC is much better making it more suitable for the examination of complex biological mixtures.

Whereas aforementioned separation technologies provide the information on retention time of eluting metabolites, the accurate measurements of masses and abundances of specific compounds depend on the type of mass analyzers (Forcisi et al., 2013). In turn, the performance for a certain task relies on physical principles behind the instrumentation and the possibility for their implementation. Frequently used mass analyzers capable for global metabolic profiling include, in the ascending order of their resolving power, time-of-flight (ToF), Orbitrap™, and Fourier Transform Ion Cyclotron Resonance (FT-ICR) mass spectrometers (Junot et al., 2014). ToF-MS measures the masses (in the form of mass-to-charge ratio, m/z) according to the time that molecular ions require to travel from the starting point to a detector via acceleration in an electric field (Forcisi et al., 2013). The resolving power of this instrument type grows proportionally to the length of the flight path that often includes reflectrons or ion mirrors for improving the clustering of ions of the same m/z ratio. The Orbitrap™ and FT-ICR-MS belong to the Fourier transform family of instruments. The Orbitrap™ measures the m/z ratios based on the harmonic oscillations of the ions introduced into electrostatic field generated by the inner and outer electrodes that trap the molecules inside the system. The m/z ratios in FT-ICR-MS are measured based on the cyclotron frequencies of the molecular ions introduced into a homogenous magnetic field whose strength greatly affects the characteristics of the instrument. Often all three types of the aforementioned mass analyzers are combined with a quadrupole (Q) MS or an ion trap (IT) for performing fragmentation experiments, *i.e.* tandem MS (MS/MS) (Junot et al., 2014). The introduction of a mixture of metabolites into a mass spectrometer is often performed by electrospray ionization (ESI) or by atmospheric pressure ionization (Gibson et al.) techniques

because of their relatively soft ionization nature and no requirements on prior chemical modification.

The performance of metabolomics experiments does not only depend on advanced analytical facilities but greatly relies on the very first steps that include sample collection, storage, and preparation (Forcisi et al., 2013). The workflow for sample collection has to be remarkably reproducible and robust, avoiding any contaminants that are incompatible with the analytical methods for metabolite measurement, *e.g.* polyethylene glycol (PEG). The main requirement on sample preparation protocols lies in extracting as many compounds as possible from the biological matrix of interest (Shulaev, 2006). No single method is capable to retrieve all metabolites from a sample and the extraction methodology is often adapted to the required metabolite range and the utilized analytical technique. In any case, the procedure has to minimize the amount of necessary passages in order to diminish the metabolite loss and possible sources of contamination (Forcisi et al., 2013). Moreover, the ongoing metabolism in a sample has to be halted by quenching methods in order to prevent degradation or alteration of metabolites being extracted (Shulaev, 2006; Smirnov et al., 2016).

1.2.3. Analysis of metabolomics data

Data analysis represents an integral part of any metabolomics experiment encompassing many aspects from the beginning to the end (De Livera et al., 2013). The tasks vary from the identification, quantification, and validation of metabolites to revealing and explaining hidden patterns in the large networks of interconnected compounds. Independently of the scientific field, any experiment towards answering a question of interest should be designed in a right way to be correctly interpretable by data evaluation strategies. Therefore, a careful study design is required that aims to control experimental variation and ensure no presence of potential confounders (Ren et al., 2015). Sample collection, preparation, and storage are one of the possible sources of experimental variation if not properly handled. Therefore, the conditions and procedures have to be standardized in order to provide reproducible and reliable results. A sufficient amount of biological replicates (*i.e.* different samples belonging to a group of interest) is necessary for extrapolating the outcome of an experiment to a wider population (Saccenti et al., 2013). Attention has to be paid to technical replicates (*i.e.* same samples measured several times) as well, because their utilization allows to estimate technical variability. Sample randomization during the preparation or measurements is another

important aspect to avoid the presence of confounding factors that can possibly interfere with a biological question of interest. For assessing the statistical methods utilized, it is recommended to use positive and negative controls, *i.e.* metabolites that are known to change or not, respectively, in response to the investigated phenomena. It is worth pointing out that all the aforementioned requirements are stricter for human trials, where, compared to animal studies, many confounding factors cannot be well controlled (Ren et al., 2015).

Following all the guides on the study and experimental design does not fulfill the requirements for actual data analysis yet (De Livera et al., 2013). Preliminary data preprocessing step is necessary for improving the metabolite quantification and comparability of their abundance across the samples (De Livera et al., 2013; Ren et al., 2015). The preprocessing starts with raw NMR or MS spectral files that have to be subjected to different types of filters to extract as much suitable information as possible while maximally reducing any kinds of interferences. After performing these procedures, the refined files are aligned in order to produce a data matrix where rows normally represent samples and columns correspond to the metabolic features. A typical matrix, containing information on metabolite abundances, will have a substantial amount of signals showing no presence in some samples, namely missing values (De Livera et al., 2013). Such a phenomenon can emerge due to many reasons, such as a genuine absence of a metabolite in a sample, analytical or technical errors, or low abundance of a compound leading to a non-detectable signal. Some data analysis tools are able to tolerate the presence of missing values. However, the majority of methods can deal only with complete datasets, thus the ways to reduce the amount of missing values are required. Complete exclusion of the features, characterized by patterns of substantial absence, from further consideration is one approach. However, there is a risk to lose valuable information. Thereby, it is preferable to substitute missing values by some small number, normally less than the detection threshold, or by the mean or median of the metabolite abundances across different samples. Furthermore, more complicated algorithms exist based on metrical or probabilistic approaches. Other challenges in the preprocessing step concern data transformation, normalization, and scaling. Generally, the metabolomics datasets can be characterized by heteroscedasticity with a right skewed distribution. Therefore, logarithmic, square root, or any other power transformations are commonly applied. The aim behind normalization lies in the identification and removal of unwanted experimental and/or biological variation in order to obtain a better focus on variation corresponding to phenomena of interest. Human mistakes, instrumental error, measurements on separate days are common

sources of unwanted experimental variation, whereas the unwanted biological variation can include the difference in concentrations or enzymatic activities. Various normalization strategies exist, each having own advantages and drawbacks together with requirements on their appropriate utilization. The use of internal or external standards, scaling factors, quality controls, or non-changing metabolites are among the most commonly utilized methods for reducing the effects of interfering sources. Scaling is applied to make metabolic features comparable to each other, especially when the differences between them are in the order of magnitudes (Ren et al., 2015). It is often conducted prior to any statistical data analysis and can significantly affect the corresponding results. The commonly utilized scaling approaches include autoscaling, Pareto scaling, and range scaling.

Information on a certain phenomenon may be available as the abundance levels of a single metabolite or the set of compounds (Saccenti et al., 2013). Normally metabolomics experiments produce a large data matrix **X**, where every metabolic signal can represent a single dimension. **X** has size of ($n \times p$), where n depicts the number of samples/rows and p depicts the number of metabolic features/columns. The statistical analysis of such massive datasets includes the use of univariate as well as multivariate methods in order to unveil useful information. Results of the two approaches do not necessarily coincide but often complement each other. Univariate analysis normally focuses on independent changes in metabolite levels, whereas multivariate methods concentrate on the interactions between compounds and their mutual involvement into biological processes. Since the results of the two approaches may differ, it is generally recommended to work in both directions. Univariate methods have the advantage of being easy to apply, to interpret, and to compare. However, the use of them is often not enough to describe the full picture behind biological phenomenon of interest. Features, that do not show significant responses independently, may be essential acting in combination. Due to a high experimental and biological variation, certain effects can be seen only when a large amount of features is taken into account, namely «consistency at large». Since metabolomics experiments are characterized by measuring a large amount of metabolites, univariate approaches require a multiple testing correction procedure that diminishes the risk of false positive discoveries, *i.e.* situations when a null hypothesis is rejected when it is actually true. However, such a scenario often leads to the increase in false negative discoveries, *i.e.* situations when a null hypothesis is accepted when it is actually false. The advantage of multivariate methods is their ability to make use of all features simultaneously taking into account their interrelationships. However, most of the

algorithms depend on the estimation of covariance or correlation matrices, which, in turn, greatly influences the performance of a method, especially when the measurements are done on relatively few samples. Non-informative features often affect the outcome of multivariate techniques by masking metabolites, genuinely involved in the phenomenon of interest. Moreover, this scenario may lead to the problem known as overfitting when a mathematical model is biased too much by noise and artifacts present in the data at hand. Therefore, a proper validation is necessary in order to test the multivariate models on their generalizability.

Examples of univariate methods, frequently utilized in metabolomics studies, include non-paired and paired Student's *t* test, ANOVA, and their non-parametric counterparts (*e.g.* Mann-Whitney *U* test, Wilcoxon signed rank test, and Friedman test, respectively) (Saccenti et al., 2013). Among multivariate approaches, many unsupervised as well as supervised methods are currently in use. The former approaches are normally implemented first in order to have a primary and unbiased look on data (Ren et al., 2015). Therefore, unsupervised analysis is explorative in nature, enabling to discover informative patterns and trends. More formally, these methods do not include factors (*e.g.* gender, genetic mutation) into corresponding calculations. Principal component analysis (PCA) is one of the most commonly utilized unsupervised multivariate techniques that stays at the beginning of almost any data analysis workflow related to metabolomics research. The method lies in rotating the coordinate system around the cloud of data points in such a way that the direction of the first axis will coincide with the direction of maximal variance in the cloud (with respect to the new coordinate system). The directions of subsequent axes have to be found correspondingly with a restriction to be orthogonal to each other and to the first axis. Putting it into mathematical terms, the original data matrix can be represented as a product of two matrices:

$$\mathbf{X} = \mathbf{T}\cdot\mathbf{P}^{\mathrm{T}} = \sum_{\mathrm{i}=1}^{\min\,(n,p)} \mathbf{t}_i \cdot \mathbf{p}_i^{\mathrm{T}} \qquad \text{Eq. 1}$$

having following properties:

1) $\mathbf{P}^{\mathrm{T}}\cdot\mathbf{P} = \mathbf{I}$

2) $\mathbf{t}_1^{\mathrm{T}} \cdot \mathbf{t}_1 \geq \mathbf{t}_2^{\mathrm{T}} \cdot \mathbf{t}_2 \geq \cdots \geq \mathbf{t}_{\min\,(n,p)}^{\mathrm{T}} \cdot \mathbf{t}_{\min\,(n,p)}$

X is an original data matrix, **T** is a so-called matrix of scores $\mathbf{t}_i$, **P** is a so-called orthogonal matrix of loadings $\mathbf{p}_i$, **I** is an identity matrix, *n* is the number of samples, *p* is the number of features. The major property of PCA is that the first *c* axes found can be characterized by substantially larger variances in the corresponding directions than the rest of them. Therefore,

original data may be approximated by decomposing **X** using only these first *c* terms called components:

$$\mathbf{X} = \mathbf{T}\cdot\mathbf{P}^{\mathrm{T}} + \mathbf{E} = \sum_{\mathrm{i}=1}^{c} \mathbf{t}_i \cdot \mathbf{p}_i^{\mathrm{T}} + \mathbf{E} \qquad \text{Eq. 2}$$

where **E** is an error matrix. In this decomposition, new coordinates of sample points represent the linear combination of the coordinates in the original coordinate system:

$$t_{ij} = \sum_{k=1}^{p} x_{ik} p_{kj}, \ \ (1 < j < c) \qquad \text{Eq. 3}$$

The examination of scores is mainly used for revealing patterns, whereas the examination of loadings is performed to seek the metabolic features responsible for generating these patterns. As a primary tool, PCA often provides the idea for further directions during scientific investigation. However, although the output from PCA may result in observing clusters, the method is not intended for clustering as it is occasionally incorrectly referred. For this purpose, different clustering algorithms exist that represent an essential part within unsupervised framework in metabolomics research. Most of them are based on estimating the similarity between sample points. Existing algorithms may use different similarity measures including distances (*e.g.* Euclidean distance, Mahalanobis distance *etc.*) and relationship measures (*e.g.* correlation coefficient, mutual information criterion *etc.*). Examples of frequently utilized techniques include K-means clustering, hierarchical cluster analysis (HCA), self-organizing maps (SOMs) *etc*. In contrast to unsupervised methods, the supervised approach directly implements the prior knowledge on factors of interest for the purposes of biomarker discovery, classification, or prediction. Depending on the nature of the factors, namely response variables, supervised algorithms are subdivided into classification and regression problems. In this division, response variables represent either discrete or quantitative values, respectively. Determining association between the response variables and the predictor variables (represented by metabolic features) by building mathematical models and making accurate predictions is the purpose of supervised methods. Partial least squares (PLS) regression and discriminant analysis (PLS-R and PLS-DA, respectively) are one of the most commonly utilized supervised multivariate techniques in metabolomics. The methods represent a way to find coefficients of a linear model:

$$\mathbf{Y} = \mathbf{XB} + \mathbf{E} \qquad \text{Eq. 4}$$

X is the matrix of predictor variables, **Y** is the matrix of response variables, **B** is the matrix of coefficients, **E** is an error matrix. Since metabolomics experiments often produce matrices **X**

with the amount of features much greater than the amount of samples, the convenient way to solve this linear equation cannot be applied because of the construction of a singular matrix $\mathbf{X}^{\mathrm{T}}\mathbf{X}$ that cannot be inverted. Similar to PCA, the PLS algorithm lies in rotating the original multidimensional space, which eventually results in simultaneous decomposition of matrices **X** and **Y**:

$$\mathbf{X} = \mathbf{T_X}\mathbf{P_X^T} = \sum_{\mathrm{i}=1}^{\min\,(n,p)} \mathbf{t}_{\mathbf{X},i} \cdot \mathbf{p}_{\mathbf{X},i}^{\mathrm{T}} \qquad \text{Eq. 5}$$

$$\mathbf{Y} = \mathbf{T_Y}\mathbf{P_Y^T} = \sum_{\mathrm{i}=1}^{\min\,(n,p)} \mathbf{t}_{\mathbf{Y},i} \cdot \mathbf{p}_{\mathbf{Y},i}^{\mathrm{T}} \qquad \text{Eq. 6}$$

having following properties:

1) $\mathbf{P_X^T} \cdot \mathbf{P_X} = \mathbf{I}$ and $\mathbf{P_Y^T} \cdot \mathbf{P_Y} = \mathbf{I}$

2) $\mathbf{t}_{\mathbf{X},1}^{\mathrm{T}} \cdot \mathbf{t}_{\mathbf{Y},1} \geq \mathbf{t}_{\mathbf{X},2}^{\mathrm{T}} \cdot \mathbf{t}_{\mathbf{Y},2} \geq \cdots \geq \mathbf{t}_{\mathbf{X},\min\,(n,p)}^{\mathrm{T}} \cdot \mathbf{t}_{\mathbf{Y},\min\,(n,p)}$

$\mathbf{T_X}$ and $\mathbf{T_Y}$ are the matrices of scores $\mathbf{t}_{\mathbf{X},i}$ and $\mathbf{t}_{\mathbf{Y},i}$, $\mathbf{P_X}$ and $\mathbf{P_Y}$ are the matrices of loadings $\mathbf{p}_{\mathbf{X},i}$ and $\mathbf{p}_{\mathbf{Y},i}$, **I** is an identity matrix, n is the number of samples, p is the number of variables. The score vectors represent the linear combination of the coordinates in the original coordinate system:

$$t_{\mathbf{X},ij} = \sum_{k=1}^{p} x_{ik} w_{\mathbf{X},kj}, \quad (1 < j < \min\,(n,p)) \qquad \text{Eq. 7}$$

$$t_{\mathbf{Y},ij} = \sum_{k=1}^{q} y_{ik} w_{\mathbf{Y},kj}, \quad (1 < j < \min\,(n,p)) \qquad \text{Eq. 8}$$

where $w_{\mathbf{X},\mathrm{kj}}$ and $w_{\mathbf{Y},\mathrm{kj}}$ are the weights used to transform the coordinates from the original coordinate system to the new coordinate system. The axes are searched in such a way that the direction of the first axis will coincide with the direction leading to the maximum covariance between $\mathbf{t}_{\mathbf{X},1}$ and $\mathbf{t}_{\mathbf{Y},1}$, and the search for the directions of the subsequent axes will follow the same rule together with preserving orthogonality. Similar to PCA, PLS represents a dimension reduction technique and only c first terms, namely latent variables, can be retained that, in turn, may potentially carry chemical or biological meaning.

The selection of an appropriate model (especially constructed by supervised techniques) classically includes training, validation, and testing steps with three corresponding sample sets, namely training, validation, and test set, respectively (Ren et al., 2015). However, limited resources and expensiveness of data gathering frequently puts restrictions on data availability,

underlining particular importance of various resampling methods, *e.g.* cross validation or bootstrapping. Often, especially in metabolomics research, it is necessary to extract a set of features substantially contributing to the prediction of the information hidden in response variables. Such a procedure, called feature selection, can be done by several approaches. For example, «Filter» methods focus on choosing features prior to multivariate data analysis, mainly according to some simple measure, *e.g. t* test or Pearson correlation coefficient. «Wrapper» methods are based on evaluating subsets of variables simultaneously with respect to the performance of a model and choosing the subset producing the best score. «Embedded» methods are characterized by estimating the importance of features during model construction.

Frequently, very few or ambiguous information can be obtained based solely on individual metabolites shown to be significant in a study (Ren et al., 2015). Therefore, special attention is paid towards investigating mutual behavior of the groups of metabolites or their cooperative dynamics. Metabolites are involved into different biochemical pathways that may be affected by a certain biological phenomenon of interest. To assess these effects mathematically, several methods have been extensively utilized. One good example is the over-representation analysis (ORA) that represents a knowledge-driven method, commonly used for estimating the significance of specific pathways involved in the investigated phenomenon. First, the metabolic features are scored (*e.g. t* test) and projected, if possible, on the corresponding biochemical pathways. Second, a small subset is taken from the entire set of features according to the calculated score. Then, the probability is calculated indicating whether a certain pathway is significantly enriched by assessing whether corresponding metabolites are over-represented in the subset. Chi-square and Fisher's exact test are among the most frequently used tests to answer this question. Despite of its simplicity, ORA has several drawbacks. The use of only a fraction of metabolites ignoring the rest, arbitrary threshold for compound selection, and improper assumption of independence between features represent the weak sides of the method. Some of these limitations can be addressed by another approach, namely functional class scoring (FCS). The main difference of FCS is in estimating the significance of a pathway based on all corresponding metabolic features found in an experiment. The importance of a biochemical pathway can be assessed univariately (*e.g.* via averaging or summing up the scores of individual metabolites) or multivariately (*e.g.* via calculating Hotelling's T^2 statistic using all metabolites in a group). The drawbacks of FCS lie in paying no attention to interactions between metabolites that may lead to the same result if

two or more pathways share completely the same metabolites. This can be partially addressed by calculating the correlation measures, which facilitates the choice towards the most suitable pathway. More complex methods for assessing whether regulation of a certain pathway is affected by a phenomenon of interest include metabolic network reconstruction and simulation that involves mathematical modelling and measuring the output of the constructed system. Generally, such methods rely on solving system of linear or ordinary/partial differential equations depending on the model considered (whether it is static or dynamic, respectively).

Metabolomics research relies on an extensive use and further development of the appropriate databases that organize the information on metabolites in a way that could simplify the analysis and interpretation of data (Ren et al., 2015). Nowadays, there are many databases containing records on specific metabolites including their concentration within certain anatomical location, NMR and MS spectra, and involvement into different metabolic pathways. This information has to be continuously updated to support novel metabolomics studies. The metabolite link (METLIN) was the first metabolomics web-based database emerged in 2004 and currently represents one of the most commonly used resources in this scientific field. Other frequently used databases include the human metabolome database (HMDB), lipid metabolites and pathways strategy (LIPID MAPS), Kyoto encyclopedia of genes and genomes (KEGG). Despite of their potential, metabolomics databases often lack common language, which hampers the systematic search for information. Moreover, the use of different types of instruments further aggravates this issue. Therefore, it is very important to establish and support common reporting standards and data formats that would make working with metabolomics databases much easier.

1.2.4. Nutritional aspects of metabolomics

Nutrition represents one of the cornerstones towards health (McNiven et al., 2011). From ancient history it has been known that food can be responsible for modulating the health of an organism (Astarita and Langridge, 2013). Currently, it is known that a poor diet promotes such metabolic imbalances as obesity, diabetes, malignancy, or inflammatory diseases (McNiven et al., 2011). However, the intrinsic mechanisms are still mostly unknown, essentially due to the limited knowledge on the molecular composition of food that can include heterogeneous plant- and animal-based nutrients (Astarita and Langridge, 2013; Jones

et al., 2012). The complexity of the task to reveal the connections between diet and host metabolism stimulates the development of holistic approaches to investigate and understand the corresponding interactions (Astarita and Langridge, 2013). As the part of this pathway, metabolomics tools are currently widely utilized to uncover food metabolome, to define association of its components to physiological responses, and to evaluate the role of gut bacteria in the processing of the corresponding molecules. For example, numerous studies investigate the effects of nutraceuticals, nutrition products that represent intermediates between food and drugs. Dietary supplements (*e.g.* vitamin D) or processed food containing biologically active compounds (*e.g.* vitamin C in juices) fall into this category. Nowadays, the way of thinking of the medical community as well as general population is gradually shifting from the focus on sufficient nutrition to avoid disease towards the focus on nutrition for optimizing overall health and function via paying much more attention to diet regimes and food intake (Astarita and Langridge, 2013; Jones et al., 2012). To a first approximation, population-based nutritional needs, based on normative descriptions, can be used to promote health and decrease the risk of a disease onset (Jones et al., 2012). The advances in technologies, including metabolomics, enable to go beyond the reductionist framework by investigating the complexity of interactions of all nutrients within a unique subject providing, in perspective, individual treatment through a personal nutrition plan. Therefore, the application of metabolomics research to nutrition science, establishing the field of nutritional metabolomics, is inevitable (Astarita and Langridge, 2013). Nutritional metabolomics aims to understand the association of entire metabolomes with changes in diet and to retrieve a complex view on the corresponding regulatory mechanisms (McNiven et al., 2011).

Diet can be considered as the part of the so-called exposome that encompasses environmental exposures through the course of life and plays a significant role in health maintenance (Jones et al., 2012). Modern metabolomics analysis allows detection and identification of thousands of chemical entities present in foods and beverages (Astarita and Langridge, 2013). Such advances facilitate investigations that go beyond classical measurements on nutrients (*e.g.* amount of carbohydrates, fats, proteins, water, vitamins, and minerals), their ratios (*e.g.* protein to carbohydrate ratio), or number of calories. For instance, metabolites, belonging to the same compound class but different subclasses, can affect human health in a distinct manner. Two subclasses of polyunsaturated fatty acids (PUFAs), ω-3 PUFA and ω-6 PUFA, are good examples of this concept: ω-3 PUFAs, considered deficient in Western diets, are mainly associated with health benefits and anti-inflammatory responses, whereas ω-6 PUFAs

contribute to a disease pathogenesis (*e.g.* cardiovascular disease). Essential nutrients required by a human body for homeostasis can be considered as a core nutritional metabolome (Astarita and Langridge, 2013; Jones et al., 2012). However, most of the food-derived chemicals are not necessary for sustaining life but can actively affect overall well-being. Modern metabolomics tools provide the possibility to analyze many of these exogenous dietary compounds (Astarita and Langridge, 2013). For example, a large proportion of food metabolome consists of phytochemicals, plant metabolites that may be extensively metabolized in the body and play a role as antioxidants and inducers of detoxification systems (Astarita and Langridge, 2013; Jones et al., 2012). Other components that can be found in diet include compounds of non-natural origin, such as herbicides, insecticides, fungicides *etc.* Moreover, diet can be characterized by the presence of different contaminants. Although the two aforementioned groups do not represent a central component of nutritional metabolomics research, their relevance is marked by the substantial amount of these compounds detected in metabolomics studies and by their possible interactions with nutrients (Jones et al., 2012). Such a big diversity of dietary components has facilitated the development of extensive databases storing information on food metabolome, *e.g.* the Food Database (FooDB) or METLIN (Astarita and Langridge, 2013; Jones et al., 2012). Molecular composition can differ between representatives of the same type of ingested dietary substance (Astarita and Langridge, 2013). The so-called metabolic phenotype can depend on several factors including genotype, environment (*e.g.* location or growing seasons) as well as the way to process (*e.g.* frying, steaming) and preserve (*e.g.* freezing, drying) the food. Therefore, modulation of metabolic phenotypes by enriching a dietary product with compounds beneficial for an organism and optimizing its organoleptic features represents one of the crucial tasks for food industry.

The aforementioned objective can be further facilitated not only by improving the food quality itself but by monitoring the corresponding responses via screening changes in human metabolism (Astarita and Langridge, 2013). Certain dietary patterns can potentially reduce the risk of various diseases, such as cancer, cardiovascular disease, or Alzheimer's disease. For example, consumption of fruits and vegetables with high levels of antioxidants can reduce the risk of cancer without considerable side effects. (McNiven et al., 2011). Thus, studies on revealing the effects associated with a reported dietary intake are of great importance in nutritional research. Characterization of food-specific biomarkers can be used for epidemiological or dietary intervention studies, where examination of the nutritional patterns

during the trial can represent supplementary information in the form of a diet questionnaire (Astarita and Langridge, 2013). Furthermore, nutritional deficiencies and unbalances can be assessed through the development of inexpensive tests on biomarkers of food intake. After such an assay, supplementation enriched with natural antioxidants, vitamins, and phytochemicals can be subscribed. However, it is important to remember that high intake of products, exhibiting protective properties at moderate consumption, may have harmful effects. This can be true even for essential nutrients whose excessive consumption can be damaging for an organism (McNiven et al., 2011). Such a contradictory behavior emerges due to the complex nature of the involvement of dietary components in host metabolism (Astarita and Langridge, 2013). The metabolites deriving from food can interact with the genes, proteins, enzymes, and microenvironment of an organism. First, these compounds may represent building blocks for molecular structures of a higher order, *e.g.* DNA, polysaccharides, cell membranes. Therefore, food metabolome can substantially influence the physical and chemical properties of such large macromolecules, especially in case of lipid membranes. Second, dietary metabolites serve as an energy source or play a role in regulation of corresponding pathways. Third, they can participate in cell signaling mechanisms or modulating enzyme activities. Fourth, some dietary metabolites act as antioxidants protecting cells against oxidative stress that can damage their components.

Following ingestion, the food components are either metabolized in gastrointestinal tract (GIT) by the commensal bacteria and/or enterocytes or secreted from an organism in an intact form (Astarita and Langridge, 2013). In turn, gut microbiota composition is modulated by the diet providing an opportunity for some microorganisms to expand due to the availability of nourishment necessary for proliferation. Resulting microbial phenotypes may greatly contribute to the variability of the host metabolome. The components derived from microbial metabolism may exhibit beneficial properties as well as be potentially harmful for health. After absorption through GIT, dietary metabolites are mainly transported to the liver followed by various modifications and transportation of the resulting compounds into the blood stream for their delivery to different tissues of the body. Summing up, the regulation of dietary components in humans occurs on different levels including food intake, gut absorption, and cell metabolism. Therefore, a holistic view on metabolome is required by screening metabolites in various tissues and biofluids in order to fully understand the effects of a diet on genes, proteins, and microenvironment and rationally design the dietary regimes for manipulating cell functions and enhancing overall health. Following a certain diet enables to

estimate the nutritional status of a subject, which assesses the nutrition-wise tendency towards healthy or disease condition (Zeisel et al., 2005). In a scale of metabolites, metabolomics is able to provide snapshots of the nutritional status, which, together with unique genotypes and environments, gives rise to so-called metabolic phenotypes that can remain constant for long periods (McNiven et al., 2011). Integration of genetic, proteomic, metabolomic, functional, and behavioral factors can represent the basis of a more global concept, namely nutritional phenotype (Zeisel et al., 2005). The individual nutritional phenotype concerns prediction of a response of a subject to certain perturbations and the extent to which they might affect health. Together with the identification of individual variations in dietary requirements (represented by nutritional phenotype), the aforementioned holistic strategy undoubtedly contributes to the development of personalized nutrition aiming at satisfying nutritional needs of individual patients for the purpose of decreasing the risk of a disease and achieving overall wellness (Astarita and Langridge, 2013; Zeisel et al., 2005).

1.2.5. Triggering the gut microbiome

The human gut can be considered as a bioreactor harboring trillions of microbes, a number that far exceeds the total amount of all eukaryotic cells of the host (Sonnenburg and Backhed, 2016; Xie et al., 2013). These bacteria altogether compose a system, namely gut microbiota (Vernocchi et al., 2016). The collective genome of this complex structure, namely microbiome, is about two orders of magnitude (100-150 times) greater than the size of the human nuclear genome (Heinken and Thiele, 2015; Xie et al., 2013). Such a striking outnumbering implies a broad range of biochemical and metabolic functions of this complex consortium of commensal bacteria, many of which can be complementary in maintaining homeostasis of the host (Xie et al., 2013). Despite of this coding potential, the knowledge on the annotation and biological function of many of the corresponding genes is relatively poor (Sonnenburg and Backhed, 2016). The gut ecosystem exhibits a hugely variable dynamic range of intrinsic microbes that can reach several orders of magnitude (Dorrestein et al., 2014). Bacterial taxa inhabiting the gut predominantly belong to two phyla, namely *Bacteroidetes* and *Firmicutes*, followed by less prevalent phyla including *Actinobacteria*, *Proteobacteria*, *Fusobacteria*, and *Verrucomicrobia* (Heinken and Thiele, 2015; Sonnenburg and Backhed, 2016). Interestingly, while at the higher levels of taxonomic hierarchy there are no considerable differences between individuals, high interpersonal variation can be observed at the genus and species level even for closely related subjects (Heinken and Thiele, 2015).

Such highly individualized microbial signatures are relatively stable through the lifespan of a subject (Dorrestein et al., 2014; Smirnov et al., 2016). Recently, the concept of an enterotype has been proposed that describes the classification scheme based on the composition of the bacterial community in the gut (Heinken and Thiele, 2015). Taking into account such diversity between subjects, it has been suggested that universality should be anticipated at the functional level described by the gut microbiome rather than at the compositional level (Heinken and Thiele, 2015; Smirnov et al., 2016).

The symbiotic bacteria form a system that is highly adaptable to environmental changes and can vary with age, diet, and health status (Xie et al., 2013). Therefore, in contrast to the genome of a host, the microbiome can dynamically change its components depending on the requirements of the individual constituents, the whole community, or the entire organism. On the other side, alterations of the microbiota composition, reflected by the presence of individual bacterial species or notable shifts in microbial communities, can prompt disease-inducing or disease-protective effects due to the modifications of the bacterial metabolic activity and functions (Holmes et al., 2011; Vernocchi et al., 2016; Xie et al., 2013). Different GI disorders and metabolic diseases, that have been shown to be associated with perturbations in a subtle equilibrium of bacterial communities in the gut, include cystic fibrosis, inflammatory bowel diseases (*e.g.* Crohn's disease, ulcerative colitis), diabetes, obesity, rheumatoid arthritis, some allergic disorders, and even neuropathologies such as Parkinson's disease (Dorrestein et al., 2014; Heinken and Thiele, 2015; Vernocchi et al., 2016). It has been proposed that metabolic health is associated with relatively high biodiversity within the microbial ecosystem (but not always), which can serve as a measure of its stability and robustness (Sonnenburg and Backhed, 2016). Many lifestyle-associated problems (*e.g.* adiposity, insulin resistance, inflammation) have been suggested to be especially connected to the «Western» diet that leads to a less diverse (*i.e.* dysbiotic) microbiota (Heinken and Thiele, 2015). Taking the aforementioned facts into account, it is reasonable to suggest that the modulation of the microbial ecosystem may have positive effects on health, indicating that the gut microbiota may serve as a nutritional target for drugs and other interventions (Xie et al., 2013). Characterization of the complex interactions between the host and its commensal bacteria is possible within the framework of systems biology approaches. The advent of different «omics» platforms has played a crucial role in this respect (Vernocchi et al., 2016). As part of the global view on biological systems, metabolomics provides exceptional opportunities to explore the interplay between mammalian and bacterial metabolic processes

by analyzing low molecular weight compounds in biofluids, tissues, and intestinal contents (Xie et al., 2013). Indeed, several studies have been reported on successful application of metabolomics to reveal metabolites associated with changes in gut microbiota composition (Vernocchi et al., 2016). It is reasonable to assume that substantial amount of metabolites within a human body is not of a human origin, comprising dietary and microbial compounds (Dorrestein et al., 2014). Similarly to the gut microbiota, metabolome can be very diverse between the subjects, providing unique and relatively stable metabolic phenotype as the reflection of the interactions between the host and other factors including commensal bacteria (Dorrestein et al., 2014; Smirnov et al., 2016). Thereby, metabolome can be considered as a window, which enables to monitor the activity of bacterial ecosystem in the gut through microbial-mammalian co-metabolism (Holmes et al., 2011).

Gut microbes can be tightly involved in the control of metabolism in the human body (Xie et al., 2013). Many studies have moved beyond describing the gut microbiota composition towards investigating the functionality of this consortium (Heinken and Thiele, 2015). In addition to the most evident role of food processing and energy harvesting, other activities of the microbial community include the maintenance of the epithelial homeostasis, stimulation of angiogenesis, protection against pathogens, development and regulation of the immune system as well as regulation of the nervous system (Heinken and Thiele, 2015; Holmes et al., 2011; Smirnov et al., 2016; Vernocchi et al., 2016; Xie et al., 2013). The composition and diversity of the bacterial population markedly increases along GIT starting from stomach, through small intestine, and towards colon (Xie et al., 2013). Therefore, functions of the gut microbiota are not homogeneously distributed but rather specialized for each GIT compartment, which is expressed in the form of differences in interactions within microbial community and between microbes and the host (*e.g.* through signaling via low molecular weight metabolites, peptides, proteins, or through immune-mediated pathways). Participating in multiple primary and secondary metabolic pathways, gut microbiota itself produces a large variety of small molecules, whose diversity can be affected by many environmental stimuli, *e.g.* lifestyle or diet (Sonnenburg and Backhed, 2016; Vernocchi et al., 2016; Xie et al., 2013). These compounds may exhibit a variety of properties, relevant for the etiology and prevention of complex diseases (Heinken and Thiele, 2015). They can be excreted with feces or absorbed by epithelial cells leading to different possible scenarios including their direct involvement into host metabolism with an eventual secretion in the urine (Sonnenburg and Backhed, 2016; Xie et al., 2013). Together with metabolites of endogenous origin, these small molecules can

be measured by MS or NMR spectroscopy of tissue or biofluid samples (*e.g.* blood, urine, or fecal extracts), providing an opportunity to evaluate the metabolic status of a human host as well as to determine chemical signatures associated with changes in gut microbiota composition due to specific physiological and pathological conditions (Xie et al., 2013). In other words, metabolic phenotypes can be measured as a result of the co-metabolism of the microbial community and the host together with an exchange of metabolic information between them. To uncover the inherent associations between commensal bacteria and metabolome at a more global level, integration of high-throughput metabolic phenotyping with gut microbial profiling is necessary.

Short-chain fatty acids (SCFAs) are one of the most known metabolites associated with bacterial activity in the gut and produced as a result of human-microbial co-metabolism (Xie et al., 2013). Being end-products of anaerobic bacteria fermentation of indigestible oligo- and polysaccharides, fiber, indigested proteins as well as endogenous epithelial-derived mucus, SCFAs play an important role in the energy metabolism of a host and *de novo* lipogenesis. Acetic, propionic, and butyric acid are the major products of such a process. Other SCFAs include formic, fumaric, malonic acid *etc*. In addition to be an energy source for cells belonging to various tissues, SCFAs have been shown to represent essential nutrients for colonic epithelium, to modulate intestinal environment, to regulate cell proliferation and gene expression, to act as transmitters of neural signals, to enhance the innate and adaptive immune system (Dorrestein et al., 2014; Xie et al., 2013). SCFAs exhibit a protective role against GI disorders and cardiovascular diseases (Xie et al., 2013). Moreover, their administration has been shown to be beneficial in the treatment of inflammatory bowel diseases, obesity, and cancer. (Vernocchi et al., 2016). Choline metabolism represents another example of the active involvement of gut microbiota into processes within a host (Xie et al., 2013). A wide range of biological functions can be associated with choline, a molecule representing an essential nutrient, primarily metabolized in the liver. In addition to di- and trimethylglycine, formed during oxidation of choline in host biochemical pathways, choline can be metabolized by commensal bacteria to produce di- and trimethylamine (DMA and TMA, respectively). TMA, after its absorption from the gut into the bloodstream, can be further enzymatically oxidized in the liver, forming trimethylamine N-oxide (TMAO) (Sonnenburg and Backhed, 2016; Xie et al., 2013). This compound is associated with several diseases such as liver disease, cardiovascular disease, and diabetes. In addition to choline, accumulation of TMA can occur as a consequence of a diet, rich in L-carnitine (*e.g.* red meat) (Sonnenburg and Backhed,

2016). Gut microbiota is actively involved in bile acid metabolism, reflected in various chemical modifications of the corresponding metabolites (*e.g.* deconjugation, dehydrogenation, dihydroxylation) by different members of bacterial community (Vernocchi et al., 2016). Being derivatives of cholesterol, bile acids play an important role in cholesterol secretion, dietary fat absorption, preserving gut barrier function as well as modulation of lipid, glucose, and energy metabolism (Vernocchi et al., 2016; Xie et al., 2013). Deconjugation performed by commensal bacteria largely contributes to reabsorption of bile acids, secreted into the duodenum (Xie et al., 2013). Gut microbiota plays a significant role in the production of vitamins, since most of them cannot be synthesized by the host alone (Vernocchi et al., 2016). Vitamins are essential substances for a human organism (especially in the infancy), participating in different biochemical reactions (Dorrestein et al., 2014; Vernocchi et al., 2016). Some vitamins arising from microbial activity include thiamine (*i.e.* vitamin B_1), riboflavin (*i.e.* vitamin B_2), niacin (*i.e.* vitamin B_3), pantothenic acid (*i.e.* vitamin B_5), pyridoxine (*i.e.* vitamin B_6), biotin (*i.e.* vitamin B_7), folic acid (*i.e.* vitamin B_9), and cobalamin (*i.e.* vitamin B_{12}) (Vernocchi et al., 2016). Bacterial metabolism of dietary polyphenols, undigested amino acids, or carbohydrates can result in the increase of organic acids (*e.g.* benzoic, hippuric, lactic acid). Hyperproduction of these compounds serves as a sign of the overgrowth of certain bacterial species. It is also worth to mention polyphenols, bioactive components largely present in a diet. Two major classes, hydroxycinnamic acids and flavonoids, are the source of many secondary metabolites of bacterial origin that can be involved in the host metabolism.

Examining aforementioned examples, it is possible to see that metabolomics together with other «omics» technologies (especially, metagenomics for the analysis of microbiome) can provide a broad spectrum of microbe-relevant metabolites together with their specific biological functions (Xie et al., 2013). This can potentially facilitate the development of an engaging area of future drug discovery and therapy. Ideally, studies on human gut microbiota and related metabolome have to be conducted using mucosal biopsies as samples (Smirnov et al., 2016). However, due to associated challenges, the majority of the research rely on stool samples since this matrix is relatively easy-to-handle and provides a partial representation of the reality taking place in the GIT (Smirnov et al., 2016; Sonnenburg and Backhed, 2016). Analyzing urine and blood samples represents an important complementary strategy to characterize metabolites of microbial origin (Xie et al., 2013). One very important aspect in the direction of uncovering the metabolic handshake between the host and the resident gut

microbiota is the use of different animal models with simplified populations of commensal bacteria (Holmes et al., 2011). Such models include germ-free animals to study the potential of the host alone, animals treated with antibiotics to investigate the effects when certain bacterial group is absent, animals with transplanted microbiota (*e.g.* so-called Schaedler microbiota or human infant microbiota) to examine patterns and interactions related to specific species. Although the use of animal models is an approximation of the reality in a human organism, the importance of some of the corresponding findings have been supported by human trials (Sonnenburg and Backhed, 2016). Besides studies on metabolism, exploration of the interactions between gut and brain activity is gaining strong interest (Dorrestein et al., 2014; Holmes et al., 2011). Finding the corresponding links responsible for behavioral patterns and the ways to influence these connections is an exciting area of research (Holmes et al., 2011). Overall, the gut microbiota that co-exists with the human host can be considered as a superorganism, whose metabolic capacities most likely outperform the metabolic capacities of the host alone (Heinken and Thiele, 2015; Holmes et al., 2011). Therefore, the significance in uncovering the corresponding mechanisms is enormous.

1.3. High resolution mass spectrometry

1.3.1. General description

Nowadays, high resolution mass spectrometry (HRMS) is a cutting-edge technology for a global metabolome analysis (Junot et al., 2014). As was mentioned before, instruments falling into this category include ToF-MS, Orbitrap, and FT-ICR-MS, each associated to its own advantages and drawbacks with respect to a specific problem (Junot et al., 2014; Rathahao-Paris et al., 2015). The excellence of HRMS can be naturally characterized by parameters that describe the quality of a mass spectrometer (Brenton and Godfrey, 2010). In order to understand the meaning behind some of the parameters, it is important to grasp the basic terminology used in MS research. The references on the corresponding terms and their usage can be found in the International Union of Pure and Applied Chemistry (IUPAC) recommendations for nomenclature and symbolism

Mass spectrometers measure mass-to-charge ratios (m/z) of ions generated by some ionization technique (*e.g.* ESI) (Brenton and Godfrey, 2010). Every experimentally determined mass of an ion refers to an «accurate mass» (*i.e.* «measured accurate mass») that has certain

interpretation capabilities depending on the instrument. The primary goal of MS is to define the elemental composition (*i.e.* the molecular formula) that stands behind the accurate mass. The calculated mass of an ion corresponding to this elemental composition refers to an «exact mass» (*i.e.* «calculated exact mass») (Brenton and Godfrey, 2010). The calculation implies the summation of the exact masses of all the individual atoms included into a molecular formula (Pleil and Isaacs, 2016). The proximity of the exact mass to the accurate mass of an ion in a single measurement run describes the parameter called «accuracy» (*i.e.* mass measurement error) that is commonly represented in three different forms (Brenton and Godfrey, 2010):

$$\begin{aligned} \text{Accuracy (in Da)} &= \left(m/z_{exp} - m/z_{th}\right) \\ \text{Accuracy (in mDa)} &= 10^3 \cdot \left(m/z_{exp} - m/z_{th}\right) \\ \text{Accuracy (in ppm)} &= 10^6 \cdot \frac{\left(m/z_{exp} - m/z_{th}\right)}{m/z_{th}} \end{aligned} \qquad \text{Eq. 9}$$

Here, m/z_{exp} stands for an accurate mass and m/z_{th} stands for an exact mass. The most frequently used notation corresponds to the accuracy in the «parts-per-million (ppm)» form. Related terms refer to mass measurement accuracy (*i.e.* mass accuracy) describing the average of a mass measurement error:

$$\begin{aligned} \text{Mass accuracy (in Da)} &= \frac{1}{n}\sum_i \left(m/z_{exp,i} - m/z_{th}\right) \\ \text{Mass accuracy (in mDa)} &= \frac{10^3}{n}\sum_i \left(m/z_{exp,i} - m/z_{th}\right) \\ \text{Mass accuracy (in ppm)} &= \frac{10^6}{n}\sum_i \frac{\left(m/z_{exp,i} - m/z_{th}\right)}{m/z_{th}} \end{aligned} \qquad \text{Eq. 10}$$

Here, *i* stands for a single measurement and *n* stands for their total amount. An accurate mass of an ion, measured several times, will not preserve its original value but rather will differ from measurement to measurement due to inherent random errors. The closeness and repeatability of the results is reflected by the parameter called «precision». A useful way to describe precision is to measure the standard deviation of an accurate mass:

$$\text{Precision} = \sqrt{\frac{1}{n-1}\sum_i \left(m/z_{exp,i} - \overline{m/z}_{exp}\right)^2} \qquad \text{Eq. 11}$$

$$\overline{m/z}_{exp} = \frac{1}{n}\sum_i m/z_{exp,i} \qquad \text{Eq. 12}$$

Here, $\overline{m/z}_{exp}$ stands for an average experimental mass. According to this notation, the definition for accuracy can be complemented by the statement, that this parameter describes the proximity of an accurate mass to the expected result, namely m/z_{th}. Theoretically, high mass accuracy (close to 0) can provide but does not imply the possibility to detect numerous metabolites present in a complex mixture (Pleil and Isaacs, 2016). An overlap between signals (especially, extremely close ones) may hinder the accurate mass analysis. A minimal distance between two ion signals to be considered as distinct, is reflected in the parameter called «resolution». It can be defined as the ratio of an accurate mass to the width of the corresponding peak at half of its height, *i.e.* full width at half maximum (FWHM) (Junot et al., 2014):

$$\text{Resolution} = \frac{m/z_{exp}}{\Delta_{1/2} m/z_{exp}} \qquad \text{Eq. 13}$$

Here, FWHM is represented by $\Delta_{1/2} m/z_{exp}$. As it is obviously and naturally implied, the term HRMS is associated to the instruments having high resolution.

Before the technological advances in HRMS, global metabolite profiling was mainly performed by low resolution instruments, such as triple quadrupole (QQQ) or IT, whose current use in metabolomics is mostly focused on the tasks of metabolite identification and MS/MS experiments (Junot et al., 2014). Since the middle of 2000s, HRMS has been extensively applied to metabolomics research due to the inherent potential to cover and detect numerous metabolites present in a sample. The constant development in this field brings new instruments with even better qualities as well as new computational tools to analyze growing amounts of spectral data. The mass accuracy and resolution of the corresponding instruments are typically below 5 ppm and above 10.000, respectively, which significantly improves the detection of metabolites, their identification and structural characterization. Theoretically, high mass accuracy is sufficient to assign an elemental composition to a metabolite signal (Rathahao-Paris et al., 2015). In turn, high resolution provides information on isotopic patterns, further facilitating characterization of metabolites. HRMS provides deep insights into the information hidden behind the nominal masses, *i.e.* ion masses represented as the sum of the exact masses of the constituent elements rounded to the nearest integer value (in the calculation only the most abundant isotope of each constituent element is taken into account) (Brenton and Godfrey, 2010; Junot et al., 2014). Therefore isobaric compounds (*i.e.* compounds that have the same nominal mass but different exact masses) can be revealed. Thus, the quality of the resulting metabolome data is immense with the possibility to measure

thousands of metabolites in a single run (Rathahao-Paris et al., 2015). In addition to the quantitative parameters such as mass accuracy and resolution, HRMS instruments can be compared by their potential to identify compounds (Junot et al., 2014). This feature implies the ability to perform MS/MS analysis and to detect isotopic patterns together with accurate measurements of the corresponding relative isotope abundances. Due to the high metabolome coverage, a natural extension of HRMS for metabolomics has been found in the closely related fields of lipidomics and glycomics. Despite describing a very specific class of compounds, lipidome and glycome are highly diverse because of the huge natural complexity and heterogeneity of the corresponding constituents. Therefore, the use of HRMS, especially combined with separation techniques (*e.g.* LC), has proven to be almost mandatory to analyze complex lipid or glycan mixtures.

The analysis of metabolome by HRMS can be performed either by DI of a sample into the mass analyzer or using hyphenated methods that enable the sequential injection of the sample fractions (Junot et al., 2014). Generally, DIMS is used for a primary data examination and screening for potentially relevant patterns that can be further investigated in much more details. The attractive features of the approach are the ability to analyze many samples in a short time (*i.e.* high-throughput screening) and relatively simple data processing due to working only with the m/z domain. However, severe matrix effects can be observed, especially when highly concentrated samples are introduced into the mass spectrometer leading to oversaturation. There is no possibility to discriminate between isomeric compounds (Junot et al., 2014; Rathahao-Paris et al., 2015). Moreover, isobaric compounds with very close m/z ratios can hamper the assignment of a peak to a unique elemental formula. The two aforementioned issues can be also addressed for MS/MS experiments, when metabolite identification can be obstructed by the difficulty to select the precursor ion. In order to overcome the aforementioned issues to some extent, HRMS instruments can be coupled to separation techniques (*e.g.* GC, CE, LC). However, this comes at the sacrifice of a high-throughput analysis (Junot et al., 2014). Moreover, for the instruments, based on Fourier transformation (FT-ICR-MS, Orbitrap), the resolution depends on the acquisition rate, which limits their coupling to separation techniques with high rate of the sample flow (Forcisi et al., 2013; Junot et al., 2014; Rathahao-Paris et al., 2015). ToF-MS does not exhibit such a behavior (Rathahao-Paris et al., 2015). The big advantage of hyphenated methods over DIMS is the addition of a second dimension, represented in a retention time, to the m/z domain (Junot et al., 2014). This feature potentially increases the capability of the technique to

discriminate isomers and isobars with extremely close m/z ratios. Although the identification of metabolites has been drastically improved with the development of HRMS, this task still represents the challenge number one in metabolomics analysis. It is worth to point out that not only the performance of an analytical tool contributes to metabolite identification but the efficiency of bioinformatics approaches as well (Rathahao-Paris et al., 2015). Therefore, many informatics and computational tools have been developed in this direction (Junot et al., 2014). Naturally, initial steps towards metabolite identification involve determination of elemental composition that can be assigned to experimentally measured accurate masses (Rathahao-Paris et al., 2015). Additionally, the use of metabolomics databases enables to find matches of accurate masses to the real compounds (Junot et al., 2014; Rathahao-Paris et al., 2015). Thus, first hints regarding metabolite identity can be obtained. However, this information is often insufficient and additional MS/MS experiments are required to match the experimentally obtained MS/MS fragmentation patterns to the ones stored in a database. In case of the lack of spectral data for a certain compound, there are computational methods that are capable to generate fragmentation patterns *in silico*, thereby enabling the comparison of experimental MS/MS spectra to the predicted ones. The final identification is achieved if two experimental metabolite characteristics (*e.g.* accurate mass and MS/MS spectrum) match to the characteristics obtained for an authentic compound under identical conditions. As a summary, four levels of metabolite identification can be defined (mainly for non-novel compounds) according to the metabolomics standards initiative (Sumner et al., 2007):

1) Compound is identified. This level requires a match between an authentic compound and a compound from a sample with respect to a minimum of two independent and orthogonal results obtained under identical experimental conditions (*e.g.* accurate mass and MS/MS spectra).
2) Compound is putatively identified. This level requires that the properties of a compound of interest match to the properties of an authentic compound stored in a database.
3) Compound class is putatively identified. This level requires that properties of a compound of interest match to the properties of a certain class of compounds.
4) Unknown compound. This level can be addressed to the compounds, for which no sufficient information was found to be classified to the above levels.

It is recommended to follow this nomenclature in order to provide a clear summary for the identification levels of all metabolites reported in a study. Nevertheless, much of the metabolites detected in an experiment often remain unidentified, mainly due to the lack of

information in spectral databases and, as a consequence, an authentic compound necessary for comparison (Rathahao-Paris et al., 2015). Therefore, the development of highly sophisticated approaches is necessary to mine the unknowns.

1.3.2. Theoretical aspects of FT-ICR-MS

FT-ICR-MS is a sophisticated technique combining advanced physics, instrumentation, and electronics, which has been widely used for chemical and biomedical research (Qi and O'Connor, 2014). It is based on the detection of an image current generated by ions trapped inside an ICR cell and implicated in rotational motions induced by a magnetic field (Marshall and Hendrickson, 2002). Initially ions are produced externally by an ion source (*e.g.* ESI) (Qi and O'Connor, 2014). After their accumulation in the ion optics, they are transferred into the ICR cell and subjected to a spatially uniform magnetic field and electric fields, necessary for ion trapping. Assuming that **i**, **j**, and **k** are unit vectors representing the axes x, y, and z, respectively, of a Cartesian coordinate system, a charged particle or an ion introduced in a spatially uniform magnetic field $\mathbf{B} = 0 \cdot \mathbf{i} + 0 \cdot \mathbf{j} - B_0 \cdot \mathbf{k}$ will be subjected to a force (Marshall et al., 1998):

$$\mathbf{F} = m\frac{d\mathbf{v}}{dt} = q\mathbf{v} \times \mathbf{B} \qquad \text{Eq. 14}$$

Here, q, m, and **v** correspond to the charge, mass, and velocity vector of the ion, respectively. The "×" sign means the cross product between the vectors **v** and **B**, resulting in a vector, perpendicular to both of them. Therefore, at a constant speed, the ion subjected to this force (*i.e.* Lorentz force) will experience a circular motion, also known as the «cyclotron motion» (Fig. 1).

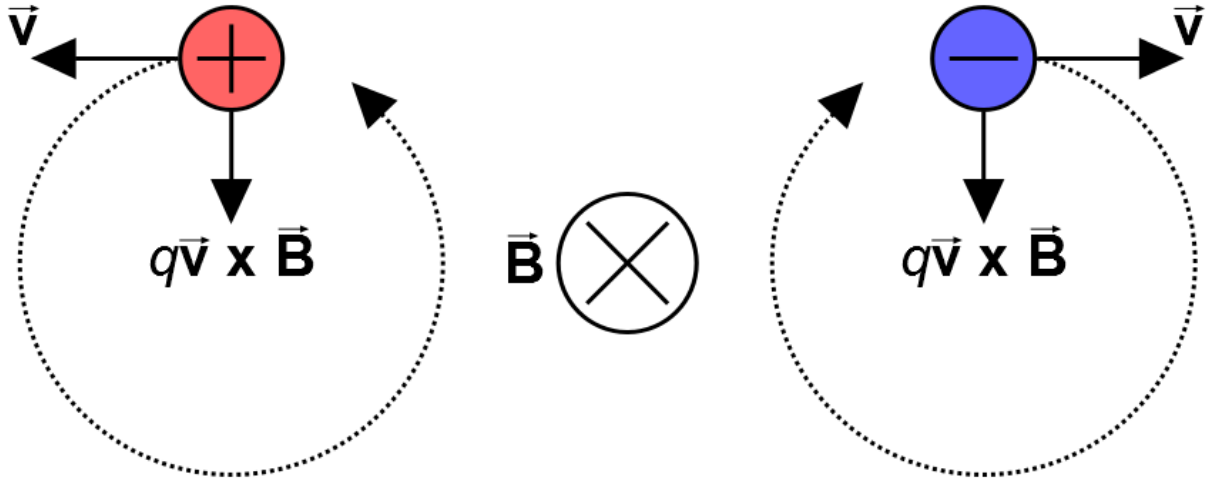

Fig. 1. The path of an ion subjected to a force generated by a spatially uniform magnetic field directed onto the plane. Positive and negative ions exhibit opposite behavior.

Projecting the behavior of the ion onto the *xy*-plane, the Eq. 14 can be modified in a following way:

$$F_{xy} = \frac{mv_{xy}^2}{r} = qv_{xy}B_0 \qquad \text{Eq. 15}$$

Here, $v_{xy} = \sqrt{v_x^2 + v_y^2}$ represents the velocity of the ion in the *xy*-plane and r is the radius of an orbit where cyclotron motion takes place. Since the angular velocity is $\omega = v_{xy}/r$, further modifications will lead to the so-called "cyclotron" equation:

$$\omega_c = \omega = \frac{qB_0}{m} = \frac{eB_0}{m/z} \qquad \text{Eq. 16}$$

Here, ω_c stays for an "unperturbed" ion cyclotron frequency and e is an elementary charge. Thus, the ion of a given m/z ratio introduced in the aforementioned static magnetic field will move around the z axis with a certain cyclotron frequency. The fact, that ions of the same m/z ratios have the same ω_c independently of their velocities, represents a remarkable feature because, in this case, the precise determination of m/z ratio does not rely on the ion kinetic energy. Consequently, this is the reason why FT-ICR-MS supports high resolution capabilities, since many other mass spectrometric techniques are affected by kinetic energy spread (Qi and O'Connor, 2014).

Although it is possible to see a straightforward way to calculate m/z ratios from the corresponding ion cyclotron frequencies ω_c, the real measurements are more complicated in nature (Marshall et al., 1998). The mass spectrometric analysis of ions takes place in an ICR cell, schematically represented on Fig. 2. The magnetic field applied along the opposite direction of the *z*-axis can confine ions only in the *xy*-plane of the ICR cell, which does not prevent their movement in the perpendicular direction (Qi and O'Connor, 2014). After entering the cell, the ions are additionally stabilized by applying an electrostatic trapping potential to the «end caps» electrodes (on Fig. 2 are represented by the front and rear plates, perpendicular to the *z*-axis), which prevents their escape along the *z*-axis. The detector plates of the ICR cell (on Fig. 2 are represented by lower and upper plates perpendicular to the *y*-axis) are used to register the electrical signal from moving ions (Marshall et al., 1998). In ideal conditions, an ion of charge q generates an «image» charge on these two opposite plates and the corresponding difference $\Delta Q(y)$ will be equal:

$$\Delta Q(y) = -\frac{2qy}{d} \qquad \text{Eq. 17}$$

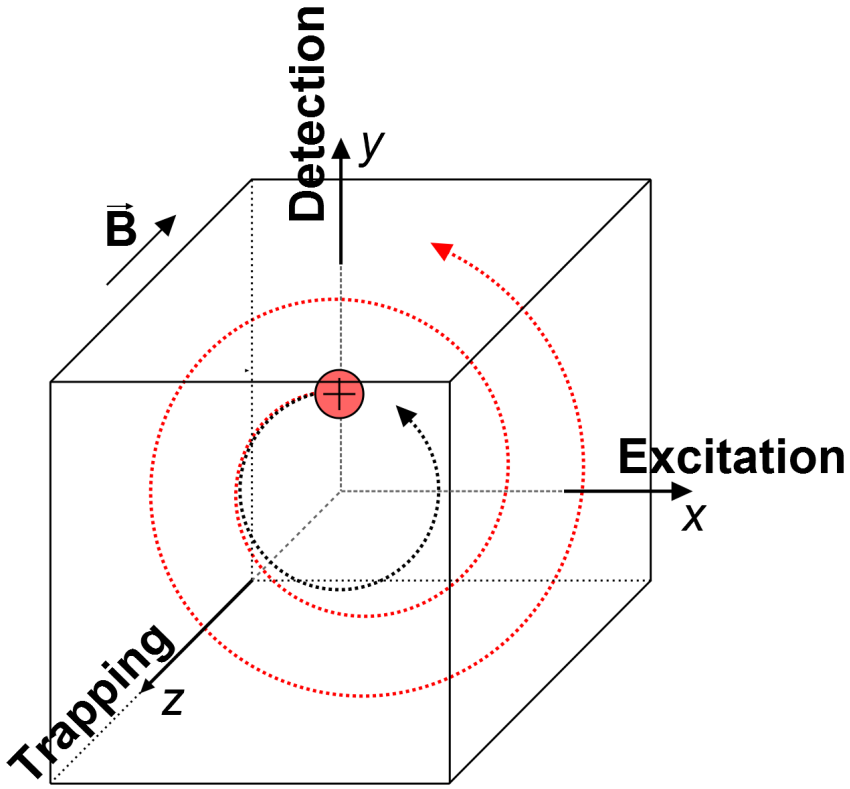

Fig. 2. A schematic representation of an ICR cell. An ion enters the ICR cell following the direction of the *z*-axis (opposite to the magnetic field). Its motion is confined in the *xy*-plane by cyclotron motion as a consequence of the Lorentz force and along the *z*-axis by applying a trapping potential on the corresponding electrodes. Application of a resonant excitation pushes the ion to the orbit of bigger radius, which eventually leads to the detection of an «image» current on the detection plates.

Here, d is the distance between the detector plates and y is the coordinate of the ion along the *y*-axis. The ICR signal, proportional to the induced current, is independent of the strength of the magnetic field. Moreover, according to the principle of «superposition», the signals from any number of ions of different m/z ratios can be measured simultaneously, simply summing up at the detector. However, ion cyclotron motion by itself is not sufficient to perform observable measurements. Ions of the same m/z ratio, entering the ICR cell, have different phases when they start their orbital movement. Therefore, due to incoherent movement, the difference in charge between the two opposite plates will be equal or close to zero. In addition, the initial cyclotron radius of ions (*i.e.* «thermal» radius), just entered the ICR cell, is too small to generate a detectable signal. In order to create a coherent ion movement as well as to increase their cyclotron radius a resonance excitation is applied. It can be achieved by introducing a spatially uniform electric field $\mathbf{E}(t)$ oscillating with time along the *y*-axis with frequency ω_c:

$$\mathbf{E}(t) = E_0 \cos(\omega_c t) \cdot \mathbf{j} \qquad \text{Eq. 18}$$

Here, the amplitude E_0 depends on the voltages $+V_0$ and $-V_0$ applied to the excitation plates (on Fig. 2 represented by the left and right plates, perpendicular to the *x*-axis). This process

pushes the ions of the corresponding cyclotron frequencies off their orbits (Fig. 2, red spiral). Applying the resonant excitation for a period of time T_{exc}, the post-excitation ion cyclotron radius r will be equal:

$$r_{exc} = \frac{E_0 T_{exc}}{2B_0} \quad \text{Eq. 19}$$

Interestingly, r_{exc} does not depend on the m/z ratios of ions. Therefore, by application of an electric field with a constant magnitude all ions can be pushed towards an orbital radius that is sufficient to generate a detectable signal. Moreover, during the excitation, the selected ions start to move coherently within an organized ion packet, inducing a differential current between the detection plates. In turn, the amplitude of the current is proportional to the number of ions within the packet (Marshall and Hendrickson, 2002).

The aforementioned ion movement was described for an idealized experiment (Marshall et al., 1998). However, the finite size of trapping and excitation electrodes results in nonlinear electric fields that will affect the analysis. In addition to ion retaining inside the ICR cell, application of a trapping potential results in the ion oscillation along the *z*-axis with an angular frequency ω_z (Qi and O'Connor, 2014):

$$\omega_z = \sqrt{\frac{2qV_t\alpha}{ma^2}} \quad \text{Eq. 20}$$

Here, V_t is the trapping potential applied on the trapping plates, α is the trapping scale factor (depends on the cell geometry), and a is the distance between the trapping plates. Moreover, the trapping potential produces a radial force directed oppositely to the Lorentz force, resulting in the outward shift of an ion. In this case, the force acting on an ion in the *xy*-plane becomes:

$$F_{xy} = m\omega^2 r = qB_0\omega r - F_{rad} = qB_0\omega r - \frac{qV_t\alpha}{a^2}r \quad \text{Eq. 21}$$

Solving this equation results in two rotational frequencies with respect to the *xy*-plane, namely reduced cyclotron frequency, ω_+, and magnetron frequency, ω_-:

$$\omega_+ = \frac{\omega_c}{2} + \sqrt{\left(\frac{\omega_c}{2}\right)^2 - \frac{\omega_z^2}{2}} \quad \text{Eq. 22}$$

$$\omega_- = \frac{\omega_c}{2} - \sqrt{\left(\frac{\omega_c}{2}\right)^2 - \frac{\omega_z^2}{2}} \quad \text{Eq. 23}$$

Thereby, the motion of an ion is a combination of three factors representing the basis for the FT-ICR-MS to measure its m/z ratio (Fig. 3):

1) Cyclotron motion in the *xy*-plane induced by the magnetic field.
2) Magnetron motion in the *xy*-plane representing the shift of the cyclotron center of the ion.
3) Harmonic oscillation along the *z*-axis (*i.e.* trapping motion).

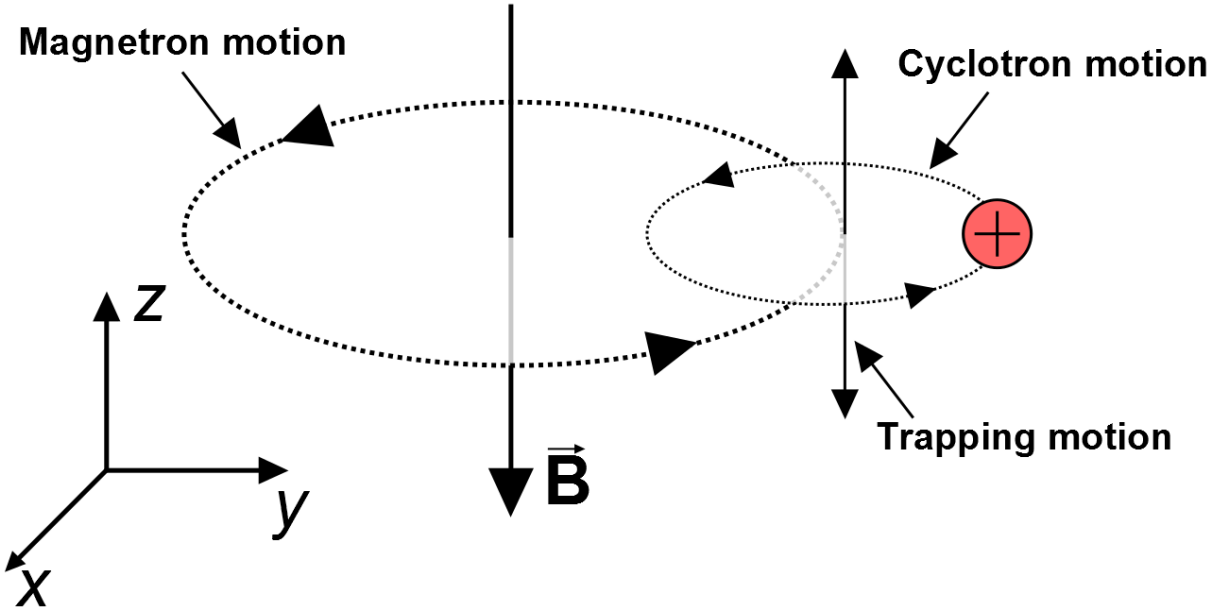

Fig. 3. The motion of an ion in the ICR cell as the combination of three modes, namely the cyclotron motion, the magnetron motion, and the trapping motion.

Because the trapping and magnetron frequency are normally much lower than the cyclotron frequency, they are usually not detected and often disregarded. Nevertheless, undesirable effects can be seen as a consequence of the perturbation of the ion motion by applying trapping electric fields.

Manifesting m/z ratio of ions as a frequency represents one of the most unique advantages of FT-ICR-MS because frequency can be measured very accurately (Marshall et al., 1998). Taking the first derivative of ω_c with respect to m in Eq. 16, it is possible to obtain a useful relation:

$$\frac{\omega_c}{d\omega_c} = \frac{m}{dm} \qquad \text{Eq. 24}$$

Eq. 24 shows that in the FT-ICR-MS the resolution can be described in terms of mass resolving power as well as in terms of frequency resolving power, thereby emphasizing that these two definitions correspond to the same phenomenon. Since ω_c can be approximately

described by Eq. 16, it is possible to rewrite the definition for resolution using Eq. 24 in a following way :

$$\frac{m}{\Delta_{1/2}m} = \frac{\omega_c}{\Delta_{1/2}\omega_c} = \frac{qB_0}{\Delta_{1/2}\omega_c} \sim \frac{qB_0T_{acq}}{m} = \omega_c T_{acq} \qquad \text{Eq. 25}$$

Here, T_{acq} represents the signal acquisition time. Eq. 25 implies the interpretation of resolution as the number of times an ion completes a round of cyclotron motion on its orbit during the acquisition period (Marshall and Hendrickson, 2002). Although in theory resolution grows linearly with increasing T_{acq}, this effect can be seen initially but does not hold for further increase in T_{acq} (Qi and O'Connor, 2014). This occurs because ions, subjected to resonant excitation, naturally experience collisions with other ions and particles, which affects the ion motion and eventually results in the signal damping. According to Eq. 16 the strength of the magnetic field directly affects ion cyclotron motion and, correspondingly, will affect the resolution as it can be seen from Eq. 25. In addition, the upper limit for m/z detection and maximum number of ions that can be confined without coalescence of their FT-ICR signals increases as B_0^2 (Marshall and Hendrickson, 2002). Stronger magnetic fields also decrease the «thermal» cyclotron radius of ions, thereby making the corresponding ion packet spatially more coherent. However, although increasing the magnetic field would represent the most straightforward way to improve the resolution and other parameters, the corresponding costs are very high with the price increasing drastically for stronger fields (Qi and O'Connor, 2014).

Compared to most of the mass analyzers, FT-ICR instrument is an ion trap characterized by discretization in time (but not in space) of the events of ionization, isolation, and detection (Qi and O'Connor, 2014). A basic sequence of events controlling the FT-ICR hardware (also called as a «pulse program») consists of cell quenching, ion injection, excitation, and detection. The use of cell quenching is necessary to eject ions left from the previous measurements. It can be achieved by applying voltages of different polarities on the trapping plates (Fig. 2). Afterwards, the new ions can enter the ICR cell followed by their trapping and cyclotron motion at «thermal» orbits. Earlier the excitation of ions of the same m/z ratios (and, as a consequence, of the same ω_+) was described. In order to apply a resonant excitation to ions of a wide range of m/z ratios, the corresponding electric field can represent a stepwise sweep with constant amplitude across the entire frequency range of interest. Sequentially generated ion packets of different ω_+ induce an «image» current every time passing the

detection plates. The recorded signal, namely «transient» or «free induction decay (FID)», represents a sum of N sinusoidal functions damping with time:

$$F(t) = \sum_{i=1}^{N} K_i \exp\left(-\frac{t}{\tau_i}\right) \cos\left(\omega_{+,i} t + \varphi_0\right), \qquad 0 < t < T_{acq} \qquad \text{Eq. 26}$$

Here, K_i is a scaling factor proportional to the number of ions, φ_0 is the initial phase shift arising when ions enter the ICR cell, τ_i is the damping factor of the corresponding ion associated with inherent collision with other ions and particles. Sampling of the FID with a certain acquisition frequency f_{acq} produces a discrete transient, *i.e.* it has a finite amount of data points. Since the choice of f_{acq} naturally affects the interpretation of the FID, it is required that this parameter has to be at least twice the highest frequency (corresponding to the lowest m/z ratio) that is detected in the transient. The data from the time domain represented as the FID is further transformed into the frequency domain. This process produces a complex output consisting of an absorption-mode and dispersion-mode spectrum ($A(\omega)$ and $D(\omega)$, respectively):

$$\text{Fourier transformation}\big(F(t)\big) = A(\omega) + iD(\omega) \qquad \text{Eq. 27}$$

Although there are several advantages in the analysis of the absorption-mode spectral data (*e.g.* the possibility to get higher resolution and signal-to-noise ratio), many commercial instruments usually report the magnitude-mode spectrum $M(\omega)$ due to the intrinsic difficulty to calculate the phase shifts for each peak in $A(\omega)$:

$$M(\omega) = \sqrt{A^2(\omega) + D^2(\omega)} \qquad \text{Eq. 28}$$

From the other side, the signal-to-noise ratio can be improved by sequential measurements of the same sample of ions several times followed by the summation of the corresponding output (Marshall and Hendrickson, 2002). This is possible because the detection with FT-ICR-MS is non-destructive and allows repeating the relaxation/excitation/detection cycle, where relaxation means returning of an ion to the original «thermal» radius.

1.3.3. Direct infusion FT-ICR-MS in non-targeted metabolomics

Non-targeted metabolomics is often considered as an «unbiased» perspective on metabolome, since capturing of metabolite signals is performed in a relatively non-selective way (Christians et al., 2011; Ohta et al., 2010). Of course, in reality different factors with respect to an experimental workflow (*e.g.* sample preparation, analytical technique) put certain limitations on the metabolite coverage, thus implying that the corresponding output will be

inherently biased (Christians et al., 2011). Nevertheless, the significance of the non-targeted approach lies in the possibility to uncover new mechanisms involved in a phenomenon of interest that cannot be revealed by a targeted screening (Naz et al., 2014). Therefore, non-targeted metabolomics is a data driven and discovery-oriented field aiming at the generation of hypotheses. This is achieved by measuring all possible metabolites under a specific set of conditions and revealing patterns mostly involved in the studied phenomenon with the potential to detect and identify candidate biomarkers. The corresponding results are often qualitative in nature because of the large amount of signals that are difficult to quantify and assign to real metabolites. The correct biological interpretation of these results represents one of the major challenges towards the construction of a reliable hypothesis. Therefore, non-targeted studies should be planned carefully from the beginning to the final step in order to provide a certain level of confidence for the entire approach that includes selection of biological samples, their pre-treatment, analytical measurements, data handling, and identification of the most significant metabolites followed by their projection onto biochemical pathways for the purpose of biological interpretation. Non-targeted metabolomics undoubtedly benefits from HRMS since an essential part of the analysis covers the interpretation of metabolite signals that can be assigned to molecular formulas and, subsequently, to real compounds (Christians et al., 2011; Ohta et al., 2010). The possibility to attribute an elemental composition to a MS peak is crucial for the characterization of unknown and potentially novel metabolites (Ohta et al., 2010). Among available MS techniques, FT-ICR-MS offers the best performance in terms of resolution with the capability to get over the value of 10^6 at $m/z = 400$ (Junot et al., 2014). Together with the opportunity to reach the mass accuracy of sub-ppm range, FT-ICR-MS can be used for high-throughput analysis in a DI mode, avoiding prior chromatographic steps (Christians et al., 2011; Draper et al., 2012; Fuhrer and Zamboni, 2015; Ghaste et al., 2016). Such an implementation has a great impact on both experimental design and data processing (Draper et al., 2012).

Prior entering a mass analyzer, metabolites in a sample have to gain charge, *i.e.* get ionized (Banerjee and Mazumdar, 2012). ESI represents one of the most commonly used ionization sources for non-targeted profiling in DI MS (Draper et al., 2012). ESI, first reported by John Bennett Fenn in 1984, is considered as a soft ionization technique, meaning that no fragmentation occurs upon the process with the possibility to preserve even weak non-covalent interactions (Banerjee and Mazumdar, 2012). The schematic representation of ESI and basic principles of ion generation are shown on Fig. 4.

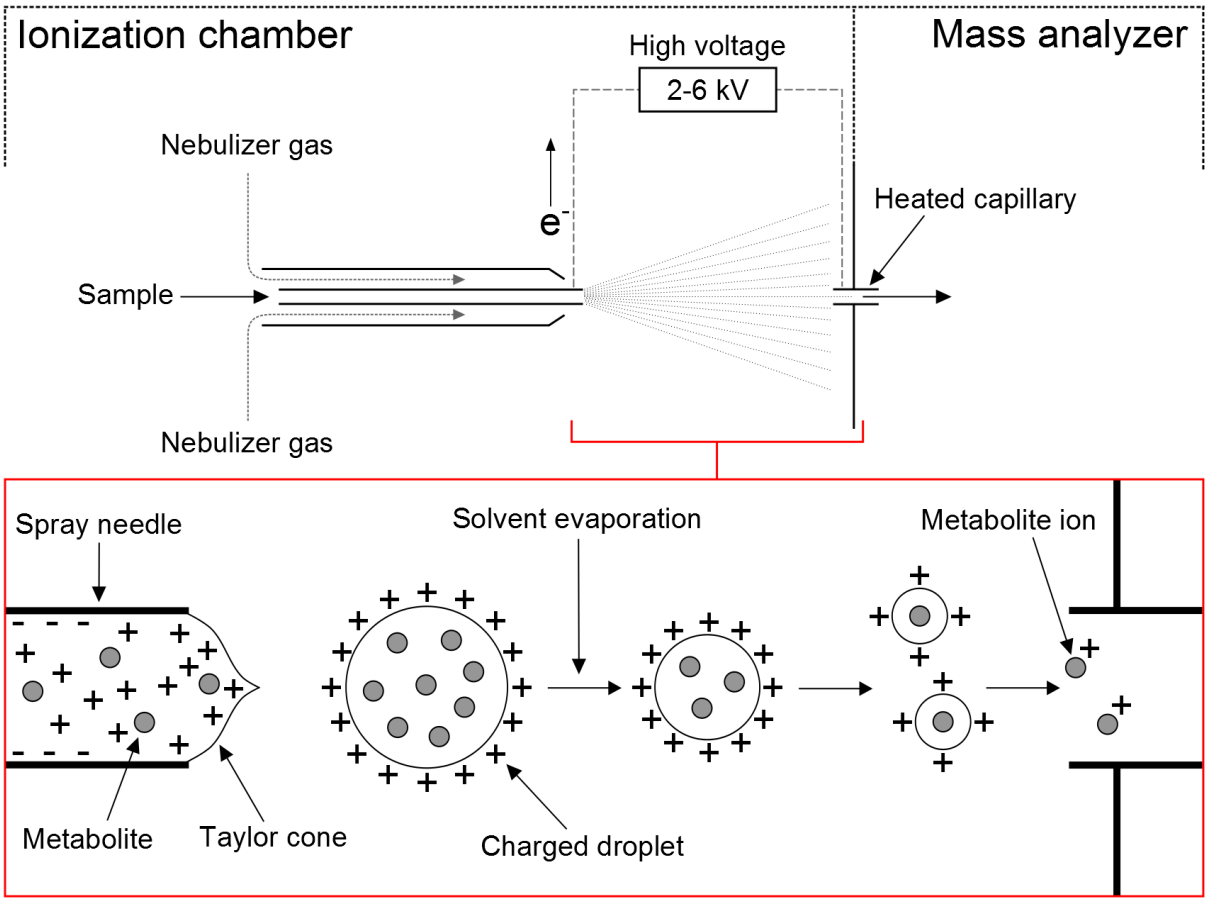

Fig. 4. The graphical representation of basic principles of ion generation in ESI. Formation of positive ions is shown. In case of negative ion formation, the applied voltage is -2-6 kV and the droplets hold a negative charge.

Ionization takes place in an ionization chamber kept at atmospheric pressure. The whole process lies in producing gas-phase ions from molecules in a solution and consists of three major steps described in more detail later (Banerjee and Mazumdar, 2012; Ho et al., 2003):

- Production of charged droplets containing molecules to be ionized.
- Solvent evaporation leading to the droplet disintegration.
- Formation of gas-phase ions from the molecules.

A sufficiently diluted sample can be introduced inside the chamber by the injection of the solution through a stainless steel capillary using a mechanical syringe pump. The tip of the capillary is kept under a high voltage (±2–6 kV) relative to a heated capillary that transfers the generated ions to the mass analyzer. Depending on the electrical polarity, it causes an electron flow from or to the stainless steel capillary. This process results in redox reactions in the solvent, which lead to the accumulation of positive or negative ions in the solution that subsequently drift towards the capillary outlet. The competition between electrical forces and surface tension of the liquid drives the formation of a cone (*i.e.* Taylor cone) that immediately ejects a charged jet from its apex that breaks up into droplets. Thereby, the sample is dispersed into an aerosol consisting of highly charged electrospray droplets moving in the

direction of counter electrode. The use of a nebulizer gas (usually N_2), whose flow is directed along the capillary towards the injection process, contributes to a better nebulization as well as helps to direct the charged droplets to the inlet of the heated capillary. The forces acting on the charged droplets consist of surface tension and Coulomb repulsion (between the charged particles on the droplet surface), acting in opposite directions and trying to preserve or break down the spherical shape, respectively. Because of the solvent evaporation assisted by an elevated temperature in the chamber and/or the flow of a drying gas (usually N_2), the droplets gradually diminish in size and, reaching a certain point when the surface tension does not sustain Coulomb forces of repulsion (*i.e.* Rayleigh limit), eventually disintegrate into smaller offspring droplets. This process eventually leads to the release of a charged molecule from a droplet, that subsequently passes through the heated capillary (serving for the complete desolvation of moving ions) into the low pressure region of the mass analyzer. Depending on the ionization mode (positive/negative), positively charged molecules are generally characterized by protonation (marked as $[M + H^+]^+$), whereas negatively charged molecules are normally formed through deprotonation (marked as $[M - H^+]^-$) (Banerjee and Mazumdar, 2012). However, naturally occurring ions (*e.g.* M^+ and M^-, respectively), formed by the loss or gain of an electron, can be present as well. Other types of charged compounds formed during the ESI process include adducts containing chlorine, sodium, and potassium ions ($[M + Cl^-]^-$, $[M + Na^+]^+$, $[M + K^+]^+$, respectively) as well as multiply charged molecules (Brown et al., 2005; Draper et al., 2012).

ESI-based MS is adaptable for analyzing both polar and lipophilic compounds with respect to non-targeted profiling (Draper et al., 2012). The use of DI with ESI in HRMS can represent an ideal choice for high throughput analysis that provides a raw perspective on the data at hand. At this level, early indications on the differences between groups of interest can be revealed and put in the context of metabolites. However, as was mentioned before, DI HRMS can be drastically affected by ion suppression (*i.e.* «matrix effect») resulting in the loss or shift of ionization efficacy. Moreover, it is important to remember that quantification in almost any non-targeted metabolomics study is limited to relative rather than absolute values of intensity signals, thus making a DI ESI HRMS approach in most cases semi-quantitative. Nevertheless, even the presence of such phenomena enables to obtain useful information from the raw screening. Concerning FT-ICR-MS, many applications can be found utilizing the DI approach with an ESI source ranging from environmental and food analysis to profiling of human biofluids for the purpose of searching for disease specific compounds. DI FT-ICR-MS

has the potential to generate an enormous amount of data represented by m/z ratio signals, thereby requiring proper handling of this information, especially in the context of molecular formula assignment (Ohta et al., 2010). Once the spectra are obtained, the corresponding m/z ratios can be assigned to elemental compositions (*e.g.* restricted to C, H, N, O, S, P elements) either by direct enumeration of possibilities (consistent with chemical laws) or by searching against the databases (Brown et al., 2005). Interestingly, even the knowledge on the elemental compositions can drive potential hypotheses to be generated about a biological system without complementary information on possible metabolites behind the formulas (Ohta et al., 2010). It can be exemplified by building so-called van Krevelen diagrams where elemental compositions are decomposed into the ratios $\mathrm{H/C}$, $\mathrm{O/C}$, $\mathrm{N/C}$, *etc*., which, in turn, can be visualized as projections onto the axes of a Cartesian coordinate system. Such a representation allows making conclusions on the metabolite degree of saturation or the prevalence of certain compound classes. Another example includes building so-called mass-difference networks (MDiNs) where the connections are constructed according to the masses of molecular formula modifications associated with particular enzymatic reactions. Such a representation allows drawing conclusions on possible biochemical transformations characteristic for a studied phenomenon.

DI HRMS has been proven to be a useful approach in studying biological systems with a broad range of applications (Ghaste et al., 2016). Simplicity, limited sample preparation together with the high-throughput analysis represent the factors that are especially advantageous for the large scale metabolomics studies. In turn, the use of FT-ICR-MS provides a tremendous increase in the metabolite space, implying the usefulness of the instrument in non-targeted screening. Such a property facilitates studying complex systems (*e.g.* the interplay between intestinal microbiota and the host) that can be described in much more detail (Ohta et al., 2010). Therefore, the importance of FT-ICR-MS in constructing of a holistic and systemic view on metabolome is indubitable.

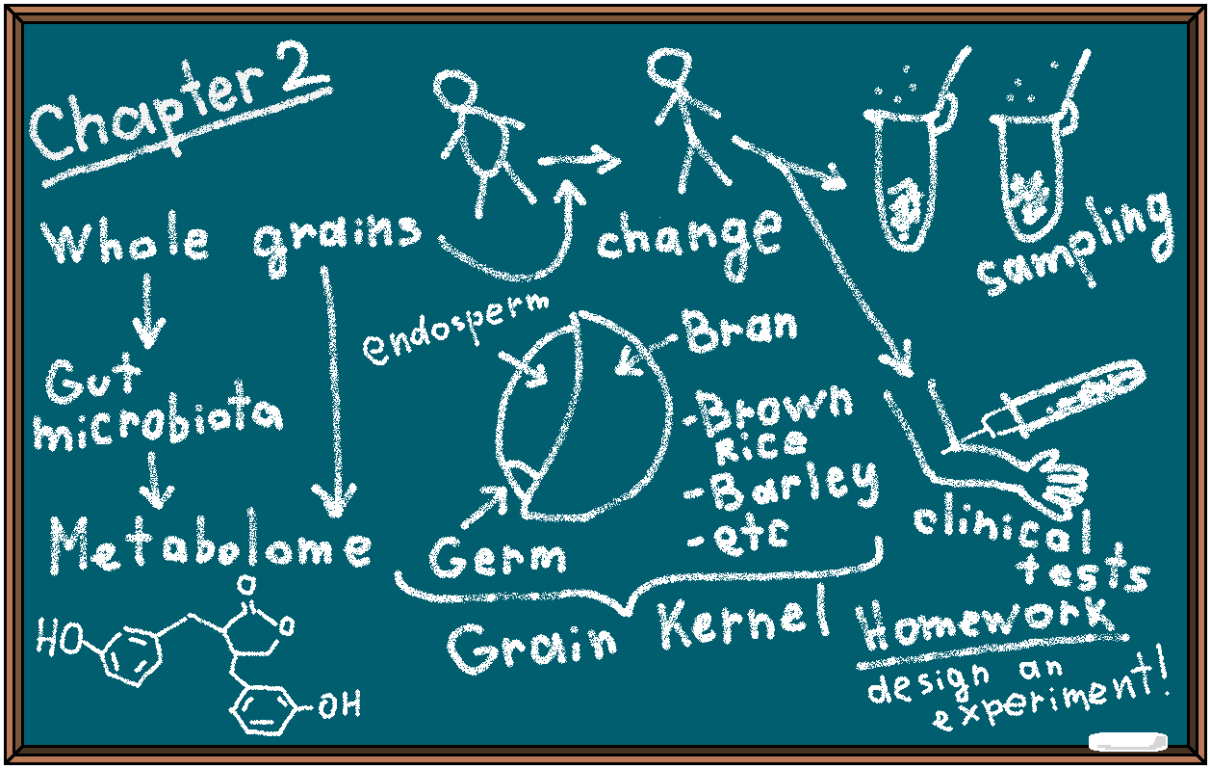
Chapter 2
Whole grains
Gut microbiota
Metabolome
HO
OH
change
sampling
endosperm
Bran
-Brown rice
-Barley
-etc
Germ
Grain Kernel
clinical tests
Homework
design an experiment!

Chapter II

2. Whole grain diet and associated responses

2.1. Metabolomics studies on whole grain consumption

By definition, whole grains are intact, ground, cracked, or flaked grain kernels whose major components – the endosperm, germ, and bran – are present in the same relative proportions as they exist in the intact grain (Cooper et al., 2015). Inedible parts such as hull and husk are removed. The most widely consumed and commonly studied whole grains are wheat, corn/maize, rice, oats, barley, and rye. The intake of whole grains is encouraged because of the associated beneficial health effects. Their consumption has been reported to play a positive role in cardiovascular diseases, metabolic syndrome, type 2 diabetes, body weight management, and cancer. However, the general interpretation is tricky as each type of whole grain is unique in the content of fiber, bioactive compounds, micro- and macronutrients. Therefore, the effects can vary. Moreover, the knowledge of the content alone is often not sufficient for understanding the corresponding mechanisms (Ross, 2015). It may make sense to investigate also the synergetic action of a combination of different grains, since this better represents a plausible human diet (Cooper et al., 2015). The beneficial effects of whole grains can be associated by the induced changes in the gut microbiota composition and function (Moco and Ross, 2015; Ross, 2015). Therefore, related studies are of particular importance, especially when assisted by metabolomics research, since it becomes possible to observe changes in endogenous as well as microbial metabolites in order to describe alterations in host metabolism. Before applying metabolomics towards studying responses to whole grain diet in the context of health improvements, the research was mainly focused on clinically relevant endpoints such as blood lipids, glucose, and inflammation markers (Ross, 2015). The beneficial properties were mostly explained by high content of fiber, vitamins, minerals, and phytochemicals. Naturally, the first studies, utilizing metabolomics and global screenings of the effects associated with whole grain consumption, used animal models. Detecting changes in the metabolome of human subjects is different and more complicated due to many more sources of variation that need to be taken into account. Nevertheless, several reports have indicated the changes in the metabolite landscape induced by whole grain consumption in humans.

Lankinen *et al.* (Lankinen et al., 2011b) investigated the metabolite profiles of blood samples taken from postmenopausal Finnish women recruited in a crossover designed study, where the

subjects followed either a diet including high fiber rye bread or a diet including refined wheat bread. In total 540 metabolites were examined by using a UPLC-ToF-MS platform for measuring lipids and GC×GC-ToF-MS for measuring other compounds such as organic acids, sterols, alcohols, *etc*. Interestingly, considering the amount of analyzed metabolites, only a small fraction of them was reported to have significant changes. Ribitol, ribonic acid, and indoleacetic acid showed elevated levels with respect to rye bread diet. The two former compounds are the precursors of tryptophan, whereas the latter one is its breakdown product. In addition, rye bread diet was characterized by decreased levels of myristoleic and oleic acid. These effects were hypothesized to be connected to satiety and weight maintenance associated with rye bread consumption. In the follow-up study using NMR spectroscopy for metabolite profiling Moazzami *et al*. (Moazzami et al., 2012) reported four other compounds associated with rye bread diet. Plasma levels of leucine and isoleucine were shown to decrease in response to the intervention, whereas betaine and N,N-dimethylglycine exhibited the opposite behavior. Leucine and isoleucine are branched-chain amino acids (BCAA) which have been reported to be biomarkers of type 2 diabetes. Therefore, their decrease may indicate a positive effect with respect to this disorder. N,N-dimethylglycine is a product of betaine that acts as a methyl donor in the reaction of conversion of homocysteine to methionine. Sufficient supply of betaine, represented by its elevated levels, may indicate the decrease in homocysteine as it is actively transformed. In turn, high levels of homocysteine in plasma have been shown to represent a risk factor for cardiovascular diseases, thereby emphasizing that rye bread diet may be favorable against the corresponding disorders. Similar results were shown in another work of Moazzami *et al*. (Moazzami et al., 2011). Men, diagnosed with an early stage prostate cancer, were recruited for a crossover designed study on investigating the differences in metabolite signatures associated with a diet rich in whole grain rye together with rye bran product and a diet rich in refined white wheat product. Metabolite profiling was done by NMR spectroscopy. In addition to increased levels of betaine and N,N-dimethylglycine with respect to whole grain rye diet, this work showed the corresponding decrease in homocysteine, thereby strengthening the hypothesis about the aforementioned reaction. The intervention caused an increase in ketone bodies 3-hydroxybutyric acid and acetone, which may indicate a shift from anabolic to catabolic status because higher levels of such compounds occur during starvation and fasting. In addition, the increase in dimethyl sulfone was observed, indicating a higher rate of intestinal fermentation as a consequence of the whole grain rye diet. Notable results were obtained in a study on effects of whole grain products, additionally supplemented with fatty fish and bilberries, on glucose metabolism,

plasma fatty acids and lipids (Lankinen et al., 2011a). This diet was compared to a regime containing whole grain products without any supplements and to a control represented by refined wheat breads. Participants recruited in the study provided blood samples used for fatty acid measurements by GC and lipidomics experiments by UPLC-ToF-MS. Interestingly, significant results were mainly obtained for the case of the combination of whole grains, fish, and bilberries emphasizing the increase of docosapentaenoic acid, eicosapentaenoic acid, docosahexaenoic acid, α-linolenic acid, and several lipids including triacylglycerols, lysophosphatidylcholines, and phosphatidylcholines. From the other side, dihomo-γ-linolenic acid, some lysophosphatidylcholines and phosphatidylserines were reported to have lower levels with respect to this diet. Although there were no changes observed for the intervention containing whole grain products alone, it was suggested that they may act synergistically within the combination containing fish and bilberries. In the follow-up study Hanhineva *et al*. (Hanhineva et al., 2015) performed a non-targeted metabolomics profiling of the plasma samples using UPLC-ToF-MS in order to find diet-specific compounds. Some of the aforementioned metabolites were reaffirmed for the case of the combination of whole grain products, fish, and bilberries. However, it was possible to detect metabolites being discriminative for the intervention involving whole grain products alone. The most prominent ones included nonadecyl-benzenediol glucuronide and heneicosenyl-benzenediol glucuronide showing an increase after the intervention. Moreover, the trend towards an increase in several amino acids (lysine, arginine, ornithine) as well as betaine-related compounds (pipecolic acid, propionylcarnitine, γ-butyrobetaine) was observed. De Angelis *et al*. (De Angelis et al., 2015) presented a complex approach to study the response to whole grain consumption by combining metabolomics and metagenomics data. Healthy subjects were recruited to examine the differences in fecal microbiota and metabolome associated with the consumption of durum wheat flour or whole grain barley pasta. The latter diet was characterized by lower levels of amino acids (proline, tryptophan, threonine, and arginine) and higher levels of SCFAs (2-methyl-propanoic acid, acetic acid, butanoic acid., propanoic acid). Despite of the metabolite signatures, there were no significant changes observed with respect to the diversity of microbial composition. However, alterations in relative abundances were observed together with correlations of some bacteria with SCFAs, indicating that whole grain diet may modulate the composition and functional profiles of gut microbiota. Mentioning another complex study, in the work of Ross *et al.* (Ross et al., 2013) metabolite profiling of urine, plasma, and stool samples was done in order to investigate the effects of whole grain consumption and to compare the results to the output related to refined diet. NMR spectroscopy and GC-ToF-MS

platforms were used to achieve this goal. Interestingly, in contrast to the other aforementioned studies there were no significant results found regarding plasma metabolome, except of higher levels of urea after whole grain intervention. Urine profiles were characterized by a decrease in carnitine, acetylcarnitine, urea, and taurine levels with respect to this diet. Intriguingly, the changes were substantially affected by gender. Regarding whole grain diet, an increase in fumarate level was observed for women, whereas in men many more metabolites were reported. Among them, an increase in creatinine was detected, while an opposite behavior was observed for 4-hydroxyphenylacetate, dimethylamine, trimethylamine, methylguanadine, pyruvate, citrate, succinate, 3-hydroxyisovalerate, and N-acetylglycoproteins. With respect to stool metabolome, whole grain diet was characterized by elevated levels of nicotinurate, acetate, and butyrate, whereas lower levels of isovalerate was observed. Only samples taken from female subjects showed decrease in succinate levels after the diet. Overall, the reported results indicate that whole grain consumption may affect protein (especially, in men), lipid, energy, and microbial metabolism.

It is worth mentioning that much of the current research is mainly focused on the health benefits associated with whole grain products, whereas eating the outer layers of the grain corresponds to a greater exposure to contaminants possibly being toxic (Ross, 2015). For example, high concentrations of deoxynivalenol – a compound that is potentially deleterious for human health – can be found in the bran fraction of the grain. Therefore, not only beneficial properties but also harmful effects have to be thoroughly studied. This emphasizes the importance to move beyond «changes» and to concentrate on the role of reported metabolites and their involvement into different biochemical pathways. Although there has been little research done in understanding the link between whole grain consumption, alterations in gut microbiota, and changes in metabolome, this direction is potentially important in deciphering molecular mechanisms connecting diet and overall health status.

2.2. Study on the influence of whole grain diet on metabolite profiles

2.2.1. Study design

The study presented in the current thesis is an expansion of the work described by Martinez *et al*. (Martinez et al., 2013). Diets, enriched in whole grain consumption, were investigated by means of changes in immunological parameters and alternations in gut microbiota

composition. The human trial involved 28 healthy individuals of both genders and followed a randomized crossover design (Fig. 5). Three types of whole grain supplements were investigated namely brown rice (BR), barley (WGB), and the mixture of both (COMB). The study period lasted for 17 weeks. After the 1st week, served as a baseline, each subject was randomly assigned to a specific order of the aforementioned diet regimes. The treatments, each lasting for 4 weeks, were separated by a 2-week wash-out period. There were no dietary restrictions, implying free-living conditions during the entire trial.

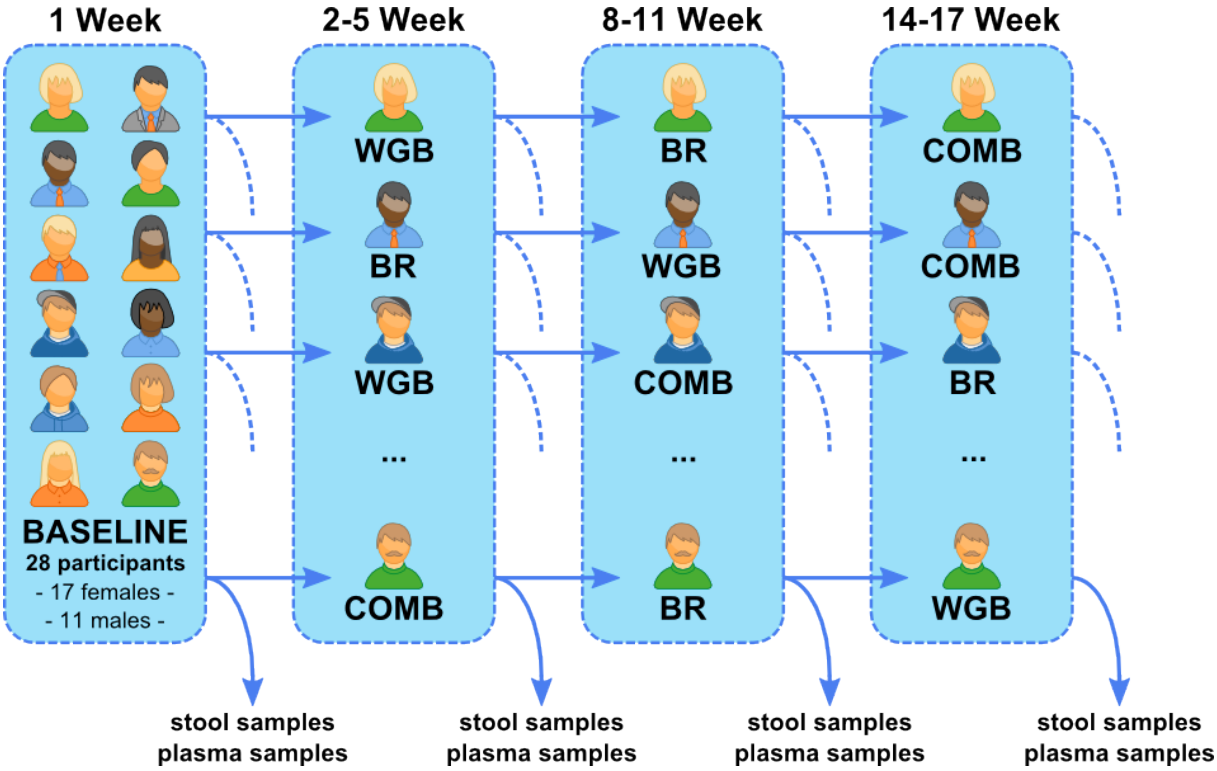

Fig. 5. Study design of the human trial where the responses to whole grain enriched diets were investigated. The 1st week served as a baseline. Afterwards participants were randomly assigned for a specific order of diet regimes. After the baseline and after each treatment period, lasting for 4 weeks, stool and plasma samples were taken.

After the baseline and each of the 4-week treatment periods, stool and plasma samples were collected. Different clinical parameters were taken into consideration. Body mass index (BMI) and percentage of body fat were assessed only after the baseline period. Plasma glucose and insulin levels were measured after overnight fastening (FGlu and FIns, respectively) and corresponding calculations of the Matsuda and insulinogenic indices (MI and IGI, respectively) were performed as well as quantification of insulin resistance by homeostatic model assessment (HOMA-IR). Examined plasma lipid profiles included total cholesterol (TChol), high- and low-density lipoproteins (HDL and LDL, respectively) levels. Among inflammatory markers, plasma concentrations of interleukin 6 (IL-6), high-sensitive

C-reactive protein (CRP), and lipopolysaccharide-binding protein (LBP) were measured. The information on participants together with the clinical data is shown in Table S1-4 (Appendix).

Whereas plasma samples were mainly used to evaluate clinical parameters, stool samples were used to assess gut microbiota composition (Martinez et al., 2013). Certainly, stool microbiota only partially reconstitutes the presence and relative abundance of specific species in the gut (Smirnov et al., 2016). However, due to the simplicity to collect stool samples compared to mucosal biopsy, analysis of fecal content is often performed. Despite the aforementioned limitation, fecal genome, transcriptome, proteome, and metabolome have certain potential to reveal distinct members in the gut microbial ecosystem together with defining their functions. In addition to assessing the gut microbiota composition, stool samples were used to quantify SCFAs, since bacteria are known to produce these metabolites (Martinez et al., 2013).

2.2.2. Objectives

The study of Martinez *et al*. (Martinez et al., 2013) has provided some new insights and has supported the existing knowledge on the relationship between whole grain consumption and the corresponding changes in gut microbiota and host metabolism. All the test meals caused an increase in bacterial diversity within the subjects, most likely associated to compositional complexity of the whole grains. The enrichment of a regular diet with whole grains (especially, in case of COMB treatment) was associated with immunological and metabolic improvements. Moreover, all three diet regimes were characterized by shifts in fecal microbiota composition with a clear response for the diet enriched in WGB, most likely due to the high content of β-glucans. As a consequence, the links were proposed to describe the relation of changes in gut microbiota, caused by whole grain consumption, to the observed anti-inflammatory effects.

The current thesis takes on a metabolomics perspective on the responses associated with whole grain consumption. The aim is to find and describe the corresponding changes in stool and plasma metabolite profiles obtained through HRMS experiments. The path towards this goal does not only require the availability of a good MS platform but the existence of a sophisticated data elaboration pipeline. Therefore, the associated subgoal is to adapt or

develop intelligent tools, capable for reasonable data handling in order to obtain a biologically relevant outcome.

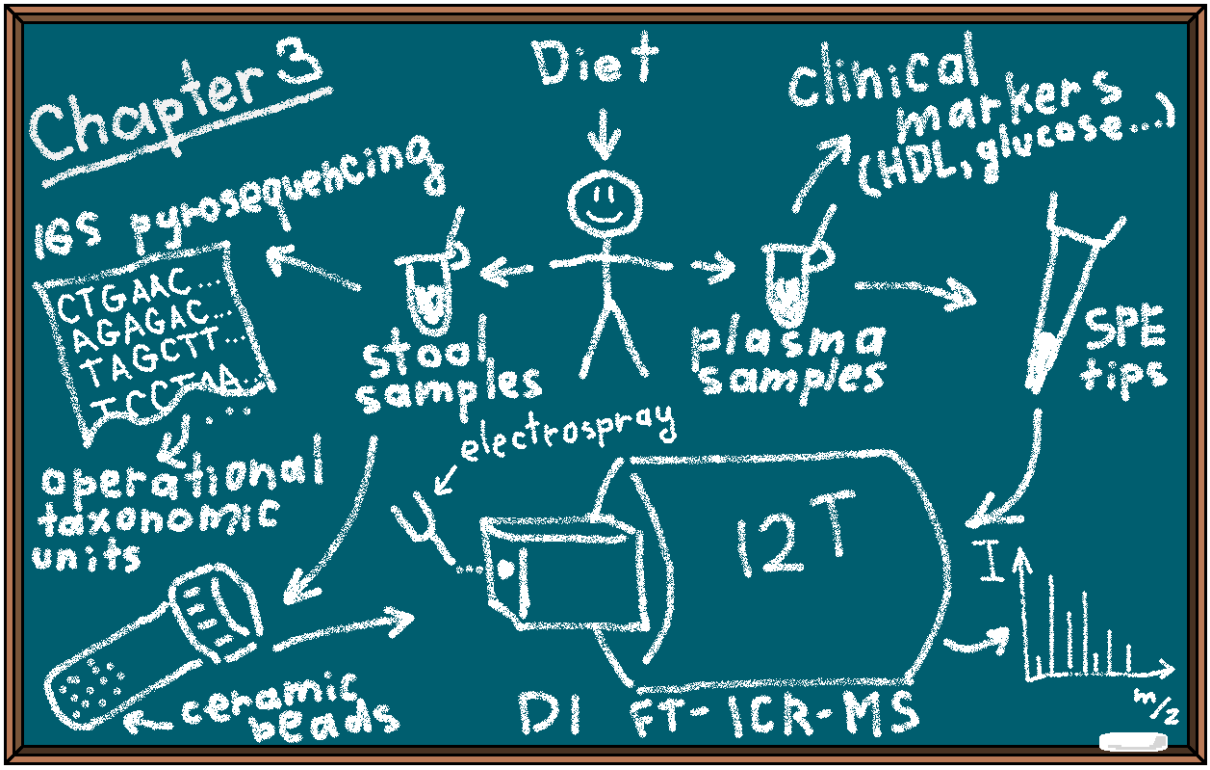
Chapter 3
Diet
clinical markers (HDL, glucose...)
IGS pyrosequencing
CTGAAC....
AGAGAC....
TAGCTT....
stool samples
plasma samples
SPE tips
electrospray
operational taxonomic units
12T
I
ceramic beads
DI FT-ICR-MS
m/z

Chapter III

3. Experimental workflow

3.0. Diet regimes

The test meals, used in the study, included whole grain brown rice (Insta Grains® Brown Rice Flakes, Briess, Chilton, Wisconsin, USA) and whole grain barley (Sustagrain® Barley Quick Flakes, ConAgra Mills, Omaha, Nebraska, USA). The participants had to follow three diet regimes, each lasting for 4 weeks. They were provided individual bags containing a daily dose of the test meal (60 g of flakes). Depending on the regime, the latter represented 60 g of brown rice (BR) or 60 g of barley (WGB), or 30 g of each test meal (COMB). The subjects were instructed to supplement their normal diet with a daily consumption of the provided flakes differing by the total amount of dietary fiber.

3.1. Sampling procedure

Blood samples were collected after a 12 h overnight fasting at the end of the baseline as well as each of the dietary intervention periods. Prior conducting a glucose tolerance test, an initial blood sample was drawn. Afterwards, the test beverage containing 75 g of glucose (Fisher Scientific, Pittsburg, Pennsylvania, USA) was consumed within 10 min followed by collecting blood samples after 15, 30, 45, 60, 90, and 120 min for postprandial glucose and insulin response determination. Blood was drawn directly in tubes with K_2-EDTA (Vacutainer, Becton, Dickinson and Company, Franklin Lakes, New Jersey, USA) followed by centrifugation at 1000 – 1500 ×g for 13 min at 5 – 10 ^{o}C. The resulting supernatant, representing blood plasma, was transferred into new tubes and stored at – 80 ^{o}C until further processing. Stool samples were provided by participants within 24 h after blood sampling and within 2 h after defecation. Collected samples as well as fecal homogenates, prepared by diluting the material in phosphate-buffered saline (PBS, pH 7.0) in the proportion of 1 to 10, were immediately placed in – 80 ^{o}C freezer and stored until further processing. Blood plasma clinical and immunological parameters as well as fecal SCFAs were measured according to Martinez *et al*. (Martinez et al., 2013).

3.2. 16S rRNA gene pyrosequencing and compositional analysis

Fecal homogenates were used for bacterial DNA extraction. The diluted material was transferred into bead beating tubes containing 300 mg of 0.1 mm zirconium beads (Biospec products, Bartlesville, Oklahoma, USA) followed by centrifugation at 8000 ×g for 5 min at room temperature. The washing procedure was performed twice by adding ice-cold PBS to the formed cell pellets. Enzymatic lysis was conducted at 37 °C for 30 min after adding 100 µL of lysis buffer (200 mM NaCl, 100 mM Tris, 20 mM EDTA, 20 mg.mL Lysozyme, pH 8.0). The stool lysis buffer ASL from QUAamp DNA Stool Mini Kit (Qiagen, Hilden, Germany) was added to each sample in the quantity of 1.6 mL. Afterwards, the samples were subjected to mechanical homogenization by Mini-BeadBeater-8 (BioSpec Products, Bartlesville, Oklahoma, USA) for 2 min at maximum speed. Following the instructions provided by the manufacturer, 1.2 mL of the resulting supernatant was used for DNA purification with the QIAamp DNA Stool Mini Kit.

The V1-V3 region of the 16S rRNA gene was amplified by PCR using universal primers as described in Martinez *et al.* (Martinez et al., 2010). Pyrosequencing was conducted using the 454 Genome Sequencer FLX with GS FLX Titanium series reagents (Roche, Basel, Switzerland) and following the protocol provided by the manufacturer. The processing of the resulting sequences was performed using the bioinformatics pipelines from the Quantitative Insights Into Microbial Ecology (QIIME) and the Ribosomal Database Project (RDP). The sequences were assigned to bacteria with respect to taxonomical ranks (*e.g.* phylum, family, genus) as well as to operational taxonomic units (OTUs).

3.3. Sample preparation for MS analysis

3.3.1. Preparation of stool samples

The preparation of stool samples for the FT-ICR-MS analysis was conducted according to the protocol of Walker *et al*. (Walker et al., 2014) with slight modifications. The whole procedure required keeping raw as well as prepared samples in a box with dry ice. For each original sample, 50 mg of crude fecal material was transferred into a bead tube containing 0.6-0.8 mm ceramic beads (NucleoSpin® Bead Tubes, Macherey-Nagel, Düren, Germany) followed by adding 1 mL of ice-cold methanol (Fluka Methanol, LC-MS Chromasolv®, Sigma-Aldrich,

St. Louis, Missouri, USA). Extraction of metabolites by disrupting cell walls was conducted by mechanical homogenization using TissueLyser II (Qiagen, Hilden, Germany) for 5 min at the frequency of 30 Hz. After centrifugation at 20800 ×g for 10 min at 4 °C, the supernatant was collected into a new tube, which was stored at – 80 °C until further processing.

3.3.2. Preparation of plasma samples

The preparation of blood plasma samples for the FT-ICR-MS analysis was conducted according to the protocol of Forcisi *et al*. (Forcisi et al., 2015). Prior to the procedure, the initially frozen plasma samples were thawed on ice and vortex mixed for 30 s. Afterwards, 50 µL of plasma was transferred into a tube containing 50 µL of 2% phosphoric acid. The resulting 100 µL solution was vortex mixed for 30 s. The extraction of metabolites was performed by solid phase extraction (SPE) technology using Omix C18 100 µL tips (Varian, Palo Alto, California, USA) and following the instructions provided by the manufacturer. The conditioning and equilibration steps (before loading the sample onto the SPE tip) included flushing the tips with methanol and 2% formic acid, respectively. After loading the sample, the tips were washed with 2% formic acid three times followed by elution step using methanol. The eluate was stored in a new tube at – 80 °C until further processing.

3.4. FT-ICR-MS measurements

The measurements were performed, as described in Walker *et al*. (Walker et al., 2014) with respect to stool samples and in Forcisi *et al*. (Forcisi et al., 2015) with respect to plasma samples, using FT-ICR mass spectrometer (Bruker, Bremen, Germany) equipped with a 12 T superconducting magnet and an Apollo II ESI source. The summary of the parameters used in the measurements can be found in Table 1. The metabolite ions were acquired in the negative and positive ionization mode for stool and plasma samples, respectively, by DI approach. The instrument was externally calibrated by injecting a 5 µg/mL solution of arginine and observing the corresponding peaks (m/z = 173.10440 $[M\text{-}H^+]^-$, 347.21607 $[2M\text{-}H^+]^-$, 521.32775 $[3M\text{-}H^+]^-$, 695.43943 $[4M\text{-}H^+]^-$ for the negative ionization mode; m/z = 175.11895 $[M+H^+]^+$, 349.23062 $[2M+H^+]^+$, 523.34230 $[3M+H^+]^+$, 697.45397 $[4M+H^+]^+$ for the positive ionization mode). Before conducting the MS experiment, the prepared samples were diluted in methanol in the proportion of 1 to 32 for stool samples and in 75% methanol in the proportion of 1 to 25 for plasma samples. Afterwards, the diluted samples were placed into a

Gilson autosampler system (Gilson Inc., Middleton, Wisconsin, USA) for performing their sequential infusion at a constant rate of 120 µL/h. The well plate of the autosampler was kept at a temperature of 4 °C. The acquisition of spectra was conducted in the range of 122.9 – 1000.0 m/z using 500 scans with the individual spectrum size of 2 MW for stool samples and 400 scans with the individual spectrum size of 4 MW for plasma samples. For positive ionization mode the capillary and spray shield voltage were set to + 3600 V and + 500 V, respectively, whereas - 3500 V and - 500 V corresponded to the acquisitions in the negative ionization mode. With respect to stool samples, the ion accumulation time was set to 0.3 s, whereas 0.2 s was used in plasma sample measurements. For both scenarios the time of flight was set to 1.0 ms. The flow rate of the nebulizer gas was kept at 2.0 bar. The drying gas flow rate and temperature were set to 4.0 L/min and 180 °C, respectively.

Table 1. Parameters used for FT-ICR-MS measurements of stool and plasma samples.

Parameter name	Stool samples	Plasma samples
Ionization mode	Negative	Positive
Infusion flow rate	120 µL/h	120 µL/h
Number of scans	500	400
Data size	2 MW	4 MW
Capillary voltage	+ 3500 V	- 3500 V
Spray shield voltage	+ 500 V	- 500 V
Ion accumulation time	0.3 s	0.2 s
Time of flight	1.0 ms	1.0 ms
Nebulizer gas pressure	2.0 bar	2.0 bar
Drying gas flow rate	4.0 L/min	4.0 L/min
Drying gas temperature	180 °C	180 °C

In an additional FT-ICR-MS run with the same parameters, several plasma samples were spiked with internal standards represented by deuterated compounds listed in Table S5. The exact masses of their ions were used to assess the quality of the calibration method described in the next chapters.

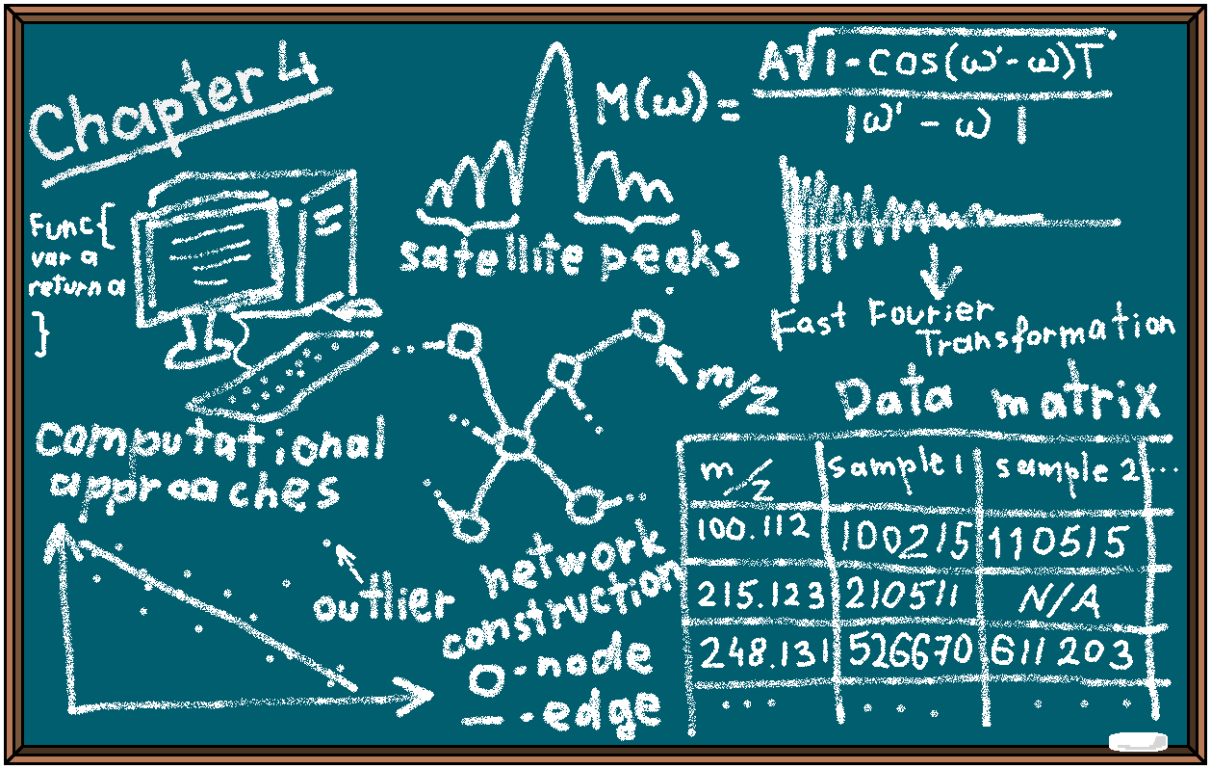
Chapter 4
M(ω) = A√1 - cos(ω' - ω)T / |ω' - ω|
satellite peaks
Fast Fourier Transformation
Func{
var a
return a
}
m/z
Data matrix
computational approaches
outlier
network construction
0 - node
— - edge
m/z | sample 1 | sample 2
100.112 | 100215 | 110515
215.123 | 210511 | N/A
248.131 | 526670 | 611203

Chapter IV

4. Digging into preprocessing of FT-ICR-MS derived metabolomics data

4.1. Spectral calibration

4.1.1. Overview on the calibration of FT-ICR-MS spectra

Given the possibility of FT-ICR-MS to resolve many signals, it becomes extremely important to have high mass accuracies, allowing for unambiguous determination of ion elemental compositions (Qi and O'Connor, 2014). This requirement emphasizes the importance of the calibration procedure, converting experimentally measured frequencies ω_+ of ions into the corresponding m/z values. From Eq. 16, Eq. 20, and Eq. 22 it is possible to derive the Eq. 29, sometimes referred as the Ledford equation:

$$\frac{m}{z} = \frac{C_1}{\omega_+} + \frac{C_2}{\omega_+^2} \qquad \text{Eq. 29}$$

$$\text{where} \quad C_1 = eB_0 \quad \text{and} \quad C_2 = \frac{eV_t\alpha}{a^2}$$

This equation can be normally used to transform the scale of frequencies ω_+ to the scale of m/z ratios. Although the constants C_1 and C_2 are principally known, they are usually determined experimentally by least squares fitting of Eq. 29 to the frequencies of two or more peaks of known m/z values. For this purpose either internal or external calibration scheme can be applied (Marshall et al., 1998). Internal calibration implies the presence of calibrant ions within a sample of interest, whereas for the latter approach a separate solution of known molecules is used for calibration. Normally, internal calibration is preferred because the calibrants are exposed to identical experimental environment as the molecules in a sample and, therefore, the mass accuracy over a wide m/z range can be improved drastically compared to external calibration (Marshall et al., 1998; Qi and O'Connor, 2014). However, sometimes using internal calibrants is not feasible, especially if samples are unknown (Qi and O'Connor, 2014). The best way to use external calibration is by using calibrant ions that are excited to the same cyclotron radius as the sample ions, while assuring that the number of ions in the ICR trap is the same for both experiments (Marshall et al., 1998).

According to all the prerequisites to derive Eq. 29, this formulation should be valid only for a single ion approximation (Marshall et al., 1998). Practically, an ion cloud is generated within an ICR cell. Thereby the ions are constantly exposed to space charge effects, originating from

columbic interaction forces between them. Such a phenomenon is associated to frequency shifts, which are substantially influenced by the total ion number in the ICR cell (Qi and O'Connor, 2014). Therefore, the ability to convert the frequency scale to m/z scale by Eq. 29 can be drastically impaired if significant changes in space charge conditions are present. As a consequence, the rule of thumb in FT-ICR-MS measurements implies acquiring spectra with sufficiently small ion populations to make the space charge effects negligible and averaging the signal of multiple spectra (Marshall and Hendrickson, 2002; Qi and O'Connor, 2014). Since the aforementioned perturbations can affect sample as well as calibrant ions, the internal calibration procedure is recommended (Marshall et al., 1998).

4.1.2. Re-calibration by searching the maximum density path

Often, after the form of the calibration function is found (for example, the constants C_1 and C_2 in Eq. 29), the re-calibration procedure is required to correct for subtle systematic shifts (Becker et al., 2007; Kozhinov et al., 2013; Petyuk et al., 2008). When the default mass calibration is performed, it is possible to examine the residual error associated with experimentally derived m/z ratios according to Eq. 9 (Kozhinov et al., 2013). However, these calculations require knowing real compounds ciphered behind the experimental m/z values in order to retrieve the corresponding theoretical counterparts. This requirement does not hold in case of non-targeted metabolomics studies, since there is no *a priori* knowledge on the measured molecules. For this scenario, it is possible to use a sufficiently long list of theoretical m/z ratios, assuring the reasonable amount of true positive assignments to experimental m/z ratios. In turn, the information on a sample matrix (*e.g.* feces, blood plasma, urine), used for MS measurements, can facilitate construction of such a list. Plotting the residual error versus the corresponding theoretical m/z ratios may reveal the systematic error component that needs to be eliminated (Petyuk et al., 2008). Thereby, spectra, containing thousands of signals, might contain sufficient amount of information necessary for re-calibration.

To demonstrate the aforementioned concept, the spectra, corresponding to plasma samples spiked with the deuterated standards, were used. The long list of reference masses was constructed by retrieving entries on theoretical masses from KEGG, HMDB, LipidMAPS, and MetaCYC databases and unifying them into one list. Selection of these databases can be reasoned as they may comprise a sufficient amount of biochemical compounds present in a

plasma sample. In order to make the collected masses comparable to the experimental ones, they were additionally modified to represent positively charged ions in the form of $[M+H^+]^+$ and $[M+Na^+]^+$. The total amount of generated entries was equal to 31354 (15677 for each adduct type). The FT-ICR-MS measurements of plasma samples followed by spectral preprocessing resulted in 11704 experimental signals. These included 33 signals from the internal standards in the protonated and sodiated forms. For further considerations, only the signals above $3 \cdot 10^6$ relative intensity units as well as those falling into the range of 200.0 – 900.0 m/z were included, resulting in the reduced amount of 7442 peaks. All the pairwise differences between the experimental and theoretical list were calculated according to the Eq. 9. The plots of the residual error versus the corresponding theoretical m/z values are shown on Fig. 6.

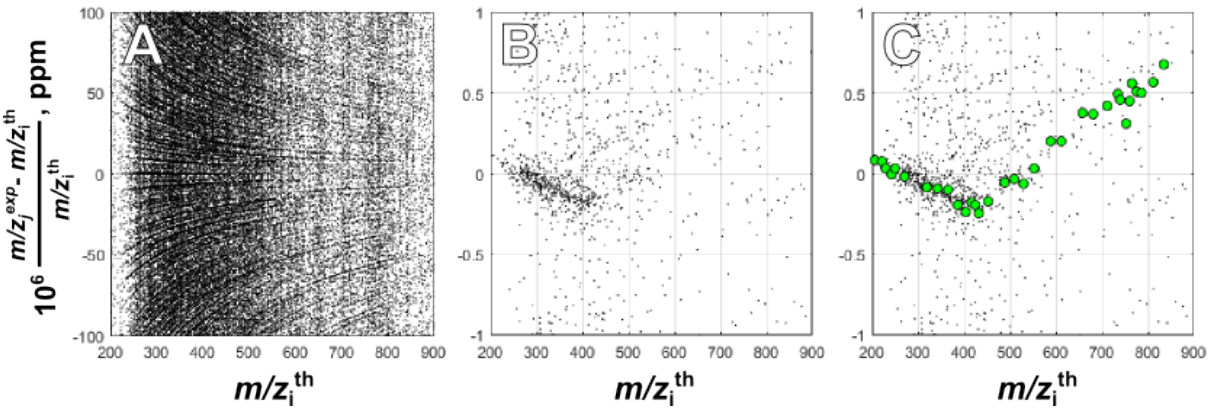

Fig. 6. The residual error versus the corresponding theoretical $\boldsymbol{m/z}$ ratio. A) The plot is built in the range of -100 to 100 ppm. B) The plot is built in the range of -1 to 1 ppm. C) The plot is built in the range of -1 to 1 ppm together with mass accuracies corresponding to the internal standards (marked as green circles).

Fig. 6A shows the residual error in the range from -100 to 100 ppm. It is possible to observe a pattern of converging curves. The emergence of each curve can be easily explained, taking into account that the differences between exact masses of any of two biochemical compounds are mainly caused by the differences in the amounts of the constituent elements (Eq. 30):

$$m_{\text{compound } i} - m_{\text{compound } j} = \sum_e \left(n_{ie} - n_{je}\right) \cdot m_{\text{element } e} \qquad \text{Eq. 30}$$

$$\text{where} \quad e \in \mathrm{E} = \{\mathrm{E}_1, \mathrm{E}_2, \ldots, \mathrm{E}_N\}, \quad n_{..} \geq 0$$

In Eq. 30, E represents a set comprising chemical elements E_1, E_2 *etc.* (*e.g.* C, H, O) and $n_{.e}$ is the amount of a certain element e in the structure of a considered compound. Since the same calculations can be easily extended to m/z ratios, every curve on Fig. 6A is associated to a specific combination of elements to be added to or subtracted from the horizontal zero line in the form of a mass difference. By building the residual error plot in a smaller range from -1 to 1 ppm in order to examine the central line (Fig. 6B), it is possible to observe the potential

presence of a systematic error component that becomes more evident when the mass accuracies, corresponding to the internal standards, are projected on the figure (marked as green circles on Fig. 6C).

Despite of supposedly many false positive assignments due to lack of restrictions on matches between experimental and theoretical data, the regions of higher density can be seen. Therefore, it is reasonable to apply methods to estimate the density on the residual error plot followed by algorithms to search for a maximum density path. For the first of the two tasks, the kernel density estimation approach, using Gaussian functions, was chosen as being relatively easy to perform. For this purpose, an initial grid of points has to be constructed. Assigning a coordinate (x_i, y_i) to every data point on Fig. 6B, the set of points defining the grid of size $H \times V$ was built in a following way:

$$x(h) = \min(x_1, x_2, \dots) + \frac{\max(x_1, x_2, \dots) - \min(x_1, x_2, \dots)}{H} \cdot h$$

$$y(v) = \min(y_1, y_2, \dots) + \frac{\max(y_1, y_2, \dots) - \min(y_1, y_2, \dots)}{V} \cdot v \qquad \text{Eq. 31}$$

$$\text{where} \quad 1 \le h \le H \quad \text{and} \quad 1 \le v \le V$$

For every coordinate $(x(h), y(v))$ on the grid the density estimation was performed according to Eq. 32:

$$f(x(h), y(v)) = \frac{1}{2\pi n} \sum_i \exp\left(-\frac{1}{2}\left(\begin{bmatrix} x(h) - x_i \\ y(v) - y_i \end{bmatrix}^{\mathrm{T}} \mathbf{B} \begin{bmatrix} x(h) - x_i \\ y(v) - y_i \end{bmatrix}\right)\right) \qquad \text{Eq. 32}$$

In this equation, **B** represents a bandwidth symmetric matrix, whose entries were chosen according to the rule of thumb (Scott and Sain, 2005):

$$\mathbf{B} = n^{-\frac{1}{6}} \begin{bmatrix} \frac{1}{n-1}\sum_i (x_i - \bar{x})^2 & 0 \\ 0 & \frac{1}{n-1}\sum_i (y_i - \bar{y})^2 \end{bmatrix} \qquad \text{Eq. 33}$$

$$\text{where} \quad \bar{x} = \frac{1}{n}\sum_i x_i \quad \text{and} \quad \bar{y} = \frac{1}{n}\sum_i y_i$$

After the density was estimated for every coordinate $(x(h), y(v))$ on the grid, the additional normalization step was conducted in order to compensate for unequal distribution of data points on the residual error plot shown on Fig. 6B:

$$f_n(x(h), y(v)) = \frac{f(x(h), y(v))}{\sum_{i=1}^{V} f(x(h), y(i))} \quad \text{Eq. 34}$$

The second task of finding a maximum density path was carried out by an adapted version of the particle swarm optimization algorithm (Poli et al., 2007). A predefined number of particles, P, was chosen with every particle, p, assigned to its own set of coordinates $\left\{\left(x(h_{1p}), y(v_{1p})\right), \left(x(h_{2p}), y(v_{2p})\right), \ldots, \left(x(h_{Hp}), y(v_{Hp})\right)\right\}$ that changed during the algorithm run. The indices h_{ip}, responsible for horizontal partition of the grid, were simply equal to i, meaning that each particle covers all the m/z range of Fig. 6B, leaving only v_{ip} indices to vary. The initial assignment of coordinates was done in a way that P particles represented equally distanced horizontal lines. All the next steps were performed repeatedly until convergence or a predefined number of iterations.

- Scoring each particle:

$$\text{score}(p) = \sum_{i=1}^{H} f_n\left(x(i), y(v_{ip})\right) \quad \text{Eq. 35}$$

- Choosing the particle, p, with the highest score.
- Selecting the $\left(x(i), y(v_{ip})\right)$ with the highest $f_n\left(x(i), y(v_{ip})\right)$, corresponding to the chosen particle (as a consequence, selecting the index i).
- Changing the v_{ip} components of other particles, k, at the chosen index i according to the rule:

$$\begin{gathered} v_{ik} \rightarrow v_{ik} + 1 \quad \text{if} \quad v_{ik} < v_{ip} \\ v_{ik} \rightarrow v_{ik} - 1 \quad \text{if} \quad v_{ik} > v_{ip} \\ v_{ik} \rightarrow v_{ik} \quad \text{if} \quad v_{ik} = v_{ip} \\ k \neq p \end{gathered} \quad \text{Eq. 36}$$

The changes shown by Eq. 36 followed a restriction that the absolute distance between adjacent v indices of a particle did not exceed 1, *i.e.* $\left|v_{ik} - v_{(i\pm1)k}\right| \leq 1$. Therefore, if necessary, adjacent indices modified their values in the direction of the main change. The aforementioned algorithm is deterministic, meaning that there is no occurrence of any random fluctuations. Therefore, the solution stays the same given the same starting conditions.

The final arrangement of the particle coordinates is equal among all of them in case if the algorithm converges. However, only the particle with the best score, according to the Eq. 35, was chosen. Although the corresponding coordinates can be already used for re-calibrating the

experimental m/z values, an additional smoothing step was applied by using a simple running average algorithm. It was conducted twice by setting the span equal to 3 for the first run and 5 for the second run. This operation leads to slightly modified y-coordinates of the chosen particle:

$$\left\{\left(x(1), y\left(v_{1p}\right)\right), \left(x(2), y\left(v_{2p}\right)\right), \ldots, \left(x(H), y\left(v_{Hp}\right)\right)\right\}$$
$$\downarrow \qquad \text{Eq. 37}$$
$$\{(x(1), \tilde{y}_1), (x(2), \tilde{y}_2), \ldots, (x(H), \tilde{y}_H)\}$$

This arrangement of the coordinates served as the basis for re-calibrating the experimental m/z ratios. At any given m/z^{exp} within the range from $x(i)$ to $x(i+1)$ the corresponding correction ε^{corr} was calculated by a linear approximation:

$$\varepsilon^{corr} = \frac{\tilde{y}_{i+1} - \tilde{y}_i}{x(i+1) - x(i)} \cdot m/z^{exp} + \frac{\tilde{y}_i x(i+1) - \tilde{y}_{i+1} x(i)}{x(i+1) - x(i)} \qquad \text{Eq. 38}$$

The values of ε^{corr} were used for adjusting experimentally derived data in a following way:

$$m/z^{adj} = \frac{(1 - \varepsilon^{corr})}{10^6} \cdot m/z^{exp} \qquad \text{Eq. 39}$$

The adjusted m/z ratios, obtained by the described re-calibration procedure, can be used over again for the aforementioned operations until satisfying conditions are found.

The results of the aforementioned re-calibration scheme can be seen on Fig. 7. The quality of the procedure was estimated by visual inspection of the arrangement of data points, corresponding to the internal standards, before and after re-calibration. Moreover, root mean squared error (RMSE) was calculated to examine the deviation of these data points from zero. This measure was chosen because the form of the corresponding equation is similar to the one of the sample standard deviation in case when the sample mean equals to zero. Therefore, the calculations were slightly modified due to this likeness:

$$\text{RMSE} = \sqrt{\frac{1}{n-1} \sum_{i=1}^{n} \left(m/z_i^{adj}\right)^2} \qquad \text{Eq. 40}$$

Computing the kernel density, using the data points shown in the residual error plot on Fig. 7A, resulted in a density map represented on Fig. 7B. Interestingly, even in the absence of a visual evidence of the systematic error increasing after approximately 400 m/z, it is possible to observe this pattern on the density map. Fig. 7C shows the re-calibration curve calculated by applying the adapted version of the particle swarm optimization algorithm. It can be seen that it almost perfectly repeats the behavior of the data points corresponding to the mass

accuracies with respect to the internal standards. Fig. 7D shows the residual error plot from Fig. 7A after correction. Application of the re-calibration centered the error distribution as can be seen by the data points, corresponding to the internal standards. Moreover, there was a decrease in RMSE from 0.32 before the procedure to 0.11 after. These facts emphasize the possibility to apply the described re-calibration method to other samples.

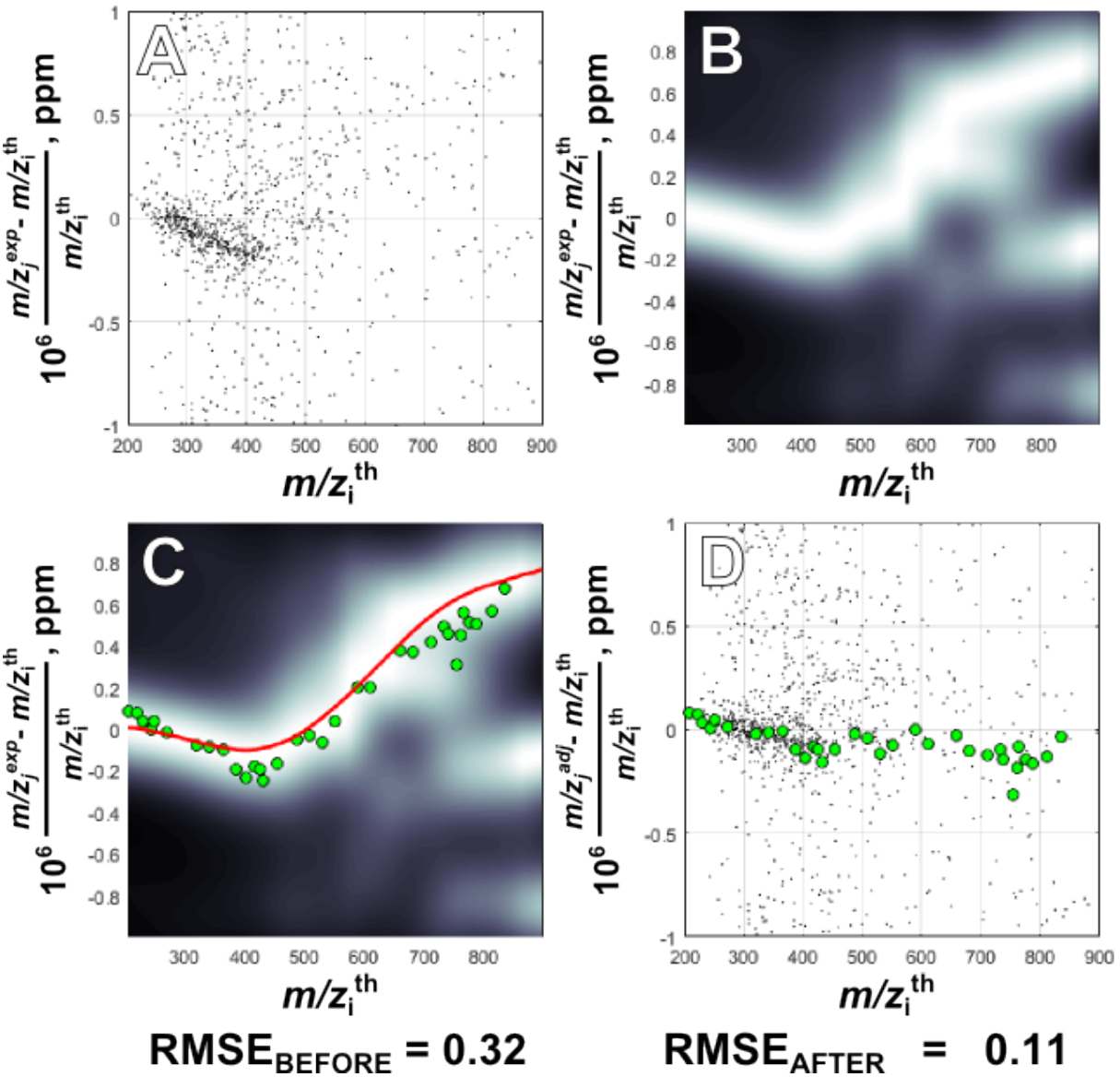

Fig. 7. The re-calibration of the experimental m/z ratios obtained by DI FT-ICR-MS measurements. Data points marked as green circles correspond to the internal standards. A) The residual error plot showing the differences between experimental and theoretical m/z ratios in the range from 200 to 900 m/z. B) Kernel density estimation using Gaussian functions. C) Resulting re-calibration curve obtained by an adapted version of the particle swarm optimization algorithm. D) The residual error plot after correction.

The aforementioned approach has several advantages. It is tolerant to the presence of false positive assignments. Even in the absence of true positives and, as a consequence, a lack of a central line in a residual error plot, any other curve, if visible, can be used for re-calibration. The only requirement is to shift the experimental m/z ratios by the corresponding mass

difference, perform the correction, and shift the adjusted values back. Another advantage is the non-parametric nature of the fitting procedure, which provides flexibility that lacks in many parametric methods. The described re-calibration scheme can be applied to other sample types and metabolomics platforms, since the algorithm is based purely on theoretical prerequisites. However, it is necessary to provide a sufficiently long reference list, preferably resembling a sample matrix to be analyzed.

The described re-calibration method was applied to all the samples included in the study presented in the current thesis. The reference list was composed out of unique masses retrieved from the HMDB database followed by their modification to represent $[M\text{-}H^+]^-$ and $[M+Cl^-]^-$ adducts in case of stool samples and $[M+H^+]^+$ and $[M+Na^+]^+$ adducts in case of plasma samples.

4.1.3. Graphical user interface

In order to adapt the re-calibration procedure for common users, a graphical user interface (GUI) was created (Fig. 8). All the code was written in MATLAB (The MathWorks Inc., Natick, Massachusetts, USA). The GUI requires MATLAB compiler runtime v9.1. The program supports importing spectra in the form of text files with the first two columns being reserved for experimental m/z ratios and the corresponding intensities. The reference list has to contain only theoretical m/z values. Optionally, it is possible to import the raw spectral data before applying the peak picking algorithm. It can be necessary for the visual inspection of the re-calibration procedure by examining the alignment of spectral peaks. After all the required files are imported, the processing can be launched. The varying parameters include:

- Error ranging: the interval for residual errors (in ppm) to be used for plotting
- m/z ranging: the interval for m/z to be used for plotting
- Intensity threshold: the threshold for intensities corresponding to m/z ratios to be excluded for further processing
- Grid resolution: the size of the grid for the density estimation
- N particles: number of particles used to fit a curve
- N iterations: number of iterations used to fit a curve
- Cut m/z value: the parameter used if the behavior of systematic error is not monotonous

- Normalize the density: the parameter that has to be on if data points on the residual error plot are not equally distributed along all the considered m/z range.

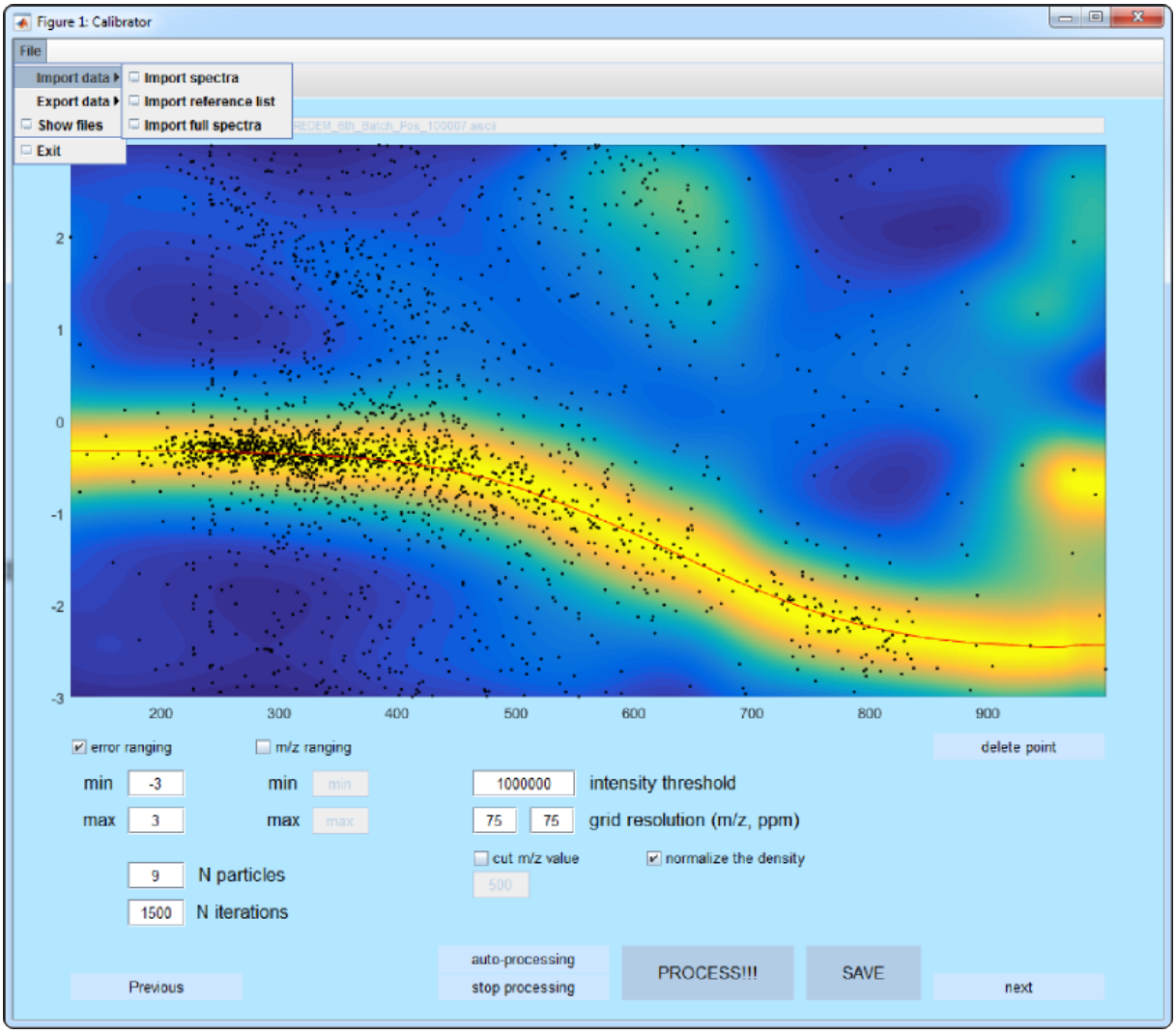

Fig. 8. The GUI for the re-calibration procedure.

The program supports «on-line» elimination of data points that can significantly influence the behavior of the re-calibration curve. In case of relatively similar patterns, observed for all the imported spectra, the processing can be done automatically. Otherwise, every spectrum has to be processed manually. After performing the re-calibration on one file, the results can be exported to a predefined folder. In this case, four output files are created:

- The re-calibrated spectrum
- The file containing original m/z values and their corrected counter parts
- The file containing data points to recover the residual error plot
- The file containing data points to recover the re-calibration curve

4.2. Satellite peak elimination

4.2.1. Overview on the peak shapes in FT-ICR-MS experiments

Application of FT to the FID, represented by Eq. 26, results in a mathematical expression of the frequency spectrum that, for the conventional magnitude-mode (Eq. 28), can be written as (Qi and O'Connor, 2014):

$$M(\omega) = \frac{KN_0\tau\sqrt{1 - 2\exp\left(\frac{-T_{acq}}{\tau}\right)\cos\left((\omega' - \omega)T_{acq}\right) + \exp\left(\frac{-2T_{acq}}{\tau}\right)}}{2\pi\sqrt{1 + (\omega' - \omega)^2\tau^2}} \qquad \text{Eq. 41}$$

Here, ω' represents the frequency of the ion of interest and ω stands for the observed frequency, whereas N_0 is the initial amount of excited ions at the time zero (Marshall et al., 1979). There are two extreme models to study the generated peak shape in the frequency spectrum. Since the overall amount of ion-ion and ion-neutral collisions in the ICR cell depends on the acquisition time, T_{acq}, these models are built considering the zero-pressure limit, $T_{acq} \ll \tau$ (no collisions), and high-pressure limit. $T_{acq} \gg \tau$ (damping of the signal). The corresponding peak shapes can be expressed as:

$$M(\omega) = \frac{KN_0\sqrt{2}}{2\pi|\omega' - \omega|}\sqrt{1 - \cos\left((\omega' - \omega)T_{acq}\right)} \quad \text{if} \quad T_{acq} \ll \tau \qquad \text{Eq. 42}$$

$$M(\omega) = \frac{KN_0\tau}{2\pi\sqrt{1 + (\omega' - \omega)^2\tau^2}} \quad \text{if} \quad T_{acq} \gg \tau \qquad \text{Eq. 43}$$

The two aforementioned scenarios can be seen on Fig. 9. In case of a low-pressure model (Fig. 9A), the corresponding peak shape is similar to a sinc function that is characterized by the presence of side bands on either side of the peak maximum. In case of a high-pressure model (Fig. 9B), the corresponding peak shape represents a Lorentzian function. Although extreme models provide useful insights into the theory of FT-ICR-MS, peak shapes, observed in real experiments, have characteristics of both scenarios.

It is important to mention that an FID is not recorded continuously but rather it is rather sampled at a certain acquisition frequency, f_{acq} (Qi and O'Connor, 2014). Therefore, the transient consists of a finite amount of data points. As a consequence, the choice on f_{acq} is crucial for reconstruction of the original signal. The Nyquist theorem states that this frequency has to be at least twice as big as the highest frequency to be recorded in a FID. As

the transient is discrete, special algorithms should be applied to transform the data into the frequency domain.

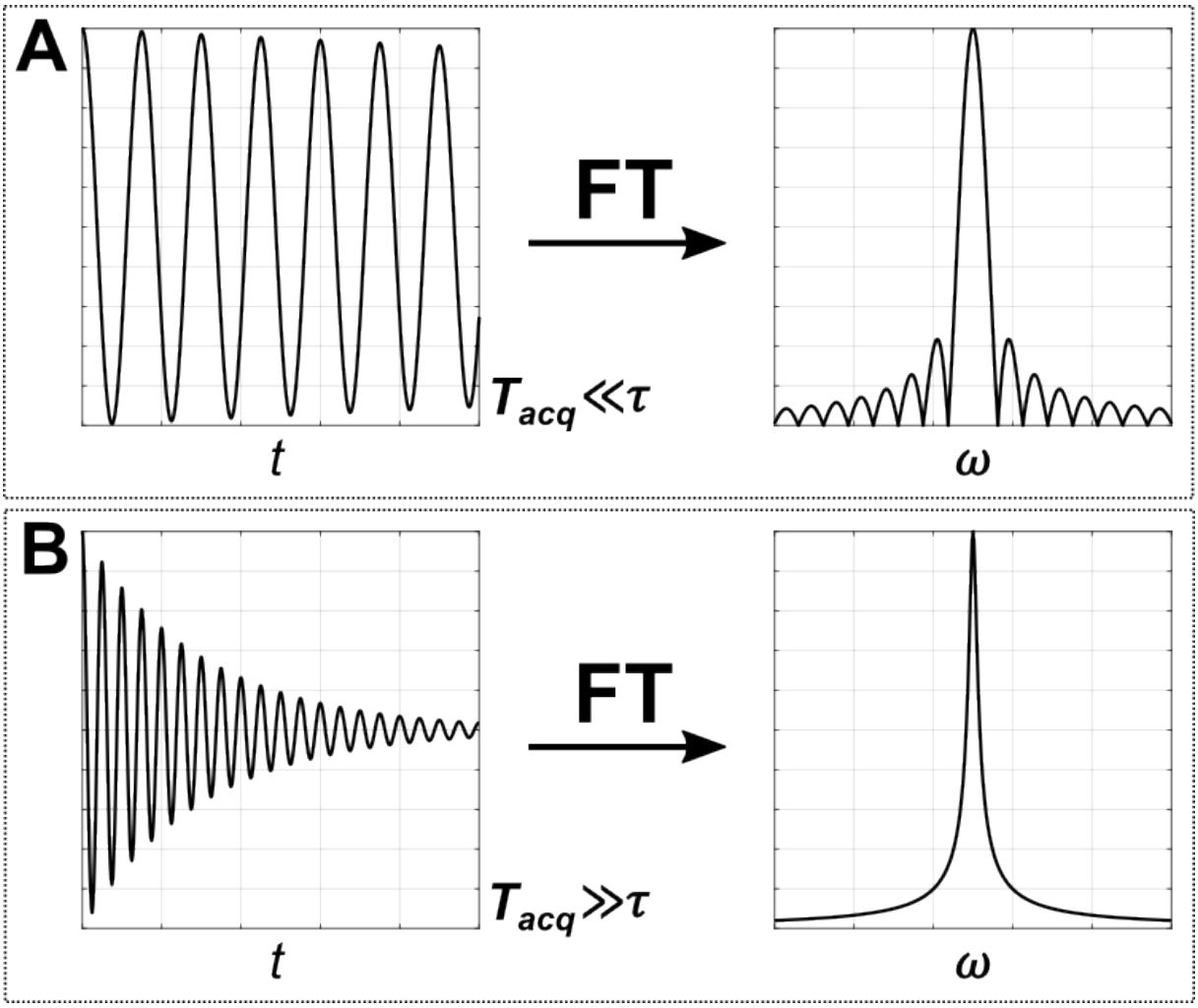

Fig. 9. Peak shapes in case of A) low-pressure model and B) high-pressure models.

A common choice is the so-called «Fast Fourier Transform» algorithm (Marshall and Hendrickson, 2002). Although a transient consists of N discrete data points, FT produces $N/2$ data points represented by complex numbers, containing information on amplitudes and phases (Qi and O'Connor, 2014). This amount of data points is often not enough to obtain a representative magnitude-mode spectrum. Therefore, in order to improve the peak and line shapes, before the FT procedure a zero filling is normally applied, extending FID by adding zeros at the end of the transient. Moreover, performing this operation can significantly improve resolution. However, it can induce the emergence of side bands/satellite peaks and sinc-like behavior. Besides, too extensive zero filling is redundant because of computational requirements and no further improvements in the spectral quality.

As described earlier, spectral acquisition or zero filling prior FT can lead to the emergence of side bands (Qi and O'Connor, 2014). These peaks are undesirable components of a spectrum because no useful information is associated with them. Moreover, they can hamper the detection of adjacent peaks of low intensity. Partially, the problem can be resolved by a procedure called «apodization», which implies multiplying the transient by a window function prior performing FT. Apodization is a standard procedure in the FT-ICR-MS data processing because it smooths the peak shapes and overall spectrum. Although an optimal choice of the window function can smooth the side bands as well, the desired outcome may come at sacrifice of signal-to-noise ratio as well as resolution of the spectrum. Therefore, care should be taken while using apodization.

4.2.2. Empirical approach to delete satellite peaks from FT-ICR-MS spectra

The spectra acquired for the study, presented in the current thesis, contained satellite peaks even after sine-bell apodization of the corresponding FIDs (Fig. 10). Moreover, these non-informative signals were selected by the peak picking algorithm. Therefore, it is necessary to find a method capable to eliminate them.

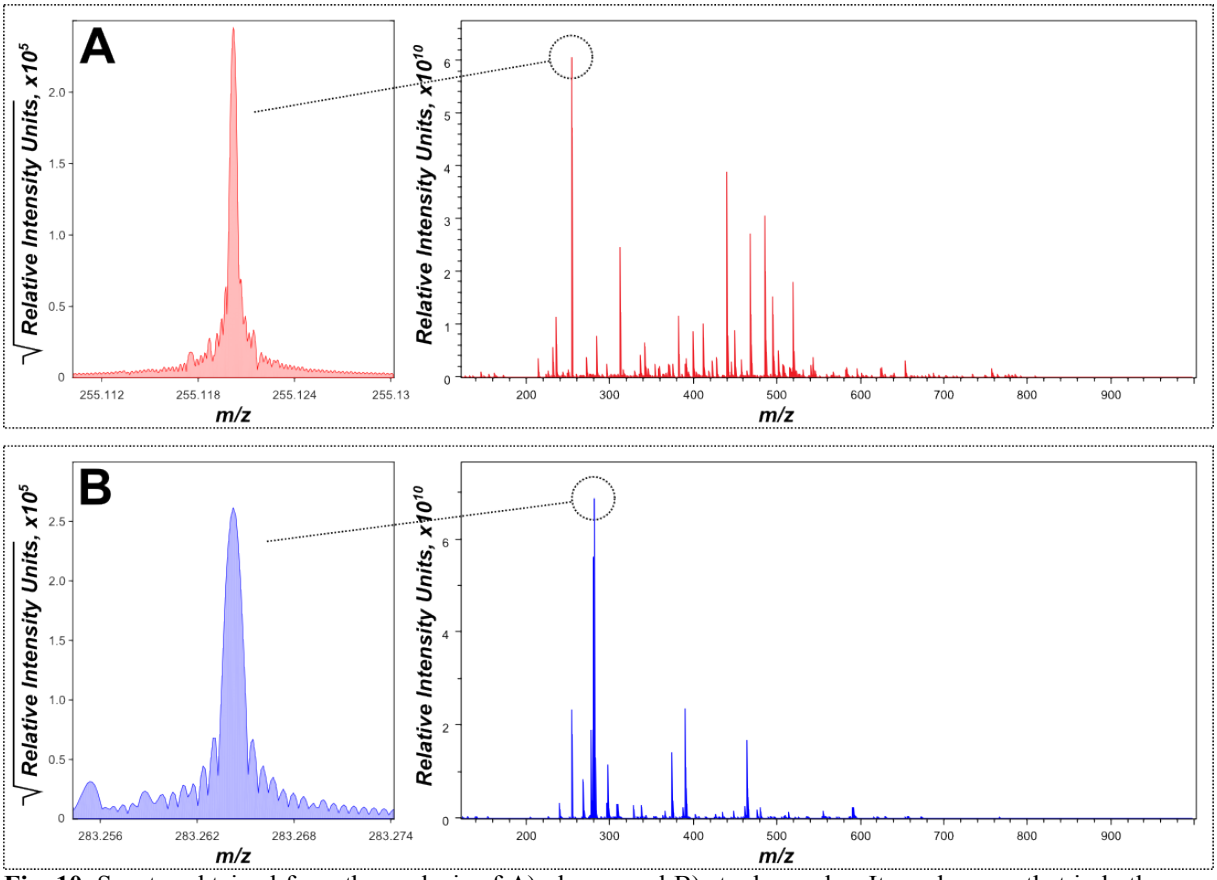

Fig. 10. Spectra obtained from the analysis of A) plasma and B) stool samples. It can be seen that in both cases satellite peaks are present.

In order to delete the peaks, corresponding to the side bands, an algorithm was developed based on empirical observation on the dependence between the intensity value of a side band and its position with respect to the same quantities of the central peak. For further considerations the position of the central peak and the corresponding intensity will be denoted as m/z_c and I_c, respectively, whereas the positions of the side bands with the corresponding intensities will be denoted as $m/z_{\pm i}$ and $I_{\pm i}$, respectively. Index i defines the proximity of a satellite peak to the central peak on the left or on the right side. Investigating the dependence of the side band intensities on their positions, the following linear relation was found empirically:

$$log_{10}\left(\frac{I_c}{I_{\pm i}}\right) \sim A \cdot log_{10}\left(\frac{m/z_c^2}{|m/z_c - m/z_{\pm i}|}\right) + B \qquad \text{Eq. 44}$$

In the Eq. 44 A and B are constant terms to be calculated. Fig. 11 depicts this relation, with respect to a stool (Fig. 11A) and plasma (Fig. 11B) matrix.

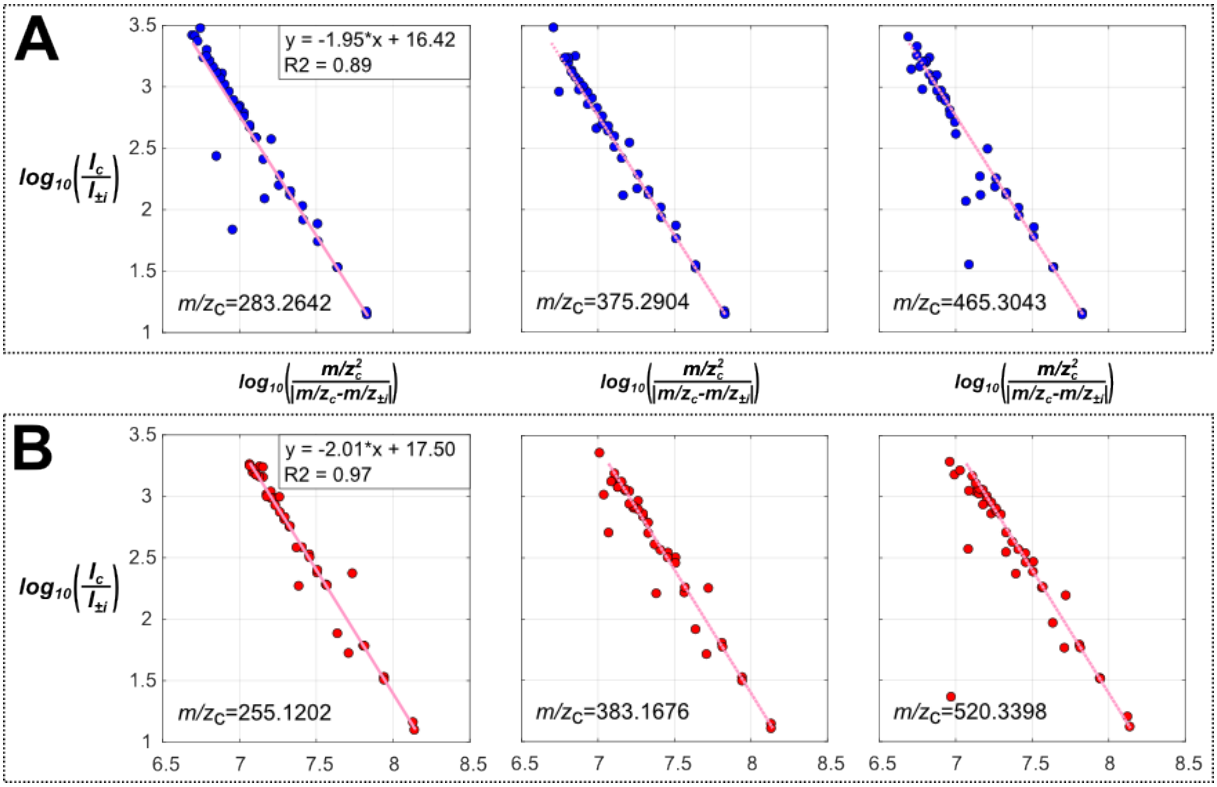

Fig. 11. Scatter plots showing the dependence between the intensity of a satellite peak and its position with respect to the same quantities of the central peak. Three peaks were chosen out of spectra corresponding to A) stool samples and B) plasma samples. Each plot on the left side was used to perform simple linear regression. The constructed line was projected onto other plots in the middle and on the right side.

One spectrum from each sample matrix was chosen to portray the concept. For each case, the scatter plots were built for three peaks of different m/z_c, considering the 20 closest signals from each side of the central peak. As can be seen, the arrangement of data points follows a linear trend. The presence of outliers implies that genuine signals may be hidden among the

side bands. A simple linear regression was performed with respect to a peak of the highest intensity in each spectrum (Fig. 11, left) and the constructed curve was projected onto the remaining scatter plots. It can be observed that the line fits very well the behavior of the corresponding data points. Therefore, it can be suggested that for each individual spectrum, a procedure can be developed that uses one of the peaks to perform a linear regression to generate a model that can represent a rule to eliminate satellite peaks.

The proposed algorithm works as follows. First, a peak of the highest intensity is found and a range around the corresponding m/z_c is chosen. Second, the corresponding quantities according to the Eq. 44 are calculated using $m/z_{\pm i}$ with the corresponding $I_{\pm i}$ within the selected m/z range. Third, an initial model has to be built. However, the presence of outliers can hamper this process. Therefore, additional refinements are done to account for this possibility by using the Grubbs' test, implying calculating the following test statistic using the model residuals, r_i's:

$$G = \max_i \frac{|r_i - \bar{r}|}{s} \qquad \text{Eq. 45}$$

The null hypothesis of no outlier presence at a significance level α is rejected if:

$$G > \frac{n-1}{\sqrt{n}} \sqrt{\frac{t^2_{\frac{\alpha}{2n}, n-2}}{n-2+t^2_{\frac{\alpha}{2n}, n-2}}} \qquad \text{Eq. 46}$$

Here, $t^2_{\frac{\alpha}{2n}, n-2}$ denotes the upper critical value, corresponding to the t-distribution with $n-2$ degrees of freedom and a significance level of $\frac{\alpha}{2n}$, where n is the number of data points used for linear model construction. Taking into account the aforementioned step, the procedure for model construction consists of the following steps, repeated until satisfying conditions are reached:

- Fitting a linear model using Eq. 44 and extracting the residuals.
- Checking for the outliers by performing the Grubbs' test. A significance level of 5% was used for the examined spectra.
- Accepting the constructed model if the null hypothesis of no outlier presence is accepted. Otherwise, deleting the most distant outlier and repeating the steps from the beginning.

At this point, the created model can be used for satellite peak elimination. Further steps are performed repeatedly starting with the peak of the highest intensity:

- Choosing a m/z range around the m/z_c, corresponding to the selected peak.
- Calculating the quantities according to the Eq. 44 using $m/z_{\pm i}$ with the corresponding $I_{\pm i}$ within the selected m/z range.
- Checking if the values of $I_{\pm i}$ lie within the prediction intervals calculated for the corresponding values of $m/z_{\pm i}$. A significance level of 1% was used for the examined spectra.
- Deleting the data points, whose values of $I_{\pm i}$ are within the prediction intervals.
- Selecting the next highest peak in the spectrum and repeating the steps from the beginning.

The procedure repeats until the selected peaks reach a predefined lower limit of intensity.

The described procedure was performed for all the calibrated spectra corresponding to stool and plasma samples. A visual representation of an output of the aforementioned algorithm in case of a spectrum, obtained for one of the stool samples, is shown on Fig. 12.

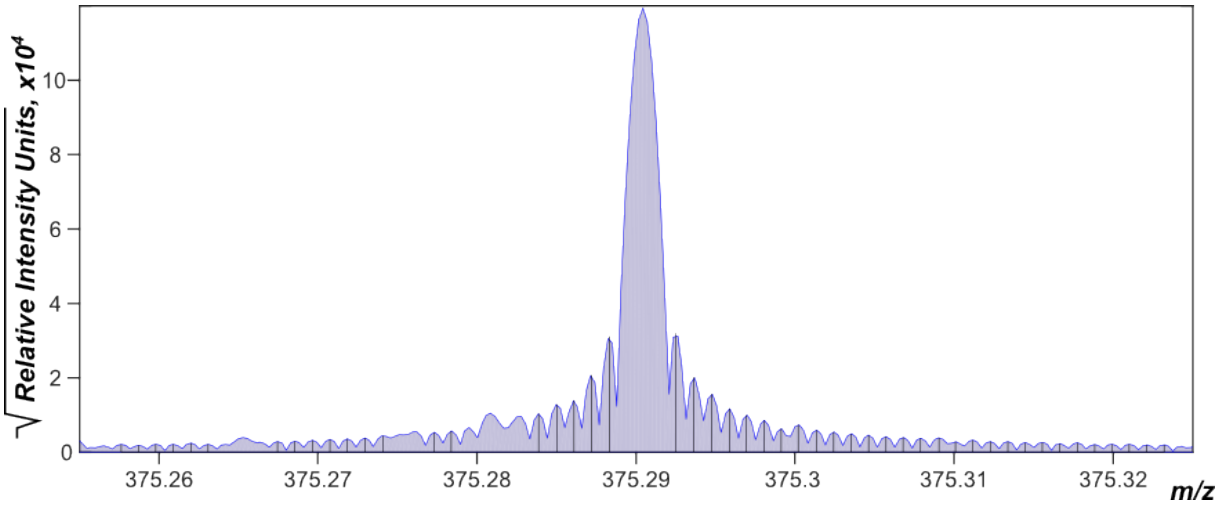

Fig. 12. One of the peaks from a spectrum, corresponding to a stool sample. Vertical bars denote the peaks deleted by the algorithm for satellite peak elimination.

In this example deleted peaks are denoted by vertical bars. It is possible to indicate the potential of the algorithm to delete satellite peaks, while leaving other signals, not following the rule defined by the linear model, intact. Table S6 lists regression coefficients calculated for linear models in each individual spectrum as well as the amount of filtered out peaks. Additionally, Fig. 13 depicts the distributions of the calculated coefficients depending on a sample matrix. Intriguingly, it can be seen that spectra, belonging to the same experiment (*e.g.* analysis of stool samples), are similar in their satellite peak arrangement. Therefore, it can be suggested that a linear model, calculated only for one spectrum, can be used to filter out side bands from other spectra in the same experiment.

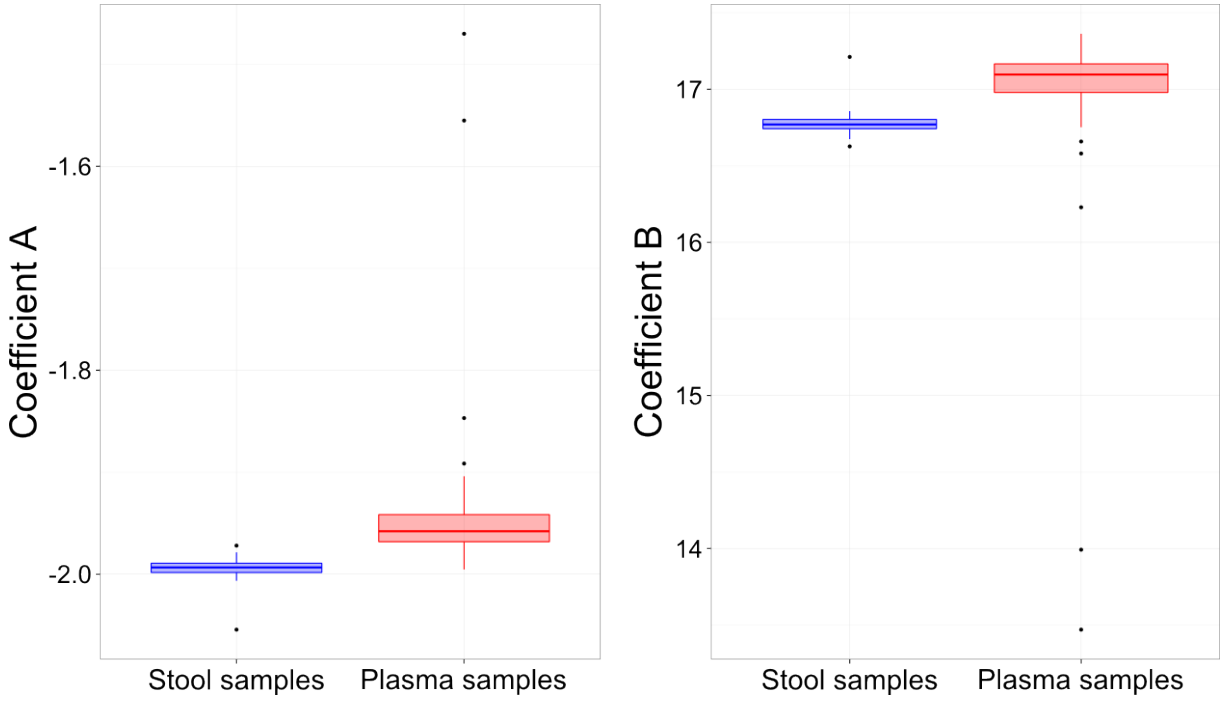

Fig. 13. The distribution of the coefficients A and B from Eq. 44 calculated for each individual spectrum.

Validation of the aforementioned approach was conducted only by visual inspection of the corresponding output because there is no training and test data available.

4.2.3. Graphical user interface

In order to adapt the procedure of satellite peak elimination for common users, a GUI was created (Fig. 14). All the code was written in MATLAB (The MathWorks Inc., Natick, Massachusetts, USA). The GUI requires MATLAB compiler runtime v9.1. The program supports importing files in the form of text files with the first two columns being reserved for experimental m/z ratios and the corresponding intensities. Launching the program starts the process of fitting a linear model with respect to the highest peak in a spectrum followed by eliminating peaks lying within calculated prediction intervals. The varying parameters include:

- Ppm window: the range calculated with respect to a m/z of a central peak and defining the surrounding peaks that can be potentially filtered out
- Exclusion criterion for the higher peaks: this parameters defines the magnitude of a prediction interval with respect to the points lying below the line corresponding to a linear model

- Exclusion criterion for the lower peaks: this parameters defines the magnitude of a prediction interval with respect to the points lying above the line corresponding to a linear model

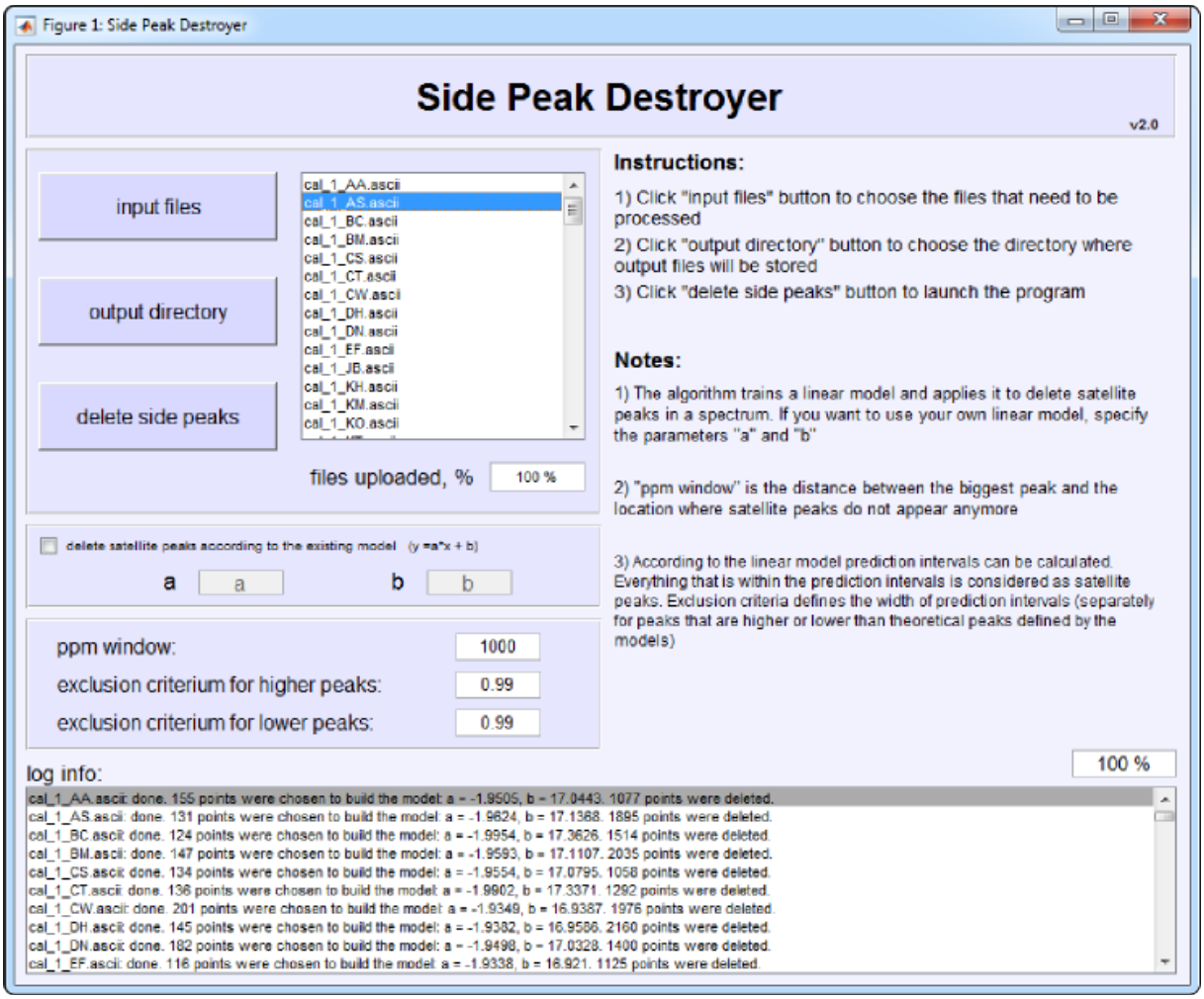

Fig. 14. The GUI for filtering out satellite peaks from mass spectral data.

Additionally, it is possible to apply a user-defined model to eliminate satellite peaks in all of the imported spectra. After selecting an output directory and launching the program, three output files are created:

- The filtered file
- The file to check which signals were filtered out
- The list of regression coefficients

4.3. Matrix generation

4.3.1. Construction of a primary matrix

After re-calibration and filtering out non-informative satellite peaks, the spectral files containing the information on m/z ratios with corresponding intensities were aligned to generate a primary data matrix using an in-house written software «Matrix generator». In short, this program takes all available m/z values, sorts them and divides into groups according to the distances between consecutive entries. In the study presented in the current thesis this distance was chosen to be 1 ppm. Afterwards, unique m/z ratios are calculated for each group by averaging the corresponding entries, while preserving original intensity values. At the end, a matrix is generated where rows represent the averaged m/z values (*i.e.* features), columns correspond to the samples, and each entry within the matrix represents an intensity level. In case of a peak absence in a certain sample, the corresponding entry in the matrix was marked as missing.

Two data matrices, corresponding to the stool and plasma sample measurements, were built in the aforementioned way. With respect to stool samples, the primary matrix was constructed from 108 spectral files and contained 86861 features. With respect to plasma samples, the primary matrix was constructed from 102 spectral files and contained 281751 features. The rows, characterized by only one available entry with the rest missing, were deleted resulting in matrices comprising 44263 and 131750 features, respectively. At this point, these matrices still contain high prevalence of non-informative signals. Moreover, it is necessary to handle missing values, *e.g.* signals that were not detected in some of the samples. Therefore, further processing is required to obtain data, suitable for statistical and multivariate data analysis.

4.3.2. Initial missing value imputation

Metabolomics datasets, derived from DI FT-ICR-MS measurements, can be characterized by a considerable amount of missing values (Hrydziuszko and Viant, 2012). They can originate due to biological and/or technical reasons. For example, the absence of a certain peak can be genuine meaning no presence of the corresponding metabolite in a sample. Moreover, the abundance of a specific compound may be below the detection limit of a mass spectrometer. Additionally, the absence of a peak might take place due to temporal impairment of ionization

process during measurements. Large amount of missing values can influence further data analysis, since a wide range of the corresponding methods relies on having complete records. Particularly, the data of small sample sizes may be affected because of an insufficient number of detected measurements/metabolites, necessary to perform statistical tests. Therefore, missing value imputation can represent a practical solution for the aforementioned challenges.

Naturally, some of the missing data can emerge due to limitations or strict filters of a peak picking algorithm. Therefore, certain missing values can be imputed by examining the corresponding m/z location in the raw spectral data containing the information on the full profile. This approach served as a first step aiming to partially reduce the amount of missing data. It included following steps, equal for both data matrices corresponding to stool and plasma samples:

- Locating rows in the data matrix where at least one missing value was present.
- For each selected row, locating samples/columns where no value was recorded.
- For each selected sample, taking the corresponding raw spectral data and choosing the two adjacent m/z values to the m/z value associated with the selected row.
- Taking an average of the intensities corresponding to the two selected m/z values.
- Performing a test if the calculated value is bigger than the 90% of the minimum intensity value across the entire data matrix.
- Performing an imputation with the calculated value for the selected row and column if the aforementioned test is valid.

The reasoning behind the testing procedure prior imputation is associated with the necessity to enrich the data matrix with genuine values rather than noise. As a result of the aforementioned steps, the percentage of the missing values in the data matrices, corresponding to stool and plasma samples, was reduced from 76% to 58% and from 87% to 75%, respectively.

4.3.3. Noise reduction and final missing value imputation

A substantial amount of features in the primary data matrices represent non-informative values because of inevitable insertion of signals, corresponding to noise, during the alignment process. The removal of possible noise was done for each row by comparing the maximum intensity level per feature to a pre-calculated threshold. Initially, an artificial spectrum in a reduced-profile mode was constructed by taking the minimum intensity levels per each row in a data matrix. As can be seen from Fig. 15, the created spectrum is fairly comparable to the

ones corresponding to the real samples. Since no intensity value in a data matrix can be less than the corresponding intensity value in the generated spectrum with respect to a row, it is possible to use this data to approximate the behavior of a baseline noise level. To do so, the operation of taking an average value in moving average algorithm was substituted by the operation of taking a minimum value. The procedure was repeated 10 times spanning 100 data points in the calculations of modified values. As a result, a curve is generated that is always below the profile of the artificial spectrum or any other spectra corresponding to real samples.

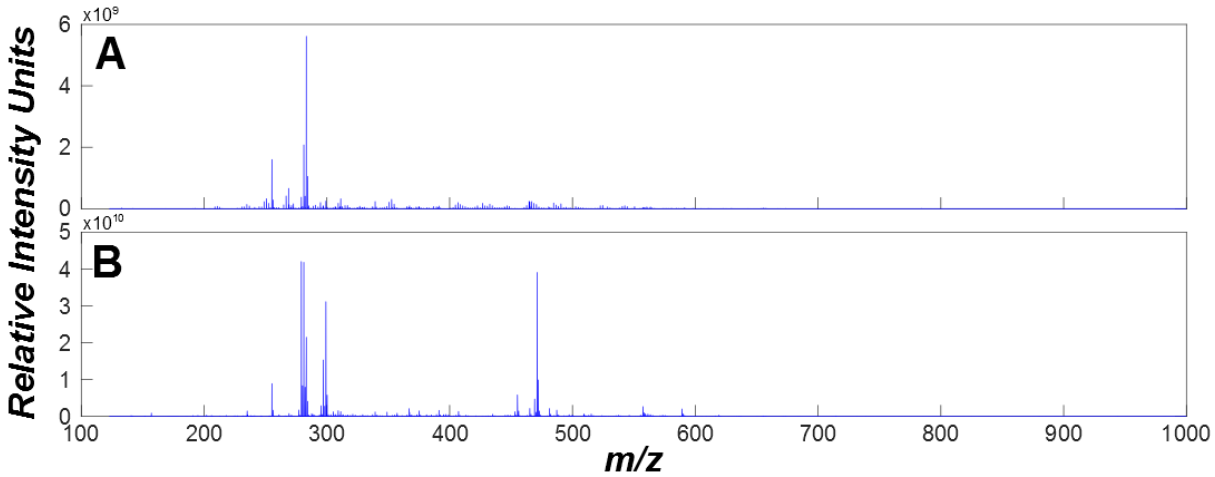

Fig. 15. The plots emphasizing, with respect to stool samples, the similarity between A) an artificial reduced-profile spectrum constructed by taking minimum non-zero intensity values per each row in a primary data matrix and B) one of the reduced-profile spectrum from the data matrix.

In order to define a threshold, to which the maximum intensity values per feature in a data matrix are compared, the level of the generated curve was elevated by raising the corresponding values to the power of 1.1. Afterwards, a testing procedure was applied checking if the maximum intensity values per feature in a data matrix were lower than the defined threshold, meaning the removal of the corresponding row. The filter was additionally restricted to reject features with more than 90% of missing values. The resulting data matrices after applying the aforementioned filtering procedure were reduced to 29513 features in case of stool samples and to 35029 features in case of plasma samples. The respective percentage of missing values was diminished to 46% and 59%.

4.3.4. Molecular formula assignment

Further refinement of the data matrices involved assignments of molecular formulas to the corresponding features through the construction of mass-difference networks (MDiNs). The approach was introduced and described by Breitling *et al.* (Breitling et al., 2006). Based on this work, an adapted version was developed (Tziotis et al., 2011) followed by further

extensions (Moritz et al., 2016). The network is created according to the distances between recorded values in a spectrum or a data matrix (Fig. 16). These distances can correspond to theoretical masses associated to differences in elements between the considered entries. Therefore, having a predefined list of such transformations allows creating a network where every node represents a feature and every edge represents the type of a transformation. This network can be used for assigning molecular formulas to the m/z values in the spectrum or the data matrix. The only requirement is to have nodes with known elemental compositions because they serve as the starters in the assignment algorithm (marked as red circle on Fig. 16).

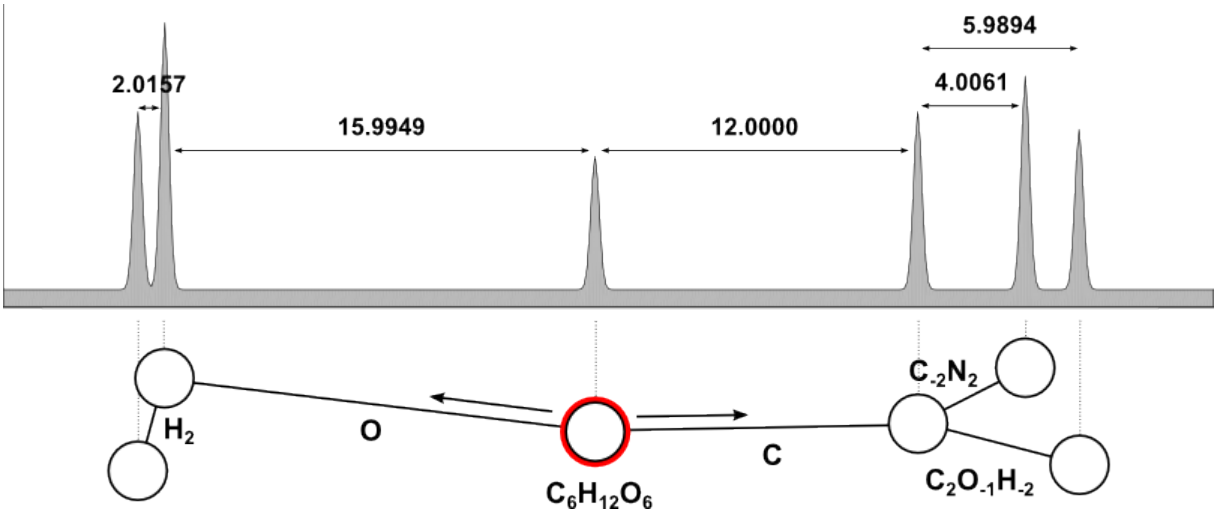

Fig. 16. The process of generating a mass difference network. Peaks of specific $\boldsymbol{m/z}$ values can be connected via theoretical masses corresponding to the addition and subtraction of certain elements. Having a molecular formula assigned to some of the $\boldsymbol{m/z}$ values (marked as red) enables to predict elemental compositions corresponding to other $\boldsymbol{m/z}$ values.

By default, the adapted version of the procedure of generating MDiN considers only $[\mathrm{M}-\mathrm{H}^+]^-$ and $[\mathrm{M}+\mathrm{H}^+]^+$ adducts for the negative and positive ionization mode, respectively. The implementation was improved by taking into account $[\mathrm{M}+\mathrm{Cl}^-]^-$ as well as $[\mathrm{M}+\mathrm{Na}^+]^+$ adducts. The transformation list used for the initial implementation of the MDiN construction for data matrices, corresponding to stool and plasma samples, is listed in

Table S7. With respect to each of the transformations, the following test was performed in order to decide whether two features m/z_i and m/z_j will be connected in a network:

$$\left|m/z_i - m/z_j - m_{tr}\right| < a\frac{\left(m/z_i + m/z_j\right)}{2 \cdot 10^6} \qquad \text{Eq. 47}$$

In Eq. 47 m_{tr} is a theoretical mass of a transformation and a is a parameter defining how strict the test should be. For the initial implementation it was chosen to be 0.1. After the network construction, the assignment algorithm was launched using as a starter the m/z value of the $[\mathrm{M}+\mathrm{Na}^+]^+$ adduct of glucose. The annotations procedure was restricted only to

molecular formulas containing the six most prevalent elements in biological life forms, namely C (carbon), H (hydrogen), N (nitrogen), O (oxygen), P (phosphorus), S (sulfur). During the annotation process many connections can be discarded because they may essentially contribute to false assignments. Therefore, the network containing assignments can differ from its initial counterpart because of the consequent removal of some of the nodes.

After initial calculations are done, the final step is to consider generated molecular formulas in their neutral form without differentiating them by an adduct type. Moreover, primary MDiN construction deals with experimental values, thereby it is not possible to comprise the map of the entire connectivity. Therefore, theoretical masses corresponding to the molecular formulas in their neutral form were calculated and served as an input for another run of mass-difference network reconstruction. The parameter a in Eq. 47 in this case was set to 0.001 because it is assumed that no or very small error can occur. Moreover, the initial transformation list (

Table S7) was substituted by its extended version containing transformations corresponding to biologically relevant reactions (

Table S8). This list was constructed by mining the corresponding entries from the KEGG database and creating a list of unique records. The final version of the network served as the basis for searching for compounds associated with whole grain consumption.

In order to adapt the procedure of MDiN construction for common users, a GUI was created (Fig. 14). All the code was written in MATLAB (The MathWorks Inc., Natick, Massachusetts, USA). The GUI requires MATLAB compiler runtime v8.3. The program supports importing files in the form of text or excel files with the first two columns being reserved for masses and their ids. Other required input files include the reference list, containing the information on the starters, and the transformation list. Prior the main workflow, it is possible to apply in-house written filtering algorithms for removing non-informative features corresponding to satellite peaks, isotope peaks, and peaks with an unusual mass defect calculated as:

$$\text{mass defect} = m/z - \text{floor}(m/z) \qquad \text{Eq. 48}$$

The varying parameters for the MDiN construction and the assignment algorithm include:

- Network tolerance: the parameter defining how strict is the testing procedure to determine if two features can be connected.
- Ref. list tolerance: the error specifying the correspondence between input m/z values and starters.
- Annotation tolerance: the allowed error between input m/z values and the theoretical ones calculated from assigned molecular formulas.
- Edge cutoff: the amount of times an edge in the network is allowed to change the assignments to the adjacent nodes during the annotation procedure. Otherwise, the edge is discarded.
- Cycles to repeat: the amount of iterations to wait before deciding if the assigning algorithm is finished. The counter launches if the assignments from the current iteration are exactly the same as from the previous iteration.
- Range factor: the allowed range between errors associated to the neighboring nodes.

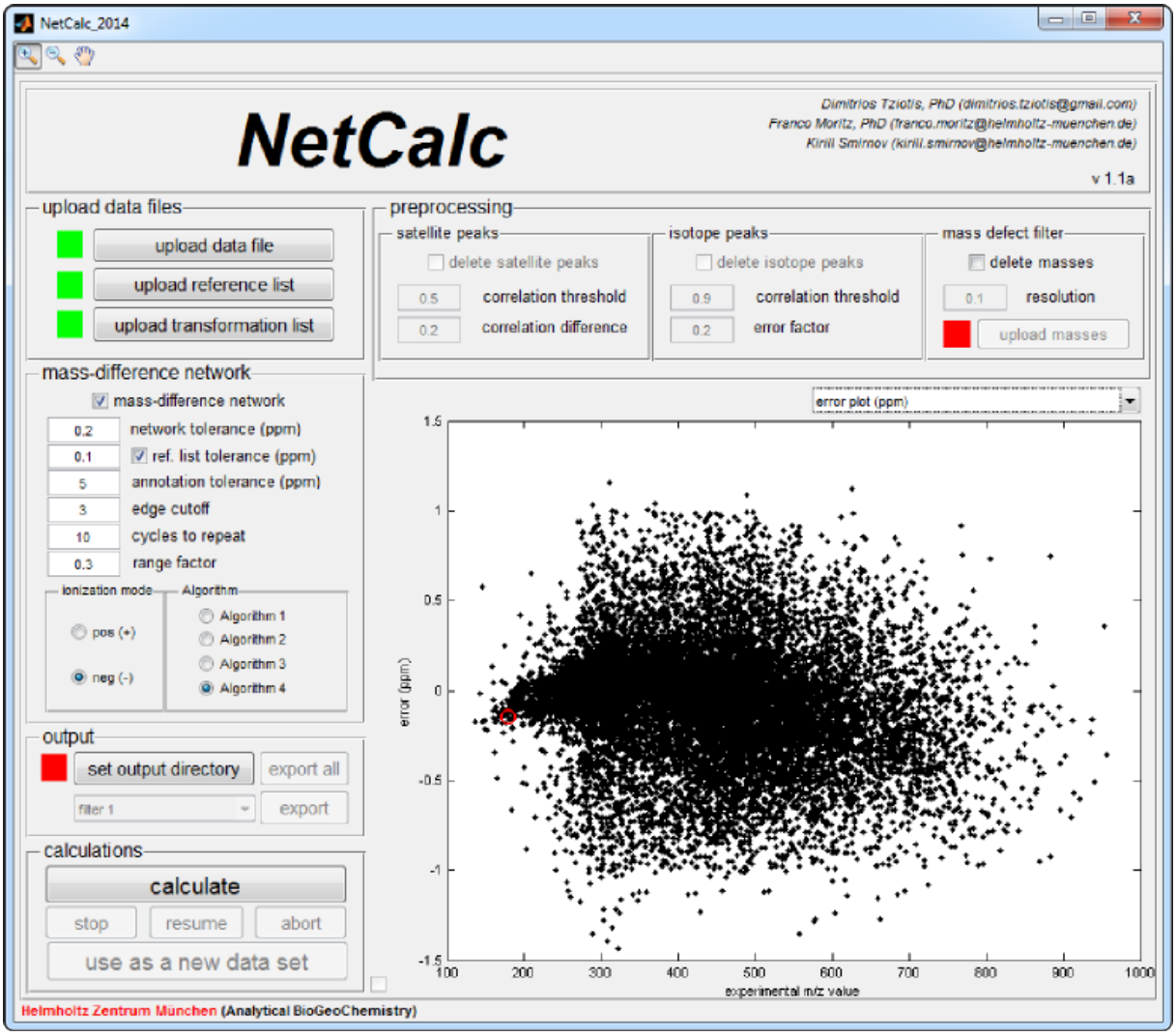

Fig. 17. The GUI for the MDiN construction and further molecular formula assignments.

It is possible to apply one of the four algorithms differing by the implementation of assignment strategy. In the current work, the 4th algorithm was used, characterized by testing the validity of the molecular formula, every time when a feature is annotated, according to the Senior rule (Kind and Fiehn, 2007):

$$\sum_i n_i v_i > 2\left(\sum_i n_i - 1\right) \qquad \text{Eq. 49}$$

$$\text{where} \quad i \in \{\mathrm{E}_1, \mathrm{E}_2 \ldots\}$$

In the Eq. 49 index i goes through the set of considered elements E_1, E_2 *etc.* (*e.g.* C, H, O), n_i and v_i are the amount and the valence, respectively, of a corresponding element in the molecular formula. As the expected valences of such elements as phosphorus and sulfur are not known *a priori* during the validation step using the Eq. 49, the corresponding values were set to 5 and 2 as the most prevalent in biological systems.

4.3.5. Final data matrices

Since MDiN construction followed by the assignment algorithm can be viewed as a filtering procedure, all the features that were not considered in the final network and were not given an annotation by means of molecular formula were filtered out from the corresponding data matrices. As a result, the data matrix, describing the stool metabolome, was reduced to 14651 features and the data matrix, describing the plasma metabolome, was reduced to 15972 features. The respective percentage of missing values was diminished to 42% and 29%. The rest of them were substituted by the 90% of the minimum intensity levels from the corresponding rows. In addition to the annotations in the form of molecular formulas, the features were assigned to the putative metabolites from the HMDB database searching for matches, using a 1 ppm error window, with $[\mathrm{M}-\mathrm{H}^+]^-$ and $[\mathrm{M}+\mathrm{Cl}^-]^-$ adducts with respect to stool metabolome data or with $[\mathrm{M}+\mathrm{H}^+]^+$ and $[\mathrm{M}+\mathrm{Na}^+]^+$ adducts with respect to plasma metabolome data. The retrieved information was supplemented by the chemical taxonomy of the corresponding compounds. For the data analysis routines the entries in the data matrices were modified using logarithm transformation to approximate the behavior of normally distributed data (Zhurov et al., 2014).

An additional data matrix containing OTU counts was created comprising 866 features recorded for all the 112 stool samples. The features having only one present entry with the rest missing were removed from further consideration. This procedure did not significantly reduce the percentage of missing values with 79% before and 76% after the filtering, whereas the amount of features decreased to 774. Other missing values were substituted by 0. The OTUs were assigned to the 5 closest species (with respect to the sequence) using a SeqMatch tool from Ribosomal Database Project. For the data analysis routines the entries in the created data matrix were modified according to Eq. 50:

$$x_{mod} = \log_{10}(100 \cdot x + 1) \qquad \text{Eq. 50}$$

Adding a pseudo OTU can be useful meaning a very little presence of an OTU in a sample where it is missing. However, in order to avoid bias, all the entries were scaled up by the factor of 100 prior adding the pseudo count. After the modification, all the count records were subjected to the logarithm transformation in order to approximate the behavior of normally distributed data.

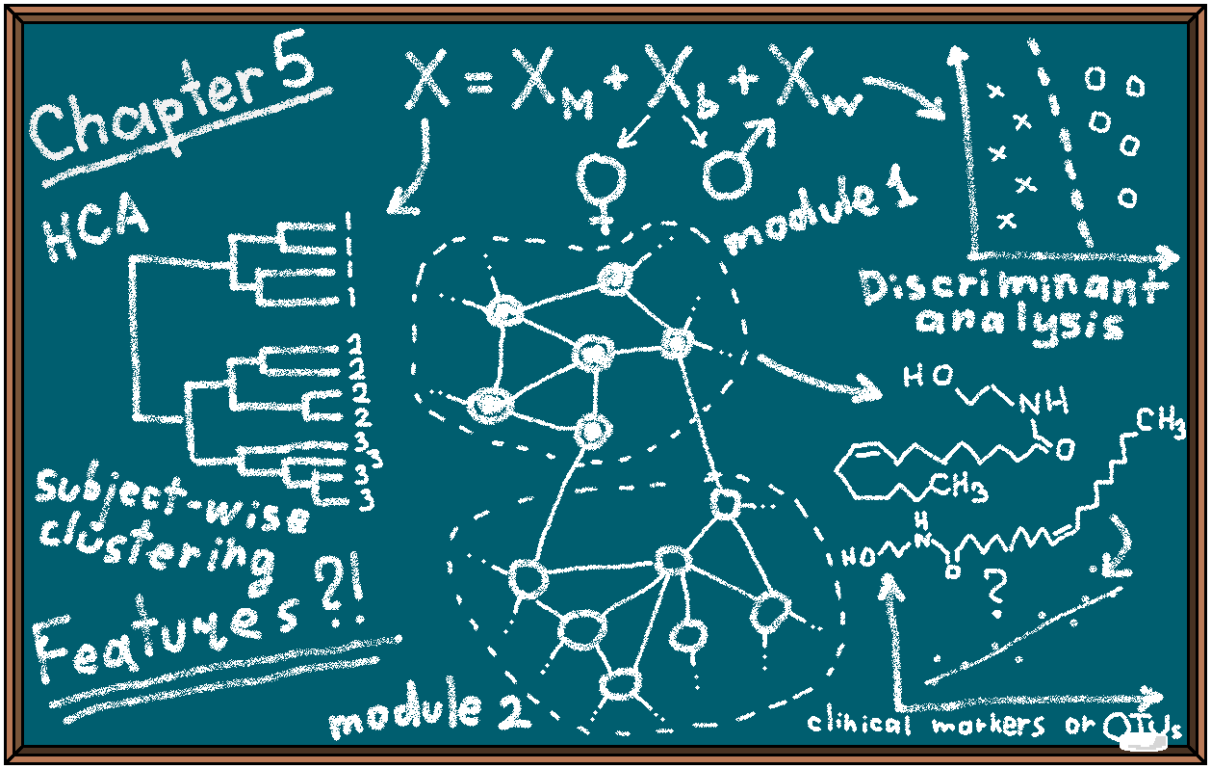
Chapter 5
X = X_M + X_b + X_w
HCA
module 1
Discriminant analysis
Subject-wise clustering
Features ?!
module 2
clinical markers or OTUs

CHAPTER V

5. Revealing metabolic patterns via multivariate data analysis

5.1. Introduction to multilevel methods

Metabolomics data derived from human trials can be frequently characterized by large variation between the subjects because usually no strict conditions are imposed as compared to animal studies (Westerhuis et al., 2010). Due to this issue the responses, associated with a certain stimulus (*e.g.* nutritional intervention), may differ between individuals and, as a consequence, be concealed. One possible solution is to conduct cross-over designed experiments where the subjects act as their own control. This paired data structure implies that the treatment effects can be distinguished from the between-subject variation component, thereby enabling to study the resulting constituents separately. However, the task might be complicated by the huge amount of features presented in metabolomics datasets because, in addition to considering different sources of variation, it is necessary to take into account the interactions between the variables (van Velzen et al., 2008; Zwanenburg et al., 2011). Although the most traditional methods to analyze multivariate metabolomics datasets include PCA and PLS, they do not tale into account an experimental design and, as a consequence, an optimal exploration of the paired data structure is omitted (van Velzen et al., 2008). In cases when the number of variables is less than the number of samples, such methods as multivariate ANOVA (MANOVA) may overcome the aforementioned issue but metabolomics datasets normally reflect the opposite scenario (Smilde et al., 2005). Therefore, other approaches are required that are capable for the analysis of multivariate data with thousands of features while taking into consideration the experimental design as well as the interrelation between variables. Multilevel methods can represent a natural choice because of the potential to handle data characterized by multiple types of variation, *i.e.* multilevel structure (Jansen et al., 2005). The corresponding framework involves creating a model consisting of different submodels, each associated to its own source of variation. Two of the methods are presented in the current work, namely multilevel simultaneous component analysis (ML-SCA) and multilevel PLS discriminant analysis (ML-PLS-DA).

5.2. Overview of the feature space covered by different datasets

As previously described, each out of 774 OTUs was assigned to the 5 closest bacterial species. The reason for increasing the space of feasible assignments was to embrace the

possible diversity of species with respect to different ranks within the taxonomic classification ranging from phylum to genus level. Table S9 lists the abundances of species at the phylum level followed by their possible classification in the lower taxonomic ranks. Depicting it visually on Fig. 18, it is possible to observe the prevalence of *Firmicutes* (76.74%), *Bacteroidetes* (16.67%), and *Actinobacteria* (4.39%), which agrees with the results shown by Martinez *et al.* (Martinez et al., 2013).

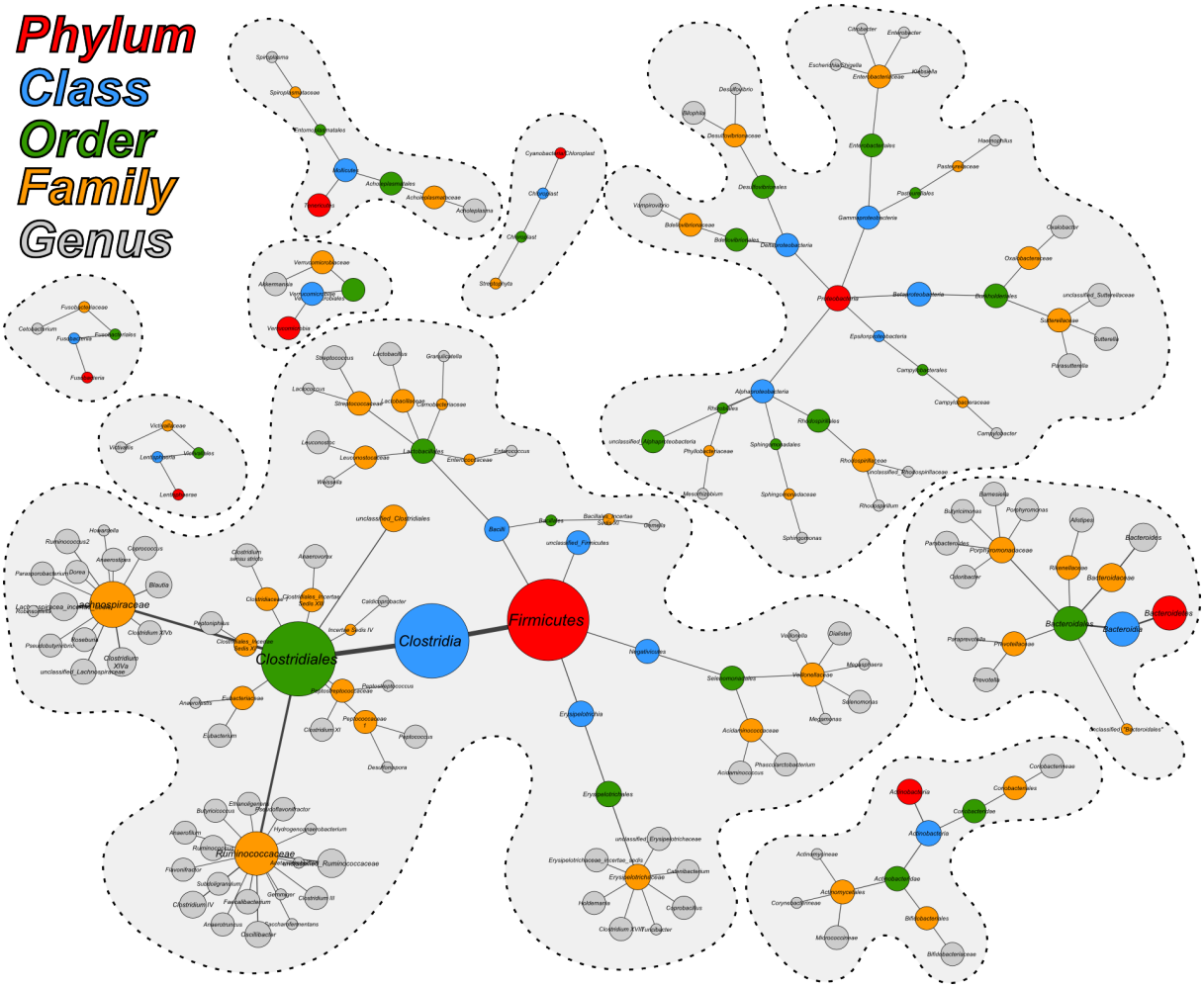

Fig. 18. The abundances of species with respect to their taxonomic ranks. The size of the nodes is proportional to the abundance of species of specific taxonomic level, whereas links depict how different levels are connected. Disconnected graphs emphasize that the corresponding species belong to distinct phyla.

Despite the filtering processes, metabolomics datasets were characterized by the presence of a big amount of features. As a result of MDiN construction followed by molecular formula assignment two distinct networks were built for stool and plasma metabolome data (Fig. 19). Although in both cases the connections form an extremely dense structure, projection of the information on the types of assigned molecular formulas reveals observable order in it. The types depend on the constituents within the corresponding elemental composition. Calculating their relative abundance, it is possible to see that for both datasets, the formulas comprising

the elements of CHO, CHON, CHOS, and CHONS groups are the most prevalent with some slight differences in the corresponding proportions of CHO and CHONS.

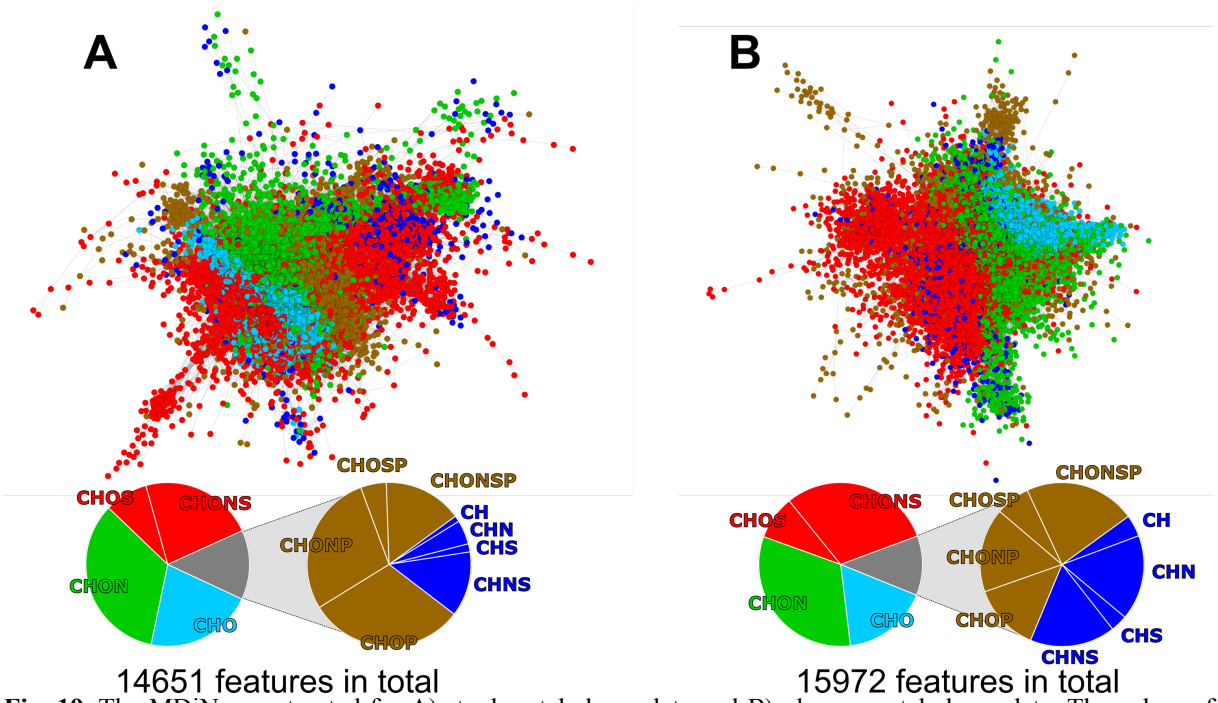

Fig. 19. The MDiNs constructed for A) stool metabolome data and B) plasma metabolome data. The colors of the nodes correspond to the type of elemental composition depending on which constituents are present in the molecular formula associated with a node. The pie charts below the networks depict the proportions of different types of elemental compositions.

Concerning the annotations done by matching the data matrix features to the entries from the HMDB database, 3216 (21.95 %) and 2801 (17.54 %) hits were found, respectively, for the stool and plasma metabolome dataset. Fig. 20 depicts the abundances of the most prevalent compound classes. In this representation redundant annotations were omitted meaning that if a feature was assigned to several compounds of the same class, it was only counted once. Moreover, since during the search two adduct forms are considered ($[M-H^+]^-$ and $[M+Cl^-]^-$ for the negative ionization mode, $[M+H^+]^+$ and $[M+Na^+]^+$ for the positive ionization mode), two entries within a data matrix can be potentially assigned to the same compound. Therefore, the corresponding corrections were done prior calculating the class abundances. Examining the Fig. 20, it is possible to see that the two datasets differ with respect to the relative order of the most prevalent compound classes, having only the steroid class being the most dominant. However, the interpretation of such data can be complicated as a feature may be assigned to several compounds belonging to different classes. Therefore, the Fig. 20 is supplied by the information on the amount of features that are shared between two classes, depicted by the width of the corresponding link. Such representation implies a certain level of ambiguity that has to be taken into account while interpreting results.

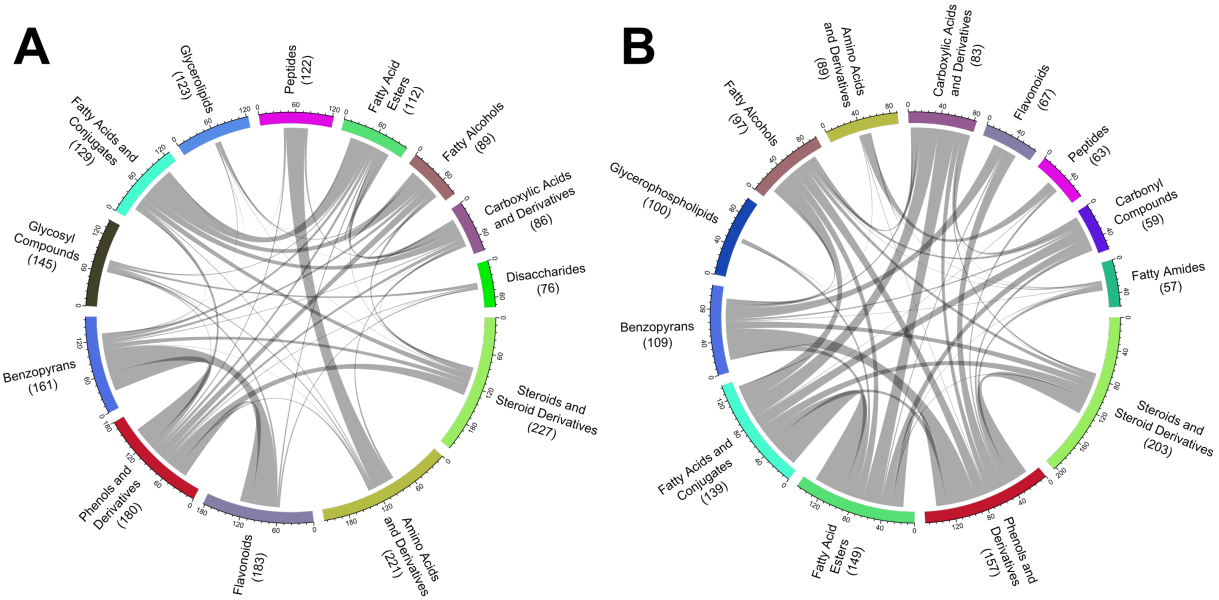

Fig. 20. Chord diagrams depicting the abundances of the most prevalent compound classes within A) stool metabolome dataset and B) plasma metabolome dataset. The links between two classes emphasize the possibility of features to belong to either of them, whereas the corresponding width is proportional to the amount of the features that are currently shared.

It is possible to conclude that the datasets, corresponding to OTU counts or metabolite features over the samples, represent very complicated structures. Therefore, the statistical and multivariate analysis of such data requires care to be taken at each step in the corresponding workflow.

5.3. Taxonomic and metabolic phenotyping

5.3.1. Implemented techniques

5.3.1.1. Multilevel simultaneous component analysis

A detailed description of the technique can be found in Jansen *et al.* (Jansen et al., 2005). ML-SCA can be seen as an extension of PCA that can be used to split the static and dynamic fraction of the total variation kept within a data matrix. In mathematical terms, it corresponds to the following decomposition:

$$\mathbf{X} = \mathbf{1}_N \cdot \mathbf{m}^{\mathrm{T}} + \mathbf{X}_b + \mathbf{X}_w \qquad \text{Eq. 51}$$

In Eq. 51, $\mathbf{X}$ is a data matrix of size $N \times P$ (where N is the number of samples and P is the number of variables), $\mathbf{1}_N$ is a column vector of ones (of size $N \times 1$), $\mathbf{m}$ is a column vector of size $P \times 1$ containing mean values of all the features within $\mathbf{X}$, $\mathbf{X}_b$ and $\mathbf{X}_w$ are the matrices storing information on between- and within-subject variation component, respectively. The

matrix $\mathbf{X}_b$ is constructed by taking the mean values for each column of the centered matrix $\mathbf{X}_c = \mathbf{X} - \mathbf{1}_N \cdot \mathbf{m}^{\mathrm{T}}$ over rows corresponding to the i^{th} individual (where $i = 1,2,\dots,I$) measured in K different occasions. In turn, the matrix $\mathbf{X}_w$ is a term that is obtained by subtracting the matrix $\mathbf{X}_b$ from the matrix $\mathbf{X}_c$. Further actions in building an ML-SCA model include decomposition of the matrices $\mathbf{X}_b$ and $\mathbf{X}_w$ by PCA algorithm to produce the corresponding submodels:

$$\mathbf{X} = \mathbf{1}_N \cdot \mathbf{m}^{\mathrm{T}} + \mathbf{T}_b\mathbf{P}_b^{\mathrm{T}} + \mathbf{T}_w\mathbf{P}_w^{\mathrm{T}} + \mathbf{E} \qquad \text{Eq. 52}$$

In Eq. 52, the matrices $\mathbf{T}_b$, $\mathbf{P}_b$, $\mathbf{T}_w$, $\mathbf{P}_w$, and $\mathbf{E}$ have the same meaning as in the Eq. 2 for PCA decomposition. However, the number of components for each of the submodels can differ. Every term in Eq. 52 can be examined separately, thereby providing a deeper way to study patterns responsible for between- and within-subject variability as compared to the classical PCA approach.

5.3.1.2. Hierarchical cluster analysis and its sparse extension

Hierarchical cluster analysis (HCA) corresponds to clustering methods used for dividing samples/observations stored in a data matrix $\mathbf{X}$ of size $N \times P$ (where N is the number of samples and P is the number of variables) into groups according to some measure of similarity or dissimilarity calculated between pairs of variables/features (Witten and Tibshirani, 2010). The optimization criteria for many clustering methods can be depicted in the following form:

$$\max_{\boldsymbol{\Theta} \in \mathbf{D}} \sum_{j=1}^{P} f_j(\mathbf{X}_{.j}, \boldsymbol{\Theta}) \qquad \text{Eq. 53}$$

In Eq. 53, $\mathbf{X}_{.j}$ denotes the column vector describing the j^{th} feature, $f_j(\mathbf{X}_{.j}, \boldsymbol{\Theta})$ is a function involving this feature and $\boldsymbol{\Theta}$ is a parameter defined as a subset of a bigger set $\mathbf{D}$ (*e.g.* one of the partitions of the observations into groups). In case of HCA, the clustering takes place after defining a dissimilarity matrix $\mathbf{U}$ of size $N \times N$. Therefore, following the form of Eq. 53, a classical HCA can represent an optimization problem to find the entries within this matrix:

$$\max_{\mathbf{U}} \sum_{j=1}^{P} \sum_{i,i'}^{N} d_{i,i',j}\, \mathbf{U}_{i,i'} \quad \text{subject to} \quad \sum_{i,i'}^{N} \mathbf{U}_{i,i'}^2 \leq 1 \qquad \text{Eq. 54}$$

The solution to the problem, depicted by Eq. 54, is $\mathbf{U}_{i,i'} \propto \sum_{i,i'}^{N} d_{i,i',j}$, representing exactly the form of a dissimilarity matrix used in the standard HCA. Afterwards, a dendrogram can be constructed followed by choosing an arbitrary cut to produce 1 to N individual clusters.

It is reasonable to assume that only a small fraction of features from **X** is responsible for observation of clusters (Witten and Tibshirani, 2010). Extraction of such information might represent an important task and sparse clustering methods can be used to solve this problem. The corresponding optimization criteria can be defined in a following way, representing a modified version of Eq. 53:

$$\max_{\mathbf{w};\,\boldsymbol{\Theta}\in\mathbf{D}} \sum_{j=1}^{P} w_j f_j\left(\mathbf{X}_{\cdot j}, \boldsymbol{\Theta}\right) \qquad \text{Eq. 55}$$

$$\text{subject to} \quad \|\mathbf{w}\|^2 \leq 1, \;\; \|\mathbf{w}\|_1 \leq s, \;\; w_j \geq 0$$

In Eq. 55, w_j is a weight associated with the j^{th} feature and s is a tuning parameter, which affects the amount of features taken into account while dividing observations into groups. Therefore, it is possible to select features, mostly responsible for clustering. In case of HCA, the problem of finding the dissimilarity matrix **U**, while considering Eq. 55, can be rewritten as:

$$\max_{\mathbf{w};\,\mathbf{U}} \sum_{j=1}^{P} w_j \sum_{i,i'} d_{i,i',j}\, \mathbf{U}_{i,i'} \qquad \text{Eq. 56}$$

$$\text{subject to} \quad \sum_{i,i'}^{N} \mathbf{U}_{i,i'}^2 \leq 1, \;\; \|\mathbf{w}\|^2 \leq 1, \;\; \|\mathbf{w}\|_1 \leq s, \;\; w_j \geq 0$$

Performing hierarchical clustering using the matrix **U** derived from Eq. 56 provides a solution built on a fraction of the total amount of features. Smaller the value of the tuning parameter s, less features is included into the final model. The aforementioned approach can be referred as a sparse hierarchical cluster analysis (SHCA) which potentially can be used for feature selection in a non-supervised manner.

5.3.1.3. Exploration of the feature space determined by SHCA

Despite finding an optimal value of the tuning parameter s in SHCA, the resulting clustering may not be satisfactory. Therefore, it can be interesting to investigate the feature space covered by SHCA output for larger values of s. However, it is important to evaluate the quality of the corresponding clustering in order to choose an acceptable value for the tuning parameter. As a consequence, an approach was developed assessing how well the data points, belonging to the same individuals, group together. It is based on calculating a clustering score for each subject for every possible cut on a dendrogram resulting from the application of SHCA. Denoting by $g_{j_i}^{i}$ (where $i = 1,2,\ldots,I$ and $j_i = 1,2,\ldots,J_i$) the elements of the

corresponding sets G_i (*e.g.* different samples taken from the same subject) and D_k (where $k = 1,2,\dots,K$) the sets created by cutting a dendrogram at a certain level (which produces K clusters containing different elements $g_{j_i}^i$), the following measure can be calculated:

$$S_i = \frac{\sum_{k=1}^{K} |D_k \cap G_i|}{\sum_{j=1}^{n} I(|D_k \cap G_i| \neq 0)} \quad \text{Eq. 57}$$

In Eq. 57, $I(x)$ represents an indicator function that is equal to 1 if the expression in the argument is true and 0 otherwise. The measure S_i can be considered as a clustering score for a group denoted by the index i. An overall clustering score can be generated by simple summation of the corresponding constituents S_i:

$$S = \sum_{i=1}^{I} S_i \quad \text{Eq. 58}$$

The measure in Eq. 58 can serve as an optimization criterion where S is to be maximized with respect to the tuning parameter s. It is worth pointing out that such formulation of the problem is not limited to SHCA but can be applied in combination with evolutionary algorithms while searching an optimal set of features for HCA.

5.3.2. Features involved in taxonomic and metabolic phenotyping

In order to have an overview on the proximity of the samples, the datasets, corresponding to OTU counts as well as stool and plasma metabolome, were subjected to HCA (Fig. 21). Euclidean distance and Ward's method were used as the metrics and linkage, respectively. It is possible to see that in case of OTU counts (Fig. 21A) as well as stool metabolome (Fig. 21B), the samples belonging to the same individual exhibit strong clustering behavior, whereas for plasma metabolome data no observable groups were detected. These results can suggest strong individual-specific inter-dependence between stool metabolome and gut microbiota composition. Only a fraction of the total amount of features within the corresponding data matrices may be responsible for the observed patterns. Therefore, it is important to find a way to extract this information. Since the observed clustering is relatively strong, it can be appealing to use unsupervised feature selection methods in order to investigate, whether the corresponding algorithms will lead to the same or better output, emphasizing the significance of the between-subject variation. In this regard, SHCA was used as described in the previous section together with finding an optimal tuning parameter s for the problem depicted by Eq. 56.

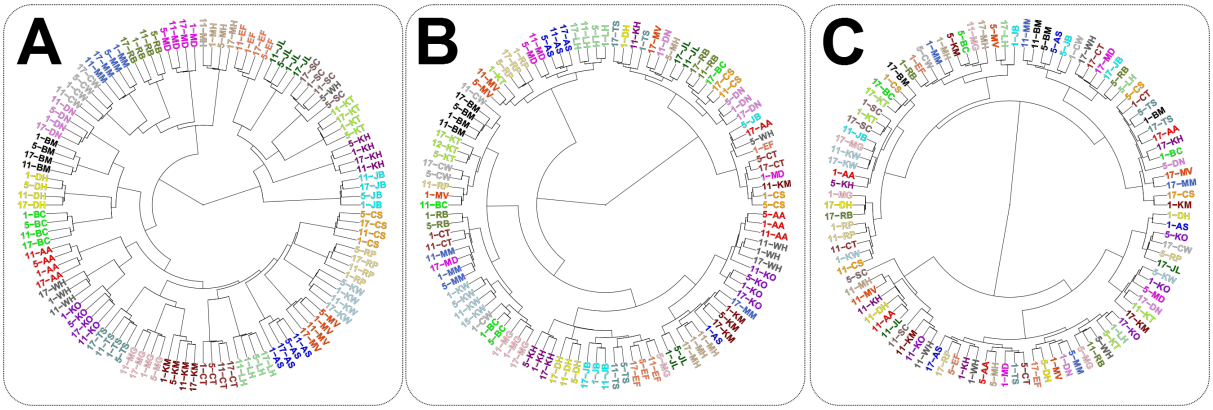

Fig. 21. HCA performed on the datasets corresponding to A) OTU counts, B) stool metabolome, and C) plasma metabolome. The analysis was conducted by using Euclidean distance and Ward's method as the distance metrics and linkage, respectively.

Since HCA results, corresponding to OTU counts and stool metabolome, showed an obvious clustering of data points belonging to the same individuals, the respective data matrices were further examined by applying SHCA using the same metrics and linkage as for HCA. In order to find an approximate optimal solution for Eq. 56, the algorithm was performed using different values of the tuning parameter s. For the dataset, containing OTU counts, SHCA was conducted for all the values between 1.1 and 30 with a step of 0.1. For the data, corresponding to stool metabolome, SHCA output was evaluated for all the values between 1.1 and 100 with the same step of 0.1. The performance was evaluated at each s by calculating the gap statistic. The resulting plots, depicting the performance of the SHCA algorithm versus the tuning parameter s, are shown on Fig. 22. The optimal value for the tuning parameter s is defined by the location of the maximal value of the gap statistic. In case of OTU counts, this corresponded to s equal to 4.6 with 33 features selected (Fig. 22A), whereas in case of stool metabolome dataset, the optimal s was equal to 3.2 with 25 features selected (Fig. 22B). The respective dendrograms, taking into consideration only the extracted variables, are shown on Fig. 23. With respect to OTU counts, using only 33 features out of 774 resulted in nearly the same perfect individual-wise clustering as depicted on Fig. 21A, meaning that the differences between subjects can be described only by this small fraction. In case of stool metabolome, although the grouping became less obvious, 25 features were capable to explain strong clustering for some individuals. It is possible to conclude that SHCA performed well in the context of unsupervised feature selection, while preserving overall trend seen at a primary look on the data. Nevertheless, it can be assumed that the features corresponding to the location of maximal gap statistic may not be sufficiently representative. As a consequence, it is reasonable to investigate the expansion of the feature space by moving along the increase of the tuning parameter s.

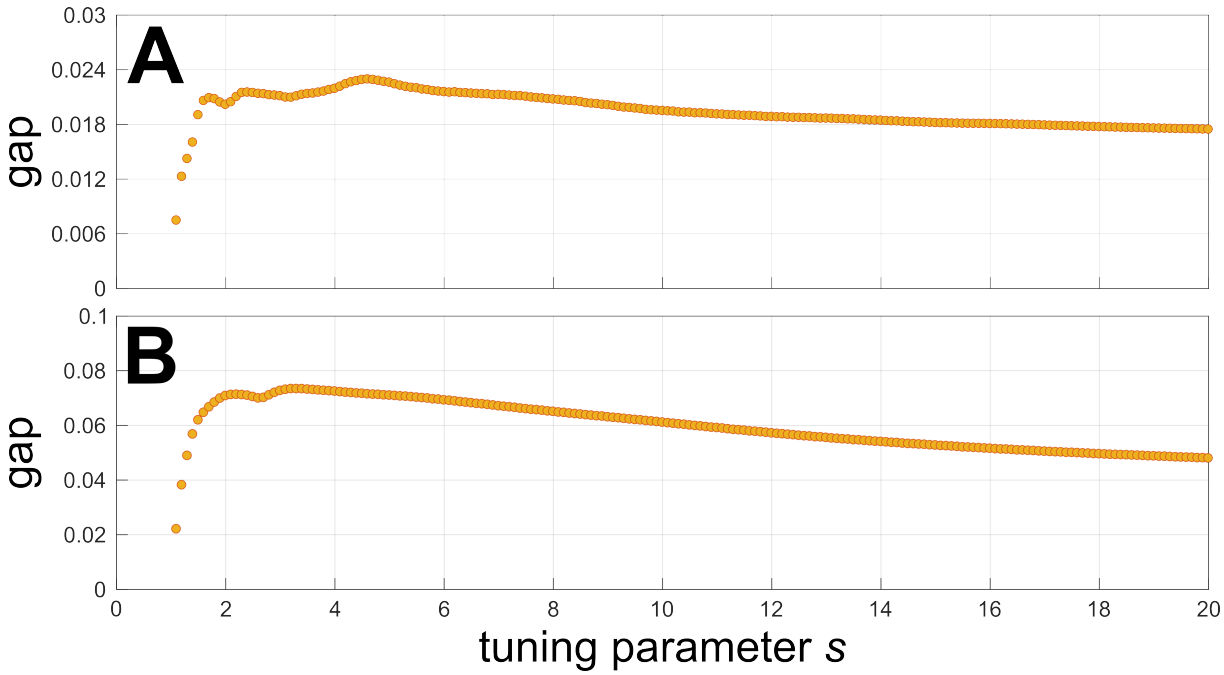

Fig. 22. SHCA performance versus the tuning parameter ***s*** for the datasets corresponding to A) OTU counts and B) stool metabolome. Global maxima reflect the features leading to the optimal solution of the optimization problem of SHCA.

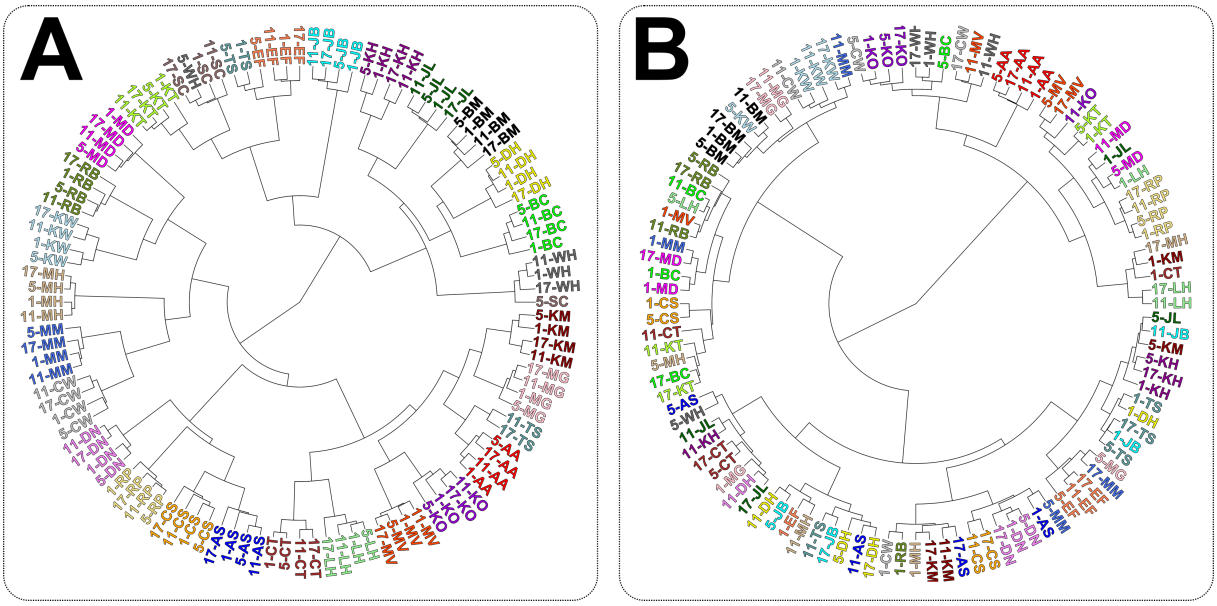

Fig. 23. Resulting dendrograms after running SHCA algorithm and selecting features corresponding to the tuning parameter ***s*** associated with the maximal value of the gap statistic. The dendrograms are built for the data corresponding to A) OTU counts and B) stool metabolome.

By calculating the clustering score using Eq. 58 for every output from SHCA corresponding to the different values of a tuning parameter *s*, it was possible to find an optimal set of features for both datasets in order to achieve the best grouping of the data points belonging to the same individuals. The corresponding dendrograms are shown on Fig. 24. The respective amount of features, chosen for HCA was 87 (11.2 % from the total amount) for the OTU counts dataset and 1211 (8.5% from the total amount) for the stool metabolome dataset. As

can be seen from Fig. 24 nearly identical clustering was obtained comparing the results to Fig. 21A and Fig. 21B but with much less amount of features.

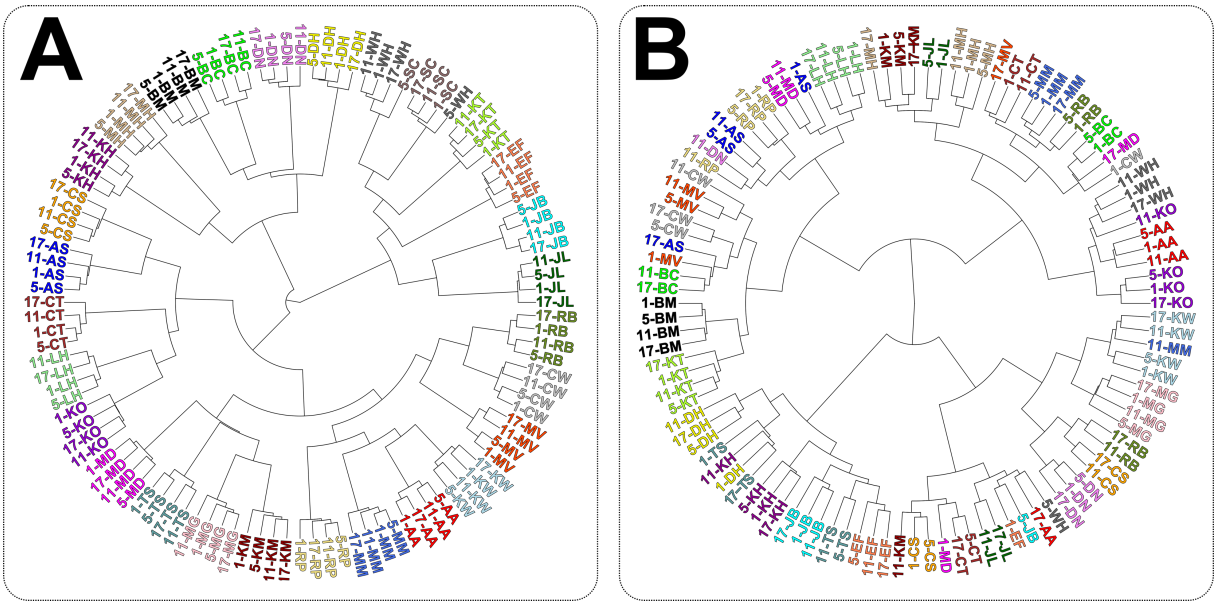

Fig. 24. Resulting dendrograms using features selected by finding an optimal solution for the tuning parameter $\boldsymbol{s}$ with respect to the Eq. 58. The dendrograms are built for the data corresponding to A) OTU counts and B) stool metabolome

Performing SHCA, it is possible to rank a feature by finding the minimal value of the tuning parameter s necessary for its inclusion into the clustering model. The corresponding results are shown in Table S10 and Table S11 covering all the features selected before the tuning parameter is equal to an optimal value for achieving the best clustering score (Eq. 58). The first entries (*i.e.* the highest ranks) in the Table S10 correspond to genera *Dialister* and *Ruminococcus*, both belonging to the *Firmicutes* phylum. Interestingly, in the work of Martinez *et al*. (Martinez et al., 2013) the abundances of these two genera showed a trend of opposite behavior with respect to diet responses as well as correlation to clinical parameters. Fig. 25 depicts the abundances of *Dialister* and *Ruminococcus* by means of the matrix $\mathbf{X}_b$ from Eq. 51 in order to concentrate on the between-subject variation component. It is possible to see that individuals with lesser prevalence of *Ruminococcus* genus have higher values for *Dialister* genus, and *vice versa*. Taking into account that they can be affected by the diet regime (as shown by Martinez *et al.*), it is possible to assume that the treatment might drive individual-specific changes depending on the gut microbiota composition.

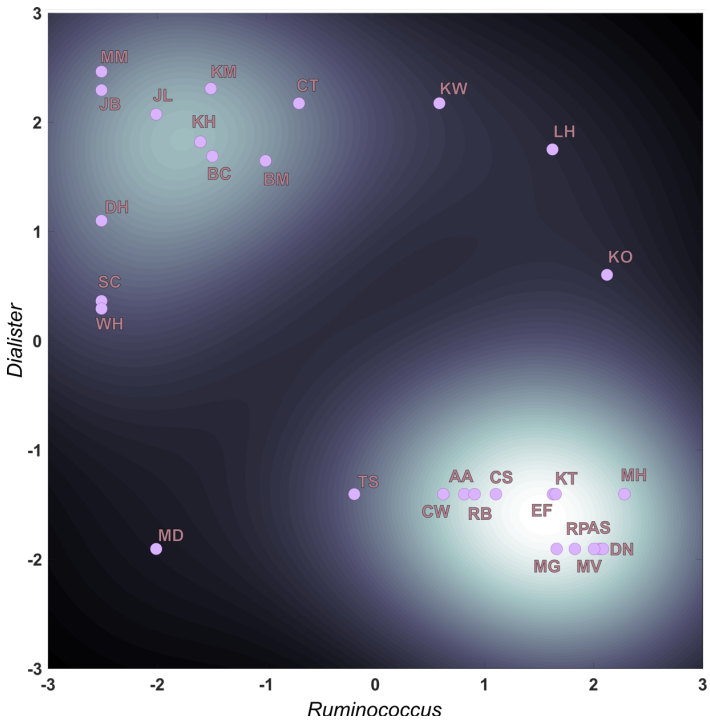

Fig. 25. The scatter plot depicting the dependence of the mean abundances between *Dialister* and *Ruminococcus* genera within subjects. Using density estimation, it is possible to see two distinct regions which emphasizes the contrary behavior of these two genera.

Regarding the stool metabolome dataset, the first entries in the Table S11, listing the features highly responsible for the differences between individuals, correspond to the same metabolite, sucralose, as annotated by the HMDB database. This compound is described by two signals in the mass spectra ($[M - H^+]^-$ and $[M + Cl^-]^-$) and is featured by the presence of 3 covalently bond chlorine atoms substituting hydroxyl groups in galactosucrose. The evidence of the compound identity can be supported by the corresponding isotopic pattern for both deprotonated as well as chlorinated adducts (Fig. 26). Moreover, the two signals, corresponding to the monoisotopic mass of sucralose, have a high value of Spearman correlation coefficient, supporting the assumption of a common precursor compound. Since sucralose is a sweetener that is poorly absorbed in gastrointestinal tract and excreted mostly unchanged (Roberts et al., 2000), its contribution to inter-individual differences by means of stool metabolome is evident.

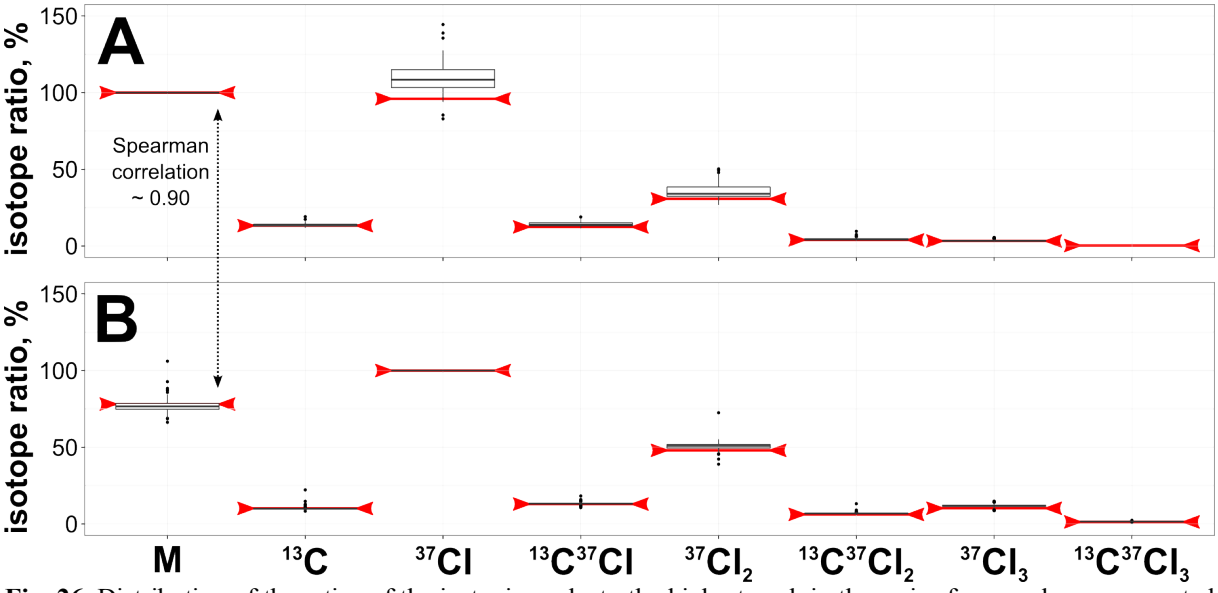

Fig. 26. Distribution of the ratios of the isotopic peaks to the highest peak in the series for sucralose represented as A) a deprotonated adduct and B) a chlorinated adduct. The red bars show the theoretical values for isotopic ratios.

Using the optimized set of features, a MSCA was performed on the matrix $\mathbf{X}_b$ in order to examine whether the chosen metabolite signals correspond to some individual characteristics (Fig. 27). Intriguingly, by representing the data in 3 dimensions and choosing the first 3 principal components, it was possible to observe that the data points, belonging to different gender groups, form distinguishable clusters. Interestingly, such a behavior was already observed by performing MSCA using the entire set of features meaning that gender is a factor that strongly influences the between-subject variability. Therefore, the selected features may partially explain the differences associated with gender on the level of OTU counts and stool metabolome.

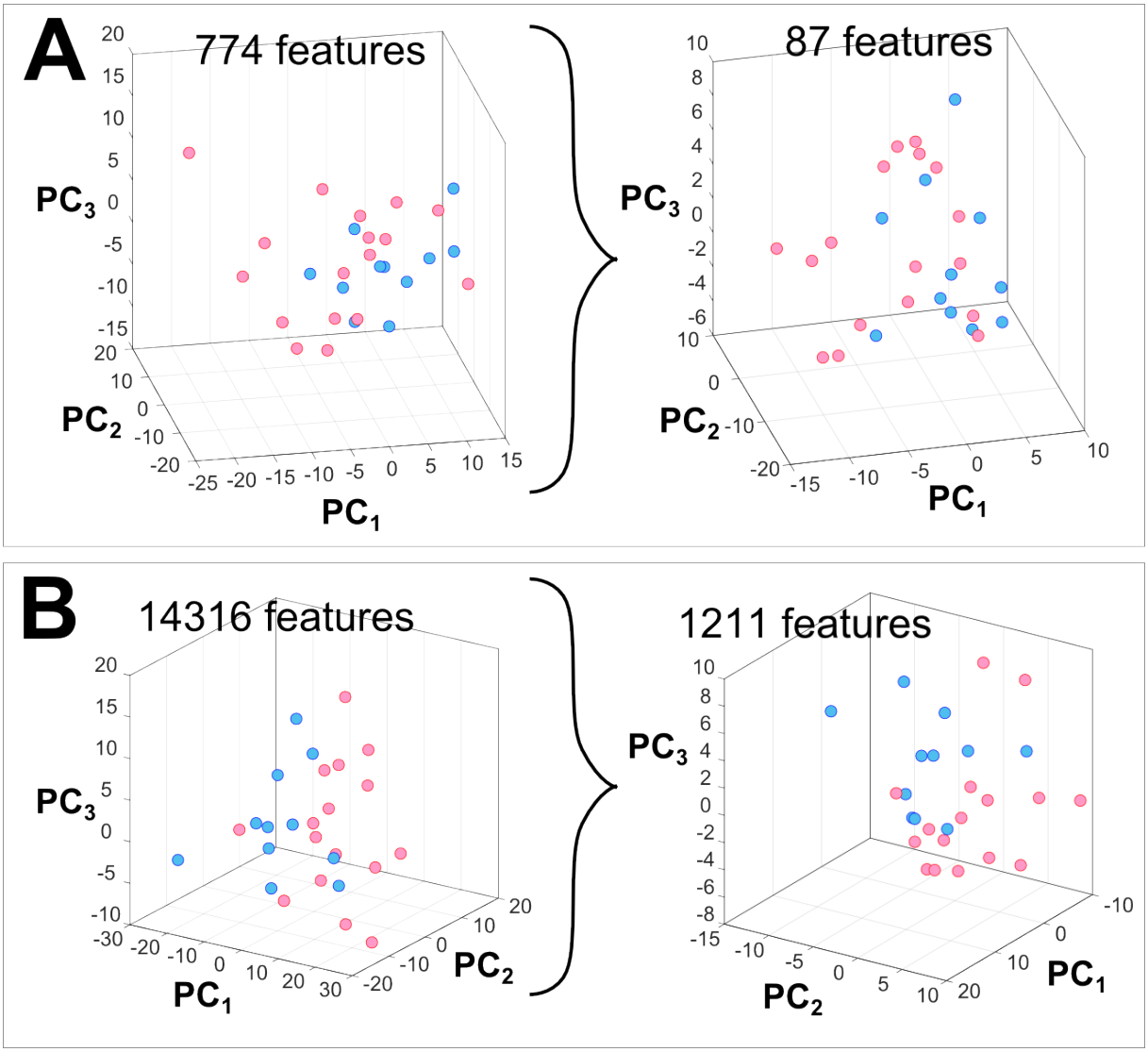

Fig. 27. MSCA applied for the A) OTU counts dataset and B) stool metabolome dataset before and after feature selection done by HSCA.

As a summary, by examining natural clustering of data points, corresponding to different samples, it was possible to see the strong influence of the between-subject variation component in the data, especially evident for OTU counts and stool metabolome datasets. Such an observation might imply a tight link between gut microbiota composition and metabolites detected in stool samples. Selecting features in an unsupervised manner using SHCA preserved the initial clustering behavior, thereby emphasizing the significance of the possible influence of inter-individual differences on further data analysis. Therefore, exploring the diet responses will require multivariate methods, capable for reducing the impact of the corresponding variation component.

5.4. Impact of whole grain diet on human gut microbiota and metabolome

5.4.1. Implemented techniques

5.4.1.1. Multilevel partial least squares discriminant analysis

A detailed description of the technique can be found in van Velzen *et al.* (van Velzen et al., 2008). ML-PLS-DA can be seen as an extension of conventional PLS-DA when paired samples are present due to longitudinal or crossover-designed experiments. As in the case of ML-SCA, the initial step involves matrix decomposition according to Eq. 51. Depending on the question of interest (for simplicity, in case of two classes, vector $\mathbf{y}$ of size $N \times 1$ containing the information on the class correspondence), either the matrix $\mathbf{X}_b$ or $\mathbf{X}_w$ can be used for further analysis. Similar to Eq. 5 and Eq. 6, it is possible to construct the following PLS decomposition, while choosing a predefined number of components:

$$\mathbf{X}_{b/w} = \mathbf{T}_{\mathbf{X}_{b/w}} \mathbf{P}_{\mathbf{X}_{b/w}}^{\mathrm{T}} + \mathbf{E}_{\mathbf{X}_{b/w}} \quad \text{Eq. 59}$$

$$\mathbf{y} = \mathbf{T}_{\mathbf{y}} \mathbf{P}_{\mathbf{y}}^{\mathrm{T}} + \mathbf{E}_{\mathbf{Y}} \quad \text{Eq. 60}$$

The task is to find the vector of regression coefficients $\mathbf{b}$ in the Eq. 4. Following the PLS routines, it is possible to show that this vector is equal to (Abdi, 2010):

$$\mathbf{b} = \left(\mathbf{P}_{\mathbf{X}_{b/w}}^{\mathrm{T}}\right)^{+} \mathbf{B}_{\mathrm{PLS}} \mathbf{P}_{\mathbf{y}}^{\mathrm{T}}$$

$$\text{where} \quad \left(\mathbf{P}_{\mathbf{X}_{b/w}}^{\mathrm{T}}\right)^{+} = \left(\mathbf{P}_{\mathbf{X}_{b/w}} \mathbf{P}_{\mathbf{X}_{b/w}}^{\mathrm{T}}\right)^{-1} \mathbf{P}_{\mathbf{X}_{b/w}} \quad \text{Eq. 61}$$

$$\text{and} \quad \mathbf{B}_{\mathrm{PLS}} = \left(\mathbf{T}_{\mathbf{X}_{b/w}}^{\mathrm{T}} \mathbf{T}_{\mathbf{X}_{b/w}}\right)^{-1} \mathbf{T}_{\mathbf{X}_{b/w}}^{\mathrm{T}} \mathbf{T}_{\mathbf{y}}$$

After finding an approximation $\hat{\boldsymbol{y}}$ for $\boldsymbol{y}$, it is possible to estimate the training error (since all the data was used to build the model) by the sum of squares of the model residuals:

$$SS_{res} = \frac{1}{N} \sum_{i=1}^{N} (y_i - \hat{y}_i)^2 \quad \text{Eq. 62}$$

It is also possible to calculate the coefficient of determination that is commonly used in evaluating PLS output:

$$R^2 = 1 - \frac{\sum_{i=1}^{N} (y_i - \hat{y}_i)^2}{\sum_{i=1}^{N} (y_i - \bar{y})^2} \quad \text{Eq. 63}$$

Nevertheless, knowing the training error is not enough for estimating the model quality. Therefore, it is necessary to assess the model on a testing set of observations or by performing a cross-validation procedure. In the latter case the total set of observations is usually divided

into several distinct subsets of approximately the same size. In each case, all but one of the subsets (training set) are used to train the model and the corresponding leftover subset is used for estimating the cross-validation error. Assuming the division onto K distinct subsets, the sum of squares after the cross-validation procedure is calculated as:

$$SS_{res}^{\mathrm{CV}} = \frac{1}{K}\sum_{k=1}^{K}\frac{1}{N_k}\sum_{i=1}^{N_k}(y_i - \hat{y}_i)^2 \qquad \text{Eq. 64}$$

In Eq. 64, N_k stands for the amount of the elements in the k^{th} subset. Similar to R^2, the measure Q^2, describing the predictive power of a model, can be defined as:

$$Q^2 = 1 - \frac{\frac{1}{K}\sum_{k=1}^{K}\frac{1}{N_k}\sum_{i=1}^{N_k}(y_i - \hat{y}_i)^2}{\sum_{i=1}^{N}(y_i - \bar{y})^2} \qquad \text{Eq. 65}$$

It is important to mention that in every cross-validation step the parameters for centering and scaling the data, corresponding to test sets, are the same as for the data, corresponding to training sets. Cross-validation can be conducted several times by randomly splitting the data into distinct subsets, estimating the associated errors and averaging them:

$$\overline{SS}_{res}^{\mathrm{CV}} = \frac{1}{N_{CV}}\sum_{i=1}^{N_{\mathrm{CV}}} SS_{res,i}^{\mathrm{CV}} \qquad \text{Eq. 66}$$

$$\bar{Q}^2 = \frac{1}{N_{CV}}\sum_{i=1}^{N_{\mathrm{CV}}} Q_{\mathrm{i}}^2 \qquad \text{Eq. 67}$$

In Eq. 66 and Eq. 67, N_{CV} is the number of repetitions of the cross-validation step. In addition to the cross-validation procedure, it is important to perform a permutation test assessing whether a reliable model can be built if the entries in the **y** vector are randomized. Repeating this process several times results in a distribution of error values calculated by Eq. 66 and Eq. 67. Comparing the values of $\overline{SS}_{res}^{\mathrm{CV}}$ and $\bar{Q}^2$, derived from the selected model, with the associated distribution, enables to estimate the corresponding p-value as:

$$\mathrm{p-value} = \frac{1}{N_{perm}+1}\left(1 + \sum_{i=1}^{N_{perm}} I\left(\bar{Q}^2 > \bar{Q}_{perm,i}^2\right)\right) \qquad \text{Eq. 68}$$

$$\mathrm{p-value} = \frac{1}{N_{perm}+1}\left(1 + \sum_{i=1}^{N_{perm}} I\left(\overline{SS}_{res}^{\mathrm{CV}} < \overline{SS}_{res(perm),i}^{\mathrm{CV}}\right)\right) \qquad \text{Eq. 69}$$

In the Eq. 68 and Eq. 69, N_{perm} is the number of permutation tests performed. The pseudo-count is added in order to avoid a scenario when the p-value equals zero.

5.4.1.2. Feature selection with ML-PLS-DA

The workflow for feature selection was based on the work of van Velzen *et al.* (van Velzen et al., 2008) describing an iterative process of fitting a ML-PLS-DA model and retrieving a subset of features with the highest values of regression coefficients. After defining an initial data matrix $\mathbf{X}_0 = \mathbf{X}$, the following steps were repeated a certain amount of times or until optimal conditions were found:

- Performing the decomposition of $\mathbf{X}_i$ according to Eq. 51 ($i = 0$ at the first iteration round).
- Depending on the question of interest, fitting a PLS model, using either the matrix $\mathbf{X}_{b,i}$ or $\mathbf{X}_{w,i}$, by finding an optimal amount of components based on the corresponding values of $\overline{SS}_{res}^{\mathrm{CV}}$ calculated by cross-validation procedure.
- Retrieving the vector of regression coefficients **b** and calculating their absolute values.
- Selecting a pre-specified amount of top $|b_k|$ and using the corresponding features to construct a new data matrix $\mathbf{X}_{i+1}$.

After finishing the aforementioned procedure, the consistency of the final ML-PLS-DA model was evaluated by projecting the corresponding $\bar{Q}^2$ value onto the null-distribution of $\bar{Q}^2_{perm}$ generated by performing a permutation test several times. Afterwards, the corresponding p-value was calculated using Eq. 68.

For the current study the ML-PLS-DA together with feature selection was conducted targeting the matrix $\mathbf{X}_w$ from Eq. 51, since it contains the information regarding the diet responses. For all the datasets (OTU counts, stool and plasma metabolome) separate models were built, describing the distinction between the baseline and either of the three treatment group (*i.e.* Baseline vs BR, Baseline vs WGB, Baseline vs COMB). Table S12 lists all the parameters used for the aforementioned procedure of feature selection followed by finding the final ML-PLS-DA classification model.

5.4.1.3. Elimination of the effects associated with time

The study, presented in the current thesis, does not include sampling after each wash-out period, thereby limiting the analysis by comparing the diet responses to the baseline characteristics. Such a limitation inevitably leads to the issue of possible effects associated with the differences in the sampling time. In other words, the features, included in the final

ML-PLS-DA models, may be important in describing the distinct time periods rather than diet responses. Therefore, an approach was developed aiming to diminish such possibilities.

In addition to describing the differences between the baseline and the treatment groups via ML-PLS-DA, the same feature selection scheme was applied to distinguish the baseline and either of the three time point groups (*i.e.* Baseline vs Week 5, Baseline vs Week 11, Baseline vs Week 17). Therefore, for each dataset there were six ML-PLS-DA models in total. With respect to every model, describing the diet responses, the selected features were matched, if applicable, to the absolute values of the regression coefficients $\left|b_k^{t_5}\right|$, $\left|b_k^{t_{11}}\right|$, and $\left|b_k^{t_{17}}\right|$, deriving from the final models on the changes associated with the corresponding time points. In case of no match, the regression coefficient was assumed to be zero (*i.e.* no change in time). These three values were averaged to produce a score s_k describing the influence associated with time. Thereby, every feature in a final model on either of the diet responses was associated to its own absolute value of the regression coefficient $\left|b_k^{d_i}\right|$ ($d_i \in \{\mathrm{BR}, \mathrm{WGB}, \mathrm{COMB}\}$) and the aforementioned score s_k (Fig. 28).

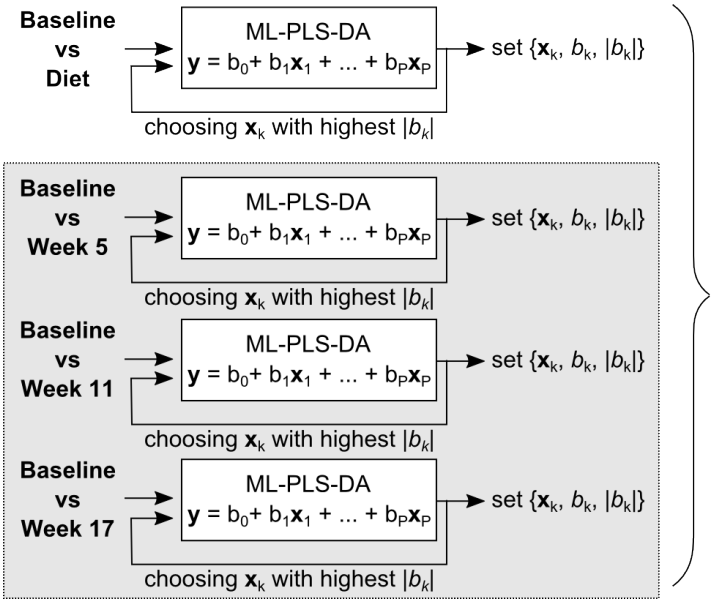

selected feature	|b| diet	|b| week 5	|b| week 11	|b| week 17	S
$\mathbf{x}_{s_1}$	0.051	0.023	0	0.014	0.0123(3)
$\mathbf{x}_{s_2}$	0.072	0.112	0.115	0.099	0.1086(6)
$\mathbf{x}_{s_3}$	0.024	0.111	0	0	0.37
$\mathbf{x}_{s_4}$	0.095	0.016	0.022	0.012	0.0166(6)
$\mathbf{x}_{s_5}$	0.044	0.039	0.011	0.022	0.024
...	...	...	...	...	...
$\mathbf{x}_{s_m}$	0.033	0.011	0.01	0	0.007

Fig. 28. The workflow for generating a score for every feature chosen in the ML-PLS-DA model. The score shows whether a change in a selected feature can be associated with time rather than diet.

The regression coefficients, deriving from the model on a diet response, and the associated scores were plotted against each other (Fig. 29). This representation can give an idea regarding the features, whose alternation is due to time rather than diet. Therefore, it is possible to filter out variables with high score and low $\left|b_k^{d_i}\right|$ values. However, it is necessary to define a rule, according to which certain features will be omitted from further consideration as being too much influenced by time. It was decided to take into account only features,

whose locations on the aforementioned scatter plot were captured by an ellipse centered at a reference point with the pre-defined coordinates calculated in a following way:

$$x_{ref} = \max\left(\{\left|b_k^{d_i}\right|\}\right)$$
$$y_{ref} = \min(\{|s_k|\}) \qquad \text{Eq. 70}$$

In other words, the reference point represents the feature having the strongest association with a diet and the weakest association with time. The shape of the ellipse can be regulated according to the question of interest.

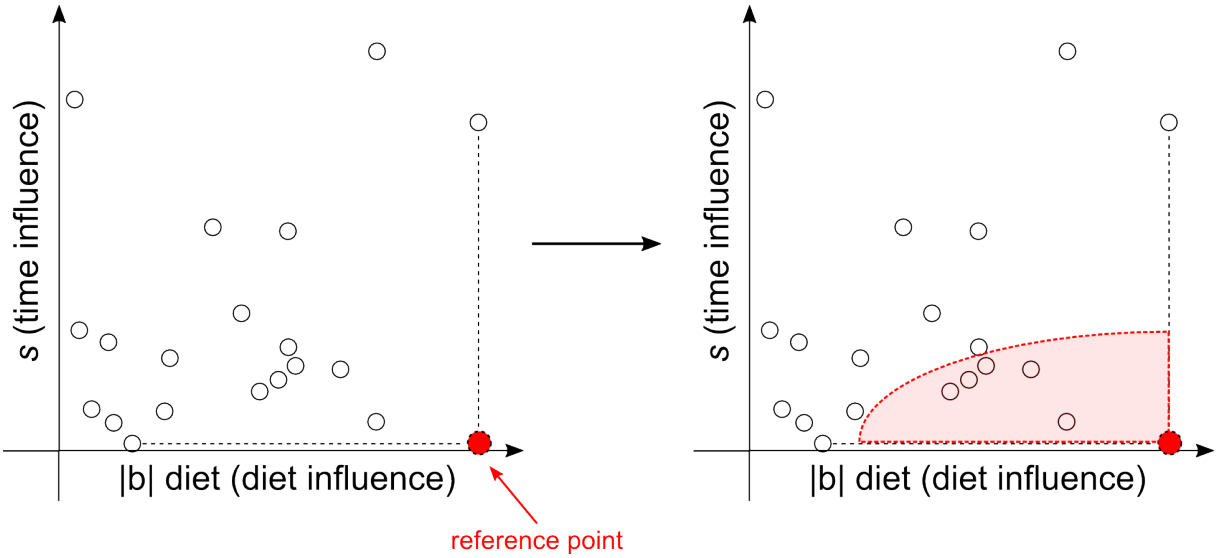

Fig. 29. A simplified example of the distribution of data points on a scatter plot where the coordinates on the horizontal axis represent the absolute values of regression coefficients, deriving from the model on a diet response, and the coordinates on the vertical axis are the associated scores, describing whether the corresponding feature is affected by time. In order to select features, mostly influenced by the diet, it is possible to include only those variables that are within an ellipse of a certain size centered at the coordinate of a pre-defined reference point.

For the study, described in the current thesis, the shape and size of the ellipse were adjusted in such a way in order to select, per each considered diet group, 50 features with respect to the dataset, containing OTU counts, and 500 features with respect to metabolome datasets. It is important to mention that the described procedure is not optimal in cases when a feature is genuinely associated to all three diets because it will have high absolute values for all three regression coefficients $\left|b_k^{t_5}\right|$, $\left|b_k^{t_{11}}\right|$, and $\left|b_k^{t_{17}}\right|$, deriving from the ML-PLS-DA models describing the time effect, and, according to the aforementioned criteria, will be excluded from further consideration. Therefore, mainly features, uniquely associated with a diet, will be selected, which is a necessary sacrifice towards obtaining informative results. Such limitations could be avoided in case if the sampling was performed after each wash-out period.

5.4.1.4. Overrepresentation analysis

The task of an ORA concerns finding out whether the presence of a certain quality in a subset, selected from a larger set, represents an informative piece of data or not. To perform an ORA, the simplest way is to use the workflow based on hypergeometric distribution. Given a set of N elements that can be divided into G groups g_1, g_2, …, g_G of sizes K_1, K_2, …, K_G, respectively, the probability that a random sample of size n, drawn without repetitions, will contain k_i or more elements, belonging to the group g_i, can be calculated in a following way:

$$P(x \geq k_i \mid n, K_i, N) = \sum_{i=x}^{\min(n,K_i)} \frac{\binom{K_i}{i}\binom{N-K_i}{n-i}}{\binom{N}{n}} \qquad \text{Eq. 71}$$

$$\text{where} \quad \binom{a}{b} = \frac{a!}{b!\,(a-b)!}$$

Therefore, knowing the way how the data can be divided into groups, it is possible to make the corresponding calculations and to estimate whether some subset contains much more elements of a certain kind than expected (Fig. 30). In case of a positive result, the corresponding quality can be considered significant for further consideration and interpretation.

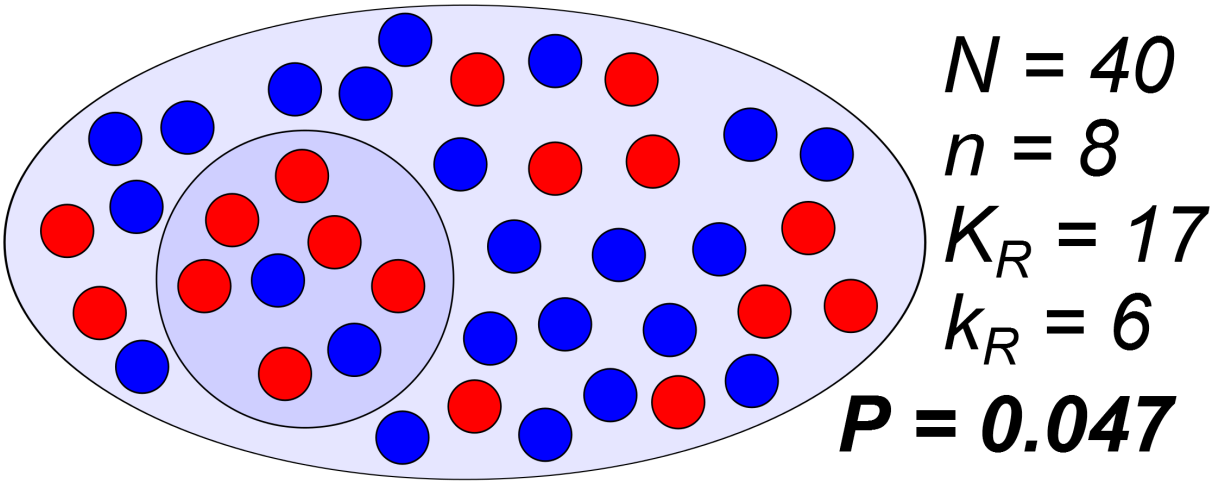

Fig. 30. An example on applying the hypergeometric distribution to find out whether the red circles are overrepresented in a subset within a larger set containing two types of colored shapes. By examining the obtained p-value, it is possible to conclude that the probability of this happening at random is very small. Therefore, such a result can represent an essential hint for further consideration.

The aforementioned scheme was applied for stool and plasma metabolome datasets. Since the features were assigned to the entries from the HMDB database, it was possible to evaluate whether certain compound classes were overrepresented in the subsets, containing features selected by ML-PLS-DA (followed by filtering out features associated with time effect). In this case, N stood for the total amount of features in a data matrix, n was the amount of

features selected by ML-PLS-DA, K_i and k_i stood for the amount of features from the entire set and the subset, respectively, assigned to a certain compound class. Since many features were not given any annotations from the HMDB database, they were taken into consideration during the calculations by classifying them as «unknowns». In addition to the aforementioned procedure, the ORA was performed by discriminating the features according to a diet response, reflected in the corresponding signs of the regression coefficients deriving from the ML-PLS-DA models. In this case, it was possible to investigate whether a certain compound class could be associated with the positive or negative change after the intervention.

The same scheme, as described for ORA with respect to compound classes, was applied to biochemical transformations listed in Table S8. Having a MDiN built, it is possible to locate a subset from the entire set of edges by considering only those connections where one of the adjacent nodes corresponds to a feature selected by ML-PLS-DA and associated with a higher, relative to its neighbor, mass (Fig. 31). Therefore, this subset can be seen as the assemble of biochemical transformations responsible for «generating» the response associated with a diet treatment. As a consequence, performing ORA has the potential to reveal major reactions involved in the corresponding changes. In this case, following the notations in Eq. 71, N stood for the total amount of edges in the MDiN, n was the amount of edges constituting the subset of connections as in Fig. 31B. The values K_i and k_i can be put into correspondence to the amount of edges from the entire set and the subset, respectively, assigned to a certain biochemical transformation. However, slightly modified values were used. First, the Spearman correlation coefficients were calculated for every pair in the subset of «generating» edges with respect to the matrix $\mathbf{X}_w$ from Eq. 51. Afterwards, considering only the edges of a specific transformation, the coefficient modes were located on density plots estimated using Gaussian kernels. By considering only positive mode values, the values K_i and k_i , in addition to the aforementioned notation, were modified by taking the edges with Spearman correlation coefficients larger than the calculated mode. Such a procedure was necessary for eliminating possible noise that may lead to non-informative results. In addition, ORA was performed by discriminating the edges with respect to the sign of the value of regression coefficients associated with the node belonging to the subset of features selected by ML-PLS-DA. In this case, it was possible to investigate whether a specific reaction plays a key role in the overall positive or negative metabolite responses.

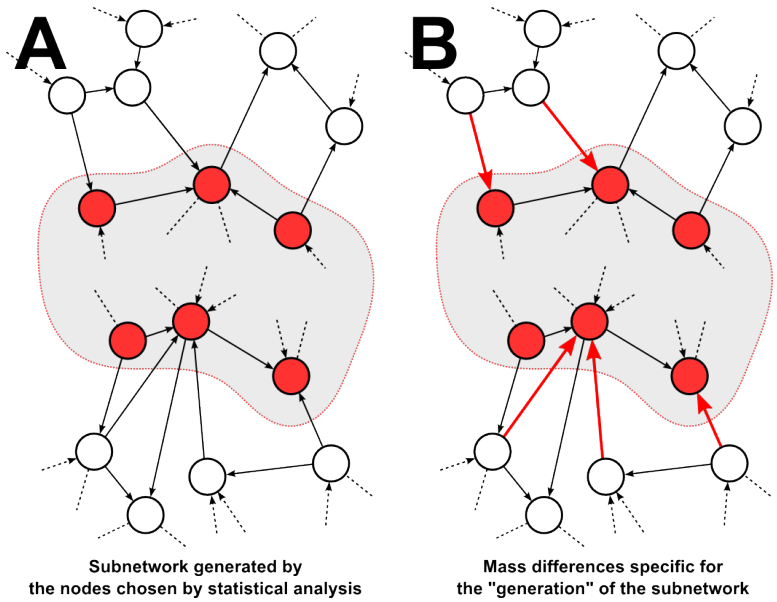

Fig. 31. Creating a representation suitable for ORA. The edges are directed toward the feature corresponding to a higher mass A) The subset built out of nodes selected by ML-PLS-DA. B) The subset of edges built by considering connections directed toward nodes selected by ML-PLS-DA.

5.4.1.5. Box-Cox transformation of clinical parameters

The clinical parameters, measured in the presented study, can be characterized by different distributions and ranges/scales of the corresponding values. Therefore, each case requires individual treatment by means of data transformation in order to achieve approximate normality. For overcoming this issue, the Box-Cox transformation can be used providing an opportunity to avoid extensive search to determine the best option (Sakia, 1992). The idea behind this technique is that many transformations, commonly used in practice, can be considered as different representations of power transformations (*e.g.* square root $\sqrt{x}$, inverse $1/x$). Also logarithm transformation (*i.e.* $\log(x)$) can be included into this category. This idea of potential continuum of similar mathematical functions, providing a range of opportunities for data normalization, can be eventually reflected using the following form:

$$x_{mod} = \begin{cases} \dfrac{x^{\lambda} - 1}{\lambda} & \text{if } \lambda \neq 0 \\ \log_e(x) & \text{if } \lambda = 0 \end{cases} \qquad \text{Eq. 72}$$

In the Eq. 72, λ is a parameter that can take on infinite number of values. Therefore, the problem lies in finding λ that results in the maximally effective transformation in terms of normality. The Box-Cox transformation was applied to all 13 clinical records.

5.4.1.6. Data integration

All the obtained information on OTU counts, stool and plasma metabolome as well as clinical data was integrated by means of calculating the Spearman correlation coefficients between the corresponding entries followed by examination of the resulting interaction patterns. To investigate the dynamics of the interplay between different constituents of the entire data pool with respect to the considered diet, distinct correlation maps were constructed using the matrices corresponding to the baseline and treatment groups as well as the matrix containing the information on intra-individual variation component ($\mathbf{X}_w$ in Eq. 51).

5.4.2. Analysis of metabolome datasets

Feature selection by ML-PLS-DA followed by partial elimination of variables potentially associated with time, resulted, for each of the datasets (OTU counts, stool and plasma metabolome), in three feature subsets (Table S15, Table S16, Table S17) corresponding to diet treatments (BR, WGB, or COMB). The final ML-PLS-DA models were constructed using 50 selected features per diet in case of OTU counts dataset and 500 selected features per diet in case of stool and plasma metabolome datasets. For the OTU counts dataset the resulting Q^2 values were equal 0.84, 0.93 and 0.77 for the models built for description of BR, WGB, and COMB group, respectively. For the stool and plasma metabolome datasets the respective values of Q^2 were equal to 0.97, 0.99, 0.97 and 0.97, 0.97, 0.97 (the group order is the same as described above). All the models were characterized by the p-values $< 5 \cdot 10^{-4}$ found by conducting the permutation tests. As expected, due to the filtering procedure after ML-PLS-DA, the intersection between the feature subsets was relatively small with only few representatives shared by all the three diet groups (Fig. 32). Thereby, the selected variables can be considered as relatively unique signatures of the intervention responses.

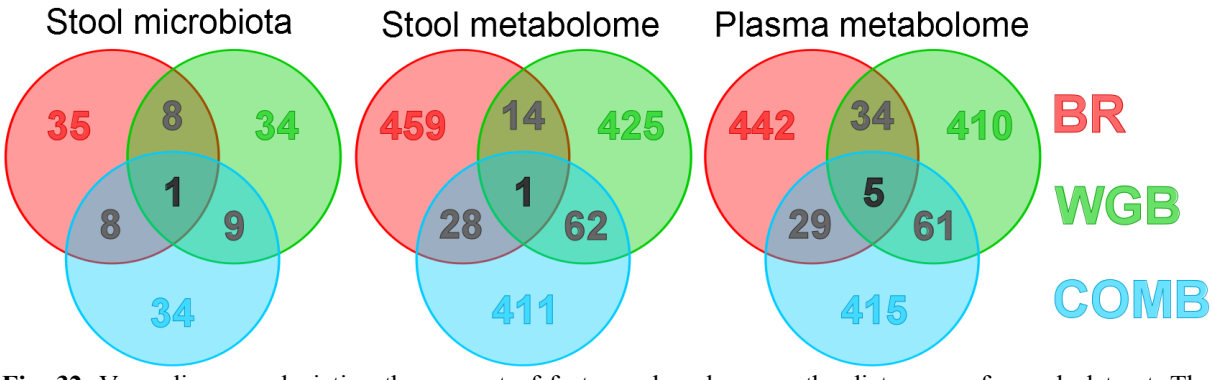

Fig. 32. Venn diagrams depicting the amount of features shared among the diet groups for each dataset. The features were chosen by ML-PLS-DA followed by eliminations of variables potentially associated with time.

By searching against the HMDB database, 3216 and 2801 features from stool and plasma metabolome datasets, respectively, were assigned to putative metabolites. These numbers corresponded to ~22 % and 18 %, respectively, of the total amount of the features present in the final data matrices. The subsequent ORA revealed compound classes significantly contributing to the subsets of selected features and potentially associated with the diet responses (Fig. 33). As can be seen, BR intervention can be characterized by changes in levels of fatty alcohols, fatty amides, and trichothecenes in stool content, whereas no specific profiles were observed for blood plasma. The compound classes contributing to the response to WGB diet included amino-, carboxylic-, and linoleic acid derivatives, glycerolipids, and steroid derivatives in case of stool metabolome. The plasma metabolome for the same diet was characterized by a remarkable decrease in the levels of fatty acid esters, mostly represented by different acylcarnitines. Considering the changes associated with the COMB diet, it is worth mentioning the plasma metabolome with many classes showing the decrease in the abundances of the corresponding metabolites. Despite of seemingly promising outcome, it can be misleading due to the aforementioned ambiguity in the metabolite assignments (Fig. 20). Therefore, any result from the performed ORA should be examined carefully in order to have a reliable conclusion.

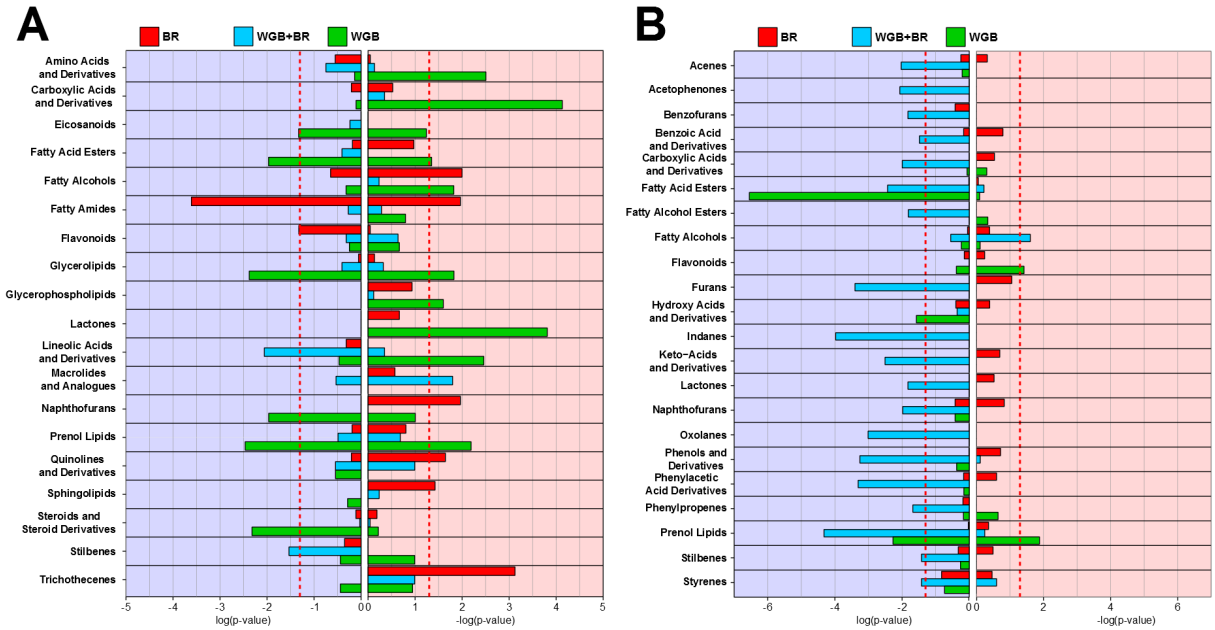

Fig. 33. The ORA depicting, by the calculated p-values, whether the response to a diet can be described in terms of overall changes in features assigned to a certain compound class. These changes are either negative or positive depending on the behavior of the corresponding features after a diet intervention. The results are presented for the A) stool metabolome dataset and B) plasma metabolome dataset.

The features selected by ML-PLS-DA were used to retrieve subnetworks from the original MDiNs (Fig. 19) by considering only the corresponding nodes. Thereby, reduced MDiNs were built for every diet group with respect to the stool and plasma metabolome datasets (Fig.

S1). Interestingly, although the relative abundances of elemental composition types are very similar for all subnetworks, it was possible to observe graph-specific patterns by projecting the information of the metabolite responses associated with the diets. Using the edges within the constructed networks, the ORA was performed in order to reveal transformations potentially associated with the treatments (Fig. 34, Table S13, Table S14). Examining the profiles obtained for stool metabolome, it is possible to observe very distinct signatures for the WGB group. The corresponding transformations, belonging to the high mass region, were mainly associated to the reactions of condensation with long chain fatty acids (LCFAs), such as hexadecanoic, linoleic, oleic, stearic acids *etc*. Moreover, it can be assumed that these transformations lead to both positive and negative regulation of the associated metabolic products. Interestingly, the COMB group shows similar but much weaker profiles with respect to the behavior of the target metabolites. Regarding the plasma metabolome, BR group can be characterized by an essential amount of transformations leading to the increase in levels of the associated features as opposed to WGB and COMB groups. Altogether, these results suggest that the diets enriched in WGB and COMB are more similar in their response, whereas BR treatment has much more unique profiles.

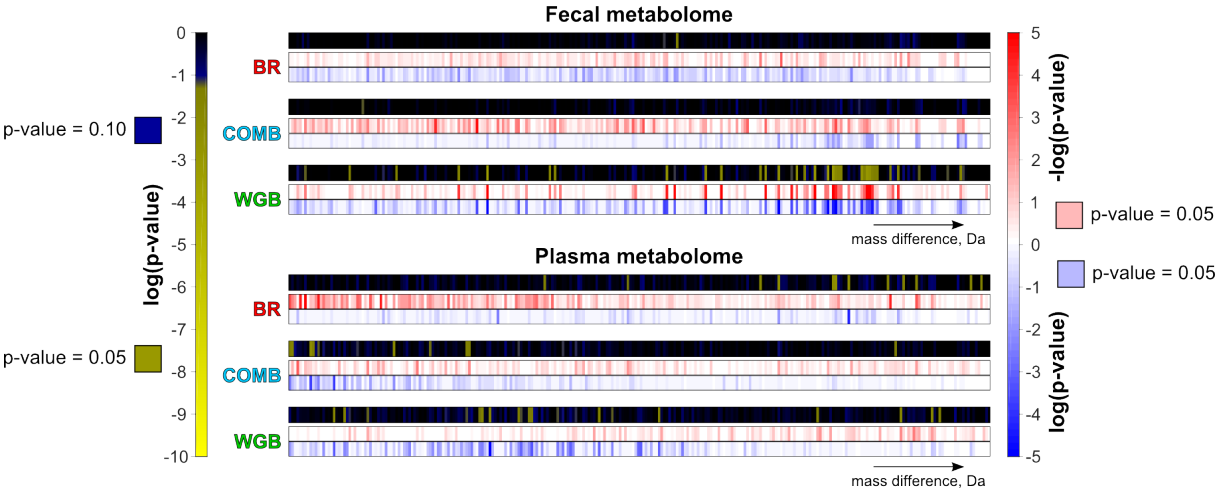

Fig. 34. The profiles of p-values obtained by performing ORA using edges from MDiNs constructed for stool and plasma metabolome datasets. Each diet group corresponds to three stripes corresponding to three different implementations of ORA. The upper stripe corresponds to ORA where all the edges were taken into account. The middle and the bottom stripe correspond to ORA using edges directed towards the nodes associated with positive or negative regression coefficients, respectively. Each bar on a stripe corresponds to a transformation.

Taking into account the outcomes from ORA, ML-PLS-DA as well as the structure of the constructed MDiNs, several putative metabolites were chosen as potential biomarkers of the diet treatments. Inspecting the MDiNs, built from the selected features (Fig. 19), the most prominent patterns were observed for BR and WGB groups (Fig. 35-37). Within the networks, it was possible to define the approximate locations of compound classes (represented by respective metabolites), accentualized by ORA using the entries from the

HMDB database (Fig. 33). This procedure simply involved observing whether certain modules in the MDiNs have prevalent amount of assigned compounds of similar structure. In addition to have a descriptive purpose, knowing the location of compound classes can provide hints on the properties of features that were not assigned to any real molecule (only to molecular formula), thereby remaining partially unknown.

Analyzing the MDiN with features describing the response of stool metabolome to BR diet, particular attention was paid to the classes of trichothecenes, steroid derivatives, and fatty amides. As previously described, trichothecenes were shown to be significantly associated with the BR treatment (Fig. 33A). This class of compounds comprises different mycotoxins whose presence in rice has been extensively studied (Ferre, 2016; Serrano et al., 2012). Deoxynivalenol (DON) is one of the widely known representatives. This contaminant and its derivatives can be synthesized by the fungi belonging to *Fusarium* genera, whose occurrence on the grains can lead to their scabbing (Tanaka et al., 2004). Inspecting the MDiN, four connected metabolites of this class were taken for further investigation, namely isotrichodermol (ITDmol), isotrichodermin (ITDmin), deacetylcalonectrin (deACAL), and acetoxyscirpenol (AOS). They can be characterized by sharing the same substructure of nivalenol. ITDmol, ITDmin, and deACAL, whose levels show an increase after the diet intervention, represent intermediate products in the *Fusarium* trichothecene biosynthesis (Kimura et al., 2014). It was reasonable to inspect mass spectra if the related compounds can be potentially present in the stool samples. By doing so, several additional compounds of the same class were taken into consideration, although the corresponding features were not selected in ML-PLS-DA procedure. DON, nivalenol, acetyldeoxynivalenol (ADON), and Fusarenone X (FusX) showed promising correlation patterns to the four aforementioned compounds (Fig. 36), thereby making them appealing candidates for further investigation because of their possible contribution to the effects associated with the diet. Although steroid derivatives were not shown to be significant with respect to ORA (Fig. 33A), it was possible to reveal two representatives within the MDiN, whose presence can be directly associated to BR consumption, namely campesteryl ferulate (CSF) and sitosterol ferulate (SSF). These molecules represent the derivatives of cycloartanyl ferulate (CAF) (Miller and Engel, 2006). The corresponding peak was detected in the mass spectra. However, it was not selected by ML-PLS-DA, although the feature correlated strongly with CSF and SSF. Such an output may be a consequence of the aforementioned filtering procedure, where time influence was examined. CAF was initially shown to be essential for all three diet group but, due to this

reason, was eliminated as time dependent. This is an example, where a partial sacrifice of the selected features leads to an undesired outcome. CSF, SSF, and CAF are constituents of γ-oryzanol, a mixture of steryl ferulates (ferulic acid esters of phytosterols) exhibiting antioxidant activity. Along with other bioactive phytochemicals present in BR, such as tocopherols and tocotrienols, γ-oryzanol has been reported to be associated with beneficial health effects (Moongngarm et al., 2012). Interestingly, examining the correlation patterns between sterol ferulates and trichothecenes, a potential relation between these two classes can be observed. Such a result may reflect their direct ingestion from the diet. As was shown by ORA (Fig. 33A), fatty amides exhibit both increasing as well as decreasing behavior in response to BR consumption. The former case can be described by palmitoyl-, oleoyl-, and steraoyl ethanolamide (PEA, OEA, and SEA, respectively), whereas the latter case includes docosahexaenoyl-, docosapentaenoyl-, and tetraenoyl ethanolamide (DHEA, DPEA, and DTEA, respectively). Interestingly, the major difference between these two groups is the degree of saturation of the corresponding carbon chains (PEA and SEA have only single bonds in the aliphatic regions, OEA has one double bond). Moreover, they have distinct locations within the MDiN, although, in the overall scale, the respective nodes are in a close proximity to each other (Fig. 35A). The aforementioned compounds belong to the group of N-acylethanolamines (NEAs), bioactive lipids that can be considered as endocannabinoid analogues, normally synthesized in a two-step enzymatic process (Cani et al., 2016; Fezza et al., 2014). It involves the formation of acylphosphatodylethanolamine (NAPE) by transferring a fatty acyl chain from membrane phospholipids to a phosphatydilethanolamine followed by a subsequent hydrolysis of the resulting product (Fezza et al., 2014). The biosynthesis of endocannabionoids and their analogues takes place in various organs including brain, liver, adipose tissue, and GIT (Cani et al., 2016; Chen et al., 2014). Interestingly, the commensal bacteria in the gut can actively participate in this process. One of the key functions of the endocannabinoid system include regulation of gut and adipose tissue physiology, providing adequate inflammatory responses, preserving intestinal integrity, and energy metabolism. The role of NEAs involves interactions with cannabinoid receptors CB_1 and CB_2, peroxisome proliferator-activated receptors PRAP-α and PRAP-γ, capsaicin receptor TRPV1, G-protein coupled receptors GRP55 and GRP119 *etc*. It has been shown that the involvement of endocannabinoids in the mediation of CB_1 can influence the production of ceramides by reducing their diet-induced synthesis when the receptor is blocked (Cinar et al., 2014; Velasco et al., 2005). Intriguingly, one of the ceramide members was observed in the MDiN within the cluster containing PEA, OEA, and SEA. It can be assumed that the elevated levels of this

metabolite due to BR consumption represent the response to the increase in the aforementioned NEAs.

Promising patterns were observed for the responses of stool and plasma metabolome to WGB diet (Fig. 35B, Fig. 35C). Special attention was paid to amino acid derivatives, glycerolipids, linoleic acid derivatives, and steroid derivatives in case of stool metabolome (Fig. 35B) and fatty acid esters in case of plasma metabolome (Fig. 35C). Compared to BR treatment, the intervention involving WGB was characterized by higher protein percentage in its content (Martinez et al., 2013). Therefore, it can be reasonable to observe the positive changes in corresponding compounds in fecal content. Within the class of amino acid derivatives, three metabolites were of particular interest, namely glutamate (Glu), acetylglutamate (AGlu), and acetylglutamate semialdehyde (AGlu-sA). Among them, Glu has the most direct connection to food intake, since it is often present in the diet in the free form or as a sodium salt (Blachier et al., 2009). It can also originate from alimentary as well as endogenous proteins or be synthesized by gut microbiota (Blachier et al., 2009; Portune et al., 2016). Glu, present in gut, can undergo its consumption by epithelial or bacterial cells with the subsequent metabolic fate depending on the part of GIT considered, corresponding microbiota composition, or the host health status (Portune et al., 2016). One of the metabolic paths, requiring Glu, is the eight-step process of arginine biosynthesis by commensal bacteria, where AGlu and AGlu-sA are intermediate products. AGlu can also be produced by intestinal mucosa and enterocytes due to the presence of required enzymes. The metabolites representing linoleic acid derivatives included oxo-, hydroxyl-, and hyroxyperoxyoctadecadienoic acid (OxoODE, HODE, and HPODE, respectively). The peak corresponding to linoleic acid (LA) was detected in the mass spectra but not selected by ML-PLS-DA. Interestingly, this feature exhibited high correlation values to the three aforementioned compounds (Fig. 37). LA, belonging to the group of ω-6 PUFAs, is an essential metabolite for a human organism and must be delivered from food because it cannot be synthesized endogenously (Marion-Letellier et al., 2016). Dietary LA can be further metabolized by gut microorganisms to produce conjugated LAs (Sun and Chang, 2014). Formation of HPODE from LA takes place by the action of lipoxygenase, an enzyme catalyzing region- and stereo-specific deoxygenation of PUFAs (Mosblech et al., 2009). Emergence of OxoODE and HODE takes place due to further modifications of HPODE. The class of glycerolipids was mainly represented by diacylglycerols (DAGs). As in case of fatty amides in BR group, it was possible to observe the positive as well as negative changes of the respective compounds in response to WGB consumption, dividing the putative metabolites

into two subclusters. Intriguingly, the AGs, having in their structure fatty acids of higher degree of unsaturation, exhibited decreasing behavior after the diet, whereas an opposite behavior was characteristic to other AGs. The production and composition of DAGs highly depends on the fiber content in a diet (Pajari et al., 2000). Commensal bacteria in the gut can participate in this process producing DAGs with 1,2-*sn* configuration (Vulevic et al., 2004). These metabolites might be further involved in the stimulation of protein kinase C playing a crucial role in the growth control and signal transduction. Among the class of steroid derivatives two metabolites, namely carbaldehyde and carboxylate of hydroxymethylcholetene (HMCCyde and HMCCate, respectively), were chosen as prominent representatives. They exhibited decreasing behavior in response to the WGB consumption. Their change can be explained by the promoted synthesis of SCFAs. The diet enriched in WGB has been shown to facilitate the production of these small molecules that, in turn, may be involved in the inhibition of cholesterol biosynthesis pathway (Alvaro et al., 2008; De Angelis et al., 2015). The most prominent players in this process are propionic and butyric acids (Alvaro et al., 2008). Methylsterol monooxygenase represents one of the enzymes involved in the aforementioned pathway catalazing the reaction of the transformation of HMCCyde to HMCCate. With respect to plasma metabolome, fatty acid esters, shown by ORA to substantially decrease after WGB consumption, were represented by different acylcarnitines (ACs) and derivatives with the aliphatic chains ranging from 6 to 18 carbon atoms. These metabolites form a dense cluster in the corresponding MDiN (Fig. 35C). ACs play a role of carriers in the process of fatty acid β-oxidation in mitochondria, where they are involved in the transportation of these molecules through the inner membrane of the organelle (Rinaldo et al., 2002). The deficiency of the involved enzymes, including carnitine palmitoyltransferase I and II, lead to various health disorders characterized in changes of AC profiles in blood. Obesity, type 2 diabetes, renal disease, and human immunodeficiency virus can all exhibit elevated levels of these metabolites (Adams et al., 2009; Mihalik et al., 2010; Reuter et al., 2005). Interestingly, the results for the latter disorders are not definitive, since there are reports showing both high and low levels of ACs, which suggests that both scenarios may represent a sign of illness (Cassol et al., 2013; Waagsbo et al., 2016). Moreover, apart from describing the disorders, elevated levels of ACs can be observed after moderately intense exercises (Lehmann et al., 2010).

Summing up, it was possible to observe features, changed in response to whole grain diet. Some of them were assigned to putative metabolites with their subsequent clustering into

groups. The analysis of these groups, using the support of MDiNs, revealed promising patterns with respect to BR and WGB diets, whereas much less of substantial description was obtained for COMB diet. However, it is important to remember that more evidence is required for unambiguous identification of the aforementioned metabolites. Nevertheless, the descriptive level, provided by DI FT-ICR-MS analysis, supplies useful data necessary to define further directions.

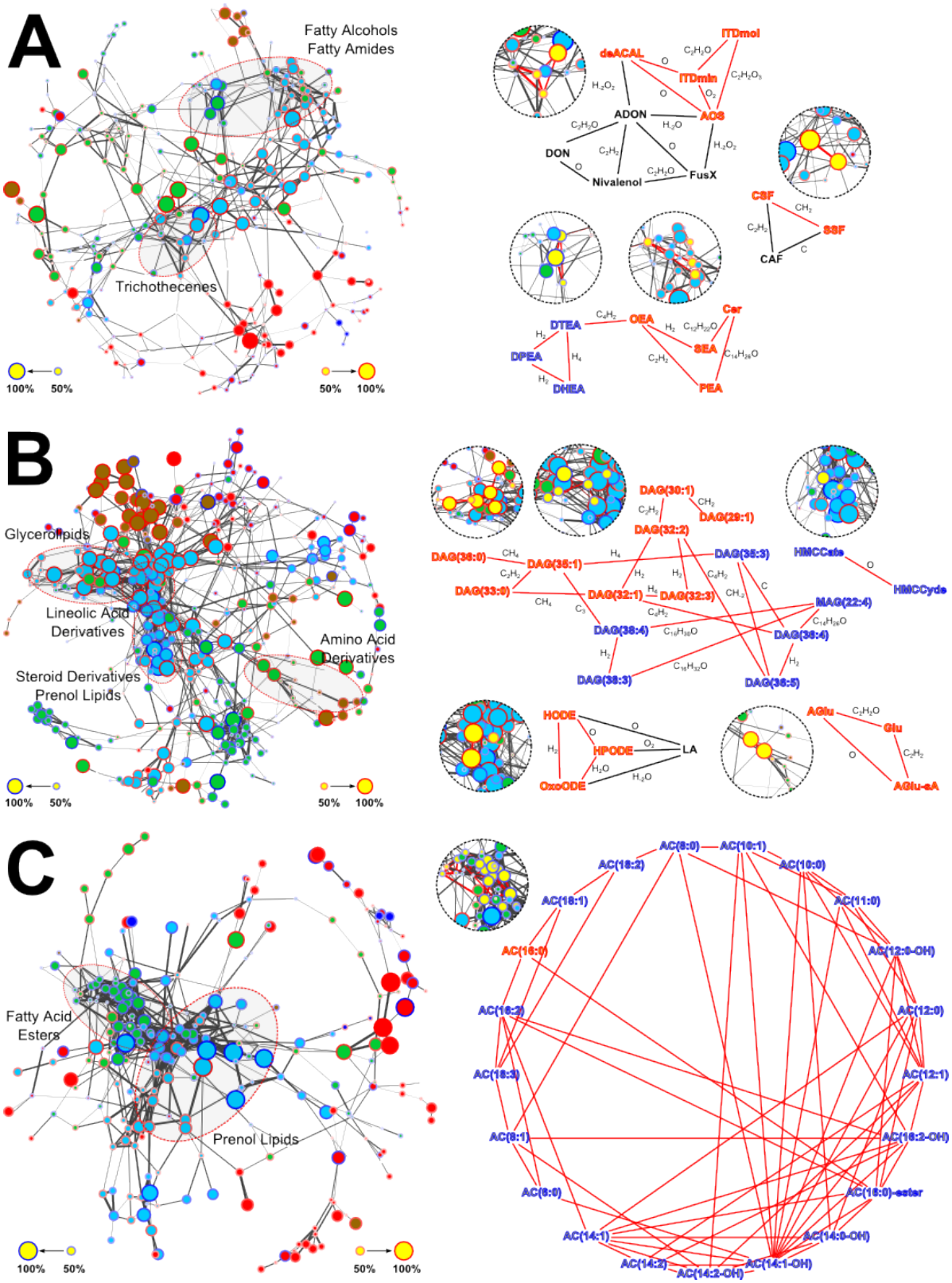

Fig. 35. Selection of putative metabolites potentially involved in the diet responses. The subnetworks and the corresponding metabolites are associated with A) stool metabolome and the BR treatment, B) stool metabolome and WGB treatment, C) plasma metabolome and the WGB treatment. The sizes of the nodes are proportional to the mean differences of the intensity values between a diet group and the baseline. The color of the node border corresponds to the sign of the differences. The color of the node interior corresponds to the type of elemental composition: lightblue – CHO, green – CHNO, red – CHOS or CHNOS, brown – CHOP, CHNOP, CHOPS, or CHNOPS, darkblue – others. The edge width corresponds to the absolute value of the Spearman correlation coefficient between features represented by the adjacent nodes. To the right of the subnetworks, smaller graphs are depicted, showing the interconnections between the selected putative metabolites.

5.4.3. Revealing connections between metabolome and taxonomic datasets

To study possible relationships between the described metabolites as well as their link to clinical markers and selected OTUs, the interactions maps for each of the aforementioned scenarios (response to BR diet with respect to stool metabolome, response to WGB with respect to stool and plasma metabolome) were built (Fig. 36, Fig. 37, Fig. 38). The metabolites were grouped according to the similarity of their chemical properties (*e.g.* the trichothecenes were put in one cluster). The construction of the maps was done to describe the interaction patterns at the baseline as well as follow-up. Such representation provides the information on the differences between static components in the study. Moreover, the interaction maps were built for describing the behavior of the patterns on a dynamic basis, *i.e.* the subject-wise differences between the post-treatment and baseline group. The combination of the constructed maps should provide hints on the evolution of the interplay between different constituents of the biological system.

Describing the interaction patterns for the BR group (Fig. 36), it can be seen that trichothecenes exhibit strong correlation behavior within the corresponding group that becomes weaker after the treatment. The opposite scenario can be observed for sterol ferulates. Together with Cer, these two groups show promising evolutionary behavior by changing the partner metabolites as depicted by the alternations of the magnitude of the correlation coefficients. It can be also seen with respect to TChol level, where positive correlations are observed within the baseline and post-treatment group. Fatty amides were divided into two subgroups according to the presence/absence of unsaturated acyl chain. Intriguingly, at the baseline the intra-group correlations are positive, whereas the inter-group values are negative. This behavior disappears after the treatment. It is probable that the explanation can be found in the emerged link between «unsaturated» fatty amides and HDL level that can be seen on the interaction map describing the dynamical change of the variables. Investigating the connection of the metabolites to OTUs, trichothecenes and sterol ferulates exhibit the most prominent patterns. Since these compounds come directly from the diet, such a behavior may represent a direct link between microbes in the gut and ingested molecules.

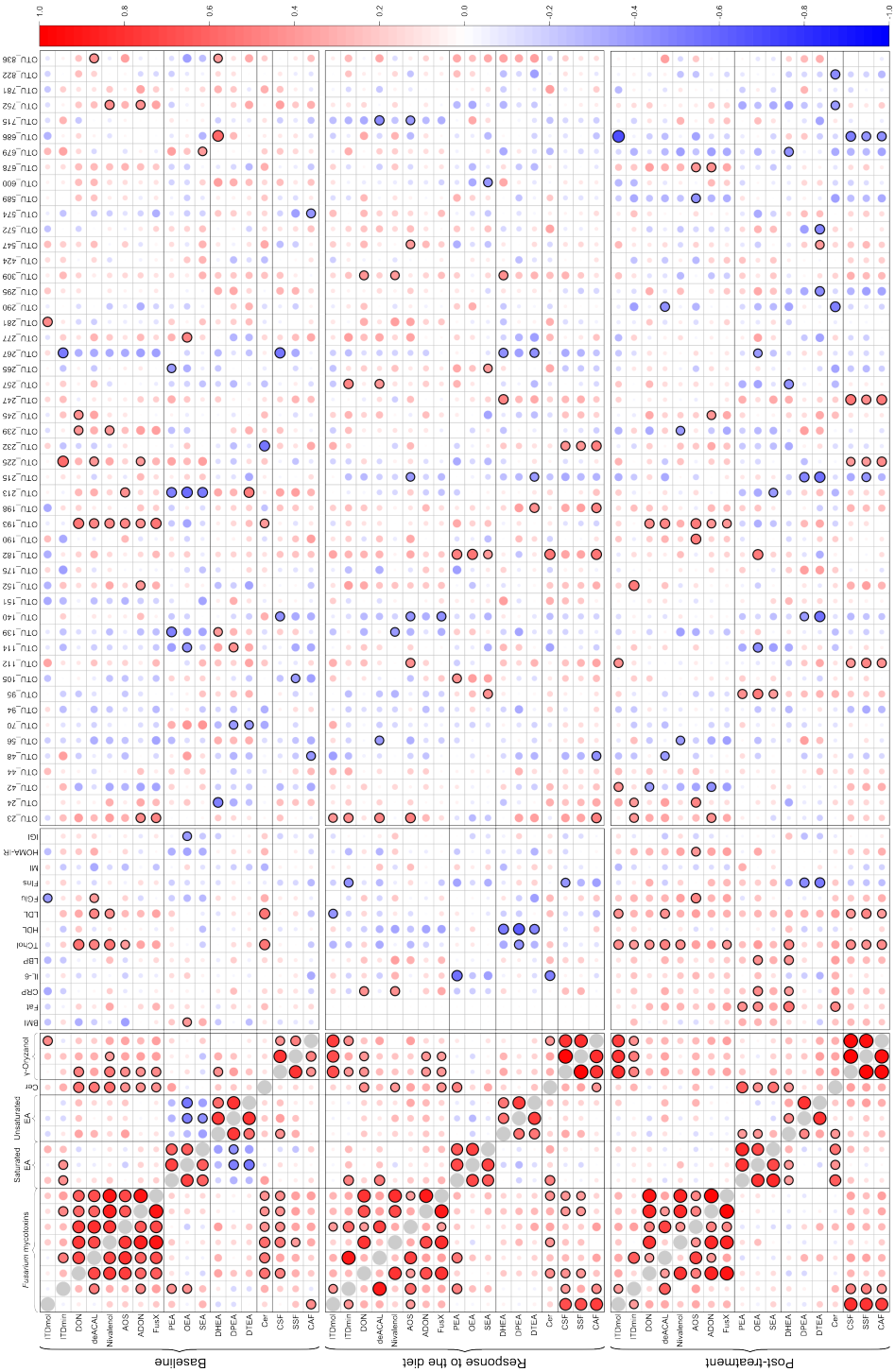

Fig. 36. Interaction maps built for stool metabolome data with respect to BR group and emphasizing the correlation of selected metabolites between themselves and to clinical markers as well as OTU counts. Each entry represents the value of Spearman correlation coefficient calculated between the corresponding pairs of variables. The circle sizes and colors are proportional to its absolute and signed value. The correlation coefficients are calculated by dividing the dataset into three different subsets (from left to right): 1) the subset corresponding only to the Baseline group; 2) the subset corresponding to the difference between the BR and Baseline group represented by the pairwise differences in values within each subject; 3) the subset corresponding to the BR group. Such a representation enables to investigate the evolution of dependencies between different variables during the course of the diet.

Concerning the stool metabolome for the WGB group, it is also possible to see the evolutionary trend in respect to the interactions among the described metabolites. The

negative correlations that are prevalent at the baseline time point between DAGs, LA derivatives, and amino acid derivatives become weaker after the diet. Strong connection at the baseline can be seen between LA derivatives and DAGs exhibiting positive changes after the diet. Interestingly, although this connection vanishes after the treatment, a new pattern can be observed with repsect to their mutual correlation to BMI. The interaction map, describing the dynamical change of the metabolites, can be characterized by a promising pattern of positive correlations between amino acid derivatives, steroid derivatives, and DAGs linked to negative changes after the diet. These DAGs as well LA derivatives can be considered as compounds acting as intermediates in shaping the gut microbiota composition as can be seen on the corresponding interaction patterns. Concerning the plasma metabolome, very strong positive correlations can be seen between almost all described ACs. This behavior becomes even more emphasized after the WGB treatment. At the baseline, positive correlation can be observed between ACs and HDL as well as MI, whereas LDL and HOMA-IR can be characterized by negative correlation values with these metabolites. Interestingly, this pattern vanishes after the treatment. With respect to microbial data, each interaction map can be characterized by distinct OTUs exhibiting a strong link to ACs. This result may imply the dynamical changes of the activities carried out by gut microbiota during the course of the treatment.

It was possible to see that dividing the datasets into groups, holding the information on static and dynamical components, can be beneficial for examining the evolution of interaction patterns between metabolites, clinical markers, and commensal bacterial. Nevertheless, further investigation is required to obtain deeper knowledge on the mechanisms underlying the obtained results describing the alternations within the biological system. The health effects, associated with a diet, can be examined according to the changes in interplay between metabolites and clinical markers. Therefore, measuring such parameters can facilitate the interpretation. As can be seen by means of interaction maps, the whole grain diet affects the human organism driving the machinery of cellular mechanisms in a certain way. Therefore, unraveling this machinery is crucial for understanding the complexity behind the host-metabolome-microbiota axis.

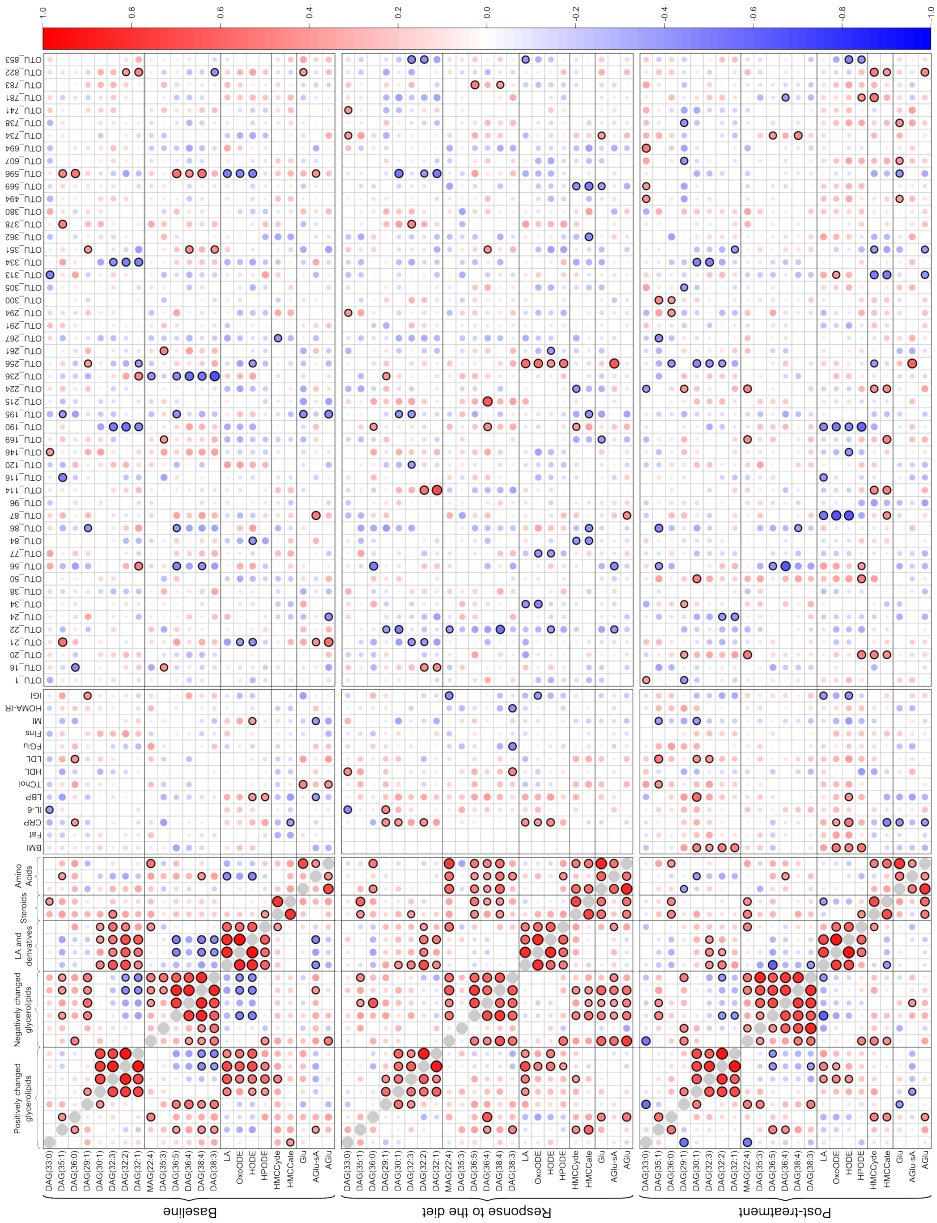

Fig. 37. Interaction maps built for stool metabolome data with respect to WGB group and emphasizing the correlation of selected metabolites between themselves and to clinical markers as well as OTU counts. Each entry represents the value of Spearman correlation coefficient calculated between the corresponding pairs of variables. The circle sizes and colors are proportional to its absolute and signed value. The correlation coefficients are calculated by dividing the dataset into three different subsets (from left to right): 1) the subset corresponding only to the Baseline group; 2) the subset corresponding to the difference between the WGB and Baseline group represented by the pairwise differences in values within each subject; 3) the subset corresponding to the WGB group. Such a representation enables to investigate the evolution of dependencies between different variables during the course of the diet.

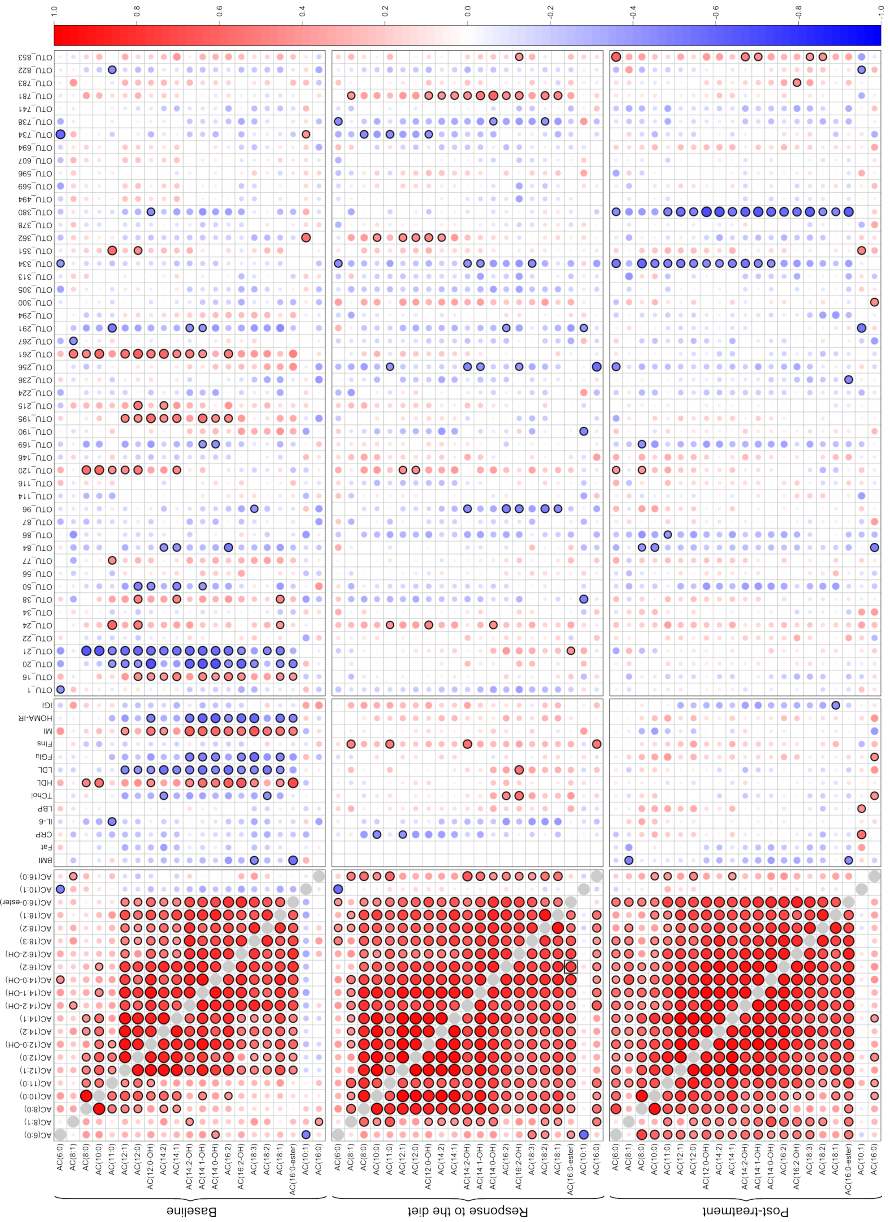

Fig. 38. Interaction maps built for plasma metabolome data with respect to WGB group and emphasizing the correlation of selected metabolites between themselves and to clinical markers as well as OTU counts. Each entry represents the value of Spearman correlation coefficient calculated between the corresponding pairs of variables. The circle sizes and colors are proportional to its absolute and signed value. The correlation coefficients are calculated by dividing the dataset into three different subsets (from left to right): 1) the subset corresponding only to the Baseline group; 2) the subset corresponding to the difference between the WGB and Baseline group represented by the pairwise differences in values within each subject; 3) the subset corresponding to the WGB group. Such a representation enables to investigate the evolution of dependencies between different variables during the course of the diet.

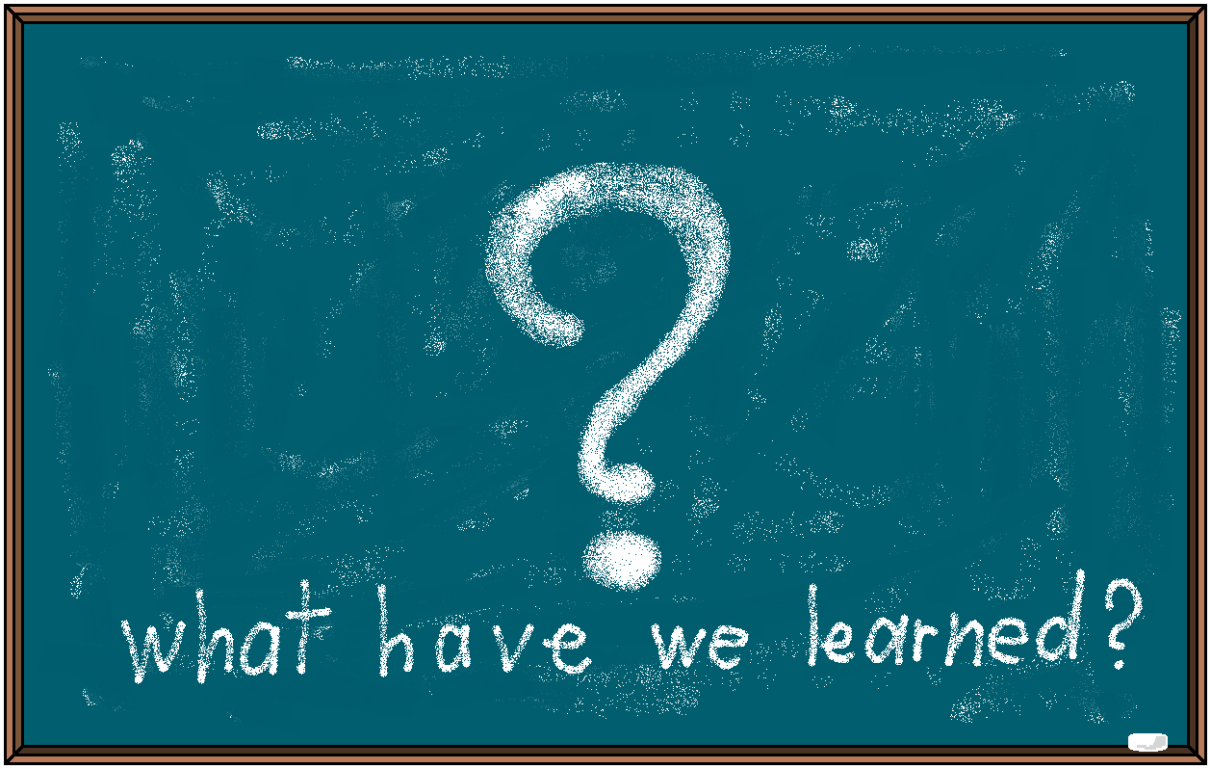

Conclusion

6. Summary and outlook

In the current work, the analysis of the responses of human stool and plasma metabolome to whole grain diet was performed. Non-targeted profiling was conducted using DI FT-ICR-MS that can be characterized by high resolution and accuracy, necessary for obtaining thousands of mass spectrometric signals with a potential for unambiguous assignment of elemental compositions. Distinct signatures corresponding to three different diet regimes (namely, BR, WGB, and COMB) were revealed and the subsequent analysis concentrated on the interaction patterns between metabolites, clinical markers, and data on OTU counts derived from 16S pyrosequencing. Nevertheless, these results heavily depend upon the quality of the data that can be only achieved by using appropriate pre- and post-processing methods as well as data analysis algorithms. Therefore, this work was also extensively focused on computational approaches for obtaining refined data, appropriate for further examination.

The raw mass spectrometric data is a complex union of meaningful as well as non-informative signals. In the current work, several methods presented were devoted to enrich subsequent analysis with useful information. The described re-calibration technique was shown to be beneficial in reaching higher mass accuracy, thereby allowing better quality of assignments of experimental m/z ratios to corresponding molecular formulas. It is worth pointing out that the reported method is only based on observing the calibration curve by plotting all the possible residual errors against reference m/z values, thereby making it possible to extend the approach to other mass spectrometry based metabolomics platforms, *e.g.* LC-MS or CE-MS. The re-calibration was followed by detection and elimination of satellite peaks, non-informative signals that emerge at both sides of a genuine mass peak. The technique, based on empirical assumptions, was shown to be successful in filtering out obstructive signals, while leaving nearby non-satellite peaks intact. Such an approach can be applied to any Fourier transform based measurements because of identical theoretical bases. After data matrix generation, a post-processing pipeline was presented to filter out leftover noise and to assign molecular formulas to the rest of the metabolic features. Final matrices represented the core inputs for multivariate statistical analysis. Certainly, different strategies can be applied to get refined data structures appropriate for further investigations. However, they all have to concern calibration, peak picking, alignment, handling missing values, and enriching the dataset in meaningful information.

Obtaining a refined data matrix is certainly not enough because appropriate statistical analysis has to be chosen to reflect the study design of the corresponding experiment. It was shown that the datasets are highly influenced by an inter-individiual variation component, implying that the diet effects can be concealed or misinterpreted if no suitable data analysis technique is selected. The dominance of between-subject differences over within-subject differences indicates that the diet responses are subtle, making data points belonging to the same individuals cluster together. Despite such observations in many metabolomics studies, there are only few reports, utilizing multivariate techniques, taking into account the high influence of inter-individual variation component. The ML-PLS-DA modelling was chosen as an appropriate statistical analysis technique that is based on decomposing the original data matrix into several matrices, each associated with its own variation component. The ML-PLS-DA was adapted for the purpose of feature selection, meaning choosing metabolic signals/OTU counts mostly associated with a specific diet. The subsequent models, built using selected features, were shown to be significant, implying that BR, WGB, and COMB consumption leads to physiological responses.

Combination of the output from ML-PLS-DA with MDiNs resulted in hypotheses regarding metabolites associated with diet responses. Interestingly, only the BR and WGB groups were characterized by prominent compounds, whereas no considerable patterns were observed for the COMB group. Most likely, it is due to the fact that COMB diet included mixture of both BR and WGB, thereby making the information more diluted. The stool metabolome response to BR consumption was characterized by several metabolites that can be directly associated to corresponding food components, such as trichothecenes and sterol ferulates. Moreover, these compounds were shown to interact with gut microbiota, making them even more appealing targets in unraveling the interplay between nutrition and alterations in microbial community within GIT. Other compounds, such as fatty amides may be involved in this activity, representing the products of bacterial activity. The responses to WGB diet were observable in stool as well as plasma metabolome. Taking into account the structure of the selected metabolites, it may be hypothesized that fatty acid as well as amino acid metabolism are strongly involved in these responses. Moreover, ACs showed prominent correlation patterns with clinical markers, making them promising targets in evaluating their association with health benefits.

This work presented that obtaining meaningful information in discovery-oriented non-targeted metabolomics is only possible by paying very careful attention to every step in the experiment starting from sample preparation and, through measurements, to pre- and post-processing pipelines as well as data analysis routines. The importance can be argued by the fact that non-targeted profiling is concentrated on hypothesis generation rather than on providing the proofs for already hypothesized concept. Therefore, the corresponding experiments will be inevitably characterized by complexity in the path towards retrieving reliable information. The current work showed a sophisticated pipeline with respect to finding responses of stool and plasma metabolome to whole grain diet by means of measurements done with DI FT-ICR-MS. The corresponding results are promising and further experiments are required to test the proposed hypotheses, for example by performing targeted experiments involving potential metabolites. In this way, it will be possible to come closer to the understanding of very subtle mechanisms involved in dietary responses, an important step towards the much more global aim of personalized treatment and medicine.


That's all Folks!

7. Appendix

Table S1. The information on the baseline characteristics of the participants involved in the study on the influence of whole grain consumption.

Id	Gender	BMI kg/m^2	Fat %	Weight	FGlu mmol/L	FIns mIU/mL	MI	IGI	HOMA-IR	TChol mmol/L	HDL mmol/L	LDL mmol/L	IL-6 pg/mL	CRP mg/L	LBP µg/mL
AA	Male	20.95	12.50	NW	4.71	9.76	7.30	3.55	2.04	4.01	1.50	2.51	0.82	0.12	1.24
AS	Female	20.31	19.20	NW	4.72	7.17	9.28	1.10	1.51	5.13	2.36	2.80	0.06	0.00	1.22
BC	Male	22.91	13.60	NW	5.27	5.53	6.13	0.29	1.30	3.75	1.42	2.36	0.36	0.05	1.01
BM	Female	31.62	52.50	OW	4.63	7.83	5.58	0.78	1.61	4.81	1.83	3.01	2.71	3.22	88.05
CS	Male	27.03	16.40	NW	4.42	6.74	11.85	0.15	1.33	4.31	1.89	2.42	2.59	0.36	6.01
CT	Female	24.28	37.70	OW	4.52	6.80	9.86	0.99	1.37	5.87	2.57	3.33	0.65	0.56	4.16
CW	Male	31.01	27.10	OW	5.55	5.04	12.10	3.03	1.24	3.89	1.18	2.74	0.69	0.30	7.96
DH	Female	17.82	14.60	NW	5.49	3.50	14.29	0.42	0.85	3.63	2.27	1.39	1.36	0.00	0.12
DN	Male	23.87	16.30	NW	4.72	3.94	10.63	0.27	0.83	3.75	1.42	2.33	0.33	0.10	3.24
EF	Female	26.43	40.50	OW	5.00	8.55	5.77	1.45	1.90	5.46	1.71	3.75	2.50	2.85	49.78
JB	Female	22.00	36.30	OW	4.87	5.58	9.22	0.25	1.21	3.51	1.77	1.74	4.88	6.70	22.26
JL	Female	24.30	42.80	OW	5.05	5.85	7.60	0.57	1.31	5.43	2.01	3.45	1.35	1.98	22.04
KH	Female	21.95	29.20	NW	4.67	4.82	10.55	0.28	1.00	5.55	1.80	3.75	0.45	1.94	15.04
KM	Female	20.01	26.00	NW	5.14	4.67	8.64	0.53	1.07	6.20	1.98	4.19	2.26	7.04	28.51
KO	Female	21.37	30.00	NW	4.83	8.40	7.11	3.44	1.81	5.49	1.45	4.04	1.04	0.06	1.14
KT	Female	30.66	45.50	OW	5.97	9.65	3.42	1.30	2.56	7.94	1.65	6.28	3.71	34.13	40.25
KW	Male	25.83	17.80	NW	5.58	7.79	10.10	8.65	1.93	3.60	1.03	2.57	6.89	24.67	8.17
LH	Female	21.25	19.20	NW	5.00	4.90	7.44	0.67	1.09	5.63	1.45	4.19	5.17	0.11	3.04
MD	Female	22.82	29.80	NW	5.48	6.11	7.61	9.75	1.49	4.75	1.83	2.89	0.50	2.05	23.35
MG	Male	34.02	36.20	OW	6.67	5.59	5.54	1.01	1.66	4.75	1.39	3.39	2.58	0.26	2.50
MH	Female	21.22	28.80	NW	4.85	10.73	6.32	0.50	2.31	6.90	-	-	0.72	0.87	7.86
MM	Female	26.96	44.20	OW	5.07	7.67	8.37	0.35	1.73	4.45	1.15	3.27	2.64	5.13	22.26
MV	Male	35.98	37.00	OW	5.54	7.08	4.28	0.42	1.75	5.63	1.00	4.63	1.03	0.80	4.09
RB	Male	23.49	24.70	NW	4.28	8.61	4.77	1.12	1.64	3.86	1.03	2.83	1.35	0.36	2.63
RP	Female	22.54	34.40	OW	7.70	4.41	9.90	2.77	1.51	4.34	2.09	2.24	0.70	0.11	3.03
SC	Female	25.76	47.40	OW	4.58	9.79	5.30	0.52	2.00	3.72	1.48	2.24	3.44	5.51	23.39
TS	Male	29.53	21.40	NW	-	-	-	-	-	-	-	-	0.89	0.54	9.61
WH	Male	26.99	27.60	OW	4.70	6.20	5.50	1.94	1.30	3.16	1.12	2.04	1.21	0.26	2.12

Table S2. The information on the characteristics of the participants involved in the study on the influence of whole grain consumption with respect to diet enriched in BR.

Id	Week	FGlu mmol/L	FIns mIU/mL	MI	IGI	HOMA-IR	TChol mmol/L	HDL mmol/L	LDL mmol/L	IL-6 pg/mL	CRP mg/L	LBP µg/mL
AA	17	4.78	5.28	5.62	1.00	1.17	4.63	1.56	3.10	0.53	0.09	0.57
AS	17	4.31	7.98	9.70	12.70	1.78	4.54	2.01	2.54	0.38	0.02	0.48
BC	11	4.71	6.43	6.19	0.32	1.45	4.10	1.30	2.77	0.61	0.07	2.91
BM	5	4.77	8.99	7.23	1.00	1.88	4.78	1.65	2.86	2.12	6.23	91.99
CS	17	4.67	4.78	10.35	0.24	1.10	4.19	1.68	2.51	0.70	0.36	3.52
CT	11	4.43	4.11	14.11	0.58	0.87	4.66	1.53	3.13	0.34	0.24	3.65
CW	11	5.23	4.39	9.92	0.45	0.91	4.16	1.12	3.07	1.69	0.38	7.85
DH	11	5.17	5.32	13.08	0.67	1.09	4.25	2.18	2.07	0.69	0.00	0.35
DN	5	4.72	4.17	14.59	0.13	1.20	4.54	2.01	2.54	0.21	0.14	1.88
EF	5	4.95	11.15	3.34	0.42	2.54	5.52	1.77	3.75	2.27	6.77	62.60
JB	17	5.10	5.80	11.88	0.32	1.18	3.30	1.45	1.83	1.32	3.44	18.38
JL	5	3.88	7.15	6.79	0.45	1.31	5.49	1.65	3.84	0.49	2.67	21.79
KH	11	4.42	7.31	6.37	1.39	1.69	5.22	1.62	3.57	0.92	0.89	12.18
KM	5	4.44	8.06	7.85	0.72	1.63	6.14	2.27	3.89	1.00	1.95	20.09
KO	17	4.67	5.02	10.60	1.00	0.99	5.43	1.24	4.16	1.14	0.18	2.65
KT	17	4.97	9.40	4.84	1.95	1.92	5.78	1.56	4.25	3.23	8.98	38.48
KW	5	4.46	4.85	11.28	0.52	0.98	4.45	1.50	2.95	0.65	0.33	4.87
LH	11	6.63	5.95	7.10	0.51	1.28	5.58	1.56	4.01	0.99	0.04	0.82
MD	17	4.21	4.84	9.44	0.48	0.92	4.66	1.71	2.95	0.66	3.45	25.09
MG	11	4.98	7.01	5.17	0.75	1.78	5.10	1.36	3.75	1.23	0.36	4.02
MH	17	4.63	8.68	6.19	0.54	1.80	5.46	2.39	3.07	0.97	0.55	5.09
MM	5	4.92	4.33	12.72	0.33	0.92	5.22	1.06	4.16	0.63	0.62	9.17
MV	11	5.68	9.31	-	0.28	2.36	6.37	0.94	5.43	4.90	3.77	16.59
RB	17	4.58	9.42	5.41	0.24	2.03	4.01	1.12	2.89	1.40	0.36	3.08
RP	11	4.94	4.92	8.24	0.79	1.10	4.63	2.15	2.48	0.39	0.14	1.24
SC	5	4.67	10.61	5.43	0.74	2.33	4.10	1.56	2.54	2.28	3.15	15.15
TS	5	4.75	4.50	12.52	0.25	0.86	3.22	1.59	1.62	0.90	0.56	7.21
WH	5	4.92	5.12	6.27	1.15	1.04	3.78	1.33	2.45	2.07	2.28	15.45

Table S3. The information on the characteristics of the participants involved in the study on the influence of whole grain consumption with respect to diet enriched in WGB.

Id	Week	FGlu mmol/L	FIns mIU/mL	MI	IGI	HOMA-IR	TChol mmol/L	HDL mmol/L	LDL mmol/L	IL-6 pg/mL	CRP mg/L	LBP µg/mL
AA	11	4.96	7.97	4.90	1.05	1.69	4.60	1.39	3.25	1.21	0.15	1.77
AS	5	4.31	7.98	9.70	12.70	1.78	4.54	2.01	2.54	0.38	0.02	0.48
BC	5	4.71	6.43	6.19	0.32	1.45	4.10	1.30	2.77	0.61	0.07	2.91
BM	17	4.77	8.99	7.23	1.00	1.88	4.78	1.65	2.86	2.12	6.23	91.99
CS	11	4.67	4.78	10.35	0.24	1.10	4.19	1.68	2.51	0.70	0.36	3.52
CT	5	4.43	4.11	14.11	0.58	0.87	4.66	1.53	3.13	0.34	0.24	3.65
CW	17	5.23	4.39	9.92	0.45	0.91	4.16	1.12	3.07	1.69	0.38	7.85
DH	17	5.17	5.32	13.08	0.67	1.09	4.25	2.18	2.07	0.69	0.00	0.35
DN	11	4.72	4.17	14.59	0.13	1.20	4.54	2.01	2.54	0.21	0.14	1.88
EF	11	4.95	11.15	3.34	0.42	2.54	5.52	1.77	3.75	2.27	6.77	62.60
JB	5	5.10	5.80	11.88	0.32	1.18	3.30	1.45	1.83	1.32	3.44	18.38
JL	17	3.88	7.15	6.79	0.45	1.31	5.49	1.65	3.84	0.49	2.67	21.79
KH	5	4.42	7.31	6.37	1.39	1.69	5.22	1.62	3.57	0.92	0.89	12.18
KM	11	4.44	8.06	7.85	0.72	1.63	6.14	2.27	3.89	1.00	1.95	20.09
KO	5	4.67	5.02	10.60	1.00	0.99	5.43	1.24	4.16	1.14	0.18	2.65
KT	5	4.97	9.40	4.84	1.95	1.92	5.78	1.56	4.25	3.23	8.98	38.48
KW	17	4.46	4.85	11.28	0.52	0.98	4.45	1.50	2.95	0.65	0.33	4.87
LH	5	6.63	5.95	7.10	0.51	1.28	5.58	1.56	4.01	0.99	0.04	0.82
MD	11	4.21	4.84	9.44	0.48	0.92	4.66	1.71	2.95	0.66	3.45	25.09
MG	5	4.98	7.01	5.17	0.75	1.78	5.10	1.36	3.75	1.23	0.36	4.02
MH	11	4.63	8.68	6.19	0.54	1.80	5.46	2.39	3.07	0.97	0.55	5.09
MM	17	4.92	4.33	12.72	0.33	0.92	5.22	1.06	4.16	0.63	0.62	9.17
MV	17	5.68	9.31	-	0.28	2.36	6.37	0.94	5.43	4.90	3.77	16.59
RB	5	4.58	9.42	5.41	0.24	2.03	4.01	1.12	2.89	1.40	0.36	3.08
RP	17	4.94	4.92	8.24	0.79	1.10	4.63	2.15	2.48	0.39	0.14	1.24
SC	11	4.67	10.61	5.43	0.74	2.33	4.10	1.56	2.54	2.28	3.15	15.15
TS	17	4.75	4.50	12.52	0.25	0.86	3.22	1.59	1.62	0.90	0.56	7.21
WH	11	4.92	5.12	6.27	1.15	1.04	3.78	1.33	2.45	2.07	2.28	15.45

Table S4. The information on the characteristics of the participants involved in the study on the influence of whole grain consumption with respect to diet enriched in COMB.

Id	Week	FGlu mmol/L	FIns mIU/mL	MI	IGI	HOMA-IR	TChol mmol/L	HDL mmol/L	LDL mmol/L	IL-6 pg/mL	CRP mg/L	LBP µg/mL
AA	5	5.55	7.68	5.53	7.52	1.90	4.16	1.30	2.86	0.60	0.09	0.96
AS	11	4.44	6.98	8.00	0.57	1.38	4.22	2.07	2.15	0.39	0.01	1.00
BC	17	5.04	4.46	6.98	0.30	1.00	3.25	1.30	1.95	12.27	4.85	23.41
BM	11	4.64	7.35	8.41	0.50	1.52	5.10	1.56	3.54	1.52	3.40	39.92
CS	5	4.34	4.09	12.30	0.27	0.79	4.81	1.89	2.92	1.24	0.26	4.51
CT	17	4.28	3.01	19.32	0.61	0.57	3.30	1.12	2.21	0.56	0.90	8.19
CW	5	4.84	8.03	7.30	0.35	1.73	4.10	0.89	3.04	0.79	0.32	6.63
DH	5	4.98	2.62	18.10	0.85	0.58	4.16	2.39	1.77	1.21	0.00	0.29
DN	17	4.53	4.58	11.71	1.46	0.92	3.22	1.30	1.92	0.45	0.13	2.50
EF	17	5.48	7.17	5.12	0.31	1.75	4.28	1.59	2.68	1.59	14.04	80.03
JB	11	4.88	6.35	11.10	0.48	1.38	3.16	1.36	1.83	2.12	1.10	10.91
JL	11	4.31	9.40	7.25	0.19	1.80	4.96	1.98	2.98	0.31	4.78	53.98
KH	17	4.11	9.54	5.65	0.66	1.74	5.58	1.59	3.98	0.92	2.02	16.75
KM	17	4.35	5.33	10.38	0.42	1.03	6.02	2.66	3.36	0.99	2.15	23.31
KO	11	5.44	7.89	5.95	0.67	1.91	5.34	1.53	3.81	0.67	0.18	1.11
KT	11	4.85	7.01	5.65	0.55	1.51	6.25	1.48	4.78	3.88	8.57	33.63
KW	11	4.65	5.32	10.84	0.67	1.10	3.84	1.33	2.51	0.61	0.41	6.06
LH	17	5.11	3.54	9.68	0.40	0.80	5.02	1.30	3.72	1.03	0.04	1.95
MD	5	4.87	7.36	7.40	0.44	1.59	5.02	1.56	3.25	0.95	1.91	16.60
MG	17	5.58	8.14	5.16	0.62	2.02	4.54	0.94	3.60	0.81	0.20	2.53
MH	5	4.36	8.99	6.92	0.73	1.74	5.75	2.27	3.48	0.37	0.28	2.12
MM	11	4.83	5.83	7.57	0.60	1.25	3.98	0.74	3.27	0.54	2.36	21.50
MV	5	4.90	6.24	8.23	0.51	1.36	5.90	1.06	4.81	0.98	0.90	4.36
RB	11	4.77	9.68	4.86	0.45	2.05	5.31	1.39	3.92	1.56	0.23	2.65
RP	5	4.95	4.48	8.34	1.15	0.99	4.28	2.04	2.24	0.71	0.09	1.21
SC	17	4.82	9.27	6.06	0.75	1.99	4.54	1.56	2.98	0.97	0.72	10.57
TS	11	4.75	5.57	-	0.39	1.18	3.48	1.74	1.74	0.47	0.36	6.25
WH	17	5.08	6.37	8.03	4.72	1.44	4.19	1.53	2.66	0.79	0.29	7.74

Table S5. Internal standards spiked into several plasma samples measured by DI FT-ICR-MS.

Name	Formula	Exact Mass	Initial/Prepared concentration, µg/mL	Final concentration, µg/mL
Acyl-L-Carnitines (Avanti Polar Lipids Inc.)				
Acetyl-L-Carnitine	$C_9H_{14}D_3NO_4$	206.134588	1000	0.5
Propionyl-L-Carnitine	$C_{10}H_{16}D_3NO_4$	220.150238	1000	0.5
Valeryl-L-Carnitine	$C_{12}H_{20}D_3NO_4$	248.181538	1000	0.5
Decanoyl-L-Carnitine	$C_{17}H_{30}D_3NO_4$	318.259789	1000	0.02
Hexadecanoyl-L-Carnitine	$C_{23}H_{42}D_3NO_4$	402.353689	1000	0.02
Octadecanoyl-L-Carnitine	$C_{25}H_{46}D_3NO_4$	430.384989	1000	0.02
SPLASH LipidoMIX (Avanti Polar Lipids Inc.)				
PC(15:0/18:1)	$C_{41}H_{73}D_7NO_8P$	752.606092	160.7	2.25
PE(15:0/18:1)	$C_{38}H_{67}D_7NO_8P$	710.559142	5.7	0.08
PS(15:0/18:1) Na salt	$C_{39}H_{66}D_7NNaO_{10}P$	776.530916	4.2	0.06
PG(15:0/18:1) Na salt	$C_{39}H_{67}D_7NaO_{10}P$	763.535667	29.1	0.41
PI(15:0/18:1) NH_4 salt	$C_{42}H_{75}D_7NO_{13}P$	846.596316	9.1	0.13
PA(15:0/18:1) Na salt	$C_{36}H_{61}D_7NaO_8P$	689.498887	7.4	0.10
LysoPC(18:1)	$C_{26}H_{45}D_7NO_7P$	528.392077	25.5	0.36
LysoPE(18:1)	$C_{23}H_{39}D_7NO_7P$	486.345127	5.3	0.07
CE(18:1)	$C_{45}H_{71}D_7O_2$	657.644119	356.1	5.00
MAG(18:1)	$C_{21}H_{33}D_7O_4$	363.336597	2.0	0.03
DAG(15:0/18:1)	$C_{36}H_{61}D_7O_5$	587.550612	9.4	0.13
TAG(15:0/18:1/15:0)	$C_{51}H_{89}D_7O_6$	811.764628	57.3	0.80
SM(d18:1/18:1)	$C_{41}H_{72}D_9N_2O_6P$	737.639716	30.9	0.43
Cholesterol	$C_{27}H_{39}D_7O$	393.398803	98.4	1.38

Abbreviations: **PC**, phosphocholine; **PE**, phosphoethanolamine; **PS**, phosphatidylserine; **PG**, phosphatidylglycerol; **PI**, phosphatidylinositol; **PA**, phosphatidic acid; **CE**, cholesterol ester; **MAG**, monoacylglycerol; **DAG**, diacylglycerol; **TAG**, triacylglycerol; **SM**, sphingomyelin.

Table S6. Coefficients of the linear models used to eliminate satellite peaks within an individual spectrum.

			Stool sample				Plasma samples			
Id	Week	Diet	N original peaks	N deleted peaks	Coef A	Coef B	N original peaks	N deleted peaks	Coef A	Coef B
AA	1	Baseline	12103	2097	-2.0544	17.2114	19533	1445	-1.9505	17.0443
AA	5	COMB	12036	2123	-1.9989	16.8029	20567	1677	-1.9481	17.0107
AA	11	WGB	11738	2113	-1.9947	16.7837	16883	1232	-1.9690	17.1806
AA	17	BR	8102	1233	-2.0046	16.8523	23153	1864	-1.9655	17.1410
AS	1	Baseline	13009	2201	-1.9879	16.7430	24403	1792	-1.9624	17.1368
AS	5	WGB	12433	1997	-2.0008	16.8171	24478	2091	-1.9596	17.1103
AS	11	COMB	11905	2040	-1.9860	16.7231	N/A	N/A	N/A	N/A
AS	17	BR	11423	1814	-1.9966	16.7945	18619	1688	-1.9356	16.9205
BC	1	Baseline	9120	1498	-1.9854	16.7129	20957	1694	-1.9954	17.3626
BC	5	WGB	10371	1773	-2.0035	16.8377	20088	1444	-1.9740	17.2055
BC	11	BR	10274	1988	-1.9932	16.7714	N/A	N/A	N/A	N/A
BC	17	COMB	9128	1680	-1.9875	16.7335	20209	1531	-1.9542	17.0698
BM	1	Baseline	11166	2155	-2.0065	16.8574	21834	2002	-1.9593	17.1107
BM	5	BR	11446	1946	-2.0061	16.8570	21935	2088	-1.9424	16.9845
BM	11	COMB	11379	2076	-1.9937	16.7689	25658	2156	-1.9799	17.2595
BM	17	WGB	11520	1882	-1.9870	16.7183	21207	1907	-1.9324	16.9022
CS	1	Baseline	5433	1634	-1.9912	16.7534	20502	1397	-1.9554	17.0795
CS	5	COMB	6111	1691	-1.9878	16.7350	22613	1685	-1.9422	16.9860
CS	11	WGB	7381	1797	-1.9786	16.6746	19574	1790	-1.9516	17.0557
CS	17	BR	7632	1848	-1.9902	16.7524	25323	1743	-1.5551	13.9921
CT	1	Baseline	10686	2331	-1.9887	16.7416	21717	1699	-1.9902	17.3371
CT	5	WGB	7056	1941	-1.9844	16.7133	16860	1319	-1.9612	17.1229
CT	11	BR	10975	2455	-1.9950	16.7817	16710	1143	-1.9597	17.1019
CT	17	COMB	6638	1723	-1.9887	16.7423	25109	2183	-1.9361	16.9453
CW	1	Baseline	10466	1933	-2.0027	16.8397	24020	2120	-1.9349	16.9387
CW	5	COMB	10279	2196	-2.0023	16.8299	20833	1167	-1.9040	16.6590
CW	11	BR	11472	1176	-1.9900	16.7458	N/A	N/A	N/A	N/A
CW	17	WGB	10060	2138	-1.9893	16.7442	20776	1518	-1.9594	17.1147
DH	1	Baseline	9042	2041	-1.9911	16.7557	23034	1885	-1.9382	16.9586
DH	5	COMB	12032	2161	-2.0026	16.8302	18459	1173	-1.9662	17.1539
DH	11	BR	11548	2046	-1.9994	16.8110	22251	1672	-1.9652	17.1516
DH	17	WGB	13301	2054	-1.9972	16.7926	22242	1917	-1.9531	17.0670
DN	1	Baseline	9712	1911	-1.9823	16.6969	19298	1636	-1.9498	17.0328
DN	5	BR	9700	2176	-1.9905	16.7537	22447	1507	-1.9456	17.0085
DN	11	WGB	10185	1428	-1.9989	16.8051	N/A	N/A	N/A	N/A
DN	17	COMB	9822	1906	-1.9851	16.7161	19710	1720	-1.9657	17.1564
EF	1	Baseline	8024	778	-1.9865	16.7400	20666	1360	-1.9338	16.9210
EF	5	BR	12361	2166	-1.9935	16.7661	16904	1476	-1.9568	17.0892
EF	11	WGB	11790	2232	-1.9956	16.7844	N/A	N/A	N/A	N/A
EF	17	COMB	12387	1855	-2.0021	16.8284	17902	1275	-1.9479	17.0256
JB	1	Baseline	10694	2537	-1.9892	16.7386	25217	1494	-1.9744	17.2174
JB	5	WGB	6787	1055	-1.9878	16.7404	25230	2073	-1.9650	17.1550
JB	11	COMB	11768	2581	-1.9982	16.8036	19353	1684	-1.9580	17.1044
JB	17	BR	12978	2262	-2.0007	16.8144	24427	2066	-1.9342	16.9235
JL	1	Baseline	13309	1851	-2.0061	16.8570	N/A	N/A	N/A	N/A
JL	5	BR	12873	2028	-1.9920	16.7556	N/A	N/A	N/A	N/A
JL	11	COMB	9903	1669	-1.9963	16.7868	17708	1082	-1.9687	17.1730
JL	17	WGB	8476	1958	-1.9963	16.7930	20063	1341	-1.9489	17.0410
KH	1	Baseline	13161	1980	-1.9931	16.7611	18865	1501	-1.9806	17.2523
KH	5	WGB	13557	1873	-1.9942	16.7683	20243	1387	-1.9199	16.8152
KH	11	BR	9419	1560	-1.9877	16.7323	12635	619	-1.9338	16.9168
KH	17	COMB	13511	1867	-1.9949	16.7758	21366	1935	-1.9732	17.2116
KM	1	Baseline	11983	1930	-1.9945	16.7815	25428	1805	-1.9776	17.2303
KM	5	BR	13396	2089	-2.0041	16.8436	20322	1591	-1.9797	17.2437

KM	11	WGB	5005	1538	-1.9912	16.7580	24470	1707	-1.9427	16.9914
KM	17	COMB	12603	2288	-1.9960	16.7865	21879	2022	-1.9597	17.1145
KO	1	Baseline	10730	2048	-1.9917	16.7544	18584	1914	-1.9666	17.1655
KO	5	WGB	11958	2113	-1.9836	16.7123	19737	1455	-1.9586	17.0954
KO	11	COMB	11965	1333	-1.9907	16.7540	20143	1670	-1.9796	17.2498
KO	17	BR	12747	1710	-1.995	16.7795	16235	1310	-1.9493	17.0385
KT	1	Baseline	12881	1812	-1.9979	16.7983	19618	1621	-1.9653	17.1525
KT	5	WGB	11311	1841	-1.9889	16.7397	15780	1287	-1.9745	17.2197
KT	11	COMB	11758	1829	-1.9949	16.7810	18717	1594	-1.9678	17.1681
KT	17	BR	11108	1981	-1.9908	16.7544	20744	1986	-1.9607	17.1156
KW	1	Baseline	10171	2171	-1.9903	16.7464	18659	1742	-1.9495	17.0402
KW	5	BR	10559	2359	-2.0046	16.8460	19148	1698	-1.9683	17.1716
KW	11	COMB	11234	2012	-1.9900	16.7449	19336	1521	-1.9190	16.8207
KW	17	WGB	11311	1918	-1.9987	16.8044	20524	1411	-1.9096	16.7524
LH	1	Baseline	12324	1957	-1.9874	16.7322	17279	1502	-1.9746	17.2235
LH	5	WGB	11515	1864	-1.9955	16.7831	25974	1863	-1.9396	16.9646
LH	11	BR	11395	1886	-1.9983	16.8019	N/A	N/A	N/A	N/A
LH	17	COMB	12993	2093	-1.9795	16.6839	23632	1483	-1.8469	16.2291
MD	1	Baseline	6977	1664	-1.9949	16.7839	18765	1546	-1.9570	17.0833
MD	5	COMB	13228	1831	-1.9963	16.7862	18826	1307	-1.9589	17.1080
MD	11	WGB	12384	1928	-1.9888	16.7405	N/A	N/A	N/A	N/A
MD	17	BR	11713	2359	-2.0034	16.8388	24707	1965	-1.9218	16.8262
MG	1	Baseline	10855	1782	-1.9944	16.7751	22484	1752	-1.9394	16.9521
MG	5	WGB	11128	2164	-1.9955	16.7845	17565	977	-1.9588	17.0990
MG	11	BR	11907	2356	-1.9997	16.8119	20523	1342	-1.4700	13.4698
MG	17	COMB	9080	1438	-1.9985	16.8096	19269	1472	-1.9521	17.0526
MH	1	Baseline	12783	1949	-2.0060	16.8536	18902	966	-1.9519	17.0358
MH	5	COMB	10303	1777	-1.9907	16.7545	21191	1875	-1.9690	17.1732
MH	11	WGB	11730	1715	-1.9800	16.6816	17949	1171	-1.9603	17.1182
MH	17	BR	12928	2065	-1.9906	16.7624	18291	1128	-1.8915	16.5804
MM	1	Baseline	10498	2064	-1.9921	16.7653	21577	1298	-1.9827	17.2699
MM	5	BR	11615	2099	-2.0023	16.8312	18560	1327	-1.9712	17.1965
MM	11	COMB	10373	1924	-1.9929	16.7701	23845	1993	-1.9414	16.9776
MM	17	WGB	12448	2112	-1.9849	16.7194	21043	1461	-1.9761	17.2308
MV	1	Baseline	10722	1875	-1.9950	16.7821	18818	1307	-1.9599	17.1134
MV	5	COMB	12710	1580	-1.9933	16.7664	24927	1290	-1.9709	17.1632
MV	11	BR	12653	1814	-2.0029	16.8341	18801	1439	-1.9830	17.2709
MV	17	WGB	10113	2050	-1.9952	16.7848	24012	1820	-1.9425	16.9862
RB	1	Baseline	12564	2079	-1.9914	16.7616	20888	1404	-1.9489	17.0181
RB	5	WGB	11546	1962	-1.9893	16.7417	26538	1973	-1.9755	17.2281
RB	11	COMB	8845	1992	-1.9851	16.7174	17188	1284	-1.9619	17.1264
RB	17	BR	8354	1877	-1.9874	16.7357	23638	1957	-1.9239	16.8556
RP	1	Baseline	12213	1941	-1.9999	16.8137	21475	1995	-1.9471	17.0232
RP	5	COMB	12395	1915	-1.9900	16.7425	19351	1099	-1.9288	16.8908
RP	11	BR	10485	1882	-1.9931	16.7698	17571	1312	-1.9363	16.9396
RP	17	WGB	12322	2064	-1.9937	16.7747	14744	1010	-1.9511	17.0439
SC	1	Baseline	N/A	N/A	N/A	N/A	18575	1541	-1.9714	17.1968
SC	5	BR	N/A	N/A	N/A	N/A	20130	407	-1.9741	17.1661
SC	11	WGB	N/A	N/A	N/A	N/A	26201	1582	-1.9360	16.9437
SC	17	COMB	N/A	N/A	N/A	N/A	19847	2057	-1.9578	17.1021
TS	1	Baseline	10637	2147	-1.9865	16.7232	18131	1334	-1.9355	16.9375
TS	5	BR	12919	2405	-1.9901	16.7495	23836	2043	-1.9136	16.7807
TS	11	COMB	12710	2100	-1.9933	16.7717	N/A	N/A	N/A	N/A
TS	17	WGB	8675	1951	-1.9945	16.7797	21539	1555	-1.9608	17.0975
WH	1	Baseline	10597	1544	-1.9993	16.8076	18519	1790	-1.9569	17.0905
WH	5	BR	7933	1001	-1.9720	16.6268	16644	1269	-1.9668	17.1545
WH	11	WGB	12022	1968	-1.9926	16.7704	21039	1685	-1.9765	17.2295
WH	17	COMB	11460	1494	-2.0047	16.8518	25420	2149	-1.9873	17.3138

Table S7. The transformation list used for the initial implementation of the MDiN construction.

Id	C	H	N	O	P	S	Transformation	Mass
1	0	-1	-1	1	0	0	H-1N-1O	0.984016
2	0	3	1	-1	0	0	H3NO-1	1.031634
3	-1	-2	0	1	0	0	C-1H-2O	1.979265
4	0	2	0	0	0	0	H2	2.015650
5	1	0	0	0	0	0	C	12.000000
6	1	3	1	-1	0	0	CH3NO-1	13.031634
7	1	2	0	0	0	0	CH2	14.015650
8	0	1	1	0	0	0	HN	15.010899
9	1	3	0	0	0	0	CH3	15.023475
10	0	0	0	-1	0	1	O-1S	15.977156
11	0	0	0	1	0	0	O	15.994915
12	0	2	0	1	0	0	H2O	18.010565
13	1	-2	0	1	0	0	CH-2O	25.979265
14	2	2	0	0	0	0	C2H2	26.015650
15	3	6	0	-1	0	0	C3H6O-1	26.052035
16	1	1	1	0	0	0	CHN	27.010899
17	2	5	1	-1	0	0	C2H5NO-1	27.047284
18	1	0	0	1	0	0	CO	27.994915
19	2	4	0	0	0	0	C2H4	28.031300
20	0	-1	1	1	0	0	H-1NO	28.990164
21	0	-2	0	0	0	1	H-2S	29.956421
22	1	2	0	1	0	0	CH2O	30.010565
23	0	0	0	0	0	1	S	31.972071
24	0	0	0	2	0	0	O2	31.989830
25	2	2	0	1	0	0	C2H2O	42.010565
26	1	2	2	0	0	0	CH2N2	42.021798
27	1	1	1	1	0	0	CHNO	43.005814
28	2	5	1	0	0	0	C2H5N	43.042199
29	1	0	0	2	0	0	CO2	43.989830
30	2	4	0	1	0	0	C2H4O	44.026215
31	0	-1	1	2	0	0	H-1NO2	44.985079
32	-1	1	0	1	1	0	C-1HOP	35.976502
33	4	7	1	-1	0	0	C4H7NO-1	53.062934
34	4	6	0	0	0	0	C4H6	54.046950
35	5	10	0	-1	0	0	C5H10O-1	54.083335
36	4	9	1	-1	0	0	C4H9NO-1	55.078584
37	2	0	0	2	0	0	C2O2	55.989830
38	3	4	0	1	0	0	C3H4O	56.026215
39	2	3	1	1	0	0	C2H3NO	57.021464
40	3	7	1	0	0	0	C3H7N	57.057849
41	2	2	0	0	0	1	C2H2S	57.987721
42	2	5	1	-1	0	1	C2H5NO-1S	59.019355
43	2	5	1	1	0	0	C2H5NO	59.037114
44	2	4	0	2	0	0	C2H4O2	60.021130
45	5	8	0	0	0	0	C5H8	68.062600
46	3	3	1	1	0	0	C3H3NO	69.021464
47	4	7	1	0	0	0	C4H7N	69.057849
48	5	11	1	-1	0	0	C5H11NO-1	69.094234
49	3	2	0	2	0	0	C3H2O2	70.005480
50	4	6	0	1	0	0	C4H6O	70.041865
51	3	6	2	0	0	0	C3H6N2	70.053098
52	4	10	2	-1	0	0	C4H10N2O-1	70.089483
53	3	5	1	1	0	0	C3H5NO	71.037114
54	2	0	0	3	0	0	C2O3	71.984745
55	4	8	0	1	0	0	C4H8O	72.057515
56	2	3	1	2	0	0	C2H3NO2	73.016379
57	3	7	1	1	0	0	C3H7NO	73.052764

58	3	6	0	2	0	0	C3H6O2	74.036780
59	2	4	0	1	0	1	C2H4OS	75.998286
60	0	0	0	3	0	1	O3S	79.956816
61	0	1	0	3	1	0	HO3P	79.966332
62	7	14	0	-1	0	0	C7H14O-1	82.114635
63	4	5	1	1	0	0	C4H5NO	83.037114
64	5	9	1	0	0	0	C5H9N	83.073499
65	4	4	0	2	0	0	C4H4O2	84.021130
66	5	8	0	1	0	0	C5H8O	84.057515
67	4	8	2	0	0	0	C4H8N2	84.068748
68	5	12	2	-1	0	0	C5H12N2O-1	84.105133
69	4	7	1	1	0	0	C4H7NO	85.052764
70	3	2	0	3	0	0	C3H2O3	86.000395
71	4	6	0	0	0	1	C4H6S	86.019021
72	5	10	0	1	0	0	C5H10O	86.073165
73	3	5	1	2	0	0	C3H5NO2	87.032029
74	4	9	1	-1	0	1	C4H9NO-1S	87.050655
75	4	9	1	1	0	0	C4H9NO	87.068414
76	3	4	0	3	0	0	C3H4O3	88.016045
77	3	7	1	2	0	0	C3H7NO2	89.047679
78	5	4	2	0	0	0	C5H4N2	92.037448
79	5	7	3	-1	0	0	C5H7N3O-1	93.069082
80	5	7	1	1	0	0	C5H7NO	97.052764
81	5	6	0	2	0	0	C5H6O2	98.036780
82	6	10	0	1	0	0	C6H10O	98.073165
83	5	9	1	1	0	0	C5H9NO	99.068414
84	4	4	0	3	0	0	C4H4O3	100.016045
85	4	7	1	2	0	0	C4H7NO2	101.047679
86	5	11	1	1	0	0	C5H11NO	101.084064
87	3	2	0	2	0	1	C3H2O2S	101.977551
88	4	6	0	3	0	0	C4H6O3	102.031695
89	8	6	0	0	0	0	C8H6	102.046950
90	3	5	1	1	0	1	C3H5NOS	103.009185
91	4	9	1	2	0	0	C4H9NO2	103.063329
92	8	9	1	-1	0	0	C8H9NO-1	103.078584
93	4	8	0	1	0	1	C4H8OS	104.029586
94	3	7	1	1	0	1	C3H7NOS	105.024835
95	2	5	1	2	0	1	C2H5NO2S	107.004100
96	2	7	1	2	0	1	C2H7NO2S	109.019750
97	5	6	2	1	0	0	C5H6N2O	110.048013
98	9	18	0	-1	0	0	C9H18O-1	110.145935
99	5	9	3	0	0	0	C5H9N3	111.079647
100	6	8	0	2	0	0	C6H8O2	112.052430
101	7	12	0	1	0	0	C7H12O	112.088815
102	5	12	4	-1	0	0	C5H12N4O-1	112.111281
103	4	3	1	3	0	0	C4H3NO3	113.011294
104	5	7	1	2	0	0	C5H7NO2	113.047679
105	6	11	1	1	0	0	C6H11NO	113.084064
106	4	2	0	4	0	0	C4H2O4	113.995310
107	5	6	0	3	0	0	C5H6O3	114.031695
108	4	6	2	2	0	0	C4H6N2O2	114.042928
109	5	10	2	1	0	0	C5H10N2O	114.079313
110	4	5	1	3	0	0	C4H5NO3	115.026944
111	6	13	1	1	0	0	C6H13NO	115.099714
112	4	8	2	2	0	0	C4H8N2O2	116.058578
113	5	12	2	1	0	0	C5H12N2O	116.094963
114	4	7	1	3	0	0	C4H7NO3	117.042594
115	8	6	0	1	0	0	C8H6O	118.041865

116	8	9	1	0	0	0	C8H9N	119.073499
117	8	8	0	1	0	0	C8H8O	120.057515
118	2	6	1	3	1	0	C2H6NO3P	123.008531
119	8	14	0	1	0	0	C8H14O	126.104465
120	5	5	1	3	0	0	C5H5NO3	127.026944
121	6	9	1	2	0	0	C6H9NO2	127.063329
122	5	4	0	4	0	0	C5H4O4	128.010960
123	6	8	0	3	0	0	C6H8O3	128.047345
124	5	8	2	2	0	0	C5H8N2O2	128.058578
125	6	12	2	1	0	0	C6H12N2O	128.094963
126	5	7	1	3	0	0	C5H7NO3	129.042594
127	5	11	3	1	0	0	C5H11N3O	129.090212
128	5	6	0	2	0	1	C5H6O2S	130.008851
129	5	10	2	2	0	0	C5H10N2O2	130.074228
130	6	14	2	1	0	0	C6H14N2O	130.110613
131	5	9	1	1	0	1	C5H9NOS	131.040485
132	5	9	1	3	0	0	C5H9NO3	131.058244
133	5	11	1	1	0	1	C5H11NOS	133.056135
134	6	4	2	2	0	0	C6H4N2O2	136.027278
135	8	8	0	2	0	0	C8H8O2	136.052430
136	10	16	0	0	0	0	C10H16	136.125200
137	6	7	3	1	0	0	C6H7N3O	137.058912
138	11	22	0	-1	0	0	C11H22O-1	138.177235
139	6	9	3	1	0	0	C6H9N3O	139.074562
140	9	16	0	1	0	0	C9H16O	140.120115
141	10	7	1	0	0	0	C10H7N	141.057849
142	7	10	0	3	0	0	C7H10O3	142.062995
143	10	10	2	-1	0	0	C10H10N2O-1	142.089483
144	9	6	0	2	0	0	C9H6O2	146.036780
145	9	9	1	1	0	0	C9H9NO	147.068414
146	9	11	1	1	0	0	C9H11NO	149.084064
147	3	7	0	5	1	0	C3H7O5P	154.003112
148	10	18	0	1	0	0	C10H18O	154.135765
149	6	9	3	2	0	0	C6H9N3O2	155.069477
150	8	12	0	3	0	0	C8H12O3	156.078645
151	6	12	4	1	0	0	C6H12N4O	156.101111
152	6	14	4	1	0	0	C6H14N4O	158.116761
153	10	9	1	1	0	0	C10H9NO	159.068414
154	9	6	0	3	0	0	C9H6O3	162.031695
155	6	10	0	5	0	0	C6H10O5	162.052825
156	9	9	1	2	0	0	C9H9NO2	163.063329
157	9	11	1	2	0	0	C9H11NO2	165.078979
158	13	26	0	-1	0	0	C13H26O-1	166.208535
159	3	6	1	5	1	0	C3H6NO5P	166.998361
160	9	14	0	3	0	0	C9H14O3	170.094295
161	6	8	0	6	0	0	C6H8O6	176.032090
162	12	22	0	1	0	0	C12H22O	182.167065
163	10	16	0	3	0	0	C10H16O3	184.109945
164	11	7	1	2	0	0	C11H7NO2	185.047679
165	11	10	2	1	0	0	C11H10N2O	186.079313
166	11	12	2	1	0	0	C11H12N2O	188.094963
167	15	30	0	-1	0	0	C15H30O-1	194.239835
168	15	24	0	0	0	0	C15H24	204.187800
169	14	26	0	1	0	0	C14H26O	210.198365
170	5	9	0	7	1	0	C5H9O7P	212.008592
171	16	30	0	1	0	0	C16H30O	238.229665
172	6	11	0	8	1	0	C6H11O8P	242.019157
173	20	32	0	0	0	0	C20H32	272.250400

174	8	18	1	5	1	0	C8H18NO5P	239.092261
175	5	13	1	3	1	0	C5H13NO3P	166.063306

Table S8. The transformation list used for the final implementation of the MDiN construction.

Id	C	H	N	O	P	S	Transformation	Mass
1	0	-1	-1	1	0	0	H-1N-1O	0.984016
2	0	3	1	-1	0	0	H3NO-1	1.031634
3	0	2	0	0	0	0	H2	2.015650
4	-1	1	1	-2	0	1	C-1HNO-2S	2.993140
5	0	4	0	0	0	0	H4	4.031300
6	4	6	1	-2	-1	0	C4H6NO-2P-1	5.086432
7	0	6	0	0	0	0	H6	6.046950
8	-1	1	-1	0	0	1	C-1HN-1S	6.976822
9	1	-2	0	0	0	0	CH-2	9.984350
10	1	0	0	0	0	0	C	12.000000
11	0	-1	1	0	0	0	H-1N	12.995249
12	0	-2	0	1	0	0	H-2O	13.979265
13	1	2	0	0	0	0	CH2	14.015650
14	0	1	1	0	0	0	HN	15.010899
15	0	0	0	1	0	0	O	15.994915
16	1	4	0	0	0	0	CH4	16.031300
17	0	4	2	-1	0	0	H4N2O-1	16.042533
18	0	-1	-1	2	0	0	H-1N-1O2	16.978931
19	3	-1	1	-2	0	0	C3H-1NO-2	17.005419
20	0	3	1	0	0	0	H3N	17.026549
21	0	2	0	1	0	0	H2O	18.010565
22	0	1	-1	2	0	0	HN-1O2	18.994581
23	0	5	1	0	0	0	H5N	19.042199
24	-10	-2	0	5	2	0	C-10H-2O5P2	19.906449
25	2	2	0	0	0	0	C2H2	26.015650
26	2	2	0	2	0	-1	C2H2O2S-1	26.033409
27	1	1	1	0	0	0	CHN	27.010899
28	1	0	0	1	0	0	CO	27.994915
29	15	22	0	-7	-2	0	C15H22O-7P-2	28.260221
30	0	-1	1	1	0	0	H-1NO	28.990164
31	0	-2	0	0	0	1	H-2S	29.956421
32	0	-2	0	2	0	0	H-2O2	29.974180
33	1	2	0	1	0	0	CH2O	30.010565
34	0	0	0	-2	0	2	O-2S2	31.954312
35	0	0	0	0	0	1	S	31.972071
36	0	0	0	2	0	0	O2	31.989830
37	0	3	1	-1	0	1	H3NO-1S	33.003705
38	0	2	0	2	0	0	H2O2	34.005480
39	4	4	1	0	-1	0	C4H4NP-1	35.060612
40	-1	1	0	1	1	0	C-1HOP	35.976502
41	3	0	0	0	0	0	C3	36.000000
42	-7	-2	0	4	2	0	C-7H-2O4P2	39.911534
43	2	2	0	1	0	0	C2H2O	42.010565
44	1	2	2	0	0	0	CH2N2	42.021798
45	1	1	1	1	0	0	CHNO	43.005814
46	2	5	1	0	0	0	C2H5N	43.042199
47	1	0	0	2	0	0	CO2	43.989830
48	2	4	0	1	0	0	C2H4O	44.026215
49	1	2	0	2	0	0	CH2O2	46.005480
50	1	5	1	-1	0	1	CH5NO-1S	47.019355
51	4	2	0	0	0	0	C4H2	50.015650
52	3	4	2	-1	0	0	C3H4N2O-1	52.042533
53	-7	-4	0	5	2	0	C-7H-4O5P2	53.890799
54	3	4	0	1	0	0	C3H4O	56.026215
55	2	3	1	1	0	0	C2H3NO	57.021464
56	3	7	1	0	0	0	C3H7N	57.057849
57	3	10	2	-1	0	0	C3H10N2O-1	58.089483

58	2	5	1	1	0	0	C2H5NO	59.037114
59	2	4	0	2	0	0	C2H4O2	60.021130
60	1	4	2	1	0	0	CH4N2O	60.032363
61	1	3	1	0	0	1	CH3NS	60.998620
62	1	2	0	3	0	0	CH2O3	62.000395
63	0	0	0	2	0	1	O2S	63.961901
64	4	5	1	0	0	0	C4H5N	67.042199
65	4	5	1	2	0	-1	C4H5NO2S-1	67.059958
66	5	8	0	0	0	0	C5H8	68.062600
67	3	2	0	2	0	0	C3H2O2	70.005480
68	4	6	0	1	0	0	C4H6O	70.041865
69	3	5	1	1	0	0	C3H5NO	71.037114
70	4	9	1	0	0	0	C4H9N	71.073499
71	3	4	0	2	0	0	C3H4O2	72.021130
72	4	8	0	1	0	0	C4H8O	72.057515
73	4	12	2	-1	0	0	C4H12N2O-1	72.105133
74	2	3	1	2	0	0	C2H3NO2	73.016379
75	2	2	0	3	0	0	C2H2O3	74.000395
76	3	6	0	2	0	0	C3H6O2	74.036780
77	8	10	0	-2	0	0	C8H10O-2	74.088420
78	2	5	1	2	0	0	C2H5NO2	75.032029
79	2	4	0	3	0	0	C2H4O3	76.016045
80	5	3	1	0	0	0	C5H3N	77.026549
81	5	7	3	-2	0	0	C5H7N3O-2	77.074167
82	0	0	0	3	0	1	O3S	79.956816
83	0	1	0	3	1	0	HO3P	79.966332
84	5	7	1	0	0	0	C5H7N	81.057849
85	0	2	-1	4	1	0	H2N-1O4P	82.965998
86	4	4	0	2	0	0	C4H4O2	84.021130
87	4	4	0	4	0	-1	C4H4O4S-1	84.038889
88	5	8	0	1	0	0	C5H8O	84.057515
89	5	11	1	0	0	0	C5H11N	85.089149
90	3	2	0	3	0	0	C3H2O3	86.000395
91	4	6	0	2	0	0	C4H6O2	86.036780
92	5	10	0	1	0	0	C5H10O	86.073165
93	3	5	1	2	0	0	C3H5NO2	87.032029
94	3	4	0	3	0	0	C3H4O3	88.016045
95	3	3	-1	4	0	0	C3H3N-1O4	89.000061
96	3	6	0	3	0	0	C3H6O3	90.031695
97	2	6	2	2	0	0	C2H6N2O2	90.042928
98	2	4	0	4	0	0	C2H4O4	92.010960
99	4	2	2	1	0	0	C4H2N2O	94.016713
100	5	5	1	1	0	0	C5H5NO	95.037114
101	0	1	0	4	1	0	HO4P	95.961247
102	4	4	2	1	0	0	C4H4N2O	96.032363
103	0	3	0	4	1	0	H3O4P	97.976897
104	4	2	0	3	0	0	C4H2O3	98.000395
105	6	10	0	1	0	0	C6H10O	98.073165
106	4	5	1	2	0	0	C4H5NO2	99.032029
107	8	5	1	-1	0	0	C8H5NO-1	99.047284
108	4	4	0	3	0	0	C4H4O3	100.016045
109	4	7	1	2	0	0	C4H7NO2	101.047679
110	4	6	0	3	0	0	C4H6O3	102.031695
111	3	5	1	1	0	1	C3H5NOS	103.009185
112	6	4	2	0	0	0	C6H4N2	104.037448
113	6	3	1	1	0	0	C6H3NO	105.021464
114	3	7	1	1	0	1	C3H7NOS	105.024835
115	7	6	0	1	0	0	C7H6O	106.041865

116	2	6	1	2	1	0	C2H6NO2P	107.013616
117	1	4	-1	5	1	0	CH4N-1O5P	112.976563
118	5	6	0	3	0	0	C5H6O3	114.031695
119	5	10	2	1	0	0	C5H10N2O	114.079313
120	4	5	1	3	0	0	C4H5NO3	115.026944
121	8	5	1	0	0	0	C8H5N	115.042199
122	4	4	0	4	0	0	C4H4O4	116.010960
123	5	8	0	1	0	1	C5H8OS	116.029586
124	4	7	1	1	0	1	C4H7NOS	117.024835
125	4	7	1	3	0	0	C4H7NO3	117.042594
126	5	3	5	-1	0	0	C5H3N5O-1	117.043930
127	8	7	1	0	0	0	C8H7N	117.057849
128	4	6	0	4	0	0	C4H6O4	118.026610
129	7	5	1	1	0	0	C7H5NO	119.037114
130	5	5	5	-1	0	0	C5H5N5O-1	119.059580
131	6	7	3	0	0	0	C6H7N3	121.063997
132	2	6	1	3	1	0	C2H6NO3P	123.008531
133	2	5	0	4	1	0	C2H5O4P	123.992547
134	8	14	0	1	0	0	C8H14O	126.104465
135	5	7	1	3	0	0	C5H7NO3	129.042594
136	6	11	1	2	0	0	C6H11NO2	129.078979
137	7	19	3	-1	0	0	C7H19N3O-1	129.162982
138	5	6	0	4	0	0	C5H6O4	130.026610
139	9	6	0	1	0	0	C9H6O	130.041865
140	6	10	0	3	0	0	C6H10O3	130.062995
141	6	14	2	1	0	0	C6H14N2O	130.110613
142	8	5	1	1	0	0	C8H5NO	131.037114
143	5	9	1	3	0	0	C5H9NO3	131.058244
144	5	8	0	4	0	0	C5H8O4	132.042260
145	4	10	2	1	0	1	C4H10N2OS	134.051384
146	10	16	0	0	0	0	C10H16	136.125200
147	7	7	1	2	0	0	C7H7NO2	137.047679
148	7	6	0	3	0	0	C7H6O3	138.031695
149	9	14	0	1	0	0	C9H14O	138.104465
150	2	8	1	4	1	0	C2H8NO4P	141.019096
151	7	10	0	3	0	0	C7H10O3	142.062995
152	6	9	1	3	0	0	C6H9NO3	143.058244
153	3	1	2	3	1	0	C3HN2O3P	143.972480
154	6	8	0	4	0	0	C6H8O4	144.042260
155	10	8	0	1	0	0	C10H8O	144.057515
156	9	6	0	2	0	0	C9H6O2	146.036780
157	7	1	1	3	0	0	C7HNO3	146.995644
158	5	8	0	5	0	0	C5H8O5	148.037175
159	3	8	2	1	0	2	C3H8N2OS2	152.007805
160	3	7	0	5	1	0	C3H7O5P	154.003112
161	10	18	0	1	0	0	C10H18O	154.135765
162	7	8	0	4	0	0	C7H8O4	156.042260
163	6	11	3	2	0	0	C6H11N3O2	157.085127
164	0	2	0	6	2	0	H2O6P2	159.932664
165	5	8	2	2	0	1	C5H8N2O2S	160.030649
166	6	8	0	5	0	0	C6H8O5	160.037175
167	13	20	0	-1	0	0	C13H20O-1	160.161585
168	0	1	-1	7	2	0	HN-1O7P2	160.916680
169	9	6	0	3	0	0	C9H6O3	162.031695
170	6	10	0	3	0	1	C6H10O3S	162.035066
171	6	10	0	5	0	0	C6H10O5	162.052825
172	6	12	0	5	0	0	C6H12O5	164.068475
173	4	9	0	5	1	0	C4H9O5P	168.018762

174	1	0	0	6	2	0	CO6P2	169.917014
175	3	7	0	6	1	0	C3H7O6P	169.998027
176	9	16	0	3	0	0	C9H16O3	172.109945
177	6	14	4	2	0	0	C6H14N4O2	174.111676
178	0	2	0	7	2	0	H2O7P2	175.927579
179	4	0	0	8	0	0	C4O8	175.959320
180	6	8	0	6	0	0	C6H8O6	176.032090
181	10	8	0	3	0	0	C10H8O3	176.047345
182	7	7	5	1	0	0	C7H7N5O	177.065060
183	0	4	0	7	2	0	H4O7P2	177.943229
184	12	22	0	1	0	0	C12H22O	182.167065
185	4	9	0	6	1	0	C4H9O6P	184.013677
186	10	7	1	3	0	0	C10H7NO3	189.042594
187	10	8	0	4	0	0	C10H8O4	192.042260
188	12	16	0	2	0	0	C12H16O2	192.115030
189	15	30	0	-1	0	0	C15H30O-1	194.239835
190	7	9	5	2	0	0	C7H9N5O2	195.075625
191	4	9	0	7	1	0	C4H9O7P	200.008592
192	8	13	1	5	0	0	C8H13NO5	203.079374
193	11	8	0	4	0	0	C11H8O4	204.042260
194	15	24	0	0	0	0	C15H24	204.187800
195	11	10	0	4	0	0	C11H10O4	206.057910
196	14	26	0	1	0	0	C14H26O	210.198365
197	5	10	1	6	1	0	C5H10NO6P	211.024576
198	5	9	0	7	1	0	C5H9O7P	212.008592
199	12	20	0	3	0	0	C12H20O3	212.141245
200	15	22	0	1	0	0	C15H22O	218.167065
201	8	12	0	7	0	0	C8H12O7	220.058305
202	14	20	0	2	0	0	C14H20O2	220.146330
203	16	28	0	0	0	0	C16H28	220.219100
204	3	2	2	6	2	0	C3H2N2O6P2	223.938812
205	6	10	0	7	0	1	C6H10O7S	226.014726
206	10	14	2	2	0	1	C10H14N2O2S	226.077599
207	14	26	0	2	0	0	C14H26O2	226.193280
208	19	32	0	-2	0	0	C19H32O-2	228.260570
209	8	12	2	4	0	1	C8H12N2O4S	232.051779
210	19	36	0	-2	0	0	C19H36O-2	232.291870
211	19	38	0	-2	0	0	C19H38O-2	234.307520
212	19	26	0	-1	0	0	C19H26O-1	238.208535
213	16	30	0	1	0	0	C16H30O	238.229665
214	6	10	1	7	1	0	C6H10NO7P	239.019491
215	0	3	0	9	3	0	H3O9P3	239.898996
216	11	12	0	6	0	0	C11H12O6	240.063390
217	16	32	0	1	0	0	C16H32O	240.245315
218	6	11	0	8	1	0	C6H11O8P	242.019157
219	16	24	0	2	0	0	C16H24O2	248.177630
220	7	12	3	5	1	0	C7H12N3O5P	249.051459
221	10	11	5	3	0	0	C10H11N5O3	249.086190
222	20	34	0	-1	0	0	C20H34O-1	258.271135
223	18	28	0	1	0	0	C18H28O	260.214015
224	18	30	0	1	0	0	C18H30O	262.229665
225	18	32	0	1	0	0	C18H32O	264.245315
226	18	34	0	1	0	0	C18H34O	266.260965
227	20	12	0	1	0	0	C20H12O	268.088815
228	20	32	0	0	0	0	C20H32	272.250400
229	14	15	1	5	0	0	C14H15NO5	277.095024
230	5	12	0	9	2	0	C5H12O9P2	277.995659
231	8	14	1	8	1	0	C8H14NO8P	283.045706

232	20	28	0	1	0	0	C20H28O	284.214015
233	20	30	0	1	0	0	C20H30O	286.229665
234	20	32	0	1	0	0	C20H32O	288.245315
235	10	15	3	5	0	1	C10H15N3O5S	289.073243
236	20	38	0	1	0	0	C20H38O	294.292265
237	14	12	6	2	0	0	C14H12N6O2	296.102174
238	11	15	5	3	0	1	C11H15N5O3S	297.089561
239	9	12	3	7	1	0	C9H12N3O7P	305.041289
240	10	15	3	6	0	1	C10H15N3O6S	305.068158
241	9	11	2	8	1	0	C9H11N2O8P	306.025305
242	10	17	3	6	0	1	C10H17N3O6S	307.083808
243	22	30	0	1	0	0	C22H30O	310.229665
244	22	32	0	1	0	0	C22H32O	312.245315
245	11	13	2	7	1	0	C11H13N2O7P	316.046040
246	11	12	1	8	1	0	C11H12NO8P	317.030056
247	9	12	3	8	1	0	C9H12N3O8P	321.036204
248	9	14	3	8	1	0	C9H14N3O8P	323.051854
249	12	20	0	10	0	0	C12H20O10	324.105650
250	17	12	0	7	0	0	C17H12O7	328.058305
251	10	12	5	6	1	0	C10H12N5O6P	329.052522
252	10	11	4	7	1	0	C10H11N4O7P	330.036538
253	9	14	4	4	2	1	C9H14N4O4P2S	336.021101
254	9	15	4	8	1	0	C9H15N4O8P	338.062753
255	9	14	3	9	1	0	C9H14N3O9P	339.046769
256	11	21	2	6	1	1	C11H21N2O6PS	340.085796
257	10	12	5	7	1	0	C10H12N5O7P	345.047437
258	10	14	5	7	1	0	C10H14N5O7P	347.063087
259	12	17	3	7	0	1	C12H17N3O7S	347.078723
260	25	34	0	1	0	0	C25H34O	350.260965
261	24	40	0	2	0	0	C24H40O2	360.302830
262	24	38	0	3	0	0	C24H38O3	374.282095
263	11	18	4	5	2	1	C11H18N4O5P2S	380.047316
264	30	48	0	0	0	0	C30H48	408.375600
265	10	13	5	9	2	0	C10H13N5O9P2	409.018854
266	11	22	2	9	2	1	C11H22N2O9P2S	420.052128
267	12	18	4	7	2	1	C12H18N4O7P2S	424.037146
268	19	21	7	5	0	0	C19H21N7O5	427.160418
269	17	19	4	8	1	0	C17H19N4O8P	438.094053
270	9	14	5	12	3	0	C9H14N5O12P3	476.985186
271	25	38	2	5	0	1	C25H38N2O5S	478.250144
272	18	30	0	15	0	0	C18H30O15	486.158475
273	9	16	5	13	3	0	C9H16N5O13P3	494.995751
274	15	17	5	10	2	1	C15H17N5O10P2S	521.017140
275	46	78	-2	-5	0	0	C46H78N-2O-5	522.629627
276	15	21	5	13	2	0	C15H21N5O13P2	541.061114
277	40	64	0	0	0	0	C40H64	544.500800
278	44	72	0	-2	0	0	C44H72O-2	568.573570
279	14	24	7	10	3	1	C14H24N7O10P3S	575.051825
280	14	26	7	11	3	1	C14H26N7O11P3S	593.062390
281	45	72	0	0	0	0	C45H72	612.563400
282	34	63	1	8	0	0	C34H63NO8	613.455369
283	30	32	2	13	0	0	C30H32N2O13	628.190443
284	16	26	7	12	3	1	C16H26N7O12P3S	633.057305
285	15	30	7	13	3	1	C15H30N7O13P3S	641.083520
286	15	30	7	14	3	1	C15H30N7O14P3S	657.078435
287	19	32	7	12	3	1	C19H32N7O12P3S	675.104255
288	28	38	5	13	1	0	C28H38N5O13P	683.220377
289	19	29	6	15	3	1	C19H29N6O15P3S	706.062451

290	20	34	7	14	3	1	C20H34N7O14P3S	721.109735
291	19	29	6	16	3	1	C19H29N6O16P3S	722.057366
292	21	34	7	15	3	1	C21H34N7O15P3S	749.104650
293	21	32	7	16	3	1	C21H32N7O16P3S	763.083915
294	21	34	7	16	3	1	C21H34N7O16P3S	765.099565
295	29	49	3	17	2	0	C29H49N3O17P2	773.253726
296	23	36	7	16	3	1	C23H36N7O16P3S	791.115215
297	23	38	7	17	3	1	C23H38N7O17P3S	809.125780
298	31	52	7	17	1	0	C31H52N7O17P	825.315735
299	26	40	7	16	3	1	C26H40N7O16P3S	831.146515
300	32	52	7	19	1	0	C32H52N7O19P	869.305565
301	30	48	7	18	3	1	C30H48N7O18P3S	919.198945

Table S9. The abundances of species at the phylum level with respect to a dataset containing OTU counts. Further division shows possible species, present at the levels of class, order, family, and genus.

Phylum	Phylum counts	Phylum relative abundance	Class	Order	Family	Genus
Actinobacteria	34	4.39%	*Actinobacteria*	*Actinobacteridae*	*Actinomycetales*	*Actinomycineae*
						Corynebacterineae
						Micrococcineae
					Bifidobacteriales	*Bifidobacteriaceae*
				Coriobacteridae	*Coriobacteriales*	*Coriobacterineae*
Bacteroidetes	129	16.67%	*Bacteroidia*	*Bacteroidales*	*Bacteroidaceae*	*Acetomicrobium*
						Anaerorhabdus
						Bacteroides
					Marinilabiliaceae	*Alkalitalea*
					Porphyromonadaceae	*Barnesiella*
						Butyricimonas
						Odoribacter
						Parabacteroides
						Porphyromonas
						Tannerella
						Unclassified
					Prevotellaceae	*Paraprevotella*
						Prevotella
					Rikenellaceae	*Alistipes*
					Unclassified	*Unclassified*
Cyanobacteria / Chloroplast	2	0.26%	*Chloroplast*	*Chloroplast*	*Streptophyta*	*Unclassified*
			Cyanobacteria	*Family II*	*GpIIa*	*Unclassified*
				Family IV	*GpIV*	*Unclassified*
				Family XI	*GpXI*	*Unclassified*
Firmicutes	594	76.74%	*Bacilli*	*Bacillales*	*Bacillales_Incertae Sedis XI*	*Gemella*
					Bacillaceae 1	*Bacillus*
					Paenibacillaceae 1	*Paenibacillus*
					Planococcaceae	*Planococcaceae_incertae_sedis*
				Lactobacillales	*Carnobacteriaceae*	*Granulicatella*
					Enterococcaceae	*Enterococcus*
					Lactobacillaceae	*Lactobacillus*
					Leuconostocaceae	*Leuconostoc*
						Weissella
					Streptococcaceae	*Lactococcus*
						Streptococcus
			Clostridia	*Clostridiales*	*Clostridiaceae 1*	*Anaerosporobacter*
						Clostridium sensu stricto
					Clostridiales_Incertae Sedis XI	*Peptoniphilus*
					Clostridiales_Incertae Sedis XII	*Unclassified*
					Clostridiales_Incertae Sedis XIII	*Anaerovorax*

					Eubacteriaceae	*Anaerofustis*
						Eubacterium
					Gracilibacteraceae	*Lutispora*
					Lachnospiraceae	*Anaerostipes*
						Blautia
						Clostridium XlVa
						Clostridium XlVb
						Coprococcus
						Dorea
						Howardella
						Lachnospira
						Lachnospiracea_incertae_sedis
						Lactonifactor
						Parasporobacterium
						Pseudobutyrivibrio
						Robinsoniella
						Roseburia
						Ruminococcus2
						Unclassified
					Natranaerovirga	*Unclassified*
					Peptococcaceae 1	*Dehalobacter*
						Desulfonispora
						Peptococcus
						Thermincola
					Peptococcaceae 2	*Desulfotomaculum*
					Peptostreptococcaceae	*Clostridium XI*
						Peptostreptococcus
					Ruminococcaceae	*Acetanaerobacterium*
						Anaerofilum
						Anaerotruncus
						Butyricicoccus
						Clostridium III
						Clostridium IV
						Ethanoligenens
						Faecalibacterium
						Flavonifractor
						Gemmiger
						Hydrogenoanaerobacterium
						Oscillibacter
						Pseudoflavonifractor
						Ruminococcus
						Saccharofermentans
						Subdoligranulum
						Unclassified
					Syntrophomonadaceae	*Syntrophomonas*

					Unclassified	*Unclassified*
			Erysipelotrichia	*Erysipelotrichales*	*Erysipelotrichaceae*	*Catenibacterium*
						Clostridium XVIII
						Coprobacillus
						Erysipelothrix
						Erysipelotrichaceae_incertae_sedis
						Holdemania
						Turicibacter
						Unclassified
			Negativicutes	*Selenomonadales*	*Acidaminococcaceae*	*Acidaminococcus*
						Phascolarctobacterium
					Veillonellaceae	*Centipeda*
						Dialister
						Megamonas
						Selenomonas
						Veillonella
			Unclassified	*Unclassified*	*Unclassified*	*Unclassified*
Fusobacteria	1	0.13%	*Fusobacteriia*	*Fusobacteriales*	*Fusobacteriaceae*	*Cetobacterium*
Lentisphaerae	1	0.13%	*Lentisphaeria*	*Victivallales*	*Victivallaceae*	*Victivallis*
				Unclassified	*Unclassified*	*Unclassified*
			Unclassified	*Unclassified*	*Unclassified*	*Unclassified*
Proteobacteria	29	3.75%	*Alphaproteobacteria*	*Rhizobiales*	*Hyphomicrobiaceae*	*Devosia*
				Rhodospirillales	*Rhodospirillaceae*	*Rhodospirillum*
						Caenispirillum
						Magnetospira
						Unclassified
				Kiloniellales	*Kiloniellaceae*	*Kiloniella*
				Sphingomonadales	*Sphingomonadaceae*	*Sphingomonas*
				Unclassified	*Unclassified*	*Unclassified*
			Betaproteobacteria	*Burkholderiales*	*Oxalobacteraceae*	*Massilia*
						Oxalobacter
					Sutterellaceae	*Parasutterella*
						Sutterella
						Unclassified
					Burkholderiales_incertae_sedis	*Piscinibacter*
					Comamonadaceae	*Schlegelella*
					Unclassified	*Unclassified*
			Deltaproteobacteria	*Bdellovibrionales*	*Bdellovibrionaceae*	*Vampirovibrio*
				Desulfovibrionales	*Desulfovibrionaceae*	*Bilophila*
						Desulfovibrio
						Unclassified
				Unclassified	*Unclassified*	*Unclassified*
			Epsilonproteobacteria	*Campylobacterales*	*Campylobacteraceae*	*Campylobacter*
			Gammaproteobacteria	*Enterobacteriales*	*Enterobacteriaceae*	*Citrobacter*

						Enterobacter
						Escherichia/Shigella
						Klebsiella
						Unclassified
				Pasteurellales	*Pasteurellaceae*	*Haemophilus*
				Vibrionales	*Vibrionaceae*	*Photobacterium*
Tenericutes	3	0.39%	*Mollicutes*	*Acholeplasmatales*	*Acholeplasmataceae*	*Acholeplasma*
				Entomoplasmatales	*Spiroplasmataceae*	*Spiroplasma*
Verrucomicrobia	4	0.52%	*Verrucomicrobiae*	*Verrucomicrobiales*	*Verrucomicrobiaceae*	*Akkermansia*
						Haloferula
						Prosthecobacter
						Verrucomicrobium
Unclassified	21	2.71%	*Unclassified*	*Unclassified*	*Unclassified*	*Unclassified*

Table S10. The features selected from the OTU counts dataset by finding an optimal tuning parameter ***s*** through scoring the generated clustering dendrograms. In addition, their ranks are shown as the minimal value of the tuning parameter that is necessary to include a feature into calculations in regard to clustering.

id	s	Phylum	Class	Order	Family	Genus
OTU_22	1.1	*Firmicutes*	*Negativicutes*	*Selenomonadales*	*Veillonellaceae*	*Dialister*
OTU_8	1.1	*Firmicutes*	*Clostridia*	*Clostridiales*	*Ruminococcaceae*	*Ruminococcus*
OTU_17	1.3	*Firmicutes*	*Clostridia*	*Clostridiales*	*Lachnospiraceae*	*Coprococcus*
OTU_38	1.6	*Bacteroidetes*	*Bacteroidia*	*Bacteroidales*	*Bacteroidaceae*	*Bacteroides*
OTU_9	1.7	*Bacteroidetes*	*Bacteroidia*	*Bacteroidales*	*Rikenellaceae*	*Alistipes*
OTU_124	1.8	*Bacteroidetes*	*Bacteroidia*	*Bacteroidales*	*Bacteroidaceae*	*Bacteroides*
OTU_34	1.9	*Bacteroidetes*	*Bacteroidia*	*Bacteroidales*	*Bacteroidaceae*	*Bacteroides*
OTU_30	2.2	*Firmicutes*	*Negativicutes*	*Selenomonadales*	*Acidaminococcaceae*	*Phascolarctobacterium*
OTU_19	2.4	*Firmicutes*	*Clostridia*	*Clostridiales*	*Ruminococcaceae*	*Ruminococcus*
OTU_21	2.4	*Actinobacteria*	*Actinobacteria*	*Actinobacteridae*	*Bifidobacteriales*	*Bifidobacteriaceae*
OTU_12	2.5	*Firmicutes*	*Erysipelotrichia*	*Erysipelotrichales*	*Erysipelotrichaceae*	*Clostridium XVIII* *unclassified_Erysipelotrichaceae*
OTU_15	2.7	*Actinobacteria*	*Actinobacteria*	*Actinobacteridae*	*Bifidobacteriales*	*Bifidobacteriaceae*
OTU_4	3.1	*Bacteroidetes*	*Bacteroidia*	*Bacteroidales*	*Bacteroidaceae*	*Bacteroides*
OTU_59	3.1	*Bacteroidetes*	*Bacteroidia*	*Bacteroidales*	*Bacteroidaceae*	*Bacteroides*
OTU_406	3.2	*Bacteroidetes*	*Bacteroidia*	*Bacteroidales*	*Bacteroidaceae*	*Bacteroides*
OTU_304	3.4	*Verrucomicrobia*	*Verrucomicrobiae*	*Verrucomicrobiales*	*Verrucomicrobiaceae*	*Akkermansia* *Haloferula*
OTU_36	3.4	*Firmicutes*	*Clostridia*	*Clostridiales*	*Ruminococcaceae*	*Ruminococcus*
OTU_40	3.4	*Bacteroidetes*	*Bacteroidia*	*Bacteroidales*	*Rikenellaceae*	*Alistipes*
OTU_155	3.6	*Bacteroidetes*	*Bacteroidia*	*Bacteroidales*	*Bacteroidaceae*	*Bacteroides*
OTU_37	3.6	*Verrucomicrobia*	*Verrucomicrobiae*	*Verrucomicrobiales*	*Verrucomicrobiaceae*	*Akkermansia* *Verrucomicrobium*
OTU_372	3.6	*Bacteroidetes*	*Bacteroidia*	*Bacteroidales*	*Bacteroidaceae*	*Bacteroides*
OTU_433	3.6	*Bacteroidetes*	*Bacteroidia*	*Bacteroidales*	*Bacteroidaceae*	*Bacteroides*
OTU_69	3.6	*Proteobacteria*	*Betaproteobacteria*	*Burkholderiales*	*Oxalobacteraceae*	*Massilia*
	3.6				*Sutterellaceae*	*Parasutterella*
	3.6					*Sutterella*
OTU_70	3.6	*Bacteroidetes*	*Bacteroidia*	*Bacteroidales*	*Bacteroidaceae*	*Bacteroides*
OTU_205	4.0	*Bacteroidetes*	*Bacteroidia*	*Bacteroidales*	*Porphyromonadaceae*	*Parabacteroides*
OTU_32	4.0	*Firmicutes*	*Erysipelotrichia*	*Erysipelotrichales*	*Erysipelotrichaceae*	*Erysipelotrichaceae_incertae_sedis*
OTU_31	4.3	*Actinobacteria*	*Actinobacteria*	*Actinobacteridae*	*Bifidobacteriales*	*Bifidobacteriaceae*
OTU_35	4.3	*Actinobacteria*	*Actinobacteria*	*Coriobacteridae*	*Coriobacteriales*	*Coriobacterineae*
OTU_405	4.3	*Bacteroidetes*	*Bacteroidia*	*Bacteroidales*	*Bacteroidaceae*	*Bacteroides*
OTU_14	4.4	*Bacteroidetes*	*Bacteroidia*	*Bacteroidales*	*Bacteroidaceae*	*Bacteroides*
OTU_599	4.4	*Proteobacteria*	*Betaproteobacteria*	*Burkholderiales*	*Oxalobacteraceae*	*Massilia*
					Sutterellaceae	*Parasutterella*
						Sutterella
OTU_50	4.6	*Firmicutes*	*Clostridia*	*Clostridiales*	*Lachnospiraceae*	*Roseburia*
OTU_53	4.6	*Firmicutes*	*Clostridia*	*Clostridiales*	*Lachnospiraceae*	*Clostridium XlVa*
						unclassified_Lachnospiraceae
					unclassified_Clostridiales	-
OTU_589	4.7	*Firmicutes*	*Clostridia*	*Clostridiales*	*Lachnospiraceae*	*Roseburia*
OTU_623	4.7	*Firmicutes*	*Clostridia*	*Clostridiales*	*Lachnospiraceae*	*Roseburia*
OTU_99	4.7	*Bacteroidetes*	*Bacteroidia*	*Bacteroidales*	*Bacteroidaceae*	*Bacteroides*
OTU_268	4.8	*Bacteroidetes*	*Bacteroidia*	*Bacteroidales*	*Porphyromonadaceae*	*Parabacteroides*
OTU_62	4.8	*Firmicutes*	*Clostridia*	*Clostridiales*	*Lachnospiraceae*	*Lachnospiracea_incertae_sedis*
OTU_87	4.8	*Bacteroidetes*	*Bacteroidia*	*Bacteroidales*	*Porphyromonadaceae*	*Parabacteroides*
OTU_92	4.8	*Firmicutes*	*Clostridia*	*Clostridiales*	*Lachnospiraceae*	*Lachnospiracea_incertae_sedis*
OTU_395	4.9	*Firmicutes*	*Clostridia*	*Clostridiales*	*Lachnospiraceae*	*Blautia*
						unclassified_Lachnospiraceae
OTU_622	4.9	*Bacteroidetes*	*Bacteroidia*	*Bacteroidales*	*Bacteroidaceae*	*Bacteroides*
OTU_142	5	*Firmicutes*	*Clostridia*	*Clostridiales*	*Lachnospiraceae*	*Coprococcus*
OTU_142	5.0	*Firmicutes*	*Clostridia*	*Clostridiales*	*Lachnospiraceae*	*Lachnospiracea_incertae_sedis*
						unclassified_Lachnospiraceae
OTU_857	5	*Bacteroidetes*	*Bacteroidia*	*Bacteroidales*	*Bacteroidaceae*	*Bacteroides*
OTU_270	5.1	*Bacteroidetes*	*Bacteroidia*	*Bacteroidales*	*Bacteroidaceae*	*Bacteroides*
OTU_68	5.1	*Firmicutes*	*Clostridia*	*Clostridiales*	*Ruminococcaceae*	*Oscillibacter*
OTU_97	5.1	*Firmicutes*	*Clostridia*	*Clostridiales*	*Ruminococcaceae*	*Oscillibacter*
						unclassified_Ruminococcaceae
OTU_98	5.1	*Firmicutes*	*Erysipelotrichia*	*Erysipelotrichales*	*Erysipelotrichaceae*	*Clostridium XVIII*
						unclassified_Erysipelotrichaceae
OTU_33	5.2	*Firmicutes*	*Clostridia*	*Clostridiales*	*Ruminococcaceae*	*Anaerotruncus*
						unclassified_Ruminococcaceae
OTU_348	5.2	*Bacteroidetes*	*Bacteroidia*	*Bacteroidales*	*Porphyromonadaceae*	*Parabacteroides*
OTU_713	5.2	*Bacteroidetes*	*Bacteroidia*	*Bacteroidales*	*Bacteroidaceae*	*Bacteroides*
OTU_25	5.3	*Firmicutes*	*Clostridia*	*Clostridiales*	*Ruminococcaceae*	*Ruminococcus*

OTU_72	5.3	*Firmicutes*	*Clostridia*	*Clostridiales*	*Ruminococcaceae*	*Oscillibacter*
OTU_130	5.4	*Firmicutes*	*Negativicutes*	*Selenomonadales*	*Acidaminococcaceae*	*Phascolarctobacterium*
OTU_134	5.4	*Firmicutes*	*Clostridia*	*Clostridiales*	*Lachnospiraceae*	*Lachnospiracea_incertae_sedis*
OTU_454	5.4	*Bacteroidetes*	*Bacteroidia*	*Bacteroidales*	*Bacteroidaceae*	*Bacteroides*
OTU_254	5.5	*Firmicutes*	*Clostridia*	*Clostridiales*	*Lachnospiraceae*	*Blautia*
						unclassified_Lachnospiraceae
OTU_80	5.5	*Firmicutes*	*Clostridia*	*Clostridiales*	*Eubacteriaceae*	*Eubacterium*
					Ruminococcaceae	*Clostridium IV*
						Ruminococcus
OTU_284	5.6	*Bacteroidetes*	*Bacteroidia*	*Bacteroidales*	*Porphyromonadaceae*	*Parabacteroides*
OTU_825	5.6	*Firmicutes*	*Clostridia*	*Clostridiales*	*Ruminococcaceae*	*Oscillibacter*
						unclassified_Ruminococcaceae
OTU_111	5.7	*Firmicutes*	*Clostridia*	*Clostridiales*	*unclassified_Clostridiales*	-
OTU_67	5.7	*Firmicutes*	*Clostridia*	*Clostridiales*	*Lachnospiraceae*	*Clostridium XlVa*
						Lachnospiracea_incertae_sedis
OTU_686	5.7	*Firmicutes*	*Clostridia*	*Clostridiales*	*Ruminococcaceae*	*Faecalibacterium*
OTU_93	5.7	*Bacteroidetes*	*Bacteroidia*	*Bacteroidales*	*Rikenellaceae*	*Alistipes*
OTU_56	5.8	*Firmicutes*	*Clostridia*	*Clostridiales*	*Ruminococcaceae*	*Clostridium IV*
OTU_91	5.8	*Bacteroidetes*	*Bacteroidia*	*Bacteroidales*	*Bacteroidaceae*	*Bacteroides*
OTU_140	5.9	*Firmicutes*	*Clostridia*	*Clostridiales*	*Lachnospiraceae*	*Coprococcus*
OTU_94	5.9	*Bacteroidetes*	*Bacteroidia*	*Bacteroidales*	*Rikenellaceae*	*Alistipes*
OTU_13	6.0	*Firmicutes*	*Clostridia*	*Clostridiales*	*Ruminococcaceae*	*Gemmiger*
						Subdoligranulum
						unclassified_Ruminococcaceae
OTU_146	6	*Bacteroidetes*	*Bacteroidia*	*Bacteroidales*	*Porphyromonadaceae*	*Odoribacter*
OTU_295	6	*Bacteroidetes*	*Bacteroidia*	*Bacteroidales*	*Bacteroidaceae*	*Bacteroides*
OTU_107	6.1	*Proteobacteria*	*Gammaproteobacteria*	*Enterobacteriales*	*Enterobacteriaceae*	*Escherichia/Shigella*
OTU_794	6.1	*Bacteroidetes*	*Bacteroidia*	*Bacteroidales*	*Porphyromonadaceae*	*Parabacteroides*
OTU_16	6.2	*Verrucomicrobia*	*Verrucomicrobiae*	*Verrucomicrobiales*	*Verrucomicrobiaceae*	*Akkermansia*
						Prosthecobacter
OTU_362	6.2	*Bacteroidetes*	*Bacteroidia*	*Bacteroidales*	*Bacteroidaceae*	*Bacteroides*
OTU_42	6.2	*Bacteroidetes*	*Bacteroidia*	*Bacteroidales*	*Bacteroidaceae*	*Bacteroides*
OTU_426	6.3	*Firmicutes*	*Clostridia*	*Clostridiales*	*Lachnospiraceae*	*Lachnospira*
						unclassified_Lachnospiraceae
OTU_838	6.3	*Firmicutes*	*Clostridia*	*Clostridiales*	*Ruminococcaceae*	*Faecalibacterium*
OTU_11	6.4	*Firmicutes*	*Clostridia*	*Clostridiales*	*Lachnospiraceae*	*Lachnospiracea_incertae_sedis*
OTU_333	6.4	*Firmicutes*	*Clostridia*	*Clostridiales*	*Lachnospiraceae*	*Blautia*
OTU_81	6.5	*Firmicutes*	*Clostridia*	*Clostridiales*	*Eubacteriaceae*	*Eubacterium*
					Ruminococcaceae	*Clostridium IV*
						unclassified_Ruminococcaceae
OTU_826	6.5	*Firmicutes*	*Clostridia*	*Clostridiales*	*Ruminococcaceae*	*Ruminococcus*
OTU_174	6.6	*Firmicutes*	*Clostridia*	*Clostridiales*	*Ruminococcaceae*	*Anaerotruncus*
						Clostridium IV
OTU_374	6.6	*Bacteroidetes*	*Bacteroidia*	*Bacteroidales*	*Bacteroidaceae*	*Bacteroides*
OTU_169	6.7	*Firmicutes*	*Clostridia*	*Clostridiales*	*Ruminococcaceae*	*Oscillibacter*
						unclassified_Ruminococcaceae
OTU_240	6.7	*Firmicutes*	*Clostridia*	*Clostridiales*	*Lachnospiraceae*	*Lachnospiracea_incertae_sedis*
						unclassified_Lachnospiraceae
OTU_120	6.8	*Firmicutes*	*Clostridia*	*Clostridiales*	*Lachnospiraceae*	*Clostridium XlVa*
						Ruminococcus2
						unclassified_Lachnospiraceae

Table S11. The features selected from the stool metabolome dataset by finding an optimal tuning parameter through scoring the generated clustering dendrograms. In addition, their ranks are shown as the minimal value of the tuning parameter that is necessary to include a feature into calculations in regard to clustering. Only features assigned to one or more entries from the HMDB database are shown.

Experimental mass	s	HMDB id	Name	Molecular formula	Adduct type
395.007226	1.1	HMDB31554	Sucralose	C12H19Cl3O8	[M-H]-
430.983960	1.1	HMDB31554	Sucralose	C12H19Cl3O8	[M+Cl]-
471.242194	1.6	HMDB02522	Chenodeoxycholic acid sulfate	C24H40O7S	[M-H]-
		HMDB02586	Chenodeoxycholic acid 3-sulfate		
		HMDB02642	Ursodeoxycholic acid 3-sulfate		
681.276065	1.7	HMDB36528	Myricanol 5-laminaribioside	C33H46O15	[M-H]-
		HMDB36529	Myricanol 5-beta-sophoroside		
305.069954	1.7	HMDB60568	10,11-Dihydroxycarbamazepine	C15H14N2O3	[M+Cl]-
475.233740	2.6	HMDB03141	Retinoyl b-glucuronide	C26H36O8	[M-H]-
		HMDB30153	Austalide H		
491.228749	2.7	HMDB60123	rac-5,6-Epoxy-retinoyl-beta-D-glucuronide	C26H36O9	[M-H]-
493.244470	2.7	HMDB33655	7,11-Bisdeacetylvaltrate 7-(3-methylpentanoate) 11-(3-hydroxy-3-methylbutanoate)	C26H38O9	[M-H]-
481.272618	2.7	HMDB30913	Cepagenin	C27H42O5	[M+Cl]-
		HMDB31079	12-Ketoporrigenin		
		HMDB32680	Neoporrigenin B		
		HMDB33583	Leontogenin		
		HMDB34189	Taccagenin		
		HMDB34424	Spirotaccagenin		
		HMDB60129	24-Oxo-1alpha,23,25-trihydroxyvitamin D3		
259.181566	3.0	HMDB14413	Ropinirole	C16H24N2O	[M-H]-
		HMDB15070	Oxymetazoline		
335.197586	3.2	HMDB15324	Acebutolol	C18H28N2O4	[M-H]-
517.244405	4.0	HMDB30154	Austalide G	C28H38O9	[M-H]-
277.253651	4.2	HMDB33609	2-Pentadecylfuran	C19H34O	[M-H]-
593.334631	4.4	HMDB04159	L-Urobilin	C33H46N4O6	[M-H]-
455.247294	4.7	HMDB00907	Sulfolithocholic acid	C24H40O6S	[M-H]-
489.213110	5.0	HMDB34434	Austalide F	C26H34O9	[M-H]-
		HMDB35073	Deacetylnomilinic acid		
		HMDB39120	alpha-Crocetin glucosyl ester		
		HMDB60122	4-Oxo-9-cis-retinoyl-beta-glucuronide		
439.379305	5.6	HMDB11559	MG(0:0/24:1(15Z)/0:0)	C27H52O4	[M-H]-
		HMDB11589	MG(24:1(15Z)/0:0/0:0)		
343.124505	5.7	HMDB02928	Maltitol	C12H24O11	[M-H]-
		HMDB06791	Melibiitol		
		HMDB29911	1-O-alpha-D-Glucopyranosyl-D-mannitol		
		HMDB40937	Lactitol		
455.353074	5.7	HMDB02364	Oleanolic acid	C30H48O3	[M-H]-
		HMDB02388	Boswellic acid		
		HMDB02395	Ursolic acid		
		HMDB30094	Betulinic acid		
		HMDB31882	Sandosapogenol		
		HMDB32256	(+-)-Ethyl 3-hydroxy-2-methylbutyrate		
		HMDB33020	Ganodermanondiol		
		HMDB34652	Soyasapogenol E		
		HMDB34654	Katonic acid		
		HMDB34655	3-Epikatonic acid		
		HMDB34961	beta-Elemolic acid		
		HMDB34962	3alpha-3-Hydroxytirucalla-7,24-dien-21-oic acid		
		HMDB34964	alpha-Elemolic acid		
		HMDB35119	Isomangiferolic acid		
		HMDB35263	Oxyallobetulin		
		HMDB35315	Ganodermatriol		
		HMDB35353	Epoxyganoderiol C		
		HMDB35511	Trametenolic acid B		
		HMDB35775	11-Deoxoglycyrrhetinic acid		
		HMDB36675	3beta-Hydroxy-28,13-ursanolide		
		HMDB36757	Bryonolic acid		
		HMDB36962	3-Epioleanolic acid		
		HMDB38177	3-Hydroxycycloart-24-en-21-oic acid		
		HMDB38703	Carissic acid		
		HMDB39690	Glycyrrhetol		
		HMDB40455	Lucidadiol		
		HMDB40456	Ganoderic acid Z		
		HMDB40652	3-Hydroxy-28,13-lupanolide		
		HMDB40976	3-Epimasticadienolic acid		

315.087436	5.8	HMDB30111	Homoferreirin	C17H16O6	[M-H]-
		HMDB33298	3-(3,4-Dihydroxybenzyl)-7-hydroxy-5-methoxy-4-chromanone		
		HMDB33683	Melilotocarpan E		
		HMDB33692	Melilotocarpan D		
		HMDB33797	Olivin		
		HMDB33924	Cajanol		
		HMDB37251	5,8-Dihydroxy-3-(4-hydroxybenzyl)-7-methoxy-4-chromanone		
		HMDB37477	5,7-Dihydroxy-3-(3-hydroxy-4-methoxybenzyl)-4-chromanone		
		HMDB37481	3',5-Dihydroxy-4',7-dimethoxyflavanone		
		HMDB37749	4',7-Dihydroxy-2',5-dimethoxyisoflavanone		
		HMDB41234	Artocarpanone A		
		HMDB41790	Violanone		
367.158443	5.8	HMDB01032	Dehydroepiandrosterone sulfate	C19H28O5S	[M-H]-
		HMDB02833	Testosterone sulfate		
		HMDB13230	Epitestosterone sulfate		
377.085613	5.8	HMDB00048	Melibiose	C12H22O11	[M+Cl]-
		HMDB00055	Cellobiose		
		HMDB00163	D-Maltose		
		HMDB00186	Alpha-Lactose		
		HMDB00258	Sucrose		
		HMDB00740	Lactulose		
		HMDB00975	Trehalose		
		HMDB02923	Isomaltose		
		HMDB05826	Galactinol		
		HMDB06603	3-b-Galactopyranosyl glucose		
		HMDB06792	Epimelibiose		
		HMDB11740	Turanose		
		HMDB11742	Kojibiose		
		HMDB29880	Neotrehalose		
		HMDB29882	Sakebiose		
		HMDB29898	Inulobiose		
		HMDB29902	Galabiose		
		HMDB29919	Maltulose		
		HMDB29933	Mannobiose		
		HMDB33368	DEAE-cellulose		
		HMDB38489	Allolactose		
		HMDB39237	Glucinol		
		HMDB39727	Trehalulose		
		HMDB39876	Fagopyritol A1		
		HMDB41627	beta-Lactose		
		HMDB60068	Glucose-1,3-mannose oligosaccharide		
411.347989	5.9	HMDB11552	MG(0:0/22:1(13Z)/0:0)	C25H48O4	[M-H]-
		HMDB11582	MG(22:1(13Z)/0:0/0:0)		
307.085608	5.9	HMDB35191	(2S,4R)-4-(9H-Pyrido[3,4-b]indol-1-yl)-1,2,4-butanetriol	C15H16N2O3	[M+Cl]-
289.192168	6.0	HMDB13962	Verapamil metabolite D-617	C17H26N2O2	[M-H]-
		HMDB60962	3-hydroxyropivacaine		
261.076875	6.1	HMDB30882	(S)-Rutaretin	C14H14O5	[M-H]-
		HMDB32838	Dorsteniol		
		HMDB39027	Celereoin		
369.174082	6.2	HMDB02759	Androsterone sulfate	C19H30O5S	[M-H]-
		HMDB06278	5a-Dihydrotestosterone sulfate		
		HMDB13232	Etiocholanolone sulfate		
		HMDB41918	Lorcainide	C22H27ClN2O	[M-H]-
		HMDB38223	Carnocin U I49	C22H26N2O	[M+Cl]-
589.303136	6.4	HMDB04158	D-Urobilinogen	C33H42N4O6	[M-H]-
		HMDB04160	I-Urobilin		
275.238001	6.5	HMDB05830	5a-Androstan-3b-ol	C19H32O	[M-H]-
517.221193	6.6	HMDB10351	11-beta-Hydroxyandrosterone-3-glucuronide	C25H38O9	[M+Cl]-
276.160485	6.8	HMDB36325	Dinorcapsaicin	C16H23NO3	[M-H]-
225.007466	6.9	HMDB15491	Nitroxoline	C9H6N2O3	[M+Cl]-
487.237088	7.0	HMDB02421	7-Sulfocholic acid	C24H40O8S	[M-H]-
		HMDB15048	Repaglinide	C27H36N2O4	[M+Cl]-
359.077293	7.2	HMDB03572	Rosmarinic acid	C18H16O8	[M-H]-
		HMDB30812	Acerosin		
		HMDB33819	Jaceidin		
		HMDB37334	Majoranin		
		HMDB37335	Sudachitin		
		HMDB38356	Sideritiflavone		
		HMDB40344	3,5,6-Trihydroxy-3',4',7-trimethoxyflavone		
		HMDB40472	Agamanone		
		HMDB40877	3,5,8-Trihydroxy-3',4',7-trimethoxyflavone		
373.071870	7.3	HMDB29538	Neodiospyrin	C22H14O6	[M-H]-

413.163920	7.3	HMDB61127	4R-Hydroxy solifenacin	C23H26N2O3	[M+Cl]-
427.262068	7.3	HMDB00348	3b,12a-Dihydroxy-5a-cholanoic acid	C24H40O4	[M+Cl]-
		HMDB00361	3b,7a-Dihydroxy-5b-cholanoic acid		
		HMDB00384	3a,7a-Dihydroxycholanoic acid		
		HMDB00411	3a,12b-Dihydroxy-5b-cholanoic acid		
		HMDB00438	3b,12a-Dihydroxy-5b-cholanoic acid		
		HMDB00478	Allodeoxycholic acid		
		HMDB00514	Allochenodeoxycholic acid		
		HMDB00518	Chenodeoxycholic acid		
		HMDB00626	Deoxycholic acid		
		HMDB00664	Isohyodeoxycholic acid		
		HMDB00686	Isoursodeoxycholic acid		
		HMDB00733	Hyodeoxycholic acid		
		HMDB00811	Murocholic acid		
		HMDB00946	Ursodeoxycholic acid		
		HMDB02451	7b,12a-Dihydroxycholanoic acid		
		HMDB02488	7a,12b-dihydroxy-5b-Cholan-24-oic acid		
		HMDB02536	Isodeoxycholic acid		
		HMDB02585	3b,12b-Dihydroxy-5b-cholanoic acid		
316.090707	7.4	HMDB61168	N2-Monodes-methylnizatidine	C11H19N5O2S2	[M-H]-
511.342939	7.4	HMDB31879	11a,12a-Epoxy-3b-hydroxy-28,13-oleananolide 3-acetate	C32H48O5	[M-H]-
		HMDB34646	3beta-Acetoxy-12-oxo-28,13beta-oleananolide		
		HMDB35313	Ganoderic acid S		
		HMDB35330	Ganoderic acid Mf		
		HMDB35332	Ganoderic acid X		
		HMDB36672	3alpha-Acetoxy-11-keto-beta-boswellic acid		
235.039440	7.5	HMDB28750	Aspartyl-Cysteine	C7H12N2O5S	[M-H]-
		HMDB28771	Cysteinyl-Aspartate		
395.189649	7.5	HMDB00774	Pregnenolone sulfate	C21H32O5S	[M-H]-
		HMDB60382	3beta-Hydroxypregn-5-en-20-one sulfate		
274.144860	7.6	HMDB41488	4,5-Dihydropiperlonguminine	C16H21NO3	[M-H]-
		HMDB60989	4'-hydroxypropanolol		
216.033602	7.7	HMDB06409	Tyramine-O-sulfate	C8H11NO4S	[M-H]-
525.358568	7.9	HMDB36673	3alpha-Acetomethoxy-11alpha-oxo-12-ursen-24-oic acid	C33H50O5	[M-H]-
195.052378	8.0	HMDB01857	1,3-Dimethyluric acid	C7H8N4O3	[M-H]-
		HMDB01982	3,7-Dimethyluric acid		
		HMDB02026	1,9-Dimethyluric acid		
		HMDB04308	7,9-Dimethyluric acid		
		HMDB11103	1,7-Dimethyluric acid		
		HMDB59704	3,9-Dimethyluric acid		
301.165648	8.4	HMDB31094	Glycerol tributanoate	C15H26O6	[M-H]-
498.289352	8.5	HMDB00874	Tauroursodeoxycholic acid	C26H45NO6S	[M-H]-
		HMDB00896	Taurodeoxycholic acid		
		HMDB00951	Taurochenodesoxycholic acid		
767.583376	8.5	HMDB12087	SM(d18:0/18:0)	C41H85N2O6P	[M+Cl]-
285.113201	8.7	HMDB30152	4'-Hydroxy-5,7-dimethoxyflavan	C17H18O4	[M-H]-
		HMDB30521	Sativan		
		HMDB34024	Isosativan		
		HMDB41168	Myrigalone G		
		HMDB41169	Myrigalone H		
		HMDB41671	4'-Hydroxy-3,4,5-trimethoxystilbene		
		HMDB41680	4-Hydroxy-3,5,4'-trimethoxystilbene		
319.191513	9.0	HMDB12798	5'-Carboxy-alpha-chromanol	C19H28O4	[M-H]-
		HMDB37591	Oryzalide A		
		HMDB37592	Oryzalide B		
		HMDB39276	[8]-Gingerdione		
		HMDB39821	10-Acetylpanaxytriol		
199.170372	9.1	HMDB00638	Dodecanoic acid	C12H24O2	[M-H]-
		HMDB30998	Ethyl decanoate		
		HMDB32310	2-Heptyl butyrate		
		HMDB32440	Nonanal propyleneglycol acetal		
		HMDB33619	Hexyl hexanoate		
		HMDB34128	Isopropyl nonanoate		
		HMDB34136	Octyl butanoate		
		HMDB34137	Octyl 2-methylpropanoate		
		HMDB35410	(R)-Dihydrocitronellol acetate		
		HMDB36225	Pentyl heptanoate		
		HMDB40166	Decyl acetate		
		HMDB59868	Isobutyl octanoate		
489.140264	9.2	HMDB40512	4',5,6-Trimethylscutellarein 7-glucoside	C24H26O11	[M-H]-
		HMDB14703	Methotrexate	C20H22N8O5	[M+Cl]-
411.267134	9.3	HMDB00381	Allolithocholic acid	C24H40O3	[M+Cl]-

		HMDB00713	Isoallolithocholic acid		
		HMDB00717	Isolithocholic acid		
		HMDB00761	Lithocholic acid		
		HMDB02431	12b-Hydroxy-5b-cholanoic acid		
		HMDB02492	7a-Hydroxy-5b-cholanic acid		
413.200296	9.3	HMDB14701	Doxapram	C24H30N2O2	[M+Cl]-
575.431460	9.5	HMDB33949	beta-Sitosterol 3-O-beta-D-galactopyranoside	C35H60O6	[M-H]-
		HMDB34185	Schottenol 3-glucoside		
317.103066	9.7	HMDB30663	4',7-Di-O-methylcatechin	C17H18O6	[M-H]-
471.202533	9.7	HMDB35684	Deacetylnomilin	C26H32O8	[M-H]-
381.097753	9.8	HMDB33339	Mollicellin A	C21H18O7	[M-H]-
		HMDB33340	Mollicellin B		
		HMDB40673	Artonin K		
331.060507	9.8	HMDB60759	4-Carboxynevirapine	C15H12N4O3	[M+Cl]-
631.530946	10.0	HMDB56183	DG(18:1n7/0:0/18:2n6)	C40H72O5	[M-H]-
		HMDB56185	DG(18:1n7/0:0/20:2n6)		
		HMDB56202	DG(18:1n9/0:0/18:2n6)		
		HMDB56204	DG(18:1n9/0:0/20:2n6)		
531.229581	10.1	HMDB03080	Leukotriene D4	C25H40N2O6S	[M+Cl]-
272.129244	10.2	HMDB30187	(E,E)-Piperlonguminine	C16H19NO3	[M-H]-
		HMDB38834	(2E)-Piperamide-C5:1		
305.066751	10.2	HMDB38361	(-)-Epigallocatechin	C15H14O7	[M-H]-
		HMDB38365	(+)-Gallocatechin		
457.223166	10.2	HMDB34760	Hydroxystrobilurin D	C26H34O7	[M-H]-
527.337863	10.3	HMDB33079	Ganoderic acid V	C32H48O6	[M-H]-
		HMDB35225	(22S)-Acetoxy-3alpha,15alpha-dihydroxylanosta-7,9(11),24-trien-26-oic acid		
		HMDB35335	(24E)-3alpha-Acetoxy-15alpha,22S-dihydroxylanosta-7,9(11),24-trien-26-oic acid		
343.085530	10.3	HMDB37521	C.I. Solvent Red 80	C18H16N2O3	[M+Cl]-
		HMDB40367	Azacridone A		
307.082327	10.4	HMDB40692	4R,5R,6S-Trihydroxy-2-hydroxymethyl-2-cyclohexen-1-one 6-(2-hydroxy-6-methylbenzoate)	C15H16O7	[M-H]-
329.248523	10.4	HMDB01976	Docosapentaenoic acid (22n-6)	C22H34O2	[M-H]-
		HMDB06528	Docosapentaenoic acid		
		HMDB32257	Ethyl abietate		
		HMDB35024	ent-16-Kauren-19-ol acetate		
		HMDB35581	1-Phenyl-1,3-hexadecanedione		
		HMDB38909	2-Methyl-5-(8,11-pentadecadienyl)-1,3-benzenediol		
		HMDB39133	4,8,12,15,19-Docosapentaenoic acid		
		HMDB39530	Ethyl icosapentate		
		HMDB60113	Docosa-4,7,10,13,16-pentaenoic acid		
425.246467	10.4	HMDB00328	12-Ketodeoxycholic acid	C24H38O4	[M+Cl]-
		HMDB00460	7-Hydroxy-3-oxocholanoic acid		
		HMDB00467	Nutriacholic acid		
		HMDB00503	7a-Hydroxy-3-oxo-5b-cholanoic acid		
		HMDB12866	9'-Carboxy-alpha-chromanol		
		HMDB41454	D8'-Merulinic acid A		
357.279883	10.5	HMDB06322	Tetracosapentaenoic acid (24:5n-6)	C24H38O2	[M-H]-
		HMDB06323	Tetracosapentaenoic acid (24:5n-3)		
		HMDB35583	1-Phenyl-1,3-octadecanedione		
617.515187	10.5	HMDB07059	DG(14:1(9Z)/22:2(13Z,16Z)/0:0)	C39H70O5	[M-H]-
		HMDB07110	DG(16:0/20:3(5Z,8Z,11Z)/0:0)		
		HMDB07111	DG(16:0/20:3(8Z,11Z,14Z)/0:0)		
		HMDB07138	DG(16:1(9Z)/20:2(11Z,14Z)/0:0)		
		HMDB07162	DG(18:0/18:3(6Z,9Z,12Z)/0:0)		
		HMDB07163	DG(18:0/18:3(9Z,12Z,15Z)/0:0)		
		HMDB07190	DG(18:1(11Z)/18:2(9Z,12Z)/0:0)		
		HMDB07219	DG(18:1(9Z)/18:2(9Z,12Z)/0:0)		
		HMDB07246	DG(18:2(9Z,12Z)/18:1(11Z)/0:0)		
		HMDB07247	DG(18:2(9Z,12Z)/18:1(9Z)/0:0)		
		HMDB07274	DG(18:3(6Z,9Z,12Z)/18:0/0:0)		
		HMDB07303	DG(18:3(9Z,12Z,15Z)/18:0/0:0)		
		HMDB07418	DG(20:2(11Z,14Z)/16:1(9Z)/0:0)		
		HMDB07446	DG(20:3(5Z,8Z,11Z)/16:0/0:0)		
		HMDB07475	DG(20:3(8Z,11Z,14Z)/16:0/0:0)		
		HMDB07647	DG(22:2(13Z,16Z)/14:1(9Z)/0:0)		
		HMDB56019	DG(16:0/0:0/20:3n9)		
		HMDB56025	DG(16:0/0:0/20:3n6)		
		HMDB56049	DG(18:0/0:0/18:3n6)		
		HMDB56056	DG(18:0/0:0/18:3n3)		
		HMDB56147	DG(14:1n5/0:0/22:2n6)		
315.290447	10.6	HMDB32112	1,2,4-Nonadecanetriol	C19H40O3	[M-H]-
463.342885	10.6	HMDB02163	Trihydroxycoprostanoic acid	C28H48O5	[M-H]-
		HMDB41135	2-Deoxybrassinolide		

321.130388	10.7	HMDB30416	Avenic acid A	C12H22N2O8	[M-H]-
		HMDB33105	N2-Galacturonyl-L-lysine		
		HMDB33106	N6-Galacturonyl-L-lysine		
343.082313	10.7	HMDB29469	Eupatilin	C18H16O7	[M-H]-
		HMDB34013	Lathycarpin		
		HMDB37600	Xanthomicrol		
		HMDB37692	5,7-Dihydroxy-3',4',5'-trimethoxyflavone		
		HMDB38807	Aflatoxin Ex2B1		
		HMDB40321	3',8-Dihydroxy-4',5',7-trimethoxyflavone		
659.562254	10.7	HMDB56220	DG(20:1n9/0:0/18:2n6)	C42H76O5	[M-H]-
		HMDB56222	DG(20:1n9/0:0/20:2n6)		
206.045880	10.8	HMDB00978	4-(2-Aminophenyl)-2,4-dioxobutanoic acid	C10H9NO4	[M-H]-
		HMDB60328	1-Nitro-5,6-dihydroxy-dihydronaphthalene		
514.284222	10.8	HMDB00036	Taurocholic acid	C26H45NO7S	[M-H]-
		HMDB00889	Tauroursocholic acid		
		HMDB00922	Taurallocholic acid		
		HMDB00932	Tauro-b-muricholic acid		
		HMDB11637	Taurohyocholate		
297.113261	10.9	HMDB04808	7C-aglycone	C18H18O4	[M-H]-
		HMDB06101	Enterolactone		
		HMDB29543	(+)-Ligballinol		
		HMDB30695	7-Hydroxy-5-methoxy-6,8-dimethylflavanone		
		HMDB37376	1-(2,4-Dihydroxy-6-methoxy-3,5-dimethylphenyl)-3-phenyl-2-propen-1-one		
		HMDB38453	5,7-Dimethoxy-6-methylflavanone		
343.045914	11.0	HMDB30477	Aflatoxin GM1	C17H12O8	[M-H]-
		HMDB37754	Wharangin		
385.092705	11.0	HMDB29277	8-8'-Dehydrodiferulic acid	C20H18O8	[M-H]-
		HMDB33876	Dehydrodiferulic dilactone		
		HMDB41277	3-[3-Carboxy-2,3-dihydro-2-(4-hydroxy-3-methoxyphenyl)-7-methoxy-5-benzofuranyl]-2-propenoic acid		
317.248583	11.1	HMDB01449	Allopregnanolone	C21H34O2	[M-H]-
		HMDB01455	Alloepipregnanolone		
		HMDB01471	Epipregnanolone		
		HMDB06012	Epimetendiol		
		HMDB06759	3a-Hydroxy-5b-pregnane-20-one		
		HMDB30983	5-(8-Pentadecenyl)-1,3-benzenediol		
		HMDB36740	(2E,5E,12Z,15Z)-1-Hydroxy-2,5,12,15-heneicosatetraen-4-one		
		HMDB60408	5alpha-Pregnan-20alpha-ol-3-one		
503.161824	11.1	HMDB01262	Maltotriose	C18H32O16	[M-H]-
		HMDB03213	Raffinose		
		HMDB03539	Levan		
		HMDB06599	3-Galactosyllactose		
		HMDB06857	Dextrin		
		HMDB11729	1-Kestose		
		HMDB11730	Melezitose		
		HMDB29910	Gentiotriose		
		HMDB29921	Neokestose		
		HMDB29922	Galactotriose		
		HMDB29929	6-O-Glucosylmaltose		
		HMDB29930	beta-D-Fructofuranosyl alpha-D-glucopyranosyl-(1->4)-D-glucopyranoside		
		HMDB29937	Panose		
		HMDB33673	6-Kestose		
		HMDB33748	Umbelliferose		
		HMDB34072	Gentianose		
		HMDB35322	Fagopyritol B2		
		HMDB38851	beta-D-Galactopyranosyl-(1->2)-[beta-D-galactopyranosyl-(1->4)]-D-galactose		
		HMDB38852	beta-D-Galactopyranosyl-(1->4)-beta-D-galactopyranosyl-(1->4)-D-galactose		
		HMDB38853	beta-D-Galactopyranosyl-(1->3)-beta-D-galactopyranosyl-(1->6)-D-galactose		
		HMDB39703	3-beta-Gentiobiosylglucose		
		HMDB39704	alpha-D-Glucopyranosyl-(1->6)-alpha-D-glucopyranosyl-(1->2)-D-glucose		
		HMDB39706	4-beta-Laminaribiosylglucose		
		HMDB39707	alpha-D-Glucopyranosyl-(1->4)-alpha-D-glucopyranosyl-(1->6)-D-glucose		
		HMDB39708	3-beta-Cellobiosylglucose		
		HMDB40181	Fagopyritol A2		
		HMDB40984	Sophorotriose		
		HMDB41948	Nephritogenoside		
		HMDB60468	D-Gal alpha 1->6D-Gal alpha 1->6D-Glucose		
511.436844	11.1	HMDB07008	DG(14:0/14:0/0:0)	C31H60O5	[M-H]-
		HMDB55952	DG(14:0/0:0/14:0)		
379.101228	11.1	HMDB02928	Maltitol	C12H24O11	[M+Cl]-
		HMDB06791	Melibiitol		
		HMDB29911	1-O-alpha-D-Glucopyranosyl-D-mannitol		
		HMDB40937	Lactitol		

265.056507	11.3	HMDB32437	Monoglyceride citrate	C9H14O9	[M-H]-
379.160747	11.5	HMDB31954	3-Methyl-3-butenyl apiosyl-(1->6)-glucoside	C16H28O10	[M-H]-
		HMDB31956	Prenyl apiosyl-(1->6)-glucoside		
		HMDB41360	Prenyl arabinosyl-(1->6)-glucoside		
500.280599	11.5	HMDB05030	Fexofenadine	C32H39NO4	[M-H]-
335.235833	11.5	HMDB10737	(R)-3-Hydroxy-Octadecanoic acid	C18H36O3	[M+Cl]-
		HMDB37396	xi-10-Hydroxyoctadecanoic acid		
275.176522	11.6	HMDB15555	Molindone	C16H24N2O2	[M-H]-
		HMDB61010	Noralfentanil		
305.248629	11.6	HMDB02925	8,11,14-Eicosatrienoic acid	C20H34O2	[M-H]-
		HMDB10378	5,8,11-Eicosatrienoic acid		
		HMDB31058	Sciadonic acid		
		HMDB36835	Sagittariol		
		HMDB60039	11,14,17-Eicosatrienoic acid		
231.098662	11.7	HMDB01199	N2-Succinyl-L-ornithine	C9H16N2O5	[M-H]-
		HMDB12161	4-(Glutamylamino) butanoate		
		HMDB28766	Aspartyl-Valine		
		HMDB28873	Hydroxyprolyl-Threonine		
		HMDB29062	Threoninyl-Hydroxyproline		
		HMDB29123	Valyl-Aspartate		
		HMDB29393	L-N-(3-Carboxypropyl)glutamine		
305.103090	11.7	HMDB39031	trans-O-Methylgrandmarin	C16H18O6	[M-H]-
		HMDB60788	6-O-Desmethyl-mycophenolic acid		
482.294581	11.8	HMDB00722	Lithocholyltaurine	C26H45NO5S	[M-H]-
615.442191	11.9	HMDB35121	Oryzanol C	C41H60O4	[M-H]-
322.275167	12.0	HMDB12252	Linoleoyl ethanolamide	C20H37NO2	[M-H]-
473.218201	12.0	HMDB30004	Austalide B	C26H34O8	[M-H]-
302.101133	12.1	HMDB15598	Voglibose	C10H21NO7	[M+Cl]-
191.107774	12.2	HMDB31571	2-Methyl-1-phenyl-2-propanyl acetate	C12H16O2	[M-H]-
		HMDB31614	4-Phenyl-2-butyl acetate		
		HMDB31618	Ethyl 4-phenylbutanoate		
		HMDB32043	Benzyl 3-methylbutanoate		
		HMDB33380	3-Methylbutyl benzoate		
		HMDB35010	2-Methylpropyl phenylacetate		
		HMDB35014	2-Phenylethyl butanoate		
		HMDB35015	2-Phenylethyl 2-methylpropanoate		
		HMDB35447	5-Isopropyl-2-methylphenol acetate		
		HMDB36388	3-Phenylpropyl propanoate		
		HMDB36734	11,12,13-Trinor-1(10)-spirovetivene-2,7-dione		
		HMDB37165	4-Methyl-2-(1-phenylethyl)-1,3-dioxolane, 9CI		
		HMDB37709	4-Methylphenyl 3-methylbutanoate		
		HMDB37716	1-Phenylethyl isobutyrate		
		HMDB37717	1-Phenylethyl butyrate		
		HMDB37792	1-Ethoxy-2-methoxy-4-(1-propenyl)benzene		
		HMDB38180	2-(2-Hydroxy-4-methylphenyl)-3-pentanone		
		HMDB39496	2-Ethoxy-1-methoxy-4-(1-propenyl)benzene		
		HMDB39643	11,12,13-Trinor-1,3,5-bisabolatrien-10-oic acid		
		HMDB39841	2-Benzyl-4,5-dimethyl-1,3-dioxolane		
		HMDB40427	Butyl phenylacetate		
471.347978	12.2	HMDB02392	Maslinic acid	C30H48O4	[M-H]-
		HMDB33233	Lucidumol A		
		HMDB34523	Queretaroic acid		
		HMDB34530	Priverogenin A		
		HMDB34567	(3beta,23xi)-3,23-Dihydroxycycloart-24-en-26-oic acid		
		HMDB35106	Pomolic acid		
		HMDB35107	20beta-Hydroxyursolic acid		
		HMDB35258	Azukisapogenol		
		HMDB35260	delta-Maslinic acid		
		HMDB35748	Sebiferenic acid		
		HMDB35758	Momordicin I		
		HMDB35962	Ganoderic acid U		
		HMDB35977	Ganodermanontriol		
		HMDB36001	Epoxyganoderiol A		
		HMDB36063	(3b,22S,24E)-3,22-Dihydroxycycloart-24-en-26-oic acid		
		HMDB36064	27-Hydroxyisomangiferolic acid		
		HMDB36638	Albigenic acid		
		HMDB36654	Rubitic acid		
		HMDB37779	Ganoderiol E		
		HMDB41043	3alpha-Corosolic acid		
485.327258	12.2	HMDB34526	Bassic acid	C30H46O5	[M-H]-
		HMDB34689	Glabric acid		
		HMDB35259	28-Hydroxyglycyrrhetic acid		

		HMDB35261	24-Hydroxyglycyrrhetic acid		
		HMDB35295	(3beta,15alpha,22S,24E)-3,15,22-Trihydroxylanosta-7,9(11),24-trien-26-oic acid		
		HMDB36652	(2xi,20beta)-2,20-Dihydroxy-3-oxo-12-ursen-28-oic acid		
		HMDB36851	Ceanothic acid		
		HMDB37963	Actinidic acid		
		HMDB38737	Melilotigenin		
		HMDB40499	18alpha-Hydroxyglycyrrhetic acid		
		HMDB41041	Lucyin A		
587.287431	12.2	HMDB04161	D-Urobilin	C33H40N4O6	[M-H]-
389.246523	12.3	HMDB11538	MG(0:0/18:2(9Z,12Z)/0:0)	C21H38O4	[M+Cl]-
		HMDB11568	MG(18:2(9Z,12Z)/0:0/0:0)		
369.097964	12.4	HMDB31941	8'-Episesaminone	C20H18O7	[M-H]-
		HMDB34119	Sesamolin		
		HMDB35527	Glycyrrhizaflavonol A		
		HMDB36555	Glycyrrhizaisoflavone A		
		HMDB38398	Gancaonin P		
		HMDB38900	2,3-Dehydrokievitol		
		HMDB38932	Justisolin		
		HMDB39731	Neouralenol		
		HMDB39732	Uralenol		
461.254463	12.4	HMDB10340	Retinyl beta-glucuronide	C26H38O7	[M-H]-
259.061180	12.5	HMDB33265	2-Methoxystypandrone	C14H12O5	[M-H]-
		HMDB39616	Orientalone		
		HMDB40630	Pratenol A		
611.408603	12.5	HMDB33949	beta-Sitosterol 3-O-beta-D-galactopyranoside	C35H60O6	[M+Cl]-
		HMDB34185	Schottenol 3-glucoside		
487.166926	12.6	HMDB02094	3-Fucosyllactose	C18H32O15	[M-H]-
		HMDB02098	2-Fucosyllactose		
		HMDB06601	B-Trisaccharide		
		HMDB06620	Fucosyllactose		
411.184646	12.7	HMDB00416	17-Hydroxypregnenolone sulfate	C21H32O6S	[M-H]-
539.138250	12.7	HMDB01262	Maltotriose	C18H32O16	[M+Cl]-
		HMDB03213	Raffinose		
		HMDB03539	Levan		
		HMDB06599	3-Galactosyllactose		
		HMDB06857	Dextrin		
		HMDB11729	1-Kestose		
		HMDB11730	Melezitose		
		HMDB29910	Gentiotriose		
		HMDB29921	Neokestose		
		HMDB29922	Galactotriose		
		HMDB29929	6-O-Glucosylmaltose		
		HMDB29930	beta-D-Fructofuranosyl alpha-D-glucopyranosyl-(1->4)-D-glucopyranoside		
		HMDB29937	Panose		
		HMDB33673	6-Kestose		
		HMDB33748	Umbelliferose		
		HMDB34072	Gentianose		
		HMDB35322	Fagopyritol B2		
		HMDB38851	beta-D-Galactopyranosyl-(1->2)-[beta-D-galactopyranosyl-(1->4)]-D-galactose		
		HMDB38852	beta-D-Galactopyranosyl-(1->4)-beta-D-galactopyranosyl-(1->4)-D-galactose		
		HMDB38853	beta-D-Galactopyranosyl-(1->3)-beta-D-galactopyranosyl-(1->6)-D-galactose		
		HMDB39703	3-beta-Gentiobiosylglucose		
		HMDB39704	alpha-D-Glucopyranosyl-(1->6)-alpha-D-glucopyranosyl-(1->2)-D-glucose		
		HMDB39706	4-beta-Laminaribiosylglucose		
		HMDB39707	alpha-D-Glucopyranosyl-(1->4)-alpha-D-glucopyranosyl-(1->6)-D-glucose		
		HMDB39708	3-beta-Cellobiosylglucose		
		HMDB40181	Fagopyritol A2		
		HMDB40984	Sophorotriose		
		HMDB41948	Nephritogenoside		
		HMDB60468	D-Gal alpha 1->6D-Gal alpha 1->6D-Glucose		
351.134989	12.8	HMDB32759	Moschamine	C20H20N2O4	[M-H]-
319.264231	12.9	HMDB02156	3a,20b-Pregnanediol	C21H36O2	[M-H]-
		HMDB04025	Pregnanediol		
		HMDB06013	7a,17-dimethyl-5b-Androstane-3a,17b-diol		
		HMDB31009	Adipostatin A		
		HMDB36741	1-Hydroxy-2,12,15-heneicosatrien-4-one		
		HMDB60409	5alpha-Pregnane-3alpha,20alpha-diol		
435.311608	12.9	HMDB02195	Varanic acid	C26H44O5	[M-H]-
509.327330	12.9	HMDB37893	Ganodermic acid TQ	C32H46O5	[M-H]-
401.124223	13.0	HMDB29308	Hexamethylquercetagetin	C21H22O8	[M-H]-
		HMDB29540	Nobiletin		
		HMDB35415	3,3',4',5,6,8-Hexamethoxyflavone		

		HMDB37755	3,3',4',5,7,8-Hexamethoxyflavone		
		HMDB39379	Chrysaloin		
227.201667	13.1	HMDB00806	Myristic acid	C14H28O2	[M-H]-
		HMDB02221	2,6,10-Trimethylundecanoic acid		
		HMDB31072	12-Methyltridecanoic acid		
		HMDB32318	Hexanal octane-1,3-diol acetal		
		HMDB32548	Undecanal propyleneglycol acetal		
		HMDB33788	Ethyl dodecanoate		
		HMDB34461	Heptyl heptanoate		
		HMDB36216	Hexyl octanoate		
		HMDB37312	Decyl butanoate		
		HMDB37495	3-Methylbutyl nonanoate		
		HMDB38034	Nonyl isovalerate		
		HMDB38969	Dodecyl acetate		
		HMDB59865	Isobutyl decanoate		
337.215055	13.1	HMDB11530	MG(0:0/14:0/0:0)	C17H34O4	[M+Cl]-
		HMDB11561	MG(14:0/0:0/0:0)		
410.283205	13.1	HMDB13626	Adrenoyl ethanolamide	C24H41NO2	[M+Cl]-
429.241307	13.1	HMDB12530	11-Hydroxyeicosatetraenoate glyceryl ester	C23H38O5	[M+Cl]-
		HMDB13651	2-(14,15-Epoxyeicosatrienoyl) Glycerol		
451.212945	13.1	HMDB15434	Forasartan	C23H28N8	[M+Cl]-
274.104456	13.2	HMDB05766	Norophthalmic acid	C10H17N3O6	[M-H]-
		HMDB11738	Gamma-Glutamyl Glutamine		
385.347565	13.3	HMDB00067	Cholesterol	C27H46O	[M-H]-
		HMDB00871	5alpha-Cholestanone		
		HMDB01170	Lathosterol		
		HMDB06841	5a-Cholest-8-en-3b-ol		
		HMDB11182	5beta-Cholestanone		
		HMDB29815	Doristerol		
		HMDB59604	5-beta-Cholestan-3-one		
399.181520	13.3	HMDB35689	Melleolide	C23H28O6	[M-H]-
		HMDB38918	Armillaritin		
443.256994	13.3	HMDB00312	3a,7a,12b-Trihydroxy-5b-cholanoic acid	C24H40O5	[M+Cl]-
		HMDB00320	3a,4b,7a-Trihydroxy-5b-cholanoic acid		
		HMDB00326	1b,3a,12a-Trihydroxy-5b-cholanoic acid		
		HMDB00330	3a,4b,12a-Trihydroxy-5b-cholanoic acid		
		HMDB00364	3a,6a,7b-Trihydroxy-5b-cholanoic acid		
		HMDB00371	1,3,12-Trihydroxycholan-24-oic acid		
		HMDB00376	3b,7a,12a-Trihydroxy-5a-Cholanoic acid		
		HMDB00390	3a,7b,12b-Trihydroxy-5b-cholanoic acid		
		HMDB00395	3b,7b,12a-Trihydroxy-5b-cholanoic acid		
		HMDB00404	2b,3a,7a-Trihydroxy-5b-cholanoic acid		
		HMDB00414	1b,3a,7a-Trihydroxy-5b-cholanoic acid		
		HMDB00415	3a,6b,7b-Trihydroxy-5b-cholanoic acid		
		HMDB00419	3b,7a,12a-Trihydroxy-5b-cholanoic acid		
		HMDB00427	3b,7b,12a-Trihydroxy-5a-Cholanoic acid		
		HMDB00432	3a,7b,12a-Trihydroxy-5a-Cholanoic acid		
		HMDB00505	Allocholic acid		
		HMDB00506	Alpha-Muricholic acid		
		HMDB00527	6a,12a-Dihydroxylithocholic acid		
		HMDB00619	Cholic acid		
		HMDB00760	Hyocholic acid		
		HMDB00865	Muricholic acid		
		HMDB00917	Ursocholic acid		
261.088095	13.5	HMDB31360	L-cis-Cyclo(aspartylphenylalanyl)	C13H14N2O4	[M-H]-
321.243549	13.5	HMDB05045	15(S)-Hydroxyeicosatrienoic acid	C20H34O3	[M-H]-
		HMDB36802	Austroinulin		
		HMDB60052	8-HETrE		
327.087414	13.5	HMDB29677	Zapotinin	C18H16O6	[M-H]-
		HMDB30596	Ugaxanthone		
		HMDB30727	Betagarin		
		HMDB30834	Americanin A		
		HMDB33169	Garbogiol		
		HMDB33318	Isoamericanin A		
		HMDB34109	Frenolicin B		
		HMDB34186	Morusignin B		
		HMDB37458	5-Hydroxy-4',7,8-trimethoxyflavone		
		HMDB39601	Americanin D		
		HMDB40303	5-Hydroxy-4,4',6-trimethoxyaurone		
		HMDB40719	8-Hydroxy-4',5,7-trimethoxyflavone		
		HMDB40935	Methyl 2-(2-methoxy-4-hydroxyphenyl)-6-methoxy-3-benzofurancarboxylate		
		HMDB41544	7-Hydroxy-3,4',8-trimethoxyflavone		

339.290441	13.5	HMDB32476	Polyoxyethylene (600) monoricinoleate	C21H40O3	[M-H]-
383.113602	13.5	HMDB29541	(+)-Zeylenol	C21H20O7	[M-H]-
		HMDB30621	Oxyisocyclointegrin		
		HMDB34914	Dulxanthone F		
		HMDB35479	Isolicopyranocoumarin		
		HMDB36281	Licofuranocoumarin		
		HMDB38396	Gancaonin D		
		HMDB38874	Licopyranocoumarin		
		HMDB38950	5-Methoxyhinokinin		
		HMDB39617	Piperenol B		
		HMDB39634	Piperenol A		
		HMDB40134	Calebin A		
		HMDB40813	3'-O-Methylgancaonin P		
		HMDB40837	3-O-Methyluralenol		
		HMDB40934	Uralene		
529.134667	13.5	HMDB29494	Formononetin 7-(6"-methylmalonylglucoside)	C26H26O12	[M-H]-
		HMDB33008	4-O-Caffeoyl-3-O-feruloylquinic acid		
		HMDB37092	3-Caffeoyl-4-feruloylquinic acid		
		HMDB41642	1-Caffeoyl-5-feruloylquinic acid		
		HMDB41643	1-Feruloyl-5-caffeoylquinic acid		
331.191506	13.6	HMDB02358	Carnosic acid	C20H28O4	[M-H]-
		HMDB04031	11b-Hydroxyprogesterone		
		HMDB12851	7'-Carboxy-gamma-tocotrienol		
		HMDB30103	Hulupone		
		HMDB30136	Adhulupone		
		HMDB31374	(1(10)E,4E,6a,9b)-9-(2-Methylbutanoyloxy)-1(10),4,11(13)-germacratrien-12,6-olide		
		HMDB31375	(1(10)E,4E,6a,9b)-9-(3-Methylbutanoyloxy)-1(10),4,11(13)-germacratrien-12,6-olide		
		HMDB35637	Petasitin		
		HMDB36146	6-Angeloylfuranofukinol		
		HMDB36623	4-Deoxycohumulone		
		HMDB36700	ent-7alpha,12beta-Dihydroxy-16-kauren-19,6beta-olide		
		HMDB36726	ent-15-Kaurene-17,19-dioic acid		
		HMDB36761	7,18-Dihydroxykaurenolide		
		HMDB38966	(9Z,11S,16S)-1-Acetoxy-9,17-octadecadiene-12,14-diyne-11,16-diol		
399.108539	13.6	HMDB40556	5-Hydroxyflavone	C21H20O8	[M-H]-
551.358985	13.6	HMDB36298	Cyclopassifloic acid E	C31H52O8	[M-H]-
573.416152	13.6	HMDB29768	Isofucosterol glucoside	C35H58O6	[M-H]-
		HMDB33775	alpha-Spinasterol 3-glucoside		
		HMDB34204	Clerosterol 3-glucoside		
		HMDB34354	Tocophersolan		
		HMDB34419	Stigmasteryl glucoside		
227.035011	13.7	HMDB13695	Urolithin A	C13H8O4	[M-H]-
		HMDB30723	1,5-Dihydroxyxanthone		
		HMDB30724	Euxanthone		
601.426317	13.7	HMDB34977	Karpoxanthin	C40H58O4	[M-H]-
		HMDB34978	6-Epikarpoxanthin		
		HMDB35891	Oryzanol A		
355.082313	13.8	HMDB33659	Dihydrohydroxy-O-methylsterigmatocystin	C19H16O7	[M-H]-
373.092864	13.8	HMDB29546	Pebrellin	C19H18O8	[M-H]-
		HMDB30611	5,8-Dihydroxy-3,3',4',7-tetramethoxyflavone		
		HMDB30660	Casticin		
		HMDB33254	Comosin		
		HMDB33276	4',5-Dihydroxy-3',5',7,8-tetramethoxyflavone		
		HMDB33306	Hymenoxin		
		HMDB33841	Menadiol disuccinate		
		HMDB35446	Methyl rosmarinate		
		HMDB41667	3-O-Methylrosmarinic acid		
371.113593	13.9	HMDB30539	Tangeritin	C20H20O7	[M-H]-
		HMDB33270	Sesamolinol		
		HMDB34278	Auranetin		
		HMDB36633	Sinensetin		
		HMDB37456	3,4',5,6,8-Pentamethoxyflavone		
		HMDB37508	Oxidihydroartocarpesin		
		HMDB37599	Isosinensetin		
		HMDB37750	Cyclokievitone hydrate		
		HMDB39775	Homoeriodictyol 4'-isobutyrate		
		HMDB40323	3',4',5',7,8-Pentamethoxyflavone		
279.087422	14.0	HMDB33884	Gravolenic acid	C14H16O6	[M-H]-
481.244345	14.0	HMDB10351	11-beta-Hydroxyandrosterone-3-glucuronide	C25H38O9	[M-H]-
487.197420	14.0	HMDB35860	Terretonin	C26H32O9	[M-H]-
		HMDB39364	Isolimonic acid 16->17-lactone		
261.007459	14.1	HMDB11719	Homovanillic acid sulfate	C9H10O7S	[M-H]-

		HMDB41648	2-Hydroxy-4-methoxyacetophenone 5-sulfate		
		HMDB41721	Dihydrocaffeic acid 3-sulfate		
		HMDB59967	3-hydroxy-3-(3-hydroxyphenyl)propanoic acid-O-sulphate		
		HMDB61117	3-(3,5-dihydroxyphenyl)-1-propanoic acid sulphate		
305.033665	14.1	HMDB59978	4-Hydroxy-5-(dihydroxyphenyl)-valeric acid-O-sulphate	C11H14O8S	[M-H]-
		HMDB59979	4-Hydroxy-5-(dihydroxyphenyl)-valeric acid-O-sulphate III		
609.510016	14.1	HMDB33753	Glycerol 1,3-didodecanoate 2-decanoate	C37H70O6	[M-H]-
		HMDB38058	Glycerol 1-dodecanoate 2-tetradecanoate 3-octanoate		
271.082300	14.2	HMDB29943	Arbutin	C12H16O7	[M-H]-
299.259186	14.2	HMDB10737	(R)-3-Hydroxy-Octadecanoic acid	C18H36O3	[M-H]-
		HMDB37396	xi-10-Hydroxyoctadecanoic acid		
377.269748	14.2	HMDB04666	2-Arachidonylglycerol	C23H38O4	[M-H]-
		HMDB11549	MG(0:0/20:4(8Z,11Z,14Z,17Z)/0:0)		
		HMDB11578	MG(20:4(5Z,8Z,11Z,14Z)/0:0/0:0)		
		HMDB11579	MG(20:4(8Z,11Z,14Z,17Z)/0:0/0:0)		
		HMDB35273	1-Acetoxy-2-hydroxy-5,12,15-heneicosatrien-4-one		
		HMDB36356	[12]-Gingerol		
		HMDB36568	Persenone A		
298.144843	14.3	HMDB04995	Codeine	C18H21NO3	[M-H]-
		HMDB15091	Hydrocodone		
		HMDB30248	Neopine		
		HMDB30255	Erysodine		
		HMDB32962	Secoclausenamide		
		HMDB38647	(2E,6E)-Piperamide-C7:2		
		HMDB38725	(R)-Juziphine		
		HMDB39767	Pandamarilactone 32		
		HMDB60319	(S)-N-Methylcoclaurine		
		HMDB60642	N-depropylpropafenone		
		HMDB60960	N-desalkylpropafenone		
324.123953	14.3	HMDB30245	Nornantenine	C19H19NO4	[M-H]-
		HMDB32143	Palaudine		
		HMDB33354	Cassythicine		
		HMDB33360	Isodomesticine		
		HMDB36987	Romucosine A		
		HMDB38145	Junosine		
327.232899	14.3	HMDB02183	Docosahexaenoic acid	C22H32O2	[M-H]-
		HMDB30053	Neogrifolin		
		HMDB30446	Grifolin		
		HMDB35185	Retinol acetate		
		HMDB38908	(Z,Z)-2-Methyl-5-(8,11,14-pentadecatrienyl)-1,3-benzenediol		
341.108912	14.3	HMDB00048	Melibiose	C12H22O11	[M-H]-
		HMDB00055	Cellobiose		
		HMDB00163	D-Maltose		
		HMDB00186	Alpha-Lactose		
		HMDB00258	Sucrose		
		HMDB00740	Lactulose		
		HMDB00975	Trehalose		
		HMDB02923	Isomaltose		
		HMDB05826	Galactinol		
		HMDB06603	3-b-Galactopyranosyl glucose		
		HMDB06792	Epimelibiose		
		HMDB11740	Turanose		
		HMDB11742	Kojibiose		
		HMDB29880	Neotrehalose		
		HMDB29882	Sakebiose		
		HMDB29898	Inulobiose		
		HMDB29902	Galabiose		
		HMDB29919	Maltulose		
		HMDB29933	Mannobiose		
		HMDB33368	DEAE-cellulose		
		HMDB38489	Allolactose		
		HMDB39237	Glucinol		
		HMDB39727	Trehalulose		
		HMDB39876	Fagopyritol A1		
		HMDB41627	beta-Lactose		
		HMDB60068	Glucose-1,3-mannose oligosaccharide		
391.285353	14.3	HMDB00348	3b,12a-Dihydroxy-5a-cholanoic acid	C24H40O4	[M-H]-
		HMDB00361	3b,7a-Dihydroxy-5b-cholanoic acid		
		HMDB00384	3a,7a-Dihydroxycholanoic acid		
		HMDB00411	3a,12b-Dihydroxy-5b-cholanoic acid		
		HMDB00438	3b,12a-Dihydroxy-5b-cholanoic acid		
		HMDB00478	Allodeoxycholic acid		

		HMDB00514	Allochenodeoxycholic acid		
		HMDB00518	Chenodeoxycholic acid		
		HMDB00626	Deoxycholic acid		
		HMDB00664	Isohyodeoxycholic acid		
		HMDB00686	Isoursodeoxycholic acid		
		HMDB00733	Hyodeoxycholic acid		
		HMDB00811	Murocholic acid		
		HMDB00946	Ursodeoxycholic acid		
		HMDB02451	7b,12a-Dihydroxycholanoic acid		
		HMDB02488	7a,12b-dihydroxy-5b-Cholan-24-oic acid		
		HMDB02536	Isodeoxycholic acid		
		HMDB02585	3b,12b-Dihydroxy-5b-cholanoic acid		
315.127143	14.4	HMDB60803	8-Hydroxydesmethylclomipramine	C18H21ClN2O	[M-H]-
505.208028	14.4	HMDB38170	Isolimonic acid	C26H34O10	[M-H]-
289.069567	14.4	HMDB06790	Galactosylglycerol	C9H18O8	[M+Cl]-
		HMDB38664	(2R)-1-O-beta-D-Galactopyranosylglycerol		
300.049041	14.5	HMDB01062	N-Acetyl-D-Glucosamine 6-Phosphate	C8H16NO9P	[M-H]-
		HMDB01121	N-Acetyl-D-mannosamine 6-phosphate		
		HMDB01367	N-Acetyl-glucosamine 1-phosphate		
		HMDB02817	N-Acetylglucosamine 6-phosphate		
		HMDB06480	N-Acetyl-D-galactosamine 1-phosphate		
		HMDB59626	N-acetyl-alpha-D-galactosamine 1-phosphate		
239.201639	14.6	HMDB29765	9-Pentadecenoic acid	C15H28O2	[M-H]-
		HMDB32347	Isobutyl 10-undecenoate		
		HMDB34455	Exaltolide		
		HMDB36426	Butyl undecylenate		
		HMDB37190	Rhodinyl isovalerate		
		HMDB37211	Menthyl isovalerate		
		HMDB37229	Citronellyl pentanoate		
		HMDB38954	Citronellyl isovalerate		
		HMDB39715	Auberganol		
		HMDB40997	15,5-Farnesanolide		
303.196553	14.6	HMDB00309	3a,16b-Dihydroxyandrostenone	C19H28O3	[M-H]-
		HMDB00322	16-Oxoandrostenediol		
		HMDB00324	3a,16a-Dihydroxyandrostenone		
		HMDB00352	16a-Hydroxydehydroisoandrosterone		
		HMDB00388	3a,16-Dihydroxyandrostenone		
		HMDB03956	7a-Hydroxytestosterone		
		HMDB04611	7a-Hydroxydehydroepiandrosterone		
		HMDB04624	7b-Hydroxydehydroepiandrosterone		
		HMDB06031	11-Ketoetiocholanolone		
		HMDB06259	6beta-Hydroxytestosterone		
		HMDB06769	19-Hydroxytestosterone		
		HMDB12533	11beta-Hydroxytestosterone		
		HMDB12654	2beta-Hydroxytestosterone		
		HMDB31464	cis-[8]-Shogaol		
		HMDB39589	Ginsenoyne G		
		HMDB39735	10-Acetoxy-8-heptadecene-4,6-diyn-3-ol		
		HMDB60089	w Hydroxy testosterone		
		HMDB60339	11beta,17beta-Dihydroxy-4-androsten-3-one		
591.390354	14.6	HMDB39054	Tuberoside	C34H56O8	[M-H]-
241.217288	14.7	HMDB00826	Pentadecanoic acid	C15H30O2	[M-H]-
		HMDB30469	Methyl tetradecanoate		
		HMDB32250	Dodecyl propionate		
		HMDB32328	Hexyl nonanoate		
		HMDB36218	Heptyl octanoate		
		HMDB36220	Octyl heptanoate		
		HMDB37306	Pentyl decanoate		
		HMDB38907	3-Methylbutyl decanoate		
		HMDB40998	7(14)-Farnesene-9,12-diol		
		HMDB41588	2,6,10-Trimethyldodecanoic acid		
		HMDB59820	Isopropyl laurate		
		HMDB59833	Ethyl tridecanoate		
275.056110	14.8	HMDB33649	O-Demethylfonsecin	C14H12O6	[M-H]-
301.129569	14.8	HMDB40462	Garcinia lactone dibutyl ester	C14H22O7	[M-H]-
359.113622	14.8	HMDB35051	Gibberellin A59	C19H20O7	[M-H]-
		HMDB40910	Heteroflavanone A		
		HMDB41196	Edulisin IV		
503.192383	14.8	HMDB31536	Myricatomentoside I	C26H32O10	[M-H]-
544.188288	14.8	HMDB06592	Lacto-N-triaose	C20H35NO16	[M-H]-
		HMDB39750	Lacto-N-triose I		
		HMDB41622	N-Acetylgalactosaminyl lactose		

253.092869	14.9	HMDB06790	Galactosylglycerol	C9H18O8	[M-H]-
		HMDB38664	(2R)-1-O-beta-D-Galactopyranosylglycerol		
325.114014	14.9	HMDB06590	2-O-a-L-Fucopyranosyl-galactose	C12H22O10	[M-H]-
		HMDB06701	3-O-a-L-Fucopyranosyl-D-glucose		
		HMDB29523	Neohesperidose		
		HMDB40154	6-O-b-D-Fructofuranosyl-2-deoxy-D-glucose		
351.087463	14.9	HMDB34019	Parvisoflavone A	C20H16O6	[M-H]-
		HMDB35184	Semilicoisoflavone B		
		HMDB37424	Citrusinol		
		HMDB37425	Cycloartocarpesin		
		HMDB38127	Lupinisoflavone A		
		HMDB38904	3-(2,4-Dihydroxyphenyl)-8,9-dihydro-5-hydroxy-8-(1-methylethenyl)-4H-furo[2,3-h]-1-benzopyran-5-one		
		HMDB40304	Cyclocommunol		
469.332380	14.9	HMDB11628	Glycyrrhetinic acid	C30H46O4	[M-H]-
		HMDB29345	Murrayenol		
		HMDB33213	(3alpha,20R,24Z)-3-Hydroxy-21-oxoeupha-8,24-dien-26-oic acid		
		HMDB34508	6beta-Hydroxy-3-oxo-12-oleanen-28-oic acid		
		HMDB34517	beta-Glycyrrhetinic acid		
		HMDB34568	23-Hydroxy-3-oxocycloart-24-en-26-oic acid		
		HMDB35252	3beta-3,24-Dihydroxy-9(11),12-oleanadien-30-oic acid		
		HMDB35327	Ganoderiol B		
		HMDB35334	Ganodermic acid Jb		
		HMDB35788	Liquiritic acid		
		HMDB35912	Pomonic acid		
		HMDB36655	Rubinic acid		
		HMDB36671	11-Keto-beta-boswellic acid		
		HMDB36786	Lansic acid		
		HMDB36847	Colubrinic acid		
		HMDB38653	Koetjapic acid		
		HMDB40415	28-Hydroxymangiferonic acid		
		HMDB40494	2-Hydroxy-3-oxo-12-oleanen-28-oic acid		
		HMDB40618	16-Hydroxy-3-oxo-12-oleanen-28-oic acid		
		HMDB40995	Secoisobryononic acid		
		HMDB40996	Secobryononic acid		
193.087037	15.0	HMDB31517	(R)-3-Hydroxy-5-phenylpentanoic acid	C11H14O3	[M-H]-
		HMDB31984	2,5-Dimethoxy-4-(2-propenyl)phenol		
		HMDB32575	Butylparaben		
		HMDB32590	Zingerone		
		HMDB34206	Ethyl 4-methylphenoxyacetate		
		HMDB34990	4-Methoxybenzyl propanoate		
		HMDB36432	Isobutyl salicylate		
		HMDB37271	2,6-Dimethoxy-4-(1-propenyl)phenol		
		HMDB40730	Butyl salicylate		
		HMDB41194	Methoxyeugenol		
		HMDB41505	5-Hydroxy-2-benzyl-1,3-dioxane		
		HMDB41506	2-Benzyl-5-hydroxymethyl-1,3-dioxolane		
		HMDB41666	3-Hydroxyphenyl-valeric acid		
		HMDB59898	Ethyl 4-ethoxybenzoate		
		HMDB59940	[2-(2-Methylphenyl)-1,3-dioxolan-4-yl]methanol		
		HMDB59941	[2-(3-Methylphenyl)-1,3-dioxolan-4-yl]methanol		
		HMDB59942	[2-(4-Methylphenyl)-1,3-dioxolan-4-yl]methanol		
		HMDB59943	2-(2-Methylphenyl)-1,3-dioxan-5-ol		
		HMDB59944	2-(3-Methylphenyl)-1,3-dioxan-5-ol		
		HMDB59945	2-(4-Methylphenyl)-1,3-dioxan-5-ol		
287.023116	15.0	HMDB29191	5'-(3',4'-Dihydroxyphenyl)-gamma-valerolactone sulfate	C11H12O7S	[M-H]-
		HMDB30228	Nigakinone	C14H8N2O3	[M+Cl]-
342.098310	15.0	HMDB29285	Avenanthramide 1s	C18H17NO6	[M-H]-
		HMDB29295	Caffeoyl tyrosine		
		HMDB29296	p-Coumaroyl 3-hydroxytyrosine		
464.301789	15.0	HMDB00138	Glycocholic acid	C26H43NO6	[M-H]-
		HMDB00331	3a,7b,12a-Trihydroxyoxocholanyl-Glycine		
		HMDB32596	Sodium glycocholate		
207.066276	15.1	HMDB12127	(R)-2-Benzylsuccinate	C11H12O4	[M-H]-
		HMDB29185	5-(3',4'-Dihydroxyphenyl)-gamma-valerolactone		
		HMDB34315	3-(3,4-Dimethoxyphenyl)-2-propenoic acid		
		HMDB36055	Furapiole		
		HMDB37308	1-(2-Methoxy-3,4-methylenedioxyphenyl)-1-propanone		
		HMDB38510	6-Methoxymellein		
		HMDB40892	3-(3-Methoxy-4,5-methylenedioxyphenyl)-2-propen-1-ol		
		HMDB41461	Anthriscinol		
		HMDB41692	5-(3',5'-Dihydroxyphenyl)-gamma-valerolactone		
343.321746	15.1	HMDB11143	MG(18:0e/0:0/0:0)	C21H44O3	[M-H]-

515.119556	15.1	HMDB29279	1,3-Dicaffeoylquinic acid	C25H24O12	[M-H]-
		HMDB29280	Dicaffeoylquinic acid		
		HMDB29493	Formononetin 7-(6"-malonylglucoside)		
		HMDB30093	1,5-Dicaffeoylquinic acid		
		HMDB30705	3,4-Di-O-caffeoylquinic acid		
		HMDB30706	3,5-Di-O-caffeoylquinic acid		
		HMDB30707	4,5-Di-O-caffeoylquinic acid		
		HMDB34766	1,4-Di-O-caffeoylquinic acid		
		HMDB37343	2",3"-Diacetylcosmosiin		
		HMDB37344	3",4"-Diacetylcosmosiin		
		HMDB40138	2",4"-Diacetylafzelin		
		HMDB40139	3",4"-Diacetylafzelin		
409.251512	15.1	HMDB00308	3b-Hydroxy-5-cholenoic acid	C24H38O3	[M+Cl]-
		HMDB38522	2-(10-Heptadecenyl)-6-hydroxybenzoic acid		
		HMDB41453	D8'-Merulinic acid C		
417.158898	15.1	HMDB15699	Tofisopam	C22H26N2O4	[M+Cl]-
300.124128	15.2	HMDB15323	Oxymorphone	C17H19NO4	[M-H]-
		HMDB29382	Genomorphine		
		HMDB41960	Noroxycodone		
303.119782	15.2	HMDB33909	2'-Deoxymugineic acid	C12H20N2O7	[M-H]-
		HMDB34894	2-(1,2,3,4-Tetrahydroxybutyl)-6-(2,3,4-trihydroxybutyl)pyrazine		
		HMDB38696	Deoxyfructosazine		
765.567842	15.2	HMDB12088	SM(d18:0/18:1(11Z))	C41H83N2O6P	[M+Cl]-
		HMDB12089	SM(d18:0/18:1(9Z))		
319.082340	15.3	HMDB29292	3-p-Coumaroyl-1,5-quinolactone	C16H16O7	[M-H]-
		HMDB29293	4-p-Coumaroyl-1,5-quinolactone		
		HMDB41295	7-Hydroxy-6-methoxy-alpha-pyrufuran		
379.139805	15.3	HMDB36893	Gibberellin A75	C19H24O8	[M-H]-
		HMDB37056	8-Oxodiacetoxyscirpenol		
		HMDB38328	(S)-Bitalin A 12-glucoside		
		HMDB38450	Gibberellin A86		
		HMDB40899	Methyl helianthenoate A glucoside		
620.249137	15.3	HMDB14700	Tigecycline	C29H39N5O8	[M+Cl]-
267.073522	15.4	HMDB00195	Inosine	C10H12N4O5	[M-H]-
		HMDB00481	Allopurinol riboside		
		HMDB03040	Arabinosylhypoxanthine		
303.087426	15.4	HMDB29175	3'-O-methyl-(-)-epicatechin	C16H16O6	[M-H]-
		HMDB29179	4'-O-methyl-(-)-epicatechin		
		HMDB29228	4-Methyl-epicatechin		
		HMDB29231	3-Methyl-epicatechin		
		HMDB30662	4'-O-Methylcatechin		
		HMDB30745	(R)-Heraclenol		
		HMDB33866	Fonsecin B		
		HMDB38519	Arachidoside		
		HMDB41294	6-Methoxy-alpha-pyrufuran		
		HMDB41507	3'-O-Methylcatechin		
387.108521	15.4	HMDB29227	5-Hydroxy-3,3',4',7,8-pentamethoxyflavone	C20H20O8	[M-H]-
		HMDB29545	3'-Hydroxy-4',5,6,7,8-pentamethoxyflavone		
		HMDB29547	4'-Hydroxy-3',5,6,7,8-pentamethoxyflavone		
		HMDB29979	2'-Hydroxy-3,4',5',7,8-pentamethoxyflavone		
		HMDB30095	Artemetin		
		HMDB31955	Dimethyl (1R*,2S*,3S*)-2-carboxy-3-(3,4-dihydroxyphenyl)-2,3-dihydro-5,6-dihydroxy-1H-indene-1-acetate		
		HMDB33275	5-Hydroxyauranetin		
		HMDB36335	2,4,6-Phenanthrenetriol 2-O-b-D-glucoside		
		HMDB37571	Demethylnobiletin		
		HMDB40722	7-Hydroxy-3',4',5,6,8-pentamethoxyflavone		
637.541424	15.4	HMDB11188	TG(12:0/12:0/12:0)	C39H74O6	[M-H]-
300.087742	15.5	HMDB29323	Citpressine I	C16H15NO5	[M-H]-
		HMDB30374	Citrusinine I		
324.290806	15.5	HMDB02088	N-Oleoylethanolamine	C20H39NO2	[M-H]-
413.124195	15.5	HMDB15310	Podofilox	C22H22O8	[M-H]-
		HMDB31452	Lignans		
		HMDB34935	Dulxanthone G		
		HMDB34936	Dulxanthone H		
		HMDB34960	Edulone A		
319.204624	15.5	HMDB35473	Avocadyne	C17H32O3	[M+Cl]-
		HMDB38685	Muricatacin		
335.044199	15.6	HMDB59977	4-Hydroxy-5-(dihydroxyphenyl)-valeric acid-O-methyl-O-sulphate	C12H16O9S	[M-H]-
367.103453	15.6	HMDB30669	3-O-Feruloylquinic acid	C17H20O9	[M-H]-
		HMDB39959	3-O-Caffeoyl-1-O-methylquinic acid		
		HMDB39960	3-O-Caffeoyl-4-O-methylquinic acid		
453.337370	15.6	HMDB34963	beta-Elemonic acid	C30H46O3	[M-H]-

		HMDB35090	Ganoderic acid Y		
		HMDB35247	Isomasticadienonic acid		
		HMDB35251	9(11)-Dehydroglycyrrhetic acid		
		HMDB35406	3beta-3-Hydroxy-11-oxolanosta-8,24-dien-26-al		
		HMDB35594	Bryononic acid		
		HMDB35615	Mangiferonic acid		
		HMDB35791	Desoxoglabrolide		
		HMDB35808	Tomentosolic acid		
		HMDB36000	Epoxyganoderiol B		
		HMDB36002	Ganoderal B		
		HMDB36007	Ursonic acid		
		HMDB36653	Micromeric acid		
		HMDB37054	Katononic acid		
		HMDB38707	Ganoderiol F		
		HMDB38758	Glypallidifloric acid		
		HMDB40454	Lucidal		
		HMDB40508	Masticadienonic acid		
263.092486	15.7	HMDB36544	1'-Acetoxyeugenol acetate	C14H16O5	[M-H]-
341.212233	15.7	HMDB02726	Guggulsterone	C22H30O3	[M-H]-
		HMDB31059	2-Hydroxy-6-(8,11,14-pentadecatrienyl)benzoic acid		
		HMDB60710	17-Hydroxymethylethisterone		
509.457538	15.7	HMDB32494	Propylene glycol mono- and diesters of fats and fatty acids	C32H62O4	[M-H]-
619.531090	15.7	HMDB07030	DG(14:0/22:2(13Z,16Z)/0:0)	C39H72O5	[M-H]-
		HMDB07058	DG(14:1(9Z)/22:1(13Z)/0:0)		
		HMDB07109	DG(16:0/20:2(11Z,14Z)/0:0)		
		HMDB07137	DG(16:1(9Z)/20:1(11Z)/0:0)		
		HMDB07161	DG(18:0/18:2(9Z,12Z)/0:0)		
		HMDB07188	DG(18:1(11Z)/18:1(11Z)/0:0)		
		HMDB07189	DG(18:1(11Z)/18:1(9Z)/0:0)		
		HMDB07217	DG(18:1(9Z)/18:1(11Z)/0:0)		
		HMDB07218	DG(18:1(9Z)/18:1(9Z)/0:0)		
		HMDB07245	DG(18:2(9Z,12Z)/18:0/0:0)		
		HMDB07389	DG(20:1(11Z)/16:1(9Z)/0:0)		
		HMDB07417	DG(20:2(11Z,14Z)/16:0/0:0)		
		HMDB07618	DG(22:1(13Z)/14:1(9Z)/0:0)		
		HMDB07646	DG(22:2(13Z,16Z)/14:0/0:0)		
		HMDB55972	DG(14:0/0:0/22:2n6)		
		HMDB56140	DG(14:1n5/0:0/22:1n9)		
		HMDB56159	DG(16:1n7/0:0/20:1n9)		
		HMDB56177	DG(18:1n7/0:0/18:1n7)		
		HMDB56178	DG(18:1n7/0:0/18:1n9)		
		HMDB56197	DG(18:1n9/0:0/18:1n9)		
427.179622	15.7	HMDB15608	Indacaterol	C24H28N2O3	[M+Cl]-
		HMDB15705	Ivacaftor		
309.098009	15.8	HMDB30293	(E)-1-O-Cinnamoyl-beta-D-glucose	C15H18O7	[M-H]-
		HMDB35880	(E)-2-O-Cinnamoyl-beta-D-glucopyranose		
		HMDB39958	1-Pentadecanecarboxylic acid		
383.153342	15.8	HMDB00386	3b,16a-Dihydroxyandrostenone sulfate	C19H28O6S	[M-H]-
423.288229	15.8	HMDB11144	LPA(18:0e/0:0)	C21H45O6P	[M-H]-
497.363493	15.8	HMDB32022	Tsugaric acid A	C32H50O4	[M-H]-
		HMDB35160	beta-Boswellic acid acetate		
		HMDB36008	Acetylursolic acid		
		HMDB36674	Ursololactone		
617.421477	15.8	HMDB29654	3,6-Epoxy-5,5',6,6'-tetrahydro-b,b-carotene-3',5,5',6'-tetrol	C40H58O5	[M-H]-
621.546391	15.8	HMDB07029	DG(14:0/22:1(13Z)/0:0)	C39H74O5	[M-H]-
		HMDB07057	DG(14:1(9Z)/22:0/0:0)		
		HMDB07108	DG(16:0/20:1(11Z)/0:0)		
		HMDB07136	DG(16:1(9Z)/20:0/0:0)		
		HMDB07159	DG(18:0/18:1(11Z)/0:0)		
		HMDB07160	DG(18:0/18:1(9Z)/0:0)		
		HMDB07187	DG(18:1(11Z)/18:0/0:0)		
		HMDB07216	DG(18:1(9Z)/18:0/0:0)		
		HMDB07360	DG(20:0/16:1(9Z)/0:0)		
		HMDB07388	DG(20:1(11Z)/16:0/0:0)		
		HMDB07589	DG(22:0/14:1(9Z)/0:0)		
		HMDB07617	DG(22:1(13Z)/14:0/0:0)		
		HMDB55965	DG(14:0/0:0/22:1n9)		
		HMDB56018	DG(16:0/0:0/20:1n9)		
		HMDB56042	DG(18:0/0:0/18:1n7)		
		HMDB56043	DG(18:0/0:0/18:1n9)		
		HMDB56066	DG(20:0/0:0/16:1n7)		
		HMDB56089	DG(22:0/0:0/14:1n5)		

289.071713	15.9	HMDB01871	Epicatechin	C15H14O6	[M-H]-
		HMDB02780	Catechin		
		HMDB29253	3-Hydroxyphloretin		
		HMDB30131	gamma-Pyrufuran		
		HMDB30144	alpha-Cotonefuran		
		HMDB32322	cis-3 and trans-2-Hexenyl propionate		
		HMDB33783	Marshrin		
		HMDB34124	Fonsecin		
		HMDB35399	Cartorimine		
		HMDB37953	(-)-Catechin		
		HMDB37954	(+)-Epicatechin		
		HMDB41293	6-Hydroxy-alpha-pyrufuran		
		HMDB41310	Luteoforol		
347.197617	15.9	HMDB15695	Roxatidine acetate	C19H28N2O4	[M-H]-
447.129693	15.9	HMDB29481	Isosakuranin	C22H24O10	[M-H]-
		HMDB31586	7-Hydroxy-8-O-methylaloin B		
		HMDB33741	Puddumin A		
		HMDB37509	Chalconosakuranetin		
		HMDB40561	Aromadendrin 4'-methyl ether 7-rhamnoside		
		HMDB41536	Piperenol C		
493.241025	15.9	HMDB14801	Flumethasone Pivalate	C27H36F2O6	[M-H]-
590.492065	15.9	HMDB10697	Cer(t18:0/16:0)	C34H69NO4	[M+Cl]-
		HMDB37105	Armillaramide		
227.128878	16.0	HMDB00933	Traumatic acid	C12H20O4	[M-H]-
		HMDB30994	5-Heptyltetrahydro-2-oxo-3-furancarboxylic acid		
235.097586	16.0	HMDB37683	Ethyl vanillin isobutyrate	C13H16O4	[M-H]-
		HMDB60564	Carboxy-ibuprofen		
323.098390	16.0	HMDB40985	Polixetonium chloride	C10H28Cl2N2OP2	[M-H]-
403.358161	16.0	HMDB06893	3a,7a-Dihydroxy-5b-cholestane	C27H48O2	[M-H]-
		HMDB31035	5-Heneicosyl-1,3-benzenediol		
		HMDB36844	Lepidiumterpenoid		
415.103307	16.0	HMDB30671	Pulmatin	C21H20O9	[M-H]-
		HMDB33162	(Z)-4',6-Dihydroxyaurone 6-glucoside		
		HMDB33651	Genistein 4'-rhamnoside		
		HMDB33991	Daidzin		
		HMDB36408	Franguloside		
		HMDB36618	Toringin		
		HMDB39098	Chrysophanein		
367.225587	16.0	HMDB30935	9,10,13-Trihydroxystearic acid	C18H36O5	[M+Cl]-
		HMDB34295	Floionolic acid		
435.288536	16.0	HMDB59929	3-(Acetyloxy)-2-hydroxypropyl octadecanoate	C23H44O5	[M+Cl]-
260.113948	16.1	HMDB13133	Methylmalonylcarnitine	C11H19NO6	[M-H]-
		HMDB33865	Lotaustralin		
		HMDB34777	Epidermin		
349.092883	16.1	HMDB29289	3-Feruloyl-1,5-quinolactone	C17H18O8	[M-H]-
		HMDB29290	4-Feruloyl-1,5-quinolactone		
361.129238	16.1	HMDB31366	Gibberellin A93	C19H22O7	[M-H]-
		HMDB33905	2',8-Dihydroxy-3',4',5',7-tetramethoxyflavan		
		HMDB35050	Gibberellin A21		
		HMDB36778	Diosbulbin C		
		HMDB39239	Gibberellin A87		
331.264290	16.2	HMDB02226	Adrenic acid	C22H36O2	[M-H]-
		HMDB35676	1-Hydroxy-1-phenyl-3-hexadecanone		
		HMDB35677	3-Hydroxy-1-phenyl-1-hexadecanone		
		HMDB38910	2-Methyl-5-(8-pentadecenyl)-1,3-benzenediol		
305.065774	16.2	HMDB28755	Aspartyl-Histidine	C10H14N4O5	[M+Cl]-
		HMDB28881	Histidinyl-Aspartate		
351.230665	16.2	HMDB11532	MG(0:0/15:0/0:0)	C18H36O4	[M+Cl]-
		HMDB11563	MG(15:0/0:0/0:0)		
		HMDB31008	(+)-15,16-Dihydroxyoctadecanoic acid		
		HMDB59633	(9S,10S)-9,10-dihydroxyoctadecanoate		
599.444788	16.2	HMDB07016	DG(14:0/18:2(9Z,12Z)/0:0)	C35H64O5	[M+Cl]-
		HMDB07043	DG(14:1(9Z)/18:1(11Z)/0:0)		
		HMDB07044	DG(14:1(9Z)/18:1(9Z)/0:0)		
		HMDB07128	DG(16:1(9Z)/16:1(9Z)/0:0)		
		HMDB07183	DG(18:1(11Z)/14:1(9Z)/0:0)		
		HMDB07212	DG(18:1(9Z)/14:1(9Z)/0:0)		
		HMDB07240	DG(18:2(9Z,12Z)/14:0/0:0)		
		HMDB31390	Annotemoyin 1		
		HMDB32094	Panatellin		
		HMDB32732	cis-Solamin		
		HMDB56136	DG(14:1n5/0:0/18:1n7)		

		HMDB56137	DG(14:1n5/0:0/18:1n9)		
		HMDB56156	DG(16:1n7/0:0/16:1n7)		
345.097963	16.3	HMDB37250	Muscomin	C18H18O7	[M-H]-
367.058916	16.3	HMDB37503	3,4',5-Trihydroxy-3',7-dimethoxyflavanone	C17H16O7	[M+Cl]-
		HMDB37504	3,3',5-Trihydroxy-4',7-dimethoxyflavanone		
		HMDB40320	3,5,7-Trihydroxy-4',6-dimethoxyflavanone		
		HMDB40482	2',3,5-Trihydroxy-5',7-dimethoxyflavanone		
255.150255	16.4	HMDB30201	(-)-Fumigaclavine B	C16H20N2O	[M-H]-
271.191461	16.4	HMDB35918	7(14)-Bisabolene-2,3,10,11-tetrol	C15H28O4	[M-H]-
323.077246	16.4	HMDB32984	Mahaleboside	C15H16O8	[M-H]-
375.326786	16.5	HMDB30956	5-Nonadecyl-1,3-benzenediol	C25H44O2	[M-H]-
483.296383	16.5	HMDB38539	Goshonoside F1	C26H44O8	[M-H]-
		HMDB38540	Goshonoside F2		
512.268469	16.5	HMDB02639	Sulfolithocholylglycine	C26H43NO7S	[M-H]-
493.113633	16.5	HMDB60705	12-Hydroxynevirapine glucuronide	C21H22N4O8	[M+Cl]-
		HMDB60720	2-Hydroxynevirapine glucuronide		
		HMDB60743	3-Hydroxynevirapine glucuronide		
		HMDB61130	8-Hydroxynevirapine glucuronide		
277.122781	16.6	HMDB03426	Pantetheine	C11H22N2O4S	[M-H]-
290.176181	16.6	HMDB15114	Cyclopentolate	C17H25NO3	[M-H]-
		HMDB15341	Levobunolol		
		HMDB36327	Norcapsaicin		
300.160524	16.6	HMDB14979	Dobutamine	C18H23NO3	[M-H]-
		HMDB32654	(E,E)-Futoamide		
		HMDB38648	(6E)-Piperamide-C7:1		
341.103125	16.6	HMDB29461	Zapotin	C19H18O6	[M-H]-
		HMDB30575	4',5,6,7-Tetramethoxyflavone		
		HMDB31289	1,4,6-Trihydroxy-5-methoxy-7-prenylxanthone		
		HMDB31992	Dulxanthone A		
		HMDB32736	Dulxanthone D		
		HMDB34182	1,5,8-Trihydroxy-3-methyl-2-prenylxanthone		
		HMDB59746	(1R,2S,5R,6S)-6-(3,4-Dihydroxyphenyl)-2-(3,4-methylenedioxyphenyl)-3,7-dioxabicyclo-[3,3,0]octane		
397.186782	16.6	HMDB34575	3'-Hydroxy-T2-triol	C20H30O8	[M-H]-
		HMDB36857	Cinncassiol E		
448.306837	16.6	HMDB00631	Deoxycholic acid glycine conjugate	C26H43NO5	[M-H]-
		HMDB00637	Chenodeoxycholic acid glycine conjugate		
		HMDB00708	Glycoursodeoxycholic acid		
		HMDB06898	Chenodeoxyglycocholic acid		
591.318925	16.6	HMDB01898	Mesobilirubinogen	C33H44N4O6	[M-H]-
371.189735	16.6	HMDB14951	Fentanyl	C22H28N2O	[M+Cl]-
315.123810	16.7	HMDB38323	Verimol B	C18H20O5	[M-H]-
		HMDB38324	Verimol A		
		HMDB38780	7-Hydroxy-2',4',5'-trimethoxyisoflavan		
		HMDB39510	7-Hydroxy-2',3',4'-trimethoxyisoflavan		
		HMDB39607	Sorgolactone		
		HMDB40534	5'-Hydroxy-3',4',7-trimethoxyflavan		
419.134732	16.7	HMDB37483	2',4',6'-Trihydroxydihydrochalcone 2'-glucoside	C21H24O9	[M-H]-
		HMDB37484	2',4',6'-Trihydroxydihydrochalcone 4'-glucoside		
273.053494	16.7	HMDB02511	3,4,5-Trimethoxycinnamic acid	C12H14O5	[M+Cl]-
		HMDB11721	Trans-2, 3, 4-Trimethoxycinnamate		
		HMDB31771	1-(2,4,5-Trimethoxyphenyl)-1,2-propanedione		
279.269264	16.8	HMDB34496	6,10,14-Trimethyl-2-methylenepentadecanal	C19H36O	[M-H]-
483.324883	16.8	HMDB34332	6-Deoxodolichosterone	C28H48O4	[M+Cl]-
		HMDB34423	2-Deoxycastasterone		
537.416096	16.8	HMDB15681	Plerixafor	C28H54N8	[M+Cl]-
229.144527	16.9	HMDB00623	Dodecanedioic acid	C12H22O4	[M-H]-
		HMDB30143	Talaromycin A		
		HMDB41613	Bis(1-methylethyl) hexanedioate		
		HMDB41614	Dipropyl hexanedioate		
301.108176	16.9	HMDB30717	(R)-3',7-Dihydroxy-2',4'-dimethoxyisoflavan	C17H18O5	[M-H]-
		HMDB33189	Isomucronulatol		
		HMDB33996	2',7-Dihydroxy-4',6-dimethoxyisoflavan		
		HMDB38128	(±)-Sphaerosin		
		HMDB41653	3'-Hydroxy-3,4,5,4'-tetramethoxystilbene		
331.082311	16.9	HMDB37503	3,4',5-Trihydroxy-3',7-dimethoxyflavanone	C17H16O7	[M-H]-
		HMDB37504	3,3',5-Trihydroxy-4',7-dimethoxyflavanone		
		HMDB40320	3,5,7-Trihydroxy-4',6-dimethoxyflavanone		
		HMDB40482	2',3,5-Trihydroxy-5',7-dimethoxyflavanone		
651.476327	16.9	HMDB07031	DG(14:0/22:4(7Z,10Z,13Z,16Z)/0:0)	C39H68O5	[M+Cl]-
		HMDB07112	DG(16:0/20:4(5Z,8Z,11Z,14Z)/0:0)		
		HMDB07113	DG(16:0/20:4(8Z,11Z,14Z,17Z)/0:0)		
		HMDB07139	DG(16:1(9Z)/20:3(5Z,8Z,11Z)/0:0)		

		HMDB07140	DG(16:1(9Z)/20:3(8Z,11Z,14Z)/0:0)		
		HMDB07164	DG(18:0/18:4(6Z,9Z,12Z,15Z)/0:0)		
		HMDB07191	DG(18:1(11Z)/18:3(6Z,9Z,12Z)/0:0)		
		HMDB07192	DG(18:1(11Z)/18:3(9Z,12Z,15Z)/0:0)		
		HMDB07220	DG(18:1(9Z)/18:3(6Z,9Z,12Z)/0:0)		
		HMDB07221	DG(18:1(9Z)/18:3(9Z,12Z,15Z)/0:0)		
		HMDB07248	DG(18:2(9Z,12Z)/18:2(9Z,12Z)/0:0)		
		HMDB07275	DG(18:3(6Z,9Z,12Z)/18:1(11Z)/0:0)		
		HMDB07276	DG(18:3(6Z,9Z,12Z)/18:1(9Z)/0:0)		
		HMDB07304	DG(18:3(9Z,12Z,15Z)/18:1(11Z)/0:0)		
		HMDB07305	DG(18:3(9Z,12Z,15Z)/18:1(9Z)/0:0)		
		HMDB07332	DG(18:4(6Z,9Z,12Z,15Z)/18:0/0:0)		
		HMDB07447	DG(20:3(5Z,8Z,11Z)/16:1(9Z)/0:0)		
		HMDB07476	DG(20:3(8Z,11Z,14Z)/16:1(9Z)/0:0)		
		HMDB07504	DG(20:4(5Z,8Z,11Z,14Z)/16:0/0:0)		
		HMDB07533	DG(20:4(8Z,11Z,14Z,17Z)/16:0/0:0)		
		HMDB07675	DG(22:4(7Z,10Z,13Z,16Z)/14:0/0:0)		
		HMDB55973	DG(14:0/0:0/22:4n6)		
		HMDB56026	DG(16:0/0:0/20:4n6)		
		HMDB56032	DG(16:0/0:0/20:4n3)		
		HMDB56057	DG(18:0/0:0/18:4n3)		
		HMDB56160	DG(16:1n7/0:0/20:3n9)		
		HMDB56166	DG(16:1n7/0:0/20:3n6)		
		HMDB56184	DG(18:1n7/0:0/18:3n6)		
		HMDB56191	DG(18:1n7/0:0/18:3n3)		
		HMDB56203	DG(18:1n9/0:0/18:3n6)		
		HMDB56210	DG(18:1n9/0:0/18:3n3)		
339.108545	17.0	HMDB30678	Linocinnamarin	C16H20O8	[M-H]-
		HMDB35441	Oenanthoside A		
		HMDB60021	trans-isoeugenol-O-glucuronide		
431.134763	17.0	HMDB31723	Trichocarposide	C22H24O9	[M-H]-
		HMDB33855	Medicocarpin		
		HMDB37689	3-Methoxynobiletin		
		HMDB39927	4'-O-Methylglucoliquiritigenin		
		HMDB40503	Pinostrobin 5-glucoside		
601.460420	17.0	HMDB07014	DG(14:0/18:1(11Z)/0:0)	C35H66O5	[M+Cl]-
		HMDB07015	DG(14:0/18:1(9Z)/0:0)		
		HMDB07042	DG(14:1(9Z)/18:0/0:0)		
		HMDB07099	DG(16:0/16:1(9Z)/0:0)		
		HMDB07127	DG(16:1(9Z)/16:0/0:0)		
		HMDB07154	DG(18:0/14:1(9Z)/0:0)		
		HMDB07182	DG(18:1(11Z)/14:0/0:0)		
		HMDB07211	DG(18:1(9Z)/14:0/0:0)		
		HMDB55961	DG(14:0/0:0/18:1n7)		
		HMDB55962	DG(14:0/0:0/18:1n9)		
		HMDB56015	DG(16:0/0:0/16:1n7)		
		HMDB56040	DG(18:0/0:0/14:1n5)		
355.264239	17.1	HMDB02007	Tetracosahexaenoic acid	C24H36O2	[M-H]-
		HMDB60117	Tetracosahexaenoic acid, n-3		
377.124177	17.1	HMDB29304	3,4-DHPEA-EA	C19H22O8	[M-H]-
		HMDB35037	Gibberellin A32		
		HMDB39137	2-(3,4-Dihydroxyphenylethyl)-6-epi-elenaiate		
441.285772	17.1	HMDB38242	Ascorbyl stearate	C24H42O7	[M-H]-
443.301476	17.1	HMDB32521	Stearyl citrate	C24H44O7	[M-H]-
		HMDB39225	2-Stearyl citrate		
329.175778	17.2	HMDB02121	Carnosol	C20H26O4	[M-H]-
		HMDB36749	Momilactone B		
		HMDB36753	Yucalexin P15		
		HMDB36755	Yucalexin P8		
		HMDB39613	3,3',4,4'-Tetrahydroxy-5,5'-diisopropyl-2,2'-dimethylbiphenyl		
441.322164	17.2	HMDB59931	2,3-Diacetoxypropyl stearate	C25H46O6	[M-H]-
531.299763	17.2	HMDB06888	5b-Cyprinol sulfate	C27H48O8S	[M-H]-
535.364038	17.2	HMDB33635	Cyclotricuspidogenin C	C31H52O7	[M-H]-
		HMDB35943	Cyclopassifloic acid A		
		HMDB35945	Cyclopassifloic acid C		
629.311226	17.2	HMDB04159	L-Urobilin	C33H46N4O6	[M+Cl]-
316.119099	17.3	HMDB30341	Piplartine	C17H19NO5	[M-H]-
395.113523	17.3	HMDB35465	6,8-Di-O-methylaverufin	C22H20O7	[M-H]-
		HMDB40674	Artonin L		
459.129729	17.3	HMDB30869	Wistin	C23H24O10	[M-H]-
		HMDB40129	5,7-Dihydroxy-2',6-dimethoxyisoflavone 7-rhamnoside		
		HMDB41385	6''-Acetylliquiritin		

287.056071	17.4	HMDB05810	Eriodictyol	C15H12O6	[M-H]-
		HMDB30847	Aromadendrin		
		HMDB31911	Porric acid B		
		HMDB32707	Dalbergioidin		
		HMDB37314	Norartocarpanone		
		HMDB40314	2,4',5,7-Tetrahydroxyflavanone		
		HMDB41651	3',4',5,7-Tetrahydroxyisoflavanone		
333.097976	17.4	HMDB30651	Mukurozidiol	C17H18O7	[M-H]-
347.161224	17.4	HMDB41886	Enalaprilat	C18H24N2O5	[M-H]-
557.245591	17.4	HMDB05006	Atorvastatin	C33H35FN2O5	[M-H]-
573.489074	17.4	HMDB29795	Montecristin	C37H66O4	[M-H]-
429.119077	17.5	HMDB10334	Ketoprofen glucuronide	C22H22O9	[M-H]-
		HMDB33098	5,7-Dihydroxy-6-methoxyflavone 5-rhamnoside		
		HMDB33987	Ononin		
571.473296	17.5	HMDB29792	Dieporeticenin	C37H64O4	[M-H]-
595.494361	17.5	HMDB31089	Glycerol triundecanoate	C36H68O6	[M-H]-
285.160875	17.6	HMDB60995	10-alpha-methoxy-9,10-dihydrolysergol	C17H22N2O2	[M-H]-
289.108145	17.6	HMDB38722	5,6-Dihydro-11-methoxyyangonin	C16H18O5	[M-H]-
165.055738	17.7	HMDB00375	3-(3-Hydroxyphenyl)propanoic acid	C9H10O3	[M-H]-
		HMDB00563	D-Phenyllactic acid		
		HMDB00748	L-3-Phenyllactic acid		
		HMDB00779	Phenyllactic acid		
		HMDB02072	4-Methoxyphenylacetic acid		
		HMDB02199	Desaminotyrosine		
		HMDB02229	3-Phenoxypropionic acid		
		HMDB05175	Homovanillin		
		HMDB29665	Ethyl vanillin		
		HMDB29817	Ethyl salicylate		
		HMDB31132	3,4-Dihydroxyphenylacetone		
		HMDB32030	Guaicyl acetate		
		HMDB32138	3,4-Dimethoxybenzaldehyde		
		HMDB32573	Ethylparaben		
		HMDB32605	Methyl 2-methoxybenzoate		
		HMDB32639	Methyl 4-methoxybenzoate		
		HMDB33752	3-(2-Hydroxyphenyl)propanoic acid		
		HMDB34243	Ipomeanine		
		HMDB34993	4-Methoxybenzyl formate		
		HMDB40645	3-Hydroxy-1-(4-hydroxyphenyl)-1-propanone		
		HMDB41611	Ethyl 2-furanacrylate		
		HMDB41683	4-Hydroxyphenyl-2-propionic acid		
		HMDB59969	3-Methoxyphenylacetic acid		
554.515434	17.7	HMDB10697	Cer(t18:0/16:0)	C34H69NO4	[M-H]-
		HMDB37105	Armillaramide		
371.116936	17.7	HMDB41519	Nb-Feruloyltryptamine	C20H20N2O3	[M+Cl]-
274.165981	17.8	HMDB13131	Hydroxyhexanoycarnitine	C13H25NO5	[M-H]-
325.092933	17.8	HMDB33581	trans-o-Coumaric acid 2-glucoside	C15H18O8	[M-H]-
		HMDB36735	Bilobalide A		
		HMDB36936	1-O-p-Coumaroyl-beta-D-glucose		
		HMDB39167	2-O-p-Coumaroyl-D-glucose		
		HMDB39169	6-O-p-Coumaroyl-D-glucose		
		HMDB39509	trans-p-Coumaric acid 4-glucoside		
		HMDB60077	cis-beta-D-Glucosyl-2-hydroxycinnamate		
335.077257	17.8	HMDB29287	3-Caffeoyl-1,5-quinolactone	C16H16O8	[M-H]-
		HMDB29288	4-Caffeoyl-1,5-quinolactone		
		HMDB30654	3-O-Caffeoylshikimic acid		
		HMDB33563	Juglone glucoside		
		HMDB33997	4-O-Caffeoylshikimic acid		
		HMDB33999	Dattelic acid		
329.103050	17.9	HMDB11672	Aflatoxin B1 dialcohol	C18H18O6	[M-H]-
		HMDB32655	(R)-2-Feruloyl-1-(4-Hydroxyphenyl)-1,2-ethanediol		
		HMDB33299	7-Hydroxy-3-(3-hydroxy-4-methoxybenzyl)-5-methoxy-4-chromanone		
		HMDB33697	Melilotocarpan C		
		HMDB33817	4-Hydroxy-2,3,9-trimethoxypterocarpan		
		HMDB37253	5-Hydroxy-3-(4-hydroxybenzyl)-7,8-dimethoxy-4-chromanone		
		HMDB37315	Cerasinone		
		HMDB37955	(±)-3',4'-Methylenedioxy-5,7-dimethylepicatechin		
		HMDB38494	Americanol		
		HMDB39381	Americanol A		
		HMDB39740	Isoamericanol A		
357.089068	17.9	HMDB01416	Pantetheine 4'-phosphate	C11H23N2O7PS	[M-H]-
		HMDB06834	D-Pantothenoyl-L-cysteine	C12H22N2O6S	[M+Cl]-
365.124180	17.9	HMDB34752	7-beta-D-Glucopyranosyloxybutylidenephthalide	C18H22O8	[M-H]-

191.056133	18.0	HMDB03072	Quinic acid	C7H12O6	[M-H]-
355.103444	18.0	HMDB36938	1-O-Feruloylglucose	C16H20O9	[M-H]-
		HMDB40664	Veranisatin B		
		HMDB40866	1-O-2'-Hydroxy-4'-methoxycinnamoyl-b-D-glucose		
225.088073	18.1	HMDB00245	Porphobilinogen	C10H14N2O4	[M-H]-
244.093928	18.1	HMDB28732	Asparaginyl-Hydroxyproline	C9H15N3O5	[M-H]-
		HMDB28858	Hydroxyprolyl-Asparagine		
371.259146	18.1	HMDB13627	Cervonoyl ethanolamide	C24H36O3	[M-H]-
		HMDB14629	Nabilone		
		HMDB41301	(3R, 6'Z)-3,4-Dihydro-8-hydroxy-3-(6-pentadecenyl)-1H-2-benzopyran-1-one		
617.385091	18.1	HMDB34539	3-O-cis-Coumaroylmaslinic acid	C39H54O6	[M-H]-
		HMDB36299	3-O-p-trans-Coumaroylalphitolic acid		
		HMDB40495	cis-p-Coumaroylcorosolic acid		
307.067032	18.2	HMDB33627	D-Erythroascorbic acid 1'-a-D-glucoside	C11H16O10	[M-H]-
397.129208	18.2	HMDB34030	Dulxanthone E	C22H22O7	[M-H]-
		HMDB38921	5'-Methoxycurcumin		
459.326929	18.2	HMDB32879	all-trans-Carophyll yellow	C32H44O2	[M-H]-
459.420752	18.2	HMDB38485	5-Pentacosyl-1,3-benzenediol	C31H56O2	[M-H]-
215.032793	18.2	HMDB00122	D-Glucose	C6H12O6	[M+Cl]-
		HMDB00143	D-Galactose		
		HMDB00169	D-Mannose		
		HMDB00211	Myoinositol		
		HMDB00346	3-Deoxyarabinohexonic acid		
		HMDB00516	Beta-D-Glucose		
		HMDB00660	D-Fructose		
		HMDB01151	Allose		
		HMDB01266	L-Sorbose		
		HMDB03345	Alpha-D-Glucose		
		HMDB03418	D-Tagatose		
		HMDB03449	Beta-D-Galactose		
		HMDB06088	Scyllitol		
		HMDB12326	L-Gulose		
		HMDB32222	Dihydroxyacetone (dimer)		
		HMDB33704	L-Galactose		
		HMDB34220	Levoinositol		
572.481646	18.2	HMDB00790	N-Palmitoylsphingosine	C34H67NO3	[M+Cl]-
		HMDB04949	Ceramide (d18:1/16:0)		
691.507061	18.2	HMDB56237	DG(20:3n9/0:0/18:2n6)	C42H72O5	[M+Cl]-
		HMDB56239	DG(20:3n9/0:0/20:2n6)		
		HMDB56285	DG(18:2n6/0:0/20:3n6)		
		HMDB56310	DG(20:2n6/0:0/20:3n6)		
197.068023	18.3	HMDB04400	5-Acetylamino-6-amino-3-methyluracil	C7H10N4O3	[M-H]-
		HMDB59771	6-amino-5[N-methylformylamino]-1-methyluracil		
225.186045	18.3	HMDB00499	5-Tetradecenoic acid	C14H26O2	[M-H]-
		HMDB00521	5Z-Tetradecenoic acid		
		HMDB02000	Myristoleic acid		
		HMDB05051	Tsuzuic acid		
		HMDB10732	trans-Tetra-dec-2-enoic acid		
		HMDB30921	(R)-14-Methyloxacyclotetradecan-2-one		
		HMDB31029	Ethyl (E)-2-dodecenoate		
		HMDB31073	12-Methyl-13-tridecanolide		
		HMDB32152	Acetaldehyde di-cis-3-hexenyl acetal		
		HMDB32321	2-Hexenyl octanoate		
		HMDB34561	Houttuynin		
		HMDB37188	Rhodinyl butyrate		
		HMDB37189	Rhodinyl isobutyrate		
		HMDB37227	Citronellyl butyrate		
		HMDB37228	Citronellyl isobutyrate		
		HMDB37369	Butyl 2-decenoate		
		HMDB37633	xi-Tetrahydro-3-nonyl-2H-pyran-2-one		
		HMDB38056	delta-Tetradecalactone		
		HMDB40228	1,1-Diethoxy-3,7-dimethyl-2,6-octadiene		
297.134324	18.3	HMDB36159	Toxin T2 tetrol	C15H22O6	[M-H]-
		HMDB37560	3,7,8,15-Scirpenetetrol		
328.119054	18.3	HMDB32805	N-trans-Feruloyloctopamine	C18H19NO5	[M-H]-
386.124500	18.3	HMDB31401	Dihydroxycitracridone I	C20H21NO7	[M-H]-
429.373808	18.3	HMDB01893	Alpha-Tocopherol	C29H50O2	[M-H]-
		HMDB12171	4alpha-Hydroxymethyl-4beta-methyl-5alpha-cholesta-8-en-3beta-ol		
		HMDB30022	Ikshusterol		
		HMDB59642	4-beta-Hydroxymethyl-4-alpha-methyl-5-alpha-cholest-7-en-3-beta-ol		
427.225856	18.3	HMDB60730	20, 22-Dihydrodigoxigenin	C23H36O5	[M+Cl]-
277.217262	18.4	HMDB01388	Alpha-Linolenic acid	C18H30O2	[M-H]-

		HMDB03073	Gamma-Linolenic acid		
		HMDB30962	Calendic acid		
		HMDB30963	Punicic acid		
		HMDB30964	Linolenelaidic acid		
285.076832	18.4	HMDB29527	Melilotocarpan B	C16H14O5	[M-H]-
		HMDB29870	3',7-Dihydroxy-4'-methoxyisoflavanone		
		HMDB30090	Sakuranetin		
		HMDB30622	(R)-Oxypeucedanin		
		HMDB30793	Moracin B		
		HMDB30807	3,4-Dihydro-8-hydroxy-3-(3-hydroxy-4-methoxyphenyl)-1H-2-benzopyran-1-one		
		HMDB30852	Asperxanthone		
		HMDB31420	Heliannone C		
		HMDB31620	Vestitone		
		HMDB33291	3,8-Dihydroxy-9-methoxypterocarpan		
		HMDB33309	Moracin F		
		HMDB34011	2-(2,4-Dihydroxyphenyl)-5,6-dimethoxybenzofuran		
		HMDB34012	3,4-Dihydroxy-9-methoxypterocarpan		
		HMDB34114	6alpha-Hydroxyisomedicarpin		
		HMDB34115	6alpha-Hydroxymedicarpin		
		HMDB34438	(R)-Pabulenol		
		HMDB37320	Licochalcone B		
		HMDB37322	Dihydrooroxylin		
		HMDB37489	Dihydrowogonin		
		HMDB38448	(-)-5,7-Dihydroxy-3-(4-hydroxybenzyl)-4-chromanone		
		HMDB41726	Dihydroglycitein		
291.171434	18.4	HMDB14662	Carteolol	C16H24N2O3	[M-H]-
304.082647	18.4	HMDB29839	Ascorbigen	C15H15NO6	[M-H]-
319.118732	18.4	HMDB15159	Mycophenolic acid	C17H20O6	[M-H]-
		HMDB30742	Helipyrone		
		HMDB37321	Oleacein		
433.114023	18.4	HMDB31347	2-O-Caffeoylarbutin	C21H22O10	[M-H]-
		HMDB33739	Floribundoside		
		HMDB37480	Eriodictin		
		HMDB38775	5,7,8-Trihydroxyflavanone 7-glucoside		
		HMDB39935	Dihydrogenistin		
		HMDB40536	(2R,3R)-3,3',4',7-Tetrahydroxyflavanone 7-O-alpha-L-Rhamnopyranoside		
		HMDB40832	5-Hydroxyaloin A		
		HMDB41150	7-Hydroxyaloin B		
		HMDB60772	4'-Hydroxyfenoprofen glucuronide		
519.369151	18.4	HMDB38388	Cyclopassifloic acid B	C31H52O6	[M-H]-
159.084917	18.5	HMDB31572	2-Methyl-4-propyl-1,3-oxathiane	C8H16OS	[M-H]-
		HMDB32426	(+/-)-3-(Methylthio)heptanal		
236.056465	18.5	HMDB34251	N-Benzoylaspartic acid	C11H11NO5	[M-H]-
		HMDB38942	Methyl 2,3-dihydro-3,5-dihydroxy-2-oxo-3-indoleacetic acid		
307.072483	18.5	HMDB33459	Flazine	C17H12N2O4	[M-H]-
326.103401	18.5	HMDB39502	N-(4-Hydroxycinnamoyl)tyrosine	C18H17NO5	[M-H]-
330.098319	18.5	HMDB37797	Citbrasine	C17H17NO6	[M-H]-
445.113993	18.5	HMDB02219	Glycitin	C22H22O10	[M-H]-
		HMDB29617	Glucoobtusifolin		
		HMDB33990	Sissotrin		
		HMDB34149	Prunitrin		
		HMDB35931	Rheochrysin		
		HMDB36630	Trifolirhizin		
		HMDB38821	Calycosin 7-galactoside		
		HMDB40511	Physcionin		
		HMDB40803	Kaempferide 3-rhamnoside		
		HMDB41455	3,6,7-Trihydroxy-4'-methoxyflavone 7-rhamnoside		
677.515360	18.5	HMDB56295	DG(18:2n6/0:0/22:6n3)	C44H70O5	[M-H]-
		HMDB56320	DG(20:2n6/0:0/22:6n3)		
307.166345	18.6	HMDB60990	8-Hydroxycarteolol	C16H24N2O4	[M-H]-
507.223648	18.6	HMDB33164	Acetyl-T2 Toxin	C26H36O10	[M-H]-
		HMDB37002	Mozambioside		
		HMDB37003	Cafamarine		
		HMDB38611	Gibberellin A37 glucosyl ester		
377.209925	18.6	HMDB40901	13-Hydroxy-9-methoxy-10-oxo-11-octadecenoic acid	C19H34O5	[M+Cl]-
415.262029	18.6	HMDB11545	MG(0:0/20:3(11Z,14Z,17Z)/0:0)	C23H40O4	[M+Cl]-
		HMDB11546	MG(0:0/20:3(5Z,8Z,11Z)/0:0)		
		HMDB11547	MG(0:0/20:3(8Z,11Z,14Z)/0:0)		
		HMDB11575	MG(20:3(11Z,14Z,17Z)/0:0/0:0)		
		HMDB11576	MG(20:3(5Z,8Z,11Z)/0:0/0:0)		
		HMDB11577	MG(20:3(8Z,11Z,14Z)/0:0/0:0)		
		HMDB32735	Isopersin		

		HMDB39403	2-Hydroxy-4-oxo-5,12-heneicosadien-1-yl acetate		
		HMDB41103	Persin		
263.103766	18.7	HMDB04259	Acetyl-N-formyl-5-methoxykynurenamine	C13H16N2O4	[M-H]-
		HMDB06344	Alpha-N-Phenylacetyl-L-glutamine		
		HMDB61136	di-Hydroxymelatonin		
369.119085	18.7	HMDB40865	Linusitamarin	C17H22O9	[M-H]-
		HMDB41115	Perilloside E		
		HMDB59980	4-Hydroxy-5-(phenyl)-valeric acid-O-glucuronide		
476.278410	18.7	HMDB11477	LysoPE(0:0/18:2(9Z,12Z))	C23H44NO7P	[M-H]-
		HMDB11507	LysoPE(18:2(9Z,12Z)/0:0)		
395.220603	18.9	HMDB59632	(9S,10S)-10-hydroxy-9-(phosphonooxy)octadecanoate	C18H37O7P	[M-H]-
435.129803	18.9	HMDB34573	Phenethyl 6-galloylglucoside	C21H24O10	[M-H]-
		HMDB36634	Phlorizin		
		HMDB37505	Trilobatin		
259.022469	19.0	HMDB00124	Fructose 6-phosphate	C6H13O9P	[M-H]-
		HMDB00213	Myo-inositol 1-phosphate		
		HMDB00645	Galactose 1-phosphate		
		HMDB00994	Dolichyl phosphate D-mannose		
		HMDB01076	Fructose 1-phosphate		
		HMDB01078	Mannose 6-phosphate		
		HMDB01313	D-Myo-inositol 4-phosphate		
		HMDB01401	Glucose 6-phosphate		
		HMDB01586	Glucose 1-phosphate		
		HMDB02985	Inositol phosphate		
		HMDB03498	Beta-D-Glucose 6-phosphate		
		HMDB03971	Beta-D-Fructose 6-phosphate		
		HMDB06328	D-Tagatose 1-phosphate		
		HMDB06330	D-Mannose 1-phosphate		
		HMDB06797	Sorbose 1-phosphate		
		HMDB06800	Beta-D-Fructose 2-phosphate		
		HMDB06814	1D-myo-Inositol 3-phosphate		
		HMDB06873	D-Tagatose 6-phosphate		
		HMDB60467	D-fructose 1-phosphate		
387.254066	19.0	HMDB30366	Cavipetin C	C24H36O4	[M-H]-
285.186005	19.1	HMDB00053	Androstenedione	C19H26O2	[M-H]-
		HMDB38957	Citronellyl cinnamate		
300.039473	19.1	HMDB00781	N-Acetylgalactosamine 4-sulphate	C8H15NO9S	[M-H]-
		HMDB00814	N-Acetylglucosamine 6-sulfate		
		HMDB00841	N-Acetylgalactosamine 6-sulfate		
		HMDB60663	Isoniazid alpha-ketoglutaric acid	C11H11N3O5	[M+Cl]-
313.108094	19.1	HMDB30567	(-)-3,4,9-Trimethoxypterocarpan	C18H18O5	[M-H]-
		HMDB32806	p-Hydroxyphenethyl trans-ferulate		
		HMDB33586	2'-Hydroxy-4,4',6'-trimethoxychalcone		
		HMDB33787	2,3,9-Trimethoxypterocarpan		
		HMDB37086	5,8-Dimethoxychalepensin		
		HMDB40936	beta,2-Dihydroxy-4,6-dimethoxy-3-methylchalcone		
		HMDB41645	2'-Hydroxyenterolactone		
		HMDB41650	2-Hydroxyenterolactone		
		HMDB41672	4'-Hydroxyenterolactone		
		HMDB41682	4-Hydroxyenterolactone		
		HMDB41694	5-Hydroxyenterolactone		
		HMDB41697	6'-Hydroxyenterolactone		
		HMDB41700	6-Hydroxyenterolactone		
		HMDB41703	7-Hydroxyenterolactone		
379.179603	19.1	HMDB14527	Oxyphencyclimine	C20H28N2O3	[M+Cl]-
573.429184	19.1	HMDB07012	DG(14:0/16:1(9Z)/0:0)	C33H62O5	[M+Cl]-
		HMDB07040	DG(14:1(9Z)/16:0/0:0)		
		HMDB07096	DG(16:0/14:1(9Z)/0:0)		
		HMDB07124	DG(16:1(9Z)/14:0/0:0)		
		HMDB55960	DG(14:0/0:0/16:1n7)		
		HMDB56014	DG(16:0/0:0/14:1n5)		
256.155432	19.2	HMDB13161	2-Hexenoylcarnitine	C13H23NO4	[M-H]-
356.113972	19.2	HMDB29330	Gravacridonetriol	C19H19NO6	[M-H]-
365.087765	19.2	HMDB29601	Furocoumarinic acid glucoside	C17H18O9	[M-H]-
317.064560	19.2	HMDB29619	Arabinopyranobiose	C10H18O9	[M+Cl]-
		HMDB29894	Xylobiose		
		HMDB29918	Arabinofuranobiose		
		HMDB38855	3-O-alpha-L-Arabinopyranosyl-L-arabinose		
		HMDB38880	5-O-a-L-Arabinofuranosyl-L-arabinose		
		HMDB38881	2-O-b-D-Xylopyranosyl-L-arabinose		
		HMDB38882	5-O-beta-D-Xylopyranosyl-L-arabinose		
575.444747	19.2	HMDB07011	DG(14:0/16:0/0:0)	C33H64O5	[M+Cl]-

		HMDB07068	DG(15:0/15:0/0:0)		
		HMDB07095	DG(16:0/14:0/0:0)		
		HMDB55954	DG(14:0/0:0/16:0)		
		HMDB55981	DG(15:0/0:0/15:0)		
314.103453	19.3	HMDB29324	Citpressine II	C17H17NO5	[M-H]-
373.129270	19.3	HMDB30598	(-)-Wikstromol	C20H22O7	[M-H]-
		HMDB32869	3',4',5,7,8-Pentamethoxyflavanone		
		HMDB33279	8-Hydroxypinoresinol		
		HMDB38111	Kievitone hydrate		
		HMDB38112	Kievitol		
393.119125	19.3	HMDB30817	6-Hydroxymusizin 8-O-b-D-glucopyranoside	C19H22O9	[M-H]-
		HMDB35734	2'-Oxoaloesol 7-glucoside		
226.039069	19.3	HMDB31769	Carbendazim	C9H9N3O2	[M+Cl]-
221.066664	19.4	HMDB10325	Ethyl glucuronide	C8H14O7	[M-H]-
353.124197	19.4	HMDB40797	Methyl helianthenoate F glucoside	C17H22O8	[M-H]-
		HMDB40898	Methyl (R)-8-Hydroxy-9-decene-4,6-diynoate glucoside		
403.139742	19.4	HMDB34117	(E)-4'-Methylresveratrol 3-glucoside	C21H24O8	[M-H]-
		HMDB37313	Citromitin		
		HMDB39273	Pinostilbenoside		
421.272558	19.4	HMDB11142	DHAP(18:0e)	C21H43O6P	[M-H]-
463.124647	19.4	HMDB30747	Hesperetin 7-glucoside	C22H24O11	[M-H]-
		HMDB37535	Hesperetin 5-O-glucoside		
498.322504	19.4	HMDB60547	Hydroxybuprenorphine	C30H45NO5	[M-H]-
603.499996	19.4	HMDB07081	DG(15:0/20:3(5Z,8Z,11Z)/0:0)	C38H68O5	[M-H]-
		HMDB07082	DG(15:0/20:3(8Z,11Z,14Z)/0:0)		
		HMDB07445	DG(20:3(5Z,8Z,11Z)/15:0/0:0)		
		HMDB07474	DG(20:3(8Z,11Z,14Z)/15:0/0:0)		
		HMDB55992	DG(15:0/0:0/20:3n9)		
		HMDB55998	DG(15:0/0:0/20:3n6)		
		HMDB56163	DG(16:1n7/0:0/18:2n6)		
		HMDB56165	DG(16:1n7/0:0/20:2n6)		
273.043801	19.5	HMDB59981	4-Hydroxy-5-(phenyl)-valeric acid-O-sulphate	C11H14O6S	[M-H]-
283.068443	19.5	HMDB00299	Xanthosine	C10H12N4O6	[M-H]-
353.087813	19.5	HMDB02336	Biflorin	C16H18O9	[M-H]-
		HMDB03164	Chlorogenic acid		
		HMDB29278	Cis-5-Caffeoylquinic acid		
		HMDB30652	1-O-Caffeoylquinic acid		
		HMDB30653	Cryptochlorogenic acid		
		HMDB32849	trans-Chlorogenic acid		
		HMDB40632	Isobiflorin		
		HMDB40690	5Z-Caffeoylquinic acid		
229.155790	19.6	HMDB28920	Isoleucyl-Valine	C11H22N2O3	[M-H]-
		HMDB28942	Leucyl-Valine		
		HMDB29130	Valyl-Isoleucine		
		HMDB29131	Valyl-Leucine		
231.135024	19.6	HMDB13075	Spermic acid 2	C10H20N2O4	[M-H]-
		HMDB28917	Isoleucyl-Threonine		
		HMDB28939	Leucyl-Threonine		
		HMDB29064	Threoninyl-Isoleucine		
		HMDB29065	Threoninyl-Leucine		
275.113604	19.6	HMDB34263	Triethyl citrate	C12H20O7	[M-H]-
297.097976	19.6	HMDB10350	2-Phenylethanol glucuronide	C14H18O7	[M-H]-
307.118696	19.6	HMDB37772	8-Acetylegelolide	C16H20O6	[M-H]-
345.109181	19.6	HMDB15247	Nifedipine	C17H18N2O6	[M-H]-
403.103451	19.6	HMDB33913	Cassiaside	C20H20O9	[M-H]-
		HMDB41711	cis-Resveratrol 3-O-glucuronide		
		HMDB41713	cis-Resveratrol 4'-O-glucuronide		
		HMDB41782	trans-Resveratrol 3-O-glucuronide		
		HMDB41783	trans-Resveratrol 4'-O-glucuronide		
417.119122	19.6	HMDB29520	Liquiritin	C21H22O9	[M-H]-
		HMDB30160	Natsudaidain		
		HMDB30161	5-Hydroxy-3,3',4',6,7,8-hexamethoxyflavone		
		HMDB32785	7-Hydroxy-3,3',4',5,6,8-hexamethoxyflavone		
		HMDB35219	Aloin		
		HMDB37317	Neoisoliquiritin		
		HMDB37318	Isoliquiritin		
		HMDB37486	Isosakuranetin 7-xyloside		
		HMDB37490	Neoliquiritin		
		HMDB37581	Naringenin 5-rhamnoside		
		HMDB39902	Dihydrodaidzin		
		HMDB40620	Gaylussacin		
		HMDB41098	2-Hydroxy-3-methyl-4H-pyran-4-one O-(6E-cinnamoyl-b-D-glucoside)		

		HMDB41359	6-Hydroxy-3,3',4',5,7,8-hexamethoxyflavone		
		HMDB41731	Equol 4'-O-glucuronide		
		HMDB41732	Equol 7-O-glucuronide		
		HMDB61142	Fenoprofen glucuronide		
457.114068	19.6	HMDB30689	6''-O-Acetyldaidzin	C23H22O10	[M-H]-
395.134737	19.7	HMDB40565	Aloesol 7-glucoside	C19H24O9	[M-H]-
		HMDB40897	Methyl (3x,4E,10R)-3,10-dihydroxy-4,11-dodecadiene-6,8-diynoate 10-glucoside		
424.154789	19.7	HMDB15315	Domperidone	C22H24ClN5O2	[M-H]-
		HMDB30381	Roquefortine	C22H23N5O2	[M+Cl]-
335.199633	19.7	HMDB11531	MG(0:0/14:1(9Z)/0:0)	C17H32O4	[M+Cl]-
		HMDB11562	MG(14:1(9Z)/0:0/0:0)		
413.246409	19.7	HMDB04666	2-Arachidonylglycerol	C23H38O4	[M+Cl]-
		HMDB11549	MG(0:0/20:4(8Z,11Z,14Z,17Z)/0:0)		
		HMDB11578	MG(20:4(5Z,8Z,11Z,14Z)/0:0/0:0)		
		HMDB11579	MG(20:4(8Z,11Z,14Z,17Z)/0:0/0:0)		
		HMDB35273	1-Acetoxy-2-hydroxy-5,12,15-heneicosatrien-4-one		
		HMDB36356	[12]-Gingerol		
		HMDB36568	Persenone A		
229.098239	19.8	HMDB37942	(1xi,3xi)-1,2,3,4-Tetrahydro-1-methyl-beta-carboline-3-carboxylic acid	C13H14N2O2	[M-H]-
		HMDB60811	cyclic Melatonin		
285.243478	19.8	HMDB31042	Avocadene	C17H34O3	[M-H]-
291.050966	19.8	HMDB34310	Cordeauxione	C14H12O7	[M-H]-
295.300653	19.8	HMDB02019	Phytol	C20H40O	[M-H]-
		HMDB03208	Thromboxane		
		HMDB34933	(Z)-11-Eicosen-1-ol		
363.144908	19.8	HMDB33420	Gibberellin A55	C19H24O7	[M-H]-
		HMDB35038	Gibberellin A50		
		HMDB35052	Gibberellin A49		
		HMDB36890	Gibberellin A72		
		HMDB36898	Gibberellin A76		
		HMDB39623	Gibberellin A79		
		HMDB40324	(7R*,8R*)-3-Methoxy-3',4,7,9,9'-pentahydroxy-8,4'-oxyneolignan		
		HMDB40651	Gibberellin A91		
513.139994	19.8	HMDB39925	2'',6''-Di-O-acetylononin	C26H26O11	[M-H]-
679.531121	19.8	HMDB56289	DG(18:2n6/0:0/22:5n6)	C44H72O5	[M-H]-
		HMDB56294	DG(18:2n6/0:0/22:5n3)		
		HMDB56314	DG(20:2n6/0:0/22:5n6)		
		HMDB56319	DG(20:2n6/0:0/22:5n3)		
260.077593	19.9	HMDB30277	Dihydromaleimide beta-D-glucoside	C10H15NO7	[M-H]-
		HMDB39127	Pisatoside		
267.269318	19.9	HMDB02384	Stearaldehyde	C18H36O	[M-H]-
		HMDB29632	Oleyl alcohol		
301.071722	19.9	HMDB05782	Hesperetin	C16H14O6	[M-H]-
		HMDB29491	Isoferreirin		
		HMDB30746	5,7,3'-Trihydroxy-4'-methoxyflavanone		
		HMDB31657	Ferreirin		
		HMDB31912	Porric acid A		
		HMDB32245	Divanillin		
		HMDB35616	3,3',4,4'-Tetrahydroxy-2-methoxychalcone		
		HMDB37507	Folerogenin		
		HMDB39377	2,3',6-Trihydroxy-4'-methoxybenzylcoumaranone		
		HMDB40316	Blumeatin		
		HMDB40560	4',5,7-Trihydroxy-3-methoxyflavanone		
		HMDB41673	4'-Methoxy-2',3,7-trihydroxyisoflavanone		
463.208435	19.9	HMDB39501	Na-Hexanoyl-Nb-inosityltryptophan	C23H32N2O8	[M-H]-
714.508305	19.9	HMDB08835	PE(14:0/20:2(11Z,14Z))	C39H74NO8P	[M-H]-
		HMDB08867	PE(14:1(9Z)/20:1(11Z))		
		HMDB08928	PE(16:0/18:2(9Z,12Z))		
		HMDB08959	PE(16:1(9Z)/18:1(11Z))		
		HMDB08960	PE(16:1(9Z)/18:1(9Z))		
		HMDB09023	PE(18:1(11Z)/16:1(9Z))		
		HMDB09056	PE(18:1(9Z)/16:1(9Z))		
		HMDB09088	PE(18:2(9Z,12Z)/16:0)		
		HMDB09251	PE(20:1(11Z)/14:1(9Z))		
		HMDB09283	PE(20:2(11Z,14Z)/14:0)		
317.054825	19.9	HMDB32560	Dinoseb acetate	C12H14N2O6	[M+Cl]-
524.299609	19.9	HMDB14573	Carboprost Tromethamine	C25H47NO8	[M+Cl]-
353.103100	20.0	HMDB30848	Artocarpesin	C20H18O6	[M-H]-
		HMDB33037	Isoartocarpesin		
		HMDB33877	1-(3,4-Dihydroxyphenyl)-7-(4-hydroxy-3-methoxyphenyl)-1,6-heptadiene-3,5-dione		
		HMDB33983	Cyclokievitone		
		HMDB34111	Glyceofuran		

		HMDB34125	Licoisoflavone A		
		HMDB34256	(+)-Sesamin		
		HMDB36595	Luteone		
		HMDB37249	Isolicoflavonol		
		HMDB37488	Albanin A		
		HMDB38395	Gancaonin C		
		HMDB38397	Gancaonin O		
		HMDB38479	Licoflavonol		
		HMDB38899	2',4',5,7-Tetrahydroxy-8-prenylisoflavone		
		HMDB38901	Gancaonin L		
433.280754	20.0	HMDB37183	Polysorbate 60	C22H42O8	[M-H]-
449.327261	20.0	HMDB00601	Coprocholic acid	C27H46O5	[M-H]-
		HMDB03873	3a,7a,12a-Trihydroxy-5b-cholestanoic acid		
		HMDB60137	3alpha,7alpha,12alpha,25-Tetrahydroxy-5beta-cholestane-24-one		
465.304380	20.0	HMDB00653	Cholesterol sulfate	C27H46O4S	[M-H]-
525.452517	20.0	HMDB07010	DG(14:0/15:0/0:0)	C32H62O5	[M-H]-
		HMDB07066	DG(15:0/14:0/0:0)		
		HMDB55953	DG(14:0/0:0/15:0)		
665.214729	20.0	HMDB00757	Glycogen	C24H42O21	[M-H]-
		HMDB01296	Maltotetraose		
		HMDB03553	Stachyose		
		HMDB29931	Mannan		
		HMDB35323	Fagopyritol B3		
		HMDB38490	Bifurcose		
		HMDB38870	Neobifurcose		
		HMDB38871	Sesamose		
		HMDB39173	3-beta-Glucosylcellotriose		
		HMDB39174	3-beta-Cellobiosylcellobiose		
		HMDB39176	Nystose		
		HMDB40182	Fagopyritol A3		
483.288457	20.0	HMDB32783	Porrigenin A	C27H44O5	[M+Cl]-
		HMDB34293	Asperagenin		
181.991754	20.1	HMDB29723	Saccharin	C7H5NO3S	[M-H]-
389.124192	20.1	HMDB30564	trans-Piceid	C20H22O8	[M-H]-
		HMDB30565	(Z)-Resveratrol 4'-glucoside		
		HMDB31422	cis-Piceid		
		HMDB36294	(E)-2-Glucosyl-3,4',5-trihydroxystilbene		
409.186780	20.1	HMDB30758	Pteroside A	C21H30O8	[M-H]-
		HMDB36603	Pteroside D		
		HMDB40713	Scorzoside		
593.551509	20.1	HMDB32260	Ethylene glycol distearate	C38H74O4	[M-H]-
225.113234	20.2	HMDB40705	Allixin	C12H18O4	[M-H]-
		HMDB59729	3,4-Methylenesebacic acid		
237.076873	20.2	HMDB02511	3,4,5-Trimethoxycinnamic acid	C12H14O5	[M-H]-
		HMDB11721	Trans-2, 3, 4-Trimethoxycinnamate		
		HMDB31771	1-(2,4,5-Trimethoxyphenyl)-1,2-propanedione		
331.248983	20.2	HMDB30935	9,10,13-Trihydroxystearic acid	C18H36O5	[M-H]-
		HMDB34295	Floionolic acid		
398.124497	20.2	HMDB33440	Narcotoline	C21H21NO7	[M-H]-
		HMDB40552	Adlumidiceine		
400.140158	20.2	HMDB31254	Margrapine A	C21H23NO7	[M-H]-
411.108367	20.2	HMDB33341	Mollicellin C	C22H20O8	[M-H]-
281.081932	20.3	HMDB30698	5,7-Dimethoxyisoflavone	C17H14O4	[M-H]-
		HMDB30719	5,6-Dimethoxyflavone		
		HMDB36620	5,7-Dimethoxyflavone		
		HMDB37255	5-Hydroxy-7-methoxy-6-methylflavone		
487.319737	20.3	HMDB00483	5b-Cholestane-3a,7a,12a,23S,25-pentol	C27H48O5	[M+Cl]-
		HMDB00513	5b-Cholestane-3a,7a,12a,23R,25-pentol		
		HMDB00556	5b-Cholestane-3a,7a,12a,24,25-pentol		
		HMDB00558	5a-Cholestane-3a,7a,12a,23,25-pentol		
		HMDB02180	5b-Cholestane-3a,7a,12a,25,26-pentol		
		HMDB02208	Cholestane-3,7,12,24,25-pentol		
325.129191	20.4	HMDB34755	1-Methoxy-3-(4-hydroxyphenyl)-2E-propenal 4'-glucoside	C16H22O7	[M-H]-
		HMDB34863	4-(4-Hydroxyphenyl)-2-butanone glucoside		
		HMDB38708	Citrusin C		
439.187328	20.4	HMDB33468	Diferuloylputrescine	C24H28N2O6	[M-H]-
273.074689	20.4	HMDB33065	(x)-1,2-Propanediol 1-O-b-D-glucopyranoside	C9H18O7	[M+Cl]-
487.124626	20.5	HMDB39489	6''-O-Acetylglycitin	C24H24O11	[M-H]-
288.120171	20.6	HMDB05765	Ophthalmic acid	C11H19N3O6	[M-H]-
311.113617	20.6	HMDB04304	Nivalenol	C15H20O7	[M-H]-
		HMDB31724	Moringyne		
		HMDB34861	3-Hydroxychavicol 1-glucoside		

411.202348	20.6	HMDB30082	5-(2,3-Dihydroxy-3-methylbutyl)-4-(3,4-epoxy-4-methylpentanoyl)-3,4-dihydroxy-2-isopentanoyl-2-cyclopenten-1-one	C21H32O8	[M-H]-
		HMDB39636	Abscisic alcohol 11-glucoside		
416.219195	20.6	HMDB15433	Cilazapril	C22H31N3O5	[M-H]-
449.363661	20.6	HMDB33984	6-Deoxocastasterone	C28H50O4	[M-H]-
259.082327	20.7	HMDB32924	3-Furanmethanol glucoside	C11H16O7	[M-H]-
465.118769	20.7	HMDB30106	Neosilyhermin A	C25H22O9	[M-H]-
		HMDB33324	Silyhermin		
		HMDB33325	Silandrin		
471.213897	20.7	HMDB60717	2-Hydroxy-imipramine glucuronide	C25H32N2O7	[M-H]-
261.028548	20.7	HMDB01904	3-Nitrotyrosine	C9H10N2O5	[M+Cl]-
281.077993	20.8	HMDB32560	Dinoseb acetate	C12H14N2O6	[M-H]-
536.504869	20.8	HMDB00790	N-Palmitoylsphingosine	C34H67NO3	[M-H]-
		HMDB04949	Ceramide (d18:1/16:0)		
357.101251	20.8	HMDB38340	N6-cis-p-Coumaroylserotonin	C19H18N2O3	[M+Cl]-
		HMDB41914	Ketophenylbutazone		
361.090657	20.8	HMDB06590	2-O-a-L-Fucopyranosyl-galactose	C12H22O10	[M+Cl]-
		HMDB06701	3-O-a-L-Fucopyranosyl-D-glucose		
		HMDB29523	Neohesperidose		
		HMDB40154	6-O-b-D-Fructofuranosyl-2-deoxy-D-glucose		
465.277514	20.8	HMDB11560	MG(0:0/24:6(6Z,9Z,12Z,15Z,18Z,21Z)/0:0)	C27H42O4	[M+Cl]-
		HMDB11590	MG(24:6(6Z,9Z,12Z,15Z,18Z,21Z)/0:0/0:0)		
		HMDB12458	7 alpha-Hydroxy-3-oxo-4-cholestenoate		
		HMDB30066	Australigenin		
		HMDB34403	Barogenin		
		HMDB36249	Schidigeragenin C		
		HMDB60127	25-Hydroxyvitamin D3-26,23-lactol		
		HMDB60128	24-Oxo-1alpha,25-dihydroxyvitamin D3		
413.378886	20.9	HMDB00649	Clionasterol	C29H50O	[M-H]-
		HMDB00852	Beta-Sitosterol		
		HMDB06840	4,4-Dimethyl-5a-cholesta-8-en-3b-ol		
		HMDB33214	Schottenol		
		HMDB37524	(3beta,5alpha,24R)-Stigmast-8(14)-en-3-ol		
		HMDB39444	24alpha-Methyllophenol		
		HMDB39699	(5alpha,14alpha,24R)-14-Methylergostan-3-one		
		HMDB59641	4,4-Dimethyl-5-alpha-cholest-7-en-3-beta-ol		
458.145681	20.9	HMDB38598	Narceinone	C23H25NO9	[M-H]-
483.129474	20.9	HMDB30584	Silidianin	C25H24O10	[M-H]-
615.499471	20.9	HMDB07031	DG(14:0/22:4(7Z,10Z,13Z,16Z)/0:0)	C39H68O5	[M-H]-
		HMDB07112	DG(16:0/20:4(5Z,8Z,11Z,14Z)/0:0)		
		HMDB07113	DG(16:0/20:4(8Z,11Z,14Z,17Z)/0:0)		
		HMDB07139	DG(16:1(9Z)/20:3(5Z,8Z,11Z)/0:0)		
		HMDB07140	DG(16:1(9Z)/20:3(8Z,11Z,14Z)/0:0)		
		HMDB07164	DG(18:0/18:4(6Z,9Z,12Z,15Z)/0:0)		
		HMDB07191	DG(18:1(11Z)/18:3(6Z,9Z,12Z)/0:0)		
		HMDB07192	DG(18:1(11Z)/18:3(9Z,12Z,15Z)/0:0)		
		HMDB07220	DG(18:1(9Z)/18:3(6Z,9Z,12Z)/0:0)		
		HMDB07221	DG(18:1(9Z)/18:3(9Z,12Z,15Z)/0:0)		
		HMDB07248	DG(18:2(9Z,12Z)/18:2(9Z,12Z)/0:0)		
		HMDB07275	DG(18:3(6Z,9Z,12Z)/18:1(11Z)/0:0)		
		HMDB07276	DG(18:3(6Z,9Z,12Z)/18:1(9Z)/0:0)		
		HMDB07304	DG(18:3(9Z,12Z,15Z)/18:1(11Z)/0:0)		
		HMDB07305	DG(18:3(9Z,12Z,15Z)/18:1(9Z)/0:0)		
		HMDB07332	DG(18:4(6Z,9Z,12Z,15Z)/18:0/0:0)		
		HMDB07447	DG(20:3(5Z,8Z,11Z)/16:1(9Z)/0:0)		
		HMDB07476	DG(20:3(8Z,11Z,14Z)/16:1(9Z)/0:0)		
		HMDB07504	DG(20:4(5Z,8Z,11Z,14Z)/16:0/0:0)		
		HMDB07533	DG(20:4(8Z,11Z,14Z,17Z)/16:0/0:0)		
		HMDB07675	DG(22:4(7Z,10Z,13Z,16Z)/14:0/0:0)		
		HMDB55973	DG(14:0/0:0/22:4n6)		
		HMDB56026	DG(16:0/0:0/20:4n6)		
		HMDB56032	DG(16:0/0:0/20:4n3)		
		HMDB56057	DG(18:0/0:0/18:4n3)		
		HMDB56160	DG(16:1n7/0:0/20:3n9)		
		HMDB56166	DG(16:1n7/0:0/20:3n6)		
		HMDB56184	DG(18:1n7/0:0/18:3n6)		
		HMDB56191	DG(18:1n7/0:0/18:3n3)		
		HMDB56203	DG(18:1n9/0:0/18:3n6)		
		HMDB56210	DG(18:1n9/0:0/18:3n3)		
241.071766	21.0	HMDB38126	Genipinic acid	C11H14O6	[M-H]-
		HMDB39136	Elenaic acid		
370.129584	21.0	HMDB30171	N-Methyl-14-O-demethylepiporphyroxine	C20H21NO6	[M-H]-
451.452111	21.0	HMDB29987	(+)-11-Hydroxy-9-triacontanone	C30H60O2	[M-H]-

		HMDB30925	Melissic acid A		
209.068043	21.1	HMDB02123	1,3,7-Trimethyluric acid	C8H10N4O3	[M-H]-
		HMDB36431	1,3,9-Trimethyluric acid		
510.489124	21.1	HMDB11759	Cer(d18:0/14:0)	C32H65NO3	[M-H]-
331.204616	21.1	HMDB04667	13S-hydroxyoctadecadienoic acid	C18H32O3	[M+Cl]-
		HMDB04670	Alpha-dimorphecolic acid		
		HMDB04701	9,10-Epoxyoctadecenoic acid		
		HMDB04702	12,13-EpOME		
		HMDB10223	9-HODE		
		HMDB29796	(Z)-13-Oxo-9-octadecenoic acid		
		HMDB29978	Avenoleic acid		
		HMDB29998	12-Hydroxy-8,10-octadecadienoic acid		
627.476372	21.1	HMDB07022	DG(14:0/20:2(11Z,14Z)/0:0)	C37H68O5	[M+Cl]-
		HMDB07050	DG(14:1(9Z)/20:1(11Z)/0:0)		
		HMDB07103	DG(16:0/18:2(9Z,12Z)/0:0)		
		HMDB07130	DG(16:1(9Z)/18:1(11Z)/0:0)		
		HMDB07131	DG(16:1(9Z)/18:1(9Z)/0:0)		
		HMDB07186	DG(18:1(11Z)/16:1(9Z)/0:0)		
		HMDB07215	DG(18:1(9Z)/16:1(9Z)/0:0)		
		HMDB07243	DG(18:2(9Z,12Z)/16:0/0:0)		
		HMDB07386	DG(20:1(11Z)/14:1(9Z)/0:0)		
		HMDB07414	DG(20:2(11Z,14Z)/14:0/0:0)		
		HMDB32714	cis-Uvariamicin IB		
		HMDB34302	Reticulatain 2		
		HMDB34560	cis-Uvariamicin IV		
		HMDB34924	Neoreticulatacin A		
		HMDB55995	DG(15:0/0:0/18:2n6)		
		HMDB55997	DG(15:0/0:0/20:2n6)		
		HMDB56138	DG(14:1n5/0:0/20:1n9)		
		HMDB56157	DG(16:1n7/0:0/18:1n7)		
		HMDB56158	DG(16:1n7/0:0/18:1n9)		
297.243503	21.2	HMDB10736	3-Oxooctadecanoic acid	C18H34O3	[M-H]-
		HMDB30979	9-Oxooctadecanoic acid		
		HMDB30980	10-Oxooctadecanoic acid		
		HMDB30981	11-Oxooctadecanoic acid		
		HMDB31127	5-Hexyltetrahydro-2-furanoctanoic acid		
		HMDB34074	5-Oxooctadecanoic acid		
		HMDB34297	Ricinoleic acid		
320.113916	21.2	HMDB32808	Niazirinin	C16H19NO6	[M-H]-
405.119106	21.2	HMDB30824	Afzelechin 7-apioside	C20H22O9	[M-H]-
		HMDB31423	omega-Salicoyisalicin		
		HMDB38330	Benzyl 2,6-dihydroxybenzoate 2-glucoside		
		HMDB39039	(R)-Apiumetin glucoside		
		HMDB39172	Flacourtin		
		HMDB40555	(E)-Oxyresveratrol 3'-O-b-D-glucoside		
		HMDB40863	Piceatannol 4'-glucoside		
		HMDB41265	Edulisin VI		
		HMDB60923	Naproxen O-glucuronide		
431.389421	21.2	HMDB38524	5-Tricosyl-1,3-benzenediol	C29H52O2	[M-H]-
590.298798	21.2	HMDB29334	Nummularine B	C32H41N5O6	[M-H]-
449.231479	21.2	HMDB39883	Ascorbyl palmitate	C22H38O7	[M+Cl]-
503.242019	21.2	HMDB10321	3,17-Androstanediol glucuronide	C25H40O8	[M+Cl]-
		HMDB10339	3-alpha-Androstanediol glucuronide		
		HMDB10359	17-Hydroxyandrostane-3-glucuronide		

Table S12. Parameters used for feature selection procedure followed by constructing an optimal ML-PLS-DA model.

	OTU counts dataset	**Stool metabolome dataset**	**Plasma metabolome dataset**
Number of iterations	4	5	5
Fraction of features chosen after the 1st iteration	2/3	1/2	1/2
Fraction of features chosen after the 2nd iteration	2/3	1/2	1/2
Fraction of features chosen after the 3rd iteration	2/3	1/2	1/2
Fraction of features chosen after the 4th iteration	2/3	1/2	1/2
Fraction of features chosen after the 5th iteration	-	1/2	1/2
Number of splits in the cross-validation procedure	7	7	7
Number of cross-validation procedures	100	100	100
Number of permutation tests	2000	2000	2000

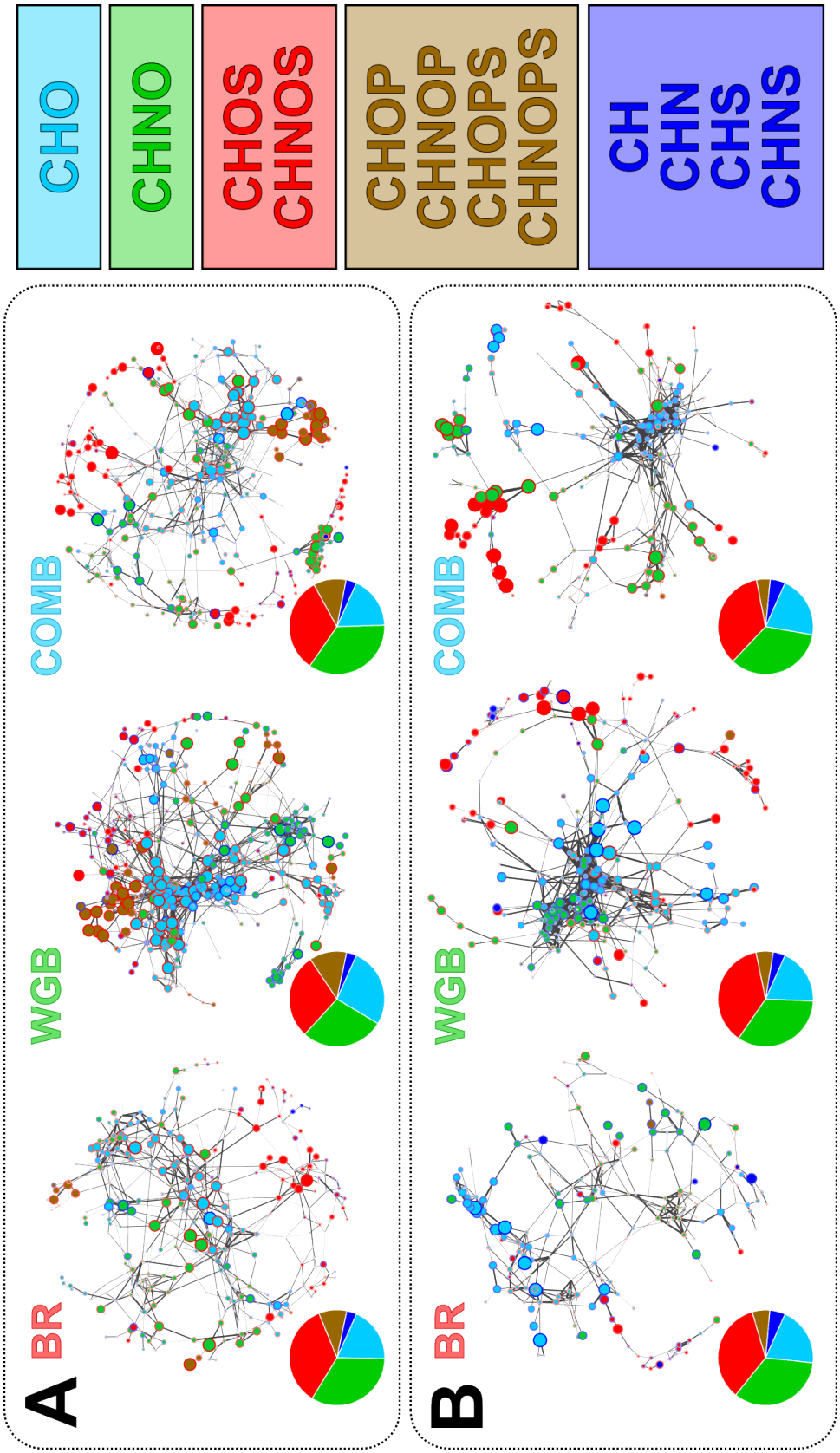

Fig. S1. The subnetworks constructed by considering the nodes corresponding to the features selected by ML-PLS-DA. The graphs were built for every diet group within A) stool metabolome dataset and B) plasma metabolome dataset. The node sizes are proportional to the mean difference of intensity values between a treatment group and the baseline. The pie charts depict the proportions of the elemental composition types within the subnetworks.

Table S13. The results of the ORA using the edges of MDiNs corresponding to fecal metabolome dataset. For each of the diet group, the calculations were done considering three scenarios differing by the amount of edges used. First scenario included edges without differentiating the corresponding nodes according to the sign of the assigned regression coefficients. The second and the third scenario involved differentiating the edges by the aforementioned scheme.

	BR, p-value			COMB, p-value			WGB, p-value		
Id	Total	Positive	Negative	Total	Positive	Negative	Total	Positive	Negative
1	1.00E+00	6.86E-01	6.22E-01	1.00E+00	9.75E-01	9.96E-01	1.00E+00	9.70E-01	4.26E-01
2	9.86E-01	5.92E-01	2.95E-01	9.98E-01	8.79E-02	7.12E-01	9.98E-01	7.95E-01	3.06E-01
3	1.00E+00	7.30E-01	4.13E-01	9.99E-01	1.45E-02	6.23E-01	9.82E-01	6.82E-01	8.21E-02
4	6.67E-01	3.61E-01	9.41E-02	7.13E-01	1.32E-01	7.85E-01	8.96E-02	3.58E-02	1.79E-02
5	1.00E+00	8.02E-01	3.24E-01	9.75E-01	6.10E-02	7.83E-01	5.26E-01	2.98E-01	4.52E-02
6	1.87E-01	7.69E-01	6.58E-02	9.40E-01	8.36E-01	4.87E-01	6.83E-01	6.01E-01	5.31E-01
7	9.87E-01	6.66E-01	1.80E-01	8.15E-01	3.52E-03	7.26E-01	5.75E-02	2.39E-03	1.34E-02
8	3.67E-01	1.07E-01	2.14E-02	8.19E-01	1.79E-01	7.53E-01	9.98E-01	9.19E-01	6.49E-01
9	1.00E+00	9.07E-01	8.69E-01	1.00E+00	7.14E-02	6.92E-01	9.41E-01	2.87E-01	1.99E-01
10	1.00E+00	8.87E-01	4.79E-01	1.00E+00	1.09E-02	7.92E-01	9.95E-01	2.00E-01	1.24E-01
11	9.45E-01	2.28E-01	7.49E-02	9.99E-01	2.56E-01	7.73E-01	9.97E-01	4.15E-01	6.29E-01
12	9.95E-01	3.36E-01	6.24E-01	9.99E-01	6.15E-02	9.47E-01	1.00E+00	4.53E-02	6.01E-01
13	1.00E+00	9.64E-01	3.18E-01	1.00E+00	6.61E-02	9.20E-01	1.00E+00	4.80E-01	1.87E-01
14	9.77E-01	1.90E-01	1.98E-01	1.00E+00	2.02E-01	8.01E-01	9.97E-01	5.96E-01	5.27E-01
15	1.00E+00	3.68E-01	7.81E-01	1.00E+00	8.66E-03	9.93E-01	1.00E+00	7.97E-01	6.45E-01
16	9.96E-01	5.02E-01	3.95E-02	1.00E+00	1.60E-01	8.58E-01	7.82E-01	7.08E-01	8.92E-02
17	9.54E-01	5.36E-01	2.75E-01	8.63E-01	2.98E-02	3.17E-01	1.00E+00	9.79E-01	3.76E-02
18	9.97E-01	7.70E-01	6.19E-01	1.00E+00	9.98E-01	9.76E-01	1.00E+00	9.90E-01	9.99E-01
19	9.98E-01	7.91E-01	3.66E-01	9.87E-01	5.19E-01	6.48E-01	9.97E-01	9.83E-01	4.17E-01
20	9.86E-01	4.81E-01	2.74E-01	9.99E-01	6.76E-02	9.28E-01	1.00E+00	9.61E-01	8.16E-01
21	1.00E+00	3.91E-01	3.64E-01	1.00E+00	5.38E-01	9.84E-01	1.00E+00	7.58E-01	7.32E-01
22	9.99E-01	7.17E-01	9.13E-01	1.00E+00	9.71E-01	9.50E-01	1.00E+00	9.59E-01	9.72E-01
23	9.85E-01	6.34E-01	3.93E-01	9.87E-01	5.86E-02	6.52E-01	9.79E-01	7.16E-01	3.13E-01
24	1.00E+00	1.00E+00	1.00E+00	1.00E+00	1.00E+00	1.00E+00	3.19E-02	3.19E-02	3.19E-02
25	1.00E+00	8.67E-01	5.00E-01	1.00E+00	1.62E-02	7.20E-01	9.57E-01	7.55E-02	2.09E-01
26	9.68E-01	7.61E-01	9.82E-01	1.00E+00	9.94E-01	9.98E-01	9.46E-01	4.98E-01	9.02E-01
27	9.67E-01	4.08E-01	1.65E-01	9.99E-01	4.76E-02	7.67E-01	1.00E+00	7.13E-01	8.48E-01
28	9.99E-01	5.98E-01	3.50E-01	1.00E+00	8.16E-03	8.21E-01	1.00E+00	8.25E-01	6.94E-01
29	1.00E+00	1.00E+00	1.00E+00	6.04E-02	8.91E-02	1.70E-01	1.00E+00	9.26E-02	1.00E+00
30	9.65E-01	2.92E-01	5.24E-01	9.97E-01	4.15E-02	8.18E-01	9.99E-01	6.66E-01	9.09E-01
31	3.07E-01	3.78E-02	7.89E-03	9.01E-01	3.68E-03	9.66E-01	9.97E-01	6.89E-01	8.76E-01
32	9.70E-01	2.84E-01	3.58E-01	1.00E+00	2.10E-01	9.84E-01	9.66E-01	2.25E-01	7.30E-01
33	9.99E-01	6.08E-01	3.68E-01	9.99E-01	2.88E-01	4.64E-01	1.00E+00	7.71E-01	2.30E-01
34	6.81E-01	1.28E-01	6.48E-01	5.88E-01	3.95E-01	3.74E-01	3.08E-01	2.38E-01	1.48E-03
35	5.65E-01	1.17E-01	6.32E-02	9.28E-01	7.63E-03	6.81E-01	9.95E-01	9.10E-01	2.61E-01
36	9.98E-01	4.16E-01	7.96E-01	1.00E+00	3.99E-01	8.31E-01	9.99E-01	6.32E-01	9.64E-01
37	4.07E-01	4.37E-01	1.14E-02	8.05E-01	3.76E-02	6.41E-01	7.91E-02	5.54E-02	3.71E-02
38	9.86E-01	4.74E-01	4.07E-01	1.00E+00	9.24E-01	9.13E-01	9.98E-01	6.21E-01	8.83E-01
39	8.02E-01	2.54E-01	6.14E-01	2.47E-01	1.15E-01	6.66E-01	2.72E-01	6.33E-01	2.18E-01
40	3.80E-01	2.70E-01	9.60E-02	8.87E-01	8.19E-01	8.08E-01	4.55E-01	2.56E-01	2.39E-01
41	1.00E+00	4.85E-01	3.86E-01	9.97E-01	3.32E-01	9.42E-01	9.80E-01	5.59E-01	4.48E-02
42	1.00E+00	1.00E+00	1.00E+00	1.00E+00	1.00E+00	1.00E+00	3.19E-02	3.19E-02	6.27E-02
43	1.00E+00	2.33E-01	4.28E-01	1.00E+00	2.62E-02	9.94E-01	1.00E+00	7.67E-02	5.67E-01
44	9.39E-01	2.50E-01	5.04E-01	9.94E-01	9.89E-02	8.29E-01	9.95E-01	9.79E-01	4.37E-01
45	9.94E-01	3.53E-01	1.64E-01	9.98E-01	5.89E-02	6.22E-01	9.99E-01	6.76E-01	7.70E-01
46	9.69E-01	4.06E-01	2.16E-01	9.97E-01	3.54E-02	8.92E-01	9.99E-01	9.77E-01	5.08E-01
47	9.90E-01	3.56E-01	5.09E-01	1.00E+00	6.37E-01	7.79E-01	1.00E+00	9.47E-01	9.46E-01
48	1.00E+00	2.02E-01	8.37E-01	1.00E+00	1.03E-01	9.39E-01	9.56E-01	9.01E-02	5.61E-01
49	9.84E-01	5.35E-01	1.78E-01	1.00E+00	4.78E-01	7.51E-01	1.00E+00	9.04E-01	9.48E-01
50	6.48E-01	2.71E-01	5.23E-02	5.41E-01	3.50E-02	3.04E-01	2.16E-01	3.06E-01	2.41E-02
51	1.00E+00	5.72E-01	6.17E-01	1.00E+00	6.57E-01	9.55E-01	9.94E-01	5.13E-01	7.05E-02
52	8.87E-01	2.94E-01	1.52E-01	9.79E-01	7.25E-02	6.50E-01	1.00E+00	9.99E-01	5.16E-01
53	1.00E+00	1.00E+00	1.00E+00	1.00E+00	1.00E+00	1.00E+00	9.26E-02	3.19E-02	6.27E-02
54	9.76E-01	5.92E-01	7.99E-02	1.00E+00	6.70E-03	9.55E-01	1.00E+00	5.15E-01	2.60E-01
55	9.67E-01	3.56E-01	2.40E-01	9.98E-01	1.48E-01	9.02E-01	1.00E+00	8.96E-01	9.70E-01
56	9.40E-01	6.50E-01	4.66E-02	9.94E-01	2.88E-02	9.38E-01	9.25E-01	4.00E-01	8.17E-02
57	9.44E-01	3.85E-01	2.35E-01	6.19E-01	7.22E-05	2.37E-01	4.28E-01	7.90E-01	1.03E-02
58	9.29E-01	3.55E-01	1.13E-01	1.00E+00	1.96E-02	9.64E-01	9.99E-01	9.84E-01	5.17E-01
59	1.00E+00	5.49E-01	2.31E-01	9.99E-01	1.93E-01	8.31E-01	9.92E-01	3.14E-01	6.38E-01
60	8.20E-01	1.46E-01	5.61E-01	9.24E-01	3.52E-02	4.93E-01	1.00E+00	9.99E-01	2.23E-01
61	5.96E-01	7.36E-01	8.59E-02	7.35E-01	2.06E-01	6.85E-01	4.15E-01	3.37E-01	1.58E-02
62	9.89E-01	6.17E-01	2.24E-01	1.00E+00	8.79E-01	9.75E-01	9.99E-01	6.08E-01	7.59E-01
63	5.99E-01	2.12E-02	2.12E-02	9.59E-01	8.18E-02	7.41E-01	9.94E-01	8.61E-01	2.59E-01
64	9.71E-01	5.60E-01	1.60E-01	1.00E+00	2.62E-01	9.04E-01	9.89E-01	7.86E-01	4.99E-01
65	6.40E-01	3.95E-01	6.03E-01	9.93E-01	9.37E-01	8.45E-01	9.21E-01	7.65E-01	8.79E-01
66	9.18E-01	5.98E-01	8.53E-03	9.75E-01	7.64E-03	7.30E-01	2.58E-02	1.69E-04	1.77E-02
67	9.94E-01	1.64E-01	6.35E-01	1.00E+00	3.36E-01	9.76E-01	1.00E+00	4.32E-01	8.65E-01
68	1.00E+00	5.10E-01	4.03E-01	1.00E+00	1.33E-02	9.59E-01	9.89E-01	1.84E-01	6.11E-01
69	9.74E-01	3.60E-01	1.17E-01	1.00E+00	7.81E-02	8.75E-01	9.98E-01	9.70E-01	4.06E-01
70	9.55E-01	1.33E-01	1.83E-02	9.54E-01	4.96E-03	6.65E-01	7.79E-01	4.91E-01	2.16E-01
71	9.98E-01	1.86E-01	6.81E-01	1.00E+00	5.15E-01	9.42E-01	9.87E-01	3.25E-01	6.71E-01
72	1.00E+00	4.44E-01	1.42E-01	9.97E-01	7.46E-02	6.10E-01	7.05E-01	2.04E-02	3.75E-01
73	9.59E-01	5.51E-01	1.92E-01	4.60E-01	1.60E-05	4.10E-01	2.02E-01	4.89E-01	3.56E-04
74	6.56E-01	7.53E-02	4.86E-01	9.89E-01	4.76E-01	7.18E-01	1.00E+00	8.92E-01	8.40E-01
75	9.59E-01	3.21E-01	4.59E-01	1.00E+00	2.32E-01	9.68E-01	9.98E-01	7.50E-01	8.74E-01
76	9.93E-01	6.94E-01	5.54E-01	1.00E+00	1.29E-01	8.35E-01	9.83E-01	3.31E-01	6.34E-01
77	9.32E-01	1.21E-01	3.73E-01	2.91E-01	1.89E-02	4.66E-02	3.97E-04	4.68E-06	3.13E-06
78	7.11E-01	1.77E-01	1.68E-01	1.00E+00	1.20E-01	8.80E-01	9.99E-01	8.29E-01	7.36E-01
79	9.59E-01	3.96E-01	4.24E-01	1.00E+00	7.97E-01	8.97E-01	9.95E-01	6.20E-01	9.41E-01
80	9.02E-01	5.37E-01	1.76E-01	1.00E+00	4.22E-01	9.97E-01	9.98E-01	9.81E-01	6.58E-01
81	9.31E-01	1.54E-01	9.64E-01	6.29E-01	1.78E-03	3.71E-01	1.00E+00	9.28E-01	5.97E-02
82	7.32E-01	2.23E-02	1.52E-01	9.19E-01	2.47E-01	8.02E-01	9.90E-01	9.19E-01	7.73E-01
83	3.29E-01	1.60E-01	5.93E-01	5.79E-01	5.50E-03	5.10E-01	3.06E-01	2.94E-02	4.24E-01

84	8.00E-01	1.57E-01	5.15E-02	9.98E-01	1.10E-01	9.04E-01	9.74E-01	7.46E-01	1.19E-01
85	7.42E-01	2.73E-01	4.70E-02	4.45E-01	1.32E-02	1.51E-01	7.50E-01	3.87E-01	6.71E-01
86	9.83E-01	2.74E-01	9.55E-02	1.00E+00	5.89E-01	8.83E-01	9.99E-01	8.23E-01	8.68E-01
87	8.58E-01	2.40E-01	9.67E-02	9.59E-01	9.36E-01	9.26E-01	9.96E-01	6.83E-01	9.70E-01
88	9.89E-01	5.89E-01	1.28E-01	9.99E-01	2.27E-03	9.54E-01	4.48E-01	8.20E-02	6.53E-02
89	8.53E-01	1.29E-01	7.36E-02	8.42E-01	1.77E-03	6.57E-01	1.20E-01	1.53E-01	1.06E-03
90	9.90E-01	5.84E-01	5.63E-01	1.00E+00	9.51E-01	9.81E-01	1.00E+00	9.67E-01	6.34E-01
91	9.48E-01	4.63E-01	5.01E-01	1.00E+00	4.30E-01	9.89E-01	9.99E-01	6.59E-01	8.30E-01
92	9.51E-01	2.80E-01	7.98E-02	9.96E-01	7.17E-03	7.60E-01	1.68E-01	7.46E-03	1.76E-03
93	9.05E-01	1.60E-01	3.70E-01	9.99E-01	4.93E-02	5.97E-01	9.98E-01	8.07E-01	7.94E-01
94	9.85E-01	2.80E-01	7.14E-01	1.00E+00	7.99E-01	9.74E-01	9.99E-01	8.23E-01	8.04E-01
95	9.95E-01	9.56E-01	5.50E-01	1.00E+00	9.95E-01	1.00E+00	1.00E+00	9.99E-01	9.18E-01
96	9.47E-01	7.09E-01	4.37E-01	1.00E+00	3.01E-01	8.99E-01	9.97E-01	6.63E-01	3.93E-01
97	6.48E-01	2.31E-01	2.98E-01	8.95E-01	2.09E-01	1.92E-01	9.92E-01	9.21E-01	3.97E-01
98	9.65E-01	6.21E-01	7.71E-01	9.98E-01	7.37E-01	6.60E-01	9.69E-01	5.87E-01	7.53E-01
99	8.95E-01	5.60E-01	6.87E-01	9.37E-01	7.01E-02	9.14E-01	9.81E-01	9.03E-01	9.52E-03
100	9.43E-01	1.69E-01	9.27E-02	1.00E+00	8.24E-01	9.55E-01	1.00E+00	8.50E-01	9.03E-01
101	4.38E-01	3.81E-01	5.37E-01	9.53E-01	1.24E-02	3.21E-01	1.33E-02	1.99E-03	2.42E-01
102	8.37E-01	5.11E-01	3.77E-01	6.35E-01	3.18E-02	4.73E-01	9.87E-01	9.90E-01	1.08E-01
103	6.48E-01	6.22E-01	1.93E-01	1.94E-01	3.68E-03	8.15E-02	2.98E-02	1.13E-02	1.68E-01
104	9.93E-01	1.65E-01	7.02E-01	1.00E+00	8.19E-01	9.87E-01	1.00E+00	9.93E-01	6.25E-01
105	7.22E-01	1.30E-01	4.40E-02	9.60E-01	1.06E-02	7.95E-01	4.13E-01	3.07E-03	3.96E-03
106	8.54E-01	3.33E-01	4.11E-01	9.99E-01	3.87E-02	9.88E-01	9.98E-01	9.59E-01	9.84E-01
107	9.99E-01	8.00E-01	5.01E-01	9.73E-01	9.32E-02	9.59E-01	9.92E-01	6.85E-01	5.16E-01
108	9.84E-01	1.64E-01	7.38E-01	1.00E+00	5.44E-01	9.84E-01	9.97E-01	6.70E-01	7.96E-01
109	8.03E-01	3.88E-01	9.69E-02	9.99E-01	2.60E-01	7.80E-01	9.89E-01	5.84E-01	7.63E-01
110	9.48E-01	4.62E-01	2.09E-01	1.00E+00	6.07E-01	9.72E-01	9.99E-01	7.27E-01	8.56E-01
111	7.90E-01	4.30E-01	1.61E-02	5.13E-01	5.07E-01	6.02E-01	2.08E-01	3.81E-01	5.63E-02
112	9.66E-01	7.83E-01	5.08E-01	9.34E-01	9.99E-02	9.51E-01	7.47E-01	8.46E-01	7.87E-03
113	7.03E-01	3.25E-01	5.02E-01	9.97E-01	1.91E-01	9.89E-01	1.00E+00	1.00E+00	7.69E-01
114	6.17E-01	1.44E-01	1.05E-02	7.44E-01	5.38E-01	4.37E-01	1.95E-01	2.34E-01	2.38E-02
115	9.83E-01	4.09E-01	2.27E-01	9.80E-01	1.21E-01	6.34E-01	9.83E-01	9.10E-01	1.98E-01
116	4.05E-01	3.35E-01	3.62E-02	3.56E-01	1.55E-01	8.71E-01	7.82E-01	9.91E-01	3.05E-01
117	6.61E-01	8.52E-01	1.93E-02	9.53E-01	2.75E-01	3.81E-01	7.52E-01	8.37E-01	6.35E-01
118	1.00E+00	8.61E-01	3.84E-01	1.00E+00	6.04E-01	9.66E-01	1.00E+00	9.48E-01	9.75E-01
119	5.27E-01	2.47E-02	3.80E-01	9.54E-01	7.10E-02	6.11E-01	9.92E-01	9.70E-01	4.17E-02
120	9.04E-01	8.08E-01	2.06E-01	9.97E-01	4.13E-01	9.14E-01	1.00E+00	9.69E-01	9.63E-01
121	9.03E-01	4.05E-01	8.76E-02	9.35E-01	6.19E-02	9.89E-01	1.00E+00	9.89E-01	8.32E-01
122	9.58E-01	1.58E-01	5.68E-01	1.00E+00	7.95E-01	9.84E-01	1.00E+00	9.68E-01	9.18E-01
123	3.34E-01	3.01E-01	4.33E-02	7.22E-01	3.19E-02	6.43E-01	9.38E-01	4.78E-01	7.39E-02
124	4.97E-01	4.52E-01	1.32E-01	3.90E-01	8.70E-02	7.82E-01	2.57E-01	2.34E-01	4.22E-02
125	8.47E-01	3.22E-01	3.02E-01	9.69E-01	2.20E-01	9.05E-01	1.00E+00	5.44E-01	9.89E-01
126	5.58E-01	3.16E-02	9.78E-01	1.19E-01	2.22E-02	6.82E-01	2.73E-01	1.48E-01	1.57E-01
127	9.90E-01	4.83E-01	3.32E-01	9.67E-01	2.66E-03	9.95E-01	9.98E-01	9.27E-01	2.71E-01
128	9.92E-01	5.87E-01	5.05E-01	9.99E-01	3.81E-01	7.22E-01	9.98E-01	8.96E-01	8.04E-01
129	8.72E-01	4.72E-01	3.43E-01	9.95E-01	2.55E-01	1.00E+00	9.99E-01	9.98E-01	6.82E-01
130	2.89E-01	1.45E-01	4.87E-02	7.02E-01	7.70E-03	8.21E-01	3.34E-01	7.95E-01	6.67E-03
131	6.45E-01	8.91E-02	5.47E-01	7.87E-01	1.13E-02	8.88E-01	9.81E-01	9.11E-01	4.52E-02
132	7.77E-01	1.61E-01	1.04E-01	3.12E-01	2.39E-01	9.53E-01	7.69E-01	6.33E-01	6.08E-01
133	1.00E-01	3.89E-01	2.78E-01	1.75E-01	1.02E-03	2.15E-01	9.51E-02	1.60E-02	2.50E-01
134	6.02E-01	1.60E-02	2.11E-02	9.26E-01	2.59E-02	4.38E-01	1.33E-01	2.04E-03	5.92E-03
135	8.26E-01	4.30E-02	7.76E-02	9.97E-01	3.61E-01	9.27E-01	9.99E-01	9.39E-01	6.54E-01
136	8.17E-01	3.20E-01	1.34E-01	9.64E-01	1.71E-02	8.54E-01	9.54E-01	3.59E-01	4.17E-01
137	7.38E-01	6.03E-02	7.58E-02	6.63E-01	4.80E-04	7.91E-01	3.50E-01	5.01E-01	2.05E-02
138	9.96E-01	6.84E-01	7.03E-01	1.00E+00	9.44E-01	9.33E-01	1.00E+00	9.85E-01	9.44E-01
139	9.77E-01	7.96E-01	2.90E-01	1.00E+00	4.59E-01	8.55E-01	9.42E-01	4.99E-01	8.67E-01
140	8.41E-01	1.51E-01	3.65E-01	9.97E-01	1.67E-01	7.93E-01	9.65E-01	1.83E-01	8.31E-01
141	6.19E-01	6.11E-02	1.98E-01	6.65E-01	2.55E-03	8.19E-01	6.84E-01	8.29E-01	3.83E-02
142	8.19E-01	6.07E-01	1.13E-01	9.74E-01	1.96E-01	9.65E-01	1.00E+00	9.92E-01	3.98E-01
143	8.12E-01	2.03E-01	1.34E-01	9.94E-01	2.51E-01	9.19E-01	9.92E-01	8.08E-01	8.15E-01
144	9.96E-01	8.70E-01	5.49E-01	1.00E+00	7.81E-01	9.84E-01	1.00E+00	9.88E-01	9.60E-01
145	7.08E-02	4.74E-02	5.45E-02	3.32E-01	2.50E-01	3.61E-01	5.29E-01	2.90E-01	2.06E-04
146	7.98E-01	3.80E-02	1.06E-02	7.96E-01	3.28E-02	1.03E-01	2.93E-03	3.20E-05	2.80E-04
147	9.91E-01	7.71E-01	2.58E-01	1.00E+00	7.46E-01	9.95E-01	9.99E-01	9.46E-01	8.54E-01
148	9.74E-01	7.04E-01	5.63E-01	1.00E+00	7.65E-01	8.26E-01	1.00E+00	7.67E-01	9.68E-01
149	6.55E-01	4.37E-01	1.24E-02	9.27E-01	3.91E-02	1.17E-01	7.13E-02	1.86E-05	9.44E-04
150	4.11E-02	2.03E-01	1.42E-02	2.21E-01	1.64E-01	1.00E+00	5.65E-01	7.40E-01	7.15E-01
151	9.49E-01	6.14E-01	3.66E-01	9.99E-01	4.57E-01	8.49E-01	9.97E-01	4.18E-01	8.44E-01
152	5.35E-01	1.09E-01	9.01E-02	1.00E+00	6.52E-01	9.72E-01	1.00E+00	9.32E-01	9.60E-01
153	8.24E-01	6.17E-01	3.32E-01	4.66E-01	3.04E-01	3.03E-01	1.32E-01	3.25E-01	3.19E-01
154	9.65E-01	3.44E-01	2.28E-01	1.00E+00	8.96E-01	9.16E-01	9.94E-01	7.86E-01	9.64E-01
155	9.93E-01	8.67E-01	1.35E-01	9.62E-01	1.92E-02	8.96E-01	9.39E-01	4.02E-01	3.21E-01
156	9.71E-01	8.03E-01	1.16E-01	9.99E-01	1.94E-01	8.62E-01	9.58E-01	9.07E-01	4.67E-01
157	8.83E-01	7.17E-01	1.61E-01	9.56E-01	6.12E-01	9.98E-01	9.88E-01	1.00E+00	9.80E-01
158	9.36E-01	6.11E-01	3.71E-01	9.99E-01	8.49E-01	9.03E-01	1.00E+00	9.26E-01	9.57E-01
159	8.92E-01	5.15E-01	6.61E-01	6.53E-01	1.12E-01	9.73E-02	7.82E-01	2.73E-01	4.17E-01
160	7.42E-01	9.26E-01	1.73E-01	2.47E-01	1.38E-02	7.43E-01	1.10E-01	7.01E-02	2.70E-01
161	5.18E-01	4.81E-02	2.28E-02	5.44E-01	1.53E-02	1.78E-01	1.43E-02	5.49E-05	1.89E-04
162	9.81E-01	6.44E-01	6.85E-01	1.00E+00	8.99E-01	9.96E-01	1.00E+00	9.79E-01	9.63E-01
163	5.67E-01	1.64E-01	1.52E-01	9.84E-01	6.49E-02	9.30E-01	9.95E-01	9.88E-01	1.85E-01
164	1.00E+00	1.00E+00	1.00E+00	1.00E+00	1.00E+00	1.00E+00	1.00E+00	1.00E+00	1.00E+00
165	5.42E-01	1.07E-01	2.20E-01	3.59E-01	7.57E-01	3.81E-01	8.52E-01	7.89E-01	1.94E-01
166	9.88E-01	6.18E-01	1.70E-01	1.00E+00	9.76E-01	9.38E-01	9.99E-01	9.31E-01	9.75E-01
167	5.63E-01	4.44E-02	1.48E-01	5.75E-01	3.89E-02	5.18E-02	7.31E-03	2.44E-08	5.30E-04
168	1.00E+00	1.00E+00	1.00E+00	1.00E+00	1.00E+00	1.00E+00	1.00E+00	1.00E+00	1.00E+00
169	9.87E-01	6.99E-01	2.56E-01	9.99E-01	6.02E-01	9.60E-01	4.66E-01	8.83E-01	9.14E-01
170	1.35E-01	1.53E-01	2.97E-02	4.25E-01	3.83E-02	2.70E-01	5.86E-01	3.12E-01	3.92E-02
171	8.61E-01	5.83E-01	1.94E-01	9.74E-01	6.72E-01	8.03E-01	1.00E+00	9.72E-01	9.77E-01
172	8.22E-01	7.77E-01	2.43E-01	9.88E-01	7.07E-01	3.82E-01	9.87E-01	6.59E-01	9.36E-01
173	8.48E-01	8.66E-01	1.50E-01	9.85E-02	1.06E-02	5.34E-01	1.15E-01	1.10E-01	3.90E-01
174	1.00E+00	1.00E+00	1.00E+00	1.00E+00	1.00E+00	1.00E+00	1.00E+00	1.00E+00	1.00E+00
175	4.29E-01	4.32E-01	8.21E-02	7.48E-01	6.91E-02	6.82E-01	6.63E-01	7.27E-01	2.99E-01
176	5.15E-01	2.76E-02	7.55E-02	9.21E-01	8.29E-03	7.83E-01	5.01E-01	8.04E-02	2.81E-01
177	8.65E-01	1.47E-01	8.03E-01	6.77E-01	8.51E-04	8.42E-01	6.76E-01	7.48E-01	4.30E-02
178	1.00E+00	1.00E+00	1.00E+00	1.00E+00	1.00E+00	1.00E+00	1.00E+00	1.00E+00	1.00E+00

179	2.00E-01	5.97E-01	2.80E-01	9.71E-01	9.39E-01	8.12E-01	9.11E-01	8.95E-01	8.42E-01
180	9.03E-01	4.45E-01	2.62E-01	9.99E-01	8.69E-01	6.98E-01	9.99E-01	9.76E-01	8.23E-01
181	9.04E-01	7.78E-01	5.76E-02	9.87E-01	2.52E-01	8.99E-01	6.60E-01	9.78E-01	9.02E-01
182	3.27E-01	2.64E-03	4.17E-01	1.90E-01	1.38E-01	9.56E-01	2.47E-02	7.80E-01	1.48E-02
183	1.00E+00	1.00E+00	1.00E+00	1.00E+00	1.00E+00	1.00E+00	1.00E+00	1.00E+00	1.00E+00
184	7.32E-01	8.33E-02	5.44E-02	4.41E-01	8.22E-04	3.59E-01	3.52E-03	2.02E-05	9.63E-04
185	5.78E-01	6.93E-01	9.13E-02	9.06E-01	1.78E-01	4.84E-01	5.27E-01	4.97E-01	3.17E-01
186	8.64E-01	7.52E-01	5.26E-01	1.00E+00	8.11E-01	1.00E+00	1.00E+00	9.99E-01	9.62E-01
187	9.90E-01	5.40E-01	2.96E-01	9.87E-01	5.26E-01	6.93E-01	9.99E-01	9.96E-01	9.99E-01
188	9.72E-01	2.75E-01	4.36E-01	8.13E-01	4.70E-02	5.36E-01	4.86E-01	1.34E-01	3.74E-02
189	6.96E-01	4.02E-01	2.17E-01	8.79E-01	6.37E-02	1.44E-02	4.74E-03	5.38E-04	5.83E-06
190	4.48E-01	6.33E-04	6.55E-01	9.36E-01	5.08E-01	8.23E-01	7.21E-01	7.75E-01	1.08E-01
191	5.90E-01	9.27E-01	2.73E-02	9.14E-01	3.62E-01	2.91E-01	7.31E-01	1.19E-01	9.44E-01
192	6.90E-01	2.89E-01	1.08E-01	9.97E-01	8.45E-01	7.30E-01	9.95E-01	6.73E-01	7.12E-01
193	9.99E-01	6.57E-01	5.57E-01	9.72E-01	2.25E-01	8.86E-01	9.87E-01	9.40E-01	9.48E-01
194	5.04E-01	9.52E-02	1.62E-02	3.24E-01	3.06E-02	1.97E-02	6.75E-02	3.29E-05	3.05E-04
195	9.97E-01	8.66E-01	5.84E-01	9.95E-01	4.83E-01	9.16E-01	1.00E+00	9.96E-01	9.94E-01
196	7.73E-01	2.13E-02	4.13E-02	2.67E-01	2.31E-02	8.59E-02	4.70E-03	5.28E-04	8.31E-04
197	1.98E-01	2.52E-01	9.98E-02	6.74E-01	7.91E-02	1.00E+00	1.00E+00	8.20E-01	6.68E-01
198	1.98E-01	5.03E-01	1.25E-02	9.17E-01	2.60E-01	6.80E-01	7.60E-01	6.96E-01	7.01E-01
199	5.58E-01	2.81E-01	1.10E-01	5.19E-01	9.75E-03	3.90E-01	4.43E-02	1.78E-02	2.00E-02
200	4.10E-01	3.30E-01	1.03E-01	7.47E-01	2.76E-01	5.15E-01	1.49E-01	6.80E-03	1.48E-03
201	9.61E-01	8.08E-01	4.32E-01	9.38E-01	9.79E-01	5.77E-01	9.99E-01	9.70E-01	5.55E-01
202	4.45E-01	7.07E-01	1.77E-01	5.63E-01	1.19E-01	4.86E-01	1.71E-01	2.00E-02	6.97E-03
203	7.85E-01	4.08E-01	2.16E-01	3.59E-01	2.01E-02	4.43E-02	1.15E-03	1.10E-06	1.66E-04
204	1.00E+00	1.00E+00	1.00E+00	1.00E+00	1.00E+00	1.00E+00	1.00E+00	1.00E+00	1.00E+00
205	4.89E-01	2.58E-02	9.29E-02	7.64E-01	3.07E-01	5.60E-01	9.48E-01	8.57E-01	8.10E-01
206	7.04E-01	4.87E-02	4.35E-01	4.09E-01	2.81E-01	5.50E-01	6.23E-01	9.46E-01	1.46E-02
207	9.06E-01	9.51E-02	2.73E-01	5.80E-01	1.32E-02	1.19E-01	8.30E-02	1.58E-03	1.12E-03
208	8.79E-01	7.10E-01	7.00E-01	3.32E-01	2.88E-02	1.55E-02	2.11E-04	2.50E-03	2.37E-06
209	3.96E-01	3.59E-01	2.95E-01	5.52E-01	5.03E-01	1.29E-01	8.18E-01	7.40E-01	7.27E-02
210	9.26E-01	2.75E-01	2.88E-01	5.15E-01	1.21E-02	1.73E-02	7.71E-04	1.30E-06	3.73E-05
211	9.23E-01	2.40E-01	3.02E-01	2.43E-01	3.04E-04	1.02E-01	1.20E-02	5.81E-05	2.45E-06
212	6.47E-01	2.50E-01	2.11E-01	5.91E-01	1.15E-01	1.70E-02	2.28E-02	1.93E-03	1.29E-02
213	7.32E-01	6.76E-01	4.66E-01	9.91E-02	8.11E-03	1.55E-01	2.27E-02	1.42E-03	8.70E-04
214	4.52E-01	2.34E-01	5.20E-01	1.00E+00	5.82E-01	1.00E+00	1.00E+00	1.00E+00	5.10E-01
216	9.71E-01	8.98E-01	3.97E-01	9.86E-01	9.97E-01	9.60E-01	9.93E-01	9.75E-01	9.86E-01
217	6.94E-01	5.22E-01	2.24E-01	4.48E-01	3.95E-03	2.18E-01	1.54E-01	2.83E-03	2.41E-03
218	3.20E-01	7.23E-01	5.76E-03	1.67E-01	8.77E-02	1.97E-01	7.60E-01	9.17E-01	4.76E-01
219	7.83E-01	9.52E-02	4.12E-01	6.77E-01	4.28E-01	3.54E-01	3.19E-01	1.05E-01	1.47E-03
220	1.00E+00	1.00E+00	3.73E-01	4.29E-01	1.00E+00	3.53E-01	1.00E+00	1.00E+00	3.65E-01
221	1.00E+00	2.56E-02	6.17E-01	7.95E-02	7.08E-02	8.59E-01	3.00E-01	4.86E-01	1.41E-01
222	7.95E-01	9.25E-01	6.11E-01	6.39E-01	3.49E-02	2.41E-01	1.89E-03	1.08E-02	1.09E-04
223	7.66E-01	1.55E-01	3.73E-01	4.88E-01	9.05E-03	1.01E-01	4.10E-02	8.63E-04	1.97E-02
224	7.60E-01	4.46E-01	1.24E-01	3.07E-01	4.29E-03	1.88E-02	1.36E-03	3.14E-06	5.12E-04
225	6.98E-01	8.00E-01	2.05E-01	4.20E-01	2.96E-02	1.70E-02	2.87E-03	9.38E-06	2.59E-04
226	8.08E-01	4.67E-01	5.48E-01	5.20E-01	4.92E-01	1.59E-02	2.74E-02	9.74E-05	3.20E-05
227	4.14E-01	7.99E-01	4.70E-01	4.63E-01	4.35E-01	7.76E-01	4.76E-02	6.63E-02	6.63E-02
228	9.08E-01	8.23E-01	8.76E-01	8.77E-01	2.68E-01	1.04E-01	3.71E-02	8.32E-02	1.67E-03
229	6.80E-01	2.95E-01	1.10E-01	9.63E-01	5.84E-01	9.81E-01	9.40E-01	9.66E-01	9.60E-01
230	1.00E+00	1.00E+00	1.00E+00	1.00E+00	1.00E+00	1.00E+00	1.00E+00	1.00E+00	1.00E+00
231	4.87E-01	3.94E-01	3.94E-01	1.00E+00	3.73E-01	1.00E+00	1.00E+00	1.00E+00	1.00E+00
232	3.89E-01	2.39E-01	7.36E-02	1.45E-01	6.36E-02	2.67E-01	5.22E-01	4.72E-02	5.92E-02
233	2.17E-01	1.66E-01	1.34E-01	3.94E-01	1.36E-02	1.26E-01	4.72E-02	2.04E-02	8.44E-03
234	5.58E-01	7.49E-01	7.74E-01	8.08E-01	6.10E-02	3.12E-01	1.05E-01	1.01E-03	2.12E-02
235	8.05E-01	3.24E-02	8.24E-01	1.00E+00	6.84E-01	1.00E+00	3.17E-01	6.98E-01	8.37E-02
236	9.05E-01	7.17E-01	3.29E-01	2.69E-01	2.04E-02	3.50E-02	4.21E-02	1.06E-04	4.12E-04
237	9.53E-02	1.20E-02	2.08E-01	1.00E+00	1.00E+00	1.00E+00	1.00E+00	3.85E-01	1.03E-03
238	1.81E-01	5.80E-01	6.33E-01	1.00E+00	5.55E-01	1.00E+00	9.26E-02	1.00E+00	2.48E-01
239	3.30E-01	1.00E+00	1.81E-01	1.00E+00	1.00E+00	1.00E+00	1.00E+00	1.00E+00	1.00E+00
240	1.81E-01	5.29E-03	1.00E+00	1.00E+00	1.00E+00	1.00E+00	1.22E-01	1.00E+00	2.48E-01
241	1.00E+00	2.34E-01	1.00E+00	1.00E+00	2.20E-01	1.00E+00	1.00E+00	1.00E+00	1.00E+00
242	9.53E-02	2.10E-01	1.00E+00	7.89E-01	5.55E-01	1.00E+00	2.03E-01	5.69E-01	2.60E-01
243	2.90E-01	1.60E-01	1.82E-01	3.80E-01	1.27E-02	1.78E-02	6.82E-01	3.82E-01	9.14E-02
244	5.73E-01	1.74E-01	3.03E-01	2.81E-01	1.24E-01	2.75E-02	5.63E-02	4.84E-01	6.65E-02
245	1.00E+00	1.00E+00	1.00E+00	1.44E-01	1.00E+00	1.00E+00	1.00E+00	2.53E-01	3.44E-01
246	1.00E+00	1.00E+00	1.00E+00	1.00E+00	1.00E+00	1.00E+00	1.00E+00	1.00E+00	1.00E+00
247	1.00E+00	1.00E+00	1.00E+00	1.00E+00	1.00E+00	1.00E+00	1.00E+00	1.77E-01	1.00E+00
248	1.00E+00	1.00E+00	2.08E-01	1.00E+00	1.00E+00	1.00E+00	1.00E+00	1.00E+00	1.00E+00
249	9.06E-01	8.69E-01	2.23E-01	9.62E-01	1.00E+00	5.29E-01	1.65E-01	3.08E-01	4.55E-02
250	9.58E-01	9.75E-01	5.39E-01	7.56E-01	8.54E-01	7.44E-01	1.40E-01	4.66E-01	2.94E-01
251	1.00E+00	1.00E+00	1.00E+00	1.00E+00	1.00E+00	1.00E+00	1.00E+00	1.00E+00	1.00E+00
252	1.00E+00	1.81E-01	1.00E+00	1.00E+00	1.70E-01	1.00E+00	1.00E+00	1.00E+00	1.00E+00
254	1.00E+00	1.25E-01	1.00E+00	1.00E+00	1.17E-01	1.70E-01	1.00E+00	1.22E-01	1.00E+00
255	1.00E+00	1.54E-01	1.00E+00	1.00E+00	1.44E-01	1.00E+00	1.00E+00	1.00E+00	1.00E+00
256	1.00E+00	1.00E+00	1.00E+00	1.00E+00	1.00E+00	1.00E+00	6.27E-02	2.03E-01	1.00E+00
257	1.00E+00	1.00E+00	1.00E+00	1.00E+00	1.00E+00	1.00E+00	1.00E+00	1.00E+00	1.00E+00
258	1.00E+00	1.00E+00	1.00E+00	1.00E+00	1.00E+00	1.00E+00	1.00E+00	1.00E+00	1.00E+00
259	1.00E+00	5.72E-02	1.00E+00	1.00E+00	1.00E+00	1.00E+00	1.00E+00	1.00E+00	3.85E-01
260	1.45E-01	3.20E-02	4.96E-01	2.43E-01	2.32E-02	2.25E-03	5.79E-01	7.95E-01	2.60E-02
261	3.01E-01	9.29E-01	3.68E-01	8.53E-01	2.34E-02	8.24E-02	1.29E-02	8.12E-03	3.51E-03
262	3.33E-01	7.72E-01	2.10E-01	9.66E-02	5.50E-03	1.50E-01	6.80E-02	2.05E-01	6.79E-02
264	6.74E-01	4.53E-01	5.90E-01	1.39E-01	6.28E-01	5.29E-03	7.60E-01	4.31E-01	1.06E-01
268	1.00E+00	1.00E+00	1.00E+00	1.00E+00	1.00E+00	1.00E+00	1.00E+00	1.00E+00	1.00E+00
269	1.00E+00	1.00E+00	1.00E+00	1.00E+00	1.00E+00	1.00E+00	1.00E+00	1.00E+00	1.00E+00
271	1.00E+00	1.00E+00	1.00E+00	1.00E+00	1.00E+00	1.00E+00	1.00E+00	1.00E+00	1.00E+00
272	1.00E+00	1.00E+00	1.00E+00	1.00E+00	1.00E+00	1.00E+00	1.00E+00	1.00E+00	1.00E+00
277	1.00E+00	1.00E+00	1.00E+00	4.29E-01	3.33E-01	1.89E-01	1.00E+00	1.00E+00	2.00E-01
278	1.00E+00	1.00E+00	1.00E+00	1.00E+00	1.00E+00	1.17E-01	1.00E+00	1.00E+00	1.00E+00
281	1.00E+00	1.00E+00	1.00E+00	1.00E+00	1.00E+00	1.00E+00	1.00E+00	1.00E+00	1.00E+00
282	1.00E+00	1.00E+00	1.00E+00	1.00E+00	1.00E+00	1.00E+00	1.00E+00	3.19E-02	1.00E+00
283	1.00E+00	1.00E+00	1.00E+00	1.00E+00	1.00E+00	1.00E+00	1.00E+00	1.00E+00	1.00E+00

Table S14. The results of the ORA using the edges of MDiNs corresponding to plasma metabolome dataset. For each of the diet group, the calculations were done considering three scenarios differing by the amount of edges used. First scenario included edges without differentiating the corresponding nodes according to the sign of the assigned regression coefficients. The second and the third scenario involved differentiating the edges by the aforementioned scheme.

	BR, p-value			COMB, p-value			WGB, p-value		
Id	Total	Positive	Negative	Total	Positive	Negative	Total	Positive	Negative
1	8.56E-01	3.03E-04	9.93E-01	4.07E-02	5.95E-01	3.10E-03	1.43E-01	1.00E+00	1.28E-01
2	3.44E-01	3.83E-03	7.38E-01	2.13E-02	3.24E-02	7.26E-02	8.54E-01	1.00E+00	1.86E-02
3	9.93E-01	1.86E-02	9.98E-01	9.55E-02	5.32E-01	2.00E-01	9.20E-01	9.67E-01	3.55E-08
4	4.48E-01	6.65E-01	6.80E-02	3.11E-01	5.33E-04	9.84E-01	2.48E-01	2.68E-02	5.43E-01
5	6.66E-01	3.48E-05	9.60E-01	3.62E-01	3.24E-01	6.10E-02	5.54E-01	5.29E-01	5.72E-03
6	1.00E+00	6.51E-01	8.52E-01	6.17E-01	1.00E+00	1.20E-01	6.25E-01	1.00E+00	1.00E+00
7	1.84E-01	1.24E-06	6.27E-01	3.61E-01	5.18E-02	4.66E-02	6.23E-01	9.04E-01	8.35E-02
8	9.49E-01	6.81E-01	7.44E-01	8.15E-01	1.13E-01	9.71E-01	5.68E-01	1.86E-01	1.00E+00
9	9.96E-01	4.99E-02	1.00E+00	5.29E-03	1.50E-01	1.89E-04	8.76E-01	9.32E-01	4.64E-02
10	9.98E-01	6.33E-02	1.00E+00	2.99E-02	3.78E-01	1.39E-01	7.97E-01	6.76E-01	2.02E-01
11	3.89E-01	5.08E-03	8.70E-01	1.53E-01	2.21E-01	2.00E-02	6.33E-01	3.57E-01	3.89E-01
12	8.60E-01	3.67E-05	9.96E-01	5.70E-02	9.37E-01	3.80E-03	6.32E-01	1.00E+00	6.98E-02
13	9.99E-01	3.39E-02	9.94E-01	9.45E-01	4.75E-01	3.70E-01	1.00E+00	4.90E-01	1.22E-02
14	4.75E-01	2.20E-03	5.49E-01	8.84E-02	2.23E-01	8.77E-02	3.13E-01	8.88E-01	6.62E-01
15	9.98E-01	1.98E-02	9.99E-01	6.58E-01	2.65E-01	1.89E-01	9.56E-01	8.79E-01	7.94E-04
16	9.98E-01	2.69E-02	9.89E-01	5.66E-01	4.04E-01	1.50E-01	7.97E-01	9.57E-01	4.13E-02
17	2.05E-01	1.05E-01	3.97E-01	9.07E-01	9.76E-01	3.14E-01	9.99E-01	7.37E-01	3.11E-01
18	9.29E-01	3.22E-03	9.05E-01	1.14E-01	8.29E-01	1.73E-04	1.23E-02	1.00E+00	4.27E-01
19	7.97E-01	4.55E-02	9.96E-01	9.15E-01	5.66E-01	8.65E-01	7.21E-01	1.00E+00	1.00E+00
20	7.89E-01	2.19E-01	9.66E-01	2.81E-01	2.06E-02	1.91E-01	9.05E-01	6.58E-01	1.65E-03
21	9.91E-01	4.50E-03	1.00E+00	9.85E-01	9.00E-01	5.29E-01	9.78E-01	1.15E-01	9.40E-03
22	9.18E-01	3.84E-02	9.95E-01	1.62E-01	2.06E-01	5.90E-03	4.02E-02	8.26E-02	4.03E-01
23	3.76E-01	4.83E-03	5.94E-01	6.15E-01	5.60E-01	1.48E-01	1.35E-01	1.00E+00	4.00E-02
24	1.00E+00	1.00E+00	1.00E+00	1.00E+00	1.00E+00	1.00E+00	7.55E-02	1.00E+00	1.00E+00
25	9.97E-01	1.38E-01	9.98E-01	4.43E-01	8.49E-01	5.38E-02	8.68E-01	8.52E-01	3.45E-07
26	8.34E-01	8.77E-02	1.00E+00	3.80E-01	8.92E-02	7.83E-01	4.53E-01	5.56E-01	6.57E-01
27	1.51E-01	9.27E-04	5.55E-01	7.22E-02	3.09E-01	6.44E-02	6.33E-01	1.00E+00	8.91E-01
28	9.99E-01	1.70E-03	1.00E+00	7.62E-01	8.73E-01	7.46E-02	7.85E-01	1.00E+00	7.25E-02
29	1.00E+00	1.00E+00	1.00E+00	1.00E+00	1.00E+00	1.00E+00	1.00E+00	1.00E+00	1.00E+00
30	8.67E-01	7.69E-02	8.15E-01	4.62E-01	3.59E-01	1.99E-01	6.80E-01	5.84E-01	6.75E-02
31	1.79E-01	4.72E-01	3.52E-01	2.21E-01	5.08E-03	9.57E-01	5.65E-02	2.13E-01	2.10E-01
32	9.63E-01	7.50E-04	1.00E+00	3.16E-01	8.29E-01	1.87E-02	3.13E-01	7.31E-01	1.00E+00
33	1.00E+00	4.07E-02	1.00E+00	9.80E-01	2.32E-01	4.72E-01	9.57E-01	9.81E-01	4.67E-02
34	7.67E-01	7.66E-01	9.59E-01	3.34E-01	1.92E-01	6.36E-01	8.76E-01	1.00E+00	1.00E+00
35	4.80E-01	9.09E-01	3.97E-01	7.82E-01	1.52E-02	9.96E-01	2.41E-01	6.31E-01	6.34E-01
36	9.73E-01	4.01E-05	9.94E-01	6.48E-01	1.85E-01	8.96E-02	4.73E-01	9.43E-01	3.65E-01
37	6.18E-01	9.29E-01	5.06E-02	3.36E-01	2.63E-02	9.95E-01	2.58E-01	8.68E-03	5.53E-01
38	9.52E-01	4.89E-03	9.76E-01	4.76E-01	3.73E-01	1.79E-01	3.05E-01	4.82E-01	4.91E-01
39	4.18E-01	4.88E-01	1.52E-01	1.00E+00	1.00E+00	7.47E-01	1.00E+00	1.00E+00	1.00E+00
40	6.72E-01	8.89E-01	6.42E-01	4.69E-01	1.72E-01	6.43E-01	6.49E-01	1.00E+00	1.00E+00
41	9.40E-01	1.20E-02	9.82E-01	1.04E-02	7.61E-01	7.45E-03	6.45E-01	8.99E-01	6.30E-01
42	1.00E+00	1.00E+00	1.00E+00	1.00E+00	1.00E+00	1.00E+00	1.00E+00	1.00E+00	1.00E+00
43	9.98E-01	1.99E-02	1.00E+00	6.70E-01	9.65E-01	2.40E-01	7.96E-01	6.31E-01	2.80E-01
44	3.97E-01	9.33E-03	6.18E-01	9.63E-01	5.67E-01	5.37E-01	9.69E-01	4.64E-01	7.57E-01
45	2.75E-01	1.32E-02	3.36E-01	5.12E-01	3.74E-01	2.26E-01	1.86E-01	1.00E+00	8.82E-01
46	1.51E-01	1.26E-02	9.28E-01	1.83E-01	1.03E-01	4.77E-02	6.62E-01	6.43E-01	2.26E-02
47	9.78E-01	3.63E-03	1.00E+00	7.34E-01	9.77E-01	3.10E-02	2.66E-01	7.46E-01	5.11E-01
48	1.00E+00	5.66E-02	9.96E-01	9.95E-01	7.51E-01	7.60E-01	9.82E-01	6.01E-02	1.05E-01
49	9.88E-01	2.66E-02	1.00E+00	8.02E-01	1.40E-01	1.27E-01	3.75E-01	8.05E-01	7.72E-01
50	2.31E-01	2.38E-01	3.77E-01	7.64E-01	3.08E-03	9.87E-01	6.37E-01	1.83E-01	1.93E-01
51	8.53E-01	3.54E-02	9.82E-01	2.01E-01	7.09E-01	3.44E-02	9.75E-01	6.52E-01	1.58E-03
52	1.40E-01	1.20E-02	2.73E-01	3.16E-01	1.03E-01	3.57E-01	9.03E-01	1.00E+00	3.45E-01
53	1.00E+00	1.00E+00	1.00E+00	1.00E+00	1.00E+00	1.00E+00	1.00E+00	1.00E+00	1.00E+00
54	9.25E-01	1.16E-02	9.96E-01	5.10E-01	8.81E-01	1.12E-01	5.58E-01	8.17E-01	2.57E-01
55	3.87E-01	4.58E-03	2.82E-01	5.19E-02	2.80E-01	1.42E-01	2.37E-01	1.00E+00	6.31E-01
56	3.41E-01	2.17E-02	7.57E-01	3.16E-01	6.47E-02	2.86E-01	3.54E-01	8.78E-01	3.27E-01
57	1.39E-01	1.02E-01	2.27E-01	7.86E-01	7.44E-01	9.37E-01	9.63E-01	6.69E-01	1.00E+00
58	4.99E-01	1.06E-01	1.33E-01	6.03E-01	3.57E-01	1.78E-01	1.69E-01	3.29E-01	3.10E-01
59	9.60E-01	5.64E-02	9.98E-01	9.70E-01	1.56E-01	3.72E-01	2.55E-01	3.64E-01	9.28E-01
60	4.63E-01	3.70E-02	4.12E-01	8.94E-01	6.49E-01	8.88E-01	9.97E-01	1.00E+00	7.18E-01
61	5.38E-01	5.70E-01	5.57E-01	3.14E-01	2.00E-02	9.83E-01	8.23E-02	5.14E-01	1.00E+00
62	9.46E-01	9.92E-04	9.99E-01	9.32E-01	7.10E-01	8.79E-01	3.07E-01	9.06E-01	6.29E-01
63	5.14E-01	7.64E-01	4.44E-01	7.92E-01	3.22E-01	9.23E-01	7.71E-01	1.00E+00	1.00E+00
64	2.23E-01	9.24E-03	6.39E-01	5.18E-01	8.56E-01	1.01E-01	5.60E-01	1.00E+00	2.95E-01
65	6.58E-01	1.83E-01	6.65E-01	4.01E-01	2.07E-02	2.98E-01	4.40E-01	1.30E-01	1.00E+00
66	9.81E-01	1.37E-02	9.97E-01	7.78E-01	2.41E-01	8.08E-02	1.81E-01	1.00E+00	1.61E-02
67	1.00E+00	1.65E-01	9.99E-01	7.40E-01	5.66E-01	2.32E-01	2.06E-01	7.08E-01	6.86E-01
68	9.85E-01	1.52E-02	9.86E-01	8.58E-01	9.42E-01	1.29E-01	4.82E-01	9.47E-01	2.45E-01
69	1.92E-01	4.01E-02	2.36E-01	3.39E-02	3.06E-01	2.98E-01	6.23E-02	8.53E-01	8.69E-01
70	7.92E-01	3.67E-01	9.12E-01	4.46E-02	5.61E-03	2.44E-01	2.29E-01	5.88E-01	3.15E-01
71	9.88E-01	1.35E-02	9.99E-01	9.89E-01	9.83E-01	8.35E-01	1.02E-01	7.69E-01	3.38E-01
72	7.15E-01	1.40E-01	6.35E-01	1.00E+00	8.23E-01	9.62E-01	7.93E-01	1.00E+00	1.54E-01
73	2.54E-01	1.69E-01	3.39E-01	5.16E-01	2.40E-01	6.69E-01	8.60E-01	6.37E-01	5.70E-01
74	6.27E-01	2.67E-01	4.56E-01	5.92E-01	4.89E-01	1.60E-01	5.07E-02	2.42E-01	1.00E+00
75	9.57E-01	1.40E-01	9.80E-01	7.86E-01	6.10E-01	3.65E-01	2.66E-02	8.96E-01	1.00E+00
76	9.94E-01	7.81E-02	9.96E-01	9.59E-01	5.64E-01	2.79E-01	5.19E-01	1.00E+00	6.31E-01
77	5.19E-01	3.07E-03	6.11E-01	2.91E-01	8.35E-01	3.20E-01	6.52E-01	7.56E-01	5.39E-01
78	7.93E-01	1.60E-01	1.26E-01	1.94E-01	2.13E-01	2.84E-01	2.11E-02	8.28E-01	2.45E-01
79	8.37E-01	1.79E-02	9.89E-01	7.95E-01	3.46E-01	3.11E-01	1.73E-01	7.15E-01	8.46E-01
80	4.95E-01	1.02E-01	8.51E-01	8.55E-01	5.66E-01	7.24E-01	3.69E-01	7.77E-01	7.62E-01
81	3.02E-01	2.44E-01	3.24E-03	5.39E-01	1.07E-01	6.43E-01	8.36E-01	1.00E+00	5.00E-01
82	7.29E-01	2.92E-01	9.76E-01	9.00E-01	6.64E-01	9.76E-01	3.54E-01	4.71E-01	5.26E-01
83	1.00E+00	1.00E+00	7.67E-01	8.61E-01	4.14E-01	3.00E-01	1.00E+00	1.00E+00	1.00E+00

84	2.32E-01	3.97E-03	7.21E-01	1.09E-01	1.37E-01	1.03E-01	1.17E-01	8.41E-01	5.49E-01
85	1.00E+00	5.18E-01	1.00E+00	7.84E-01	5.20E-01	8.16E-01	1.00E+00	1.00E+00	1.00E+00
86	9.99E-01	2.40E-01	9.99E-01	7.77E-01	9.40E-01	7.10E-02	4.43E-01	1.00E+00	1.34E-01
87	9.02E-01	8.30E-01	7.76E-01	3.16E-01	1.52E-01	5.51E-01	3.38E-01	1.00E+00	5.08E-01
88	9.37E-01	1.66E-03	8.96E-01	8.62E-01	3.98E-01	1.32E-01	4.32E-01	4.88E-01	3.28E-01
89	4.27E-01	1.39E-02	7.61E-01	7.05E-02	2.24E-01	2.59E-01	4.33E-02	5.28E-01	2.54E-01
90	9.45E-01	4.21E-02	9.95E-01	4.63E-01	8.72E-01	3.35E-01	6.35E-02	8.69E-01	3.37E-01
91	9.99E-01	8.05E-02	1.00E+00	9.47E-01	9.99E-01	2.72E-01	6.25E-01	7.56E-01	3.39E-01
92	9.79E-01	8.93E-03	9.00E-01	1.00E+00	9.30E-01	7.38E-01	5.95E-01	3.42E-01	9.14E-01
93	4.99E-01	6.86E-03	3.25E-01	2.38E-01	7.76E-01	2.67E-01	4.83E-02	1.00E+00	8.47E-01
94	9.63E-01	1.62E-02	9.99E-01	8.47E-01	6.80E-01	4.03E-01	4.90E-02	4.12E-01	6.33E-01
95	6.39E-01	2.71E-03	9.55E-01	9.89E-01	8.99E-01	9.74E-01	9.64E-02	2.84E-01	8.08E-01
96	5.50E-01	1.27E-03	9.81E-01	9.61E-01	8.17E-02	8.51E-01	1.62E-01	1.00E+00	2.53E-01
97	6.49E-01	1.01E-01	7.44E-01	8.85E-01	5.44E-01	7.47E-01	9.48E-01	1.00E+00	6.70E-01
98	6.02E-01	3.93E-02	9.26E-01	3.41E-01	1.44E-01	5.59E-01	1.08E-01	8.60E-01	9.31E-01
99	3.36E-02	7.16E-03	2.14E-01	2.29E-01	1.86E-01	9.09E-01	7.58E-01	1.00E+00	6.31E-01
100	4.38E-01	1.40E-02	5.41E-01	4.46E-01	1.45E-01	2.48E-01	2.60E-01	1.00E+00	1.00E+00
101	9.17E-01	3.20E-01	5.01E-01	3.83E-01	7.84E-01	2.79E-01	8.36E-01	1.00E+00	1.00E+00
102	2.83E-01	1.15E-03	5.13E-01	8.71E-01	6.19E-01	9.50E-01	9.99E-01	1.38E-01	1.00E+00
103	4.89E-01	5.62E-01	1.00E+00	5.03E-01	1.70E-01	7.46E-01	9.43E-01	1.00E+00	1.00E+00
104	9.81E-01	1.17E-01	9.97E-01	8.96E-01	9.21E-01	9.54E-01	6.33E-02	2.41E-01	7.05E-01
105	9.67E-01	2.63E-01	9.94E-01	9.46E-01	5.76E-01	2.17E-01	3.82E-01	7.10E-01	6.82E-01
106	7.26E-01	4.31E-01	5.87E-01	7.30E-02	1.67E-01	2.93E-01	9.18E-02	4.52E-01	5.12E-01
107	7.80E-01	4.61E-01	7.34E-01	8.07E-01	3.66E-01	7.37E-01	9.44E-01	1.00E+00	6.18E-01
108	9.73E-01	2.52E-02	9.97E-01	8.45E-01	7.22E-01	9.65E-01	3.52E-01	1.00E+00	6.00E-01
109	4.00E-01	2.30E-01	5.43E-01	1.98E-01	3.70E-01	4.36E-02	1.16E-01	7.99E-01	1.00E+00
110	9.24E-01	2.35E-02	9.80E-01	9.63E-01	9.58E-01	7.10E-01	4.25E-01	2.06E-01	9.61E-01
111	7.29E-01	8.24E-01	2.08E-01	7.80E-02	2.01E-02	9.64E-01	7.42E-02	1.00E+00	1.00E+00
112	1.11E-01	3.42E-03	2.45E-01	6.53E-01	1.96E-01	9.23E-01	9.07E-01	6.24E-01	1.00E+00
113	1.91E-01	3.82E-02	3.91E-01	8.28E-01	1.95E-01	5.87E-01	7.22E-01	6.65E-01	3.09E-01
114	7.24E-01	9.38E-01	2.82E-01	1.38E-01	2.21E-02	9.99E-01	1.75E-01	1.00E+00	1.00E+00
115	9.03E-01	4.30E-01	9.87E-01	5.98E-01	9.78E-01	8.75E-02	2.90E-01	1.00E+00	6.89E-01
116	7.38E-01	8.15E-01	7.54E-01	4.89E-01	8.52E-02	4.05E-01	8.93E-01	1.00E+00	1.00E+00
117	8.74E-01	2.07E-01	8.38E-01	7.39E-01	2.08E-01	5.39E-01	5.25E-01	9.58E-02	1.00E+00
118	9.81E-01	1.07E-01	9.76E-01	7.46E-01	8.06E-01	8.48E-01	3.64E-01	8.83E-01	3.45E-01
119	2.09E-01	2.56E-02	9.04E-01	6.07E-01	3.15E-01	9.44E-01	9.84E-01	3.77E-01	1.00E+00
120	8.62E-01	5.33E-01	9.43E-01	1.98E-01	1.57E-01	3.39E-01	2.09E-02	7.24E-01	7.66E-01
121	9.04E-01	7.39E-01	5.32E-01	8.25E-01	4.39E-01	5.36E-01	9.42E-01	6.19E-01	1.00E+00
122	9.15E-01	2.04E-01	9.78E-01	9.22E-01	8.28E-01	7.78E-01	2.22E-01	8.27E-01	4.24E-01
123	5.33E-01	6.23E-01	9.06E-01	3.95E-01	5.81E-02	9.99E-01	6.69E-01	5.59E-01	1.00E+00
124	1.54E-01	3.32E-01	2.06E-01	3.40E-01	3.15E-02	9.37E-01	6.95E-01	1.00E+00	1.00E+00
125	7.11E-01	6.13E-01	4.73E-01	5.61E-01	3.63E-01	4.00E-01	5.69E-02	1.00E+00	1.00E+00
126	8.07E-01	4.55E-01	1.52E-01	6.52E-01	9.73E-01	8.20E-01	6.01E-01	1.00E+00	1.00E+00
127	6.95E-01	4.58E-01	9.33E-01	6.27E-01	3.69E-01	5.03E-01	9.52E-01	1.00E+00	6.98E-01
128	9.77E-01	7.74E-02	9.95E-01	9.83E-01	6.38E-01	9.09E-01	4.24E-01	8.68E-01	7.35E-01
129	1.91E-01	6.55E-02	2.07E-01	9.34E-01	5.54E-01	5.50E-01	8.06E-01	6.68E-01	1.00E+00
130	5.69E-01	1.33E-01	9.30E-01	4.72E-01	2.26E-01	5.22E-01	8.67E-01	1.00E+00	3.10E-01
131	5.01E-02	2.69E-02	3.58E-02	5.60E-01	8.02E-03	9.96E-01	8.98E-01	1.00E+00	1.00E+00
132	4.37E-01	8.38E-01	1.67E-01	4.69E-01	3.34E-02	1.68E-01	6.53E-01	1.00E+00	1.00E+00
133	5.65E-01	3.94E-01	3.86E-01	8.71E-01	1.91E-01	1.85E-01	1.00E+00	1.00E+00	1.00E+00
134	9.53E-01	2.34E-01	9.97E-01	8.74E-01	4.92E-01	5.98E-01	6.69E-01	1.70E-01	1.57E-01
135	9.56E-01	8.22E-01	7.78E-01	6.90E-01	1.81E-01	7.82E-01	1.92E-01	1.00E+00	4.38E-01
136	1.53E-01	1.82E-01	2.16E-01	5.97E-01	5.61E-01	4.30E-01	1.70E-01	1.00E+00	1.00E+00
137	1.12E-01	1.34E-02	6.40E-01	8.10E-01	3.54E-01	9.96E-01	4.79E-01	1.00E+00	1.00E+00
138	9.46E-01	3.06E-01	9.96E-01	9.74E-01	9.86E-01	9.71E-01	6.29E-01	5.17E-01	4.50E-01
139	8.21E-01	4.80E-01	8.28E-01	8.31E-01	5.81E-01	8.31E-01	7.90E-01	1.00E+00	7.87E-01
140	9.96E-01	2.96E-01	9.89E-01	9.99E-01	1.00E+00	9.50E-01	7.00E-01	8.91E-01	5.83E-01
141	1.89E-01	5.47E-02	2.62E-01	8.62E-01	5.20E-01	9.68E-01	9.94E-01	6.61E-01	2.54E-01
142	8.63E-01	2.64E-01	8.00E-01	3.45E-01	1.89E-01	6.16E-01	9.81E-01	1.00E+00	6.11E-01
143	6.31E-01	1.76E-01	3.53E-01	4.90E-01	2.39E-01	8.64E-01	2.77E-02	3.97E-01	1.00E+00
144	9.64E-01	3.25E-01	8.69E-01	9.93E-01	6.12E-01	9.51E-01	3.09E-01	5.94E-01	2.62E-01
145	5.21E-01	4.98E-01	7.08E-01	3.36E-01	7.25E-02	9.90E-01	9.63E-01	1.00E+00	1.00E+00
146	8.98E-01	2.00E-01	8.05E-01	5.82E-01	6.43E-01	6.89E-01	8.01E-01	4.85E-01	1.43E-01
147	5.09E-01	6.64E-02	3.86E-01	9.57E-01	7.24E-01	9.89E-01	1.23E-01	3.22E-01	1.00E+00
148	9.92E-01	8.02E-02	9.90E-01	9.95E-01	7.69E-01	9.97E-01	7.95E-01	4.10E-01	3.33E-01
149	9.85E-01	3.33E-01	9.84E-01	6.35E-01	2.16E-01	8.64E-01	2.81E-01	5.43E-01	9.19E-01
150	7.02E-01	5.28E-01	7.21E-01	1.00E+00	9.95E-02	7.22E-01	1.00E+00	1.00E+00	1.00E+00
151	9.93E-01	3.97E-01	9.62E-01	9.44E-01	8.02E-01	9.94E-01	8.75E-01	8.74E-01	5.13E-01
152	6.53E-01	3.77E-01	8.06E-01	4.56E-01	5.68E-01	6.61E-01	1.57E-01	1.00E+00	1.00E+00
153	2.25E-01	6.40E-01	1.00E+00	1.00E+00	7.85E-02	1.00E+00	6.25E-01	1.00E+00	1.00E+00
154	8.89E-01	6.29E-02	9.40E-01	9.99E-01	9.79E-01	9.98E-01	4.81E-01	8.28E-01	7.11E-01
155	7.99E-01	4.21E-01	8.66E-01	9.33E-01	6.22E-01	9.12E-01	9.09E-01	2.94E-01	4.26E-01
156	8.00E-01	3.76E-01	8.68E-01	9.39E-01	8.38E-01	1.00E+00	1.94E-01	6.51E-01	7.84E-01
157	5.65E-01	2.14E-01	3.80E-01	4.68E-01	3.25E-01	8.74E-01	8.02E-01	4.14E-01	1.00E+00
158	9.18E-01	1.69E-01	1.00E+00	8.91E-01	9.08E-01	8.84E-01	4.62E-01	7.97E-01	6.09E-01
159	1.30E-01	2.49E-01	9.27E-01	2.20E-01	3.90E-01	8.27E-01	6.63E-01	1.00E+00	1.00E+00
160	4.47E-01	4.11E-01	2.29E-01	5.05E-01	6.80E-01	7.08E-01	9.01E-01	1.00E+00	1.00E+00
161	9.90E-01	6.70E-01	9.40E-01	9.95E-01	9.33E-01	8.42E-01	4.84E-01	8.22E-01	8.89E-01
162	9.55E-01	6.24E-01	9.05E-01	9.90E-01	9.54E-01	9.97E-01	4.23E-01	1.00E+00	6.21E-01
163	3.36E-01	5.46E-01	7.79E-02	2.59E-01	1.02E-01	7.78E-01	7.14E-01	1.81E-01	1.00E+00
164	1.00E+00	1.00E+00	1.00E+00	1.00E+00	1.00E+00	1.00E+00	1.00E+00	1.00E+00	1.00E+00
165	8.29E-01	1.19E-01	9.39E-01	6.40E-01	8.88E-01	9.40E-01	9.09E-01	1.00E+00	1.00E+00
166	9.40E-01	1.52E-01	9.84E-01	9.87E-01	8.71E-01	9.84E-01	2.92E-01	1.00E+00	5.83E-01
167	6.26E-01	2.46E-01	5.10E-01	5.39E-01	8.20E-01	7.07E-01	3.88E-01	1.00E+00	6.59E-01
168	1.00E+00	1.00E+00	1.00E+00	1.00E+00	1.00E+00	1.48E-01	1.00E+00	1.00E+00	1.00E+00
169	8.08E-01	4.83E-01	9.79E-01	9.12E-01	7.87E-01	9.98E-01	4.83E-01	6.06E-01	1.56E-01
170	9.21E-01	3.17E-01	7.99E-01	8.82E-01	3.20E-01	1.00E+00	6.52E-01	1.38E-01	1.00E+00
171	8.39E-01	4.91E-01	9.75E-01	9.67E-01	7.28E-01	9.97E-01	4.58E-01	8.06E-01	6.28E-01
172	7.46E-01	4.77E-01	9.19E-01	9.28E-01	7.12E-01	9.64E-01	7.00E-01	8.16E-01	8.82E-01
173	4.68E-01	3.69E-01	1.59E-01	6.94E-01	3.70E-01	1.60E-01	5.56E-01	1.00E+00	1.00E+00
174	1.00E+00	1.00E+00	1.00E+00	1.00E+00	1.00E+00	1.00E+00	1.00E+00	1.00E+00	1.00E+00
175	5.28E-01	3.06E-01	6.72E-01	1.00E+00	7.74E-01	6.73E-01	1.00E+00	1.00E+00	1.37E-01
176	9.98E-01	8.45E-01	8.90E-01	9.43E-01	6.67E-01	9.99E-01	5.40E-01	5.52E-01	9.18E-01
177	1.72E-01	4.64E-01	3.14E-01	6.78E-01	5.99E-01	7.96E-01	7.30E-01	4.53E-01	1.38E-01
178	1.00E+00	1.00E+00	1.00E+00	1.00E+00	1.00E+00	1.48E-01	1.00E+00	1.00E+00	1.00E+00

179	6.71E-01	3.50E-01	5.64E-01	9.68E-01	6.41E-01	9.95E-01	7.14E-01	1.33E-02	1.17E-01
180	8.83E-01	3.86E-01	9.83E-01	9.64E-01	8.25E-01	9.22E-01	4.63E-01	1.00E+00	7.88E-01
181	7.91E-01	2.46E-01	8.83E-01	9.34E-01	6.41E-01	9.99E-01	5.32E-01	6.18E-01	7.16E-01
182	1.38E-02	5.49E-01	3.87E-01	8.66E-01	3.73E-01	5.87E-01	4.26E-01	1.00E+00	1.00E+00
183	1.00E+00	1.00E+00	1.00E+00	1.00E+00	1.00E+00	1.00E+00	1.00E+00	1.00E+00	1.00E+00
184	6.58E-01	1.58E-01	8.24E-01	8.33E-01	2.85E-01	9.65E-01	7.73E-01	7.40E-01	1.00E+00
185	7.67E-01	4.93E-01	7.32E-01	4.55E-01	4.95E-01	7.34E-01	9.25E-01	1.00E+00	1.00E+00
186	6.75E-01	1.66E-01	7.33E-01	8.90E-01	3.66E-01	7.36E-01	7.28E-01	2.43E-02	4.56E-01
187	8.49E-01	2.97E-01	9.12E-01	9.08E-01	8.23E-01	1.00E+00	4.85E-01	5.59E-01	3.21E-01
188	4.06E-01	9.80E-02	9.73E-01	9.96E-01	8.65E-01	9.96E-01	9.74E-01	1.11E-01	7.92E-01
189	5.21E-03	2.90E-02	1.08E-02	9.11E-02	1.52E-02	6.98E-01	2.36E-01	4.54E-01	1.00E+00
190	2.16E-01	1.02E-01	5.99E-01	2.86E-01	3.14E-01	6.01E-01	9.10E-01	1.00E+00	1.00E+00
191	1.84E-01	6.57E-02	8.38E-01	1.00E+00	3.70E-01	1.00E+00	4.32E-01	1.00E+00	1.00E+00
192	2.20E-01	4.57E-01	6.26E-01	3.95E-01	6.55E-02	9.73E-01	3.37E-01	1.00E+00	1.00E+00
193	7.45E-01	1.04E-01	6.54E-01	9.99E-01	9.70E-01	1.00E+00	3.64E-01	1.63E-01	5.95E-01
194	7.87E-01	4.47E-01	1.47E-01	6.36E-01	4.51E-01	8.65E-01	7.38E-01	1.00E+00	1.00E+00
195	6.90E-01	3.63E-01	9.08E-01	9.38E-01	8.77E-01	9.94E-01	3.83E-01	1.90E-01	6.58E-01
196	3.49E-01	2.88E-01	3.20E-01	8.60E-01	5.69E-01	8.38E-01	8.37E-01	1.00E+00	1.00E+00
197	1.00E+00	4.78E-01	7.12E-01	1.00E+00	4.80E-01	1.00E+00	7.15E-01	1.00E+00	1.00E+00
198	9.45E-01	7.20E-01	8.82E-01	9.34E-01	1.08E-01	8.83E-01	8.23E-01	1.00E+00	1.00E+00
199	9.29E-01	5.33E-01	7.50E-01	9.61E-01	6.25E-01	9.72E-01	5.56E-01	1.00E+00	8.46E-01
200	6.23E-01	8.35E-02	6.36E-01	5.99E-01	1.94E-01	8.79E-01	7.98E-01	1.00E+00	1.00E+00
201	3.93E-01	3.41E-01	7.01E-01	9.45E-01	6.60E-01	9.92E-01	4.82E-01	1.00E+00	7.02E-01
202	3.84E-01	4.84E-02	5.08E-01	9.95E-01	4.29E-01	9.89E-01	9.94E-01	1.00E+00	1.00E+00
203	3.08E-01	5.91E-02	5.48E-01	8.72E-01	5.92E-01	9.77E-01	9.05E-01	1.00E+00	1.00E+00
204	1.00E+00	1.00E+00	1.00E+00	1.00E+00	1.00E+00	1.00E+00	3.85E-02	1.00E+00	1.00E+00
205	9.69E-01	2.72E-01	7.82E-01	1.00E+00	2.74E-01	1.00E+00	5.78E-01	1.00E+00	1.00E+00
206	3.26E-01	3.44E-01	7.68E-01	3.14E-01	7.96E-01	8.97E-01	9.04E-01	1.00E+00	1.00E+00
207	4.29E-01	8.74E-01	5.25E-01	9.79E-01	8.10E-01	8.47E-01	8.37E-01	2.72E-01	1.00E+00
208	4.78E-01	7.64E-01	6.63E-01	4.16E-01	1.93E-02	4.43E-01	8.23E-01	1.00E+00	1.00E+00
209	9.38E-01	8.23E-02	8.05E-01	7.15E-01	2.59E-01	9.17E-01	2.18E-01	1.00E+00	1.00E+00
210	5.64E-03	5.91E-02	3.62E-01	8.39E-01	6.05E-01	2.07E-01	9.41E-01	1.00E+00	1.00E+00
211	3.47E-03	4.58E-02	5.63E-02	5.34E-01	4.14E-01	2.59E-01	7.56E-01	1.00E+00	1.97E-01
212	1.36E-01	9.16E-03	3.21E-01	6.73E-01	1.49E-01	9.97E-01	7.19E-01	1.00E+00	3.00E-01
213	3.18E-01	1.86E-01	1.94E-01	8.58E-01	4.68E-01	9.23E-01	9.77E-01	2.11E-01	1.00E+00
214	1.00E+00	6.72E-01	1.00E+00	1.00E+00	3.02E-01	6.29E-01	1.00E+00	1.00E+00	6.05E-02
216	7.45E-01	3.57E-01	9.40E-01	9.38E-01	7.10E-01	1.00E+00	1.37E-01	6.62E-03	1.00E+00
217	4.20E-03	2.07E-01	5.85E-05	9.85E-01	7.47E-01	8.36E-01	2.43E-01	5.31E-01	1.00E+00
218	8.86E-01	5.92E-01	1.00E+00	2.96E-01	1.43E-02	1.00E+00	3.66E-01	1.00E+00	1.00E+00
219	8.10E-01	5.20E-01	9.55E-01	9.84E-01	6.36E-01	9.18E-01	6.81E-01	1.00E+00	1.00E+00
220	1.00E+00	3.39E-01	5.27E-02	1.00E+00	3.40E-01	1.00E+00	3.51E-01	1.00E+00	1.00E+00
221	2.89E-01	2.82E-01	4.61E-01	7.52E-01	6.64E-02	4.63E-01	6.24E-01	1.00E+00	1.00E+00
222	3.81E-01	3.54E-01	6.03E-01	6.80E-01	3.56E-01	6.05E-01	6.08E-01	1.00E+00	1.00E+00
223	2.20E-01	2.53E-01	2.60E-01	9.92E-01	4.92E-01	9.88E-01	9.68E-01	1.00E+00	1.00E+00
224	1.04E-01	5.38E-01	8.90E-02	7.51E-01	5.41E-01	9.43E-01	7.99E-01	4.72E-01	1.00E+00
225	5.04E-01	1.45E-01	4.90E-01	7.49E-01	3.34E-01	9.94E-01	8.98E-01	1.00E+00	1.00E+00
226	1.32E-01	1.61E-01	1.14E-01	6.03E-01	2.49E-01	9.46E-01	7.90E-01	1.00E+00	1.00E+00
227	5.64E-01	9.02E-01	8.92E-02	3.40E-01	8.01E-02	8.22E-01	3.50E-01	1.00E+00	1.00E+00
228	9.06E-01	2.80E-01	8.83E-01	8.92E-01	4.26E-01	9.88E-01	9.95E-01	1.00E+00	3.36E-01
229	8.53E-01	1.72E-01	9.39E-01	4.20E-01	9.50E-01	5.53E-01	5.95E-01	1.00E+00	3.18E-01
230	1.00E+00	1.00E+00	1.00E+00	1.00E+00	1.00E+00	1.00E+00	1.00E+00	1.00E+00	1.00E+00
231	1.00E+00	7.77E-01	1.00E+00	5.05E-01	1.84E-01	1.00E+00	4.45E-01	1.00E+00	1.00E+00
232	3.82E-02	1.09E-01	6.64E-01	7.89E-01	2.96E-01	9.97E-01	6.15E-01	3.70E-01	1.00E+00
233	3.62E-01	5.57E-05	5.71E-01	8.62E-01	2.01E-01	9.94E-01	7.79E-01	1.00E+00	1.00E+00
234	7.62E-01	5.71E-01	5.71E-01	8.84E-01	1.81E-01	9.29E-01	8.81E-01	3.67E-01	1.00E+00
235	8.88E-01	4.12E-01	7.50E-01	4.93E-02	1.31E-01	3.51E-01	8.64E-01	2.62E-03	1.00E+00
236	1.04E-01	6.29E-01	3.89E-02	7.13E-01	2.03E-01	8.06E-01	9.45E-01	3.40E-01	1.00E+00
237	2.96E-01	6.28E-01	2.78E-01	6.17E-01	2.55E-01	6.52E-01	1.83E-02	1.00E+00	1.00E+00
238	3.75E-02	9.86E-02	8.89E-01	2.90E-01	9.95E-02	8.90E-01	3.51E-01	1.84E-01	1.00E+00
239	1.00E+00	1.00E+00	1.00E+00	1.00E+00	1.00E+00	1.00E+00	1.00E+00	1.00E+00	1.00E+00
240	5.77E-01	7.25E-01	9.66E-01	4.59E-01	3.20E-01	9.66E-01	2.08E-01	1.00E+00	1.00E+00
241	1.00E+00	5.20E-01	1.00E+00	1.00E+00	5.21E-01	1.00E+00	3.76E-01	1.00E+00	1.00E+00
242	9.40E-01	7.30E-01	9.68E-01	3.79E-01	5.24E-01	9.68E-01	2.29E-01	1.00E+00	1.00E+00
243	2.41E-02	5.13E-04	4.85E-01	4.14E-01	1.07E-02	1.00E+00	5.35E-01	3.00E-01	1.00E+00
244	6.21E-01	9.09E-03	7.45E-01	7.13E-01	2.73E-01	1.00E+00	4.19E-01	1.00E+00	1.00E+00
245	2.25E-01	4.88E-01	1.00E+00	2.96E-01	4.89E-01	1.00E+00	3.76E-01	1.00E+00	1.00E+00
246	6.28E-01	2.78E-01	1.00E+00	1.00E+00	1.00E+00	1.00E+00	2.64E-01	1.00E+00	1.00E+00
247	1.00E+00	1.00E+00	1.00E+00	1.00E+00	1.00E+00	1.00E+00	1.00E+00	1.00E+00	1.00E+00
248	1.47E-01	3.60E-01	1.00E+00	1.00E+00	7.01E-02	1.00E+00	1.00E+00	1.00E+00	1.00E+00
249	1.29E-01	1.29E-02	3.90E-01	9.49E-01	6.22E-01	9.97E-01	1.78E-02	6.42E-02	1.00E+00
250	1.47E-01	8.69E-02	9.06E-01	4.00E-01	6.87E-01	9.06E-01	2.81E-01	1.00E+00	1.00E+00
251	1.00E+00	1.00E+00	1.00E+00	1.00E+00	2.74E-01	1.00E+00	1.00E+00	1.00E+00	1.00E+00
252	1.00E+00	2.96E-01	1.00E+00	1.00E+00	1.00E+00	1.00E+00	3.85E-02	1.00E+00	1.00E+00
254	1.00E+00	1.00E+00	1.00E+00	1.00E+00	4.89E-01	3.40E-01	1.00E+00	1.00E+00	1.00E+00
255	1.00E+00	4.18E-01	1.00E+00	1.00E+00	1.00E+00	1.00E+00	1.00E+00	1.00E+00	1.00E+00
256	1.00E+00	1.00E+00	1.00E+00	1.00E+00	3.40E-01	1.00E+00	1.00E+00	1.00E+00	1.00E+00
257	1.00E+00	1.00E+00	1.00E+00	1.00E+00	2.26E-01	1.00E+00	1.00E+00	1.00E+00	1.00E+00
258	1.00E+00	1.00E+00	1.00E+00	1.00E+00	2.26E-01	1.00E+00	1.00E+00	1.00E+00	1.00E+00
259	1.00E+00	3.48E-01	1.00E+00	1.00E+00	8.04E-01	6.66E-01	1.00E-01	1.00E+00	1.00E+00
260	1.08E-01	7.35E-01	7.83E-01	5.50E-01	5.31E-01	1.00E+00	9.81E-01	1.00E+00	1.00E+00
261	9.13E-01	6.43E-01	8.73E-01	6.26E-01	2.79E-01	9.73E-01	7.50E-01	1.00E+00	1.00E+00
262	7.20E-01	5.15E-01	7.87E-01	3.02E-01	1.05E-01	9.85E-01	3.36E-01	2.62E-01	1.00E+00
264	1.00E+00	7.90E-01	1.00E+00	6.17E-01	2.00E-01	1.00E+00	1.00E+00	1.00E+00	1.00E+00
268	1.00E+00	3.18E-01	2.25E-01	2.74E-01	3.19E-01	1.00E+00	2.69E-01	1.00E+00	1.00E+00
269	3.14E-02	1.47E-01	1.00E+00	1.00E+00	1.00E+00	1.00E+00	1.00E+00	1.00E+00	1.00E+00
271	1.00E+00	3.47E-01	1.00E+00	1.00E+00	7.13E-01	1.00E+00	5.06E-01	1.00E+00	1.00E+00
272	1.00E+00	4.37E-01	4.18E-01	2.96E-01	4.38E-01	1.00E+00	1.00E+00	1.00E+00	1.00E+00
277	1.00E+00	1.00E+00	1.00E+00	1.00E+00	2.26E-01	1.00E+00	1.00E+00	1.00E+00	1.00E+00
278	3.14E-02	3.14E-02	1.00E+00	1.00E+00	1.00E+00	1.00E+00	1.00E+00	1.00E+00	1.00E+00
281	1.00E+00	1.00E+00	1.00E+00	1.00E+00	1.00E+00	1.00E+00	1.00E+00	1.00E+00	1.00E+00
282	1.00E+00	3.60E-01	1.00E+00	1.00E+00	1.00E+00	1.00E+00	2.10E-01	1.00E+00	1.00E+00
283	1.00E+00	1.00E+00	1.00E+00	1.00E+00	1.00E+00	1.00E+00	1.00E+00	1.00E+00	1.00E+00

Table S15. Features selected by ML-PLS-DA (followed by filtering out variables most likely influenced by time) in case of stool metabolome data.

Exp. Mass	H / N	Molecular Formula	HMDB id	Name of the metabolite
Features selected for the BR group				
149.045574	H / N	C5H10O5 [M-H]-	HMDB00098	D-Xylose
149.045574	H / N	C5H10O5 [M-H]-	HMDB00283	D-Ribose
149.045574	H / N	C5H10O5 [M-H]-	HMDB00366	2-Deoxyribonic acid
149.045574	H / N	C5H10O5 [M-H]-	HMDB00621	D-Ribulose
149.045574	H / N	C5H10O5 [M-H]-	HMDB00646	L-Arabinose
149.045574	H / N	C5H10O5 [M-H]-	HMDB00751	L-Threo-2-pentulose
149.045574	H / N	C5H10O5 [M-H]-	HMDB01644	D-Xylulose
149.045574	H / N	C5H10O5 [M-H]-	HMDB03371	L-Ribulose
149.045574	H / N	C5H10O5 [M-H]-	HMDB12194	Beta-D-ribopyranose
149.045574	H / N	C5H10O5 [M-H]-	HMDB12325	Arabinofuranose
149.045574	H / N	C5H10O5 [M-H]-	HMDB29941	D-Apiose
149.045574	H / N	C5H10O5 [M-H]-	HMDB29942	Arabinose
149.045574	H / N	C5H10O5 [M-H]-	HMDB59753	2-Deoxypentonic acid
149.045574	H / N	C5H10O5 [M-H]-	HMDB60254	Aldehydo-D-xylose
160.040427	H / N	C9H7NO2 [M-H]-	HMDB02285	2-Indolecarboxylic acid
160.040427	H / N	C9H7NO2 [M-H]-	HMDB03320	Indole-3-carboxylic acid
160.040427	H / N	C9H7NO2 [M-H]-	HMDB04077	4,6-Dihydroxyquinoline
160.040427	H / N	C9H7NO2 [M-H]-	HMDB31172	3-Formyl-6-hydroxyindole
160.040427	H / N	C9H7NO2 [M-H]-	HMDB60289	Quinoline-4,8-diol
174.088434	H / N	C6H13N3O3 [M-H]-	HMDB00904	Citrulline
174.088434	H / N	C6H13N3O3 [M-H]-	HMDB03148	Argininic acid
181.973995	N	C7H5NOS2 [M-H]-	-	-
187.097607	H / N	C9H16O4 [M-H]-	HMDB00784	Azelaic acid
187.097607	H / N	C9H16O4 [M-H]-	HMDB11717	Nonate
187.097607	H / N	C9H16O4 [M-H]-	HMDB32200	cis- and trans-Ethyl 2,4-dimethyl-1,3-dioxolane-2-acetate
187.097607	H / N	C9H16O4 [M-H]-	HMDB32258	(+/-)-Ethyl 3-acetoxy-2-methylbutyrate
187.097607	H / N	C9H16O4 [M-H]-	HMDB32387	(+/-)-Methyl 5-acetoxyhexanoate
187.097607	H / N	C9H16O4 [M-H]-	HMDB36233	Butyl ethyl malonate
187.097607	H / N	C9H16O4 [M-H]-	HMDB59760	2,4-Dimethylpimelic acid
187.097607	H / N	C9H16O4 [M-H]-	HMDB59783	3-Methylsuberic acid
187.097607	H / N	C9H16O4 [M-H]-	HMDB59814	Diethyl methylsuccinate
187.097607	H / N	C9H16O4 [M-H]-	HMDB59879	Diethyl glutarate
193.017606	N	C6H10O5S [M-H]-	-	-
197.068023	H / N	C7H10N4O3 [M-H]-	HMDB04400	5-Acetylamino-6-amino-3-methyluracil
197.068023	H / N	C7H10N4O3 [M-H]-	HMDB59771	6-amino-5[N-methylformylamino]-1-methyluracil
199.108834	N	C9H16N2O3 [M-H]-	-	-
202.072093	N	C8H13NO5 [M-H]-	-	-
206.045880	H / N	C10H9NO4 [M-H]-	HMDB00978	4-(2-Aminophenyl)-2,4-dioxobutanoic acid
206.045880	H / N	C10H9NO4 [M-H]-	HMDB60328	1-Nitro-5,6-dihydroxy-dihydronaphthalene
213.007477	N	C5H10O7S [M-H]-	-	-
216.124125	H / N	C10H19NO4 [M-H]-	HMDB00824	Propionylcarnitine
225.007466	N	C6H10O7S [M-H]-	-	-
244.001742	N	C9H7NO5 [M+Cl]-	-	-
244.001742	N	C8H8NO6P [M-H]-	-	-
249.043771	N	C9H14O6S [M-H]-	-	-
249.149649	H / N	C15H22O3 [M-H]-	HMDB15371	Gemfibrozil
249.149649	H / N	C15H22O3 [M-H]-	HMDB30917	1-Hydroxyacorenone
249.149649	H / N	C15H22O3 [M-H]-	HMDB31901	Blennin A
249.149649	H / N	C15H22O3 [M-H]-	HMDB34721	Procurcumadiol
249.149649	H / N	C15H22O3 [M-H]-	HMDB35117	(3beta,6beta)-Furanoeremophilane-3,6-diol
249.149649	H / N	C15H22O3 [M-H]-	HMDB35137	Heliannuol D
249.149649	H / N	C15H22O3 [M-H]-	HMDB35148	(6beta,8alpha)-6-Hydroxy-7(11)-eremophilen-12,8-olide
249.149649	H / N	C15H22O3 [M-H]-	HMDB35358	Ketosantalic acid
249.149649	H / N	C15H22O3 [M-H]-	HMDB35760	3-Hydroxytrichothecene
249.149649	H / N	C15H22O3 [M-H]-	HMDB35798	Piperdial
249.149649	H / N	C15H22O3 [M-H]-	HMDB36036	3beta-Dihydroxymarasmene
249.149649	H / N	C15H22O3 [M-H]-	HMDB36037	13-Hydroxymarasmene
249.149649	H / N	C15H22O3 [M-H]-	HMDB36550	3-Ketoapotrichothecene
249.149649	H / N	C15H22O3 [M-H]-	HMDB36563	Valerenolic acid
249.149649	H / N	C15H22O3 [M-H]-	HMDB36664	Ketopelenolide a
249.149649	H / N	C15H22O3 [M-H]-	HMDB37064	FS4 toxin
249.149649	H / N	C15H22O3 [M-H]-	HMDB37529	Lactaronecatorin A
249.149649	H / N	C15H22O3 [M-H]-	HMDB37559	Cadabicilone
249.149649	H / N	C15H22O3 [M-H]-	HMDB39156	3beta-Hydroxycinnamolide
249.149649	H / N	C15H22O3 [M-H]-	HMDB39635	Abscisic alcohol

249.149649	H / N	C15H22O3 [M-H]-	HMDB39644	Heliannuol A
249.149649	H / N	C15H22O3 [M-H]-	HMDB40754	(3beta,8beta)-3-Hydroxy-7(11)-eremophilen-12,8-olide
250.039116	N	C8H13NO6S [M-H]-	-	-
253.180898	H / N	C15H26O3 [M-H]-	HMDB29604	Lubiminol
253.180898	H / N	C15H26O3 [M-H]-	HMDB35780	8-Hydroxy-4(6)-lactarene-5,14-diol
253.180898	H / N	C15H26O3 [M-H]-	HMDB36053	(3beta,9beta)-7-Drimene-3,11,12-triol
253.180898	H / N	C15H26O3 [M-H]-	HMDB36866	7-Drimene-11,12,14-triol
253.180898	H / N	C15H26O3 [M-H]-	HMDB37197	Kessyl glycol
253.180898	H / N	C15H26O3 [M-H]-	HMDB40276	5-Acetoxydihydrotheaespirane
259.083311	N	C12H20O2S2 [M-H]-	-	-
260.096201	N	C11H19NO4S [M-H]-	-	-
261.028548	N	C6H14O9S [M-H]-	-	-
261.158245	N	C11H18N8 [M-H]-	-	-
261.170754	H / N	C13H26O5 [M-H]-	HMDB32297	Glyceryl 5-hydroxydecanoate
265.107128	N	C8H19N4O4P [M-H]-	-	-
268.064931	N	C12H15NO4S [M-H]-	-	-
268.068334	N	C9H19NO4S2 [M-H]-	-	-
269.087832	H / N	C9H18O9 [M-H]-	HMDB29955	D-erythro-L-galacto-Nonulose
270.044182	N	C11H13NO5S [M-H]-	-	-
272.129244	H / N	C16H19NO3 [M-H]-	HMDB30187	(E,E)-Piperlonguminine
272.129244	H / N	C16H19NO3 [M-H]-	HMDB38834	(2E)-Piperamide-C5:1
273.076808	H / N	C15H14O5 [M-H]-	HMDB03306	Phloretin
273.076808	H / N	C15H14O5 [M-H]-	HMDB30377	(Z)-4-Methoxy-3,3',5,5'-tetrahydroxystilbene
273.076808	H / N	C15H14O5 [M-H]-	HMDB30541	3,3',4',7-Tetrahydroxyflavan
273.076808	H / N	C15H14O5 [M-H]-	HMDB30634	beta-Pyrufuran
273.076808	H / N	C15H14O5 [M-H]-	HMDB30635	alpha-Pyrufuran
273.076808	H / N	C15H14O5 [M-H]-	HMDB30744	Hemigossypolone
273.076808	H / N	C15H14O5 [M-H]-	HMDB30754	11-Methoxynoryangonin
273.076808	H / N	C15H14O5 [M-H]-	HMDB30822	(-)-Epiafzelechin
273.076808	H / N	C15H14O5 [M-H]-	HMDB30823	Afzelechin
273.076808	H / N	C15H14O5 [M-H]-	HMDB30949	Wyerone epoxide
273.076808	H / N	C15H14O5 [M-H]-	HMDB33017	11-Hydroxyyangonin
273.076808	H / N	C15H14O5 [M-H]-	HMDB33333	2,3-Epoxysesamone
273.076808	H / N	C15H14O5 [M-H]-	HMDB33590	(R)-Methysticin
273.076808	H / N	C15H14O5 [M-H]-	HMDB37232	(2xi,4xi)-4,4',5,7-Tetrahydroxyflavan
273.076808	H / N	C15H14O5 [M-H]-	HMDB37760	Hydroxysesamone
273.076808	H / N	C15H14O5 [M-H]-	HMDB40828	(2S,3S,4R)-3,4,4',7-Tetrahydroxyflavan
273.076808	H / N	C15H14O5 [M-H]-	HMDB41654	3'-Hydroxy-O-desmethylangolensin
273.076808	H / N	C15H14O5 [M-H]-	HMDB41685	5'-Hydroxy-O-desmethylangolensin
273.076808	H / N	C15H14O5 [M-H]-	HMDB41695	6'-Hydroxy-O-desmethylangolensin
273.189341	N	C15H30O2S [M-H]-	-	-
275.144314	N	C20H20O [M-H]-	-	-
277.112432	N	C13H26S3 [M-H]-	-	-
277.121371	H / N	C13H22O4 [M+Cl]-	HMDB30987	2-Carboxy-4-dodecanolide
277.121371	H / N	C13H22O4 [M+Cl]-	HMDB38736	(3S,5R,6R,7E)-3,5,6-Trihydroxy-7-megastigmen-9-one
277.165683	H / N	C13H26O6 [M-H]-	HMDB35028	(x)-2-Heptanol glucoside
281.027959	N	C16H10O3S [M-H]-	-	-
285.152948	N	C15H26O3S [M-H]-	-	-
285.170772	N	C15H26O5 [M-H]-	-	-
286.144826	H / N	C17H21NO3 [M-H]-	HMDB14812	Galantamine
286.144826	H / N	C17H21NO3 [M-H]-	HMDB14887	Etodolac
286.144826	H / N	C17H21NO3 [M-H]-	HMDB15005	Ritodrine
286.144826	H / N	C17H21NO3 [M-H]-	HMDB33874	Piperanine
286.144826	H / N	C17H21NO3 [M-H]-	HMDB40699	Feruperine
286.144826	H / N	C17H21NO3 [M-H]-	HMDB41956	Nordihydrocodeine
286.144826	H / N	C17H21NO3 [M-H]-	HMDB60548	Dihydromorphine
286.144826	H / N	C17H21NO3 [M-H]-	HMDB60796	6alpha-Hydroxy-hydromorphone
286.144826	H / N	C17H21NO3 [M-H]-	HMDB60798	6beta-Hydroxy-hydromorphone
286.144826	H / N	C17H21NO3 [M-H]-	HMDB60854	Nordihydroisomorphine
287.178337	H / N	C16H28O2 [M+Cl]-	HMDB00477	7Z,10Z-Hexadecadienoic acid
287.178337	H / N	C16H28O2 [M+Cl]-	HMDB29351	Geranyl hexanoate
287.178337	H / N	C16H28O2 [M+Cl]-	HMDB30429	Linalyl hexanoate
287.178337	H / N	C16H28O2 [M+Cl]-	HMDB31086	(Z)-7-Hexadecen-1,16-olide
287.178337	H / N	C16H28O2 [M+Cl]-	HMDB32340	Isoambrettolide
287.178337	H / N	C16H28O2 [M+Cl]-	HMDB37805	D6-Ambrettolide
287.178337	H / N	C16H28O2 [M+Cl]-	HMDB38255	Geranyl 2-ethylbutyrate
287.178337	H / N	C16H28O2 [M+Cl]-	HMDB39131	Ethyl (Z,Z)-5,8-tetradecadienoate
288.036331	N	C10H11NO9 [M-H]-	-	-
288.048983	N	C8H15NO8 [M+Cl]-	-	-
288.048983	N	C7H16NO9P [M-H]-	-	-
288.070016	N	C15H15NO3S [M-H]-	-	-
288.088990	N	C16H11N5O [M-H]-	-	-

289.071713	H / N	C15H14O6 [M-H]-	HMDB01871	Epicatechin
289.071713	H / N	C15H14O6 [M-H]-	HMDB02780	Catechin
289.071713	H / N	C15H14O6 [M-H]-	HMDB29253	3-Hydroxyphloretin
289.071713	H / N	C15H14O6 [M-H]-	HMDB30131	gamma-Pyrufuran
289.071713	H / N	C15H14O6 [M-H]-	HMDB30144	alpha-Cotonefuran
289.071713	H / N	C15H14O6 [M-H]-	HMDB32322	cis-3 and trans-2-Hexenyl propionate
289.071713	H / N	C15H14O6 [M-H]-	HMDB33783	Marshrin
289.071713	H / N	C15H14O6 [M-H]-	HMDB34124	Fonsecin
289.071713	H / N	C15H14O6 [M-H]-	HMDB35399	Cartorimine
289.071713	H / N	C15H14O6 [M-H]-	HMDB37953	(-)-Catechin
289.071713	H / N	C15H14O6 [M-H]-	HMDB37954	(+)-Epicatechin
289.071713	H / N	C15H14O6 [M-H]-	HMDB41293	6-Hydroxy-alpha-pyrufuran
289.071713	H / N	C15H14O6 [M-H]-	HMDB41310	Luteoforol
289.112556	N	C14H26S3 [M-H]-	-	-
290.075131	N	C9H17N5O2S2 [M-H]-	-	-
290.104610	N	C16H13N5O [M-H]-	-	-
290.176181	H / N	C17H25NO3 [M-H]-	HMDB15114	Cyclopentolate
290.176181	H / N	C17H25NO3 [M-H]-	HMDB15341	Levobunolol
290.176181	H / N	C17H25NO3 [M-H]-	HMDB36327	Norcapsaicin
291.160215	H / N	C17H24O4 [M-H]-	HMDB34658	9-Acetoxyfukinanolide
291.160215	H / N	C17H24O4 [M-H]-	HMDB34738	Isotrichodermin
291.160215	H / N	C17H24O4 [M-H]-	HMDB34930	(3beta,6beta)-Furanoeremophilane-3,6-diol 6-acetate
291.160215	H / N	C17H24O4 [M-H]-	HMDB35687	Acetylvalerenolic acid
291.160215	H / N	C17H24O4 [M-H]-	HMDB36693	Acetylbalchanolide
291.160215	H / N	C17H24O4 [M-H]-	HMDB39275	[6]-Gingerdione
291.160215	H / N	C17H24O4 [M-H]-	HMDB41249	6-Hydroxyshogaol
295.173633	N	C17H28O2S [M-H]-	-	-
297.122120	N	C11H22N2O5 [M+Cl]-	-	-
297.122120	N	C10H23N2O6P [M-H]-	-	-
298.072114	H / N	C16H13NO5 [M-H]-	HMDB29284	Avenanthramide 1c
298.072114	H / N	C16H13NO5 [M-H]-	HMDB38577	(Z)-N-Coumaroyl-5-hydroxyanthranilic acid
298.072114	H / N	C16H13NO5 [M-H]-	HMDB41141	Marshdine
298.072114	H / N	C16H13NO5 [M-H]-	HMDB41516	Avenanthramide G
298.275229	H / N	C18H37NO2 [M-H]-	HMDB00252	Sphingosine
298.275229	H / N	C18H37NO2 [M-H]-	HMDB01480	3-Dehydrosphinganine
298.275229	H / N	C18H37NO2 [M-H]-	HMDB02100	Palmitoylethanolamide
299.128802	H / N	C18H20O4 [M-H]-	HMDB30755	Myrigalone E
299.128802	H / N	C18H20O4 [M-H]-	HMDB30922	1,3-Diacetoxy-4,6,12-tetradecatriene-8,10-diyne
299.128802	H / N	C18H20O4 [M-H]-	HMDB37245	Myrigalone A
299.128802	H / N	C18H20O4 [M-H]-	HMDB37246	Myrigalon B
299.128802	H / N	C18H20O4 [M-H]-	HMDB38325	Verimol C
300.089078	N	C17H11N5O [M-H]-	-	-
300.132245	N	C12H23N5S2 [M-H]-	-	-
300.194257	N	C15H23N7 [M-H]-	-	-
300.218109	H / N	C16H31NO4 [M-H]-	HMDB06320	2,6 Dimethylheptanoyl carnitine
300.218109	H / N	C16H31NO4 [M-H]-	HMDB13288	Nonanoylcarnitine
301.105505	N	C13H14N6O3 [M-H]-	-	-
302.055127	N	C8H17NO9S [M-H]-	-	-
302.160987	H / N	C14H25NO6 [M-H]-	HMDB13328	Pimelylcarnitine
303.057175	N	C11H17N2O4PS [M-H]-	-	-
303.207727	N	C18H28N2O2 [M-H]-	-	-
304.022778	N	C10H12NO8P [M-H]-	-	-
304.102125	N	C9H19N7OS2 [M-H]-	-	-
305.079475	N	C12H19O7P [M-H]-	-	-
307.072483	H / N	C17H12N2O4 [M-H]-	HMDB33459	Flazine
307.155133	H / N	C17H24O5 [M-H]-	HMDB30496	ACRL Toxin II
307.155133	H / N	C17H24O5 [M-H]-	HMDB35724	15-Deacetylcalonectrin
307.155133	H / N	C17H24O5 [M-H]-	HMDB36489	Dihydrocumambrin A
308.075856	N	C11H15N7S2 [M-H]-	-	-
308.121799	N	C10H23N5O2S2 [M-H]-	-	-
309.174033	N	C14H30O5S [M-H]-	-	-
309.316387	N	C21H42O [M-H]-	-	-
311.107137	H	C17H17ClN4 [M-H]-	HMDB60536	Norclozapine
311.107137	H / N	C14H20N2O4S [M-H]-	HMDB28985	Methionyl-Tyrosine
311.107137	H / N	C14H20N2O4S [M-H]-	HMDB29111	Tyrosyl-Methionine
313.138194	N	C18H22N2OS [M-H]-	-	-
313.218008	N	C14H30N6S [M-H]-	-	-
314.110059	N	C11H25NO5S2 [M-H]-	-	-
314.114562	N	C16H17N3O4 [M-H]-	-	-
314.176173	H / N	C19H25NO3 [M-H]-	HMDB15382	Mitiglinide
314.176173	H / N	C19H25NO3 [M-H]-	HMDB30185	(E)-Piperolein A
315.123810	H / N	C18H20O5 [M-H]-	HMDB38323	Verimol B

315.123810	H / N	C18H20O5 [M-H]-	HMDB38324	Verimol A
315.123810	H / N	C18H20O5 [M-H]-	HMDB38780	7-Hydroxy-2',4',5'-trimethoxyisoflavan
315.123810	H / N	C18H20O5 [M-H]-	HMDB39510	7-Hydroxy-2',3',4'-trimethoxyisoflavan
315.123810	H / N	C18H20O5 [M-H]-	HMDB39607	Sorgolactone
315.123810	H / N	C18H20O5 [M-H]-	HMDB40534	5'-Hydroxy-3',4',7-trimethoxyflavan
315.173207	H / N	C17H28O3 [M+Cl]-	HMDB12535	12S-HHT
315.173207	H / N	C17H28O3 [M+Cl]-	HMDB32675	Dihydropanaxacol
315.173207	H / N	C17H28O3 [M+Cl]-	HMDB36422	Fauronyl acetate
315.173207	H / N	C17H28O3 [M+Cl]-	HMDB41388	Valeracetate
315.173207	N	C16H29O4P [M-H]-	-	-
315.222444	N	C15H32N4OS [M-H]-	-	-
316.067570	N	C12H15NO9 [M-H]-	-	-
317.132823	N	C17H22N2O2S [M-H]-	-	-
317.194625	N	C20H30OS [M-H]-	-	-
318.028853	N	C11H13NO8S [M-H]-	-	-
318.116717	N	C17H21NO3S [M-H]-	-	-
319.138048	N	C11H24N6OS2 [M-H]-	-	-
319.204624	H / N	C17H32O3 [M+Cl]-	HMDB35473	Avocadyne
319.204624	H / N	C17H32O3 [M+Cl]-	HMDB38685	Muricatacin
319.204624	N	C16H33O4P [M-H]-	-	-
321.133698	N	C12H22N4O4 [M+Cl]-	-	-
321.134364	N	C17H22O6 [M-H]-	-	-
321.153641	N	C11H26N6OS2 [M-H]-	-	-
322.039106	N	C14H13NO6S [M-H]-	-	-
322.096619	N	C12H21NO7S [M-H]-	-	-
322.150800	N	C13H25NO8 [M-H]-	-	-
323.142791	N	C11H24N6OS [M+Cl]-	-	-
323.150044	H / N	C17H24O6 [M-H]-	HMDB33504	AF Toxin II
323.150044	H / N	C17H24O6 [M-H]-	HMDB34576	3-Acetoxyscirpene-4,15-diol
323.150044	H / N	C17H24O6 [M-H]-	HMDB35357	Blumealactone C
323.150044	H / N	C17H24O6 [M-H]-	HMDB35847	4-Acetoxyscirpene-3,15-diol
323.150044	H / N	C17H24O6 [M-H]-	HMDB35848	Monoacetoxyscirpenol
324.153509	N	C11H27N5O2S2 [M-H]-	-	-
324.218052	H / N	C18H31NO4 [M-H]-	HMDB05049	10-Nitrolinoleic acid
324.218052	H / N	C18H31NO4 [M-H]-	HMDB14750	Bisoprolol
324.218052	H / N	C18H31NO4 [M-H]-	HMDB33503	Small bacteriocin
324.218052	H / N	C18H31NO4 [M-H]-	HMDB41248	N-[[3-Hydroxy-2-(2-pentenyl)cyclopentyl]acetyl]isoleucine
324.290806	H / N	C20H39NO2 [M-H]-	HMDB02088	N-Oleoylethanolamine
325.121896	N	C10H22N6O2S [M+Cl]-	-	-
325.130705	N	C17H18N4O3 [M-H]-	-	-
326.306483	H / N	C20H41NO2 [M-H]-	HMDB13078	Stearoylethanolamide
326.306483	H / N	C20H41NO2 [M-H]-	HMDB13645	N,N-Dimethylsphingosine
327.128096	N	C17H28S3 [M-H]-	-	-
329.103050	H / N	C18H18O6 [M-H]-	HMDB11672	Aflatoxin B1 dialcohol
329.103050	H / N	C18H18O6 [M-H]-	HMDB32655	(R)-2-Feruloyl-1-(4-Hydroxyphenyl)-1,2-ethanediol
329.103050	H / N	C18H18O6 [M-H]-	HMDB33299	7-Hydroxy-3-(3-hydroxy-4-methoxybenzyl)-5-methoxy-4-chromanone
329.103050	H / N	C18H18O6 [M-H]-	HMDB33697	Melilotocarpan C
329.103050	H / N	C18H18O6 [M-H]-	HMDB33817	4-Hydroxy-2,3,9-trimethoxypterocarpan
329.103050	H / N	C18H18O6 [M-H]-	HMDB37253	5-Hydroxy-3-(4-hydroxybenzyl)-7,8-dimethoxy-4-chromanone
329.103050	H / N	C18H18O6 [M-H]-	HMDB37315	Cerasinone
329.103050	H / N	C18H18O6 [M-H]-	HMDB37955	(±)-3',4'-Methylenedioxy-5,7-dimethylepicatechin
329.103050	H / N	C18H18O6 [M-H]-	HMDB38494	Americanol
329.103050	H / N	C18H18O6 [M-H]-	HMDB39381	Americanol A
329.103050	H / N	C18H18O6 [M-H]-	HMDB39740	Isoamericanol A
329.167043	N	C13H30N2O3S [M+Cl]-	-	-
329.208192	N	C16H30N2O5 [M-H]-	-	-
330.114186	N	C14H17N7OS [M-H]-	-	-
332.295873	H / N	C22H39NO [M-H]-	HMDB32033	2,4,12-Octadecatrienoic acid isobutylamide
333.186468	N	C16H26N6S [M-H]-	-	-
334.148882	N	C11H25N7OS2 [M-H]-	-	-
335.295555	N	C22H40O2 [M-H]-	-	-
336.181646	H / N	C18H27NO5 [M-H]-	HMDB29325	3,6-Ditigloyloxytropan-7-ol
338.034045	N	C14H13NO7S [M-H]-	-	-
339.156122	N	C16H24N2O6 [M-H]-	-	-
339.164300	N	C11H28N6O2S2 [M-H]-	-	-
339.167427	N	C15H24N4O5 [M-H]-	-	-
339.246195	H / N	C21H36O [M+Cl]-	HMDB33872	3-Pentadecylphenol
340.155367	H / N	C20H23NO4 [M-H]-	HMDB14842	Naltrexone
340.155367	H / N	C20H23NO4 [M-H]-	HMDB30184	(S)-Isocorydine
340.155367	H / N	C20H23NO4 [M-H]-	HMDB31998	Peroxysimulenoline
340.159547	N	C10H27N7O2S2 [M-H]-	-	-
340.212925	N	C18H31NO5 [M-H]-	-	-

341.081242	N	C14H18N2O6S [M-H]-	-	-
341.175832	H / N	C21H26O4 [M-H]-	HMDB29525	7-(4-Hydroxy-3-methoxyphenyl)-5-methoxy-1-phenyl-3-heptanone
341.249137	N	C16H34N6S [M-H]-	-	-
343.321746	H / N	C21H44O3 [M-H]-	HMDB11143	MG(18:0e/0:0/0:0)
345.217713	N	C15H30N6O [M+Cl]-	-	-
346.096453	N	C14H21NO7S [M-H]-	-	-
347.044267	N	C13H16O9S [M-H]-	-	-
349.107141	N	C15H19N4O4P [M-H]-	-	-
351.081974	N	C10H24N2O5S2 [M+Cl]-	-	-
351.163406	N	C19H28O4S [M-H]-	-	-
353.106207	N	C17H22O6S [M-H]-	-	-
353.175600	H / N	C22H26O4 [M-H]-	HMDB31877	Acetylsalvipisone
357.106898	H / N	C12H22N2O8 [M+Cl]-	HMDB30416	Avenic acid A
357.106898	H / N	C12H22N2O8 [M+Cl]-	HMDB33105	N2-Galacturonyl-L-lysine
357.106898	H / N	C12H22N2O8 [M+Cl]-	HMDB33106	N6-Galacturonyl-L-lysine
357.106898	N	C11H23N2O9P [M-H]-	-	-
357.148798	H / N	C16H26N2O5S [M-H]-	HMDB15535	Cilastatin
357.170726	H / N	C21H26O5 [M-H]-	HMDB05798	Malabaricone C
357.170726	H / N	C21H26O5 [M-H]-	HMDB14773	Prednisone
357.170726	H / N	C21H26O5 [M-H]-	HMDB30784	Normammein
357.170726	H / N	C21H26O5 [M-H]-	HMDB30792	Monascoflavin
357.170726	H / N	C21H26O5 [M-H]-	HMDB34096	Mammea B/BD
357.170726	H / N	C21H26O5 [M-H]-	HMDB34275	Mammea B/AC
357.203064	N	C17H30N2O6 [M-H]-	-	-
357.268022	N	C20H38N2O [M+Cl]-	-	-
359.182432	N	C16H28N2O7 [M-H]-	-	-
361.077553	N	C14H18O11 [M-H]-	-	-
361.131210	N	C13H18N10OS [M-H]-	-	-
361.225110	N	C12H30N10OS [M-H]-	-	-
362.070355	N	C17H17NO6S [M-H]-	-	-
362.143909	N	C12H25N7O2S2 [M-H]-	-	-
362.147577	N	C17H25N5S2 [M-H]-	-	-
362.156948	N	C14H25N3O8 [M-H]-	-	-
363.090691	N	C18H20O6S [M-H]-	-	-
363.123051	N	C14H24N2O7S [M-H]-	-	-
363.148228	N	C16H28O7S [M-H]-	-	-
364.224202	N	C19H31N3O4 [M-H]-	-	-
365.127699	N	C15H26O8S [M-H]-	-	-
365.142735	N	C19H26O5S [M-H]-	-	-
369.141703	N	C15H22N4O7 [M-H]-	-	-
370.275094	H / N	C24H37NO2 [M-H]-	HMDB13658	Docosahexaenoyl Ethanolamide
371.213914	N	C16H36N2O3S [M+Cl]-	-	-
371.218733	N	C18H32N2O6 [M-H]-	-	-
372.166289	N	C17H27NO8 [M-H]-	-	-
372.225182	N	C16H31N5O5 [M-H]-	-	-
372.290785	N	C24H39NO2 [M-H]-	-	-
373.071870	H / N	C22H14O6 [M-H]-	HMDB29538	Neodiospyrin
374.069769	N	C10H21N3O8S2 [M-H]-	-	-
374.102722	N	C14H21N3O7S [M-H]-	-	-
374.306421	H / N	C24H41NO2 [M-H]-	HMDB13626	Adrenoyl ethanolamide
375.177329	N	C16H28N2O8 [M-H]-	-	-
376.070750	N	C14H19NO9S [M-H]-	-	-
377.102471	N	C14H22N2O8S [M-H]-	-	-
378.101569	N	C18H21NO6S [M-H]-	-	-
379.261999	H / N	C20H40O4 [M+Cl]-	HMDB31923	10,20-Dihydroxyeicosanoic acid
379.261999	N	C19H41O5P [M-H]-	-	-
382.107694	N	C16H21N3O6S [M-H]-	-	-
383.044093	N	C16H16O9S [M-H]-	-	-
383.295566	N	C26H40O2 [M-H]-	-	-
384.152760	N	C15H23N5O7 [M-H]-	-	-
384.221330	N	C20H35NO4S [M-H]-	-	-
385.071059	N	C15H18N2O8S [M-H]-	-	-
386.233709	N	C23H33NO4 [M-H]-	-	-
387.027013	N	C11H16N2O9S [M+Cl]-	-	-
387.027013	N	C10H17N2O10PS [M-H]-	-	-
387.166221	H / N	C18H28O9 [M-H]-	HMDB39964	beta-D-Glucopyranosyl-11-hydroxyjasmonic acid
387.166221	H / N	C18H28O9 [M-H]-	HMDB40706	7-Epi-12-hydroxyjasmonic acid glucoside
387.166221	H / N	C18H28O9 [M-H]-	HMDB41552	2-[4-(3-Hydroxypropyl)-2-methoxyphenoxy]-1,3-propanediol 1-xyloside
387.204497	N	C13H28N10O2S [M-H]-	-	-
387.254066	H / N	C24H36O4 [M-H]-	HMDB30366	Cavipetin C
389.148458	N	C17H26N2O6 [M+Cl]-	-	-
389.148458	N	C16H27N2O7P [M-H]-	-	-

389.280248	N	C18H38N6O [M+Cl]-	-	-
391.085616	N	C19H20O7S [M-H]-	-	-
391.246103	N	C19H32N6O3 [M-H]-	-	-
393.101261	N	C19H22O7S [M-H]-	-	-
394.187202	N	C20H29NO7 [M-H]-	-	-
394.271226	N	C21H37N3O4 [M-H]-	-	-
395.192215	H / N	C17H32O10 [M-H]-	HMDB31689	1-Hexanol arabinosylglucoside
395.261709	N	C18H40N4OS [M+Cl]-	-	-
397.038143	N	C12H18N2O9S2 [M-H]-	-	-
397.205392	N	C21H34O5S [M-H]-	-	-
397.234315	N	C20H34N2O6 [M-H]-	-	-
398.076271	N	C13H21NO11S [M-H]-	-	-
398.306421	N	C26H41NO2 [M-H]-	-	-
399.117493	H / N	C14H24N2O9 [M+Cl]-	HMDB60494	N-Acetylmuramoyl-Ala
399.117493	N	C13H25N2O10P [M-H]-	-	-
399.143376	N	C17H32O4S2 [M+Cl]-	-	-
399.143376	N	C16H33O5PS2 [M-H]-	-	-
399.143376	N	C19H16N10O [M-H]-	-	-
400.103751	N	C20H19NO8 [M-H]-	-	-
401.143808	N	C15H26N6O3S2 [M-H]-	-	-
401.210084	H / N	C21H34O5 [M+Cl]-	HMDB00314	3b-Allotetrahydrocortisol
401.210084	H / N	C21H34O5 [M+Cl]-	HMDB00526	5a-Tetrahydrocortisol
401.210084	H / N	C21H34O5 [M+Cl]-	HMDB00949	Tetrahydrocortisol
401.210084	H / N	C21H34O5 [M+Cl]-	HMDB03128	Cortolone
401.210084	H / N	C21H34O5 [M+Cl]-	HMDB13221	Beta-Cortolone
401.210084	N	C20H35O6P [M-H]-	-	-
401.338805	N	C22H46N2O4 [M-H]-	-	-
402.151774	N	C16H25N3O9 [M-H]-	-	-
402.155859	N	C21H25NO7 [M-H]-	-	-
403.179574	N	C19H32O7S [M-H]-	-	-
404.228987	N	C19H35NO8 [M-H]-	-	-
404.244190	N	C23H35NO5 [M-H]-	-	-
405.037611	N	C11H18N2O10S [M+Cl]-	-	-
405.037611	N	C10H19N2O11PS [M-H]-	-	-
407.262883	N	C24H40O3S [M-H]-	-	-
407.262883	N	C17H40N6OS2 [M-H]-	-	-
407.294435	N	C23H40N4 [M+Cl]-	-	-
408.202767	N	C21H31NO7 [M-H]-	-	-
409.293463	N	C20H38N6O3 [M-H]-	-	-
410.288343	N	C19H37N7O3 [M-H]-	-	-
411.179216	N	C18H32O8 [M+Cl]-	-	-
411.179216	N	C17H33O9P [M-H]-	-	-
413.163920	N	C20H30O7S [M-H]-	-	-
413.288273	N	C19H38N6O4 [M-H]-	-	-
414.112203	N	C12H25N5O7S2 [M-H]-	-	-
415.207062	N	C16H32N8OS2 [M-H]-	-	-
415.281296	N	C21H40N2O6 [M-H]-	-	-
418.169813	N	C15H29N7O3S2 [M-H]-	-	-
419.187883	N	C27H24N4O [M-H]-	-	-
421.075326	N	C13H22O13 [M+Cl]-	-	-
421.075326	H / N	C12H23O14P [M-H]-	HMDB01124	Trehalose 6-phosphate
421.075326	H / N	C12H23O14P [M-H]-	HMDB06789	Lactose 6-phosphate
421.317312	N	C22H46O7 [M-H]-	-	-
422.185469	N	C18H33NO8S [M-H]-	-	-
423.144908	N	C24H24O7 [M-H]-	-	-
423.148460	N	C21H28O7S [M-H]-	-	-
423.285520	N	C18H40N6O3 [M+Cl]-	-	-
423.285520	N	C17H41N6O4P [M-H]-	-	-
423.326831	H / N	C29H44O2 [M-H]-	HMDB06327	Alpha-Tocotrienol
423.326831	H / N	C29H44O2 [M-H]-	HMDB38656	(22E,24R)-Stigmasta-4,22-diene-3,6-dione
425.054819	N	C18H18O10S [M-H]-	-	-
425.192837	N	C20H30N2O8 [M-H]-	-	-
425.363644	N	C26H50O4 [M-H]-	-	-
426.159316	N	C20H29NO7S [M-H]-	-	-
427.079921	N	C18H21O10P [M-H]-	-	-
427.135749	H	C19H22F2N4O3 [M+Cl]-	HMDB15339	Sparfloxacin
427.135749	H / N	C18H24N2O10 [M-H]-	HMDB60829	Lacosamide-glucuronide
427.149090	N	C16H28N2O9 [M+Cl]-	-	-
427.149090	N	C15H29N2O10P [M-H]-	-	-
427.228485	N	C22H32N6OS [M-H]-	-	-
427.233727	N	C22H36O8 [M-H]-	-	-
428.146431	N	C21H23N3O7 [M-H]-	-	-

428.247009	N	C17H39N5O3S [M+Cl]-	-	-
429.158881	N	C20H30O8S [M-H]-	-	-
429.202969	N	C23H30N2O6 [M-H]-	-	-
429.249467	N	C22H38O8 [M-H]-	-	-
430.129058	N	C17H25N3O8S [M-H]-	-	-
430.162019	N	C21H25N3O7 [M-H]-	-	-
431.155971	H / N	C19H28O11 [M-H]-	HMDB34954	Zizybeoside I
431.155971	H / N	C19H28O11 [M-H]-	HMDB41515	Benzyl gentiobioside
431.195578	N	C20H32N2O6 [M+Cl]-	-	-
431.195578	N	C17H36O10S [M-H]-	-	-
431.201488	N	C16H32N8O2S2 [M-H]-	-	-
432.311996	H / N	C26H43NO4 [M-H]-	HMDB00698	Lithocholic acid glycine conjugate
433.153830	N	C19H30O9S [M-H]-	-	-
433.174911	N	C19H30N2O7 [M+Cl]-	-	-
433.174911	N	C16H34O11S [M-H]-	-	-
435.133270	N	C18H28O10S [M-H]-	-	-
435.139435	N	C14H33N2O7PS2 [M-H]-	-	-
435.170915	N	C20H28N4O5S [M-H]-	-	-
435.246113	N	C18H36N4O8 [M-H]-	-	-
437.267477	H / N	C22H42O6 [M+Cl]-	HMDB29887	Sorbitan palmitate
437.267477	H / N	C21H43O7P [M-H]-	HMDB07850	LPA(0:0/18:0)
437.267477	H / N	C21H43O7P [M-H]-	HMDB07854	LPA(18:0/0:0)
437.363646	N	C27H50O4 [M-H]-	-	-
438.270546	N	C20H41NO9 [M-H]-	-	-
439.229219	N	C21H40O5S [M+Cl]-	-	-
439.229219	N	C20H41O6PS [M-H]-	-	-
439.231413	N	C27H36O3S [M-H]-	-	-
439.303610	N	C21H40N6O4 [M-H]-	-	-
439.361301	N	C27H52O2S [M-H]-	-	-
439.379305	H / N	C27H52O4 [M-H]-	HMDB11559	MG(0:0/24:1(15Z)/0:0)
439.379305	H / N	C27H52O4 [M-H]-	HMDB11589	MG(24:1(15Z)/0:0/0:0)
440.167496	N	C19H27N3O9 [M-H]-	-	-
440.215360	N	C19H31N5O7 [M-H]-	-	-
441.358582	N	C26H50O5 [M-H]-	-	-
441.363059	N	C24H50N4OS [M-H]-	-	-
442.216248	N	C16H37N5O5S2 [M-H]-	-	-
442.219587	N	C20H33N3O8 [M-H]-	-	-
444.252590	N	C23H39NO5 [M+Cl]-	-	-
444.252590	N	C22H40NO6P [M-H]-	-	-
445.080823	N	C18H22O11S [M-H]-	-	-
445.172869	N	C21H26N4O7 [M-H]-	-	-
445.405082	N	C30H54O2 [M-H]-	-	-
446.156942	N	C21H25N3O8 [M-H]-	-	-
447.169509	N	C20H32O9S [M-H]-	-	-
447.208718	N	C21H36N2O4S [M+Cl]-	-	-
447.208718	N	C12H33N8O8P [M-H]-	-	-
447.208718	N	C20H37N2O5PS [M-H]-	-	-
447.301006	N	C21H44N4O4S [M-H]-	-	-
449.212213	N	C16H34N8O3S2 [M-H]-	-	-
449.247014	N	C19H38N6O2S [M+Cl]-	-	-
450.145361	N	C19H25N5O6S [M-H]-	-	-
450.161656	N	C18H29NO12 [M-H]-	-	-
450.262960	N	C22H41NO6 [M+Cl]-	-	-
450.262960	H / N	C21H42NO7P [M-H]-	HMDB11474	LysoPE(0:0/16:1(9Z))
450.262960	H / N	C21H42NO7P [M-H]-	HMDB11504	LysoPE(16:1(9Z)/0:0)
451.264733	N	C17H32N12O3 [M-H]-	-	-
451.452111	H / N	C30H60O2 [M-H]-	HMDB29987	(+)-11-Hydroxy-9-triacontanone
451.452111	H / N	C30H60O2 [M-H]-	HMDB30925	Melissic acid A
452.179041	N	C19H27N5O8 [M-H]-	-	-
452.275140	N	C20H31N13 [M-H]-	-	-
453.199150	N	C20H30N4O8 [M-H]-	-	-
454.183187	N	C20H29N3O9 [M-H]-	-	-
455.174369	N	C22H32O8S [M-H]-	-	-
455.271345	N	C21H44N2O4S [M+Cl]-	-	-
455.271345	N	C20H45N2O5PS [M-H]-	-	-
457.081126	N	C19H22O11S [M-H]-	-	-
457.125227	N	C22H22N2O9 [M-H]-	-	-
457.177180	N	C27H26N2O5 [M-H]-	-	-
458.130387	H / N	C19H25NO12 [M-H]-	HMDB37551	1-(2-Hydroxyphenylamino)-1-deoxy-beta-D-gentiobioside 1,2-carbamate
458.385108	N	C26H53NO5 [M-H]-	-	-
459.183110	N	C16H32N2O13 [M-H]-	-	-
459.204400	N	C19H28N10O2S [M-H]-	-	-

459.291458	N	C24H40N6OS [M-H]-	-	-
461.167401	N	C21H34O7S2 [M-H]-	-	-
462.229859	N	C19H41NO7S [M+Cl]-	-	-
464.247552	N	C25H39NO5S [M-H]-	-	-
464.276764	N	C24H39N3O6 [M-H]-	-	-
465.199186	N	C21H30N4O8 [M-H]-	-	-
465.238847	N	C19H38N4O7S [M-H]-	-	-
465.245379	N	C20H38N2O10 [M-H]-	-	-
465.394932	N	C29H54O4 [M-H]-	-	-
465.467652	H / N	C31H62O2 [M-H]-	HMDB32682	10-Hydroxy-16-hentriacontanone
467.101866	N	C21H24O10S [M-H]-	-	-
467.341082	N	C27H48N2O2 [M+Cl]-	-	-
467.348780	N	C26H48N2O5 [M-H]-	-	-
467.410599	N	C29H56O4 [M-H]-	-	-
468.206760	N	C16H35N7O5S2 [M-H]-	-	-
468.208956	N	C19H35NO12 [M-H]-	-	-
469.252676	N	C19H42N4O5S2 [M-H]-	-	-
469.252676	N	C19H34N8O6 [M-H]-	-	-
470.348713	N	C26H49NO6 [M-H]-	-	-
470.396591	N	C26H53N3O4 [M-H]-	-	-
471.129650	N	C24H24O10 [M-H]-	-	-
471.190452	N	C19H36O11S [M-H]-	-	-
471.259686	N	C24H40O9 [M-H]-	-	-
472.158623	H	C28H27NO4S [M-H]-	HMDB14624	Raloxifene
472.158623	H / N	C20H23N7O7 [M-H]-	HMDB00972	10-Formyltetrahydrofolate
472.158623	H / N	C20H23N7O7 [M-H]-	HMDB01562	N5-Formyl-THF
472.158623	H / N	C20H23N7O7 [M-H]-	HMDB02140	Pteroyl-D-glutamic acid
473.267437	N	C25H42O6 [M+Cl]-	-	-
473.267437	N	C24H43O7P [M-H]-	-	-
475.222510	N	C15H36N8O5S [M+Cl]-	-	-
475.222510	N	C23H40N2O2S2 [M+Cl]-	-	-
475.222510	N	C20H36N4O7S [M-H]-	-	-
475.300550	N	C20H44N8OS2 [M-H]-	-	-
476.250022	N	C22H39NO10 [M-H]-	-	-
476.284026	N	C27H43NO4S [M-H]-	-	-
478.243896	N	C20H37N5O6 [M+Cl]-	-	-
478.243896	N	C19H38N5O7P [M-H]-	-	-
478.284610	N	C23H45NO7S [M-H]-	-	-
479.218576	H / N	C27H32N2O6 [M-H]-	HMDB15530	Solifenacin
479.286269	N	C23H44O10 [M-H]-	-	-
479.311208	N	C23H36N12 [M-H]-	-	-
479.410566	N	C30H56O4 [M-H]-	-	-
479.446936	H / N	C31H60O3 [M-H]-	HMDB31056	8-Hydroxy-14,16-hentriacontanedione
479.446936	H / N	C31H60O3 [M-H]-	HMDB32087	5-Hydroxy-14,16-hentriacontanedione
479.446936	H / N	C31H60O3 [M-H]-	HMDB32125	(S)-25-Hydroxy-14,16-hentriacontanedione
480.219275	N	C22H39NO6S [M+Cl]-	-	-
480.219275	N	C21H40NO7PS [M-H]-	-	-
480.237930	N	C15H39N7O6S [M+Cl]-	-	-
480.237930	N	C22H36N5O5P [M-H]-	-	-
480.293523	N	C22H47N3O4S2 [M-H]-	-	-
481.426216	N	C30H58O4 [M-H]-	-	-
482.225540	N	C21H33N5O8 [M-H]-	-	-
483.283800	N	C32H40N2S [M-H]-	-	-
483.384363	H / N	C32H52O3 [M-H]-	HMDB36404	3beta-Acetoxy-19alpha-hydroxy-12-ursene
483.420718	N	C33H56O2 [M-H]-	-	-
483.436600	N	C22H52N12 [M-H]-	-	-
484.182747	N	C22H31NO11 [M-H]-	-	-
484.255199	N	C24H39NO9 [M-H]-	-	-
485.341610	N	C26H50N2O4S [M-H]-	-	-
486.245786	N	C22H37N3O9 [M-H]-	-	-
487.135615	N	C23H24N2O10 [M-H]-	-	-
487.178127	N	C17H32N2O14 [M-H]-	-	-
487.400421	N	C28H56O6 [M-H]-	-	-
489.213109	H / N	C26H34O9 [M-H]-	HMDB34434	Austalide F
489.213109	H / N	C26H34O9 [M-H]-	HMDB35073	Deacetylnomilinic acid
489.213109	H / N	C26H34O9 [M-H]-	HMDB39120	alpha-Crocetin glucosyl ester
489.213109	H / N	C26H34O9 [M-H]-	HMDB60122	4-Oxo-9-cis-retinoyl-beta-glucuronide
489.220478	N	C20H34N4O10 [M-H]-	-	-
491.195069	N	C25H32N2O6 [M+Cl]-	-	-
491.195069	N	C24H33N2O7P [M-H]-	-	-
491.218940	N	C28H32N2O6 [M-H]-	-	-
492.195633	N	C19H35N5O6S2 [M-H]-	-	-

492.245003	N	C22H39NO11 [M-H]-	-	-
493.157076	N	C21H34O9S2 [M-H]-	-	-
493.273085	N	C21H42N6O3S [M+Cl]-	-	-
493.273085	N	C20H43N6O4PS [M-H]-	-	-
494.154483	N	C18H30N3O11P [M-H]-	-	-
495.182836	N	C19H32N2O13 [M-H]-	-	-
495.227276	N	C22H40O10S [M-H]-	-	-
495.250430	N	C28H36N2O6 [M-H]-	-	-
495.478225	N	C32H64O3 [M-H]-	-	-
496.200275	N	C19H35N5O6S [M+Cl]-	-	-
496.200275	N	C18H36N5O7PS [M-H]-	-	-
496.251780	N	C21H43N3O6S2 [M-H]-	-	-
496.312568	N	C23H47NO10 [M-H]-	-	-
497.160024	N	C22H30N2O9S [M-H]-	-	-
497.266893	N	C29H34N6O2 [M-H]-	-	-
498.161850	N	C22H29NO12 [M-H]-	-	-
498.216082	N	C19H37N5O6S [M+Cl]-	-	-
498.216082	N	C18H38N5O7PS [M-H]-	-	-
499.244090	N	C22H36N6O5 [M+Cl]-	-	-
499.244090	N	C21H37N6O6P [M-H]-	-	-
502.300770	N	C22H37N11O3 [M-H]-	-	-
506.229397	N	C28H33N3O6 [M-H]-	-	-
506.297405	N	C24H45NO10 [M-H]-	-	-
507.302225	N	C19H36N14O3 [M-H]-	-	-
508.255454	N	C26H39NO9 [M-H]-	-	-
508.473516	H / N	C32H63NO3 [M-H]-	HMDB11773	Cer(d18:1/14:0)
510.219592	N	C21H37NO13 [M-H]-	-	-
510.271102	N	C26H41NO9 [M-H]-	-	-
511.267620	N	C26H36N6O5 [M-H]-	-	-
512.307370	N	C23H47NO11 [M-H]-	-	-
514.244705	N	C28H37NO8 [M-H]-	-	-
515.086634	N	C21H24O13S [M-H]-	-	-
516.341272	N	C25H51N5O2S2 [M-H]-	-	-
518.181531	N	C21H33N3O10S [M-H]-	-	-
518.253813	N	C23H41N3O8S [M-H]-	-	-
519.219046	N	C25H40O7S [M+Cl]-	-	-
519.219046	N	C24H41O8PS [M-H]-	-	-
519.257490	N	C24H36N6O7 [M-H]-	-	-
519.324063	N	C33H40N6 [M-H]-	-	-
520.209202	N	C28H31N3O7 [M-H]-	-	-
522.307460	N	C28H45NO8 [M-H]-	-	-
522.338152	N	C21H49N9O2S2 [M-H]-	-	-
523.319808	H / N	C30H48O5 [M+Cl]-	HMDB34036	Pitheduloside I
523.319808	H / N	C30H48O5 [M+Cl]-	HMDB34502	Arjunolic acid
523.319808	H / N	C30H48O5 [M+Cl]-	HMDB34531	Camelliagenin B
523.319808	H / N	C30H48O5 [M+Cl]-	HMDB35118	Madasiatic acid
523.319808	H / N	C30H48O5 [M+Cl]-	HMDB35782	Esculentic acid (Diplazium)
523.319808	H / N	C30H48O5 [M+Cl]-	HMDB35957	Hovenolactone
523.319808	H / N	C30H48O5 [M+Cl]-	HMDB36311	Centellasapogenol A
523.319808	H / N	C30H48O5 [M+Cl]-	HMDB36639	Glyyunnansapogenin B
523.319808	H / N	C30H48O5 [M+Cl]-	HMDB36651	Euscaphic acid
523.319808	H / N	C30H48O5 [M+Cl]-	HMDB36961	(3beta,6alpha,19alpha)-3,6,19-Trihydroxy-12-ursen-28-oic acid
523.319808	H / N	C30H48O5 [M+Cl]-	HMDB37782	Ganoderiol D
523.319808	H / N	C30H48O5 [M+Cl]-	HMDB38116	Ananasic acid
523.319808	H / N	C30H48O5 [M+Cl]-	HMDB40391	16beta-Hydroxystellatogenin
523.319808	H / N	C30H48O5 [M+Cl]-	HMDB41039	21beta-Hydroxyhederagenin
525.232767	N	C23H30N10O5 [M-H]-	-	-
526.257975	N	C27H41NO7 [M+Cl]-	-	-
526.257975	N	C26H42NO8P [M-H]-	-	-
526.288622	N	C24H41N5O8 [M-H]-	-	-
526.353912	H / N	C32H49NO5 [M-H]-	HMDB30291	Daphniphylline
528.224279	N	C28H35NO9 [M-H]-	-	-
528.280068	N	C23H35N11O4 [M-H]-	-	-
528.281893	N	C26H43NO10 [M-H]-	-	-
528.318292	N	C27H47NO9 [M-H]-	-	-
529.161864	N	C29H26N2O8 [M-H]-	-	-
529.226893	N	C22H38N6O5S2 [M-H]-	-	-
529.423039	N	C30H54N6O2 [M-H]-	-	-
531.217132	N	C27H36N2O7S [M-H]-	-	-
531.234616	N	C27H36N2O9 [M-H]-	-	-
532.223330	N	C25H35N5O6S [M-H]-	-	-
533.216173	N	C25H38O10 [M+Cl]-	-	-

533.216173	N	C24H39O11P [M-H]-	-	-
535.270168	N	C32H40O7 [M-H]-	-	-
536.149158	N	C19H31N5O9S2 [M-H]-	-	-
536.206888	N	C25H35N3O8S [M-H]-	-	-
536.276920	N	C30H39N3O6 [M-H]-	-	-
536.294671	N	C23H47N5O5S2 [M-H]-	-	-
537.193875	N	C21H34N2O14 [M-H]-	-	-
539.309303	N	C27H48N4O3S2 [M-H]-	-	-
540.199016	N	C27H31N3O9 [M-H]-	-	-
543.295766	N	C23H48N2O10S [M-H]-	-	-
543.426706	N	C31H60O7 [M-H]-	-	-
544.244784	N	C23H39N5O8S [M-H]-	-	-
548.294503	N	C24H47N5O5S2 [M-H]-	-	-
548.315865	N	C29H47N3O5S [M-H]-	-	-
549.343719	N	C31H50O8 [M-H]-	-	-
550.346932	N	C25H53N5O4S2 [M-H]-	-	-
550.441175	N	C32H61N3O2S [M-H]-	-	-
551.250068	N	C28H40O11 [M-H]-	-	-
553.221116	H	C28H39ClO9 [M-H]-	HMDB31388	23-Hydroxyphysalolactone
553.221116	H / N	C28H38O9 [M+Cl]-	HMDB30154	Austalide G
553.221116	N	C27H39O10P [M-H]-	-	-
555.187259	N	C29H32O11 [M-H]-	-	-
555.245975	N	C28H36N4O8 [M-H]-	-	-
557.418980	N	C31H54N6O3 [M-H]-	-	-
559.075147	N	C19H16N10O9S [M-H]-	-	-
559.075147	N	C16H25N4O14PS [M-H]-	-	-
561.270550	N	C30H42O10 [M-H]-	-	-
561.457250	N	C33H62N4OS [M-H]-	-	-
564.271819	N	C31H39N3O7 [M-H]-	-	-
565.247768	N	C29H42O9S [M-H]-	-	-
569.442281	N	C33H62O7 [M-H]-	-	-
571.416369	N	C32H56N6OS [M-H]-	-	-
571.458155	N	C33H64O7 [M-H]-	-	-
575.410754	H / N	C38H56O4 [M-H]-	HMDB00977	3-Hexaprenyl-4-hydroxy-5-methoxybenzoic acid
575.410754	H / N	C38H56O4 [M-H]-	HMDB06820	2-Hexaprenyl-3-methyl-5-hydroxy-6-methoxy-1,4-benzoquinone
575.410754	H / N	C38H56O4 [M-H]-	HMDB36285	Campesteryl ferulate
576.285561	N	C23H43N9O4S [M+Cl]-	-	-
579.281447	N	C30H44O11 [M-H]-	-	-
579.354270	N	C32H52O9 [M-H]-	-	-
579.491442	N	C37H68O2 [M+Cl]-	-	-
580.357404	N	C26H55N5O5S2 [M-H]-	-	-
581.482573	N	C28H66N8S [M+Cl]-	-	-
581.504887	N	C38H66N2O2 [M-H]-	-	-
582.343560	N	C34H49NO7 [M-H]-	-	-
583.415711	H / N	C40H56O3 [M-H]-	HMDB29857	Cryptochrome
583.415711	H / N	C40H56O3 [M-H]-	HMDB29896	Cryptoxanthin diepoxide
583.415711	H / N	C40H56O3 [M-H]-	HMDB30537	Cryptoxanthin 5,6:5',8'-diepoxide
583.415711	H / N	C40H56O3 [M-H]-	HMDB30586	(3S,3'R,4xi)-beta,beta-Carotene-3,3',4-triol
583.415711	H / N	C40H56O3 [M-H]-	HMDB35319	Cucurbitaxanthin A
583.415711	H / N	C40H56O3 [M-H]-	HMDB35831	Antheraxanthin A
583.415711	H / N	C40H56O3 [M-H]-	HMDB36590	Capsanthin
583.415711	H / N	C40H56O3 [M-H]-	HMDB36868	Flavoxanthin
583.415711	H / N	C40H56O3 [M-H]-	HMDB36914	Triphasiaxanthin
583.415711	H / N	C40H56O3 [M-H]-	HMDB37121	Prenigroxanthin
583.415711	H / N	C40H56O3 [M-H]-	HMDB37564	Mutatoxanthin
583.415711	H / N	C40H56O3 [M-H]-	HMDB41590	Lutein 5,6-epoxide
583.494374	N	C35H68O6 [M-H]-	-	-
589.426703	H / N	C39H58O4 [M-H]-	HMDB36062	Ubiquinone 6
589.426703	H / N	C39H58O4 [M-H]-	HMDB41146	Feruloyl-beta-sitosterol
589.426703	N	C32H58N6O2S [M-H]-	-	-
590.429800	N	C33H61N5S2 [M-H]-	-	-
593.129983	H / N	C30H26O13 [M-H]-	HMDB36303	Epicatechin-(4beta->8)-gallocatechin
593.129983	H / N	C30H26O13 [M-H]-	HMDB37345	3''-O-Caffeoylcosmosiin
593.129983	H / N	C30H26O13 [M-H]-	HMDB37348	Piperitoside
593.129983	H / N	C30H26O13 [M-H]-	HMDB37651	Epigallocatechin-(4beta->8)-catechin
593.129983	H / N	C30H26O13 [M-H]-	HMDB37653	Gallocatechin-(4alpha->8)-epicatechin
593.129983	H / N	C30H26O13 [M-H]-	HMDB38766	2''-O-trans-p-Coumaroylastragalin
593.129983	H / N	C30H26O13 [M-H]-	HMDB40473	7-O-(4-Hydroxycinnamoyl) astragalin
593.129983	H / N	C30H26O13 [M-H]-	HMDB40477	Buddlenoid A
593.129983	H / N	C30H26O13 [M-H]-	HMDB40689	6''-O-p-Coumaroyltrifolin
595.258330	N	C30H44O10S [M-H]-	-	-
597.304613	N	C28H50O11 [M+Cl]-	-	-

597.304613	N	C27H51O12P [M-H]-	-	-
597.450443	N	C32H66O7 [M+Cl]-	-	-
598.277193	N	C31H41N3O9 [M-H]-	-	-
598.338672	N	C34H49NO8 [M-H]-	-	-
598.344242	N	C27H53NO13 [M-H]-	-	-
599.297333	N	C32H44N2O9 [M-H]-	-	-
599.341592	N	C28H52N6O4S2 [M-H]-	-	-
599.344230	N	C31H52O11 [M-H]-	-	-
603.405970	N	C39H56O5 [M-H]-	-	-
603.405970	N	C32H56N6O3S [M-H]-	-	-
607.498624	N	C35H68N4O2S [M-H]-	-	-
608.326206	N	C32H51NO8S [M-H]-	-	-
608.373529	N	C32H55N3O6S [M-H]-	-	-
609.182619	H	C24H30N8O9 [M+Cl]-	HMDB06825	Tetrahydrofolyl-[Glu](2)
609.182619	H / N	C28H34O15 [M-H]-	HMDB03265	Hesperidin
609.182619	H / N	C28H34O15 [M-H]-	HMDB30748	Hesperetin 7-neohesperidoside
609.182619	H / N	C28H34O15 [M-H]-	HMDB36333	4'-Hydroxyacetophenone 4'-[4-hydroxy-3,5-dimethoxybenzoyl-(->5)-apiosyl-(1->2)-glucoside]
611.289459	N	C31H48O10S [M-H]-	-	-
614.333666	N	C34H49NO9 [M-H]-	-	-
615.406115	N	C33H56N6O3S [M-H]-	-	-
615.439523	H / N	C35H64O6 [M+Cl]-	HMDB33165	4-Deoxyannoreticuin
615.439523	H / N	C35H64O6 [M+Cl]-	HMDB35183	Murisolin
615.439523	H / N	C35H64O6 [M+Cl]-	HMDB39453	Muricin H
615.439523	H / N	C35H64O6 [M+Cl]-	HMDB40870	Corossoline
615.439523	H / N	C35H64O6 [M+Cl]-	HMDB41374	cis-Murisolinone
615.439523	N	C34H65O7P [M-H]-	-	-
615.450380	N	C28H60N10O3S [M-H]-	-	-
615.450380	N	C36H56N8O [M-H]-	-	-
618.408694	N	C29H57N5O9 [M-H]-	-	-
618.468716	N	C34H70NO4PS [M-H]-	-	-
618.504328	N	C37H69N3O2S [M-H]-	-	-
619.490114	N	C33H68N2O8 [M-H]-	-	-
621.432290	N	C34H66O5S [M+Cl]-	-	-
621.432290	N	C36H58N6OS [M-H]-	-	-
621.432290	N	C33H67O6PS [M-H]-	-	-
622.378415	N	C34H57NO7S [M-H]-	-	-
623.467202	N	C32H68N2O7S [M-H]-	-	-
626.369914	N	C36H53NO8 [M-H]-	-	-
627.303359	N	C32H44N4O9 [M-H]-	-	-
630.471458	N	C34H61N7O4 [M-H]-	-	-
630.471458	N	C42H65NOS [M-H]-	-	-
635.427565	N	C35H60N2O8 [M-H]-	-	-
635.435233	N	C37H64O6S [M-H]-	-	-
642.379053	N	C32H57N3O8S [M-H]-	-	-
645.516374	N	C37H74N2O2S [M+Cl]-	-	-
646.482086	N	C36H69NO6 [M+Cl]-	-	-
646.482086	H / N	C35H70NO7P [M-H]-	HMDB08850	PE(14:0/P-16:0)
646.482086	H / N	C35H70NO7P [M-H]-	HMDB11335	PE(P-16:0/14:0)
649.444868	H / N	C35H66O8 [M+Cl]-	HMDB33087	Donhexocin
649.444868	N	C37H58N6O4 [M-H]-	-	-
649.505068	N	C39H70O7 [M-H]-	-	-
655.443242	N	C36H64O10 [M-H]-	-	-
672.452095	N	C32H63N9O2S [M+Cl]-	-	-
672.452095	N	C36H67NO8S [M-H]-	-	-
673.232033	N	C26H46N2O14S2 [M-H]-	-	-
673.232033	N	C36H39N2O9P [M-H]-	-	-
673.232033	N	C34H42O12S [M-H]-	-	-
675.228949	N	C25H44N2O17S [M-H]-	-	-
675.460255	N	C39H60N6O4 [M-H]-	-	-
675.520811	N	C41H72O7 [M-H]-	-	-
677.463615	N	C39H66O9 [M-H]-	-	-
679.551986	N	C41H76O7 [M-H]-	-	-
685.417633	N	C40H62N2O3S [M+Cl]-	-	-
685.417633	N	C37H66O7S2 [M-H]-	-	-
685.417633	N	C37H58N4O8 [M-H]-	-	-
703.551952	N	C43H76O7 [M-H]-	-	-
709.435757	N	C39H66O9S [M-H]-	-	-
727.552151	N	C45H76O7 [M-H]-	-	-
729.567920	N	C45H78O7 [M-H]-	-	-
730.570930	N	C39H81N5O3S2 [M-H]-	-	-
730.570930	N	C39H73N9O4 [M-H]-	-	-
745.562692	N	C45H78O8 [M-H]-	-	-

746.566534	N	C39H73N9O5 [M-H]-	-	-
775.500729	N	C44H72O11 [M-H]-	-	-
823.570651	N	C43H85O12P [M-H]-	-	-
883.740445	N	C56H100O7 [M-H]-	-	-
Features selected for the WGB group				
146.045908	H / N	C5H9NO4 [M-H]-	HMDB00148	L-Glutamic acid
146.045908	H / N	C5H9NO4 [M-H]-	HMDB02393	N-Methyl-D-aspartic acid
146.045908	H / N	C5H9NO4 [M-H]-	HMDB02931	N-Acetylserine
146.045908	H / N	C5H9NO4 [M-H]-	HMDB03011	O-Acetylserine
146.045908	H / N	C5H9NO4 [M-H]-	HMDB03339	D-Glutamic acid
146.045908	H / N	C5H9NO4 [M-H]-	HMDB06556	L-4-Hydroxyglutamate semialdehyde
146.045908	H / N	C5H9NO4 [M-H]-	HMDB33550	3-(Carboxymethylamino)propanoic acid
146.045908	H / N	C5H9NO4 [M-H]-	HMDB60475	DL-Glutamate
159.066301	H / N	C7H12O4 [M-H]-	HMDB00555	3-Methyladipic acid
159.066301	H / N	C7H12O4 [M-H]-	HMDB00857	Pimelic acid
159.066301	H / N	C7H12O4 [M-H]-	HMDB02441	3,3-Dimethylglutaric acid
159.066301	H / N	C7H12O4 [M-H]-	HMDB29167	2-Methyladipic acid
159.066301	H / N	C7H12O4 [M-H]-	HMDB29573	Diethyl malonate
159.066301	H / N	C7H12O4 [M-H]-	HMDB41605	Propyleneglycol diacetate
159.066301	H / N	C7H12O4 [M-H]-	HMDB59722	Mono-methyl-adipate
159.066301	H / N	C7H12O4 [M-H]-	HMDB59738	2-Ethylglutaric acid
159.066301	H / N	C7H12O4 [M-H]-	HMDB59893	Ethyl methyl succinate
170.045895	H / N	C7H9NO4 [M-H]-	HMDB12289	Tetrahydrodipicolinate
172.061556	H / N	C7H11NO4 [M-H]-	HMDB06488	N-Acetyl-L-glutamate 5-semialdehyde
184.001772	H / N	C3H8NO6P [M-H]-	HMDB00272	Phosphoserine
184.001772	H / N	C3H8NO6P [M-H]-	HMDB01721	DL-O-Phosphoserine
185.056802	N	C7H10N2O4 [M-H]-	-	-
188.056464	H / N	C7H11NO5 [M-H]-	HMDB00590	Glutarylglycine
188.056464	H / N	C7H11NO5 [M-H]-	HMDB01138	N-Acetylglutamic acid
195.052378	H / N	C7H8N4O3 [M-H]-	HMDB01857	1,3-Dimethyluric acid
195.052378	H / N	C7H8N4O3 [M-H]-	HMDB01982	3,7-Dimethyluric acid
195.052378	H / N	C7H8N4O3 [M-H]-	HMDB02026	1,9-Dimethyluric acid
195.052378	H / N	C7H8N4O3 [M-H]-	HMDB04308	7,9-Dimethyluric acid
195.052378	H / N	C7H8N4O3 [M-H]-	HMDB11103	1,7-Dimethyluric acid
195.052378	H / N	C7H8N4O3 [M-H]-	HMDB59704	3,9-Dimethyluric acid
209.081961	H / N	C11H14O4 [M-H]-	HMDB13070	Sinapyl alcohol
209.081961	H / N	C11H14O4 [M-H]-	HMDB29187	5-(3',5')-Dihydroxyphenyl-gamma-valerolactone
209.081961	H / N	C11H14O4 [M-H]-	HMDB29233	3,4-Dihydroxyphenylvaleric acid
209.081961	H / N	C11H14O4 [M-H]-	HMDB33798	3-Methyl-1-(2,4,6-trihydroxyphenyl)-1-butanone
209.081961	H / N	C11H14O4 [M-H]-	HMDB34047	2'-Hydroxy-4',6'-dimethoxy-3'-methylacetophenone
209.081961	H / N	C11H14O4 [M-H]-	HMDB36199	2-Methoxy-4-(4-methyl-1,3-dioxolan-2-yl)phenol
209.081961	H / N	C11H14O4 [M-H]-	HMDB39428	2-Methoxy-3-(4-methoxyphenyl)propanoic acid
209.081961	H / N	C11H14O4 [M-H]-	HMDB41406	Bancroftinone
209.081961	H / N	C11H14O4 [M-H]-	HMDB60737	3-(4-Hydroxy-3-methoxyphenyl)-2-methylpropionic acid
213.186036	H / N	C13H26O2 [M-H]-	HMDB00910	Tridecanoic acid
213.186036	H / N	C13H26O2 [M-H]-	HMDB29552	Ethyl undecanoate
213.186036	H / N	C13H26O2 [M-H]-	HMDB31018	Methyl dodecanoate
213.186036	H / N	C13H26O2 [M-H]-	HMDB32211	Decanal propyleneglycol acetal
213.186036	H / N	C13H26O2 [M-H]-	HMDB34140	Octyl 3-methylbutanoate
213.186036	H / N	C13H26O2 [M-H]-	HMDB36217	Pentyl octanoate
213.186036	H / N	C13H26O2 [M-H]-	HMDB36219	Octyl 2-methylbutyrate
213.186036	H / N	C13H26O2 [M-H]-	HMDB37311	Decyl propionate
213.186036	H / N	C13H26O2 [M-H]-	HMDB38729	3-Methylbutyl octanoate
213.186036	H / N	C13H26O2 [M-H]-	HMDB59900	Propyl decanoate
216.051356	H / N	C8H11NO6 [M-H]-	HMDB30417	Lycoperdic acid
226.012337	H / N	C6H9NO6 [M+Cl]-	HMDB15155	Isosorbide Mononitrate
226.012337	H / N	C6H9NO6 [M+Cl]-	HMDB41900	gamma-Carboxyglutamic acid
226.012337	H / N	C5H10NO7P [M-H]-	HMDB01228	L-Glutamic acid 5-phosphate
228.124135	H / N	C11H19NO4 [M-H]-	HMDB13126	Butenylcarnitine
235.074182	H / N	C10H16O4 [M+Cl]-	HMDB00603	cis-4-Decenedioic acid
235.074182	H / N	C10H16O4 [M+Cl]-	HMDB13227	cis-5-Decenedioic acid
235.074182	H / N	C10H16O4 [M+Cl]-	HMDB30989	5-Pentyltetrahydro-2-oxo-3-furancarboxylic acid
235.074182	H / N	C10H16O4 [M+Cl]-	HMDB30990	alpha-Carboxy-delta-nonalactone
235.074182	H / N	C10H16O4 [M+Cl]-	HMDB34491	(±)-Camphoric acid
235.074182	H / N	C10H16O4 [M+Cl]-	HMDB34971	(1R,2R,3S,1'R)-Nepetalinic acid
235.074182	H / N	C10H16O4 [M+Cl]-	HMDB36715	Matsutakic acid A
235.074182	N	C9H17O5P [M-H]-	-	-
241.123416	N	C16H18O2 [M-H]-	-	-
247.170368	H / N	C16H24O2 [M-H]-	HMDB32228	Dimethylbenzyl carbinyl hexanoate
247.170368	H / N	C16H24O2 [M-H]-	HMDB36221	[2-(Dimethoxymethyl)-1-heptenyl]benzene
247.170368	H / N	C16H24O2 [M-H]-	HMDB36640	Furanofukinin
247.170368	H / N	C16H24O2 [M-H]-	HMDB37713	Octyl phenylacetate

247.170368	H / N	C16H24O2 [M-H]-	HMDB37719	2-Phenylethyl octanoate
249.089870	H / N	C11H18O4 [M+Cl]-	HMDB30984	5-Hexyltetrahydro-2-oxo-3-furancarboxylic acid
249.089870	H / N	C11H18O4 [M+Cl]-	HMDB30985	alpha-Carboxy-delta-decalactone
249.089870	H / N	C11H18O4 [M+Cl]-	HMDB30986	2-Carboxy-5,7-dimethyl-4-octanolide
249.089870	N	C10H19O5P [M-H]-	-	-
257.060153	N	C10H14N2O4S [M-H]-	-	-
257.081969	H / N	C15H14O4 [M-H]-	HMDB04629	O-Desmethylangolensin
257.081969	H / N	C15H14O4 [M-H]-	HMDB30616	Archangin
257.081969	H / N	C15H14O4 [M-H]-	HMDB30947	Wyerone
257.081969	H / N	C15H14O4 [M-H]-	HMDB31842	Rhapontigenin
257.081969	H / N	C15H14O4 [M-H]-	HMDB32725	Acetomenaphthone
257.081969	H / N	C15H14O4 [M-H]-	HMDB33931	Xanthoxyletin
257.081969	H / N	C15H14O4 [M-H]-	HMDB33986	Demethylvestitol
257.081969	H / N	C15H14O4 [M-H]-	HMDB34144	Yangonin
257.081969	H / N	C15H14O4 [M-H]-	HMDB34255	5-Methoxyseselin
257.081969	H / N	C15H14O4 [M-H]-	HMDB40679	(2S,3R,4R)-3,4,4'-Trihydroxyflavan
257.081969	H / N	C15H14O4 [M-H]-	HMDB41652	3',4',7-Trihydroxyisoflavan
257.081969	H / N	C15H14O4 [M-H]-	HMDB41657	3'-Hydroxyequol
257.081969	H / N	C15H14O4 [M-H]-	HMDB41710	cis-4-Hydroxyequol
257.158060	N	C14H26O2S [M-H]-	-	-
259.173757	N	C14H28O2S [M-H]-	-	-
261.116603	N	C12H22O4S [M-H]-	-	-
261.185996	H / N	C17H26O2 [M-H]-	HMDB32501	Santalyl acetate
261.185996	H / N	C17H26O2 [M-H]-	HMDB33957	Crithmumdiol
261.185996	H / N	C17H26O2 [M-H]-	HMDB37209	alpha-Santalyl acetate
261.185996	H / N	C17H26O2 [M-H]-	HMDB37832	Vetiveryl acetate
261.185996	H / N	C17H26O2 [M-H]-	HMDB38024	beta-Santalyl acetate
261.185996	H / N	C17H26O2 [M-H]-	HMDB38782	1-Heptadecene-4,6-diyne-3,9-diol
261.185996	H / N	C17H26O2 [M-H]-	HMDB39358	Ginsenoyne D
261.185996	H / N	C17H26O2 [M-H]-	HMDB40374	Ginsenoyne I
263.091470	N	C8H17N4O4P [M-H]-	-	-
263.113589	H / N	C11H20O7 [M-H]-	HMDB41186	Ilicifolinoside A
263.113589	H / N	C11H20O7 [M-H]-	HMDB41187	(Z)-2-Methyl-2-butene-1,4-diol 4-O-beta-D-Glucopyranoside
263.128888	H / N	C15H20O4 [M-H]-	HMDB30102	Hulupinic acid
263.128888	H / N	C15H20O4 [M-H]-	HMDB31972	Heliespirone A
263.128888	H / N	C15H20O4 [M-H]-	HMDB33227	Curcolonol
263.128888	H / N	C15H20O4 [M-H]-	HMDB33661	4-Hydroxydehydromyoporone
263.128888	H / N	C15H20O4 [M-H]-	HMDB34719	Isoamberboin
263.128888	H / N	C15H20O4 [M-H]-	HMDB35140	(S)-Abscisic acid
263.128888	H / N	C15H20O4 [M-H]-	HMDB35715	Tanacetin
263.128888	H / N	C15H20O4 [M-H]-	HMDB35805	Thellungianin G
263.128888	H / N	C15H20O4 [M-H]-	HMDB35874	(10R,11R)-Pterosin L
263.128888	H / N	C15H20O4 [M-H]-	HMDB36043	15-Hydroxymarasmen-3-one
263.128888	H / N	C15H20O4 [M-H]-	HMDB36045	O-Formyloreadone
263.128888	H / N	C15H20O4 [M-H]-	HMDB36093	Abscisic acid
263.128888	H / N	C15H20O4 [M-H]-	HMDB36125	(1beta,8beta)-1,8-Dihydroxy-3,7(11)-eudesmadien-12,8-olide
263.128888	H / N	C15H20O4 [M-H]-	HMDB36130	Vulgarin
263.128888	H / N	C15H20O4 [M-H]-	HMDB36135	3-Epiarmefolin
263.128888	H / N	C15H20O4 [M-H]-	HMDB36202	Alkhanin
263.128888	H / N	C15H20O4 [M-H]-	HMDB36773	Tavulin
263.128888	H / N	C15H20O4 [M-H]-	HMDB36931	Tatridin B
263.128888	H / N	C15H20O4 [M-H]-	HMDB37055	Istanbulin A
263.128888	H / N	C15H20O4 [M-H]-	HMDB37528	Blennin B
263.128888	H / N	C15H20O4 [M-H]-	HMDB38156	Umbellifolide
263.128888	H / N	C15H20O4 [M-H]-	HMDB40119	Enokipodin C
263.128888	H / N	C15H20O4 [M-H]-	HMDB41227	(8betaOH,10beta)-8-Hydroxy-3-oxo-7(11)-eremophilen-12,8-olide
263.128888	H / N	C15H20O4 [M-H]-	HMDB41284	2-Methyl-1-[2,4,6-trihydroxy-3-(3-methyl-2-butenyl)phenyl]-1-propanone
264.124122	N	C14H19NO4 [M-H]-	-	-
265.147896	N	C12H26O4S [M-H]-	-	-
268.166666	N	C13H23N3O3 [M-H]-	-	-
269.095846	N	C7H18N6OS [M+Cl]-	-	-
270.047588	N	C8H17NO5S2 [M-H]-	-	-
272.096097	N	C12H19NO4S [M-H]-	-	-
272.172820	H / N	C11H23N5O3 [M-H]-	HMDB28722	Arginyl-Valine
272.172820	H / N	C11H23N5O3 [M-H]-	HMDB29121	Valyl-Arginine
275.105553	N	C13H20O4 [M+Cl]-	-	-
275.105553	N	C12H21O5P [M-H]-	-	-
277.121371	H / N	C13H22O4 [M+Cl]-	HMDB30987	2-Carboxy-4-dodecanolide
277.121371	H / N	C13H22O4 [M+Cl]-	HMDB38736	(3S,5R,6R,7E)-3,5,6-Trihydroxy-7-megastigmen-9-one
277.122781	H / N	C11H22N2O4S [M-H]-	HMDB03426	Pantetheine
277.140534	N	C11H22N2O6 [M-H]-	-	-
278.126024	N	C12H17N5O3 [M-H]-	-	-

279.064058	H / N	C11H16O6 [M+Cl]-	HMDB31237	threo-Syringoylglycerol
279.064058	N	C10H17O7P [M-H]-	-	-
279.188745	N	C18H28 [M+Cl]-	-	-
281.978739	N	C3H11NO10P2 [M-H]-	-	-
282.084373	H / N	C10H13N5O5 [M-H]-	HMDB00133	Guanosine
282.084373	H / N	C10H13N5O5 [M-H]-	HMDB03333	8-Hydroxy-deoxyguanosine
283.068443	H / N	C10H12N4O6 [M-H]-	HMDB00299	Xanthosine
284.974425	N	C7H10O8S2 [M-H]-	-	-
285.083990	N	C10H14N4O6 [M-H]-	-	-
285.113201	H / N	C17H18O4 [M-H]-	HMDB30152	4'-Hydroxy-5,7-dimethoxyflavan
285.113201	H / N	C17H18O4 [M-H]-	HMDB30521	Sativan
285.113201	H / N	C17H18O4 [M-H]-	HMDB34024	Isosativan
285.113201	H / N	C17H18O4 [M-H]-	HMDB41168	Myrigalone G
285.113201	H / N	C17H18O4 [M-H]-	HMDB41169	Myrigalone H
285.113201	H / N	C17H18O4 [M-H]-	HMDB41671	4'-Hydroxy-3,4,5-trimethoxystilbene
285.113201	H / N	C17H18O4 [M-H]-	HMDB41680	4-Hydroxy-3,5,4'-trimethoxystilbene
287.201701	H / N	C19H28O2 [M-H]-	HMDB00077	Dehydroepiandrosterone
287.201701	H / N	C19H28O2 [M-H]-	HMDB00234	Testosterone
287.201701	H / N	C19H28O2 [M-H]-	HMDB00628	Epitestosterone
287.201701	H / N	C19H28O2 [M-H]-	HMDB00899	Androstanedione
287.201701	H / N	C19H28O2 [M-H]-	HMDB03769	Etiocholanedione
287.201701	H / N	C19H28O2 [M-H]-	HMDB05962	Dehydroandrosterone
287.201701	H / N	C19H28O2 [M-H]-	HMDB06035	4-Dihydroboldenone
287.201701	H / N	C19H28O2 [M-H]-	HMDB36205	alpha-Amylcinnamyl isovalerate
288.036331	N	C10H11NO9 [M-H]-	-	-
289.123625	H / N	C20H18O2 [M-H]-	HMDB40916	2-(4-Methyl-3-pentenyl)anthraquinone
289.123625	H / N	C20H18O2 [M-H]-	HMDB60517	trans-3,4-Dihydro-3,4-dihydroxy-7,12-dimethylbenz[a]anthracene
289.123625	H / N	C20H18O2 [M-H]-	HMDB60519	trans-5,6-Dihydro-5,6-dihydroxy-7,12-dimethylbenz[a]anthracene
289.155745	H / N	C16H22N2O3 [M-H]-	HMDB15453	Procaterol
291.136612	N	C13H25O5P [M-H]-	-	-
291.144877	N	C13H24O7 [M-H]-	-	-
292.022908	N	C10H11NO7 [M+Cl]-	-	-
292.022908	N	C9H12NO8P [M-H]-	-	-
293.212179	H / N	C18H30O3 [M-H]-	HMDB04668	13-OxoODE
293.212179	H / N	C18H30O3 [M-H]-	HMDB04669	9-OxoODE
293.212179	H / N	C18H30O3 [M-H]-	HMDB10200	A-12(13)-EpODE
293.212179	H / N	C18H30O3 [M-H]-	HMDB10203	13-HOTE
293.212179	H / N	C18H30O3 [M-H]-	HMDB10206	15(16)-EpODE
293.212179	H / N	C18H30O3 [M-H]-	HMDB10220	9(10)-EpODE
293.212179	H / N	C18H30O3 [M-H]-	HMDB10224	9-HOTE
293.212179	H / N	C18H30O3 [M-H]-	HMDB11108	17-Hydroxylinolenic acid
293.212179	H / N	C18H30O3 [M-H]-	HMDB29786	10-Oxo-11-octadecen-13-olide
293.212179	H / N	C18H30O3 [M-H]-	HMDB29969	Squamostanal A
293.212179	H / N	C18H30O3 [M-H]-	HMDB30950	15,16-Epoxy-9,12-octadecadienoic acid
293.212179	H / N	C18H30O3 [M-H]-	HMDB30995	(2'E,4'Z,8E)-Colneleic acid
293.212179	H / N	C18H30O3 [M-H]-	HMDB31088	12,13-Epoxy-9,15-octadecadienoic acid
293.212179	H / N	C18H30O3 [M-H]-	HMDB31103	2-Hydroxylinolenic acid
293.212179	H / N	C18H30O3 [M-H]-	HMDB31934	(9S,10E,12Z,15Z)-9-Hydroxy-10,12,15-octadecatrienoic acid
293.212179	H / N	C18H30O3 [M-H]-	HMDB34586	(9Z,12Z,14E)-16-Hydroxy-9,12,14-octadecatrienoic acid
293.212179	H / N	C18H30O3 [M-H]-	HMDB36832	Sterebin D
293.212179	H / N	C18H30O3 [M-H]-	HMDB39603	3,4-Dimethyl-5-pentyl-2-furanheptanoic acid
294.147916	H / N	C13H25NO4 [M+Cl]-	HMDB00705	Hexanoylcarnitine
294.147916	H / N	C13H25NO4 [M+Cl]-	HMDB00756	L-Hexanoylcarnitine
294.147916	N	C12H26NO5P [M-H]-	-	-
295.070100	N	C9H17N2O7P [M-H]-	-	-
295.139829	N	C12H24O8 [M-H]-	-	-
295.156059	N	C17H28S2 [M-H]-	-	-
295.227839	H / N	C18H32O3 [M-H]-	HMDB04667	13S-hydroxyoctadecadienoic acid
295.227839	H / N	C18H32O3 [M-H]-	HMDB04670	Alpha-dimorphecolic acid
295.227839	H / N	C18H32O3 [M-H]-	HMDB04701	9,10-Epoxyoctadecenoic acid
295.227839	H / N	C18H32O3 [M-H]-	HMDB04702	12,13-EpOME
295.227839	H / N	C18H32O3 [M-H]-	HMDB10223	9-HODE
295.227839	H / N	C18H32O3 [M-H]-	HMDB29796	(Z)-13-Oxo-9-octadecenoic acid
295.227839	H / N	C18H32O3 [M-H]-	HMDB29978	Avenoleic acid
295.227839	H / N	C18H32O3 [M-H]-	HMDB29998	12-Hydroxy-8,10-octadecadienoic acid
297.047137	N	C10H18O6S2 [M-H]-	-	-
297.084025	N	C11H14N4O6 [M-H]-	-	-
299.098323	N	C10H20O10 [M-H]-	-	-
301.214899	N	C16H26N6 [M-H]-	-	-
303.160117	H / N	C18H24O4 [M-H]-	HMDB60352	2-Polyprenyl-3-methyl-5-hydroxy-6-methoxy-1,4-benzoquinone
303.160117	H / N	C18H24O4 [M-H]-	HMDB60379	3-Polyprenyl-4-hydroxy-5-methoxybenzoate
303.171403	N	C17H24N2O3 [M-H]-	-	-

306.117645	N	C9H21N7OS2 [M-H]-	-	-
306.137837	N	C13H25NO5S [M-H]-	-	-
307.166345	H / N	C16H24N2O4 [M-H]-	HMDB60990	8-Hydroxycarteolol
309.055073	N	C13H14N2O5S [M-H]-	-	-
309.119094	N	C12H22O9 [M-H]-	-	-
309.181937	N	C16H26N2O4 [M-H]-	-	-
310.010071	N	C6H14NO9P [M+Cl]-	-	-
310.010071	N	C5H15NO10P2 [M-H]-	-	-
311.222775	H / N	C18H32O4 [M-H]-	HMDB03871	13-L-Hydroperoxylinoleic acid
311.222775	H / N	C18H32O4 [M-H]-	HMDB04706	8(R)-Hydroperoxylinoleic acid
311.222775	H / N	C18H32O4 [M-H]-	HMDB06940	9(S)-HPODE
311.222775	H / N	C18H32O4 [M-H]-	HMDB10201	12,13-DiHODE
311.222775	H / N	C18H32O4 [M-H]-	HMDB10208	15,16-DiHODE
311.222775	H / N	C18H32O4 [M-H]-	HMDB10221	9,10-DiHODE
311.222775	H / N	C18H32O4 [M-H]-	HMDB40900	(±)-(E)-13-Hydroxy-10-oxo-11-octadecenoic acid
312.054726	N	C13H15NO6S [M-H]-	-	-
313.035354	H / N	C16H10O7 [M-H]-	HMDB29508	Laccaic acid D
313.157559	H / N	C17H26O3 [M+Cl]-	HMDB30801	1-(4-Hydroxy-3-methoxyphenyl)-3-decanone
313.157559	H / N	C17H26O3 [M+Cl]-	HMDB30974	8-Acetoxy-4-acoren-3-one
313.157559	H / N	C17H26O3 [M+Cl]-	HMDB31928	Panaxytriol
313.157559	H / N	C17H26O3 [M+Cl]-	HMDB39251	Panaxacol
313.157559	N	C16H27O4P [M-H]-	-	-
313.234677	N	C9H30N10 [M+Cl]-	-	-
313.238428	H / N	C18H34O4 [M-H]-	HMDB00782	Octadecanedioic acid
313.238428	H / N	C18H34O4 [M-H]-	HMDB04704	9,10-DHOME
313.238428	H / N	C18H34O4 [M-H]-	HMDB04705	12,13-DHOME
313.238428	H / N	C18H34O4 [M-H]-	HMDB31679	(9xi,10xi,12xi)-9,10-Dihydroxy-12-octadecenoic acid
313.238428	H / N	C18H34O4 [M-H]-	HMDB41220	Dibutyl decanedioate
315.171303	N	C18H24N2O3 [M-H]-	-	-
315.173207	H / N	C17H28O3 [M+Cl]-	HMDB12535	12S-HHT
315.173207	H / N	C17H28O3 [M+Cl]-	HMDB32675	Dihydropanaxacol
315.173207	H / N	C17H28O3 [M+Cl]-	HMDB36422	Fauronyl acetate
315.173207	H / N	C17H28O3 [M+Cl]-	HMDB41388	Valeracetate
315.173207	N	C16H29O4P [M-H]-	-	-
315.196616	H / N	C20H28O3 [M-H]-	HMDB00344	2-Methoxyestradiol-3-methylether
315.196616	H / N	C20H28O3 [M-H]-	HMDB05079	15-Deoxy-d-12,14-PGJ2
315.196616	H / N	C20H28O3 [M-H]-	HMDB05832	6b-Hydroxymethandienone
315.196616	H / N	C20H28O3 [M-H]-	HMDB06254	4-Hydroxyretinoic acid
315.196616	H / N	C20H28O3 [M-H]-	HMDB12451	all-trans-5,6-Epoxyretinoic acid
315.196616	H / N	C20H28O3 [M-H]-	HMDB12452	all-trans-18-Hydroxyretinoic acid
315.196616	H / N	C20H28O3 [M-H]-	HMDB31773	Phytocassane E
315.196616	H / N	C20H28O3 [M-H]-	HMDB34630	(4Z,9a)-9-(3-Methyl-2-butenoyloxy)-4,10(14)-oplopadien-3-one
315.196616	H / N	C20H28O3 [M-H]-	HMDB34631	(4Z,9a)-9-Angeloyloxy-4,10(14)-oplopadien-3-one
315.196616	H / N	C20H28O3 [M-H]-	HMDB34691	Yucalexin B9
315.196616	H / N	C20H28O3 [M-H]-	HMDB35710	Cafestol
315.196616	H / N	C20H28O3 [M-H]-	HMDB36147	Furanojaponin
315.196616	H / N	C20H28O3 [M-H]-	HMDB36725	ent-17-Oxo-15-kauren-19-oic acid
315.196616	H / N	C20H28O3 [M-H]-	HMDB36747	ent-7-Oxo-8(14),15-pimaradien-19-oic acid
315.196616	H / N	C20H28O3 [M-H]-	HMDB36750	Momilactone C
315.196616	H / N	C20H28O3 [M-H]-	HMDB36762	ent-15-Oxo-16-kauren-19-oic acid
315.196616	H / N	C20H28O3 [M-H]-	HMDB36812	7-Oxo-8,15-isopimaradien-18-oic acid
315.196616	H / N	C20H28O3 [M-H]-	HMDB37233	Rosmaridiphenol
315.196616	H / N	C20H28O3 [M-H]-	HMDB38885	Trilobinone
315.196616	H / N	C20H28O3 [M-H]-	HMDB39442	ent-15,16-Epoxy-1(10),13(16),14-halimatrien-19-oic acid
315.196616	H / N	C20H28O3 [M-H]-	HMDB39484	Gibberellin A12 7-aldehyde
315.196616	H / N	C20H28O3 [M-H]-	HMDB41056	Phytocassane A
315.196616	H / N	C20H28O3 [M-H]-	HMDB41057	Phytocassane D
315.196616	H / N	C20H28O3 [M-H]-	HMDB60093	rac-5,6-Epoxy-retinoate
315.196616	H / N	C20H28O3 [M-H]-	HMDB61095	18-Hydroxyretinoic acid
316.144696	N	C12H23N5O3S [M-H]-	-	-
316.176586	N	C15H27NO6 [M-H]-	-	-
317.128765	N	C12H22N4O4S [M-H]-	-	-
317.186983	N	C18H26N2O3 [M-H]-	-	-
317.188870	N	C17H30O3 [M+Cl]-	-	-
317.188870	N	C16H31O4P [M-H]-	-	-
319.202682	N	C18H28N2O3 [M-H]-	-	-
320.259515	H / N	C20H35NO2 [M-H]-	HMDB13624	Alpha-Linolenoyl ethanolamide
321.130388	H / N	C12H22N2O8 [M-H]-	HMDB30416	Avenic acid A
321.130388	H / N	C12H22N2O8 [M-H]-	HMDB33105	N2-Galacturonyl-L-lysine
321.130388	H / N	C12H22N2O8 [M-H]-	HMDB33106	N6-Galacturonyl-L-lysine
321.182020	N	C17H26N2O4 [M-H]-	-	-
321.228342	N	C16H34O6 [M-H]-	-	-

322.185310	N	C11H29N7S2 [M-H]-	-	-
322.275167	H / N	C20H37NO2 [M-H]-	HMDB12252	Linoleoyl ethanolamide
325.007056	N	C11H10N4O4S2 [M-H]-	-	-
325.136000	N	C13H26N2O3S [M+Cl]-	-	-
325.136000	N	C12H27N2O4PS [M-H]-	-	-
325.212656	N	C12H30N6O2 [M+Cl]-	-	-
326.197278	N	C17H29NO5 [M-H]-	-	-
326.270033	H / N	C19H37NO3 [M-H]-	HMDB13246	Margaroylglycine
327.215256	N	C14H28N6O3 [M-H]-	-	-
331.033969	N	C9H16O11S [M-H]-	-	-
331.054949	N	C8H17N2O10P [M-H]-	-	-
331.168488	H / N	C17H28O4 [M+Cl]-	HMDB35075	Tanacetol B
331.168488	H / N	C17H28O4 [M+Cl]-	HMDB38798	(1(10)E,4a,5E)-1(10),5-Germacradiene-12-acetoxy-4,11-diol
334.187118	N	C15H29NO7 [M-H]-	-	-
335.197586	H / N	C18H28N2O4 [M-H]-	HMDB15324	Acebutolol
335.201034	N	C15H32N2O4S [M-H]-	-	-
335.292974	N	C18H36N6 [M-H]-	-	-
335.295555	N	C22H40O2 [M-H]-	-	-
336.254397	N	C20H35NO3 [M-H]-	-	-
338.146918	N	C14H21N5O5 [M-H]-	-	-
338.270070	H / N	C20H37NO3 [M-H]-	HMDB13631	Oleoyl glycine
339.148066	N	C17H24N2O3 [M+Cl]-	-	-
339.148066	N	C14H28O7S [M-H]-	-	-
341.218357	N	C11H30N8O2 [M+Cl]-	-	-
343.249004	N	C19H36O5 [M-H]-	-	-
343.264218	H / N	C23H36O2 [M-H]-	HMDB35582	1-Phenyl-1,3-heptadecanedione
344.092052	N	C13H19N3O6S [M-H]-	-	-
345.097963	H / N	C18H18O7 [M-H]-	HMDB37250	Muscomin
347.132937	N	C12H24N6O2S2 [M-H]-	-	-
349.213243	N	C19H30N2O4 [M-H]-	-	-
350.160914	N	C18H25NO6 [M-H]-	-	-
350.233700	N	C20H33NO4 [M-H]-	-	-
351.088548	N	C11H24O8S [M+Cl]-	-	-
351.088548	N	C21H20OS2 [M-H]-	-	-
351.184750	N	C16H32O6S [M-H]-	-	-
351.194277	N	C17H32O5 [M+Cl]-	-	-
351.194277	N	C16H33O6P [M-H]-	-	-
351.195120	N	C18H36S2 [M+Cl]-	-	-
351.215425	N	C24H32S [M-H]-	-	-
352.049603	N	C15H15NO7S [M-H]-	-	-
353.167043	N	C15H30N2O3S [M+Cl]-	-	-
353.167043	N	C14H31N2O4PS [M-H]-	-	-
353.257626	N	C17H38N2O3 [M+Cl]-	-	-
354.130637	N	C15H21N3O7 [M-H]-	-	-
357.095650	N	C13H22O9 [M+Cl]-	-	-
357.095650	N	C12H23O10P [M-H]-	-	-
359.295520	H / N	C24H40O2 [M-H]-	HMDB06246	Tetracosatetraenoic acid (24:4n-6)
359.295520	H / N	C24H40O2 [M-H]-	HMDB35679	1-Hydroxy-1-phenyl-3-octadecanone
359.295520	H / N	C24H40O2 [M-H]-	HMDB35680	3-Hydroxy-1-phenyl-1-octadecanone
361.129237	H / N	C19H22O7 [M-H]-	HMDB31366	Gibberellin A93
361.129237	H / N	C19H22O7 [M-H]-	HMDB33905	2',8-Dihydroxy-3',4',5',7-tetramethoxyflavan
361.129237	H / N	C19H22O7 [M-H]-	HMDB35050	Gibberellin A21
361.129237	H / N	C19H22O7 [M-H]-	HMDB36778	Diosbulbin C
361.129237	H / N	C19H22O7 [M-H]-	HMDB39239	Gibberellin A87
362.200644	N	C17H33NO5S [M-H]-	-	-
363.142880	N	C13H28O9 [M+Cl]-	-	-
363.142880	N	C16H24N6S2 [M-H]-	-	-
363.144908	H / N	C19H24O7 [M-H]-	HMDB33420	Gibberellin A55
363.144908	H / N	C19H24O7 [M-H]-	HMDB35038	Gibberellin A50
363.144908	H / N	C19H24O7 [M-H]-	HMDB35052	Gibberellin A49
363.144908	H / N	C19H24O7 [M-H]-	HMDB36890	Gibberellin A72
363.144908	H / N	C19H24O7 [M-H]-	HMDB36898	Gibberellin A76
363.144908	H / N	C19H24O7 [M-H]-	HMDB39623	Gibberellin A79
363.144908	H / N	C19H24O7 [M-H]-	HMDB40324	(7R*,8R*)-3-Methoxy-3',4,7,9,9'-pentahydroxy-8,4'-oxyneolignan
363.144908	H / N	C19H24O7 [M-H]-	HMDB40651	Gibberellin A91
363.146926	N	C13H20N10OS [M-H]-	-	-
365.208176	N	C19H30N2O5 [M-H]-	-	-
367.227610	N	C24H32O3 [M-H]-	-	-
368.190405	N	C19H31NO4S [M-H]-	-	-
369.010790	N	C15H14O7S2 [M-H]-	-	-
369.158718	N	C15H30O8S [M-H]-	-	-
369.183477	H / N	C20H30O4 [M+Cl]-	HMDB01244	15-Keto-13,14-dihydroprostaglandin A2

369.183477	H / N	C20H30O4 [M+Cl]-	HMDB02710	Prostaglandin J2
369.183477	H / N	C20H30O4 [M+Cl]-	HMDB02752	Prostaglandin A2
369.183477	H / N	C20H30O4 [M+Cl]-	HMDB04234	12-Keto-leukotriene B4
369.183477	H / N	C20H30O4 [M+Cl]-	HMDB04236	Prostaglandin B2
369.183477	H / N	C20H30O4 [M+Cl]-	HMDB04238	Delta-12-Prostaglandin J2
369.183477	H / N	C20H30O4 [M+Cl]-	HMDB05073	Leukotriene B5
369.183477	H / N	C20H30O4 [M+Cl]-	HMDB12824	5-Oxo-6-trans-leukotriene B4
369.183477	H / N	C20H30O4 [M+Cl]-	HMDB12850	7'-Carboxy-gamma-chromanol
369.183477	H / N	C20H30O4 [M+Cl]-	HMDB35286	Crispanone
369.183477	H / N	C20H30O4 [M+Cl]-	HMDB35878	8alpha-8-Hydroxy-12-oxo-13-abieten-18-oic acid
369.183477	H / N	C20H30O4 [M+Cl]-	HMDB36760	(ent-16betaOH)-16,17-Dihydroxy-9(11)-kauren-19-oic acid
369.183477	H / N	C20H30O4 [M+Cl]-	HMDB36763	(ent-6alpha,7alpha)-6,7-Dihydroxy-16-kauren-19-oic acid
369.183477	H / N	C20H30O4 [M+Cl]-	HMDB36828	Dehydropinifolic acid
369.183477	H / N	C20H30O4 [M+Cl]-	HMDB41055	Phytocassane B
369.183477	H / N	C20H30O4 [M+Cl]-	HMDB60046	15d PGD2
369.183477	H / N	C20H30O4 [M+Cl]-	HMDB60054	bicyclo-PGE2
369.183477	H / N	C20H30O4 [M+Cl]-	HMDB60095	Prostaglandin-c2
369.183477	N	C19H31O5P [M-H]-	-	-
371.077190	N	C19H16O8 [M-H]-	-	-
371.137849	N	C17H24N2O5 [M+Cl]-	-	-
371.137849	N	C16H25N2O6P [M-H]-	-	-
372.275520	N	C20H39NO5 [M-H]-	-	-
374.139103	N	C15H25N3O6S [M-H]-	-	-
375.268586	N	C19H40N2O3S [M-H]-	-	-
377.139381	H / N	C23H22O5 [M-H]-	HMDB30656	Demethylcalabaxanthone
377.139381	H / N	C23H22O5 [M-H]-	HMDB40350	6,11-Dihydroxy-3-methyl-3-(4-methyl-3-pentenyl)-3H,7H-pyrano[2,3-c]xanthen-7-one
377.209925	H / N	C19H34O5 [M+Cl]-	HMDB40901	13-Hydroxy-9-methoxy-10-oxo-11-octadecenoic acid
377.209925	N	C18H35O6P [M-H]-	-	-
378.159170	N	C16H29NO7S [M-H]-	-	-
379.187460	N	C19H28N2O6 [M-H]-	-	-
379.189275	H / N	C18H32O6 [M+Cl]-	HMDB37146	5(6)-Pentyl-1,4-dioxan-2-one
379.189275	N	C17H33O7P [M-H]-	-	-
379.192560	N	C25H24N4 [M-H]-	-	-
380.234709	N	C23H31N3O2 [M-H]-	-	-
381.191842	H / N	C20H30O7 [M-H]-	HMDB12553	12-Oxo-20-trihydroxy-leukotriene B4
381.191842	H / N	C20H30O7 [M-H]-	HMDB35164	Cinncassiol A
381.191842	H / N	C20H30O7 [M-H]-	HMDB35396	T2 Triol
381.191842	H / N	C20H30O7 [M-H]-	HMDB36859	Cinncassiol C3
381.196333	N	C18H30N4O3S [M-H]-	-	-
381.203059	N	C19H30N2O6 [M-H]-	-	-
381.277596	N	C20H42O4 [M+Cl]-	-	-
381.277596	N	C22H34N6 [M-H]-	-	-
382.107694	N	C16H21N3O6S [M-H]-	-	-
383.142905	N	C13H28N4O5S2 [M-H]-	-	-
383.176163	N	C17H28N4O4S [M-H]-	-	-
383.220434	N	C18H36O6 [M+Cl]-	-	-
383.220434	N	C17H37O7P [M-H]-	-	-
385.134978	N	C14H26O12 [M-H]-	-	-
387.108521	H / N	C20H20O8 [M-H]-	HMDB29227	5-Hydroxy-3,3',4',7,8-pentamethoxyflavone
387.108521	H / N	C20H20O8 [M-H]-	HMDB29545	3'-Hydroxy-4',5,6,7,8-pentamethoxyflavone
387.108521	H / N	C20H20O8 [M-H]-	HMDB29547	4'-Hydroxy-3',5,6,7,8-pentamethoxyflavone
387.108521	H / N	C20H20O8 [M-H]-	HMDB29979	2'-Hydroxy-3,4',5',7,8-pentamethoxyflavone
387.108521	H / N	C20H20O8 [M-H]-	HMDB30095	Artemetin
387.108521	H / N	C20H20O8 [M-H]-	HMDB31955	Dimethyl (1R*,2S*,3S*)-2-carboxy-3-(3,4-dihydroxyphenyl)-2,3-dihydro-5,6-dihydroxy-1H-indene-1-acetate
387.108521	H / N	C20H20O8 [M-H]-	HMDB33275	5-Hydroxyauranetin
387.108521	H / N	C20H20O8 [M-H]-	HMDB36335	2,4,6-Phenanthrenetriol 2-O-b-D-glucoside
387.108521	H / N	C20H20O8 [M-H]-	HMDB37571	Demethylnobiletin
387.108521	H / N	C20H20O8 [M-H]-	HMDB40722	7-Hydroxy-3',4',5,6,8-pentamethoxyflavone
387.110990	N	C12H24N4O6S [M+Cl]-	-	-
387.110990	N	C11H25N4O7PS [M-H]-	-	-
387.192307	H / N	C21H28N2O5 [M-H]-	HMDB14800	Trimethobenzamide
387.192307	H / N	C21H28N2O5 [M-H]-	HMDB60579	Ramiprilat
387.230815	H / N	C21H36O4 [M+Cl]-	HMDB11539	MG(0:0/18:3(6Z,9Z,12Z)/0:0)
387.230815	H / N	C21H36O4 [M+Cl]-	HMDB11540	MG(0:0/18:3(9Z,12Z,15Z)/0:0)
387.230815	H / N	C21H36O4 [M+Cl]-	HMDB11569	MG(18:3(6Z,9Z,12Z)/0:0/0:0)
387.230815	H / N	C21H36O4 [M+Cl]-	HMDB11570	MG(18:3(9Z,12Z,15Z)/0:0/0:0)
387.230815	N	C20H37O5P [M-H]-	-	-
389.124192	H / N	C20H22O8 [M-H]-	HMDB30564	trans-Piceid
389.124192	H / N	C20H22O8 [M-H]-	HMDB30565	(Z)-Resveratrol 4'-glucoside
389.124192	H / N	C20H22O8 [M-H]-	HMDB31422	cis-Piceid
389.124192	H / N	C20H22O8 [M-H]-	HMDB36294	(E)-2-Glucosyl-3,4',5-trihydroxystilbene
390.195561	N	C18H33NO6S [M-H]-	-	-

391.225465	H / N	C20H36O5 [M+Cl]-	HMDB02685	Prostaglandin F1a
391.225465	H / N	C20H36O5 [M+Cl]-	HMDB02689	13,14-Dihydro PGE1
391.225465	H / N	C20H36O5 [M+Cl]-	HMDB04239	13,14-Dihydro PGF2a
391.225465	H / N	C19H37O6P [M-H]-	HMDB07003	CPA(16:0/0:0)
393.204929	N	C19H34O6 [M+Cl]-	-	-
393.204929	N	C18H35O7P [M-H]-	-	-
394.158875	N	C14H29N5O4S2 [M-H]-	-	-
394.208186	N	C17H33NO9 [M-H]-	-	-
395.044192	N	C17H16O9S [M-H]-	-	-
395.214212	N	C18H36N2O3S [M+Cl]-	-	-
395.214212	N	C17H37N2O4PS [M-H]-	-	-
396.223867	N	C17H35NO9 [M-H]-	-	-
396.265963	N	C24H35N3O2 [M-H]-	-	-
397.132300	N	C19H26O7S [M-H]-	-	-
397.183138	N	C15H30N2O10 [M-H]-	-	-
397.186782	H / N	C20H30O8 [M-H]-	HMDB34575	3'-Hydroxy-T2-triol
397.186782	H / N	C20H30O8 [M-H]-	HMDB36857	Cinncassiol E
397.198310	N	C19H30N2O7 [M-H]-	-	-
398.076271	N	C13H21NO11S [M-H]-	-	-
399.116760	N	C16H24N4O4S2 [M-H]-	-	-
399.169262	N	C19H28N2O5 [M+Cl]-	-	-
399.169262	N	C16H32O9S [M-H]-	-	-
401.129812	N	C14H26O13 [M-H]-	-	-
401.142111	N	C14H30N2O7S2 [M-H]-	-	-
401.184864	N	C19H30N2O5 [M+Cl]-	-	-
401.184864	N	C18H31N2O6P [M-H]-	-	-
401.306098	H / N	C26H42O3 [M-H]-	HMDB29458	Oryzarol
403.164135	N	C18H28N2O6 [M+Cl]-	-	-
403.164135	N	C17H29N2O7P [M-H]-	-	-
408.250356	N	C21H35N3O5 [M-H]-	-	-
411.187352	H / N	C17H32O11 [M-H]-	HMDB41512	Isopentyl gentiobioside
414.195654	N	C20H33NO6S [M-H]-	-	-
415.148190	N	C17H28N4O4S2 [M-H]-	-	-
415.148190	N	C17H20N8O5 [M-H]-	-	-
416.197757	N	C25H27N3O3 [M-H]-	-	-
418.213550	N	C25H29N3O3 [M-H]-	-	-
418.226937	N	C20H37NO6S [M-H]-	-	-
419.256897	N	C22H40O5 [M+Cl]-	-	-
419.256897	H / N	C21H41O6P [M-H]-	HMDB07004	CPA(18:0/0:0)
423.200356	N	C19H32N6OS2 [M-H]-	-	-
423.230964	H / N	C24H36O4 [M+Cl]-	HMDB30366	Cavipetin C
423.230964	N	C23H37O5P [M-H]-	-	-
423.293936	N	C25H44O3S [M-H]-	-	-
423.326831	H / N	C29H44O2 [M-H]-	HMDB06327	Alpha-Tocotrienol
423.326831	H / N	C29H44O2 [M-H]-	HMDB38656	(22E,24R)-Stigmasta-4,22-diene-3,6-dione
424.336391	N	C24H47N3OS [M-H]-	-	-
425.064376	N	C19H18O9 [M+Cl]-	-	-
425.064376	N	C18H19O10P [M-H]-	-	-
425.127623	N	C20H26O8S [M-H]-	-	-
425.263237	N	C26H38N2OS [M-H]-	-	-
425.342604	H / N	C29H46O2 [M-H]-	HMDB12167	4alpha-Formyl-4beta-methyl-5alpha-cholesta-8,24-dien-3beta-ol
425.342604	H / N	C29H46O2 [M-H]-	HMDB30015	7-Oxostigmasterol
425.342604	H / N	C29H46O2 [M-H]-	HMDB31080	Momordenol
425.342604	H / N	C29H46O2 [M-H]-	HMDB31931	Stigmast-22-ene-3,6-dione
425.342604	H / N	C29H46O2 [M-H]-	HMDB32084	29-Norcycloartane-3,24-dione
425.342604	H / N	C29H46O2 [M-H]-	HMDB37382	(3beta,23E)-3-Hydroxy-27-norcycloart-23-en-25-one
425.342604	H / N	C29H46O2 [M-H]-	HMDB38063	Stigmast-4-ene-3,6-dione
425.342604	H / N	C29H46O2 [M-H]-	HMDB39425	(6beta,22E)-6-Hydroxystigmasta-4,22-dien-3-one
427.079921	N	C18H21O10P [M-H]-	-	-
427.199280	N	C15H28N10O3S [M-H]-	-	-
427.262068	H / N	C24H40O4 [M+Cl]-	HMDB00348	3b,12a-Dihydroxy-5a-cholanoic acid
427.262068	H / N	C24H40O4 [M+Cl]-	HMDB00361	3b,7a-Dihydroxy-5b-cholanoic acid
427.262068	H / N	C24H40O4 [M+Cl]-	HMDB00384	3a,7a-Dihydroxycholanoic acid
427.262068	H / N	C24H40O4 [M+Cl]-	HMDB00411	3a,12b-Dihydroxy-5b-cholanoic acid
427.262068	H / N	C24H40O4 [M+Cl]-	HMDB00438	3b,12a-Dihydroxy-5b-cholanoic acid
427.262068	H / N	C24H40O4 [M+Cl]-	HMDB00478	Allodeoxycholic acid
427.262068	H / N	C24H40O4 [M+Cl]-	HMDB00514	Allochenodeoxycholic acid
427.262068	H / N	C24H40O4 [M+Cl]-	HMDB00518	Chenodeoxycholic acid
427.262068	H / N	C24H40O4 [M+Cl]-	HMDB00626	Deoxycholic acid
427.262068	H / N	C24H40O4 [M+Cl]-	HMDB00664	Isohyodeoxycholic acid
427.262068	H / N	C24H40O4 [M+Cl]-	HMDB00686	Isoursodeoxycholic acid
427.262068	H / N	C24H40O4 [M+Cl]-	HMDB00733	Hyodeoxycholic acid

427.262068	H / N	C24H40O4 [M+Cl]-	HMDB00811	Murocholic acid
427.262068	H / N	C24H40O4 [M+Cl]-	HMDB00946	Ursodeoxycholic acid
427.262068	H / N	C24H40O4 [M+Cl]-	HMDB02451	7b,12a-Dihydroxycholanoic acid
427.262068	H / N	C24H40O4 [M+Cl]-	HMDB02488	7a,12b-dihydroxy-5b-Cholan-24-oic acid
427.262068	H / N	C24H40O4 [M+Cl]-	HMDB02536	Isodeoxycholic acid
427.262068	H / N	C24H40O4 [M+Cl]-	HMDB02585	3b,12b-Dihydroxy-5b-cholanoic acid
427.262068	N	C23H41O5P [M-H]-	-	-
427.358200	H / N	C29H48O2 [M-H]-	HMDB03822	Cholesteryl acetate
427.358200	H / N	C29H48O2 [M-H]-	HMDB12168	4alpha-Formyl-4beta-methyl-5alpha-cholesta-8-en-3beta-ol
427.358200	H / N	C29H48O2 [M-H]-	HMDB12170	4alpha-Hydroxymethyl-4beta-methyl-5alpha-cholesta-8,24-dien-3beta-ol
427.358200	H / N	C29H48O2 [M-H]-	HMDB34422	3-Hydroxystigmast-5-en-7-one
427.358200	H / N	C29H48O2 [M-H]-	HMDB36018	Mangiferdesmethylursanone
427.358200	H / N	C29H48O2 [M-H]-	HMDB39498	(6beta,24R)-6-Hydroxystigmast-4-en-3-one
427.358200	H / N	C29H48O2 [M-H]-	HMDB39822	Stigmastane-3,6-dione
427.358200	H / N	C29H48O2 [M-H]-	HMDB41112	(3alpha,5alpha,7alpha)-14-Methylergosta-9(11),24(28)-dien-3,7-diol
427.358200	H / N	C29H48O2 [M-H]-	HMDB59643	3-beta-Hydroxy-4-beta-methyl-5-alpha-cholest-7-ene-4-alpha-carbaldehyde
428.149673	N	C18H27N3O7S [M-H]-	-	-
428.301763	H / N	C23H43NO6 [M-H]-	HMDB00712	Hexadecanedioic acid mono-L-carnitine ester
429.122563	N	C19H26O9S [M-H]-	-	-
429.176290	H / N	C20H30O10 [M-H]-	HMDB32622	Phenethyl rutinoside
429.222365	N	C17H34N8OS2 [M-H]-	-	-
431.124553	N	C16H24N4O8S [M-H]-	-	-
431.191174	N	C15H32N4O8 [M+Cl]-	-	-
431.191174	N	C14H33N4O9P [M-H]-	-	-
433.178142	N	C16H34N2O7S [M+Cl]-	-	-
433.178142	N	C26H22N6O [M-H]-	-	-
435.215798	N	C21H36O7 [M+Cl]-	-	-
435.215798	N	C20H37O8P [M-H]-	-	-
435.242356	N	C21H40O7S [M-H]-	-	-
437.342496	H / N	C30H46O2 [M-H]-	HMDB34726	Momordicinin
437.342496	H / N	C30H46O2 [M-H]-	HMDB35728	Ganoderol A
437.342496	H / N	C30H46O2 [M-H]-	HMDB36787	alpha,gamma-Onoceradienedione
437.342496	H / N	C30H46O2 [M-H]-	HMDB36840	Thujyl 19-trachylobanoate
438.125138	N	C16H25NO13 [M-H]-	-	-
438.170505	N	C20H29N3O6S [M-H]-	-	-
439.223720	N	C25H32N2O5 [M-H]-	-	-
440.218959	N	C24H31N3O5 [M-H]-	-	-
441.225303	N	C22H38N2O3S2 [M-H]-	-	-
441.228291	H / N	C26H34O6 [M-H]-	HMDB31958	3-O-Acetylepisamarcandin
441.228291	H / N	C26H34O6 [M-H]-	HMDB39064	Pectachol
441.272315	N	C21H38N4O6 [M-H]-	-	-
441.272315	N	C22H42N4OS2 [M-H]-	-	-
441.277950	H / N	C25H42O4 [M+Cl]-	HMDB11554	MG(0:0/22:4(7Z,10Z,13Z,16Z)/0:0)
441.277950	H / N	C25H42O4 [M+Cl]-	HMDB11584	MG(22:4(7Z,10Z,13Z,16Z)/0:0/0:0)
441.277950	N	C24H43O5P [M-H]-	-	-
442.190549	N	C21H33NO7S [M-H]-	-	-
443.254128	N	C20H36N6O3 [M+Cl]-	-	-
443.254128	N	C19H37N6O4P [M-H]-	-	-
443.292811	N	C19H40N8O2S [M-H]-	-	-
443.292811	N	C27H36N6 [M-H]-	-	-
443.353080	H / N	C29H48O3 [M-H]-	HMDB11662	3-beta-Hydroxy-4-beta-methyl-5-alpha-cholest-7-ene-4-alpha-carboxylate
443.353080	H / N	C29H48O3 [M-H]-	HMDB12165	4alpha-Carboxy-4beta-methyl-5alpha-cholesta-8-en-3beta-ol
443.353080	H / N	C29H48O3 [M-H]-	HMDB33633	(3beta,5alpha,6beta,22E,24R)-23-Methylergosta-7,22-diene-3,5,6-triol
443.353080	H / N	C29H48O3 [M-H]-	HMDB35804	Schleicherastatin 5
446.221840	N	C21H37NO7S [M-H]-	-	-
447.384407	H / N	C29H52O3 [M-H]-	HMDB30014	(3beta,5alpha,6beta,24R)-Stigmastane-3,5,6-triol
450.271139	N	C21H41NO9 [M-H]-	-	-
450.283790	N	C21H37N7O4 [M-H]-	-	-
451.198165	N	C16H32N6O7S [M-H]-	-	-
451.198165	N	C24H36O4S2 [M-H]-	-	-
453.086128	N	C20H22O10S [M-H]-	-	-
453.161160	N	C18H30O13 [M-H]-	-	-
453.193305	N	C27H26N4O3 [M-H]-	-	-
453.217594	N	C21H34N4O5S [M-H]-	-	-
453.219068	N	C22H30N8OS [M-H]-	-	-
453.337370	H / N	C30H46O3 [M-H]-	HMDB34963	beta-Elemonic acid
453.337370	H / N	C30H46O3 [M-H]-	HMDB35090	Ganoderic acid Y
453.337370	H / N	C30H46O3 [M-H]-	HMDB35247	Isomasticadienonic acid
453.337370	H / N	C30H46O3 [M-H]-	HMDB35251	9(11)-Dehydroglycyrrhetic acid
453.337370	H / N	C30H46O3 [M-H]-	HMDB35406	3beta-3-Hydroxy-11-oxolanosta-8,24-dien-26-al
453.337370	H / N	C30H46O3 [M-H]-	HMDB35594	Bryononic acid
453.337370	H / N	C30H46O3 [M-H]-	HMDB35615	Mangiferonic acid

453.337370	H / N	C30H46O3 [M-H]-	HMDB35791	Desoxoglabrolide
453.337370	H / N	C30H46O3 [M-H]-	HMDB35808	Tomentosolic acid
453.337370	H / N	C30H46O3 [M-H]-	HMDB36000	Epoxyganoderiol B
453.337370	H / N	C30H46O3 [M-H]-	HMDB36002	Ganoderal B
453.337370	H / N	C30H46O3 [M-H]-	HMDB36007	Ursonic acid
453.337370	H / N	C30H46O3 [M-H]-	HMDB36653	Micromeric acid
453.337370	H / N	C30H46O3 [M-H]-	HMDB37054	Katononic acid
453.337370	H / N	C30H46O3 [M-H]-	HMDB38707	Ganoderiol F
453.337370	H / N	C30H46O3 [M-H]-	HMDB38758	Glypallidifloric acid
453.337370	H / N	C30H46O3 [M-H]-	HMDB40454	Lucidal
453.337370	H / N	C30H46O3 [M-H]-	HMDB40508	Masticadienonic acid
453.386912	N	C29H54O [M+Cl]-	-	-
454.159220	N	C19H21N9O5 [M-H]-	-	-
454.159220	N	C27H25N3O2S [M-H]-	-	-
454.159220	N	C16H30N3O10P [M-H]-	-	-
454.227005	H / N	C23H37NO6S [M-H]-	HMDB12639	20-Hydroxy-leukotriene E4
454.244646	N	C23H37NO8 [M-H]-	-	-
454.246053	N	C24H33N5O4 [M-H]-	-	-
454.338740	N	C18H45N9O2 [M+Cl]-	-	-
455.268148	N	C24H40N2O4 [M+Cl]-	-	-
455.268148	N	C23H41N2O5P [M-H]-	-	-
455.269478	N	C22H40N4O4S [M-H]-	-	-
455.329638	H / N	C27H48O3 [M+Cl]-	HMDB01457	5-b-Cholestane-3a ,7a ,12a-triol
455.329638	H / N	C27H48O3 [M+Cl]-	HMDB03990	3b,5a,6b-Cholestanetriol
455.329638	H / N	C27H48O3 [M+Cl]-	HMDB12455	3 alpha,7 alpha,26-Trihydroxy-5beta-cholestane
455.329638	H / N	C27H48O3 [M+Cl]-	HMDB39463	(3alpha,5alpha,22R,23R)-Cholestane-3,22,23-triol
455.329638	H / N	C27H48O3 [M+Cl]-	HMDB60138	5beta-Cholestane-3alpha,7alpha,27-triol
455.329638	N	C26H49O4P [M-H]-	-	-
457.247605	N	C23H38N2O5 [M+Cl]-	-	-
457.247605	N	C22H39N2O6P [M-H]-	-	-
457.259310	H / N	C27H38O6 [M-H]-	HMDB37611	Lucidenic acid A
457.308761	N	C25H47O5P [M-H]-	-	-
459.093292	H / N	C22H20O11 [M-H]-	HMDB33818	Irilone 4'-glucoside
459.093292	H / N	C22H20O11 [M-H]-	HMDB41740	Glycitein 4'-O-glucuronide
459.093292	H / N	C22H20O11 [M-H]-	HMDB41741	Glycitein 7-O-glucuronide
459.173458	N	C18H28N4O10 [M-H]-	-	-
459.210716	N	C20H36N4O4S2 [M-H]-	-	-
459.347995	H / N	C29H48O4 [M-H]-	HMDB12555	13'-Carboxy-alpha-tocopherol
459.347995	H / N	C29H48O4 [M-H]-	HMDB33634	(3beta,5alpha,6beta,9alpha,22E,24R)-23-Methylergosta-7,22-diene-3,5,6,9-tetrol
459.420752	H / N	C31H56O2 [M-H]-	HMDB38485	5-Pentacosyl-1,3-benzenediol
460.214266	N	C19H39NO7S [M+Cl]-	-	-
460.214266	N	C29H27N5O [M-H]-	-	-
462.154575	N	C13H29N7O7S [M+Cl]-	-	-
462.154575	N	C21H33NO4S2 [M+Cl]-	-	-
463.208435	H / N	C23H32N2O8 [M-H]-	HMDB39501	Na-Hexanoyl-Nb-inosityltryptophan
463.224880	N	C18H40N2O7S [M+Cl]-	-	-
463.254573	N	C22H40O10 [M-H]-	-	-
463.280999	N	C25H40N2O6 [M-H]-	-	-
464.323490	N	C19H43N9O2 [M+Cl]-	-	-
464.323490	N	C24H51NO3S2 [M-H]-	-	-
465.353036	N	C35H46 [M-H]-	-	-
465.353036	N	C20H50N8S2 [M-H]-	-	-
465.353036	N	C20H42N12O [M-H]-	-	-
466.274254	N	C24H41N3O4S [M-H]-	-	-
467.237452	N	C27H36N2O3S [M-H]-	-	-
467.241827	N	C22H40O8 [M+Cl]-	-	-
467.241827	N	C21H41O9P [M-H]-	-	-
467.250567	N	C22H44O6S2 [M-H]-	-	-
467.256977	H / N	C26H40O5 [M+Cl]-	HMDB14792	Latanoprost
467.256977	N	C25H41O6P [M-H]-	-	-
469.332380	H / N	C30H46O4 [M-H]-	HMDB11628	Glycyrrhetinic acid
469.332380	H / N	C30H46O4 [M-H]-	HMDB29345	Murrayenol
469.332380	H / N	C30H46O4 [M-H]-	HMDB33213	(3alpha,20R,24Z)-3-Hydroxy-21-oxoeupha-8,24-dien-26-oic acid
469.332380	H / N	C30H46O4 [M-H]-	HMDB34508	6beta-Hydroxy-3-oxo-12-oleanen-28-oic acid
469.332380	H / N	C30H46O4 [M-H]-	HMDB34517	beta-Glycyrrhetinic acid
469.332380	H / N	C30H46O4 [M-H]-	HMDB34568	23-Hydroxy-3-oxocycloart-24-en-26-oic acid
469.332380	H / N	C30H46O4 [M-H]-	HMDB35252	3beta-3,24-Dihydroxy-9(11),12-oleanadien-30-oic acid
469.332380	H / N	C30H46O4 [M-H]-	HMDB35327	Ganoderiol B
469.332380	H / N	C30H46O4 [M-H]-	HMDB35334	Ganodermic acid Jb
469.332380	H / N	C30H46O4 [M-H]-	HMDB35788	Liquiritic acid
469.332380	H / N	C30H46O4 [M-H]-	HMDB35912	Pomonic acid
469.332380	H / N	C30H46O4 [M-H]-	HMDB36655	Rubinic acid

469.332380	H / N	C30H46O4 [M-H]-	HMDB36671	11-Keto-beta-boswellic acid
469.332380	H / N	C30H46O4 [M-H]-	HMDB36786	Lansic acid
469.332380	H / N	C30H46O4 [M-H]-	HMDB36847	Colubrinic acid
469.332380	H / N	C30H46O4 [M-H]-	HMDB38653	Koetjapic acid
469.332380	H / N	C30H46O4 [M-H]-	HMDB40415	28-Hydroxymangiferonic acid
469.332380	H / N	C30H46O4 [M-H]-	HMDB40494	2-Hydroxy-3-oxo-12-oleanen-28-oic acid
469.332380	H / N	C30H46O4 [M-H]-	HMDB40618	16-Hydroxy-3-oxo-12-oleanen-28-oic acid
469.332380	H / N	C30H46O4 [M-H]-	HMDB40995	Secoisobryononic acid
469.332380	H / N	C30H46O4 [M-H]-	HMDB40996	Secobryononic acid
471.155523	N	C19H28N4O8S [M-H]-	-	-
471.171789	H / N	C18H32O14 [M-H]-	HMDB39741	alpha-L-Rhamnopyranosyl-(1->3)-alpha-D-galactopyranosyl-(1->3)-L-fucose
471.173240	N	C19H28N4O10 [M-H]-	-	-
471.185208	N	C19H32N6O4S2 [M-H]-	-	-
471.347978	H / N	C30H48O4 [M-H]-	HMDB02392	Maslinic acid
471.347978	H / N	C30H48O4 [M-H]-	HMDB33233	Lucidumol A
471.347978	H / N	C30H48O4 [M-H]-	HMDB34523	Queretaroic acid
471.347978	H / N	C30H48O4 [M-H]-	HMDB34530	Priverogenin A
471.347978	H / N	C30H48O4 [M-H]-	HMDB34567	(3beta,23xi)-3,23-Dihydroxycycloart-24-en-26-oic acid
471.347978	H / N	C30H48O4 [M-H]-	HMDB35106	Pomolic acid
471.347978	H / N	C30H48O4 [M-H]-	HMDB35107	20beta-Hydroxyursolic acid
471.347978	H / N	C30H48O4 [M-H]-	HMDB35258	Azukisapogenol
471.347978	H / N	C30H48O4 [M-H]-	HMDB35260	delta-Maslinic acid
471.347978	H / N	C30H48O4 [M-H]-	HMDB35748	Sebiferenic acid
471.347978	H / N	C30H48O4 [M-H]-	HMDB35758	Momordicin I
471.347978	H / N	C30H48O4 [M-H]-	HMDB35962	Ganoderic acid U
471.347978	H / N	C30H48O4 [M-H]-	HMDB35977	Ganodermanontriol
471.347978	H / N	C30H48O4 [M-H]-	HMDB36001	Epoxyganoderiol A
471.347978	H / N	C30H48O4 [M-H]-	HMDB36063	(3b,22S,24E)-3,22-Dihydroxycycloart-24-en-26-oic acid
471.347978	H / N	C30H48O4 [M-H]-	HMDB36064	27-Hydroxyisomangiferolic acid
471.347978	H / N	C30H48O4 [M-H]-	HMDB36638	Albigenic acid
471.347978	H / N	C30H48O4 [M-H]-	HMDB36654	Rubitic acid
471.347978	H / N	C30H48O4 [M-H]-	HMDB37779	Ganoderiol E
471.347978	H / N	C30H48O4 [M-H]-	HMDB41043	3alpha-Corosolic acid
473.206960	N	C15H34N8O5S [M+Cl]-	-	-
473.206960	N	C23H38N2O2S2 [M+Cl]-	-	-
473.206960	N	C20H34N4O7S [M-H]-	-	-
473.363628	H / N	C30H50O4 [M-H]-	HMDB34505	Soyasapogenol A
473.363628	H / N	C30H50O4 [M-H]-	HMDB34528	Camelliagenin A
473.363628	H / N	C30H50O4 [M-H]-	HMDB34644	Priverogenin B
473.363628	H / N	C30H50O4 [M-H]-	HMDB34683	(3alphaOH,20S,24S)-3,19:20,24-Diepoxydammarane-3,25-diol
473.363628	H / N	C30H50O4 [M-H]-	HMDB35326	Ganoderiol A
473.363628	H / N	C30H50O4 [M-H]-	HMDB39692	20,24-Epoxy-25,26-dihydroxydammaran-3-one
474.224857	N	C24H33N3O7 [M-H]-	-	-
474.246655	N	C22H41N3O4S2 [M-H]-	-	-
474.289144	N	C24H45NO6S [M-H]-	-	-
475.218558	N	C22H36O11 [M-H]-	-	-
475.226458	N	C20H36N6O3S [M+Cl]-	-	-
475.226458	N	C17H40N4O7S2 [M-H]-	-	-
476.250022	N	C22H39NO10 [M-H]-	-	-
477.271375	N	C27H42N2OS [M+Cl]-	-	-
477.271375	N	C24H46O5S2 [M-H]-	-	-
479.098530	H / N	C25H20O10 [M-H]-	HMDB40513	2,3-Dehydrosilybin
479.098530	H / N	C25H20O10 [M-H]-	HMDB40514	2,3-Dehydrosilychristin
479.314825	N	C25H48O6 [M+Cl]-	-	-
479.314825	N	C24H49O7P [M-H]-	-	-
479.374193	N	C29H52O5 [M-H]-	-	-
479.446936	H / N	C31H60O3 [M-H]-	HMDB31056	8-Hydroxy-14,16-hentriacontanedione
479.446936	H / N	C31H60O3 [M-H]-	HMDB32087	5-Hydroxy-14,16-hentriacontanedione
479.446936	H / N	C31H60O3 [M-H]-	HMDB32125	(S)-25-Hydroxy-14,16-hentriacontanedione
480.450379	N	C25H55N9 [M-H]-	-	-
481.253623	N	C21H38N8OS2 [M-H]-	-	-
483.211133	N	C22H28N8O5 [M-H]-	-	-
483.232058	N	C27H36N2O4S [M-H]-	-	-
483.234955	N	C23H36N2O9 [M-H]-	-	-
484.237155	N	C24H39NO7S [M-H]-	-	-
485.267556	N	C26H42O6 [M+Cl]-	-	-
485.267556	H / N	C25H43O7P [M-H]-	HMDB11156	PA(20:4(5Z,8Z,11Z,14Z)e/2:0)
485.323574	N	C25H46N2O7 [M-H]-	-	-
485.375961	N	C23H50N8OS [M-H]-	-	-
486.272346	N	C25H37N5O5 [M-H]-	-	-
487.276280	N	C17H40N8O6 [M+Cl]-	-	-
487.276280	N	C24H45N2O4PS [M-H]-	-	-

487.452025	N	C33H60O2 [M-H]-	-	-
488.171740	N	C28H27NO7 [M-H]-	-	-
488.268460	N	C24H43NO7S [M-H]-	-	-
489.182495	N	C18H34O15 [M-H]-	-	-
490.338719	N	C25H49NO8 [M-H]-	-	-
493.214740	N	C22H38N2O6S [M+Cl]-	-	-
493.214740	N	C19H34N4O11 [M-H]-	-	-
493.220550	N	C25H30N6O5 [M-H]-	-	-
493.258062	N	C17H42N6O6S [M+Cl]-	-	-
493.258062	N	C25H46O3S2 [M+Cl]-	-	-
493.258062	N	C27H30N10 [M-H]-	-	-
495.172708	N	C21H36O9S2 [M-H]-	-	-
495.220649	N	C21H32N6O8 [M-H]-	-	-
495.369118	N	C29H52O6 [M-H]-	-	-
496.147737	N	C16H31N7O5S3 [M-H]-	-	-
496.270755	N	C29H39NO6 [M-H]-	-	-
496.309770	N	C27H47NO5S [M-H]-	-	-
497.200655	N	C18H38O13 [M+Cl]-	-	-
497.200655	N	C21H34N6O4S2 [M-H]-	-	-
497.340054	H / N	C29H50O4 [M+Cl]-	HMDB34430	6-Deoxohomodolichosterone
497.340054	H / N	C29H50O4 [M+Cl]-	HMDB39713	(3beta,22R,23R,24S)-3,22,23-Trihydroxystigmastan-6-one
497.340054	N	C28H51O5P [M-H]-	-	-
497.363493	H / N	C32H50O4 [M-H]-	HMDB32022	Tsugaric acid A
497.363493	H / N	C32H50O4 [M-H]-	HMDB35160	beta-Boswellic acid acetate
497.363493	H / N	C32H50O4 [M-H]-	HMDB36008	Acetylursolic acid
497.363493	H / N	C32H50O4 [M-H]-	HMDB36674	Ursololactone
499.355451	N	C23H48N8O2S [M-H]-	-	-
499.355451	N	C31H44N6 [M-H]-	-	-
500.231553	N	C19H39N5O6S [M+Cl]-	-	-
500.231553	N	C18H40N5O7PS [M-H]-	-	-
501.202748	N	C21H34N4O8S [M-H]-	-	-
502.198112	N	C20H33N5O8S [M-H]-	-	-
502.198112	N	C28H29N3O6 [M-H]-	-	-
502.219533	N	C25H33N3O8 [M-H]-	-	-
502.255819	N	C26H37N3O7 [M-H]-	-	-
504.213685	N	C20H35N5O8S [M-H]-	-	-
504.213685	N	C28H31N3O6 [M-H]-	-	-
504.263439	N	C24H43NO8S [M-H]-	-	-
504.369392	N	C30H51NO5 [M-H]-	-	-
505.211278	N	C23H38O10S [M-H]-	-	-
505.253628	N	C23H38N8OS2 [M-H]-	-	-
506.385105	N	C30H53NO5 [M-H]-	-	-
507.292474	N	C23H44N2O10 [M-H]-	-	-
507.387968	N	C31H56O3S [M-H]-	-	-
508.203657	N	C21H35NO13 [M-H]-	-	-
509.327330	H / N	C32H46O5 [M-H]-	HMDB37893	Ganodermic acid TQ
509.367198	N	C30H54O4S [M-H]-	-	-
510.289213	N	C27H45NO6S [M-H]-	-	-
510.489124	H / N	C32H65NO3 [M-H]-	HMDB11759	Cer(d18:0/14:0)
511.167054	N	C20H32O15 [M-H]-	-	-
511.415664	N	C34H56O3 [M-H]-	-	-
514.255883	N	C27H37N3O7 [M-H]-	-	-
515.205682	H / N	C25H36O9 [M+Cl]-	HMDB10338	11-Oxo-androsterone glucuronide
515.205682	H / N	C25H36O9 [M+Cl]-	HMDB33654	11-Deacetylvaltrate 11-(3-hydroxy-3-methylbutanoate)
515.205682	H / N	C25H36O9 [M+Cl]-	HMDB36161	4-Propanoyl-HT2 toxin
515.205682	H / N	C25H36O9 [M+Cl]-	HMDB38559	8-Hexanoylneosolaniol
515.205682	N	C24H37O10P [M-H]-	-	-
515.258418	N	C28H40N2O5S [M-H]-	-	-
516.335665	N	C22H51N5O4S [M+Cl]-	-	-
516.341272	N	C25H51N5O2S2 [M-H]-	-	-
517.274778	N	C21H42N8O3S2 [M-H]-	-	-
520.310050	N	C29H47NO5S [M-H]-	-	-
521.290158	N	C24H46N2O8S [M-H]-	-	-
521.324373	N	C29H42N6O3 [M-H]-	-	-
522.325863	N	C29H49NO5S [M-H]-	-	-
523.336632	N	C32H48N2O2S [M-H]-	-	-
523.339252	N	C28H48N2O7 [M-H]-	-	-
524.268678	N	C27H43NO7S [M-H]-	-	-
525.182600	H / N	C21H34O15 [M-H]-	HMDB39092	Stachyoside A
526.284438	N	C27H45NO7S [M-H]-	-	-
527.287444	N	C28H40N4O6 [M-H]-	-	-
529.389873	H / N	C33H54O5 [M-H]-	HMDB33685	alpha-Tocopherol succinate

531.063814	N	C21H24O12S2 [M-H]-	-	-
531.303801	N	C24H44N4O9 [M-H]-	-	-
532.307114	N	C33H43NO5 [M-H]-	-	-
533.457911	N	C34H62O4 [M-H]-	-	-
533.461823	N	C32H62N4S [M-H]-	-	-
535.216395	N	C21H40O13 [M+Cl]-	-	-
535.216395	N	C24H36N6O4S2 [M-H]-	-	-
535.466407	N	C33H64N2OS [M-H]-	-	-
535.473173	N	C34H64O4 [M-H]-	-	-
536.323048	N	C29H47NO8 [M-H]-	-	-
537.261785	N	C31H34N6O3 [M-H]-	-	-
539.243096	N	C26H40N2O8S [M-H]-	-	-
542.315980	N	C28H49NO7S [M-H]-	-	-
543.499466	N	C33H68O5 [M-H]-	-	-
544.261160	N	C22H43NO14 [M-H]-	-	-
544.328421	N	C24H47N7O5S [M-H]-	-	-
544.445346	N	C29H63N5S2 [M-H]-	-	-
544.445346	N	C29H55N9O [M-H]-	-	-
545.229273	N	C31H34N2O7 [M-H]-	-	-
545.271787	N	C25H42N2O11 [M-H]-	-	-
545.331900	N	C25H42N10O4 [M-H]-	-	-
545.338633	N	C34H46N2O4 [M-H]-	-	-
546.170154	N	C29H29N3O6S [M-H]-	-	-
546.329055	N	C23H45N9O4 [M+Cl]-	-	-
546.329055	N	C22H46N9O5P [M-H]-	-	-
547.328625	N	C24H48N6O6S [M-H]-	-	-
553.342950	N	C28H50N4O5S [M-H]-	-	-
554.328555	N	C26H54NO7PS [M-H]-	-	-
559.297370	N	C20H44N8O8 [M+Cl]-	-	-
559.297370	N	C27H49N2O6PS [M-H]-	-	-
559.340891	N	C30H52O7 [M+Cl]-	-	-
559.340891	N	C29H53O8P [M-H]-	-	-
559.413479	H / N	C32H60O5 [M+Cl]-	HMDB07039	DG(14:1(9Z)/15:0/0:0)
559.413479	H / N	C32H60O5 [M+Cl]-	HMDB07067	DG(15:0/14:1(9Z)/0:0)
559.413479	H / N	C32H60O5 [M+Cl]-	HMDB55987	DG(15:0/0:0/14:1n5)
559.413479	N	C31H61O6P [M-H]-	-	-
562.171508	N	C22H33N3O12S [M-H]-	-	-
562.171508	N	C30H29NO10 [M-H]-	-	-
563.155992	N	C30H28O11 [M-H]-	-	-
563.307570	N	C27H48O12 [M-H]-	-	-
564.159483	N	C24H31N5O7S2 [M-H]-	-	-
564.390524	N	C32H55NO7 [M-H]-	-	-
566.515341	N	C35H69NO4 [M-H]-	-	-
572.347410	N	C29H51N3O6 [M+Cl]-	-	-
572.361590	N	C27H47N11OS [M-H]-	-	-
573.356031	N	C33H46N6O3 [M-H]-	-	-
573.429184	H / N	C33H62O5 [M+Cl]-	HMDB07012	DG(14:0/16:1(9Z)/0:0)
573.429184	H / N	C33H62O5 [M+Cl]-	HMDB07040	DG(14:1(9Z)/16:0/0:0)
573.429184	H / N	C33H62O5 [M+Cl]-	HMDB07096	DG(16:0/14:1(9Z)/0:0)
573.429184	H / N	C33H62O5 [M+Cl]-	HMDB07124	DG(16:1(9Z)/14:0/0:0)
573.429184	H / N	C33H62O5 [M+Cl]-	HMDB55960	DG(14:0/0:0/16:1n7)
573.429184	H / N	C33H62O5 [M+Cl]-	HMDB56014	DG(16:0/0:0/14:1n5)
573.429184	N	C32H63O6P [M-H]-	-	-
575.329319	N	C29H52N2O5S [M+Cl]-	-	-
575.329319	N	C26H48N4O10 [M-H]-	-	-
575.410754	H / N	C38H56O4 [M-H]-	HMDB00977	3-Hexaprenyl-4-hydroxy-5-methoxybenzoic acid
575.410754	H / N	C38H56O4 [M-H]-	HMDB06820	2-Hexaprenyl-3-methyl-5-hydroxy-6-methoxy-1,4-benzoquinone
575.410754	H / N	C38H56O4 [M-H]-	HMDB36285	Campesteryl ferulate
575.457707	N	C30H64N4O4S [M-H]-	-	-
577.339142	N	C25H50N6O7S [M-H]-	-	-
577.339142	N	C33H46N4O5 [M-H]-	-	-
577.361085	N	C30H50N4O7 [M-H]-	-	-
579.150890	H / N	C30H28O12 [M-H]-	HMDB37583	6''-p-Coumaroylprunin
579.150890	H / N	C30H28O12 [M-H]-	HMDB38357	Gambiriin A1
580.357404	N	C26H55N5O5S2 [M-H]-	-	-
580.385540	N	C32H55NO8 [M-H]-	-	-
581.166438	N	C30H30O12 [M-H]-	-	-
581.294197	N	C26H42N6O9 [M-H]-	-	-
581.515105	H / N	C36H70O5 [M-H]-	HMDB07071	DG(15:0/18:0/0:0)
581.515105	H / N	C36H70O5 [M-H]-	HMDB07155	DG(18:0/15:0/0:0)
581.515105	H / N	C36H70O5 [M-H]-	HMDB55983	DG(15:0/0:0/18:0)
583.182266	N	C30H32O12 [M-H]-	-	-

583.458074	N	C34H64O7 [M-H]-	-	-
583.470516	N	C34H68N2OS2 [M-H]-	-	-
583.470516	N	C34H60N6O2 [M-H]-	-	-
585.379832	H / N	C35H54O7 [M-H]-	HMDB32832	(3b,16a,21b,22a)-12-Oleanene-3,16,21,23,28-pentol-22-angeloyloxy-23-al
585.379832	H / N	C35H54O7 [M-H]-	HMDB35331	Ganoderic acid Md
585.379832	H / N	C35H54O7 [M-H]-	HMDB37908	18-Dehydroursolic acid 3-arabinoside
587.203566	N	C32H32N2O9 [M-H]-	-	-
589.359770	N	C30H54O11 [M-H]-	-	-
593.419168	N	C32H62O7 [M+Cl]-	-	-
593.419168	N	C31H63O8P [M-H]-	-	-
593.425018	N	C35H62O5S [M-H]-	-	-
593.425018	N	C28H62N6O3S2 [M-H]-	-	-
596.336666	N	C25H51N7O5S [M+Cl]-	-	-
597.429013	H / N	C35H62O5 [M+Cl]-	HMDB07017	DG(14:0/18:3(6Z,9Z,12Z)/0:0)
597.429013	H / N	C35H62O5 [M+Cl]-	HMDB07018	DG(14:0/18:3(9Z,12Z,15Z)/0:0)
597.429013	H / N	C35H62O5 [M+Cl]-	HMDB07045	DG(14:1(9Z)/18:2(9Z,12Z)/0:0)
597.429013	H / N	C35H62O5 [M+Cl]-	HMDB07241	DG(18:2(9Z,12Z)/14:1(9Z)/0:0)
597.429013	H / N	C35H62O5 [M+Cl]-	HMDB07269	DG(18:3(6Z,9Z,12Z)/14:0/0:0)
597.429013	H / N	C35H62O5 [M+Cl]-	HMDB07298	DG(18:3(9Z,12Z,15Z)/14:0/0:0)
597.429013	H / N	C35H62O5 [M+Cl]-	HMDB35898	Robustocin
597.429013	H / N	C35H62O5 [M+Cl]-	HMDB55968	DG(14:0/0:0/18:3n6)
597.429013	H / N	C35H62O5 [M+Cl]-	HMDB55975	DG(14:0/0:0/18:3n3)
597.429013	N	C34H63O6P [M-H]-	-	-
597.437351	N	C34H62O8 [M-H]-	-	-
598.432529	N	C33H61NO8 [M-H]-	-	-
599.444788	H / N	C35H64O5 [M+Cl]-	HMDB07016	DG(14:0/18:2(9Z,12Z)/0:0)
599.444788	H / N	C35H64O5 [M+Cl]-	HMDB07043	DG(14:1(9Z)/18:1(11Z)/0:0)
599.444788	H / N	C35H64O5 [M+Cl]-	HMDB07044	DG(14:1(9Z)/18:1(9Z)/0:0)
599.444788	H / N	C35H64O5 [M+Cl]-	HMDB07128	DG(16:1(9Z)/16:1(9Z)/0:0)
599.444788	H / N	C35H64O5 [M+Cl]-	HMDB07183	DG(18:1(11Z)/14:1(9Z)/0:0)
599.444788	H / N	C35H64O5 [M+Cl]-	HMDB07212	DG(18:1(9Z)/14:1(9Z)/0:0)
599.444788	H / N	C35H64O5 [M+Cl]-	HMDB07240	DG(18:2(9Z,12Z)/14:0/0:0)
599.444788	H / N	C35H64O5 [M+Cl]-	HMDB31390	Annotemoyin 1
599.444788	H / N	C35H64O5 [M+Cl]-	HMDB32094	Panatellin
599.444788	H / N	C35H64O5 [M+Cl]-	HMDB32732	cis-Solamin
599.444788	H / N	C35H64O5 [M+Cl]-	HMDB56136	DG(14:1n5/0:0/18:1n7)
599.444788	H / N	C35H64O5 [M+Cl]-	HMDB56137	DG(14:1n5/0:0/18:1n9)
599.444788	H / N	C35H64O5 [M+Cl]-	HMDB56156	DG(16:1n7/0:0/16:1n7)
599.444788	N	C34H65O6P [M-H]-	-	-
601.374676	H / N	C35H54O8 [M-H]-	HMDB35999	Ganoderic acid Mg
601.444694	N	C33H58N6O4 [M-H]-	-	-
601.460420	H / N	C35H66O5 [M+Cl]-	HMDB07014	DG(14:0/18:1(11Z)/0:0)
601.460420	H / N	C35H66O5 [M+Cl]-	HMDB07015	DG(14:0/18:1(9Z)/0:0)
601.460420	H / N	C35H66O5 [M+Cl]-	HMDB07042	DG(14:1(9Z)/18:0/0:0)
601.460420	H / N	C35H66O5 [M+Cl]-	HMDB07099	DG(16:0/16:1(9Z)/0:0)
601.460420	H / N	C35H66O5 [M+Cl]-	HMDB07127	DG(16:1(9Z)/16:0/0:0)
601.460420	H / N	C35H66O5 [M+Cl]-	HMDB07154	DG(18:0/14:1(9Z)/0:0)
601.460420	H / N	C35H66O5 [M+Cl]-	HMDB07182	DG(18:1(11Z)/14:0/0:0)
601.460420	H / N	C35H66O5 [M+Cl]-	HMDB07211	DG(18:1(9Z)/14:0/0:0)
601.460420	H / N	C35H66O5 [M+Cl]-	HMDB55961	DG(14:0/0:0/18:1n7)
601.460420	H / N	C35H66O5 [M+Cl]-	HMDB55962	DG(14:0/0:0/18:1n9)
601.460420	H / N	C35H66O5 [M+Cl]-	HMDB56015	DG(16:0/0:0/16:1n7)
601.460420	H / N	C35H66O5 [M+Cl]-	HMDB56040	DG(18:0/0:0/14:1n5)
601.460420	N	C34H67O6P [M-H]-	-	-
603.499996	H / N	C38H68O5 [M-H]-	HMDB07081	DG(15:0/20:3(5Z,8Z,11Z)/0:0)
603.499996	H / N	C38H68O5 [M-H]-	HMDB07082	DG(15:0/20:3(8Z,11Z,14Z)/0:0)
603.499996	H / N	C38H68O5 [M-H]-	HMDB07445	DG(20:3(5Z,8Z,11Z)/15:0/0:0)
603.499996	H / N	C38H68O5 [M-H]-	HMDB07474	DG(20:3(8Z,11Z,14Z)/15:0/0:0)
603.499996	H / N	C38H68O5 [M-H]-	HMDB55992	DG(15:0/0:0/20:3n9)
603.499996	H / N	C38H68O5 [M-H]-	HMDB55998	DG(15:0/0:0/20:3n6)
603.499996	H / N	C38H68O5 [M-H]-	HMDB56163	DG(16:1n7/0:0/18:2n6)
603.499996	H / N	C38H68O5 [M-H]-	HMDB56165	DG(16:1n7/0:0/20:2n6)
604.479475	N	C33H67NO8 [M-H]-	-	-
605.510629	N	C33H70N2O7 [M-H]-	-	-
607.308180	N	C27H48N2O13 [M-H]-	-	-
607.313810	N	C33H44N4O7 [M-H]-	-	-
607.530739	H / N	C38H72O5 [M-H]-	HMDB07079	DG(15:0/20:1(11Z)/0:0)
607.530739	H / N	C38H72O5 [M-H]-	HMDB07387	DG(20:1(11Z)/15:0/0:0)
607.530739	H / N	C38H72O5 [M-H]-	HMDB55991	DG(15:0/0:0/20:1n9)
609.329578	N	C33H46N4O7 [M-H]-	-	-
609.364957	N	C33H54O10 [M-H]-	-	-
610.332770	N	C27H49N9O3S2 [M-H]-	-	-

612.375576	N	C32H55NO10 [M-H]-	-	-
613.483944	H / N	C39H66O5 [M-H]-	HMDB07032	DG(14:0/22:5(4Z,7Z,10Z,13Z,16Z)/0:0)
613.483944	H / N	C39H66O5 [M-H]-	HMDB07033	DG(14:0/22:5(7Z,10Z,13Z,16Z,19Z)/0:0)
613.483944	H / N	C39H66O5 [M-H]-	HMDB07060	DG(14:1(9Z)/22:4(7Z,10Z,13Z,16Z)/0:0)
613.483944	H / N	C39H66O5 [M-H]-	HMDB07114	DG(16:0/20:5(5Z,8Z,11Z,14Z,17Z)/0:0)
613.483944	H / N	C39H66O5 [M-H]-	HMDB07141	DG(16:1(9Z)/20:4(5Z,8Z,11Z,14Z)/0:0)
613.483944	H / N	C39H66O5 [M-H]-	HMDB07142	DG(16:1(9Z)/20:4(8Z,11Z,14Z,17Z)/0:0)
613.483944	H / N	C39H66O5 [M-H]-	HMDB07193	DG(18:1(11Z)/18:4(6Z,9Z,12Z,15Z)/0:0)
613.483944	H / N	C39H66O5 [M-H]-	HMDB07222	DG(18:1(9Z)/18:4(6Z,9Z,12Z,15Z)/0:0)
613.483944	H / N	C39H66O5 [M-H]-	HMDB07249	DG(18:2(9Z,12Z)/18:3(6Z,9Z,12Z)/0:0)
613.483944	H / N	C39H66O5 [M-H]-	HMDB07250	DG(18:2(9Z,12Z)/18:3(9Z,12Z,15Z)/0:0)
613.483944	H / N	C39H66O5 [M-H]-	HMDB07277	DG(18:3(6Z,9Z,12Z)/18:2(9Z,12Z)/0:0)
613.483944	H / N	C39H66O5 [M-H]-	HMDB07306	DG(18:3(9Z,12Z,15Z)/18:2(9Z,12Z)/0:0)
613.483944	H / N	C39H66O5 [M-H]-	HMDB07333	DG(18:4(6Z,9Z,12Z,15Z)/18:1(11Z)/0:0)
613.483944	H / N	C39H66O5 [M-H]-	HMDB07334	DG(18:4(6Z,9Z,12Z,15Z)/18:1(9Z)/0:0)
613.483944	H / N	C39H66O5 [M-H]-	HMDB07505	DG(20:4(5Z,8Z,11Z,14Z)/16:1(9Z)/0:0)
613.483944	H / N	C39H66O5 [M-H]-	HMDB07534	DG(20:4(8Z,11Z,14Z,17Z)/16:1(9Z)/0:0)
613.483944	H / N	C39H66O5 [M-H]-	HMDB07562	DG(20:5(5Z,8Z,11Z,14Z,17Z)/16:0/0:0)
613.483944	H / N	C39H66O5 [M-H]-	HMDB07676	DG(22:4(7Z,10Z,13Z,16Z)/14:1(9Z)/0:0)
613.483944	H / N	C39H66O5 [M-H]-	HMDB07704	DG(22:5(4Z,7Z,10Z,13Z,16Z)/14:0/0:0)
613.483944	H / N	C39H66O5 [M-H]-	HMDB07733	DG(22:5(7Z,10Z,13Z,16Z,19Z)/14:0/0:0)
613.483944	H / N	C39H66O5 [M-H]-	HMDB55974	DG(14:0/0:0/22:5n6)
613.483944	H / N	C39H66O5 [M-H]-	HMDB55979	DG(14:0/0:0/22:5n3)
613.483944	H / N	C39H66O5 [M-H]-	HMDB56033	DG(16:0/0:0/20:5n3)
613.483944	H / N	C39H66O5 [M-H]-	HMDB56148	DG(14:1n5/0:0/22:4n6)
613.483944	H / N	C39H66O5 [M-H]-	HMDB56167	DG(16:1n7/0:0/20:4n6)
613.483944	H / N	C39H66O5 [M-H]-	HMDB56173	DG(16:1n7/0:0/20:4n3)
613.483944	H / N	C39H66O5 [M-H]-	HMDB56192	DG(18:1n7/0:0/18:4n3)
613.483944	H / N	C39H66O5 [M-H]-	HMDB56211	DG(18:1n9/0:0/18:4n3)
615.499471	H / N	C39H68O5 [M-H]-	HMDB07031	DG(14:0/22:4(7Z,10Z,13Z,16Z)/0:0)
615.499471	H / N	C39H68O5 [M-H]-	HMDB07112	DG(16:0/20:4(5Z,8Z,11Z,14Z)/0:0)
615.499471	H / N	C39H68O5 [M-H]-	HMDB07113	DG(16:0/20:4(8Z,11Z,14Z,17Z)/0:0)
615.499471	H / N	C39H68O5 [M-H]-	HMDB07139	DG(16:1(9Z)/20:3(5Z,8Z,11Z)/0:0)
615.499471	H / N	C39H68O5 [M-H]-	HMDB07140	DG(16:1(9Z)/20:3(8Z,11Z,14Z)/0:0)
615.499471	H / N	C39H68O5 [M-H]-	HMDB07164	DG(18:0/18:4(6Z,9Z,12Z,15Z)/0:0)
615.499471	H / N	C39H68O5 [M-H]-	HMDB07191	DG(18:1(11Z)/18:3(6Z,9Z,12Z)/0:0)
615.499471	H / N	C39H68O5 [M-H]-	HMDB07192	DG(18:1(11Z)/18:3(9Z,12Z,15Z)/0:0)
615.499471	H / N	C39H68O5 [M-H]-	HMDB07220	DG(18:1(9Z)/18:3(6Z,9Z,12Z)/0:0)
615.499471	H / N	C39H68O5 [M-H]-	HMDB07221	DG(18:1(9Z)/18:3(9Z,12Z,15Z)/0:0)
615.499471	H / N	C39H68O5 [M-H]-	HMDB07248	DG(18:2(9Z,12Z)/18:2(9Z,12Z)/0:0)
615.499471	H / N	C39H68O5 [M-H]-	HMDB07275	DG(18:3(6Z,9Z,12Z)/18:1(11Z)/0:0)
615.499471	H / N	C39H68O5 [M-H]-	HMDB07276	DG(18:3(6Z,9Z,12Z)/18:1(9Z)/0:0)
615.499471	H / N	C39H68O5 [M-H]-	HMDB07304	DG(18:3(9Z,12Z,15Z)/18:1(11Z)/0:0)
615.499471	H / N	C39H68O5 [M-H]-	HMDB07305	DG(18:3(9Z,12Z,15Z)/18:1(9Z)/0:0)
615.499471	H / N	C39H68O5 [M-H]-	HMDB07332	DG(18:4(6Z,9Z,12Z,15Z)/18:0/0:0)
615.499471	H / N	C39H68O5 [M-H]-	HMDB07447	DG(20:3(5Z,8Z,11Z)/16:1(9Z)/0:0)
615.499471	H / N	C39H68O5 [M-H]-	HMDB07476	DG(20:3(8Z,11Z,14Z)/16:1(9Z)/0:0)
615.499471	H / N	C39H68O5 [M-H]-	HMDB07504	DG(20:4(5Z,8Z,11Z,14Z)/16:0/0:0)
615.499471	H / N	C39H68O5 [M-H]-	HMDB07533	DG(20:4(8Z,11Z,14Z,17Z)/16:0/0:0)
615.499471	H / N	C39H68O5 [M-H]-	HMDB07675	DG(22:4(7Z,10Z,13Z,16Z)/14:0/0:0)
615.499471	H / N	C39H68O5 [M-H]-	HMDB55973	DG(14:0/0:0/22:4n6)
615.499471	H / N	C39H68O5 [M-H]-	HMDB56026	DG(16:0/0:0/20:4n6)
615.499471	H / N	C39H68O5 [M-H]-	HMDB56032	DG(16:0/0:0/20:4n3)
615.499471	H / N	C39H68O5 [M-H]-	HMDB56057	DG(18:0/0:0/18:4n3)
615.499471	H / N	C39H68O5 [M-H]-	HMDB56160	DG(16:1n7/0:0/20:3n9)
615.499471	H / N	C39H68O5 [M-H]-	HMDB56166	DG(16:1n7/0:0/20:3n6)
615.499471	H / N	C39H68O5 [M-H]-	HMDB56184	DG(18:1n7/0:0/18:3n6)
615.499471	H / N	C39H68O5 [M-H]-	HMDB56191	DG(18:1n7/0:0/18:3n3)
615.499471	H / N	C39H68O5 [M-H]-	HMDB56203	DG(18:1n9/0:0/18:3n6)
615.499471	H / N	C39H68O5 [M-H]-	HMDB56210	DG(18:1n9/0:0/18:3n3)
619.432624	N	C35H60N2O7 [M-H]-	-	-
621.348846	N	C28H50N10O2S2 [M-H]-	-	-
621.448136	N	C35H62N2O7 [M-H]-	-	-
621.501524	N	C39H70O3 [M+Cl]-	-	-
621.501524	N	C38H71O4P [M-H]-	-	-
623.308819	N	C33H44N4O8 [M-H]-	-	-
623.345196	N	C34H48N4O7 [M-H]-	-	-
623.364664	N	C30H56O13 [M-H]-	-	-
623.398821	N	C35H60O7S [M-H]-	-	-
625.324685	N	C33H46N4O8 [M-H]-	-	-
626.327809	N	C27H49N9O4S2 [M-H]-	-	-
626.369914	N	C36H53NO8 [M-H]-	-	-

627.536014	N	C41H72O4 [M-H]-	-	-
631.513027	N	C40H72O3S [M-H]-	-	-
632.484392	N	C35H72NO4PS [M-H]-	-	-
635.489174	N	C38H68O7 [M-H]-	-	-
637.231991	N	C33H39N2O9P [M-H]-	-	-
637.231991	N	C31H42O12S [M-H]-	-	-
637.451202	N	C37H66O6S [M-H]-	-	-
637.451202	N	C30H66N6O4S2 [M-H]-	-	-
639.340129	N	C34H48N4O8 [M-H]-	-	-
641.226360	N	C24H43N4O12PS [M-H]-	-	-
641.355775	N	C34H50N4O8 [M-H]-	-	-
641.375635	N	C30H58O14 [M-H]-	-	-
643.530818	H / N	C41H72O5 [M-H]-	HMDB07118	DG(16:0/22:4(7Z,10Z,13Z,16Z)/0:0)
643.530818	H / N	C41H72O5 [M-H]-	HMDB07170	DG(18:0/20:4(5Z,8Z,11Z,14Z)/0:0)
643.530818	H / N	C41H72O5 [M-H]-	HMDB07171	DG(18:0/20:4(8Z,11Z,14Z,17Z)/0:0)
643.530818	H / N	C41H72O5 [M-H]-	HMDB07198	DG(18:1(11Z)/20:3(8Z,11Z,14Z)/0:0)
643.530818	H / N	C41H72O5 [M-H]-	HMDB07226	DG(18:1(9Z)/20:3(5Z,8Z,11Z)/0:0)
643.530818	H / N	C41H72O5 [M-H]-	HMDB07227	DG(18:1(9Z)/20:3(8Z,11Z,14Z)/0:0)
643.530818	H / N	C41H72O5 [M-H]-	HMDB07254	DG(18:2(9Z,12Z)/20:2(11Z,14Z)/0:0)
643.530818	H / N	C41H72O5 [M-H]-	HMDB07282	DG(18:3(6Z,9Z,12Z)/20:1(11Z)/0:0)
643.530818	H / N	C41H72O5 [M-H]-	HMDB07311	DG(18:3(9Z,12Z,15Z)/20:1(11Z)/0:0)
643.530818	H / N	C41H72O5 [M-H]-	HMDB07339	DG(18:4(6Z,9Z,12Z,15Z)/20:0/0:0)
643.530818	H / N	C41H72O5 [M-H]-	HMDB07367	DG(20:0/18:4(6Z,9Z,12Z,15Z)/0:0)
643.530818	H / N	C41H72O5 [M-H]-	HMDB07394	DG(20:1(11Z)/18:3(6Z,9Z,12Z)/0:0)
643.530818	H / N	C41H72O5 [M-H]-	HMDB07395	DG(20:1(11Z)/18:3(9Z,12Z,15Z)/0:0)
643.530818	H / N	C41H72O5 [M-H]-	HMDB07422	DG(20:2(11Z,14Z)/18:2(9Z,12Z)/0:0)
643.530818	H / N	C41H72O5 [M-H]-	HMDB07449	DG(20:3(5Z,8Z,11Z)/18:1(11Z)/0:0)
643.530818	H / N	C41H72O5 [M-H]-	HMDB07450	DG(20:3(5Z,8Z,11Z)/18:1(9Z)/0:0)
643.530818	H / N	C41H72O5 [M-H]-	HMDB07478	DG(20:3(8Z,11Z,14Z)/18:1(11Z)/0:0)
643.530818	H / N	C41H72O5 [M-H]-	HMDB07479	DG(20:3(8Z,11Z,14Z)/18:1(9Z)/0:0)
643.530818	H / N	C41H72O5 [M-H]-	HMDB07506	DG(20:4(5Z,8Z,11Z,14Z)/18:0/0:0)
643.530818	H / N	C41H72O5 [M-H]-	HMDB07535	DG(20:4(8Z,11Z,14Z,17Z)/18:0/0:0)
643.530818	H / N	C41H72O5 [M-H]-	HMDB07678	DG(22:4(7Z,10Z,13Z,16Z)/16:0/0:0)
643.530818	H / N	C41H72O5 [M-H]-	HMDB56028	DG(16:0/0:0/22:4n6)
643.530818	H / N	C41H72O5 [M-H]-	HMDB56052	DG(18:0/0:0/20:4n6)
643.530818	H / N	C41H72O5 [M-H]-	HMDB56058	DG(18:0/0:0/20:4n3)
643.530818	H / N	C41H72O5 [M-H]-	HMDB56082	DG(20:0/0:0/18:4n3)
643.530818	H / N	C41H72O5 [M-H]-	HMDB56180	DG(18:1n7/0:0/20:3n9)
643.530818	H / N	C41H72O5 [M-H]-	HMDB56186	DG(18:1n7/0:0/20:3n6)
643.530818	H / N	C41H72O5 [M-H]-	HMDB56199	DG(18:1n9/0:0/20:3n9)
643.530818	H / N	C41H72O5 [M-H]-	HMDB56205	DG(18:1n9/0:0/20:3n6)
643.530818	H / N	C41H72O5 [M-H]-	HMDB56221	DG(20:1n9/0:0/18:3n6)
643.530818	H / N	C41H72O5 [M-H]-	HMDB56228	DG(20:1n9/0:0/18:3n3)
643.530818	H / N	C41H72O5 [M-H]-	HMDB56282	DG(18:2n6/0:0/18:2n6)
643.530818	H / N	C41H72O5 [M-H]-	HMDB56284	DG(18:2n6/0:0/20:2n6)
643.530818	H / N	C41H72O5 [M-H]-	HMDB56309	DG(20:2n6/0:0/20:2n6)
645.385591	N	C33H58O12 [M-H]-	-	-
645.546667	H / N	C41H74O5 [M-H]-	HMDB07146	DG(16:1(9Z)/22:2(13Z,16Z)/0:0)
645.546667	H / N	C41H74O5 [M-H]-	HMDB07168	DG(18:0/20:3(5Z,8Z,11Z)/0:0)
645.546667	H / N	C41H74O5 [M-H]-	HMDB07169	DG(18:0/20:3(8Z,11Z,14Z)/0:0)
645.546667	H / N	C41H74O5 [M-H]-	HMDB07196	DG(18:1(11Z)/20:2(11Z,14Z)/0:0)
645.546667	H / N	C41H74O5 [M-H]-	HMDB07225	DG(18:1(9Z)/20:2(11Z,14Z)/0:0)
645.546667	H / N	C41H74O5 [M-H]-	HMDB07253	DG(18:2(9Z,12Z)/20:1(11Z)/0:0)
645.546667	H / N	C41H74O5 [M-H]-	HMDB07281	DG(18:3(6Z,9Z,12Z)/20:0/0:0)
645.546667	H / N	C41H74O5 [M-H]-	HMDB07310	DG(18:3(9Z,12Z,15Z)/20:0/0:0)
645.546667	H / N	C41H74O5 [M-H]-	HMDB07365	DG(20:0/18:3(6Z,9Z,12Z)/0:0)
645.546667	H / N	C41H74O5 [M-H]-	HMDB07366	DG(20:0/18:3(9Z,12Z,15Z)/0:0)
645.546667	H / N	C41H74O5 [M-H]-	HMDB07393	DG(20:1(11Z)/18:2(9Z,12Z)/0:0)
645.546667	H / N	C41H74O5 [M-H]-	HMDB07420	DG(20:2(11Z,14Z)/18:1(11Z)/0:0)
645.546667	H / N	C41H74O5 [M-H]-	HMDB07421	DG(20:2(11Z,14Z)/18:1(9Z)/0:0)
645.546667	H / N	C41H74O5 [M-H]-	HMDB07448	DG(20:3(5Z,8Z,11Z)/18:0/0:0)
645.546667	H / N	C41H74O5 [M-H]-	HMDB07477	DG(20:3(8Z,11Z,14Z)/18:0/0:0)
645.546667	H / N	C41H74O5 [M-H]-	HMDB07650	DG(22:2(13Z,16Z)/16:1(9Z)/0:0)
645.546667	H / N	C41H74O5 [M-H]-	HMDB56045	DG(18:0/0:0/20:3n9)
645.546667	H / N	C41H74O5 [M-H]-	HMDB56051	DG(18:0/0:0/20:3n6)
645.546667	H / N	C41H74O5 [M-H]-	HMDB56074	DG(20:0/0:0/18:3n6)
645.546667	H / N	C41H74O5 [M-H]-	HMDB56081	DG(20:0/0:0/18:3n3)
645.546667	H / N	C41H74O5 [M-H]-	HMDB56168	DG(16:1n7/0:0/22:2n6)
645.583104	N	C42H78O4 [M-H]-	-	-
651.556997	N	C40H76O6 [M-H]-	-	-
653.339332	N	C30H54O15 [M-H]-	-	-
657.350749	N	C34H50N4O9 [M-H]-	-	-

657.495903	N	C38H66N4O5 [M-H]-	-	-
659.435432	N	C39H64O6S [M-H]-	-	-
659.489615	N	C40H68O7 [M-H]-	-	-
659.538593	H / N	C39H76O5 [M+Cl]-	HMDB07028	DG(14:0/22:0/0:0)
659.538593	H / N	C39H76O5 [M+Cl]-	HMDB07107	DG(16:0/20:0/0:0)
659.538593	H / N	C39H76O5 [M+Cl]-	HMDB07158	DG(18:0/18:0/0:0)
659.538593	H / N	C39H76O5 [M+Cl]-	HMDB07359	DG(20:0/16:0/0:0)
659.538593	H / N	C39H76O5 [M+Cl]-	HMDB07588	DG(22:0/14:0/0:0)
659.538593	H / N	C39H76O5 [M+Cl]-	HMDB31012	Glycerol 1,2-dioctadecanoate
659.538593	H / N	C39H76O5 [M+Cl]-	HMDB55957	DG(14:0/0:0/22:0)
659.538593	H / N	C39H76O5 [M+Cl]-	HMDB56011	DG(16:0/0:0/20:0)
659.538593	H / N	C39H76O5 [M+Cl]-	HMDB56036	DG(18:0/0:0/18:0)
659.538593	N	C38H77O6P [M-H]-	-	-
667.588379	N	C41H80O6 [M-H]-	-	-
673.345720	N	C34H50N4O10 [M-H]-	-	-
673.417080	N	C35H62O12 [M-H]-	-	-
675.430152	N	C39H64O7S [M-H]-	-	-
683.283012	N	C28H44N8O10S [M-H]-	-	-
689.406194	N	C35H58N6O6S [M-H]-	-	-
705.294602	N	C38H47N2O9P [M-H]-	-	-
705.294602	N	C36H50O12S [M-H]-	-	-
705.555421	N	C39H78N2O6 [M+Cl]-	-	-
707.407612	N	C45H52N6O2 [M-H]-	-	-
709.443695	N	C41H62N2O8 [M-H]-	-	-
713.475050	N	C41H66N2O8 [M-H]-	-	-
714.508305	N	C40H73NO7 [M+Cl]-	-	-
714.508305	H / N	C39H74NO8P [M-H]-	HMDB08835	PE(14:0/20:2(11Z,14Z))
714.508305	H / N	C39H74NO8P [M-H]-	HMDB08867	PE(14:1(9Z)/20:1(11Z))
714.508305	H / N	C39H74NO8P [M-H]-	HMDB08928	PE(16:0/18:2(9Z,12Z))
714.508305	H / N	C39H74NO8P [M-H]-	HMDB08959	PE(16:1(9Z)/18:1(11Z))
714.508305	H / N	C39H74NO8P [M-H]-	HMDB08960	PE(16:1(9Z)/18:1(9Z))
714.508305	H / N	C39H74NO8P [M-H]-	HMDB09023	PE(18:1(11Z)/16:1(9Z))
714.508305	H / N	C39H74NO8P [M-H]-	HMDB09056	PE(18:1(9Z)/16:1(9Z))
714.508305	H / N	C39H74NO8P [M-H]-	HMDB09088	PE(18:2(9Z,12Z)/16:0)
714.508305	H / N	C39H74NO8P [M-H]-	HMDB09251	PE(20:1(11Z)/14:1(9Z))
714.508305	H / N	C39H74NO8P [M-H]-	HMDB09283	PE(20:2(11Z,14Z)/14:0)
715.511406	N	C38H72N2O10 [M-H]-	-	-
738.508294	N	C42H73NO7 [M+Cl]-	-	-
738.508294	H / N	C41H74NO8P [M-H]-	HMDB07943	PC(15:0/18:4(6Z,9Z,12Z,15Z))
738.508294	H / N	C41H74NO8P [M-H]-	HMDB08231	PC(18:4(6Z,9Z,12Z,15Z)/15:0)
738.508294	H / N	C41H74NO8P [M-H]-	HMDB08844	PE(14:0/22:4(7Z,10Z,13Z,16Z))
738.508294	H / N	C41H74NO8P [M-H]-	HMDB08937	PE(16:0/20:4(5Z,8Z,11Z,14Z))
738.508294	H / N	C41H74NO8P [M-H]-	HMDB08938	PE(16:0/20:4(8Z,11Z,14Z,17Z))
738.508294	H / N	C41H74NO8P [M-H]-	HMDB08968	PE(16:1(9Z)/20:3(5Z,8Z,11Z))
738.508294	H / N	C41H74NO8P [M-H]-	HMDB08997	PE(18:0/18:4(6Z,9Z,12Z,15Z))
738.508294	H / N	C41H74NO8P [M-H]-	HMDB09028	PE(18:1(11Z)/18:3(6Z,9Z,12Z))
738.508294	H / N	C41H74NO8P [M-H]-	HMDB09029	PE(18:1(11Z)/18:3(9Z,12Z,15Z))
738.508294	H / N	C41H74NO8P [M-H]-	HMDB09061	PE(18:1(9Z)/18:3(6Z,9Z,12Z))
738.508294	H / N	C41H74NO8P [M-H]-	HMDB09062	PE(18:1(9Z)/18:3(9Z,12Z,15Z))
738.508294	H / N	C41H74NO8P [M-H]-	HMDB09093	PE(18:2(9Z,12Z)/18:2(9Z,12Z))
738.508294	H / N	C41H74NO8P [M-H]-	HMDB09124	PE(18:3(6Z,9Z,12Z)/18:1(11Z))
738.508294	H / N	C41H74NO8P [M-H]-	HMDB09125	PE(18:3(6Z,9Z,12Z)/18:1(9Z))
738.508294	H / N	C41H74NO8P [M-H]-	HMDB09157	PE(18:3(9Z,12Z,15Z)/18:1(11Z))
738.508294	H / N	C41H74NO8P [M-H]-	HMDB09158	PE(18:3(9Z,12Z,15Z)/18:1(9Z))
738.508294	H / N	C41H74NO8P [M-H]-	HMDB09189	PE(18:4(6Z,9Z,12Z,15Z)/18:0)
738.508294	H / N	C41H74NO8P [M-H]-	HMDB09320	PE(20:3(5Z,8Z,11Z)/16:1(9Z))
738.508294	H / N	C41H74NO8P [M-H]-	HMDB09353	PE(20:3(8Z,11Z,14Z)/16:1(9Z))
738.508294	H / N	C41H74NO8P [M-H]-	HMDB09385	PE(20:4(5Z,8Z,11Z,14Z)/16:0)
738.508294	H / N	C41H74NO8P [M-H]-	HMDB09418	PE(20:4(8Z,11Z,14Z,17Z)/16:0)
738.508294	H / N	C41H74NO8P [M-H]-	HMDB09580	PE(22:4(7Z,10Z,13Z,16Z)/14:0)
740.387672	N	C38H55N5O10 [M-H]-	-	-
741.676548	N	C49H90O4 [M-H]-	-	-
751.433505	N	C39H60N8O5S [M-H]-	-	-
752.592098	N	C42H83N5O2S2 [M-H]-	-	-
752.592098	N	C42H75N9O3 [M-H]-	-	-
769.590019	N	C41H86N2O6S [M+Cl]-	-	-
769.590019	N	C43H78N8O2S [M-H]-	-	-
770.593738	N	C47H81NO7 [M-H]-	-	-
773.534224	N	C43H78O9 [M+Cl]-	-	-
773.534224	H / N	C42H79O10P [M-H]-	HMDB10605	PG(18:0/18:2(9Z,12Z))
773.534224	H / N	C42H79O10P [M-H]-	HMDB10618	PG(18:1(11Z)/18:1(11Z))
773.534224	H / N	C42H79O10P [M-H]-	HMDB10619	PG(18:1(11Z)/18:1(9Z))

773.534224	H / N	C42H79O10P [M-H]-	HMDB10633	PG(18:1(9Z)/18:1(11Z))
773.534224	H / N	C42H79O10P [M-H]-	HMDB10634	PG(18:1(9Z)/18:1(9Z))
773.534224	H / N	C42H79O10P [M-H]-	HMDB10647	PG(18:2(9Z,12Z)/18:0)
786.588697	N	C47H81NO8 [M-H]-	-	-
801.565634	N	C45H82O9 [M+Cl]-	-	-
802.568474	N	C43H81NO12 [M-H]-	-	-
807.615056	N	C51H84O7 [M-H]-	-	-
809.630569	N	C51H86O7 [M-H]-	-	-
815.581295	N	C46H84O9 [M+Cl]-	-	-
817.560379	N	C45H82O10 [M+Cl]-	-	-
817.560379	N	C44H83O11P [M-H]-	-	-
817.657023	N	C50H90O8 [M-H]-	-	-
865.714277	N	C48H94N8O3 [M+Cl]-	-	-
865.714277	N	C52H98O9 [M-H]-	-	-
867.729859	N	C48H96N8O3 [M+Cl]-	-	-
867.729859	N	C52H100O9 [M-H]-	-	-
893.576151	N	C46H87O14P [M-H]-	-	-
Features selected for the COMB group				
145.044024	N	C5H10N2OS [M-H]-	-	-
165.041827	H / N	C6H6N4O2 [M-H]-	HMDB01886	3-Methylxanthine
165.041827	H / N	C6H6N4O2 [M-H]-	HMDB01991	7-Methylxanthine
165.041827	H / N	C6H6N4O2 [M-H]-	HMDB10738	1-Methylxanthine
165.041827	H / N	C6H6N4O2 [M-H]-	HMDB59716	9-Methylxanthine
174.088434	H / N	C6H13N3O3 [M-H]-	HMDB00904	Citrulline
174.088434	H / N	C6H13N3O3 [M-H]-	HMDB03148	Argininic acid
190.072116	H / N	C7H13NO5 [M-H]-	HMDB31346	Calystegine C1
197.022152	H / N	C6H10O5 [M+Cl]-	HMDB00321	2-Hydroxyadipic acid
197.022152	H / N	C6H10O5 [M+Cl]-	HMDB00345	3-Hydroxyadipic acid
197.022152	H / N	C6H10O5 [M+Cl]-	HMDB00355	3-Hydroxymethylglutaric acid
197.022152	H / N	C6H10O5 [M+Cl]-	HMDB00368	2(R)-Hydroxyadipic acid
197.022152	H / N	C6H10O5 [M+Cl]-	HMDB00640	Levoglucosan
197.022152	H / N	C6H10O5 [M+Cl]-	HMDB29934	D-1-Deoxy-erythro-hexo-2,3-diulose
197.022152	H / N	C6H10O5 [M+Cl]-	HMDB32873	Diethyl dicarbonate
197.022152	H / N	C6H10O5 [M+Cl]-	HMDB41561	D-1,5-Anhydrofructose
197.022152	H / N	C6H10O5 [M+Cl]-	HMDB59758	2-Hydroxy-2-ethylsuccinic acid
197.022152	N	C5H11O6P [M-H]-	-	-
199.170372	H / N	C12H24O2 [M-H]-	HMDB00638	Dodecanoic acid
199.170372	H / N	C12H24O2 [M-H]-	HMDB30998	Ethyl decanoate
199.170372	H / N	C12H24O2 [M-H]-	HMDB32310	2-Heptyl butyrate
199.170372	H / N	C12H24O2 [M-H]-	HMDB32440	Nonanal propyleneglycol acetal
199.170372	H / N	C12H24O2 [M-H]-	HMDB33619	Hexyl hexanoate
199.170372	H / N	C12H24O2 [M-H]-	HMDB34128	Isopropyl nonanoate
199.170372	H / N	C12H24O2 [M-H]-	HMDB34136	Octyl butanoate
199.170372	H / N	C12H24O2 [M-H]-	HMDB34137	Octyl 2-methylpropanoate
199.170372	H / N	C12H24O2 [M-H]-	HMDB35410	(R)-Dihydrocitronellol acetate
199.170372	H / N	C12H24O2 [M-H]-	HMDB36225	Pentyl heptanoate
199.170372	H / N	C12H24O2 [M-H]-	HMDB40166	Decyl acetate
199.170372	H / N	C12H24O2 [M-H]-	HMDB59868	Isobutyl octanoate
200.129216	H / N	C10H19NO3 [M-H]-	HMDB00832	Capryloylglycine
200.129216	H / N	C10H19NO3 [M-H]-	HMDB13116	Valproylglycine
200.129216	H / N	C10H19NO3 [M-H]-	HMDB41540	N-(5-Methyl-3-oxohexyl)alanine
200.129216	H / N	C10H19NO3 [M-H]-	HMDB59745	N-Acetylaminooctanoic acid
209.118337	H / N	C12H18O3 [M-H]-	HMDB32797	Jasmonic acid
209.118337	H / N	C12H18O3 [M-H]-	HMDB32871	Sedanonic acid
209.118337	H / N	C12H18O3 [M-H]-	HMDB33102	Dihydro-3-(2-octenyl)-2,5-furandione
209.118337	H / N	C12H18O3 [M-H]-	HMDB37104	(R)-8-Acetoxycarvotanacetone
209.118337	H / N	C12H18O3 [M-H]-	HMDB37135	1-Benzyloxy-1-(2-methoxyethoxy)ethane
209.118337	H / N	C12H18O3 [M-H]-	HMDB37642	4-(Butoxymethyl)-2-methoxyphenol
209.118337	H / N	C12H18O3 [M-H]-	HMDB37735	Isoamyl 2-furonpropionate
209.118337	H / N	C12H18O3 [M-H]-	HMDB37816	Dihydro-3-(1-octenyl)-2,5-furandione
209.118337	H / N	C12H18O3 [M-H]-	HMDB41573	3-Ethenyl-2,5-dimethyl-4-oxohex-5-en-2-yl acetate
233.153958	H / N	C10H22N4 [M+Cl]-	HMDB15301	Guanethidine
234.113567	H / N	C13H17NO3 [M-H]-	HMDB33610	Pandamarilactam 3x
244.093928	H / N	C9H15N3O5 [M-H]-	HMDB28732	Asparaginyl-Hydroxyproline
244.093928	H / N	C9H15N3O5 [M-H]-	HMDB28858	Hydroxyprolyl-Asparagine
248.059818	N	C9H15NO5S [M-H]-	-	-
249.185988	H / N	C16H26O2 [M-H]-	HMDB35293	Norambreinolide
249.185988	H / N	C16H26O2 [M-H]-	HMDB37631	3-Methyl-alpha-ionyl acetate
249.185988	H / N	C16H26O2 [M-H]-	HMDB37712	[2,2-Bis(2-methylpropoxy)ethyl]benzene
250.039116	N	C8H13NO6S [M-H]-	-	-
250.144883	N	C14H21NO3 [M-H]-	-	-
253.050689	H / N	C15H10O4 [M-H]-	HMDB03312	Daidzein

253.050689	H / N	C15H10O4 [M-H]-	HMDB30670	Chrysophanol
253.050689	H / N	C15H10O4 [M-H]-	HMDB30699	5,7-Dihydroxyisoflavone
253.050689	H / N	C15H10O4 [M-H]-	HMDB30874	Phomarin
253.050689	H / N	C15H10O4 [M-H]-	HMDB33153	(Z)-4',6-Dihydroxyaurone
253.050689	H / N	C15H10O4 [M-H]-	HMDB36619	5,7-Dihydroxyflavone
253.180898	H / N	C15H26O3 [M-H]-	HMDB29604	Lubiminol
253.180898	H / N	C15H26O3 [M-H]-	HMDB35780	8-Hydroxy-4(6)-lactarene-5,14-diol
253.180898	H / N	C15H26O3 [M-H]-	HMDB36053	(3beta,9beta)-7-Drimene-3,11,12-triol
253.180898	H / N	C15H26O3 [M-H]-	HMDB36866	7-Drimene-11,12,14-triol
253.180898	H / N	C15H26O3 [M-H]-	HMDB37197	Kessyl glycol
253.180898	H / N	C15H26O3 [M-H]-	HMDB40276	5-Acetoxydihydrotheaespirane
256.028559	N	C10H11NO5S [M-H]-	-	-
257.060153	N	C10H14N2O4S [M-H]-	-	-
257.165931	N	C16H22N2O [M-H]-	-	-
261.053500	H / N	C11H14O5 [M+Cl]-	HMDB31722	3,4,5-Trimethoxyphenyl acetate
261.053500	H / N	C11H14O5 [M+Cl]-	HMDB35830	Genipin
261.053500	H / N	C11H14O5 [M+Cl]-	HMDB41560	2,4,6-Trimethoxyphenyl acetate
261.053500	H / N	C11H14O5 [M+Cl]-	HMDB41679	4-Hydroxy-(3',4'-dihydroxyphenyl)-valeric acid
261.053500	H / N	C11H14O5 [M+Cl]-	HMDB41727	Dihydrosinapic acid
261.053500	H / N	C11H14O5 [M+Cl]-	HMDB60736	3-(4-Hydroxy-3-methoxyphenyl)-2-methyllactic acid
261.053500	N	C10H15O6P [M-H]-	-	-
263.165288	H / N	C16H24O3 [M-H]-	HMDB32090	12-Oxo-2,3-dinor-10,15-phytodienoic acid
269.065633	N	C6H15N4O6P [M-H]-	-	-
269.165972	H / N	C17H22N2O [M-H]-	HMDB01936	Doxylamine
273.096161	N	C9H18N6S2 [M-H]-	-	-
275.101496	N	C8H20N2O6 [M+Cl]-	-	-
276.107219	N	C8H19N7S2 [M-H]-	-	-
278.151052	H / N	C14H21N3O3 [M-H]-	HMDB15228	Oxamniquine
281.089313	H / N	C11H14N4O5 [M-H]-	HMDB02721	1-Methylinosine
281.140662	N	C16H18N4O [M-H]-	-	-
282.120132	N	C11H25NO3S2 [M-H]-	-	-
282.215993	N	C11H25N9 [M-H]-	-	-
284.223050	H / N	C16H31NO3 [M-H]-	HMDB13250	Myristoylglycine
285.066175	N	C10H14N4O4S [M-H]-	-	-
286.060184	N	C8H17NO8S [M-H]-	-	-
286.096310	N	C12H17N3O3 [M+Cl]-	-	-
286.096310	N	C11H18N3O4P [M-H]-	-	-
287.095669	N	C13H20O5S [M-H]-	-	-
287.165305	H / N	C18H24O3 [M-H]-	HMDB00153	Estriol
287.165305	H / N	C18H24O3 [M-H]-	HMDB00338	2-Hydroxyestradiol
287.165305	H / N	C18H24O3 [M-H]-	HMDB00347	16b-Hydroxyestradiol
287.165305	H / N	C18H24O3 [M-H]-	HMDB00356	17-Epiestriol
287.165305	H / N	C18H24O3 [M-H]-	HMDB00431	16,17-Epiestriol
287.165305	H / N	C18H24O3 [M-H]-	HMDB05896	4-Hydroxyestradiol
287.165305	H / N	C18H24O3 [M-H]-	HMDB40864	O-Geranylvanillin
287.165305	H / N	C18H24O3 [M-H]-	HMDB60353	2-Polyprenyl-3-methyl-6-methoxy-1,4-benzoquinone
287.165305	H / N	C18H24O3 [M-H]-	HMDB60999	4-hydroxystradiol
288.088990	N	C16H11N5O [M-H]-	-	-
290.135834	N	C11H21N3O6 [M-H]-	-	-
290.189302	N	C15H29NO2 [M+Cl]-	-	-
291.125294	N	C17H16N4O [M-H]-	-	-
291.143679	N	C10H16N10O [M-H]-	-	-
295.070100	N	C9H17N2O7P [M-H]-	-	-
295.227839	H / N	C18H32O3 [M-H]-	HMDB04667	13S-hydroxyoctadecadienoic acid
295.227839	H / N	C18H32O3 [M-H]-	HMDB04670	Alpha-dimorphecolic acid
295.227839	H / N	C18H32O3 [M-H]-	HMDB04701	9,10-Epoxyoctadecenoic acid
295.227839	H / N	C18H32O3 [M-H]-	HMDB04702	12,13-EpOME
295.227839	H / N	C18H32O3 [M-H]-	HMDB10223	9-HODE
295.227839	H / N	C18H32O3 [M-H]-	HMDB29796	(Z)-13-Oxo-9-octadecenoic acid
295.227839	H / N	C18H32O3 [M-H]-	HMDB29978	Avenoleic acid
295.227839	H / N	C18H32O3 [M-H]-	HMDB29998	12-Hydroxy-8,10-octadecadienoic acid
297.084025	N	C11H14N4O6 [M-H]-	-	-
298.202351	N	C16H29NO4 [M-H]-	-	-
299.090169	H / N	C11H20O7 [M+Cl]-	HMDB41186	Ilicifolinoside A
299.090169	H / N	C11H20O7 [M+Cl]-	HMDB41187	(Z)-2-Methyl-2-butene-1,4-diol 4-O-beta-D-Glucopyranoside
299.090169	N	C10H21O8P [M-H]-	-	-
299.091110	N	C12H24O2S2 [M+Cl]-	-	-
299.127543	N	C13H28OS2 [M+Cl]-	-	-
299.176517	N	C18H24N2O2 [M-H]-	-	-
300.103751	N	C13H15N7S [M-H]-	-	-
301.137823	N	C17H22N2OS [M-H]-	-	-
301.192205	N	C18H26N2O2 [M-H]-	-	-

302.187409	H / N	C17H25N3O2 [M-H]-	HMDB15596	Vildagliptin
303.090527	N	C13H20O6S [M-H]-	-	-
303.230137	N	C16H28N6 [M-H]-	-	-
305.122270	N	C10H22N6OS2 [M-H]-	-	-
306.130781	N	C11H21N3O7 [M-H]-	-	-
307.108797	H / N	C18H16N2O3 [M-H]-	HMDB37521	C.I. Solvent Red 80
307.108797	H / N	C18H16N2O3 [M-H]-	HMDB40367	Azacridone A
307.111496	N	C10H20N6OS [M+Cl]-	-	-
307.129723	H / N	C15H20N2O5 [M-H]-	HMDB35173	2-Carboxy-1-[5-(2-carboxy-1-pyrrolidinyl)-2-hydroxy-2,4-pentadienylidene]pyrrolidinium
307.194756	N	C15H32O4S [M-H]-	-	-
308.158386	N	C11H27N5OS2 [M-H]-	-	-
308.223177	N	C18H31NO3 [M-H]-	-	-
309.183745	N	C15H30O4 [M+Cl]-	-	-
309.183745	N	C14H31O5P [M-H]-	-	-
309.204690	N	C14H26N6O2 [M-H]-	-	-
309.241087	N	C15H30N6O [M-H]-	-	-
311.163216	N	C14H28O5 [M+Cl]-	-	-
311.163216	N	C13H29O6P [M-H]-	-	-
312.176802	N	C14H31NO2S [M+Cl]-	-	-
313.150523	N	C12H26O9 [M-H]-	-	-
313.180907	H / N	C20H26O3 [M-H]-	HMDB06285	4-oxo-Retinoic acid
313.180907	H / N	C20H26O3 [M-H]-	HMDB12789	4-Oxo-13-cis-retinoate
313.180907	H / N	C20H26O3 [M-H]-	HMDB34712	Prexanthoperol
313.180907	H / N	C20H26O3 [M-H]-	HMDB35200	Yucalexin B5
313.180907	H / N	C20H26O3 [M-H]-	HMDB35602	Kahweol
313.180907	H / N	C20H26O3 [M-H]-	HMDB36748	Momilactone A
313.180907	H / N	C20H26O3 [M-H]-	HMDB39614	3,4,4'-Trihydroxy-5,5'-diisopropyl-2,2'-dimethylbiphenyl
313.180907	H / N	C20H26O3 [M-H]-	HMDB40746	12-Hydroxy-7-oxo-8,11,13-abietatrien-18-al
313.180907	H / N	C20H26O3 [M-H]-	HMDB41152	Methyl cis-p-coumarate 3-(3,7-dimethyl-2,6-octadienyl)
315.080966	N	C16H16N2O3S [M-H]-	-	-
315.091263	N	C7H20N6O4S2 [M-H]-	-	-
315.131690	N	C13H24N4OS2 [M-H]-	-	-
316.093747	N	C15H15N3O5 [M-H]-	-	-
316.130594	H / N	C16H19N3O4 [M-H]-	HMDB28874	Hydroxyprolyl-Tryptophan
316.130594	H / N	C16H19N3O4 [M-H]-	HMDB29084	Tryptophyl-Hydroxyproline
316.151356	N	C13H23N3O6 [M-H]-	-	-
316.176586	N	C15H27NO6 [M-H]-	-	-
317.128765	N	C12H22N4O4S [M-H]-	-	-
317.132823	N	C17H22N2O2S [M-H]-	-	-
317.142745	N	C15H26O5S [M-H]-	-	-
317.188870	N	C17H30O3 [M+Cl]-	-	-
317.188870	N	C16H31O4P [M-H]-	-	-
318.182336	N	C17H25N3O3 [M-H]-	-	-
319.202682	N	C18H28N2O3 [M-H]-	-	-
319.225403	N	C16H28N6O [M-H]-	-	-
320.168140	N	C13H27N5S [M+Cl]-	-	-
321.055083	N	C14H14N2O5S [M-H]-	-	-
321.077310	N	C12H22N2O2S3 [M-H]-	-	-
321.279871	N	C21H38O2 [M-H]-	-	-
322.185310	N	C11H29N7S2 [M-H]-	-	-
323.124650	N	C15H20N2O6 [M-H]-	-	-
323.142791	N	C11H24N6OS [M+Cl]-	-	-
324.065912	N	C13H15N3O5S [M-H]-	-	-
324.114185	N	C21H15N3O [M-H]-	-	-
324.132435	N	C14H23N5S2 [M-H]-	-	-
324.254419	N	C19H35NO3 [M-H]-	-	-
325.007056	N	C11H10N4O4S2 [M-H]-	-	-
326.114640	N	C17H17N3O4 [M-H]-	-	-
326.197278	N	C17H29NO5 [M-H]-	-	-
326.233722	N	C18H33NO4 [M-H]-	-	-
326.270033	H / N	C19H37NO3 [M-H]-	HMDB13246	Margaroylglycine
326.306483	H / N	C20H41NO2 [M-H]-	HMDB13078	Stearoylethanolamide
326.306483	H / N	C20H41NO2 [M-H]-	HMDB13645	N,N-Dimethylsphingosine
327.215256	N	C14H28N6O3 [M-H]-	-	-
329.033542	N	C13H14O8S [M-H]-	-	-
329.165489	N	C14H26N4O3S [M-H]-	-	-
330.102990	N	C15H17N5O2S [M-H]-	-	-
330.114186	N	C14H17N7OS [M-H]-	-	-
330.167000	N	C14H25N3O6 [M-H]-	-	-
331.033969	N	C9H16O11S [M-H]-	-	-
331.168488	H / N	C17H28O4 [M+Cl]-	HMDB35075	Tanacetol B
331.168488	H / N	C17H28O4 [M+Cl]-	HMDB38798	(1(10)E,4a,5E)-1(10),5-Germacradiene-12-acetoxy-4,11-diol

331.194834	N	C17H32O4S [M-H]-	-	-
332.129940	N	C14H19N7OS [M-H]-	-	-
333.055008	N	C15H14N2O5S [M-H]-	-	-
333.186468	N	C16H26N6S [M-H]-	-	-
335.091760	N	C12H20N2O7S [M-H]-	-	-
336.202769	N	C15H31NO7 [M-H]-	-	-
336.254397	N	C20H35NO3 [M-H]-	-	-
337.144416	H / N	C21H22O4 [M-H]-	HMDB29514	Licochalcone A
337.144416	H / N	C21H22O4 [M-H]-	HMDB30846	Archangelin
337.144416	H / N	C21H22O4 [M-H]-	HMDB31633	Orientanol B
337.144416	H / N	C21H22O4 [M-H]-	HMDB32665	Licoagrocarpin
337.144416	H / N	C21H22O4 [M-H]-	HMDB33671	2'-O-Methylglabridin
337.144416	H / N	C21H22O4 [M-H]-	HMDB33672	4'-O-Methylglabridin
337.144416	H / N	C21H22O4 [M-H]-	HMDB33782	Bergamottin
337.144416	H / N	C21H22O4 [M-H]-	HMDB34412	2'-O-Methylphaseollinisoflavan
337.144416	H / N	C21H22O4 [M-H]-	HMDB39309	9-[(3,7-Dimethyl-2,6-octadienyl)oxy]-7H-furo[3,2-g][1]benzopyran-7-one
337.144416	H / N	C21H22O4 [M-H]-	HMDB39438	2-Hydroxy-4-methoxy-3-(3-methyl-2-butenyl)-6-(2-phenylethenyl)benzoic acid
337.144416	H / N	C21H22O4 [M-H]-	HMDB39439	6-Hydroxy-4-methoxy-3-(3-methyl-2-butenyl)-2-(2-phenylethenyl)benzoic acid
337.144416	H / N	C21H22O4 [M-H]-	HMDB41386	Gancaonin X
337.191584	N	C13H30N4O4S [M-H]-	-	-
337.238397	H / N	C20H34O4 [M-H]-	HMDB02265	14,15-DiHETrE
337.238397	H / N	C20H34O4 [M-H]-	HMDB02311	8,9-DiHETrE
337.238397	H / N	C20H34O4 [M-H]-	HMDB02314	11,12-DiHETrE
337.238397	H / N	C20H34O4 [M-H]-	HMDB02343	5,6-DHET
337.238397	H / N	C20H34O4 [M-H]-	HMDB02995	12-Keto-tetrahydro-leukotriene B4
337.238397	H / N	C20H34O4 [M-H]-	HMDB12504	10,11-dihydro-leukotriene B4
337.238397	H / N	C20H34O4 [M-H]-	HMDB12838	6,7-dihydro-12-epi-LTB4
337.238397	H / N	C20H34O4 [M-H]-	HMDB35379	Sterebin E
337.238397	H / N	C20H34O4 [M-H]-	HMDB60106	15-Hydroperoxyeicosa-8Z,11Z,13E-trienoate
338.091449	H	C15H17N3O4 [M+Cl]-	HMDB13240	Indoleacetyl glutamine
338.091449	H / N	C12H21NO8S [M-H]-	HMDB05034	Topiramate
338.091449	H / N	C12H21NO8S [M-H]-	HMDB40829	N-(1-Deoxy-b-D-fructopyranosyl) (R)C(S)S-alliin
338.270070	H / N	C20H37NO3 [M-H]-	HMDB13631	Oleoyl glycine
340.155367	H / N	C20H23NO4 [M-H]-	HMDB14842	Naltrexone
340.155367	H / N	C20H23NO4 [M-H]-	HMDB30184	(S)-Isocorydine
340.155367	H / N	C20H23NO4 [M-H]-	HMDB31998	Peroxysimulenoline
342.117020	N	C19H21NO3S [M-H]-	-	-
342.227980	N	C13H33N5O3 [M+Cl]-	-	-
342.228590	N	C18H33NO5 [M-H]-	-	-
343.249004	N	C19H36O5 [M-H]-	-	-
345.203104	N	C16H30N2O6 [M-H]-	-	-
349.196391	N	C12H30N8S2 [M-H]-	-	-
350.233700	N	C20H33NO4 [M-H]-	-	-
351.194277	N	C17H32O5 [M+Cl]-	-	-
351.194277	N	C16H33O6P [M-H]-	-	-
351.215425	N	C24H32S [M-H]-	-	-
352.249347	N	C20H35NO4 [M-H]-	-	-
353.184085	N	C17H30N4S2 [M-H]-	-	-
353.184085	N	C17H22N8O [M-H]-	-	-
354.182458	N	C20H25N3O3 [M-H]-	-	-
355.162372	N	C15H24N4O6 [M-H]-	-	-
355.164024	N	C14H28N2O6 [M+Cl]-	-	-
355.164024	N	C13H29N2O7P [M-H]-	-	-
355.202196	N	C13H32N4O5S [M-H]-	-	-
356.111840	N	C13H23NO8 [M+Cl]-	-	-
356.111840	N	C12H24NO9P [M-H]-	-	-
357.178023	N	C15H26N4O6 [M-H]-	-	-
357.196709	N	C16H30N4O3S [M-H]-	-	-
357.217733	N	C16H30N6O [M+Cl]-	-	-
360.327168	H / N	C24H43NO [M-H]-	HMDB30385	2,4,8-Eicosatrienoic acid isobutylamide
360.327168	H / N	C24H43NO [M-H]-	HMDB32032	2,4,14-Eicosatrienoic acid isobutylamide
361.129237	H / N	C19H22O7 [M-H]-	HMDB31366	Gibberellin A93
361.129237	H / N	C19H22O7 [M-H]-	HMDB33905	2',8-Dihydroxy-3',4',5',7-tetramethoxyflavan
361.129237	H / N	C19H22O7 [M-H]-	HMDB35050	Gibberellin A21
361.129237	H / N	C19H22O7 [M-H]-	HMDB36778	Diosbulbin C
361.129237	H / N	C19H22O7 [M-H]-	HMDB39239	Gibberellin A87
361.235979	N	C18H30N6O2 [M-H]-	-	-
363.090691	N	C18H20O6S [M-H]-	-	-
365.208176	N	C19H30N2O5 [M-H]-	-	-
365.230895	N	C17H30N6O3 [M-H]-	-	-
367.209503	N	C16H36N2O3S2 [M-H]-	-	-
367.227610	N	C24H32O3 [M-H]-	-	-

371.137849	N	C17H24N2O5 [M+Cl]-	-	-
371.137849	N	C16H25N2O6P [M-H]-	-	-
372.185217	N	C18H31NO5S [M-H]-	-	-
373.193369	N	C15H34N2O4S [M+Cl]-	-	-
374.270207	N	C23H37NO3 [M-H]-	-	-
375.081012	N	C21H16N2O3S [M-H]-	-	-
375.081012	N	C10H21N2O11P [M-H]-	-	-
375.106297	N	C13H24O10 [M+Cl]-	-	-
375.106297	N	C12H25O11P [M-H]-	-	-
375.251531	N	C19H32N6O2 [M-H]-	-	-
378.155801	N	C19H25NO7 [M-H]-	-	-
378.218973	N	C23H29N3O2 [M-H]-	-	-
379.225576	N	C19H36O5 [M+Cl]-	-	-
379.225576	N	C18H37O6P [M-H]-	-	-
379.246400	N	C18H32N6O3 [M-H]-	-	-
380.228804	N	C17H35NO8 [M-H]-	-	-
381.076198	N	C16H18N2O7S [M-H]-	-	-
381.176750	H / N	C16H30O10 [M-H]-	HMDB33237	1,2,10-Trihydroxydihydro-trans-linalyl oxide 7-O-beta-D-glucopyranoside
381.203059	N	C19H30N2O6 [M-H]-	-	-
381.241226	N	C19H38O5 [M+Cl]-	-	-
381.241226	N	C18H39O6P [M-H]-	-	-
385.148872	N	C15H26N6O2S2 [M-H]-	-	-
387.110990	N	C12H24N4O6S [M+Cl]-	-	-
387.110990	N	C11H25N4O7PS [M-H]-	-	-
387.230815	H / N	C21H36O4 [M+Cl]-	HMDB11539	MG(0:0/18:3(6Z,9Z,12Z)/0:0)
387.230815	H / N	C21H36O4 [M+Cl]-	HMDB11540	MG(0:0/18:3(9Z,12Z,15Z)/0:0)
387.230815	H / N	C21H36O4 [M+Cl]-	HMDB11569	MG(18:3(6Z,9Z,12Z)/0:0/0:0)
387.230815	H / N	C21H36O4 [M+Cl]-	HMDB11570	MG(18:3(9Z,12Z,15Z)/0:0/0:0)
387.230815	N	C20H37O5P [M-H]-	-	-
387.290433	H / N	C25H40O3 [M-H]-	HMDB38523	Methyl 2-(10-heptadecenyl)-6-hydroxybenzoate
389.127680	N	C17H26O8S [M-H]-	-	-
391.206695	N	C14H32N8OS2 [M-H]-	-	-
391.223324	N	C24H36S [M+Cl]-	-	-
391.223324	N	C15H33N6O4P [M-H]-	-	-
393.178094	N	C18H26N4O6 [M-H]-	-	-
395.200080	N	C15H32N6O2S [M+Cl]-	-	-
395.277825	N	C19H36N6O3 [M-H]-	-	-
396.112074	N	C18H23NO7S [M-H]-	-	-
396.223867	N	C17H35NO9 [M-H]-	-	-
397.096194	H	C21H18N2O4 [M+Cl]-	HMDB40786	Zanthobisquinolone
397.096194	H / N	C18H22O8S [M-H]-	HMDB33623	Zearalenone 4-sulfate
397.132300	N	C19H26O7S [M-H]-	-	-
397.186782	H / N	C20H30O8 [M-H]-	HMDB34575	3'-Hydroxy-T2-triol
397.186782	H / N	C20H30O8 [M-H]-	HMDB36857	Cinncassiol E
397.190386	N	C17H34O8S [M-H]-	-	-
397.213002	H / N	C23H30N2O4 [M-H]-	HMDB41933	Mitragynine
397.213002	H / N	C23H30N2O4 [M-H]-	HMDB41984	Pholcodine
397.213002	H / N	C23H30N2O4 [M-H]-	HMDB60869	Ramipril Diketopiperazine
397.213978	N	C16H30N8O2S [M-H]-	-	-
398.216518	N	C17H33N7S2 [M-H]-	-	-
398.306421	N	C26H41NO2 [M-H]-	-	-
399.114348	N	C14H24O13 [M-H]-	-	-
399.143376	N	C17H32O4S2 [M+Cl]-	-	-
399.143376	N	C16H33O5PS2 [M-H]-	-	-
399.143376	N	C19H16N10O [M-H]-	-	-
399.167690	N	C20H24N4O5 [M-H]-	-	-
399.363203	H / N	C28H48O [M-H]-	HMDB02869	Campesterol
399.363203	H / N	C28H48O [M-H]-	HMDB11605	4-alpha-Methyl-5-alpha-cholest-7-en-3-beta-ol
399.363203	H / N	C28H48O [M-H]-	HMDB12116	(5Alpha)-campestan-3-one
399.363203	H / N	C28H48O [M-H]-	HMDB30077	(3beta,4alpha,5alpha)-4-Methyl-8(14)-cholesten-3-ol
399.363203	H / N	C28H48O [M-H]-	HMDB30123	(3beta,5alpha,24S)-Ergost-8(14)-en-3-ol
399.363203	H / N	C28H48O [M-H]-	HMDB34224	Dihydrobrassicasterol
399.363203	H / N	C28H48O [M-H]-	HMDB34418	Pollinastanol
399.363203	H / N	C28H48O [M-H]-	HMDB39700	(5alpha,14alpha)-14-Methylcholestan-3-one
401.184864	N	C19H30N2O5 [M+Cl]-	-	-
401.184864	N	C18H31N2O6P [M-H]-	-	-
401.280931	N	C24H38N2O3 [M-H]-	-	-
401.306098	H / N	C26H42O3 [M-H]-	HMDB29458	Oryzarol
401.340100	N	C23H42N6 [M-H]-	-	-
402.188223	N	C17H29N3O8 [M-H]-	-	-
403.139742	H / N	C21H24O8 [M-H]-	HMDB34117	(E)-4'-Methylresveratrol 3-glucoside
403.139742	H / N	C21H24O8 [M-H]-	HMDB37313	Citromitin

403.139742	H / N	C21H24O8 [M-H]-	HMDB39273	Pinostilbenoside
403.170344	N	C14H28N8O2S2 [M-H]-	-	-
403.181688	N	C13H28N10OS2 [M-H]-	-	-
403.181688	N	C15H32O12 [M-H]-	-	-
403.321742	N	C26H44O3 [M-H]-	-	-
405.070819	N	C12H22O13S [M-H]-	-	-
406.146763	N	C15H25N3O10 [M-H]-	-	-
407.256942	N	C21H40O5 [M+Cl]-	-	-
407.256942	N	C20H41O6P [M-H]-	-	-
407.316640	N	C25H44O4 [M-H]-	-	-
409.272568	N	C21H42O5 [M+Cl]-	-	-
409.272568	N	C20H43O6P [M-H]-	-	-
409.293463	N	C20H38N6O3 [M-H]-	-	-
410.172212	H / N	C22H25N3O5 [M-H]-	HMDB38581	Dihydroxyfumitremorgin C
411.075518	N	C18H20O9S [M-H]-	-	-
412.245363	N	C20H35N3O6 [M-H]-	-	-
413.181532	N	C20H30O9 [M-H]-	-	-
413.273270	N	C23H42O4S [M-H]-	-	-
414.200988	N	C16H33N3O7 [M+Cl]-	-	-
414.200988	N	C15H34N3O8P [M-H]-	-	-
415.145660	N	C15H28O13 [M-H]-	-	-
416.246788	N	C16H39N5O3S [M+Cl]-	-	-
417.295700	N	C18H34N12 [M-H]-	-	-
419.216610	N	C16H36N2O8 [M+Cl]-	-	-
419.274896	N	C17H32N12O [M-H]-	-	-
420.229258	N	C25H31N3O3 [M-H]-	-	-
421.272558	N	C22H42O5 [M+Cl]-	-	-
421.272558	H / N	C21H43O6P [M-H]-	HMDB11142	DHAP(18:0e)
421.307167	N	C24H42N2O4 [M-H]-	-	-
422.208469	N	C24H29N3O4 [M-H]-	-	-
423.309180	N	C21H40N6O3 [M-H]-	-	-
425.106575	N	C23H22O6S [M-H]-	-	-
425.127623	N	C20H26O8S [M-H]-	-	-
425.236799	N	C23H38O5S [M-H]-	-	-
425.251710	N	C19H34N6O5 [M-H]-	-	-
425.267506	N	C21H42O6 [M+Cl]-	-	-
425.267506	N	C20H43O7P [M-H]-	-	-
426.159316	N	C20H29NO7S [M-H]-	-	-
427.048660	N	C13H20N2O10S2 [M-H]-	-	-
427.199280	N	C15H28N10O3S [M-H]-	-	-
427.220970	N	C20H36N4O2S2 [M-H]-	-	-
429.222365	N	C17H34N8OS2 [M-H]-	-	-
429.272040	N	C20H38N4O6 [M-H]-	-	-
429.296894	N	C22H42N2O6 [M-H]-	-	-
430.195315	N	C18H33N5O3S2 [M-H]-	-	-
431.124553	N	C16H24N4O8S [M-H]-	-	-
431.267973	N	C22H40N2O4 [M+Cl]-	-	-
431.267973	N	C21H41N2O5P [M-H]-	-	-
431.313881	N	C23H40N6O2 [M-H]-	-	-
432.198859	N	C18H31N3O9 [M-H]-	-	-
433.173109	N	C20H26N4O7 [M-H]-	-	-
433.283133	N	C24H34N8 [M-H]-	-	-
434.221863	N	C20H37NO7S [M-H]-	-	-
434.258410	N	C21H41NO6S [M-H]-	-	-
435.181279	H / N	C26H28O6 [M-H]-	HMDB30849	Artocarpin
435.181279	H / N	C26H28O6 [M-H]-	HMDB33806	2'-O-Methylcajanone
435.181279	H / N	C26H28O6 [M-H]-	HMDB41212	Kanzonol K
435.249405	N	C26H40OS [M+Cl]-	-	-
435.249405	N	C17H37N6O5P [M-H]-	-	-
436.103772	N	C23H19NO8 [M-H]-	-	-
436.180050	N	C22H31NO6S [M-H]-	-	-
436.184252	N	C19H27N5O7 [M-H]-	-	-
436.184252	N	C20H31N5O2S2 [M-H]-	-	-
438.127754	N	C18H25N5O4S2 [M-H]-	-	-
439.106890	N	C20H24O9S [M-H]-	-	-
441.133733	N	C19H26N2O8S [M-H]-	-	-
441.225303	N	C22H38N2O3S2 [M-H]-	-	-
442.353858	H / N	C25H49NO5 [M-H]-	HMDB13154	12-Hydroxy-12-octadecanoylcarnitine
443.220922	N	C23H36O6 [M+Cl]-	-	-
443.220922	N	C22H37O7P [M-H]-	-	-
443.238047	N	C18H36N8OS2 [M-H]-	-	-
443.251393	N	C20H36N4O7 [M-H]-	-	-

443.254128	N	C20H36N6O3 [M+Cl]-	-	-
443.254128	N	C19H37N6O4P [M-H]-	-	-
445.077676	H / N	C21H18O11 [M-H]-	HMDB32877	Glucorhein
445.077676	H / N	C21H18O11 [M-H]-	HMDB41737	Genistein 4'-O-glucuronide
445.077676	H / N	C21H18O11 [M-H]-	HMDB41738	Genistein 5-O-glucuronide
445.077676	H / N	C21H18O11 [M-H]-	HMDB41739	Genistein 7-O-glucuronide
445.077676	H / N	C21H18O11 [M-H]-	HMDB41832	Baicalin
445.172869	N	C21H26N4O7 [M-H]-	-	-
445.231337	N	C20H38N4O3S2 [M-H]-	-	-
446.327519	N	C27H45NO4 [M-H]-	-	-
447.182715	N	C28H24N4O2 [M-H]-	-	-
448.224184	H / N	C26H31N3O4 [M-H]-	HMDB39857	Cadabicine methyl ether
448.268161	N	C21H35N7O4 [M-H]-	-	-
449.229177	N	C23H34N2O7 [M-H]-	-	-
449.309814	N	C27H46O3S [M-H]-	-	-
451.176203	H / N	C26H28O7 [M-H]-	HMDB41323	Heteroartonin A
451.223361	N	C18H36N4O7S [M-H]-	-	-
451.452111	H / N	C30H60O2 [M-H]-	HMDB29987	(+)-11-Hydroxy-9-triacontanone
451.452111	H / N	C30H60O2 [M-H]-	HMDB30925	Melissic acid A
453.086128	N	C20H22O10S [M-H]-	-	-
454.338740	N	C18H45N9O2 [M+Cl]-	-	-
455.168996	N	C19H32O10 [M+Cl]-	-	-
455.168996	N	C18H33O11P [M-H]-	-	-
455.224925	N	C18H36N2O11 [M-H]-	-	-
455.277894	N	C24H36N6O3 [M-H]-	-	-
455.277894	N	C21H45O8P [M-H]-	-	-
456.206162	N	C22H35NO7S [M-H]-	-	-
457.209840	N	C16H30N10O4S [M-H]-	-	-
457.259310	H / N	C27H38O6 [M-H]-	HMDB37611	Lucidenic acid A
457.364302	N	C25H50N2O5 [M-H]-	-	-
459.173458	N	C18H28N4O10 [M-H]-	-	-
462.234300	N	C21H37NO10 [M-H]-	-	-
463.187741	N	C26H28N2O6 [M-H]-	-	-
463.224880	N	C18H40N2O7S [M+Cl]-	-	-
463.372715	N	C28H52N2OS [M-H]-	-	-
464.286480	N	C22H43NO9 [M-H]-	-	-
464.292328	N	C21H39N9OS [M-H]-	-	-
465.245379	N	C20H38N2O10 [M-H]-	-	-
466.190480	N	C23H33NO7S [M-H]-	-	-
466.257854	N	C22H41NO7 [M+Cl]-	-	-
466.257854	N	C21H42NO8P [M-H]-	-	-
466.274254	N	C24H41N3O4S [M-H]-	-	-
467.348780	N	C26H48N2O5 [M-H]-	-	-
468.294162	N	C21H39N7O5 [M-H]-	-	-
469.202611	N	C23H30N6O3S [M-H]-	-	-
469.306334	N	C23H42N6O2 [M+Cl]-	-	-
470.224844	N	C23H37N3O3S [M+Cl]-	-	-
470.260320	N	C20H41NO11 [M-H]-	-	-
471.093307	H / N	C23H20O11 [M-H]-	HMDB38363	(-)-Epigallocatechin 3-(3-methyl-gallate)
471.093307	H / N	C23H20O11 [M-H]-	HMDB40293	(-)-Epigallocatechin 3-(4-methyl-gallate)
471.169599	N	C22H32O9S [M-H]-	-	-
471.206300	N	C16H36N6O6S2 [M-H]-	-	-
471.329052	N	C17H44N10O3 [M+Cl]-	-	-
472.167125	N	C17H31NO14 [M-H]-	-	-
472.240518	N	C23H39N3O3S [M+Cl]-	-	-
472.240518	N	C20H43NO7S2 [M-H]-	-	-
472.364401	N	C26H51NO6 [M-H]-	-	-
475.193649	N	C20H32N2O11 [M-H]-	-	-
475.222510	N	C15H36N8O5S [M+Cl]-	-	-
475.222510	N	C23H40N2O2S2 [M+Cl]-	-	-
475.222510	N	C20H36N4O7S [M-H]-	-	-
475.265449	N	C25H44O4S [M+Cl]-	-	-
475.265449	N	C24H45O5PS [M-H]-	-	-
475.319577	H / N	C26H48O5 [M+Cl]-	HMDB29804	Momordol
475.319577	N	C25H49O6P [M-H]-	-	-
476.250022	N	C22H39NO10 [M-H]-	-	-
476.292001	N	C29H39N3O3 [M-H]-	-	-
477.172577	N	C19H30N2O12 [M-H]-	-	-
477.183760	N	C18H30N4O11 [M-H]-	-	-
477.271375	N	C27H42N2OS [M+Cl]-	-	-
477.271375	N	C24H46O5S2 [M-H]-	-	-
477.392263	N	C26H50N6O2 [M-H]-	-	-

478.338742	N	C24H49NO8 [M-H]-	-	-
479.116966	N	C26H24O7S [M-H]-	-	-
479.211151	N	C25H36O7S [M-H]-	-	-
481.207779	H / N	C24H34O10 [M-H]-	HMDB36601	3'-Hydroxy-T2 Toxin
481.213036	N	C22H34N4O6S [M-H]-	-	-
481.260933	N	C30H34N4O2 [M-H]-	-	-
481.262971	N	C26H42O6S [M-H]-	-	-
481.364597	N	C27H50N2O5 [M-H]-	-	-
483.096647	N	C21H24O11S [M-H]-	-	-
483.185863	N	C20H24N10O5 [M-H]-	-	-
483.185863	N	C28H28N4O2S [M-H]-	-	-
483.185863	N	C17H33N4O10P [M-H]-	-	-
483.236909	N	C22H40O9 [M+Cl]-	-	-
483.236909	N	C21H41O10P [M-H]-	-	-
484.201164	N	C23H35NO8S [M-H]-	-	-
484.268254	N	C22H43NO8 [M+Cl]-	-	-
484.268254	N	C21H44NO9P [M-H]-	-	-
485.184940	N	C23H34O9S [M-H]-	-	-
485.261825	N	C22H38N4O8 [M-H]-	-	-
486.218164	N	C24H33N5O4S [M-H]-	-	-
487.203211	N	C19H36O14 [M-H]-	-	-
487.217603	N	C18H36N4O9 [M+Cl]-	-	-
487.217603	N	C17H37N4O10P [M-H]-	-	-
487.259203	N	C22H40N4O6S [M-H]-	-	-
487.334942	H / N	C31H48O2 [M+Cl]-	HMDB34839	2',3'-Dihydro-phytomenadione
487.334942	H / N	C31H48O2 [M+Cl]-	HMDB60502	Phylloquinol
488.149330	N	C23H27N3O7S [M-H]-	-	-
488.342705	N	C27H47N5OS [M-H]-	-	-
489.202985	N	C28H30N2O6 [M-H]-	-	-
489.232676	N	C20H38N6O4S2 [M-H]-	-	-
489.431256	N	C32H58O3 [M-H]-	-	-
490.230998	N	C23H33N5O7 [M-H]-	-	-
490.273856	N	C21H41N7O2S [M+Cl]-	-	-
490.276181	N	C25H45NO4S [M+Cl]-	-	-
492.206845	N	C18H35N7O5S2 [M-H]-	-	-
495.434293	N	C32H60O [M+Cl]-	-	-
496.147737	N	C16H31N7O5S3 [M-H]-	-	-
496.186453	N	C16H31N9O5S [M+Cl]-	-	-
496.223390	N	C22H35N5O6S [M-H]-	-	-
497.199047	N	C19H34N2O13 [M-H]-	-	-
497.323404	N	C26H46N2O7 [M-H]-	-	-
497.363493	H / N	C32H50O4 [M-H]-	HMDB32022	Tsugaric acid A
497.363493	H / N	C32H50O4 [M-H]-	HMDB35160	beta-Boswellic acid acetate
497.363493	H / N	C32H50O4 [M-H]-	HMDB36008	Acetylursolic acid
497.363493	H / N	C32H50O4 [M-H]-	HMDB36674	Ursololactone
498.366990	N	C26H53N5S2 [M-H]-	-	-
500.280599	H / N	C32H39NO4 [M-H]-	HMDB05030	Fexofenadine
501.277961	N	C30H42O4 [M+Cl]-	-	-
501.277961	N	C19H42N4O11 [M-H]-	-	-
501.283744	N	C23H46O9 [M+Cl]-	-	-
501.283744	N	C22H47O10P [M-H]-	-	-
501.371005	N	C23H50N8O2S [M-H]-	-	-
501.371005	N	C31H46N6 [M-H]-	-	-
504.177577	N	C27H27N3O7 [M-H]-	-	-
504.263439	N	C24H43NO8S [M-H]-	-	-
505.423403	N	C28H54N6O2 [M-H]-	-	-
506.281480	N	C33H37N3O2 [M-H]-	-	-
506.281480	N	C18H41N11O2S2 [M-H]-	-	-
507.193041	N	C18H36O16 [M-H]-	-	-
507.220434	N	C22H40N2O7S2 [M-H]-	-	-
508.264593	N	C22H39N9OS2 [M-H]-	-	-
509.198075	N	C23H38O8S [M+Cl]-	-	-
509.198075	N	C22H39O9PS [M-H]-	-	-
509.222533	N	C27H34N4O4S [M-H]-	-	-
511.227628	N	C21H36N8O3S2 [M-H]-	-	-
513.033867	N	C12H22N2O16S2 [M-H]-	-	-
513.033867	N	C22H15N2O11P [M-H]-	-	-
513.206934	N	C20H34N8O4S2 [M-H]-	-	-
516.236072	N	C19H35N9O6S [M-H]-	-	-
518.370015	N	C27H53NO8 [M-H]-	-	-
520.310050	N	C29H47NO5S [M-H]-	-	-
521.202958	H / N	C26H34O11 [M-H]-	HMDB32907	Isolariciresinol 9-O-beta-D-glucoside

521.202958	H / N	C26H34O11 [M-H]-	HMDB34749	Icariside E5
521.202958	H / N	C26H34O11 [M-H]-	HMDB38711	(7'R,8'R)-4,7'-Epoxy-3',5-dimethoxy-4',9,9'-lignanetriol 9'-glucoside
521.202958	H / N	C26H34O11 [M-H]-	HMDB38927	Isolariciresinol 9'-O-beta-D-glucoside
521.202958	H / N	C26H34O11 [M-H]-	HMDB40471	Isolariciresinol 4'-O-beta-D-glucoside
523.319808	H / N	C30H48O5 [M+Cl]-	HMDB34036	Pitheduloside I
523.319808	H / N	C30H48O5 [M+Cl]-	HMDB34502	Arjunolic acid
523.319808	H / N	C30H48O5 [M+Cl]-	HMDB34531	Camelliagenin B
523.319808	H / N	C30H48O5 [M+Cl]-	HMDB35118	Madasiatic acid
523.319808	H / N	C30H48O5 [M+Cl]-	HMDB35782	Esculentic acid (Diplazium)
523.319808	H / N	C30H48O5 [M+Cl]-	HMDB35957	Hovenolactone
523.319808	H / N	C30H48O5 [M+Cl]-	HMDB36311	Centellasapogenol A
523.319808	H / N	C30H48O5 [M+Cl]-	HMDB36639	Glyyunnansapogenin B
523.319808	H / N	C30H48O5 [M+Cl]-	HMDB36651	Euscaphic acid
523.319808	H / N	C30H48O5 [M+Cl]-	HMDB36961	(3beta,6alpha,19alpha)-3,6,19-Trihydroxy-12-ursen-28-oic acid
523.319808	H / N	C30H48O5 [M+Cl]-	HMDB37782	Ganoderiol D
523.319808	H / N	C30H48O5 [M+Cl]-	HMDB38116	Ananasic acid
523.319808	H / N	C30H48O5 [M+Cl]-	HMDB40391	16beta-Hydroxystellatogenin
523.319808	H / N	C30H48O5 [M+Cl]-	HMDB41039	21beta-Hydroxyhederagenin
523.375184	N	C29H52N2O6 [M-H]-	-	-
524.236338	N	C23H35N5O9 [M-H]-	-	-
526.257975	N	C27H41NO7 [M+Cl]-	-	-
526.257975	N	C26H42NO8P [M-H]-	-	-
530.279387	N	C26H45NO8S [M-H]-	-	-
530.370010	N	C28H53NO8 [M-H]-	-	-
531.129954	N	C29H24O10 [M-H]-	-	-
531.254007	N	C21H40N8O4S2 [M-H]-	-	-
531.438683	N	C30H56N6O2 [M-H]-	-	-
533.457911	N	C34H62O4 [M-H]-	-	-
534.169654	N	C20H33N5O8S2 [M-H]-	-	-
534.307506	N	C29H45NO8 [M-H]-	-	-
535.172661	N	C28H28N2O9 [M-H]-	-	-
535.172661	N	C21H36N4O6S3 [M-H]-	-	-
535.172661	N	C21H28N8O7S [M-H]-	-	-
535.203694	N	C23H36O14 [M-H]-	-	-
535.234772	N	C24H36N6O6S [M-H]-	-	-
535.234772	N	C32H32N4O4 [M-H]-	-	-
535.255235	N	C28H40O10 [M-H]-	-	-
535.273684	N	C29H44O7S [M-H]-	-	-
545.338633	N	C34H46N2O4 [M-H]-	-	-
545.397612	H / N	C31H58O5 [M+Cl]-	HMDB07009	DG(14:0/14:1(9Z)/0:0)
545.397612	H / N	C31H58O5 [M+Cl]-	HMDB07037	DG(14:1(9Z)/14:0/0:0)
545.397612	H / N	C31H58O5 [M+Cl]-	HMDB55959	DG(14:0/0:0/14:1n5)
545.397612	N	C30H59O6P [M-H]-	-	-
547.226030	N	C26H44N2O2S3 [M+Cl]-	-	-
547.226030	N	C22H36N4O12 [M-H]-	-	-
547.338456	N	C30H48N2O7 [M-H]-	-	-
549.270783	H / N	C29H42O10 [M-H]-	HMDB34362	Desglucocheirotoxin
553.353550	H / N	C34H50O6 [M-H]-	HMDB35333	Ganoderic acid Me
553.353550	H / N	C34H50O6 [M-H]-	HMDB35621	Ganoderic acid R
553.353550	H / N	C34H50O6 [M-H]-	HMDB36745	(2xi,3xi)-2,3-Dihydroxy-12,18-ursadien-28-oic acid diacetate
556.175986	N	C27H31N3O8S [M-H]-	-	-
556.324202	N	C27H47N3O9 [M-H]-	-	-
556.369203	N	C31H51N5O2S [M-H]-	-	-
557.215898	N	C27H38O10 [M+Cl]-	-	-
557.215898	N	C26H39O11P [M-H]-	-	-
559.075147	N	C19H16N10O9S [M-H]-	-	-
559.075147	N	C16H25N4O14PS [M-H]-	-	-
561.339430	N	C27H50N2O10 [M-H]-	-	-
561.379693	H / N	C33H54O7 [M-H]-	HMDB10330	Cholesterol glucuronide
563.423223	N	C35H60O3 [M+Cl]-	-	-
563.423223	N	C34H61O4P [M-H]-	-	-
567.295072	N	C28H44N4O6 [M+Cl]-	-	-
567.295072	N	C30H36N10O2 [M-H]-	-	-
567.295072	N	C27H45N4O7P [M-H]-	-	-
570.245869	N	C29H37N3O9 [M-H]-	-	-
571.277731	N	C29H40N4O8 [M-H]-	-	-
571.288948	N	C26H48O11 [M+Cl]-	-	-
571.288948	N	C25H49O12P [M-H]-	-	-
571.412964	N	C27H56N8O3S [M-H]-	-	-
571.412964	N	C35H52N6O [M-H]-	-	-
571.416369	N	C32H56N6OS [M-H]-	-	-
573.429184	H / N	C33H62O5 [M+Cl]-	HMDB07012	DG(14:0/16:1(9Z)/0:0)

573.429184	H / N	C33H62O5 [M+Cl]-	HMDB07040	DG(14:1(9Z)/16:0/0:0)
573.429184	H / N	C33H62O5 [M+Cl]-	HMDB07096	DG(16:0/14:1(9Z)/0:0)
573.429184	H / N	C33H62O5 [M+Cl]-	HMDB07124	DG(16:1(9Z)/14:0/0:0)
573.429184	H / N	C33H62O5 [M+Cl]-	HMDB55960	DG(14:0/0:0/16:1n7)
573.429184	H / N	C33H62O5 [M+Cl]-	HMDB56014	DG(16:0/0:0/14:1n5)
573.429184	N	C32H63O6P [M-H]-	-	-
575.183112	N	C21H36O18 [M-H]-	-	-
575.444747	H / N	C33H64O5 [M+Cl]-	HMDB07011	DG(14:0/16:0/0:0)
575.444747	H / N	C33H64O5 [M+Cl]-	HMDB07068	DG(15:0/15:0/0:0)
575.444747	H / N	C33H64O5 [M+Cl]-	HMDB07095	DG(16:0/14:0/0:0)
575.444747	H / N	C33H64O5 [M+Cl]-	HMDB55954	DG(14:0/0:0/16:0)
575.444747	H / N	C33H64O5 [M+Cl]-	HMDB55981	DG(15:0/0:0/15:0)
575.444747	N	C32H65O6P [M-H]-	-	-
576.447951	N	C31H63NO8 [M-H]-	-	-
576.463890	N	C35H63NO5 [M-H]-	-	-
576.463890	N	C28H63N7O3S [M-H]-	-	-
577.479440	N	C31H66N2O7 [M-H]-	-	-
579.405774	N	C37H56O5 [M-H]-	-	-
581.279136	N	C30H46O9S [M-H]-	-	-
582.198159	N	C30H33NO11 [M-H]-	-	-
582.388158	N	C30H57N5O2S2 [M-H]-	-	-
584.352413	N	C25H55N5O6S2 [M-H]-	-	-
584.352413	N	C25H47N9O7 [M-H]-	-	-
584.352413	N	C33H51N3O4S [M-H]-	-	-
585.274503	N	C22H46N6O8S2 [M-H]-	-	-
586.275219	N	C27H41N9O2S2 [M-H]-	-	-
586.277478	N	C30H41N3O9 [M-H]-	-	-
589.357636	N	C27H54N6O4S2 [M-H]-	-	-
589.458903	N	C35H62N2O5 [M-H]-	-	-
591.457878	N	C33H69O4PS [M-H]-	-	-
593.425018	N	C35H62O5S [M-H]-	-	-
593.425018	N	C28H62N6O3S2 [M-H]-	-	-
594.510570	N	C36H69NO5 [M-H]-	-	-
595.289082	N	C28H48O11 [M+Cl]-	-	-
595.289082	N	C27H49O12P [M-H]-	-	-
595.400536	N	C37H56O6 [M-H]-	-	-
596.353564	N	C27H51N9O2S2 [M-H]-	-	-
596.358847	N	C27H55N3O9S [M-H]-	-	-
596.362647	N	C32H55NO7S [M-H]-	-	-
596.364570	N	C41H47N3O [M-H]-	-	-
597.176729	N	C34H30O10 [M-H]-	-	-
597.176729	N	C19H34N8O10S2 [M-H]-	-	-
597.274048	N	C30H46O10S [M-H]-	-	-
597.304613	N	C28H50O11 [M+Cl]-	-	-
597.304613	N	C27H51O12P [M-H]-	-	-
597.357067	N	C26H54N6O5S [M+Cl]-	-	-
597.357067	N	C25H55N6O6PS [M-H]-	-	-
598.277193	N	C31H41N3O9 [M-H]-	-	-
598.361028	N	C32H49N5O6 [M-H]-	-	-
603.476346	H / N	C35H68O5 [M+Cl]-	HMDB07013	DG(14:0/18:0/0:0)
603.476346	H / N	C35H68O5 [M+Cl]-	HMDB07098	DG(16:0/16:0/0:0)
603.476346	H / N	C35H68O5 [M+Cl]-	HMDB07153	DG(18:0/14:0/0:0)
603.476346	H / N	C35H68O5 [M+Cl]-	HMDB31011	Glycerol 1,3-dihexadecanoate
603.476346	H / N	C35H68O5 [M+Cl]-	HMDB55955	DG(14:0/0:0/18:0)
603.476346	H / N	C35H68O5 [M+Cl]-	HMDB56009	DG(16:0/0:0/16:0)
603.476346	N	C34H69O6P [M-H]-	-	-
605.339930	N	C30H54N2O6S [M+Cl]-	-	-
605.339930	N	C27H50N4O11 [M-H]-	-	-
605.406027	N	C35H58O8 [M-H]-	-	-
608.380567	N	C33H55NO9 [M-H]-	-	-
609.291920	N	C31H46O12 [M-H]-	-	-
611.395496	N	C37H56O7 [M-H]-	-	-
615.439523	H / N	C35H64O6 [M+Cl]-	HMDB33165	4-Deoxyannoreticuin
615.439523	H / N	C35H64O6 [M+Cl]-	HMDB35183	Murisolin
615.439523	H / N	C35H64O6 [M+Cl]-	HMDB39453	Muricin H
615.439523	H / N	C35H64O6 [M+Cl]-	HMDB40870	Corossoline
615.439523	H / N	C35H64O6 [M+Cl]-	HMDB41374	cis-Murisolinone
615.439523	N	C34H65O7P [M-H]-	-	-
617.332304	N	C29H50N4O8 [M+Cl]-	-	-
617.332304	N	C28H51N4O9P [M-H]-	-	-
617.385091	H / N	C39H54O6 [M-H]-	HMDB34539	3-O-cis-Coumaroylmaslinic acid
617.385091	H / N	C39H54O6 [M-H]-	HMDB36299	3-O-p-trans-Coumaroylalphitolic acid

617.385091	H / N	C39H54O6 [M-H]-	HMDB40495	cis-p-Coumaroylcorosolic acid
617.385091	N	C32H54N6O4S [M-H]-	-	-
617.455123	N	C35H66O6 [M+Cl]-	-	-
617.455123	N	C34H67O7P [M-H]-	-	-
618.388315	N	C33H57N5O2S2 [M-H]-	-	-
618.458223	N	C33H65NO9 [M-H]-	-	-
620.380678	N	C34H55NO9 [M-H]-	-	-
621.401074	N	C35H58O9 [M-H]-	-	-
624.336657	N	C28H47N7O9 [M-H]-	-	-
625.159355	N	C30H31N2O11P [M-H]-	-	-
625.159355	N	C28H34O14S [M-H]-	-	-
627.390633	N	C37H56O8 [M-H]-	-	-
629.390702	N	C33H58O11 [M-H]-	-	-
631.326858	N	C30H52N2O10S [M-H]-	-	-
631.421893	H / N	C37H60O8 [M-H]-	HMDB35821	Momordicoside G
631.421893	H / N	C37H60O8 [M-H]-	HMDB36966	28-Glucopyranosyl-3-methyloleanolic acid
631.513027	N	C40H72O3S [M-H]-	-	-
633.299306	N	C31H54N2O3S3 [M+Cl]-	-	-
633.299306	N	C27H46N4O13 [M-H]-	-	-
633.306311	N	C29H50N2O11S [M-H]-	-	-
633.449181	N	C37H66N2O2S2 [M-H]-	-	-
643.421713	N	C38H60O8 [M-H]-	-	-
643.479627	N	C36H68O9 [M-H]-	-	-
647.464139	N	C37H64N2O7 [M-H]-	-	-
649.460349	H / N	C39H66O5 [M+Cl]-	HMDB07032	DG(14:0/22:5(4Z,7Z,10Z,13Z,16Z)/0:0)
649.460349	H / N	C39H66O5 [M+Cl]-	HMDB07033	DG(14:0/22:5(7Z,10Z,13Z,16Z,19Z)/0:0)
649.460349	H / N	C39H66O5 [M+Cl]-	HMDB07060	DG(14:1(9Z)/22:4(7Z,10Z,13Z,16Z)/0:0)
649.460349	H / N	C39H66O5 [M+Cl]-	HMDB07114	DG(16:0/20:5(5Z,8Z,11Z,14Z,17Z)/0:0)
649.460349	H / N	C39H66O5 [M+Cl]-	HMDB07141	DG(16:1(9Z)/20:4(5Z,8Z,11Z,14Z)/0:0)
649.460349	H / N	C39H66O5 [M+Cl]-	HMDB07142	DG(16:1(9Z)/20:4(8Z,11Z,14Z,17Z)/0:0)
649.460349	H / N	C39H66O5 [M+Cl]-	HMDB07193	DG(18:1(11Z)/18:4(6Z,9Z,12Z,15Z)/0:0)
649.460349	H / N	C39H66O5 [M+Cl]-	HMDB07222	DG(18:1(9Z)/18:4(6Z,9Z,12Z,15Z)/0:0)
649.460349	H / N	C39H66O5 [M+Cl]-	HMDB07249	DG(18:2(9Z,12Z)/18:3(6Z,9Z,12Z)/0:0)
649.460349	H / N	C39H66O5 [M+Cl]-	HMDB07250	DG(18:2(9Z,12Z)/18:3(9Z,12Z,15Z)/0:0)
649.460349	H / N	C39H66O5 [M+Cl]-	HMDB07277	DG(18:3(6Z,9Z,12Z)/18:2(9Z,12Z)/0:0)
649.460349	H / N	C39H66O5 [M+Cl]-	HMDB07306	DG(18:3(9Z,12Z,15Z)/18:2(9Z,12Z)/0:0)
649.460349	H / N	C39H66O5 [M+Cl]-	HMDB07333	DG(18:4(6Z,9Z,12Z,15Z)/18:1(11Z)/0:0)
649.460349	H / N	C39H66O5 [M+Cl]-	HMDB07334	DG(18:4(6Z,9Z,12Z,15Z)/18:1(9Z)/0:0)
649.460349	H / N	C39H66O5 [M+Cl]-	HMDB07505	DG(20:4(5Z,8Z,11Z,14Z)/16:1(9Z)/0:0)
649.460349	H / N	C39H66O5 [M+Cl]-	HMDB07534	DG(20:4(8Z,11Z,14Z,17Z)/16:1(9Z)/0:0)
649.460349	H / N	C39H66O5 [M+Cl]-	HMDB07562	DG(20:5(5Z,8Z,11Z,14Z,17Z)/16:0/0:0)
649.460349	H / N	C39H66O5 [M+Cl]-	HMDB07676	DG(22:4(7Z,10Z,13Z,16Z)/14:1(9Z)/0:0)
649.460349	H / N	C39H66O5 [M+Cl]-	HMDB07704	DG(22:5(4Z,7Z,10Z,13Z,16Z)/14:0/0:0)
649.460349	H / N	C39H66O5 [M+Cl]-	HMDB07733	DG(22:5(7Z,10Z,13Z,16Z,19Z)/14:0/0:0)
649.460349	H / N	C39H66O5 [M+Cl]-	HMDB55974	DG(14:0/0:0/22:5n6)
649.460349	H / N	C39H66O5 [M+Cl]-	HMDB55979	DG(14:0/0:0/22:5n3)
649.460349	H / N	C39H66O5 [M+Cl]-	HMDB56033	DG(16:0/0:0/20:5n3)
649.460349	H / N	C39H66O5 [M+Cl]-	HMDB56148	DG(14:1n5/0:0/22:4n6)
649.460349	H / N	C39H66O5 [M+Cl]-	HMDB56167	DG(16:1n7/0:0/20:4n6)
649.460349	H / N	C39H66O5 [M+Cl]-	HMDB56173	DG(16:1n7/0:0/20:4n3)
649.460349	H / N	C39H66O5 [M+Cl]-	HMDB56192	DG(18:1n7/0:0/18:4n3)
649.460349	H / N	C39H66O5 [M+Cl]-	HMDB56211	DG(18:1n9/0:0/18:4n3)
651.556997	N	C40H76O6 [M-H]-	-	-
653.349466	N	C32H58O9S [M+Cl]-	-	-
653.349466	N	C31H59O10PS [M-H]-	-	-
653.464477	N	C38H62N4O5 [M-H]-	-	-
654.477019	N	C37H69NO6S [M-H]-	-	-
655.363684	N	C33H56N2O9S [M-H]-	-	-
655.480509	N	C38H64N4O5 [M-H]-	-	-
661.359624	H / N	C36H54O11 [M-H]-	HMDB33729	1-Acetyl-3,27-dihydroxywitha-5,24-dienolide 3-glucoside
661.359624	H / N	C36H54O11 [M-H]-	HMDB34201	Physalolactone B 3-glucoside
661.359624	H / N	C36H54O11 [M-H]-	HMDB41131	Prosapogenin
663.375194	H / N	C36H56O11 [M-H]-	HMDB34552	Medicagenic acid 3-O-beta-D-glucoside
663.375194	H / N	C36H56O11 [M-H]-	HMDB34636	Phytolaccasaponin G
663.375194	H / N	C36H56O11 [M-H]-	HMDB41347	Elatoside G
665.319452	N	C35H46N4O9 [M-H]-	-	-
665.474831	N	C37H66N2O8 [M-H]-	-	-
670.440768	N	C34H65N5O4S2 [M-H]-	-	-
670.440768	N	C34H57N9O5 [M-H]-	-	-
672.515301	N	C48H67NO [M-H]-	-	-
672.515301	N	C33H71N9OS2 [M-H]-	-	-
675.430152	N	C39H64O7S [M-H]-	-	-

679.193951	N	C24H40O22 [M-H]-	-	-
685.309041	N	C34H46N4O11 [M-H]-	-	-
689.295784	N	C33H47N4O10P [M-H]-	-	-
691.298396	N	C36H44N4O10 [M-H]-	-	-
701.495348	N	C37H70N2O10 [M-H]-	-	-
709.443695	N	C41H62N2O8 [M-H]-	-	-
714.508305	N	C40H73NO7 [M+Cl]-	-	-
714.508305	H / N	C39H74NO8P [M-H]-	HMDB08835	PE(14:0/20:2(11Z,14Z))
714.508305	H / N	C39H74NO8P [M-H]-	HMDB08867	PE(14:1(9Z)/20:1(11Z))
714.508305	H / N	C39H74NO8P [M-H]-	HMDB08928	PE(16:0/18:2(9Z,12Z))
714.508305	H / N	C39H74NO8P [M-H]-	HMDB08959	PE(16:1(9Z)/18:1(11Z))
714.508305	H / N	C39H74NO8P [M-H]-	HMDB08960	PE(16:1(9Z)/18:1(9Z))
714.508305	H / N	C39H74NO8P [M-H]-	HMDB09023	PE(18:1(11Z)/16:1(9Z))
714.508305	H / N	C39H74NO8P [M-H]-	HMDB09056	PE(18:1(9Z)/16:1(9Z))
714.508305	H / N	C39H74NO8P [M-H]-	HMDB09088	PE(18:2(9Z,12Z)/16:0)
714.508305	H / N	C39H74NO8P [M-H]-	HMDB09251	PE(20:1(11Z)/14:1(9Z))
714.508305	H / N	C39H74NO8P [M-H]-	HMDB09283	PE(20:2(11Z,14Z)/14:0)
714.516417	N	C39H73NO10 [M-H]-	-	-
721.422864	N	C38H58N8O4S [M-H]-	-	-
722.506033	N	C37H73NO12 [M-H]-	-	-
725.536420	N	C45H74O7 [M-H]-	-	-
734.504372	N	C35H73N7O5S2 [M-H]-	-	-
735.593608	N	C48H80O5 [M-H]-	-	-
753.661543	N	C46H90O7 [M-H]-	-	-
755.619817	N	C48H84O6 [M-H]-	-	-
757.501128	N	C43H70N2O9 [M-H]-	-	-
765.576577	N	C41H82N2O8 [M+Cl]-	-	-
779.583315	N	C49H80O7 [M-H]-	-	-
789.588994	N	C47H82O9 [M-H]-	-	-
807.615056	N	C51H84O7 [M-H]-	-	-
817.560379	N	C45H82O10 [M+Cl]-	-	-
817.560379	N	C44H83O11P [M-H]-	-	-
895.739993	N	C57H100O7 [M-H]-	-	-

Abbreviations: H – annotated with HMDB, N – annotated with NetCalc.

Table S16. Features selected by ML-PLS-DA (followed by filtering out variables most likely influenced by time) in case of plasma metabolome data.

Exp. Mass	H / N	Molecular Formula	HMDB id	Name of the metabolite
Features selected for the BR group				
169.122263	H / N	C10H16O2 [M+H]+	HMDB13105	trans-4,5-epoxy-2(E)-decenal
169.122263	H / N	C10H16O2 [M+H]+	HMDB31156	Ethyl (4Z)-4,7-octadienoate
169.122263	H / N	C10H16O2 [M+H]+	HMDB31273	Methyl octynecarboxylate
169.122263	H / N	C10H16O2 [M+H]+	HMDB32219	(+/-)-Dihydromintlactone
169.122263	H / N	C10H16O2 [M+H]+	HMDB32312	2,4-Hexadienyl butyrate
169.122263	H / N	C10H16O2 [M+H]+	HMDB32313	2,4-Hexadienyl isobutyrate
169.122263	H / N	C10H16O2 [M+H]+	HMDB32319	cis-3-Hexenyl crotonate
169.122263	H / N	C10H16O2 [M+H]+	HMDB32434	(+/-)-2-(5-Methyl-5-vinyltetrahydrofuran-2-yl)propionaldehyde
169.122263	H / N	C10H16O2 [M+H]+	HMDB33700	(-)-(Z)-Tetrahydro-6-(2-pentenyl)-2H-pyran-2-one
169.122263	H / N	C10H16O2 [M+H]+	HMDB34452	5,6-Dihydro-6-pentyl-2H-pyran-2-one
169.122263	H / N	C10H16O2 [M+H]+	HMDB34670	6-Hydroxy-2,6-dimethyl-2,7-octadien-4-one
169.122263	H / N	C10H16O2 [M+H]+	HMDB35714	Epoxyartemisia ketone
169.122263	H / N	C10H16O2 [M+H]+	HMDB35766	Ascaridole
169.122263	H / N	C10H16O2 [M+H]+	HMDB35829	Dihydronepetalactone
169.122263	H / N	C10H16O2 [M+H]+	HMDB36067	Epoxycampholenic aldehyde
169.122263	H / N	C10H16O2 [M+H]+	HMDB36103	Geranic acid
169.122263	H / N	C10H16O2 [M+H]+	HMDB37014	gamma-Diosphenol
169.122263	H / N	C10H16O2 [M+H]+	HMDB37175	4-Isopropyl-3-cyclohexene-1-carboxylic acid
169.122263	H / N	C10H16O2 [M+H]+	HMDB37821	xi-1,8,8-Trimethyl-2-oxabicyclo[3.2.1]octan-3-one
169.122263	H / N	C10H16O2 [M+H]+	HMDB40639	(xi)-(Z)-5-(3-Hexenyl)dihydro-2(3H)-furanone
171.101519	H / N	C9H14O3 [M+H]+	HMDB30471	1,4-Ipomeadiol
171.101519	H / N	C9H14O3 [M+H]+	HMDB38276	cis-3-Hexenyl pyruvate
177.054597	H / N	C10H8O3 [M+H]+	HMDB29758	Herniarin
177.054597	H / N	C10H8O3 [M+H]+	HMDB31054	10-Hydroxy-2,8-decadiene-4,6-diynoic acid
177.054597	H / N	C10H8O3 [M+H]+	HMDB32883	1,4,5-Naphthalenetriol
177.054597	H / N	C10H8O3 [M+H]+	HMDB32990	7-Hydroxy-6-methyl-2H-1-benzopyran-2-one
177.054597	H / N	C10H8O3 [M+H]+	HMDB33813	3-(3,4-Methylenedioxyphenyl)propenal
177.054597	H / N	C10H8O3 [M+H]+	HMDB59622	4-Methylumbelliferone
177.090967	H / N	C11H12O2 [M+H]+	HMDB29699	Cinnamyl acetate
177.090967	H / N	C11H12O2 [M+H]+	HMDB33834	Ethyl cinnamate
177.090967	H / N	C11H12O2 [M+H]+	HMDB36905	2-Propenyl phenylacetate
177.090967	H / N	C11H12O2 [M+H]+	HMDB37142	2-(Phenylethenyl)-1,3-dioxolane
177.090967	H / N	C11H12O2 [M+H]+	HMDB37145	3-(4-Methoxyphenyl)-2-methyl-2-propenal
184.169567	N	C11H21NO [M+H]+	-	-
187.094074	N	C7H16O4 [M+Na]+	-	-
200.128135	H / N	C10H17NO3 [M+H]+	HMDB06406	Ecgonine methyl ester
200.128135	H / N	C10H17NO3 [M+H]+	HMDB31820	Neotussilagine
205.060029	N	C6H15O4P [M+Na]+	-	-
208.133198	H / N	C12H17NO2 [M+H]+	HMDB15319	Ciclopirox
208.133198	H / N	C12H17NO2 [M+H]+	HMDB29370	O-Methylcorypalline
208.133198	H / N	C12H17NO2 [M+H]+	HMDB37697	Isobutyl N-methylanthranilate
208.133198	H / N	C12H17NO2 [M+H]+	HMDB39939	Synephrine acetonide
208.133198	H / N	C12H17NO2 [M+H]+	HMDB40010	1-(2,3-Dihydro-6,7-dimethyl-1H-pyrrolizin-5-yl)-2-hydroxy-1-propanone
211.144064	H / N	C11H18N2O2 [M+H]+	HMDB34276	L,L-Cyclo(leucylprolyl)
215.028340	H / N	C6H12N2OS2 [M+Na]+	HMDB31186	N-Nitrosothialdine
221.128419	N	C12H16N2O2 [M+H]+	-	-
221.189947	H / N	C15H24O [M+H]+	HMDB13688	Nootkatol
221.189947	H / N	C15H24O [M+H]+	HMDB30232	(2R,6S,7S,10Z)-beta-Santala-3(15),10-dien-12-ol
221.189947	H / N	C15H24O [M+H]+	HMDB32220	Dihydronootkatone
221.189947	H / N	C15H24O [M+H]+	HMDB33826	2,6-Di-tert-butyl-4-methylphenol
221.189947	H / N	C15H24O [M+H]+	HMDB34661	alpha-Valerenol
221.189947	H / N	C15H24O [M+H]+	HMDB34718	Isospathulenol
221.189947	H / N	C15H24O [M+H]+	HMDB34940	alpha-Santal-10-en-12-ol
221.189947	H / N	C15H24O [M+H]+	HMDB35020	Acolamone
221.189947	H / N	C15H24O [M+H]+	HMDB35026	alpha-Cyperol
221.189947	H / N	C15H24O [M+H]+	HMDB35097	beta-Costol
221.189947	H / N	C15H24O [M+H]+	HMDB35306	Epishyobunone
221.189947	H / N	C15H24O [M+H]+	HMDB35391	Preisocalamendiol
221.189947	H / N	C15H24O [M+H]+	HMDB35645	Epoxyguaiene
221.189947	H / N	C15H24O [M+H]+	HMDB35704	Acorenone
221.189947	H / N	C15H24O [M+H]+	HMDB35718	Isocyperol
221.189947	H / N	C15H24O [M+H]+	HMDB35720	Isoacolamone
221.189947	H / N	C15H24O [M+H]+	HMDB35739	(R)-2,7(14),9-Bisabolatrien-11-ol
221.189947	H / N	C15H24O [M+H]+	HMDB35793	Fukinone
221.189947	H / N	C15H24O [M+H]+	HMDB36118	(3S,6E)-6-Caryophyllen-15-al

221.189947	H / N	C15H24O [M+H]+	HMDB36192	Apritone
221.189947	H / N	C15H24O [M+H]+	HMDB36402	alpha-Bergamotenol
221.189947	H / N	C15H24O [M+H]+	HMDB36420	Spathulenol
221.189947	H / N	C15H24O [M+H]+	HMDB36716	beta-Santalol
221.189947	H / N	C15H24O [M+H]+	HMDB36717	trans-beta-Santalol
221.189947	H / N	C15H24O [M+H]+	HMDB36788	beta-Betulenol
221.189947	H / N	C15H24O [M+H]+	HMDB36789	Caryophyllene alpha-oxide
221.189947	H / N	C15H24O [M+H]+	HMDB36793	3,15-Epoxy-6-caryophyllene
221.189947	H / N	C15H24O [M+H]+	HMDB36798	8alpha-3-Copaen-8-ol
221.189947	H / N	C15H24O [M+H]+	HMDB37069	Acoragermacrone
221.189947	H / N	C15H24O [M+H]+	HMDB37392	4(15)-Copaen-11-ol
221.189947	H / N	C15H24O [M+H]+	HMDB37395	11-Copaen-4-ol
221.189947	H / N	C15H24O [M+H]+	HMDB37811	Vetiverol
221.189947	H / N	C15H24O [M+H]+	HMDB38119	Eremofukinone
221.189947	H / N	C15H24O [M+H]+	HMDB38123	1,5-Epoxy-4(14)-salvialene
221.189947	H / N	C15H24O [M+H]+	HMDB38134	Bisabolene oxide
221.189947	H / N	C15H24O [M+H]+	HMDB38146	Calacone
221.189947	H / N	C15H24O [M+H]+	HMDB38160	7(14)-Isodaucen-10-one
221.189947	H / N	C15H24O [M+H]+	HMDB38193	Isoshyobunone
221.189947	H / N	C15H24O [M+H]+	HMDB38208	Humuladienone
221.189947	H / N	C15H24O [M+H]+	HMDB38209	Humulene epoxide I
221.189947	H / N	C15H24O [M+H]+	HMDB38210	Humulene epoxide II
221.189947	H / N	C15H24O [M+H]+	HMDB38211	Humulenol I
221.189947	H / N	C15H24O [M+H]+	HMDB38212	Humulenol II
221.189947	H / N	C15H24O [M+H]+	HMDB38512	Bisacurol
221.189947	H / N	C15H24O [M+H]+	HMDB38982	4-Nonylphenol
221.189947	H / N	C15H24O [M+H]+	HMDB39532	(6Z,9Z,12Z)-6,9,12-Pentadecatrien-2-one
221.189947	H / N	C15H24O [M+H]+	HMDB39711	Aromadendrene epoxide
221.189947	H / N	C15H24O [M+H]+	HMDB40763	Italicene ether
221.189947	H / N	C15H24O [M+H]+	HMDB59836	Cabreuva oxide D
221.189947	H / N	C15H24O [M+H]+	HMDB60356	2-trans,6-trans-Farnesal
223.144055	H / N	C12H18N2O2 [M+H]+	HMDB60678	3-Hydroxymonoethylglycinexylidide
229.085938	H / N	C14H12O3 [M+H]+	HMDB03747	Resveratrol
229.085938	H / N	C14H12O3 [M+H]+	HMDB15497	Oxybenzone
229.085938	H / N	C14H12O3 [M+H]+	HMDB15575	Trioxsalen
229.085938	H / N	C14H12O3 [M+H]+	HMDB29818	Benzyl salicylate
229.085938	H / N	C14H12O3 [M+H]+	HMDB32217	2,4-Difurfurylfuran
229.085938	H / N	C14H12O3 [M+H]+	HMDB34118	(Z)-Resveratrol
229.085938	H / N	C14H12O3 [M+H]+	HMDB34257	Seselin
229.085938	H / N	C14H12O3 [M+H]+	HMDB34270	5,6-Dihydro-5-hydroxy-6-methyl-2H-pyran-2-one
229.085938	H / N	C14H12O3 [M+H]+	HMDB37667	o-Tolyl salicylate
233.211067	N	C13H28O3 [M+H]+	-	-
235.190395	N	C12H26O4 [M+H]+	-	-
237.133227	N	C10H20O6 [M+H]+	-	-
237.139593	N	C11H22N2S [M+Na]+	-	-
237.149074	N	C7H20N6OS [M+H]+	-	-
239.139034	H / N	C12H18N2O3 [M+H]+	HMDB14562	Secobarbital
239.175361	N	C13H22N2O2 [M+H]+	-	-
241.176921	N	C10H20N6O [M+H]+	-	-
241.195041	N	C18H24 [M+H]+	-	-
242.153909	H / N	C16H19NO [M+H]+	HMDB33527	Dehydroisochalciporone
242.153909	H / N	C16H19NO [M+H]+	HMDB60535	N-Desmethyldiphenhydramine
242.153909	H / N	C16H19NO [M+H]+	HMDB61165	N,N-Didemethyl orphenadrine
243.053240	N	C7H14O7S [M+H]+	-	-
243.087653	N	C12H10N4O2 [M+H]+	-	-
245.153615	N	C16H20O2 [M+H]+	-	-
247.026284	N	C8H8N4O2S [M+Na]+	-	-
248.167822	N	C12H25NO2S [M+H]+	-	-
251.148874	H / N	C11H22O6 [M+H]+	HMDB34750	Isopentyl beta-D-glucoside
252.193426	N	C13H27NO2 [M+Na]+	-	-
253.136841	N	C13H20N2OS [M+H]+	-	-
253.162042	N	C15H24OS [M+H]+	-	-
253.195098	N	C19H24 [M+H]+	-	-
255.170310	N	C13H22N2O3 [M+H]+	-	-
256.263451	H / N	C16H33NO [M+H]+	HMDB12273	Palmitic amide
259.203266	H / N	C16H28O [M+Na]+	HMDB31851	3-(5,6,6-Trimethylbicyclo[2.2.1]hept-1-yl)cyclohexanol
259.203266	H / N	C16H28O [M+Na]+	HMDB36831	Ambronide
261.206023	N	C14H28O4 [M+H]+	-	-
263.176778	N	C18H24 [M+Na]+	-	-
265.191004	N	C15H24N2O2 [M+H]+	-	-
267.076439	H / N	C15H10N2O3 [M+H]+	HMDB60566	Carbamazepine-O-quinone
267.143835	N	C11H22O7 [M+H]+	-	-

267.206658	N	C15H26N2O2 [M+H]+	-	-
270.217615	N	C14H27N3O2 [M+H]+	-	-
270.315482	H / N	C18H39N [M+H]+	HMDB29586	Octadecylamine
271.111054	H / N	C12H18N2O3S [M+H]+	HMDB15256	Tolbutamide
273.180927	N	C13H24N2O4 [M+H]+	-	-
274.134180	N	C18H15N3 [M+H]+	-	-
274.159050	N	C20H19N [M+H]+	-	-
275.164094	H / N	C17H22O3 [M+H]+	HMDB32697	1b-Furanoeudesm-4(15)-en-1-ol acetate
275.164094	H / N	C17H22O3 [M+H]+	HMDB33090	[6]-Dehydroshogaol
275.164094	H / N	C17H22O3 [M+H]+	HMDB38939	Panaquinquecol 4
275.164094	H / N	C17H22O3 [M+H]+	HMDB40926	2-Butyl-5-[2-(4-hydroxy-3-methoxyphenyl)ethyl]furan
275.164094	H / N	C17H22O3 [M+H]+	HMDB60354	2-Polyprenyl-6-methoxy-1,4-benzoquinone
275.164094	H / N	C17H22O3 [M+H]+	HMDB60388	4-Hydroxy-3-polyprenylbenzoate
276.199133	N	C14H29NO2S [M+H]+	-	-
277.118292	N	C14H16N2O4 [M+H]+	-	-
277.161715	N	C9H20N6O4 [M+H]+	-	-
279.062916	H / N	C15H12O4 [M+Na]+	HMDB05760	Dihydrodaidzein
279.062916	H / N	C15H12O4 [M+Na]+	HMDB29462	(E)-2,4,4'-Trihydroxychalcone
279.062916	H / N	C15H12O4 [M+Na]+	HMDB29519	(2S)-Liquiritigenin
279.062916	H / N	C15H12O4 [M+Na]+	HMDB30808	(S)-Pinocembrin
279.062916	H / N	C15H12O4 [M+Na]+	HMDB32577	4'-Methoxybenzophenone-2-carboxylic acid
279.062916	H / N	C15H12O4 [M+Na]+	HMDB33904	7E-Mycosinyl acetate
279.062916	H / N	C15H12O4 [M+Na]+	HMDB36457	Emodinanthranol
279.062916	H / N	C15H12O4 [M+Na]+	HMDB37316	Isoliquiritigenin
279.062916	H / N	C15H12O4 [M+Na]+	HMDB41647	2-Dehydro-O-desmethylangolensin
279.304664	H / N	C20H38 [M+H]+	HMDB41106	3-Eicosyne
279.304664	H / N	C20H38 [M+H]+	HMDB41107	5-Eicosyne
279.304664	H / N	C20H38 [M+H]+	HMDB41108	9-Icosyne
281.042087	H / N	C14H10O5 [M+Na]+	HMDB15471	Salsalate
281.042087	H / N	C14H10O5 [M+Na]+	HMDB30831	Alternariol
281.042087	H / N	C14H10O5 [M+Na]+	HMDB30871	Isogentisin
281.042087	H / N	C14H10O5 [M+Na]+	HMDB31760	Gentisin
281.042087	H / N	C14H10O5 [M+Na]+	HMDB31898	Porric acid C
281.042087	H / N	C14H10O5 [M+Na]+	HMDB33088	(±)-2-(3,4-Dihydroxyphenyl)-1,3-benzodioxole-5-carboxaldehyde
281.042087	H / N	C14H10O5 [M+Na]+	HMDB33911	5,6,8-Trihydroxy-2-methylbenzo[g]chromen-4-one
281.042087	H / N	C14H10O5 [M+Na]+	HMDB38677	Alfafuran
281.113196	H / N	C13H16N2O5 [M+H]+	HMDB00706	L-Aspartyl-L-phenylalanine
281.113196	H / N	C13H16N2O5 [M+H]+	HMDB11167	L-beta-aspartyl-L-phenylalanine
281.113196	H / N	C13H16N2O5 [M+H]+	HMDB28760	Aspartyl-Phenylalanine
281.113196	H / N	C13H16N2O5 [M+H]+	HMDB28991	Phenylalanyl-Aspartate
281.185914	N	C15H24N2O3 [M+H]+	-	-
283.047422	N	C8H12N4O4S [M+Na]+	-	-
284.237312	N	C20H29N [M+H]+	-	-
285.178396	N	C12H26N2O4 [M+Na]+	-	-
285.184924	H / N	C19H24O2 [M+H]+	HMDB03422	Boldione
285.184924	H / N	C19H24O2 [M+H]+	HMDB30432	Linalyl cinnamate
285.184924	H / N	C19H24O2 [M+H]+	HMDB38050	alpha-Terpinyl cinnamate
287.085825	N	C10H20N2O2S2 [M+Na]+	-	-
289.036850	N	C10H10N4O3S [M+Na]+	-	-
289.097863	N	C13H18N2O2S [M+Na]+	-	-
289.175849	N	C13H24N2O5 [M+H]+	-	-
290.107917	N	C8H21N5OS2 [M+Na]+	-	-
294.181168	H / N	C15H23N3O3 [M+H]+	HMDB28958	Lysyl-Phenylalanine
294.181168	H / N	C15H23N3O3 [M+H]+	HMDB29000	Phenylalanyl-Lysine
294.181168	H / N	C15H23N3O3 [M+H]+	HMDB60996	N-Acetyl-3-hydroxyprocainamide
294.279111	H / N	C19H35NO [M+H]+	HMDB60644	cis-Hydroxy Perhexiline
294.279111	H / N	C19H35NO [M+H]+	HMDB61155	Monohydroxyperhexiline
295.144017	H / N	C18H18N2O2 [M+H]+	HMDB41061	Nigellidine
295.175100	N	C13H26O7 [M+H]+	-	-
295.181516	N	C14H28N2OS [M+Na]+	-	-
297.167284	H / N	C14H26O5 [M+Na]+	HMDB00394	3-Hydroxytetradecanedioic acid
299.094748	N	C14H18O5S [M+H]+	-	-
301.202430	N	C17H24N4O [M+H]+	-	-
301.248615	N	C16H32N2O3 [M+H]+	-	-
303.304609	N	C22H38 [M+H]+	-	-
304.188224	N	C16H27NO3 [M+Na]+	-	-
306.251713	N	C16H33N3O [M+Na]+	-	-
307.142703	N	C10H20N8S [M+Na]+	-	-
309.031124	N	C7H16O9S2 [M+H]+	-	-
313.113215	N	C11H14N8O2 [M+Na]+	-	-
314.229631	N	C13H27N7O2 [M+H]+	-	-
317.053037	N	C8H14N4O6S [M+Na]+	-	-

318.178709	N	C15H25N3O3 [M+Na]+	-	-
318.217588	N	C18H27N3O2 [M+H]+	-	-
326.107826	N	C11H21N5OS2 [M+Na]+	-	-
326.245518	H / N	C20H33NO [M+Na]+	HMDB37270	Fenpropimorph
328.307382	N	C17H37N5O [M+H]+	-	-
329.104556	N	C14H18N4O2S [M+Na]+	-	-
331.136388	N	C13H24O8 [M+Na]+	-	-
331.297102	N	C21H40O [M+Na]+	-	-
332.146518	N	C14H17N7O3 [M+H]+	-	-
332.183075	H / N	C17H27NO4 [M+Na]+	HMDB15334	Nadolol
332.183075	H / N	C17H27NO4 [M+Na]+	HMDB15345	Metipranolol
332.294792	N	C22H37NO [M+H]+	-	-
335.171173	N	C16H22N4O4 [M+H]+	-	-
335.192573	N	C13H26N4O6 [M+H]+	-	-
336.264562	N	C19H33N3O2 [M+H]+	-	-
337.258462	N	C17H36O6 [M+H]+	-	-
338.193611	N	C16H29NO5 [M+Na]+	-	-
339.201365	N	C15H30O8 [M+H]+	-	-
341.120647	N	C14H22O8 [M+Na]+	-	-
343.209127	N	C16H32O6 [M+Na]+	-	-
343.295539	N	C19H38N2O3 [M+H]+	-	-
344.222106	H / N	C21H29NO3 [M+H]+	HMDB30340	Piperolein B
344.222106	H / N	C21H29NO3 [M+H]+	HMDB33959	Isopiperolein B
344.225405	N	C18H33NO3S [M+H]+	-	-
345.224708	N	C16H34O6 [M+Na]+	-	-
345.263581	N	C19H36O5 [M+H]+	-	-
345.311161	N	C19H40N2O3 [M+H]+	-	-
346.237740	N	C21H31NO3 [M+H]+	-	-
347.096451	N	C13H16N4O6 [M+Na]+	-	-
349.210659	N	C10H30N8O2S [M+Na]+	-	-
350.243944	N	C19H31N3O3 [M+H]+	-	-
350.266429	H / N	C19H37NO3 [M+Na]+	HMDB13246	Margaroylglycine
351.145901	N	C14H24N4O3S [M+Na]+	-	-
352.126570	N	C17H19N3O4 [M+Na]+	-	-
353.185997	H / N	C21H24N2O3 [M+H]+	HMDB30389	Quebrachidine
353.185997	H / N	C21H24N2O3 [M+H]+	HMDB30390	(+)-Quebrachidine
355.260746	H / N	C22H36O2 [M+Na]+	HMDB02226	Adrenic acid
355.260746	H / N	C22H36O2 [M+Na]+	HMDB35676	1-Hydroxy-1-phenyl-3-hexadecanone
355.260746	H / N	C22H36O2 [M+Na]+	HMDB35677	3-Hydroxy-1-phenyl-1-hexadecanone
355.260746	H / N	C22H36O2 [M+Na]+	HMDB38910	2-Methyl-5-(8-pentadecenyl)-1,3-benzenediol
356.191456	N	C14H29NO9 [M+H]+	-	-
356.261769	N	C20H37NO2S [M+H]+	-	-
357.206807	N	C15H28N6O2S [M+H]+	-	-
360.215231	N	C12H31N7O2S [M+Na]+	-	-
361.174693	N	C18H22N6O [M+Na]+	-	-
362.181235	N	C16H21N9 [M+Na]+	-	-
362.194660	N	C19H33NS2 [M+Na]+	-	-
363.219987	N	C18H34O5S [M+H]+	-	-
363.225612	N	C18H32N2O4 [M+Na]+	-	-
364.247082	N	C20H31N5 [M+Na]+	-	-
365.207093	N	C19H28N2O5 [M+H]+	-	-
367.269018	N	C18H38O7 [M+H]+	-	-
368.138102	N	C15H29NO3S3 [M+H]+	-	-
369.351551	N	C27H44 [M+H]+	-	-
372.207360	N	C24H25N3O [M+H]+	-	-
372.347230	N	C22H45NO3 [M+H]+	-	-
374.213808	N	C13H25N11O [M+Na]+	-	-
375.110083	N	C15H20N4O4S [M+Na]+	-	-
375.274103	N	C20H38O6 [M+H]+	-	-
376.291670	N	C17H37N5O4 [M+H]+	-	-
377.352647	N	C24H44N2O [M+H]+	-	-
378.224822	N	C17H27N7O3 [M+H]+	-	-
378.279257	N	C26H35NO [M+H]+	-	-
379.193828	N	C15H32O9 [M+Na]+	-	-
379.251913	N	C20H42S3 [M+H]+	-	-
380.156348	N	C16H21N5O6 [M+H]+	-	-
381.409132	H / N	C26H52O [M+H]+	HMDB29695	Hexacosanal
382.170587	H / N	C15H27NO10 [M+H]+	HMDB33965	(R)-Pantothenic acid 4'-O-b-D-glucoside
382.219770	N	C18H33NO6 [M+Na]+	-	-
384.067483	N	C11H24NO6PS2 [M+Na]+	-	-
384.144006	H / N	C21H21NO6 [M+H]+	HMDB32878	13-Oxocryptopine
384.144006	H / N	C21H21NO6 [M+H]+	HMDB38554	Gravacridonediolacetate

384.274419	H / N	C21H37NO5 [M+H]+	HMDB13332	3-Hydroxy-5, 8-tetradecadiencarnitine
386.223035	N	C25H27N3O [M+H]+	-	-
387.186613	N	C15H24N8O3 [M+Na]+	-	-
387.196246	N	C21H32O3S [M+Na]+	-	-
388.267835	N	C17H29N11 [M+H]+	-	-
390.321414	N	C21H43NO5 [M+H]+	-	-
391.155665	N	C12H28N6O3S2 [M+Na]+	-	-
391.157389	H / N	C15H28O10 [M+Na]+	HMDB41255	(2S)-2-Butanol O-[b-D-Apiofuranosyl-(1->6)-b-D-glucopyranoside]
392.148805	N	C15H25N3O7S [M+H]+	-	-
393.311012	N	C23H40N2O3 [M+H]+	-	-
400.256911	N	C21H35N3O3 [M+Na]+	-	-
401.228957	N	C20H36N2O2S2 [M+H]+	-	-
401.239312	N	C18H32N4O6 [M+H]+	-	-
401.241692	N	C14H34N8O2S [M+Na]+	-	-
402.269701	N	C17H41N5S2 [M+Na]+	-	-
403.081259	N	C16H22N2O4S3 [M+H]+	-	-
404.228247	N	C19H27N9 [M+Na]+	-	-
404.232617	N	C17H33N5O4S [M+H]+	-	-
404.241405	N	C14H35N7O3S [M+Na]+	-	-
409.269699	N	C22H36N2O5 [M+H]+	-	-
410.102819	N	C12H25N3O7S2 [M+Na]+	-	-
412.202160	N	C26H25N3O2 [M+H]+	-	-
413.193323	H / N	C22H30O6 [M+Na]+	HMDB30844	6,7-Dimethoxy-7-epirosmanol
413.193323	H / N	C22H30O6 [M+Na]+	HMDB31933	11,12-Dihydroxy-7,14-dimethoxy-8,11,13-abietatrien-20,6-olide
413.193323	H / N	C22H30O6 [M+Na]+	HMDB35206	Bakkenolide B
413.193323	H / N	C22H30O6 [M+Na]+	HMDB35922	Nigakihemiacetal B
413.198319	N	C20H30N4O2S [M+Na]+	-	-
413.323764	N	C22H46O5 [M+Na]+	-	-
415.111408	N	C24H18N2O3S [M+H]+	-	-
415.208777	N	C20H26N6O4 [M+H]+	-	-
415.250241	N	C21H36N4OS [M+Na]+	-	-
416.274546	N	C19H35N7O2 [M+Na]+	-	-
418.224987	N	C19H33N5O2S [M+Na]+	-	-
419.137222	N	C18H26O9S [M+H]+	-	-
419.148453	N	C17H26N2O8S [M+H]+	-	-
420.247613	N	C21H39N3S2 [M+Na]+	-	-
420.265361	N	C21H39N3O2S [M+Na]+	-	-
421.221273	N	C22H30N4O3 [M+Na]+	-	-
421.232806	N	C14H30N12S [M+Na]+	-	-
422.323955	H / N	C23H45NO4 [M+Na]+	HMDB00222	L-Palmitoylcarnitine
423.456062	H / N	C29H58O [M+H]+	HMDB33190	15-Nonacosanone
423.456062	H / N	C29H58O [M+H]+	HMDB33719	10-Nonacosanone
423.456062	H / N	C29H58O [M+H]+	HMDB40884	(-)-1-Cyclohexyl-4-tricosanol
424.221806	N	C15H31N9O2S [M+Na]+	-	-
425.229906	H / N	C24H34O5 [M+Na]+	HMDB35844	Lucidone A
425.305003	N	C28H40O3 [M+H]+	-	-
427.254470	N	C20H42O5S2 [M+H]+	-	-
427.291667	N	C21H38N4O5 [M+H]+	-	-
429.303522	N	C24H44O4S [M+H]+	-	-
429.347554	N	C27H44N2O2 [M+H]+	-	-
430.228224	N	C17H37N5O2S2 [M+Na]+	-	-
432.347289	H / N	C27H45NO3 [M+H]+	HMDB38836	Solanocardinol
433.204416	N	C18H34O10 [M+Na]+	-	-
433.277217	N	C20H42O8 [M+Na]+	-	-
433.331164	H / N	C27H44O4 [M+H]+	HMDB06228	24-Hydroxycalcitriol
433.331164	H / N	C27H44O4 [M+H]+	HMDB12454	3 beta,7 alpha-Dihydroxy-5-cholestenoate
433.331164	H / N	C27H44O4 [M+H]+	HMDB30702	Neochlorogenin
433.331164	H / N	C27H44O4 [M+H]+	HMDB33769	Rockogenin
433.331164	H / N	C27H44O4 [M+H]+	HMDB60134	23S,25,26-Trihydroxyvitamin D3
435.065536	N	C17H20N2O6S2 [M+Na]+	-	-
435.185186	H / N	C18H28N4O7 [M+Na]+	HMDB00569	Deoxypyridinoline
435.252938	N	C28H34O4 [M+H]+	-	-
437.189465	N	C19H30N2O8 [M+Na]+	-	-
437.276498	N	C23H40N4S2 [M+H]+	-	-
439.231813	N	C22H32N4O4 [M+Na]+	-	-
439.331933	N	C28H42N2O2 [M+H]+	-	-
442.230977	N	C22H33N3O5 [M+Na]+	-	-
443.220237	N	C20H32N6O2S [M+Na]+	-	-
444.179894	N	C19H29N3O7S [M+H]+	-	-
444.250732	H / N	C27H35NO3 [M+Na]+	HMDB38568	PC-M6
446.193375	N	C17H33N3O7S [M+Na]+	-	-
447.168379	N	C20H30O9S [M+H]+	-	-

447.202407	N	C19H36O8S [M+Na]+	-	-
448.235541	N	C20H35N5O3S [M+Na]+	-	-
449.199349	N	C18H34O11 [M+Na]+	-	-
449.235793	N	C19H38O10 [M+Na]+	-	-
450.310165	N	C19H41N9S [M+Na]+	-	-
450.329471	N	C21H47N5OS2 [M+H]+	-	-
452.164093	N	C18H27N3O9 [M+Na]+	-	-
452.269927	N	C30H33N3O [M+H]+	-	-
453.125413	N	C19H32O4S4 [M+H]+	-	-
455.178370	N	C14H32N4O9S [M+Na]+	-	-
455.327860	N	C23H48N2O3S [M+Na]+	-	-
455.373028	N	C27H50O5 [M+H]+	-	-
456.246676	N	C23H35N3O5 [M+Na]+	-	-
457.195419	N	C15H30N8O5S [M+Na]+	-	-
457.349988	N	C24H50O6 [M+Na]+	-	-
458.271437	N	C18H33N11O2 [M+Na]+	-	-
459.160763	N	C19H28N6O2S2 [M+Na]+	-	-
459.453556	H / N	C30H60O [M+Na]+	HMDB29993	2-Methyl-3-nonacosanone
459.453556	H / N	C30H60O [M+Na]+	HMDB30296	(±)-2-Nonylheneicosanal
459.453556	H / N	C30H60O [M+Na]+	HMDB32868	Triacontanal
463.306185	N	C20H42N6O4S [M+H]+	-	-
464.193167	N	C24H25N5O5 [M+H]+	-	-
464.254897	N	C20H33N9O2S [M+H]+	-	-
464.279791	N	C29H37NO4 [M+H]+	-	-
465.502977	N	C32H64O [M+H]+	-	-
466.386741	N	C26H53NO4 [M+Na]+	-	-
468.192208	N	C28H25N3O4 [M+H]+	-	-
469.386382	N	C26H54O5 [M+Na]+	-	-
469.388774	N	C28H52O5 [M+H]+	-	-
473.292312	N	C24H42N4O2S [M+Na]+	-	-
473.302239	N	C30H42O3 [M+Na]+	-	-
474.316471	N	C22H41N7O3 [M+Na]+	-	-
477.215899	N	C23H40O4S3 [M+H]+	-	-
477.230621	H	C29H33ClN2O2 [M+H]+	HMDB04999	Loperamide
477.230621	H / N	C20H38O11 [M+Na]+	HMDB29925	Methyl cellulose
477.230621	H / N	C20H38O11 [M+Na]+	HMDB33370	Ethyl cellulose
477.233790	N	C23H40O6S2 [M+H]+	-	-
479.173395	N	C18H32O13 [M+Na]+	-	-
479.323762	N	C26H46N4S2 [M+H]+	-	-
479.345519	N	C25H48N2O5 [M+Na]+	-	-
480.243946	N	C21H37NO11 [M+H]+	-	-
480.293675	N	C23H41N7S2 [M+H]+	-	-
483.275904	N	C30H34N4O2 [M+H]+	-	-
484.241646	N	C24H35N3O6 [M+Na]+	-	-
484.333953	N	C20H45N5O8 [M+H]+	-	-
486.239105	N	C29H31N3O4 [M+H]+	-	-
488.284929	N	C16H39N11O3S [M+Na]+	-	-
491.443466	N	C30H60O3 [M+Na]+	-	-
493.201737	N	C27H34O5S [M+Na]+	-	-
493.261962	N	C21H42O11 [M+Na]+	-	-
494.285328	N	C21H46NO8P [M+Na]+	-	-
496.214644	N	C16H36N5O9P [M+Na]+	-	-
496.281164	N	C21H37N9O3S [M+H]+	-	-
497.114527	N	C19H28O11S2 [M+H]+	-	-
497.401966	N	C30H56O3S [M+H]+	-	-
498.303719	H / N	C24H45NO8 [M+Na]+	HMDB15291	Dinoprost Tromethamine
498.339371	N	C23H51N3O4S2 [M+H]+	-	-
499.215062	N	C22H36O11 [M+Na]+	-	-
499.261115	N	C19H38N4O11 [M+H]+	-	-
501.336534	N	C34H44O3 [M+H]+	-	-
501.376222	N	C26H54O7 [M+Na]+	-	-
501.378644	N	C28H52O7 [M+H]+	-	-
504.259186	N	C27H37NO8 [M+H]+	-	-
504.265007	N	C20H43N5O4S2 [M+Na]+	-	-
505.252552	N	C17H38N8O6S [M+Na]+	-	-
505.277230	N	C26H42O8 [M+Na]+	-	-
506.244131	N	C19H41N5O5S2 [M+Na]+	-	-
507.277478	N	C22H44O11 [M+Na]+	-	-
507.332186	N	C22H46N6O5S [M+H]+	-	-
508.285372	N	C21H39N7O6 [M+Na]+	-	-
508.998817	N	C16H16N2O11S3 [M+H]+	-	-
510.226480	N	C16H39N5O9S2 [M+H]+	-	-

510.345103	N	C24H49N5O3S [M+Na]+	-	-
511.248370	N	C20H44N2O7S2 [M+Na]+	-	-
511.249432	N	C21H38N2O12 [M+H]+	-	-
511.292416	N	C23H44N4O5S [M+Na]+	-	-
512.282495	N	C22H45N3O6S2 [M+H]+	-	-
513.051824	N	C12H22N2O16P2 [M+H]+	-	-
513.412628	N	C28H58O6 [M+Na]+	-	-
517.280599	N	C24H46O8S [M+Na]+	-	-
517.371112	N	C26H54O8 [M+Na]+	-	-
517.495469	H / N	C33H66O2 [M+Na]+	HMDB39537	18-Hydroxy-16-tritriacontanone
518.259167	N	C24H39NO11 [M+H]+	-	-
518.280570	N	C21H45N5O4S2 [M+Na]+	-	-
518.337386	N	C24H47N5O5S [M+H]+	-	-
518.374259	N	C33H47N3O2 [M+H]+	-	-
519.131396	N	C17H30N2O12S2 [M+H]+	-	-
519.278581	N	C30H38N4O2S [M+H]+	-	-
519.372341	N	C29H50N4O2S [M+H]+	-	-
521.285374	N	C23H47O9P [M+Na]+	-	-
521.366702	N	C24H52N6O2S2 [M+H]+	-	-
524.197908	N	C18H36N3O11P [M+Na]+	-	-
524.331489	N	C26H51N3O2S2 [M+Na]+	-	-
525.194233	N	C23H34O12 [M+Na]+	-	-
526.366634	N	C27H49N7S [M+Na]+	-	-
527.122229	N	C20H29N2O9PS [M+Na]+	-	-
527.174337	N	C21H30N6O6S2 [M+H]+	-	-
529.219033	N	C22H38N2O9S [M+Na]+	-	-
529.239737	N	C25H40N2O6S2 [M+H]+	-	-
529.276720	N	C26H36N6O6 [M+H]+	-	-
531.274170	N	C26H46N2O3S3 [M+H]+	-	-
533.194754	N	C18H36N4O10S2 [M+H]+	-	-
533.351122	N	C28H52O7S [M+H]+	-	-
534.227013	N	C26H35N3O7S [M+H]+	-	-
534.238892	N	C20H41N5O6S2 [M+Na]+	-	-
537.263464	N	C28H44N2O2S3 [M+H]+	-	-
538.213699	N	C19H38N3O11P [M+Na]+	-	-
538.309687	N	C25H45N3O8 [M+Na]+	-	-
539.240398	N	C32H36O6 [M+Na]+	-	-
540.322967	N	C29H47N3O3S [M+Na]+	-	-
540.350702	N	C27H51NO8 [M+Na]+	-	-
541.117520	N	C17H25N4O14P [M+H]+	-	-
541.213063	N	C22H30N8O7 [M+Na]+	-	-
542.262979	N	C23H43NO11S [M+H]+	-	-
543.293366	N	C22H44N6O6S [M+Na]+	-	-
544.389912	N	C35H49N3O2 [M+H]+	-	-
545.402470	N	C28H58O8 [M+Na]+	-	-
549.278821	N	C25H40N8O2S2 [M+H]+	-	-
549.307479	N	C31H40N4O5 [M+H]+	-	-
551.357784	N	C31H50O8 [M+H]+	-	-
551.377814	N	C27H52N4O6 [M+Na]+	-	-
553.324427	N	C28H40N8O4 [M+H]+	-	-
553.362520	N	C32H46N6O [M+Na]+	-	-
554.341734	N	C27H53N3O3S2 [M+Na]+	-	-
555.172790	N	C19H34N6O7S3 [M+H]+	-	-
555.393388	N	C29H54N4O4S [M+H]+	-	-
557.359901	H / N	C35H50O4 [M+Na]+	HMDB35899	Pyrohyperforin
557.438846	N	C30H62O7 [M+Na]+	-	-
558.368929	N	C35H47N3O3 [M+H]+	-	-
559.137521	N	C18H30N4O12S2 [M+H]+	-	-
560.331149	N	C21H47N9O5S [M+Na]+	-	-
561.397211	N	C28H58O9 [M+Na]+	-	-
568.248470	N	C25H43N3O6S2 [M+Na]+	-	-
568.357935	N	C28H47N7O4 [M+Na]+	-	-
569.329504	N	C28H50O10 [M+Na]+	-	-
570.233510	N	C23H43N3O7S3 [M+H]+	-	-
571.105925	N	C20H29N4O8PS2 [M+Na]+	-	-
572.348673	N	C35H45N3O4 [M+H]+	-	-
573.198974	N	C25H34N4O8S [M+Na]+	-	-
573.307120	N	C33H40N4O5 [M+H]+	-	-
573.348542	N	C26H46N8O5 [M+Na]+	-	-
574.306624	N	C24H49N5O5S2 [M+Na]+	-	-
575.376828	N	C28H56O10 [M+Na]+	-	-
575.434545	N	C33H66OS3 [M+H]+	-	-

579.370832	N	C25H50N6O9 [M+H]+	-	-
583.090035	N	C20H26N2O14S2 [M+H]+	-	-
583.276872	N	C23H38N10O6S [M+H]+	-	-
586.234221	N	C23H39NO16 [M+H]+	-	-
587.313489	N	C23H46N4O13 [M+H]+	-	-
587.340290	N	C28H52O11 [M+Na]+	-	-
589.334847	N	C31H50O9 [M+Na]+	-	-
589.428543	N	C30H62O9 [M+Na]+	-	-
593.308680	N	C33H46O8 [M+Na]+	-	-
594.340169	N	C33H49NO7 [M+Na]+	-	-
597.369061	N	C38H48N2O4 [M+H]+	-	-
598.147262	N	C29H28NO11P [M+H]+	-	-
598.253802	N	C26H47NO8S3 [M+H]+	-	-
600.368974	N	C33H55NO5S [M+Na]+	-	-
601.450203	N	C35H68OS3 [M+H]+	-	-
601.464986	N	C32H66O8 [M+Na]+	-	-
603.127100	N	C23H33O13PS [M+Na]+	-	-
604.356786	N	C30H51N3O8 [M+Na]+	-	-
605.296272	N	C25H44N6O9S [M+H]+	-	-
605.481327	N	C35H72OS3 [M+H]+	-	-
606.342200	N	C28H45N11OS [M+Na]+	-	-
606.472999	N	C36H63NO6 [M+H]+	-	-
607.200845	N	C20H36N6O12S [M+Na]+	-	-
607.217420	N	C26H42N2O8S3 [M+H]+	-	-
607.418161	H / N	C33H60O8 [M+Na]+	HMDB33336	Antibiotic X 14889A
609.161974	N	C22H41O11PS3 [M+H]+	-	-
609.296114	H / N	C37H40N2O6 [M+H]+	HMDB30172	Oxyacanthine
609.346485	N	C34H48N4O4S [M+H]+	-	-
609.373171	N	C31H50N6O5 [M+Na]+	-	-
610.134958	N	C23H34N5O5PS3 [M+Na]+	-	-
610.312884	N	C26H43N9O6S [M+H]+	-	-
610.371133	N	C34H53NO7 [M+Na]+	-	-
613.267230	N	C22H42N10O5S2 [M+Na]+	-	-
613.364466	N	C33H54N2O5S [M+Na]+	-	-
613.411438	N	C38H52N4O3 [M+H]+	-	-
613.486621	N	C37H72S3 [M+H]+	-	-
614.340639	N	C29H51N5O5S2 [M+H]+	-	-
614.364067	N	C37H53NO3S [M+Na]+	-	-
614.381704	N	C37H53NO5 [M+Na]+	-	-
617.152368	N	C20H33N4O14PS [M+H]+	-	-
617.327725	N	C29H48N2O12 [M+H]+	-	-
617.430266	N	C31H60N4O6S [M+H]+	-	-
617.460350	N	C32H66O9 [M+Na]+	-	-
621.424818	N	C29H58N8O3S [M+Na]+	-	-
623.325503	N	C26H50N6O7S2 [M+H]+	-	-
628.231333	N	C27H44NO10PS [M+Na]+	-	-
628.291894	N	C32H47NO8S [M+Na]+	-	-
628.367947	N	C31H51N5O7 [M+Na]+	-	-
629.215406	N	C27H43O11PS [M+Na]+	-	-
630.389816	N	C30H55N5O7S [M+H]+	-	-
631.436793	N	C36H64O5S [M+Na]+	-	-
633.455089	N	C32H66O10 [M+Na]+	-	-
638.288308	N	C25H37N13O6 [M+Na]+	-	-
639.315037	N	C35H44N4O6 [M+Na]+	-	-
640.439715	N	C33H63NO9 [M+Na]+	-	-
641.306153	N	C30H51O11P [M+Na]+	-	-
643.257959	N	C27H42N6O8S2 [M+H]+	-	-
649.338741	N	C26H54N6O7S2 [M+Na]+	-	-
650.278270	N	C30H45NO13 [M+Na]+	-	-
651.159414	N	C23H37N2O14PS [M+Na]+	-	-
651.299130	N	C31H48O13 [M+Na]+	-	-
654.354289	N	C39H47N3O6 [M+H]+	-	-
655.439466	N	C34H64O10 [M+Na]+	-	-
655.475775	N	C35H68O9 [M+Na]+	-	-
658.411289	N	C36H61NO6S [M+Na]+	-	-
658.422220	N	C35H61N3O5S [M+Na]+	-	-
659.558768	H / N	C40H76O5 [M+Na]+	HMDB07087	DG(15:0/22:1(13Z)/0:0)
659.558768	H / N	C40H76O5 [M+Na]+	HMDB07619	DG(22:1(13Z)/15:0/0:0)
659.558768	H / N	C40H76O5 [M+Na]+	HMDB55993	DG(15:0/0:0/22:1n9)
663.298704	N	C32H48O13 [M+Na]+	-	-
665.350573	N	C33H54O12 [M+Na]+	-	-
665.353974	N	C28H52N6O10S [M+H]+	-	-

665.364308	N	C34H52N2O11 [M+H]+	-	-
666.317755	N	C39H43N3O7 [M+H]+	-	-
666.357479	N	C37H51N3O6S [M+H]+	-	-
666.639501	N	C42H83NO4 [M+H]+	-	-
667.400849	N	C31H58N2O13 [M+H]+	-	-
669.243074	N	C29H48O11S3 [M+H]+	-	-
669.490911	N	C34H64N6O7 [M+H]+	-	-
671.492105	N	C39H74O2S3 [M+H]+	-	-
675.230954	N	C29H40N4O11S [M+Na]+	-	-
675.251025	N	C31H38N4O13 [M+H]+	-	-
675.347534	N	C34H56N2O6S2 [M+Na]+	-	-
677.265502	N	C30H38N8O9 [M+Na]+	-	-
677.350772	N	C34H54O12 [M+Na]+	-	-
679.266103	N	C34H44N2O9S [M+Na]+	-	-
681.337587	N	C29H52N4O12S [M+H]+	-	-
683.341448	N	C37H48N4O7 [M+Na]+	-	-
687.248423	N	C30H40N4O13 [M+Na]+	-	-
693.336377	N	C29H50N8O8S [M+Na]+	-	-
693.476311	N	C34H70O12 [M+Na]+	-	-
697.340959	N	C33H54O14 [M+Na]+	-	-
699.283652	N	C31H48O16 [M+Na]+	-	-
701.605841	H / N	C43H82O5 [M+Na]+	HMDB07123	DG(16:0/24:1(15Z)/0:0)
701.605841	H / N	C43H82O5 [M+Na]+	HMDB07151	DG(16:1(9Z)/24:0/0:0)
701.605841	H / N	C43H82O5 [M+Na]+	HMDB07174	DG(18:0/22:1(13Z)/0:0)
701.605841	H / N	C43H82O5 [M+Na]+	HMDB07202	DG(18:1(11Z)/22:0/0:0)
701.605841	H / N	C43H82O5 [M+Na]+	HMDB07231	DG(18:1(9Z)/22:0/0:0)
701.605841	H / N	C43H82O5 [M+Na]+	HMDB07369	DG(20:0/20:1(11Z)/0:0)
701.605841	H / N	C43H82O5 [M+Na]+	HMDB07397	DG(20:1(11Z)/20:0/0:0)
701.605841	H / N	C43H82O5 [M+Na]+	HMDB07594	DG(22:0/18:1(11Z)/0:0)
701.605841	H / N	C43H82O5 [M+Na]+	HMDB07595	DG(22:0/18:1(9Z)/0:0)
701.605841	H / N	C43H82O5 [M+Na]+	HMDB07622	DG(22:1(13Z)/18:0/0:0)
701.605841	H / N	C43H82O5 [M+Na]+	HMDB07795	DG(24:0/16:1(9Z)/0:0)
701.605841	H / N	C43H82O5 [M+Na]+	HMDB07823	DG(24:1(15Z)/16:0/0:0)
701.605841	H / N	C43H82O5 [M+Na]+	HMDB56021	DG(16:0/0:0/24:1n9)
701.605841	H / N	C43H82O5 [M+Na]+	HMDB56046	DG(18:0/0:0/22:1n9)
701.605841	H / N	C43H82O5 [M+Na]+	HMDB56069	DG(20:0/0:0/20:1n9)
701.605841	H / N	C43H82O5 [M+Na]+	HMDB56091	DG(22:0/0:0/18:1n7)
701.605841	H / N	C43H82O5 [M+Na]+	HMDB56092	DG(22:0/0:0/18:1n9)
701.605841	H / N	C43H82O5 [M+Na]+	HMDB56113	DG(24:0/0:0/16:1n7)
703.351363	N	C32H56O15 [M+Na]+	-	-
703.366646	N	C36H56O12 [M+Na]+	-	-
712.312252	N	C34H45N7O8S [M+H]+	-	-
713.263447	N	C30H44N6O10S2 [M+H]+	-	-
713.408324	N	C35H62O13 [M+Na]+	-	-
715.315046	H / N	C32H52O16 [M+Na]+	HMDB37125	Pisumoside B
719.177695	N	C23H39N6O14PS2 [M+H]+	-	-
721.477290	N	C34H66N8O5S [M+Na]+	-	-
721.507468	N	C36H74O12 [M+Na]+	-	-
723.367256	N	C34H56N2O13 [M+Na]+	-	-
725.530735	N	C40H72N2O9 [M+H]+	-	-
727.314336	N	C31H54N2O13S2 [M+H]+	-	-
727.574859	N	C46H76N2O3 [M+Na]+	-	-
732.481795	N	C36H67N7O5S [M+Na]+	-	-
735.465997	N	C38H66N6O4S2 [M+H]+	-	-
739.212630	N	C20H45N8O14PS2 [M+Na]+	-	-
741.299367	N	C34H49N2O14P [M+H]+	-	-
741.463590	N	C36H62N8O7 [M+Na]+	-	-
751.351894	N	C37H60O10S2 [M+Na]+	-	-
753.368719	N	C37H54N4O11 [M+Na]+	-	-
753.547309	N	C38H76N2O12 [M+H]+	-	-
757.441068	N	C37H72O9S3 [M+H]+	-	-
757.475157	N	C34H64N10O7S [M+H]+	-	-
759.482106	N	C46H64N4O4 [M+Na]+	-	-
761.408059	H / N	C39H62O13 [M+Na]+	HMDB30132	Isonuatigenin 3-[rhamnosyl-(1->2)-glucoside]
761.408059	H / N	C39H62O13 [M+Na]+	HMDB33803	Nuatigenin 3-[rhamnosyl-(1->2)-glucoside]
761.408059	H / N	C39H62O13 [M+Na]+	HMDB34337	Polypodosaponin
761.408059	H / N	C39H62O13 [M+Na]+	HMDB39003	Fistuloside A
761.408059	H / N	C39H62O13 [M+Na]+	HMDB40744	Polypodoside B
761.408059	H / N	C39H62O13 [M+Na]+	HMDB40949	Melongoside F
762.476025	N	C40H69NO11 [M+Na]+	-	-
770.458596	N	C42H63N3O10 [M+H]+	-	-
771.288346	N	C35H48N4O12S [M+Na]+	-	-

773.435415	N	C36H62N8O7S [M+Na]+	-	-
775.473752	N	C38H73O12P [M+Na]+	-	-
776.536512	N	C50H69N3O4 [M+H]+	-	-
778.617267	H / N	C44H85NO8 [M+Na]+	HMDB04973	Glucosylceramide (d18:1/20:0)
778.617267	H / N	C44H85NO8 [M+Na]+	HMDB10710	Galactosylceramide (d18:1/20:0)
780.491166	N	C36H65N11O6S [M+H]+	-	-
780.503006	N	C37H71N7O7S [M+Na]+	-	-
787.364805	N	C32H52N12O8S [M+Na]+	-	-
805.275149	N	C33H52N6O9S4 [M+H]+	-	-
814.484951	N	C44H67N3O11 [M+H]+	-	-
821.409357	N	C37H62N6O11S [M+Na]+	-	-
826.578947	N	C44H79N3O11 [M+H]+	-	-
828.486189	N	C42H73N3O9S2 [M+H]+	-	-
833.472029	N	C39H75N2O11PS [M+Na]+	-	-
841.392940	N	C40H67O13PS [M+Na]+	-	-
843.201338	N	C29H50N2O18S4 [M+H]+	-	-
844.319997	N	C41H51N5O11S [M+Na]+	-	-
859.319979	N	C38H59N4O10PS3 [M+H]+	-	-
860.541974	N	C50H73N3O9 [M+H]+	-	-
864.495971	N	C39H76N3O14P [M+Na]+	-	-
865.498121	N	C43H70N8O7S [M+Na]+	-	-
889.371098	N	C31H63N8O16PS [M+Na]+	-	-
900.639504	N	C54H85N5O4S [M+H]+	-	-
937.540440	N	C49H76N8O6S2 [M+H]+	-	-
947.431591	N	C46H66N4O15S [M+H]+	-	-
968.641706	N	C51H89N3O14 [M+H]+	-	-
976.647429	N	C54H93N3O8S2 [M+H]+	-	-
990.587477	N	C45H88N3O18P [M+H]+	-	-
Features selected for the WGB group				
172.169539	H / N	C10H21NO [M+H]+	HMDB36195	N,2,3-Trimethyl-2-(1-methylethyl)butanamide
181.158635	H / N	C12H20O [M+H]+	HMDB31181	Homodihydrojasmone
181.158635	H / N	C12H20O [M+H]+	HMDB32531	2-trans-6-cis-Dodecadienal
181.158635	H / N	C12H20O [M+H]+	HMDB38108	cis-Quinceoxepane
181.158635	H / N	C12H20O [M+H]+	HMDB39339	Tricycloekasantalol
181.158635	H / N	C12H20O [M+H]+	HMDB39590	(2E,4E)-2,4-Dodecadienal
185.128406	N	C9H16N2O2 [M+H]+	-	-
195.122544	N	C8H18O5 [M+H]+	-	-
199.097831	H / N	C11H10N4 [M+H]+	HMDB29706	2-Amino-3-methylimidazo[4,5-f]quinoline
199.097831	H / N	C11H10N4 [M+H]+	HMDB29749	2-Amino-6-methyldipyrido[1,2-a:3',2'-d]imidazole
217.104612	N	C8H18O5 [M+Na]+	-	-
220.136530	N	C10H21NO2S [M+H]+	-	-
222.055925	H / N	C9H13NO2S [M+Na]+	HMDB32424	2-(4-Methyl-5-thiazolyl)ethyl propionate
239.094962	N	C9H18O5S [M+H]+	-	-
241.176921	N	C10H20N6O [M+H]+	-	-
241.195041	N	C18H24 [M+H]+	-	-
243.108699	H / N	C9H14N4O4 [M+H]+	HMDB28894	Histidinyl-Serine
243.108699	H / N	C9H14N4O4 [M+H]+	HMDB29041	Serinyl-Histidine
243.108699	H / N	C9H14N4O4 [M+H]+	HMDB40248	(S,S)-Nt-Histidinylalanine
243.108699	H / N	C9H14N4O4 [M+H]+	HMDB40249	(S,S)-Np-Histidinylalanine
243.159062	H / N	C13H22O4 [M+H]+	HMDB30987	2-Carboxy-4-dodecanolide
243.159062	H / N	C13H22O4 [M+H]+	HMDB38736	(3S,5R,6R,7E)-3,5,6-Trihydroxy-7-megastigmen-9-one
245.092091	H / N	C13H12N2O3 [M+H]+	HMDB06005	Indolylacryloylglycine
245.092091	H / N	C13H12N2O3 [M+H]+	HMDB40734	Haematopodin
248.125694	H / N	C12H19NO3 [M+Na]+	HMDB15009	Terbutaline
248.167822	N	C12H25NO2S [M+H]+	-	-
251.095878	N	C11H14N4OS [M+H]+	-	-
253.090714	N	C8H14N4O4 [M+Na]+	-	-
259.153029	N	C12H20N4O [M+Na]+	-	-
259.153941	N	C13H22O5 [M+H]+	-	-
260.185591	H / N	C13H25NO4 [M+H]+	HMDB00705	Hexanoylcarnitine
260.185591	H / N	C13H25NO4 [M+H]+	HMDB00756	L-Hexanoylcarnitine
262.154975	H / N	C14H19N3O2 [M+H]+	HMDB61150	Hydroxyl frovatriptan
266.196209	N	C12H27NO5 [M+H]+	-	-
267.135430	N	C16H20O2 [M+Na]+	-	-
267.143835	N	C11H22O7 [M+H]+	-	-
268.103151	N	C9H11N9 [M+Na]+	-	-
270.217615	N	C14H27N3O2 [M+H]+	-	-
271.127518	N	C11H24N2S2 [M+Na]+	-	-
271.132050	N	C9H22N2O5S [M+H]+	-	-
271.190331	H / N	C15H26O4 [M+H]+	HMDB40459	Ethylene brassylate
275.186787	N	C15H22N4O [M+H]+	-	-
277.263769	N	C18H32N2 [M+H]+	-	-

278.232614	N	C14H31NO4 [M+H]+	-	-
279.051078	N	C8H16O7S [M+Na]+	-	-
279.062916	H / N	C15H12O4 [M+Na]+	HMDB05760	Dihydrodaidzein
279.062916	H / N	C15H12O4 [M+Na]+	HMDB29462	(E)-2,4,4'-Trihydroxychalcone
279.062916	H / N	C15H12O4 [M+Na]+	HMDB29519	(2S)-Liquiritigenin
279.062916	H / N	C15H12O4 [M+Na]+	HMDB30808	(S)-Pinocembrin
279.062916	H / N	C15H12O4 [M+Na]+	HMDB32577	4'-Methoxybenzophenone-2-carboxylic acid
279.062916	H / N	C15H12O4 [M+Na]+	HMDB33904	7E-Mycosinyl acetate
279.062916	H / N	C15H12O4 [M+Na]+	HMDB36457	Emodinanthranol
279.062916	H / N	C15H12O4 [M+Na]+	HMDB37316	Isoliquiritigenin
279.062916	H / N	C15H12O4 [M+Na]+	HMDB41647	2-Dehydro-O-desmethylangolensin
281.114751	H	C14H12N6O [M+H]+	HMDB15058	Levosimendan
281.114751	H / N	C16H18O3 [M+Na]+	HMDB30420	Strobilurin A
284.237312	N	C20H29N [M+H]+	-	-
285.070849	N	C10H10N6O3 [M+Na]+	-	-
285.169678	H / N	C15H24O5 [M+H]+	HMDB60593	Alpha-dihydroartemisinin
285.169678	H / N	C15H24O5 [M+H]+	HMDB61088	Dihydroartemisinin (DHA)
285.206015	N	C16H28O4 [M+H]+	-	-
286.201309	H / N	C15H27NO4 [M+H]+	HMDB13324	2-Octenoylcarnitine
287.085825	N	C10H20N2O2S2 [M+Na]+	-	-
288.216981	H / N	C15H29NO4 [M+H]+	HMDB00791	L-Octanoylcarnitine
291.112997	N	C18H14N2O2 [M+H]+	-	-
291.159122	H	C18H22NO [M+Na]+	HMDB30347	N-(p-Hydroxyphenethyl)actinidine
291.159122	H / N	C17H22O4 [M+H]+	HMDB29474	[6]-Dehydrogingerdione
291.159122	H / N	C17H22O4 [M+H]+	HMDB36771	Laurenobiolide
291.159122	H / N	C17H22O4 [M+H]+	HMDB39949	Oudemansin A
291.159122	H / N	C17H22O4 [M+H]+	HMDB60380	3-Polyprenyl-4,5-dihydroxybenzoate
292.248224	N	C15H33NO4 [M+H]+	-	-
293.066666	N	C9H18O7S [M+Na]+	-	-
293.147184	N	C13H22N2O4 [M+Na]+	-	-
293.174758	H / N	C17H24O4 [M+H]+	HMDB34658	9-Acetoxyfukinanolide
293.174758	H / N	C17H24O4 [M+H]+	HMDB34738	Isotrichodermin
293.174758	H / N	C17H24O4 [M+H]+	HMDB34930	(3beta,6beta)-Furanoeremophilane-3,6-diol 6-acetate
293.174758	H / N	C17H24O4 [M+H]+	HMDB35687	Acetylvalerenolic acid
293.174758	H / N	C17H24O4 [M+H]+	HMDB36693	Acetylbalchanolide
293.174758	H / N	C17H24O4 [M+H]+	HMDB39275	[6]-Gingerdione
293.174758	H / N	C17H24O4 [M+H]+	HMDB41249	6-Hydroxyshogaol
294.170003	N	C16H23NO4 [M+H]+	-	-
294.178048	N	C11H27N5S2 [M+H]+	-	-
297.206091	H / N	C17H28O4 [M+H]+	HMDB35075	Tanacetol B
297.206091	H / N	C17H28O4 [M+H]+	HMDB38798	(1(10)E,4a,5E)-1(10),5-Germacradiene-12-acetoxy-4,11-diol
301.162168	H / N	C13H26O6 [M+Na]+	HMDB35028	(x)-2-Heptanol glucoside
301.201004	N	C16H28O5 [M+H]+	-	-
302.136145	H / N	C15H21NO4 [M+Na]+	HMDB31802	(±)-Metalaxyl
302.196193	N	C15H27NO5 [M+H]+	-	-
303.180249	H / N	C15H26O6 [M+H]+	HMDB31094	Glycerol tributanoate
304.211914	N	C15H29NO5 [M+H]+	-	-
305.268657	N	C17H36O4 [M+H]+	-	-
307.112608	N	C10H16N6O4 [M+Na]+	-	-
307.154046	H	C18H22NO2 [M+Na]+	HMDB33483	6,7-Dihydro-4-(hydroxymethyl)-2-(p-hydroxyphenethyl)-7-methyl-5H-2-pyrindinium
307.154046	H / N	C17H22O5 [M+H]+	HMDB35781	Naematolone
307.154046	H / N	C17H22O5 [M+H]+	HMDB36487	Achillicin
307.154046	H / N	C17H22O5 [M+H]+	HMDB36643	Matricin
310.149497	N	C12H23NO8 [M+H]+	-	-
310.185945	N	C13H27NO7 [M+H]+	-	-
310.201277	H / N	C17H27NO4 [M+H]+	HMDB15334	Nadolol
310.201277	H / N	C17H27NO4 [M+H]+	HMDB15345	Metipranolol
311.185359	H / N	C17H26O5 [M+H]+	HMDB40756	3-Hydroxy-6,8-dimethoxy-7(11)-eremophilen-12,8-olide
311.185359	H / N	C17H26O5 [M+H]+	HMDB40980	Valdiate
311.204564	N	C11H30N6S2 [M+H]+	-	-
312.185542	N	C14H25N5OS [M+H]+	-	-
313.113215	N	C11H14N8O2 [M+Na]+	-	-
314.141963	N	C15H23NO4S [M+H]+	-	-
314.234752	N	C13H33N5S [M+Na]+	-	-
316.106021	N	C10H21NO8S [M+H]+	-	-
316.248265	H / N	C17H33NO4 [M+H]+	HMDB00651	Decanoylcarnitine
317.058279	N	C11H19O5PS [M+Na]+	-	-
317.187486	N	C21H26O [M+Na]+	-	-
318.181259	H / N	C17H23N3O3 [M+H]+	HMDB28918	Isoleucyl-Tryptophan
318.181259	H / N	C17H23N3O3 [M+H]+	HMDB28940	Leucyl-Tryptophan
318.181259	H / N	C17H23N3O3 [M+H]+	HMDB29086	Tryptophyl-Isoleucine
318.181259	H / N	C17H23N3O3 [M+H]+	HMDB29087	Tryptophyl-Leucine

319.149319	N	C20H24S [M+Na]+	-	-
320.233204	N	C18H29N3O2 [M+H]+	-	-
321.109923	H / N	C18H18O4 [M+Na]+	HMDB04808	7C-aglycone
321.109923	H / N	C18H18O4 [M+Na]+	HMDB06101	Enterolactone
321.109923	H / N	C18H18O4 [M+Na]+	HMDB29543	(+)-Ligballinol
321.109923	H / N	C18H18O4 [M+Na]+	HMDB30695	7-Hydroxy-5-methoxy-6,8-dimethylflavanone
321.109923	H / N	C18H18O4 [M+Na]+	HMDB37376	1-(2,4-Dihydroxy-6-methoxy-3,5-dimethylphenyl)-3-phenyl-2-propen-1-one
321.109923	H / N	C18H18O4 [M+Na]+	HMDB38453	5,7-Dimethoxy-6-methylflavanone
326.199883	N	C14H31NO5S [M+H]+	-	-
328.160302	N	C12H25NO9 [M+H]+	-	-
329.135337	N	C15H24N2O2S2 [M+H]+	-	-
329.136096	H / N	C17H22O5 [M+Na]+	HMDB35781	Naematolone
329.136096	H / N	C17H22O5 [M+Na]+	HMDB36487	Achillicin
329.136096	H / N	C17H22O5 [M+Na]+	HMDB36643	Matricin
330.124931	N	C15H21N3O2S [M+Na]+	-	-
330.263948	H / N	C18H35NO4 [M+H]+	HMDB06202	4,8 Dimethylnonanoyl carnitine
330.263948	H / N	C18H35NO4 [M+H]+	HMDB13321	Undecanoylcarnitine
331.134360	N	C10H24N6OS2 [M+Na]+	-	-
332.206807	N	C16H29NO6 [M+H]+	-	-
336.214489	H / N	C17H31NO4 [M+Na]+	HMDB13205	9-Decenoylcarnitine
339.087265	N	C14H20O6S [M+Na]+	-	-
340.183431	N	C12H29N5O2S2 [M+H]+	-	-
340.217832	N	C11H27N9O2 [M+Na]+	-	-
342.227521	N	C18H31NO5 [M+H]+	-	-
342.263861	H / N	C19H35NO4 [M+H]+	HMDB13326	trans-2-Dodecenoylcarnitine
343.221953	N	C16H28N6O [M+Na]+	-	-
343.247891	H / N	C19H34O5 [M+H]+	HMDB40901	13-Hydroxy-9-methoxy-10-oxo-11-octadecenoic acid
344.140521	H / N	C16H23N3O2S [M+Na]+	HMDB61011	N-desmethylalmotriptan
344.179358	N	C13H27N3O6 [M+Na]+	-	-
344.225405	N	C18H33NO3S [M+H]+	-	-
344.279552	H / N	C19H37NO4 [M+H]+	HMDB02250	Dodecanoylcarnitine
345.188396	N	C15H30O7 [M+Na]+	-	-
346.258812	N	C18H35NO5 [M+H]+	-	-
348.213061	N	C15H29N3O6 [M+H]+	-	-
349.177293	H / N	C21H26O3 [M+Na]+	HMDB03039	Isoacitretin
349.177293	H / N	C21H26O3 [M+Na]+	HMDB14602	Acitretin
351.200167	N	C15H28N4O4 [M+Na]+	-	-
353.172267	H / N	C20H26O4 [M+Na]+	HMDB02121	Carnosol
353.172267	H / N	C20H26O4 [M+Na]+	HMDB36749	Momilactone B
353.172267	H / N	C20H26O4 [M+Na]+	HMDB36753	Yucalexin P15
353.172267	H / N	C20H26O4 [M+Na]+	HMDB36755	Yucalexin P8
353.172267	H / N	C20H26O4 [M+Na]+	HMDB39613	3,3',4,4'-Tetrahydroxy-5,5'-diisopropyl-2,2'-dimethylbiphenyl
354.188704	N	C16H29NO6 [M+Na]+	-	-
354.202279	N	C17H27N3O5 [M+H]+	-	-
355.136351	N	C15H24O8 [M+Na]+	-	-
356.174407	N	C15H33NO2S3 [M+H]+	-	-
356.261769	N	C20H37NO2S [M+H]+	-	-
358.156043	N	C12H28N3O5PS [M+H]+	-	-
358.221218	N	C17H29N5O2 [M+Na]+	-	-
358.277447	N	C20H39NO2S [M+H]+	-	-
358.295168	N	C20H39NO4 [M+H]+	-	-
360.215231	N	C12H31N7O2S [M+Na]+	-	-
360.274440	H / N	C19H37NO5 [M+H]+	HMDB13164	2-Hydroxylauroylcarnitine
361.139369	H / N	C18H20N2O6 [M+H]+	HMDB06045	Dityrosine
361.139369	H / N	C18H20N2O6 [M+H]+	HMDB15187	Nitrendipine
361.173525	N	C17H26N2O5 [M+Na]+	-	-
361.357764	N	C24H44N2 [M+H]+	-	-
362.191188	N	C14H25N7O3 [M+Na]+	-	-
363.194042	N	C15H28N6OS [M+Na]+	-	-
364.195542	N	C15H27N5O4 [M+Na]+	-	-
364.248238	N	C21H33NO4 [M+H]+	-	-
366.225088	N	C18H33NO5 [M+Na]+	-	-
366.263887	N	C21H35NO4 [M+H]+	-	-
368.191421	N	C15H29NO9 [M+H]+	-	-
368.278550	N	C20H35N5 [M+Na]+	-	-
368.279517	H / N	C21H37NO4 [M+H]+	HMDB13331	3, 5-Tetradecadiencarnitine
369.372699	H / N	C24H48O2 [M+H]+	HMDB02003	Tetracosanoic acid
369.372699	H / N	C24H48O2 [M+H]+	HMDB35633	5-Hydroxy-7-tetracosanone
369.372699	H / N	C24H48O2 [M+H]+	HMDB35636	4-Hydroxy-6-tetracosanone
369.372699	H / N	C24H48O2 [M+H]+	HMDB40887	20-Tetracosene-1,18-diol
370.295196	H / N	C21H39NO4 [M+H]+	HMDB02014	cis-5-Tetradecenoylcarnitine
370.295196	H / N	C21H39NO4 [M+H]+	HMDB13329	trans-2-Tetradecenoylcarnitine

371.078742	N	C15H16N4O4S [M+Na]+	-	-
373.198478	H / N	C20H30O5 [M+Na]+	HMDB02341	8-iso-15-keto-PGE2
373.198478	H / N	C20H30O5 [M+Na]+	HMDB02664	Prostaglandin E3
373.198478	H / N	C20H30O5 [M+Na]+	HMDB03034	Prostaglandin D3
373.198478	H / N	C20H30O5 [M+Na]+	HMDB03175	15-Keto-prostaglandin E2
373.198478	H / N	C20H30O5 [M+Na]+	HMDB10410	Resolvin E1
373.198478	H / N	C20H30O5 [M+Na]+	HMDB12552	12-Oxo-20-hydroxy-leukotriene B4
373.198478	H / N	C20H30O5 [M+Na]+	HMDB12588	15-Epi-lipoxin B5
373.198478	H / N	C20H30O5 [M+Na]+	HMDB12590	15-Oxo-lipoxin A4
373.198478	H / N	C20H30O5 [M+Na]+	HMDB12641	20-oxo-leukotriene B4
373.198478	H / N	C20H30O5 [M+Na]+	HMDB13040	PGH3
373.198478	H / N	C20H30O5 [M+Na]+	HMDB36701	(ent-6alpha,7alpha,12alpha)-6,7,12-Trihydroxy-16-kauren-19-oic acid
373.198478	H / N	C20H30O5 [M+Na]+	HMDB37593	Oryzalic acid A
373.198478	H / N	C20H30O5 [M+Na]+	HMDB38693	Oryzalic acid B
373.198478	H / N	C20H30O5 [M+Na]+	HMDB60096	5,12,18R-TriHEPE
373.213264	N	C16H34N2O4S [M+Na]+	-	-
374.065809	N	C14H19N3O3S3 [M+H]+	-	-
374.302987	N	C22H41NO2 [M+Na]+	-	-
375.220734	N	C20H38S3 [M+H]+	-	-
376.223973	N	C15H35N3O4S [M+Na]+	-	-
378.224822	N	C17H27N7O3 [M+H]+	-	-
379.184128	N	C17H28N2O6 [M+Na]+	-	-
380.175836	N	C25H21N3O [M+H]+	-	-
381.210135	N	C14H32N6O2S2 [M+H]+	-	-
381.211200	N	C16H30N4O5 [M+Na]+	-	-
383.167670	N	C17H28O8 [M+Na]+	-	-
383.204046	N	C18H32O7 [M+Na]+	-	-
383.205117	N	C19H36O2S2 [M+Na]+	-	-
383.315643	H / N	C23H42O4 [M+H]+	HMDB11544	MG(0:0/20:2(11Z,14Z)/0:0)
383.315643	H / N	C23H42O4 [M+H]+	HMDB11574	MG(20:2(11Z,14Z)/0:0/0:0)
383.315643	H / N	C23H42O4 [M+H]+	HMDB35959	Persenone B
383.315643	H / N	C23H42O4 [M+H]+	HMDB36865	Lepidiumterpenyl ester
384.163310	N	C15H25N7OS2 [M+H]+	-	-
384.164134	N	C17H23N5O4 [M+Na]+	-	-
384.164953	H / N	C18H25NO8 [M+H]+	HMDB38630	Niazimin A
384.166133	N	C19H29NO3S2 [M+H]+	-	-
384.204261	N	C15H31N5O3S [M+Na]+	-	-
384.274419	H / N	C21H37NO5 [M+H]+	HMDB13332	3-Hydroxy-5, 8-tetradecadiencarnitine
384.310872	N	C22H41NO4 [M+H]+	-	-
385.210681	N	C13H30N8O2S [M+Na]+	-	-
385.222075	H / N	C20H32O7 [M+H]+	HMDB12643	20-Trihydroxy-leukotriene-B4
385.222075	H / N	C20H32O7 [M+H]+	HMDB36010	Cinnzeylanol
385.245185	N	C19H36N4S2 [M+H]+	-	-
386.225436	N	C14H35N5O3S2 [M+H]+	-	-
386.246856	N	C19H35N3O3S [M+H]+	-	-
386.290095	H / N	C21H39NO5 [M+H]+	HMDB13330	3-Hydroxy-cis-5-tetradecenoylcarnitine
388.198870	N	C14H31N5O4S [M+Na]+	-	-
388.305731	H / N	C21H41NO5 [M+H]+	HMDB13166	2-Hydroxymyristoylcarnitine
389.147005	N	C13H26N4O6S [M+Na]+	-	-
389.199176	N	C19H32O6S [M+H]+	-	-
389.214579	N	C17H34O8 [M+Na]+	-	-
389.216931	H / N	C19H32O8 [M+H]+	HMDB31676	5a,6a-Epoxy-7E-megastigmene-3a,9e-diol 3-glucoside
389.216931	H / N	C19H32O8 [M+H]+	HMDB36318	9,13-Dihydroxy-4-megastigmen-3-one 9-glucoside
389.216931	H / N	C19H32O8 [M+H]+	HMDB36846	Icariside B8
389.216931	H / N	C19H32O8 [M+H]+	HMDB38306	5a,6a-Epoxy-7E-megastigmene-3b,9e-diol 9-glucoside
389.216931	H / N	C19H32O8 [M+H]+	HMDB40614	Dihydroroseoside
390.233295	N	C15H37N5OS2 [M+Na]+	-	-
391.209160	H / N	C20H32O6 [M+Na]+	HMDB01908	19-Hydroxy-PGE2
391.209160	H / N	C20H32O6 [M+Na]+	HMDB01979	6,15-Diketo,13,14-dihydro-PGF1a
391.209160	H / N	C20H32O6 [M+Na]+	HMDB03235	Prostaglandin G2
391.209160	H / N	C20H32O6 [M+Na]+	HMDB03247	20-Hydroxy-PGE2
391.209160	H / N	C20H32O6 [M+Na]+	HMDB04241	6-Ketoprostaglandin E1
391.209160	H / N	C20H32O6 [M+Na]+	HMDB04242	11-Dehydro-thromboxane B2
391.209160	H / N	C20H32O6 [M+Na]+	HMDB05099	Thromboxane B3
391.209160	H / N	C20H32O6 [M+Na]+	HMDB12110	5(6)-Epoxy Prostaglandin E1
391.209160	H / N	C20H32O6 [M+Na]+	HMDB12633	20-COOH-10,11-dihydro-LTB4
391.209160	H / N	C20H32O6 [M+Na]+	HMDB12635	20-dihydroxyleukotriene B4
391.209160	H / N	C20H32O6 [M+Na]+	HMDB34678	Cinncassiol D2
391.209160	H / N	C20H32O6 [M+Na]+	HMDB36854	Cinncassiol D3
392.083610	N	C12H24N3O4PS2 [M+Na]+	-	-
394.189449	N	C17H31NO7S [M+H]+	-	-
394.295254	N	C23H39NO4 [M+H]+	-	-

395.062428	N	C13H24O6S3 [M+Na]+	-	-
395.216915	N	C19H28N6O2 [M+Na]+	-	-
395.226409	N	C17H32N4O5 [M+Na]+	-	-
395.298544	N	C17H42N6S2 [M+H]+	-	-
396.310830	H / N	C23H41NO4 [M+H]+	HMDB13334	9,12-Hexadecadienoylcarnitine
397.254993	N	C17H30N10 [M+Na]+	-	-
398.223020	N	C26H27N3O [M+H]+	-	-
399.283762	N	C20H44N2S2 [M+Na]+	-	-
399.358136	N	C23H46N2O3 [M+H]+	-	-
401.193664	H / N	C21H30O6 [M+Na]+	HMDB00418	18-Hydroxycortisol
401.193664	H / N	C21H30O6 [M+Na]+	HMDB30045	Isohumulinone A
401.193664	H / N	C21H30O6 [M+Na]+	HMDB30105	Humulinone
401.193664	H / N	C21H30O6 [M+Na]+	HMDB32770	Eremopetasitenin C1
401.193664	H / N	C21H30O6 [M+Na]+	HMDB32773	Eremopetasitenin D1
401.193664	H / N	C21H30O6 [M+Na]+	HMDB36889	11-Dihydro-12-norneoquassin
401.193664	H / N	C21H30O6 [M+Na]+	HMDB40702	Sugetriol triacetate
401.193664	H / N	C21H30O6 [M+Na]+	HMDB61033	6-beta-hydrocortisol
403.209092	H / N	C21H32O6 [M+Na]+	HMDB40568	[6]-Gingerdiol 3,5-diacetate
403.229060	N	C15H28N10O2 [M+Na]+	-	-
403.230193	N	C18H36O8 [M+Na]+	-	-
405.084270	N	C15H18N4O6S [M+Na]+	-	-
405.156968	N	C17H26N4O4S [M+Na]+	-	-
405.209363	N	C17H34O9 [M+Na]+	-	-
405.215963	N	C16H30N8OS [M+Na]+	-	-
407.195096	N	C15H28N8O2S [M+Na]+	-	-
409.078099	N	C14H26O6S3 [M+Na]+	-	-
409.183262	H / N	C19H30O8 [M+Na]+	HMDB29772	Corchoionol C 9-glucoside
409.183262	H / N	C19H30O8 [M+Na]+	HMDB30370	Citroside A
409.183262	H / N	C19H30O8 [M+Na]+	HMDB35212	Sonchuionoside C
410.223096	N	C27H27N3O [M+H]+	-	-
410.290123	N	C23H39NO5 [M+H]+	-	-
411.141561	H / N	C21H24O7 [M+Na]+	HMDB33284	8-Hydroxy-4'-methoxypinoresinol
411.141561	H / N	C21H24O7 [M+Na]+	HMDB35110	8-Epidiosbulbin E acetate
411.141561	H / N	C21H24O7 [M+Na]+	HMDB36557	MS 3
411.141561	H / N	C21H24O7 [M+Na]+	HMDB39059	(R)-Heraclenol 2'-(3-methylbutanoate)
411.141561	H / N	C21H24O7 [M+Na]+	HMDB41197	Edulisin III
411.187596	N	C18H26N4O7 [M+H]+	-	-
411.271712	N	C21H40O6 [M+Na]+	-	-
412.164325	N	C17H33NO4S3 [M+H]+	-	-
412.238647	N	C27H29N3O [M+H]+	-	-
412.305788	H / N	C23H41NO5 [M+H]+	HMDB13335	3-Hydroxyhexadecadienoylcarnitine
414.139925	N	C15H26N3O7P [M+Na]+	-	-
414.212253	N	C20H31NO8 [M+H]+	-	-
415.215829	N	C14H34N6O4S2 [M+H]+	-	-
415.245555	H / N	C23H36O5 [M+Na]+	HMDB60730	20, 22-Dihydrodigoxigenin
416.212482	N	C16H35N5O2S2 [M+Na]+	-	-
417.105310	N	C13H22N4O8S [M+Na]+	-	-
417.224819	H / N	C22H34O6 [M+Na]+	HMDB31964	(3b,6b,8b,12a)-8,12-Epoxy-7(11)-eremophilene-6-angeloyloxy-8,12-dimethoxy-3-ol
417.224819	H / N	C22H34O6 [M+Na]+	HMDB40569	3'-Methoxy-[6]-Gingerdiol 3,5-diacetate
417.247169	N	C20H34N4O4 [M+Na]+	-	-
419.100857	N	C17H22O10S [M+H]+	-	-
419.281873	N	C21H40N4OS [M+Na]+	-	-
420.317787	N	C19H41N5O5 [M+H]+	-	-
421.202640	N	C14H34N6O3S2 [M+Na]+	-	-
422.323955	H / N	C23H45NO4 [M+Na]+	HMDB00222	L-Palmitoylcarnitine
422.326523	H / N	C25H43NO4 [M+H]+	HMDB06318	Gamma-linolenyl carnitine
422.326523	H / N	C25H43NO4 [M+H]+	HMDB06319	Alpha-linolenyl carnitine
423.130161	N	C16H32O5S3 [M+Na]+	-	-
424.282410	N	C25H39NO3 [M+Na]+	-	-
424.342144	H / N	C25H45NO4 [M+H]+	HMDB06461	Linoelaidyl carnitine
424.342144	H / N	C25H45NO4 [M+H]+	HMDB06469	Linoleyl carnitine
426.357753	H / N	C25H47NO4 [M+H]+	HMDB05065	Oleoylcarnitine
426.357753	H / N	C25H47NO4 [M+H]+	HMDB06351	Vaccenyl carnitine
426.357753	H / N	C25H47NO4 [M+H]+	HMDB06464	Elaidic carnitine
426.357753	H / N	C25H47NO4 [M+H]+	HMDB13338	11Z-Octadecenylcarnitine
427.147030	N	C12H28N4O9S [M+Na]+	-	-
428.230495	N	C17H35N5O4S [M+Na]+	-	-
429.152130	N	C21H26O8 [M+Na]+	-	-
430.228224	N	C17H37N5O2S2 [M+Na]+	-	-
430.273054	N	C21H39N3O4S [M+H]+	-	-
430.316413	H / N	C23H43NO6 [M+H]+	HMDB00712	Hexadecanedioic acid mono-L-carnitine ester
431.276701	H / N	C24H40O5 [M+Na]+	HMDB00312	3a,7a,12b-Trihydroxy-5b-cholanoic acid

431.276701	H / N	C24H40O5 [M+Na]+	HMDB00320	3a,4b,7a-Trihydroxy-5b-cholanoic acid
431.276701	H / N	C24H40O5 [M+Na]+	HMDB00326	1b,3a,12a-Trihydroxy-5b-cholanoic acid
431.276701	H / N	C24H40O5 [M+Na]+	HMDB00330	3a,4b,12a-Trihydroxy-5b-cholanoic acid
431.276701	H / N	C24H40O5 [M+Na]+	HMDB00364	3a,6a,7b-Trihydroxy-5b-cholanoic acid
431.276701	H / N	C24H40O5 [M+Na]+	HMDB00371	1,3,12-Trihydroxycholan-24-oic acid
431.276701	H / N	C24H40O5 [M+Na]+	HMDB00376	3b,7a,12a-Trihydroxy-5a-Cholanoic acid
431.276701	H / N	C24H40O5 [M+Na]+	HMDB00390	3a,7b,12b-Trihydroxy-5b-cholanoic acid
431.276701	H / N	C24H40O5 [M+Na]+	HMDB00395	3b,7b,12a-Trihydroxy-5b-cholanoic acid
431.276701	H / N	C24H40O5 [M+Na]+	HMDB00404	2b,3a,7a-Trihydroxy-5b-cholanoic acid
431.276701	H / N	C24H40O5 [M+Na]+	HMDB00414	1b,3a,7a-Trihydroxy-5b-cholanoic acid
431.276701	H / N	C24H40O5 [M+Na]+	HMDB00415	3a,6b,7b-Trihydroxy-5b-cholanoic acid
431.276701	H / N	C24H40O5 [M+Na]+	HMDB00419	3b,7a,12a-Trihydroxy-5b-cholanoic acid
431.276701	H / N	C24H40O5 [M+Na]+	HMDB00427	3b,7b,12a-Trihydroxy-5a-Cholanoic acid
431.276701	H / N	C24H40O5 [M+Na]+	HMDB00432	3a,7b,12a-Trihydroxy-5a-Cholanoic acid
431.276701	H / N	C24H40O5 [M+Na]+	HMDB00505	Allocholic acid
431.276701	H / N	C24H40O5 [M+Na]+	HMDB00506	Alpha-Muricholic acid
431.276701	H / N	C24H40O5 [M+Na]+	HMDB00527	6a,12a-Dihydroxylithocholic acid
431.276701	H / N	C24H40O5 [M+Na]+	HMDB00619	Cholic acid
431.276701	H / N	C24H40O5 [M+Na]+	HMDB00760	Hyocholic acid
431.276701	H / N	C24H40O5 [M+Na]+	HMDB00865	Muricholic acid
431.276701	H / N	C24H40O5 [M+Na]+	HMDB00917	Ursocholic acid
431.324413	N	C24H44N2O3 [M+Na]+	-	-
434.238355	N	C20H35NO9 [M+H]+	-	-
434.270355	N	C23H41NO3S [M+Na]+	-	-
437.181908	N	C23H24N4O5 [M+H]+	-	-
437.206483	N	C17H32N4O7S [M+H]+	-	-
439.172895	H / N	C23H28O7 [M+Na]+	HMDB37040	Armillaric acid
439.172895	H / N	C23H28O7 [M+Na]+	HMDB38786	10-Hydroxymelleolide
439.193890	H / N	C20H32O9 [M+Na]+	HMDB36340	Ethyl 7-epi-12-hydroxyjasmonate glucoside
439.200387	N	C20H38O4S3 [M+H]+	-	-
439.287713	N	C25H42O4S [M+H]+	-	-
439.318289	H / N	C27H44O3 [M+Na]+	HMDB00430	24,25-Dihydroxyvitamin D
439.318289	H / N	C27H44O3 [M+Na]+	HMDB01420	25,26-dihydroxyvitamin D
439.318289	H / N	C27H44O3 [M+Na]+	HMDB01903	Calcitriol
439.318289	H / N	C27H44O3 [M+Na]+	HMDB02197	7a,12a-Dihydroxy-cholestene-3-one
439.318289	H / N	C27H44O3 [M+Na]+	HMDB06226	24R,25-Dihydroxyvitamin D3
439.318289	H / N	C27H44O3 [M+Na]+	HMDB06720	23S,25-dihydroxyvitamin D3
439.318289	H / N	C27H44O3 [M+Na]+	HMDB12453	3 beta-Hydroxy-5-cholestenoate
439.318289	H / N	C27H44O3 [M+Na]+	HMDB12457	7 alpha,24-Dihydroxy-4-cholesten-3-one
439.318289	H / N	C27H44O3 [M+Na]+	HMDB12459	7 alpha,26-Dihydroxy-4-cholesten-3-one
439.318289	H / N	C27H44O3 [M+Na]+	HMDB15046	Paricalcitol
439.318289	H / N	C27H44O3 [M+Na]+	HMDB30024	Sarsasapogenin
439.318289	H / N	C27H44O3 [M+Na]+	HMDB30047	Neotigogenin
439.318289	H / N	C27H44O3 [M+Na]+	HMDB30048	Smilagenin
439.318289	H / N	C27H44O3 [M+Na]+	HMDB35300	Octadecyl cis-p-coumarate
439.318289	H / N	C27H44O3 [M+Na]+	HMDB60133	(24R)-24,25-Dihydroxycalciol
439.318289	H / N	C27H44O3 [M+Na]+	HMDB60425	7alpha,25-Dihydroxy-4-cholesten-3-one
439.318289	H / N	C27H44O3 [M+Na]+	HMDB60508	Secalciferol
440.273099	N	C20H39N3O6 [M+Na]+	-	-
441.098029	N	C21H22O7S [M+Na]+	-	-
441.141611	N	C16H26N4O7S [M+Na]+	-	-
441.295213	N	C22H38N6O2 [M+Na]+	-	-
441.357434	H / N	C26H48O5 [M+H]+	HMDB29804	Momordol
442.185765	N	C16H25N11OS [M+Na]+	-	-
443.263927	N	C23H38O8 [M+H]+	-	-
445.326559	N	C22H42N6O2 [M+Na]+	-	-
447.220143	N	C19H36O10 [M+Na]+	-	-
448.119095	N	C23H23NO5S [M+Na]+	-	-
449.111400	N	C18H24O11S [M+H]+	-	-
449.261006	N	C19H30N12 [M+Na]+	-	-
450.243670	N	C18H33N7O5 [M+Na]+	-	-
452.281468	N	C16H35N11O3 [M+Na]+	-	-
452.286301	N	C22H45NO4S2 [M+H]+	-	-
458.186738	N	C17H33N5O4S2 [M+Na]+	-	-
458.190998	N	C22H33N3O2S2 [M+Na]+	-	-
459.415691	N	C26H54N2O4 [M+H]+	-	-
463.157550	N	C21H28O10 [M+Na]+	-	-
463.297589	N	C17H44N8OS2 [M+Na]+	-	-
465.195006	N	C17H32N6O5S2 [M+H]+	-	-
465.230798	N	C19H38O11 [M+Na]+	-	-
465.324820	N	C24H48O6S [M+H]+	-	-
467.172632	N	C22H28N4O4S [M+Na]+	-	-

467.200893	N	C21H36N2O4S2 [M+Na]+	-	-
471.101748	N	C21H24N2O5S2 [M+Na]+	-	-
471.167532	N	C21H28N4O5S [M+Na]+	-	-
472.256597	N	C19H39N5O5S [M+Na]+	-	-
473.137789	N	C23H24N2O7S [M+H]+	-	-
473.308708	N	C23H46O8 [M+Na]+	-	-
474.151868	N	C17H29N3O9S [M+Na]+	-	-
475.199379	N	C22H34O9S [M+H]+	-	-
479.140282	N	C20H30O9S2 [M+H]+	-	-
480.280148	N	C22H41NO10 [M+H]+	-	-
483.147441	H / N	C20H28O12 [M+Na]+	HMDB33138	Methyl salicylate O-[rhamnosyl-(1->6)-glucoside]
483.164305	N	C18H30N2O11S [M+H]+	-	-
483.249233	N	C27H34N2O6 [M+H]+	-	-
484.259735	N	C30H33N3O3 [M+H]+	-	-
484.333953	N	C20H45N5O8 [M+H]+	-	-
485.214781	H / N	C25H34O8 [M+Na]+	HMDB10337	6-Dehydrotestosterone glucuronide
486.217998	N	C19H37N5O4S2 [M+Na]+	-	-
487.291601	N	C26H38N4O5 [M+H]+	-	-
488.284929	N	C16H39N11O3S [M+Na]+	-	-
488.288874	N	C21H45NO9S [M+H]+	-	-
489.377366	N	C26H50N4O3 [M+Na]+	-	-
490.167719	N	C20H31N3O7S2 [M+H]+	-	-
492.223117	N	C25H33NO9 [M+H]+	-	-
493.164120	N	C23H28N2O8S [M+H]+	-	-
494.293353	N	C27H43NO5S [M+H]+	-	-
496.364741	N	C29H45N5O2 [M+H]+	-	-
497.383550	N	C29H52O6 [M+H]+	-	-
500.242334	N	C23H37N3O7S [M+H]+	-	-
500.325281	N	C23H49NO8S [M+H]+	-	-
500.328963	N	C20H45N5O9 [M+H]+	-	-
503.157485	N	C21H28N4O7S [M+Na]+	-	-
505.292077	N	C30H42O5 [M+Na]+	-	-
507.138777	N	C18H34O10S3 [M+H]+	-	-
507.171608	N	C22H34O9S2 [M+H]+	-	-
507.277478	N	C22H44O11 [M+Na]+	-	-
509.185934	N	C15H27N12O5P [M+Na]+	-	-
509.381604	N	C28H54O6 [M+Na]+	-	-
509.529238	H / N	C34H68O2 [M+H]+	HMDB30954	Grewinol
509.529238	H / N	C34H68O2 [M+H]+	HMDB35278	28-Hydroxy-6-methyl-5-tritriacontanone
511.298419	N	C22H46N4O5S2 [M+H]+	-	-
512.212444	N	C24H33NO11 [M+H]+	-	-
515.074511	N	C19H25O11PS [M+Na]+	-	-
516.332468	N	C23H45N7O4S [M+H]+	-	-
517.298310	N	C24H46O10 [M+Na]+	-	-
519.176050	N	C28H26N2O8 [M+H]+	-	-
523.248284	N	C21H44N2O7S2 [M+Na]+	-	-
523.396977	N	C29H56O6 [M+Na]+	-	-
524.269969	N	C23H41NO12 [M+H]+	-	-
524.331489	N	C26H51N3O2S2 [M+Na]+	-	-
525.203509	N	C19H32N4O13 [M+H]+	-	-
525.281871	N	C27H36N6O5 [M+H]+	-	-
526.366634	N	C27H49N7S [M+Na]+	-	-
527.079920	N	C18H23O16P [M+H]+	-	-
527.174337	N	C21H30N6O6S2 [M+H]+	-	-
527.202459	N	C20H38N4O6S3 [M+H]+	-	-
527.304560	N	C21H46N6O5S2 [M+H]+	-	-
528.160936	N	C25H25N3O10 [M+H]+	-	-
530.203540	N	C28H27N5O6 [M+H]+	-	-
531.511151	H / N	C34H68O2 [M+Na]+	HMDB30954	Grewinol
531.511151	H / N	C34H68O2 [M+Na]+	HMDB35278	28-Hydroxy-6-methyl-5-tritriacontanone
533.351122	N	C28H52O7S [M+H]+	-	-
534.140577	N	C23H29NO10S [M+Na]+	-	-
535.258244	N	C26H38N4O6S [M+H]+	-	-
536.147118	N	C28H26NO8P [M+H]+	-	-
537.087675	N	C16H28N2O12S3 [M+H]+	-	-
538.295979	N	C30H45NO4S [M+Na]+	-	-
539.147389	N	C23H33O9PS [M+Na]+	-	-
540.173812	N	C20H31N5O9S [M+Na]+	-	-
541.225599	H / N	C24H38O12 [M+Na]+	HMDB29773	6S,9R-Dihydroxy-4,7E-megastigmadien-3-one 9-[apiosyl-(1->6)-glucoside]
541.225599	H / N	C24H38O12 [M+Na]+	HMDB35520	Vomifoliol 9-[xylosyl-(1->6)-glucoside]
541.225599	H / N	C24H38O12 [M+Na]+	HMDB38923	Cinnamoside
541.227753	N	C18H34N10O6S [M+Na]+	-	-

541.282239	N	C27H42N4O4S [M+Na]+	-	-
542.173917	N	C22H31N5O7S2 [M+H]+	-	-
542.338041	N	C34H43N3O3 [M+H]+	-	-
544.099716	N	C17H26N3O13PS [M+H]+	-	-
548.291230	N	C22H47N5O5S2 [M+Na]+	-	-
549.336862	N	C25H46N6O6 [M+Na]+	-	-
551.304028	N	C24H48O12 [M+Na]+	-	-
552.301621	N	C25H45NO12 [M+H]+	-	-
553.195478	N	C24H40O8S3 [M+H]+	-	-
555.161229	N	C20H34N4O8S3 [M+H]+	-	-
555.256653	N	C29H40O9 [M+Na]+	-	-
555.311798	N	C31H48O5S [M+Na]+	-	-
555.361553	N	C27H52N2O8 [M+Na]+	-	-
559.002677	N	C17H17N2O14PS [M+Na]+	-	-
559.137521	N	C18H30N4O12S2 [M+H]+	-	-
559.438873	N	C32H62O5S [M+H]+	-	-
563.342556	N	C28H50O11 [M+H]+	-	-
567.241588	H / N	C26H40O12 [M+Na]+	HMDB35165	Cinncassiol A 19-glucoside
569.248063	N	C21H38N8O7S [M+Na]+	-	-
569.249510	N	C23H44N4O6S3 [M+H]+	-	-
569.250621	N	C31H32N6O5 [M+H]+	-	-
569.251928	N	C26H38N6O5S [M+Na]+	-	-
569.256946	H / N	C26H42O12 [M+Na]+	HMDB36317	Canavalioside
569.259305	H / N	C28H40O12 [M+H]+	HMDB38682	Musabalbisiane C
569.264836	H / N	C34H36N2O6 [M+H]+	HMDB31751	y-Morphine
570.248174	N	C26H39N3O9S [M+H]+	-	-
570.252928	N	C26H45NO7S2 [M+Na]+	-	-
573.328933	N	C25H50N4O7S [M+Na]+	-	-
577.360308	N	C31H52N4O2S2 [M+H]+	-	-
582.229686	N	C26H29N11O4 [M+Na]+	-	-
583.262295	N	C29H40N2O9 [M+Na]+	-	-
583.363230	N	C28H50N6O5S [M+H]+	-	-
585.253466	N	C27H38N4O9 [M+Na]+	-	-
587.270090	N	C28H42O13 [M+H]+	-	-
587.340290	N	C28H52O11 [M+Na]+	-	-
588.358760	N	C26H55N5O4S2 [M+Na]+	-	-
589.274269	N	C29H46N2O5S2 [M+Na]+	-	-
591.173585	N	C24H32N4O10S [M+Na]+	-	-
591.419664	N	C27H58N8O2S2 [M+H]+	-	-
594.340169	N	C33H49NO7 [M+Na]+	-	-
595.529643	H / N	C37H70O5 [M+H]+	HMDB07021	DG(14:0/20:1(11Z)/0:0)
595.529643	H / N	C37H70O5 [M+H]+	HMDB07049	DG(14:1(9Z)/20:0/0:0)
595.529643	H / N	C37H70O5 [M+H]+	HMDB07101	DG(16:0/18:1(11Z)/0:0)
595.529643	H / N	C37H70O5 [M+H]+	HMDB07102	DG(16:0/18:1(9Z)/0:0)
595.529643	H / N	C37H70O5 [M+H]+	HMDB07129	DG(16:1(9Z)/18:0/0:0)
595.529643	H / N	C37H70O5 [M+H]+	HMDB07157	DG(18:0/16:1(9Z)/0:0)
595.529643	H / N	C37H70O5 [M+H]+	HMDB07185	DG(18:1(11Z)/16:0/0:0)
595.529643	H / N	C37H70O5 [M+H]+	HMDB07214	DG(18:1(9Z)/16:0/0:0)
595.529643	H / N	C37H70O5 [M+H]+	HMDB07357	DG(20:0/14:1(9Z)/0:0)
595.529643	H / N	C37H70O5 [M+H]+	HMDB07385	DG(20:1(11Z)/14:0/0:0)
595.529643	H / N	C37H70O5 [M+H]+	HMDB55963	DG(14:0/0:0/20:1n9)
595.529643	H / N	C37H70O5 [M+H]+	HMDB56016	DG(16:0/0:0/18:1n7)
595.529643	H / N	C37H70O5 [M+H]+	HMDB56017	DG(16:0/0:0/18:1n9)
595.529643	H / N	C37H70O5 [M+H]+	HMDB56041	DG(18:0/0:0/16:1n7)
595.529643	H / N	C37H70O5 [M+H]+	HMDB56065	DG(20:0/0:0/14:1n5)
597.280069	N	C24H44N4O11S [M+H]+	-	-
597.282751	N	C28H42N6O5S [M+Na]+	-	-
597.290861	N	C30H38N8O4 [M+Na]+	-	-
597.296365	H / N	C36H40N2O6 [M+H]+	HMDB36361	Pipercyclobutanamide B
597.296365	H / N	C36H40N2O6 [M+H]+	HMDB40521	Dipiperamide D
597.300906	N	C28H42N6O7 [M+Na]+	-	-
597.324659	N	C29H50O11 [M+Na]+	-	-
598.283333	N	C27H45NO12 [M+Na]+	-	-
598.285953	N	C29H43NO12 [M+H]+	-	-
598.294116	N	C24H47N5O8S2 [M+H]+	-	-
598.327849	N	C36H43N3O5 [M+H]+	-	-
599.286816	H / N	C34H38N4O6 [M+H]+	HMDB00668	Hematoporphyrin IX
600.059882	N	C17H27N3O13S3 [M+Na]+	-	-
602.397292	N	C25H49N13O3 [M+Na]+	-	-
605.225552	N	C26H38N4O9S [M+Na]+	-	-
606.255541	N	C25H45NO12S [M+Na]+	-	-
607.369217	N	C30H48N8O4 [M+Na]+	-	-

607.372392	N	C27H52N8O4S [M+Na]+	-	-
610.312884	N	C26H43N9O6S [M+H]+	-	-
613.238210	N	C27H43O12P [M+Na]+	-	-
615.209064	N	C27H36N4O9S [M+Na]+	-	-
615.486985	N	C32H64N8S [M+Na]+	-	-
616.353125	N	C26H51N5O10 [M+Na]+	-	-
617.209346	N	C21H40N6O9S3 [M+H]+	-	-
617.278241	N	C27H46O14 [M+Na]+	-	-
618.393838	N	C28H57N3O10 [M+Na]+	-	-
621.205373	N	C22H38N4O13S [M+Na]+	-	-
623.415558	N	C35H58O9 [M+H]+	-	-
623.432387	N	C40H54N4O2 [M+H]+	-	-
624.298863	N	C29H47NO12 [M+Na]+	-	-
624.364793	N	C35H49N3O7 [M+H]+	-	-
625.279468	N	C31H48N2O5S3 [M+H]+	-	-
628.393306	N	C33H55N3O7 [M+Na]+	-	-
629.278101	N	C28H46O14 [M+Na]+	-	-
632.404795	N	C30H57N5O7S [M+H]+	-	-
637.319302	N	C31H50O12 [M+Na]+	-	-
640.302622	N	C32H47N3O7S [M+Na]+	-	-
641.426228	N	C35H60O10 [M+H]+	-	-
643.272860	N	C32H44O12 [M+Na]+	-	-
645.400434	N	C30H56N6O7S [M+H]+	-	-
645.451994	N	C35H60N6O3S [M+H]+	-	-
647.196158	N	C25H35N4O14P [M+H]+	-	-
647.380091	N	C31H60O10S [M+Na]+	-	-
647.461852	N	C28H64N8O5S [M+Na]+	-	-
648.235001	N	C27H42N3O11PS [M+H]+	-	-
649.355897	H / N	C33H54O11 [M+Na]+	HMDB34091	Ponasteroside A
651.395835	N	C33H62O8S2 [M+H]+	-	-
653.460448	N	C34H64N6O2S2 [M+H]+	-	-
656.225837	N	C23H45NO16S2 [M+H]+	-	-
658.239182	N	C31H42NO11P [M+Na]+	-	-
659.206699	N	C30H40N2O9S2 [M+Na]+	-	-
661.356018	H / N	C34H54O11 [M+Na]+	HMDB40405	26-Glucosyl-1,3,11,22-tetrahydroxyergosta-5,24-dien-26-oate
663.408158	N	C35H60O10 [M+Na]+	-	-
663.411270	N	C32H64O10S [M+Na]+	-	-
663.442049	N	C33H62N2O11 [M+H]+	-	-
665.350573	N	C33H54O12 [M+Na]+	-	-
665.355735	N	C31H54N4O8S [M+Na]+	-	-
665.411545	N	C34H64O8S2 [M+H]+	-	-
665.417501	N	C40H52N6O3 [M+H]+	-	-
667.301709	N	C39H42N2O8 [M+H]+	-	-
667.357798	N	C36H48N6O5 [M+Na]+	-	-
669.558121	H / N	C45H74O2 [M+Na]+	HMDB10369	CE(18:3(6Z,9Z,12Z))
669.558121	H / N	C45H74O2 [M+Na]+	HMDB10370	CE(18:3(9Z,12Z,15Z))
670.177701	N	C22H40NO18PS [M+H]+	-	-
670.428201	N	C35H63N3O5S2 [M+H]+	-	-
670.450224	N	C34H65NO10 [M+Na]+	-	-
671.304125	N	C34H48O12 [M+Na]+	-	-
671.325486	N	C30H50N6O7S2 [M+H]+	-	-
671.346012	N	C28H56O16 [M+Na]+	-	-
675.251025	N	C31H38N4O13 [M+H]+	-	-
675.434256	N	C39H60N2O6 [M+Na]+	-	-
677.227327	N	C28H46O13S2 [M+Na]+	-	-
677.451498	N	C33H64N4O8S [M+H]+	-	-
679.253922	N	C27H48N2O12S2 [M+Na]+	-	-
679.428981	N	C38H60N2O7 [M+Na]+	-	-
683.327938	N	C31H53N2O11P [M+Na]+	-	-
683.341448	N	C37H48N4O7 [M+Na]+	-	-
683.455966	N	C39H62N4O4S [M+H]+	-	-
685.271740	N	C26H48N6O9S3 [M+H]+	-	-
685.335195	N	C32H50N6O7S [M+Na]+	-	-
695.361115	N	C34H56O13 [M+Na]+	-	-
696.525327	N	C36H73NO11 [M+H]+	-	-
699.392205	N	C32H54N6O11 [M+H]+	-	-
701.261434	N	C24H47N4O16P [M+Na]+	-	-
701.440233	N	C43H58N4O3 [M+Na]+	-	-
702.345412	N	C33H55N3O9S2 [M+H]+	-	-
702.457777	N	C40H63NO9 [M+H]+	-	-
703.262251	N	C31H44N4O11S [M+Na]+	-	-
703.338952	N	C38H52N2O7S [M+Na]+	-	-

705.258309	N	C28H44N6O11S2 [M+H]+	-	-
705.266400	N	C32H46N2O12S [M+Na]+	-	-
705.306599	N	C38H50O9S [M+Na]+	-	-
706.441191	N	C32H61N9O5S [M+Na]+	-	-
711.427134	N	C33H62N2O14 [M+H]+	-	-
713.444534	N	C36H66O12 [M+Na]+	-	-
713.449027	N	C32H60N10O6S [M+H]+	-	-
721.450256	N	C37H64N6O4S2 [M+H]+	-	-
725.254079	N	C32H47O15P [M+Na]+	-	-
728.354957	N	C36H55N3O9S [M+Na]+	-	-
735.254235	N	C22H49N8O12PS2 [M+Na]+	-	-
741.299367	N	C34H49N2O14P [M+H]+	-	-
741.309922	N	C29H56N2O14P2 [M+Na]+	-	-
741.442555	N	C36H67N2O10P [M+Na]+	-	-
744.365967	N	C33H61NO13S2 [M+H]+	-	-
745.279640	N	C35H50N2O10S2 [M+Na]+	-	-
745.353269	N	C34H59O14P [M+Na]+	-	-
747.325214	N	C34H52N4O11S [M+Na]+	-	-
753.327533	N	C37H48N6O9S [M+H]+	-	-
753.478593	H / N	C41H68O12 [M+H]+	HMDB34596	Hebevinoside VI
753.478593	H / N	C41H68O12 [M+H]+	HMDB41465	Melilotoside B
757.452289	N	C36H64N6O9S [M+H]+	-	-
757.475157	N	C34H64N10O7S [M+H]+	-	-
759.288003	N	C29H59O14PS3 [M+H]+	-	-
761.382544	N	C35H60N4O10S2 [M+H]+	-	-
761.408059	H / N	C39H62O13 [M+Na]+	HMDB30132	Isonuatigenin 3-[rhamnosyl-(1->2)-glucoside]
761.408059	H / N	C39H62O13 [M+Na]+	HMDB33803	Nuatigenin 3-[rhamnosyl-(1->2)-glucoside]
761.408059	H / N	C39H62O13 [M+Na]+	HMDB34337	Polypodosaponin
761.408059	H / N	C39H62O13 [M+Na]+	HMDB39003	Fistuloside A
761.408059	H / N	C39H62O13 [M+Na]+	HMDB40744	Polypodoside B
761.408059	H / N	C39H62O13 [M+Na]+	HMDB40949	Melongoside F
764.500303	N	C35H73NO16 [M+H]+	-	-
772.489581	N	C46H65N3O7 [M+H]+	-	-
774.286182	N	C36H50NO14P [M+Na]+	-	-
775.301747	N	C35H52N4O10S2 [M+Na]+	-	-
794.430934	N	C40H61N5O10 [M+Na]+	-	-
805.239152	N	C34H46N4O13S2 [M+Na]+	-	-
810.557419	N	C41H79NO14 [M+H]+	-	-
823.308747	N	C36H59N2O11PS3 [M+H]+	-	-
823.408553	N	C40H64O16 [M+Na]+	-	-
823.525599	N	C51H70N2O7 [M+H]+	-	-
828.500565	N	C45H69N3O11 [M+H]+	-	-
833.560605	N	C43H78N4O10 [M+Na]+	-	-
844.349975	N	C38H64NO12PS2 [M+Na]+	-	-
850.572991	N	C53H75N3O6 [M+H]+	-	-
851.440016	H / N	C42H68O16 [M+Na]+	HMDB35449	1beta,2alpha,3beta,19alpha-Tetrahydroxy-12-ursen-28-oic acid 28-O-[b-D-Glucopyranosyl-(1->2)-b-D-glucopyranosyl] ester
851.440016	H / N	C42H68O16 [M+Na]+	HMDB40123	Centellasaponin B
851.471869	N	C36H66N8O15 [M+H]+	-	-
859.319979	N	C38H59N4O10PS3 [M+H]+	-	-
876.485464	N	C45H69N3O14 [M+H]+	-	-
888.632798	N	C53H87NO8 [M+Na]+	-	-
900.483963	N	C46H67N7O10 [M+Na]+	-	-
910.614417	N	C52H83N3O10 [M+H]+	-	-
955.521317	N	C49H74N6O11S [M+H]+	-	-
975.411763	N	C43H60N12O11S [M+Na]+	-	-
Features selected for the COMB group				
169.122263	H / N	C10H16O2 [M+H]+	HMDB13105	trans-4,5-epoxy-2(E)-decenal
169.122263	H / N	C10H16O2 [M+H]+	HMDB31156	Ethyl (4Z)-4,7-octadienoate
169.122263	H / N	C10H16O2 [M+H]+	HMDB31273	Methyl octynecarboxylate
169.122263	H / N	C10H16O2 [M+H]+	HMDB32219	(+/-)-Dihydromintlactone
169.122263	H / N	C10H16O2 [M+H]+	HMDB32312	2,4-Hexadienyl butyrate
169.122263	H / N	C10H16O2 [M+H]+	HMDB32313	2,4-Hexadienyl isobutyrate
169.122263	H / N	C10H16O2 [M+H]+	HMDB32319	cis-3-Hexenyl crotonate
169.122263	H / N	C10H16O2 [M+H]+	HMDB32434	(+/-)-2-(5-Methyl-5-vinyltetrahydrofuran-2-yl)propionaldehyde
169.122263	H / N	C10H16O2 [M+H]+	HMDB33700	(-)-(Z)-Tetrahydro-6-(2-pentenyl)-2H-pyran-2-one
169.122263	H / N	C10H16O2 [M+H]+	HMDB34452	5,6-Dihydro-6-pentyl-2H-pyran-2-one
169.122263	H / N	C10H16O2 [M+H]+	HMDB34670	6-Hydroxy-2,6-dimethyl-2,7-octadien-4-one
169.122263	H / N	C10H16O2 [M+H]+	HMDB35714	Epoxyartemisia ketone
169.122263	H / N	C10H16O2 [M+H]+	HMDB35766	Ascaridole
169.122263	H / N	C10H16O2 [M+H]+	HMDB35829	Dihydronepetalactone
169.122263	H / N	C10H16O2 [M+H]+	HMDB36067	Epoxycampholenic aldehyde

169.122263	H / N	C10H16O2 [M+H]+	HMDB36103	Geranic acid
169.122263	H / N	C10H16O2 [M+H]+	HMDB37014	gamma-Diosphenol
169.122263	H / N	C10H16O2 [M+H]+	HMDB37175	4-Isopropyl-3-cyclohexene-1-carboxylic acid
169.122263	H / N	C10H16O2 [M+H]+	HMDB37821	xi-1,8,8-Trimethyl-2-oxabicyclo[3.2.1]octan-3-one
169.122263	H / N	C10H16O2 [M+H]+	HMDB40639	(xi)-(Z)-5-(3-Hexenyl)dihydro-2(3H)-furanone
171.101519	H / N	C9H14O3 [M+H]+	HMDB30471	1,4-Ipomeadiol
171.101519	H / N	C9H14O3 [M+H]+	HMDB38276	cis-3-Hexenyl pyruvate
177.090967	H / N	C11H12O2 [M+H]+	HMDB29699	Cinnamyl acetate
177.090967	H / N	C11H12O2 [M+H]+	HMDB33834	Ethyl cinnamate
177.090967	H / N	C11H12O2 [M+H]+	HMDB36905	2-Propenyl phenylacetate
177.090967	H / N	C11H12O2 [M+H]+	HMDB37142	2-(Phenylethenyl)-1,3-dioxolane
177.090967	H / N	C11H12O2 [M+H]+	HMDB37145	3-(4-Methoxyphenyl)-2-methyl-2-propenal
190.086224	H / N	C11H11NO2 [M+H]+	HMDB02302	3-Indolepropionic acid
190.086224	H / N	C11H11NO2 [M+H]+	HMDB14970	Phensuximide
190.086224	H / N	C11H11NO2 [M+H]+	HMDB29738	Indole-3-methyl acetate
195.137945	H / N	C12H18O2 [M+H]+	HMDB14018	4-Hydroxypropofol
195.137945	H / N	C12H18O2 [M+H]+	HMDB31840	(S,Z)-Lyratol acetate
195.137945	H / N	C12H18O2 [M+H]+	HMDB32567	Hexylresorcinol
195.137945	H / N	C12H18O2 [M+H]+	HMDB34450	Neocnidilide
195.137945	H / N	C12H18O2 [M+H]+	HMDB35126	(±)-Myrtenyl acetate
195.137945	H / N	C12H18O2 [M+H]+	HMDB35375	Ethyl (2E,4E,7Z)-Decatrienoate
195.137945	H / N	C12H18O2 [M+H]+	HMDB35376	Ethyl (2E,4Z,7Z)-Decatrienoate
195.137945	H / N	C12H18O2 [M+H]+	HMDB35801	(2S,4R)-p-Mentha-1(7),5-dien-2-ol acetate
195.137945	H / N	C12H18O2 [M+H]+	HMDB37018	(S)-p-Mentha-1,8-dien-10-yl acetate
195.137945	H / N	C12H18O2 [M+H]+	HMDB37231	Perillyl acetate
195.137945	H / N	C12H18O2 [M+H]+	HMDB37389	(R)-2-Acetoxy-p-mentha-1,8-diene
195.137945	H / N	C12H18O2 [M+H]+	HMDB38046	Carvyl acetate
195.137945	H / N	C12H18O2 [M+H]+	HMDB38292	Menthadienyl acetate
195.137945	H / N	C12H18O2 [M+H]+	HMDB39685	8-Ocimenyl acetate
195.137945	H / N	C12H18O2 [M+H]+	HMDB40439	1-(2-Furanyl)-1-octanone
195.137945	H / N	C12H18O2 [M+H]+	HMDB41497	(S)-Neolyratyl acetate
195.137945	H / N	C12H18O2 [M+H]+	HMDB41610	(2,2-Diethoxyethyl)benzene
199.109309	H / N	C12H16O [M+Na]+	HMDB31569	4-Methyl-1-phenyl-2-pentanone
199.109309	H / N	C12H16O [M+Na]+	HMDB34177	(S)-4-(4-Methylphenyl)-2-pentanone
199.109309	H / N	C12H16O [M+Na]+	HMDB36021	Rhubafuran
199.109309	H / N	C12H16O [M+Na]+	HMDB36171	3-(4-Isopropylphenyl)propanal
201.112052	H / N	C10H16O4 [M+H]+	HMDB00603	cis-4-Decenedioic acid
201.112052	H / N	C10H16O4 [M+H]+	HMDB13227	cis-5-Decenedioic acid
201.112052	H / N	C10H16O4 [M+H]+	HMDB30989	5-Pentyltetrahydro-2-oxo-3-furancarboxylic acid
201.112052	H / N	C10H16O4 [M+H]+	HMDB30990	alpha-Carboxy-delta-nonalactone
201.112052	H / N	C10H16O4 [M+H]+	HMDB34491	(±)-Camphoric acid
201.112052	H / N	C10H16O4 [M+H]+	HMDB34971	(1R,2R,3S,1'R)-Nepetalinic acid
201.112052	H / N	C10H16O4 [M+H]+	HMDB36715	Matsutakic acid A
205.122258	H / N	C13H16O2 [M+H]+	HMDB30770	4-Hydroxy-3-(3-methyl-2-butenyl)acetophenone
205.122258	H / N	C13H16O2 [M+H]+	HMDB30904	alpha,alpha-Dimethylanisalacetone
205.122258	H / N	C13H16O2 [M+H]+	HMDB31553	6-(1-Hydroxyethyl)-2,2-dimethyl-2H-1-benzopyran
205.122258	H / N	C13H16O2 [M+H]+	HMDB31661	3-Isovalidene-3alpha,4-dihydrophthalide
205.122258	H / N	C13H16O2 [M+H]+	HMDB33379	cis-3-Hexenyl benzoate
205.122258	H / N	C13H16O2 [M+H]+	HMDB36224	Benzyl 2,3-dimethyl-2-butenoate
205.122258	H / N	C13H16O2 [M+H]+	HMDB37628	Phenethyl tiglate
205.122258	H / N	C13H16O2 [M+H]+	HMDB37702	Butyl cinnamate
205.122258	H / N	C13H16O2 [M+H]+	HMDB37703	Isobutyl cinnamate
205.122258	H / N	C13H16O2 [M+H]+	HMDB37721	2-Phenylethyl 3-methyl-2-butenoate
205.122258	H / N	C13H16O2 [M+H]+	HMDB41316	Cinnamyl butyrate
205.122258	H / N	C13H16O2 [M+H]+	HMDB41317	Cinnamyl isobutyrate
207.137914	H / N	C13H18O2 [M+H]+	HMDB01925	Ibuprofen
207.137914	H / N	C13H18O2 [M+H]+	HMDB29669	Eremopetasinorone A
207.137914	H / N	C13H18O2 [M+H]+	HMDB32176	Benzyl hexanoate
207.137914	H / N	C13H18O2 [M+H]+	HMDB33196	(E)-6-Methyl-6-(5-methyl-2-furanyl)-3-hepten-2-one
207.137914	H / N	C13H18O2 [M+H]+	HMDB34469	2-Phenylpropyl butyrate
207.137914	H / N	C13H18O2 [M+H]+	HMDB34470	2-Phenylpropyl isobutyrate
207.137914	H / N	C13H18O2 [M+H]+	HMDB34472	3-Phenylpropyl 2-methylpropanoate
207.137914	H / N	C13H18O2 [M+H]+	HMDB34556	3-Acetoxy-3-methyl-1-phenylbutane
207.137914	H / N	C13H18O2 [M+H]+	HMDB35008	3-Methylbutyl phenylacetate
207.137914	H / N	C13H18O2 [M+H]+	HMDB35016	2-Phenylethyl pentanoate
207.137914	H / N	C13H18O2 [M+H]+	HMDB35017	2-Phenylethyl 3-methylbutanoate
207.137914	H / N	C13H18O2 [M+H]+	HMDB35181	xi-8,9-Dehydrotheaspirone
207.137914	H / N	C13H18O2 [M+H]+	HMDB36025	2,4,6-Trimethyl-4-phenyl-1,3-dioxane
207.137914	H / N	C13H18O2 [M+H]+	HMDB36240	Methyl 4-tert-butylphenylacetate
207.137914	H / N	C13H18O2 [M+H]+	HMDB36386	1-Phenylpropyl butyrate
207.137914	H / N	C13H18O2 [M+H]+	HMDB36391	alpha-Methylphenethyl butyrate
207.137914	H / N	C13H18O2 [M+H]+	HMDB37194	Ethyl (±)-2-ethyl-3-phenylpropanoate

207.137914	H / N	C13H18O2 [M+H]+	HMDB37604	10beta-12,13-Dinor-8-oxo-6-eremophilen-11-al
207.137914	H / N	C13H18O2 [M+H]+	HMDB37623	1-Methyl-1-phenylethyl isobutyrate
207.137914	H / N	C13H18O2 [M+H]+	HMDB37720	2-Phenylethyl 2-methylbutanoate
207.137914	H / N	C13H18O2 [M+H]+	HMDB38605	Amyl phenylacetate
207.137914	H / N	C13H18O2 [M+H]+	HMDB39101	Etrogol
207.137914	H / N	C13H18O2 [M+H]+	HMDB40431	Hexyl benzoate
211.096464	H / N	C11H14O4 [M+H]+	HMDB13070	Sinapyl alcohol
211.096464	H / N	C11H14O4 [M+H]+	HMDB29187	5-(3',5')-Dihydroxyphenyl-gamma-valerolactone
211.096464	H / N	C11H14O4 [M+H]+	HMDB29233	3,4-Dihydroxyphenylvaleric acid
211.096464	H / N	C11H14O4 [M+H]+	HMDB33798	3-Methyl-1-(2,4,6-trihydroxyphenyl)-1-butanone
211.096464	H / N	C11H14O4 [M+H]+	HMDB34047	2'-Hydroxy-4',6'-dimethoxy-3'-methylacetophenone
211.096464	H / N	C11H14O4 [M+H]+	HMDB36199	2-Methoxy-4-(4-methyl-1,3-dioxolan-2-yl)phenol
211.096464	H / N	C11H14O4 [M+H]+	HMDB39428	2-Methoxy-3-(4-methoxyphenyl)propanoic acid
211.096464	H / N	C11H14O4 [M+H]+	HMDB41406	Bancroftinone
211.096464	H / N	C11H14O4 [M+H]+	HMDB60737	3-(4-Hydroxy-3-methoxyphenyl)-2-methylpropionic acid
211.132865	H / N	C12H18O3 [M+H]+	HMDB32797	Jasmonic acid
211.132865	H / N	C12H18O3 [M+H]+	HMDB32871	Sedanonic acid
211.132865	H / N	C12H18O3 [M+H]+	HMDB33102	Dihydro-3-(2-octenyl)-2,5-furandione
211.132865	H / N	C12H18O3 [M+H]+	HMDB37104	(R)-8-Acetoxycarvotanacetone
211.132865	H / N	C12H18O3 [M+H]+	HMDB37135	1-Benzyloxy-1-(2-methoxyethoxy)ethane
211.132865	H / N	C12H18O3 [M+H]+	HMDB37642	4-(Butoxymethyl)-2-methoxyphenol
211.132865	H / N	C12H18O3 [M+H]+	HMDB37735	Isoamyl 2-furonpropionate
211.132865	H / N	C12H18O3 [M+H]+	HMDB37816	Dihydro-3-(1-octenyl)-2,5-furandione
211.132865	H / N	C12H18O3 [M+H]+	HMDB41573	3-Ethenyl-2,5-dimethyl-4-oxohex-5-en-2-yl acetate
212.128100	H / N	C11H17NO3 [M+H]+	HMDB14861	Methoxamine
212.128100	H / N	C11H17NO3 [M+H]+	HMDB14954	Orciprenaline
212.128100	H / N	C11H17NO3 [M+H]+	HMDB15197	Isoproterenol
217.158654	H / N	C15H20O [M+H]+	HMDB31736	2-Hexyl-3-phenyl-2-propenal
217.158654	H / N	C15H20O [M+H]+	HMDB35612	(R)-ar-Turmerone
217.158654	H / N	C15H20O [M+H]+	HMDB35965	5beta-1,3,7(11)-Eudesmatrien-8-one
217.158654	H / N	C15H20O [M+H]+	HMDB36108	1,3,5,11-Bisabolatetraen-10-one
217.158654	H / N	C15H20O [M+H]+	HMDB36589	1,2-Dehydro-alpha-cyperone
217.158654	H / N	C15H20O [M+H]+	HMDB36769	Furanodiene
217.158654	H / N	C15H20O [M+H]+	HMDB38147	Isogermafurene
217.158654	H / N	C15H20O [M+H]+	HMDB59863	1,10-Oxidocalamenene
219.077922	H / N	C14H12O [M+Na]+	HMDB59631	Cis-stilbene oxide
219.137949	H / N	C14H18O2 [M+H]+	HMDB30759	(R)-Pterosin B
219.137949	H / N	C14H18O2 [M+H]+	HMDB32227	Dimethylbenzyl carbinyl crotonate
219.137949	H / N	C14H18O2 [M+H]+	HMDB37704	Isoamyl cinnamate
219.137949	H / N	C14H18O2 [M+H]+	HMDB37738	2-(3-Hydroxy-4-methylphenyl)-5-methyl-4-hexen-3-one
219.137949	H / N	C14H18O2 [M+H]+	HMDB38281	cis-3-Hexenyl phenylacetate
219.137949	H / N	C14H18O2 [M+H]+	HMDB41318	Cinnamyl isovalerate
220.167211	N	C12H23NO [M+Na]+	-	-
221.135965	N	C14H20S [M+H]+	-	-
223.094084	H / N	C10H16O4 [M+Na]+	HMDB00603	cis-4-Decenedioic acid
223.094084	H / N	C10H16O4 [M+Na]+	HMDB13227	cis-5-Decenedioic acid
223.094084	H / N	C10H16O4 [M+Na]+	HMDB30989	5-Pentyltetrahydro-2-oxo-3-furancarboxylic acid
223.094084	H / N	C10H16O4 [M+Na]+	HMDB30990	alpha-Carboxy-delta-nonalactone
223.094084	H / N	C10H16O4 [M+Na]+	HMDB34491	(±)-Camphoric acid
223.094084	H / N	C10H16O4 [M+Na]+	HMDB34971	(1R,2R,3S,1'R)-Nepetalinic acid
223.094084	H / N	C10H16O4 [M+Na]+	HMDB36715	Matsutakic acid A
223.132873	H / N	C13H18O3 [M+H]+	HMDB32121	Annuionone B
223.132873	H / N	C13H18O3 [M+H]+	HMDB36819	Dehydrovomifoliol
223.132873	H / N	C13H18O3 [M+H]+	HMDB38894	Isoamyl p-anisate
223.132873	H / N	C13H18O3 [M+H]+	HMDB60565	1-Hydroxyibuprofen
223.132873	H / N	C13H18O3 [M+H]+	HMDB60920	2-Hydroxyibuprofen
223.132873	H / N	C13H18O3 [M+H]+	HMDB60921	3-Hydroxyibuprofen
224.175705	N	C12H21N3O [M+H]+	-	-
225.148515	H / N	C13H20O3 [M+H]+	HMDB29670	Epoxyeremopetasinorol
225.148515	H / N	C13H20O3 [M+H]+	HMDB32679	Annuionone A
225.148515	H / N	C13H20O3 [M+H]+	HMDB32689	Annuionone C
225.148515	H / N	C13H20O3 [M+H]+	HMDB34564	13-Oxo-9,11-tridecadienoic acid
225.148515	H / N	C13H20O3 [M+H]+	HMDB36583	Methyl jasmonate
225.148515	H / N	C13H20O3 [M+H]+	HMDB37244	(8alpha,10beta,11beta)-3-Hydroxy-4,15-dinor-1(5)-xanthen-12,8-olide
225.148515	H / N	C13H20O3 [M+H]+	HMDB37726	Octyl 2-furoate
225.148515	H / N	C13H20O3 [M+H]+	HMDB37730	Furfuryl octanoate
225.148515	H / N	C13H20O3 [M+H]+	HMDB37736	3-Methylbutyl 2-furanbutanoate
227.059080	N	C8H18OS3 [M+H]+	-	-
228.107574	N	C7H17NO7 [M+H]+	-	-
229.119866	H / N	C13H18O2 [M+Na]+	HMDB01925	Ibuprofen
229.119866	H / N	C13H18O2 [M+Na]+	HMDB29669	Eremopetasinorone A
229.119866	H / N	C13H18O2 [M+Na]+	HMDB32176	Benzyl hexanoate

229.119866	H / N	C13H18O2 [M+Na]+	HMDB33196	(E)-6-Methyl-6-(5-methyl-2-furanyl)-3-hepten-2-one
229.119866	H / N	C13H18O2 [M+Na]+	HMDB34469	2-Phenylpropyl butyrate
229.119866	H / N	C13H18O2 [M+Na]+	HMDB34470	2-Phenylpropyl isobutyrate
229.119866	H / N	C13H18O2 [M+Na]+	HMDB34472	3-Phenylpropyl 2-methylpropanoate
229.119866	H / N	C13H18O2 [M+Na]+	HMDB34556	3-Acetoxy-3-methyl-1-phenylbutane
229.119866	H / N	C13H18O2 [M+Na]+	HMDB35008	3-Methylbutyl phenylacetate
229.119866	H / N	C13H18O2 [M+Na]+	HMDB35016	2-Phenylethyl pentanoate
229.119866	H / N	C13H18O2 [M+Na]+	HMDB35017	2-Phenylethyl 3-methylbutanoate
229.119866	H / N	C13H18O2 [M+Na]+	HMDB35181	xi-8,9-Dehydrotheaspirone
229.119866	H / N	C13H18O2 [M+Na]+	HMDB36025	2,4,6-Trimethyl-4-phenyl-1,3-dioxane
229.119866	H / N	C13H18O2 [M+Na]+	HMDB36240	Methyl 4-tert-butylphenylacetate
229.119866	H / N	C13H18O2 [M+Na]+	HMDB36386	1-Phenylpropyl butyrate
229.119866	H / N	C13H18O2 [M+Na]+	HMDB36391	alpha-Methylphenethyl butyrate
229.119866	H / N	C13H18O2 [M+Na]+	HMDB37194	Ethyl (±)-2-ethyl-3-phenylpropanoate
229.119866	H / N	C13H18O2 [M+Na]+	HMDB37604	10beta-12,13-Dinor-8-oxo-6-eremophilen-11-al
229.119866	H / N	C13H18O2 [M+Na]+	HMDB37623	1-Methyl-1-phenylethyl isobutyrate
229.119866	H / N	C13H18O2 [M+Na]+	HMDB37720	2-Phenylethyl 2-methylbutanoate
229.119866	H / N	C13H18O2 [M+Na]+	HMDB38605	Amyl phenylacetate
229.119866	H / N	C13H18O2 [M+Na]+	HMDB39101	Etrogol
229.119866	H / N	C13H18O2 [M+Na]+	HMDB40431	Hexyl benzoate
233.153620	H / N	C15H20O2 [M+H]+	HMDB30761	Pterosin O
233.153620	H / N	C15H20O2 [M+H]+	HMDB30790	6-[(3,4-Methylenedioxy)phenyl]-3,3-dimethyl-1-hexene
233.153620	H / N	C15H20O2 [M+H]+	HMDB31000	(Z)-8-Decene-4,6-diyn-1-yl 3-methylbutanoate
233.153620	H / N	C15H20O2 [M+H]+	HMDB35412	1(10),11-Eremophiladiene-2,9-dione
233.153620	H / N	C15H20O2 [M+H]+	HMDB35906	Alantolactone
233.153620	H / N	C15H20O2 [M+H]+	HMDB35934	Isoalantolactone
233.153620	H / N	C15H20O2 [M+H]+	HMDB36110	(S)-Bilobanone
233.153620	H / N	C15H20O2 [M+H]+	HMDB36119	Alloalantolactone
233.153620	H / N	C15H20O2 [M+H]+	HMDB36148	Furoeremophilone 1
233.153620	H / N	C15H20O2 [M+H]+	HMDB36206	alpha-Amylcinnamyl formate
233.153620	H / N	C15H20O2 [M+H]+	HMDB36688	Costunolide
233.153620	H / N	C15H20O2 [M+H]+	HMDB36766	Furanogermenone
233.153620	H / N	C15H20O2 [M+H]+	HMDB36881	Germacrone-13-al
233.153620	H / N	C15H20O2 [M+H]+	HMDB37563	Turmeronol B
233.153620	H / N	C15H20O2 [M+H]+	HMDB37608	Turmeronol A
233.153620	H / N	C15H20O2 [M+H]+	HMDB39011	1,3,11(13)-Eudesmatrien-12-oic acid
233.153620	H / N	C15H20O2 [M+H]+	HMDB40902	(E)-9-(3-Furanyl)-2,6-dimethyl-2,6-nonadien-4-one
233.153620	H / N	C15H20O2 [M+H]+	HMDB40981	(7b,10a)-3-Hydroxy-1,3,5-cadinatrien-9-one
233.153620	H / N	C15H20O2 [M+H]+	HMDB41038	Collybial
233.153620	H / N	C15H20O2 [M+H]+	HMDB41062	10,11-Epidioxycalamene
235.117779	N	C10H18O6 [M+H]+	-	-
236.148392	N	C9H19N5O [M+Na]+	-	-
237.088390	H / N	C14H14O2 [M+Na]+	HMDB12111	(+)-(1R,2R)-1,2-Diphenylethane-1,2-diol
237.088390	H / N	C14H14O2 [M+Na]+	HMDB29553	(E)-2-(2,4-Hexadiynylidene)-1,6-dioxaspiro[4.5]dec-3-ene
237.088390	H / N	C14H14O2 [M+Na]+	HMDB32709	Ethyl 1-naphthylacetic acid
237.148519	H / N	C14H20O3 [M+H]+	HMDB34462	Heptyl 4-hydroxybenzoate
237.148519	H / N	C14H20O3 [M+H]+	HMDB40778	Eremopetasidione
238.191420	N	C13H23N3O [M+H]+	-	-
239.111657	H / N	C8H16N4O3 [M+Na]+	HMDB04620	N-a-Acetyl-L-arginine
239.164186	H / N	C14H22O3 [M+H]+	HMDB38256	Geranyl acetoacetate
243.137965	N	C16H18O2 [M+H]+	-	-
243.159062	H / N	C13H22O4 [M+H]+	HMDB30987	2-Carboxy-4-dodecanolide
243.159062	H / N	C13H22O4 [M+H]+	HMDB38736	(3S,5R,6R,7E)-3,5,6-Trihydroxy-7-megastigmen-9-one
245.033223	N	C7H16O3S3 [M+H]+	-	-
245.117223	H / N	C15H16O3 [M+H]+	HMDB30636	Batatasin III
245.117223	H / N	C15H16O3 [M+H]+	HMDB30731	3-(1,1-Dimethylallyl)herniarin
245.117223	H / N	C15H16O3 [M+H]+	HMDB31925	5-Hydroxy-2-(5-methyl-1-oxo-4-hexenyl)benzofuran
245.117223	H / N	C15H16O3 [M+H]+	HMDB32641	Batatasin IV
245.117223	H / N	C15H16O3 [M+H]+	HMDB34723	Encelin
245.117223	H / N	C15H16O3 [M+H]+	HMDB38548	Glandulone B
247.109153	N	C16H16O [M+Na]+	-	-
247.132841	H / N	C15H18O3 [M+H]+	HMDB30911	2-Oxo-5,11(13)-eudesmadien-12,8-olide
247.132841	H / N	C15H18O3 [M+H]+	HMDB31900	Methyl (2E,4Z,6E,8E,10E)-4,8-dimethyl-12-oxo-2,4,6,8,10-dodecapentaenoate
247.132841	H / N	C15H18O3 [M+H]+	HMDB31916	5-Hydroxy-2-(1-hydroxy-5-methyl-4-hexenyl)benzofuran
247.132841	H / N	C15H18O3 [M+H]+	HMDB35902	Enokipodin B
247.132841	H / N	C15H18O3 [M+H]+	HMDB36455	Lacinilene C
247.132841	H / N	C15H18O3 [M+H]+	HMDB36473	8-Epixanthatin
247.132841	H / N	C15H18O3 [M+H]+	HMDB36488	Annuolide C
247.132841	H / N	C15H18O3 [M+H]+	HMDB36767	Zederone
247.132841	H / N	C15H18O3 [M+H]+	HMDB37558	3-Oxo-1,4,11(13)-eudesmatrien-12-oic acid
247.132841	H / N	C15H18O3 [M+H]+	HMDB37801	Annuolide A
247.132841	H / N	C15H18O3 [M+H]+	HMDB38188	Curcolone

247.132841	H / N	C15H18O3 [M+H]+	HMDB38202	Zedoarol
247.132841	H / N	C15H18O3 [M+H]+	HMDB38547	Glandulone A
247.132841	H / N	C15H18O3 [M+H]+	HMDB40903	Ipomeabisfuran
247.132841	H / N	C15H18O3 [M+H]+	HMDB41920	Loxoprofen
248.167822	N	C12H25NO2S [M+H]+	-	-
249.148536	H / N	C15H20O3 [M+H]+	HMDB01931	Gamma-CEHC
249.148536	H / N	C15H20O3 [M+H]+	HMDB30757	(S)-Pterosin A
249.148536	H / N	C15H20O3 [M+H]+	HMDB30888	Illudin C2
249.148536	H / N	C15H20O3 [M+H]+	HMDB30910	2alpha-Hydroxyalantolactone
249.148536	H / N	C15H20O3 [M+H]+	HMDB31378	4-Epiisoinuviscolide
249.148536	H / N	C15H20O3 [M+H]+	HMDB31386	(1(10)E,4beta,5alpha,8beta)-4,5-Epoxy-1(10),11(13)-germacradien-12,8-olide
249.148536	H / N	C15H20O3 [M+H]+	HMDB31387	(1beta,4E,8beta,10alpha)-1,10-Epoxy-4,11(13)-germacradien-12,8-olide
249.148536	H / N	C15H20O3 [M+H]+	HMDB31970	1beta-Hydroxyalantolactone
249.148536	H / N	C15H20O3 [M+H]+	HMDB32649	4,5-Epoxy-11(13)-guaien-12,8-olide
249.148536	H / N	C15H20O3 [M+H]+	HMDB33707	Heliannuol E
249.148536	H / N	C15H20O3 [M+H]+	HMDB34123	Eugenyl isovalerate
249.148536	H / N	C15H20O3 [M+H]+	HMDB35131	Heliannuol C
249.148536	H / N	C15H20O3 [M+H]+	HMDB35132	Heliannuol B
249.148536	H / N	C15H20O3 [M+H]+	HMDB35223	(S)-Pterosin D
249.148536	H / N	C15H20O3 [M+H]+	HMDB35503	Pseudoisoeugenol 2-methylbutanoate
249.148536	H / N	C15H20O3 [M+H]+	HMDB35708	8-Epiisoivangustin
249.148536	H / N	C15H20O3 [M+H]+	HMDB35903	Enokipodin A
249.148536	H / N	C15H20O3 [M+H]+	HMDB36005	Istanbulin B
249.148536	H / N	C15H20O3 [M+H]+	HMDB36040	Marasmen-3-one
249.148536	H / N	C15H20O3 [M+H]+	HMDB36641	Artabsin
249.148536	H / N	C15H20O3 [M+H]+	HMDB36770	Desacetyllaurenobiolide
249.148536	H / N	C15H20O3 [M+H]+	HMDB36772	Glechomafuran
249.148536	H / N	C15H20O3 [M+H]+	HMDB37022	Cichoralexin
249.148536	H / N	C15H20O3 [M+H]+	HMDB37557	1alpha-1-Hydroxy-2,4(18),11(13)-eudesmatrien-12-oic acid
249.148536	H / N	C15H20O3 [M+H]+	HMDB37800	Annuolide B
249.148536	H / N	C15H20O3 [M+H]+	HMDB38326	Annuolide E
249.148536	H / N	C15H20O3 [M+H]+	HMDB38794	2,12-Epoxy-7(14)-illudadiene-3,8-diol
249.148536	H / N	C15H20O3 [M+H]+	HMDB39859	Glandulone C
249.232569	N	C16H28N2 [M+H]+	-	-
251.234494	H / N	C15H32O [M+Na]+	HMDB13299	Pentadecanol
253.136841	N	C13H20N2OS [M+H]+	-	-
255.071412	N	C8H8N8O [M+Na]+	-	-
255.090381	N	C10H22OS3 [M+H]+	-	-
255.159073	N	C14H22O4 [M+H]+	-	-
257.153585	H / N	C17H20O2 [M+H]+	HMDB33680	Falcarindione
257.173553	N	C13H22N4 [M+Na]+	-	-
257.175926	N	C15H20N4 [M+H]+	-	-
259.093220	N	C11H18N2OS2 [M+H]+	-	-
259.102624	N	C8H12N8O [M+Na]+	-	-
259.153941	N	C13H22O5 [M+H]+	-	-
261.112139	H / N	C15H16O4 [M+H]+	HMDB30110	Celerin
261.112139	H / N	C15H16O4 [M+H]+	HMDB30578	Apigravin
261.112139	H / N	C15H16O4 [M+H]+	HMDB30690	(E)-Suberenol
261.112139	H / N	C15H16O4 [M+H]+	HMDB30788	Citrusal
261.112139	H / N	C15H16O4 [M+H]+	HMDB30853	(R)-Meranzin
261.112139	H / N	C15H16O4 [M+H]+	HMDB30854	(S)-Auraptenol
261.112139	H / N	C15H16O4 [M+H]+	HMDB30948	Dihydrowyerone
261.112139	H / N	C15H16O4 [M+H]+	HMDB32953	7-Methoxy-5-prenyloxycoumarin
261.112139	H / N	C15H16O4 [M+H]+	HMDB33015	5,6-Dihydroyangonin
261.112139	H / N	C15H16O4 [M+H]+	HMDB33016	7,8-Dihydroyangonin
261.112139	H / N	C15H16O4 [M+H]+	HMDB33771	Cyperine
261.112139	H / N	C15H16O4 [M+H]+	HMDB34133	3-(1,1-Dimethylallyl)scopoletin
261.112139	H / N	C15H16O4 [M+H]+	HMDB35254	7-Hydroxy-5-isopropyl-2-methoxy-3-methyl-1,4-naphthoquinone
261.112139	H / N	C15H16O4 [M+H]+	HMDB36050	Anhydromarasmone
261.112139	H / N	C15H16O4 [M+H]+	HMDB39142	Wyerol
261.112139	H / N	C15H16O4 [M+H]+	HMDB39592	Pergillin
261.112139	H / N	C15H16O4 [M+H]+	HMDB41192	Kanzonol Q
261.148555	H / N	C16H20O3 [M+H]+	HMDB36456	10-Hydroxy-3-methoxy-1,3,5,7-cadinatetraen-9-one
265.143456	H / N	C15H20O4 [M+H]+	HMDB30102	Hulupinic acid
265.143456	H / N	C15H20O4 [M+H]+	HMDB31972	Heliespirone A
265.143456	H / N	C15H20O4 [M+H]+	HMDB33227	Curcolonol
265.143456	H / N	C15H20O4 [M+H]+	HMDB33661	4-Hydroxydehydromyoporone
265.143456	H / N	C15H20O4 [M+H]+	HMDB34719	Isoamberboin
265.143456	H / N	C15H20O4 [M+H]+	HMDB35140	(S)-Abscisic acid
265.143456	H / N	C15H20O4 [M+H]+	HMDB35715	Tanacetin
265.143456	H / N	C15H20O4 [M+H]+	HMDB35805	Thellungianin G
265.143456	H / N	C15H20O4 [M+H]+	HMDB35874	(10R,11R)-Pterosin L

265.143456	H / N	C15H20O4 [M+H]+	HMDB36043	15-Hydroxymarasmen-3-one
265.143456	H / N	C15H20O4 [M+H]+	HMDB36045	O-Formyloreadone
265.143456	H / N	C15H20O4 [M+H]+	HMDB36093	Abscisic acid
265.143456	H / N	C15H20O4 [M+H]+	HMDB36125	(1beta,8beta)-1,8-Dihydroxy-3,7(11)-eudesmadien-12,8-olide
265.143456	H / N	C15H20O4 [M+H]+	HMDB36130	Vulgarin
265.143456	H / N	C15H20O4 [M+H]+	HMDB36135	3-Epiarmefolin
265.143456	H / N	C15H20O4 [M+H]+	HMDB36202	Alkhanin
265.143456	H / N	C15H20O4 [M+H]+	HMDB36773	Tavulin
265.143456	H / N	C15H20O4 [M+H]+	HMDB36931	Tatridin B
265.143456	H / N	C15H20O4 [M+H]+	HMDB37055	Istanbulin A
265.143456	H / N	C15H20O4 [M+H]+	HMDB37528	Blennin B
265.143456	H / N	C15H20O4 [M+H]+	HMDB38156	Umbellifolide
265.143456	H / N	C15H20O4 [M+H]+	HMDB40119	Enokipodin C
265.143456	H / N	C15H20O4 [M+H]+	HMDB41227	(8betaOH,10beta)-8-Hydroxy-3-oxo-7(11)-eremophilen-12,8-olide
265.143456	H / N	C15H20O4 [M+H]+	HMDB41284	2-Methyl-1-[2,4,6-trihydroxy-3-(3-methyl-2-butenyl)phenyl]-1-propanone
265.188608	N	C13H26N2O2 [M+Na]+	-	-
266.078055	N	C12H15N3S2 [M+H]+	-	-
266.196209	N	C12H27NO5 [M+H]+	-	-
267.107757	N	C10H12N8 [M+Na]+	-	-
267.150188	N	C12H24N2OS [M+Na]+	-	-
268.138961	H / N	C10H21NO7 [M+H]+	HMDB15598	Voglibose
269.086917	N	C9H10N8O [M+Na]+	-	-
269.134200	N	C9H20N2O7 [M+H]+	-	-
269.258698	N	C16H32N2O [M+H]+	-	-
270.109352	N	C12H19N3S2 [M+H]+	-	-
270.138452	N	C11H19N5OS [M+H]+	-	-
271.190331	H / N	C15H26O4 [M+H]+	HMDB40459	Ethylene brassylate
273.041913	H / N	C10H10N4O2S [M+Na]+	HMDB14503	Sulfadiazine
273.157313	H / N	C14H22N2O2 [M+Na]+	HMDB15124	Rivastigmine
273.157313	H / N	C14H22N2O2 [M+Na]+	HMDB60655	3-Hydroxylidocaine
275.086548	N	C17H16S [M+Na]+	-	-
275.172839	N	C14H24N2O2 [M+Na]+	-	-
275.186787	N	C15H22N4O [M+H]+	-	-
276.029082	N	C9H13N3OS3 [M+H]+	-	-
276.193419	N	C15H27NO2 [M+Na]+	-	-
277.179773	H / N	C17H24O3 [M+H]+	HMDB15586	Cyclandelate
277.179773	H / N	C17H24O3 [M+H]+	HMDB31463	[8]-Shogaol
277.179773	H / N	C17H24O3 [M+H]+	HMDB38938	Panaquinquecol 2
277.179773	H / N	C17H24O3 [M+H]+	HMDB38994	Ginsenoyne C
277.179773	H / N	C17H24O3 [M+H]+	HMDB40375	Ginsenoyne K
277.179773	H / N	C17H24O3 [M+H]+	HMDB41201	Panaquinquecol 7
277.191937	N	C9H24N8S [M+H]+	-	-
277.263769	N	C18H32N2 [M+H]+	-	-
277.990083	N	C7H7N3O5S2 [M+H]+	-	-
278.116893	H / N	C10H19N3O4S [M+H]+	HMDB28803	Glutaminyl-Methionine
278.116893	H / N	C10H19N3O4S [M+H]+	HMDB28971	Methionyl-Glutamine
278.116893	H / N	C10H19N3O4S [M+H]+	HMDB28987	Methionyl-Gamma-glutamate
278.116893	H / N	C10H19N3O4S [M+H]+	HMDB29155	Gamma-glutamyl-Methionine
278.149916	N	C14H19N3O3 [M+H]+	-	-
278.209004	N	C15H29NO2 [M+Na]+	-	-
279.051078	N	C8H16O7S [M+Na]+	-	-
279.268256	H / N	C19H34O [M+H]+	HMDB33609	2-Pentadecylfuran
283.101413	H / N	C9H16N4O5 [M+Na]+	HMDB28729	Asparaginyl-Glutamine
283.101413	H / N	C9H16N4O5 [M+Na]+	HMDB28745	Asparaginyl-Gamma-glutamate
283.101413	H / N	C9H16N4O5 [M+Na]+	HMDB28792	Glutaminyl-Asparagine
283.101413	H / N	C9H16N4O5 [M+Na]+	HMDB29144	Gamma-glutamyl-Asparagine
283.102693	N	C10H12N8O [M+Na]+	-	-
283.144130	N	C17H18N2O2 [M+H]+	-	-
283.190417	H / N	C16H26O4 [M+H]+	HMDB33630	Lactapiperanol C
284.097981	N	C9H11N9O [M+Na]+	-	-
284.237312	N	C20H29N [M+H]+	-	-
285.148517	H / N	C18H20O3 [M+H]+	HMDB00372	16-Oxoestrone
285.148517	H / N	C18H20O3 [M+H]+	HMDB12941	Estrone-2,3-quinone
285.148517	H / N	C18H20O3 [M+H]+	HMDB12942	Estrone-3,4-quinone
285.148517	H / N	C18H20O3 [M+H]+	HMDB38995	(S)-17-Hydroxy-9,11,13,15-octadecatetraynoic acid
285.180990	N	C14H24N2O4 [M+H]+	-	-
285.257717	N	C21H32 [M+H]+	-	-
286.104280	N	C12H19N3OS2 [M+H]+	-	-
286.114417	N	C10H15N5O5 [M+H]+	-	-
287.164192	H / N	C18H22O3 [M+H]+	HMDB00313	16b-Hydroxyestrone
287.164192	H / N	C18H22O3 [M+H]+	HMDB00335	16a-Hydroxyestrone
287.164192	H / N	C18H22O3 [M+H]+	HMDB00343	2-Hydroxyestrone

287.164192	H / N	C18H22O3 [M+H]+	HMDB00406	16-Ketoestradiol
287.164192	H / N	C18H22O3 [M+H]+	HMDB05895	4-Hydroxyestrone
287.164192	H / N	C18H22O3 [M+H]+	HMDB60084	17beta-Estradiol-2,3-quinone
287.164192	H / N	C18H22O3 [M+H]+	HMDB60085	17beta-Estradiol-3,4-quinone
289.056224	N	C12H16O4S2 [M+H]+	-	-
289.074681	N	C13H20OS3 [M+H]+	-	-
289.179844	H / N	C18H24O3 [M+H]+	HMDB00153	Estriol
289.179844	H / N	C18H24O3 [M+H]+	HMDB00338	2-Hydroxyestradiol
289.179844	H / N	C18H24O3 [M+H]+	HMDB00347	16b-Hydroxyestradiol
289.179844	H / N	C18H24O3 [M+H]+	HMDB00356	17-Epiestriol
289.179844	H / N	C18H24O3 [M+H]+	HMDB00431	16,17-Epiestriol
289.179844	H / N	C18H24O3 [M+H]+	HMDB05896	4-Hydroxyestradiol
289.179844	H / N	C18H24O3 [M+H]+	HMDB40864	O-Geranylvanillin
289.179844	H / N	C18H24O3 [M+H]+	HMDB60353	2-Polyprenyl-3-methyl-6-methoxy-1,4-benzoquinone
289.179844	H / N	C18H24O3 [M+H]+	HMDB60999	4-hydroxystradiol
291.087432	N	C10H20O6S [M+Na]+	-	-
291.090316	N	C13H22OS3 [M+H]+	-	-
292.224711	N	C16H31NO2 [M+Na]+	-	-
293.064473	N	C8H13N4O6P [M+H]+	-	-
293.084342	H / N	C9H18O9 [M+Na]+	HMDB29955	D-erythro-L-galacto-Nonulose
296.116897	N	C12H25NOS3 [M+H]+	-	-
297.206091	H / N	C17H28O4 [M+H]+	HMDB35075	Tanacetol B
297.206091	H / N	C17H28O4 [M+H]+	HMDB38798	(1(10)E,4a,5E)-1(10),5-Germacradiene-12-acetoxy-4,11-diol
297.290038	N	C18H36N2O [M+H]+	-	-
298.112162	N	C9H17N5O5 [M+Na]+	-	-
298.216566	N	C20H27NO [M+H]+	-	-
299.094748	N	C14H18O5S [M+H]+	-	-
300.138497	N	C21H17NO [M+H]+	-	-
301.201004	N	C16H28O5 [M+H]+	-	-
302.116629	N	C12H19N3O4S [M+H]+	-	-
302.136145	H / N	C15H21NO4 [M+Na]+	HMDB31802	(±)-Metalaxyl
303.265781	H / N	C19H36O [M+Na]+	HMDB34496	6,10,14-Trimethyl-2-methylenepentadecanal
304.211914	N	C15H29NO5 [M+H]+	-	-
306.206419	H / N	C18H27NO3 [M+H]+	HMDB02227	Capsaicin
307.085296	N	C13H22O2S3 [M+H]+	-	-
307.161348	N	C11H22N4O6 [M+H]+	-	-
308.222081	H / N	C18H29NO3 [M+H]+	HMDB14341	Betaxolol
308.222081	H / N	C18H29NO3 [M+H]+	HMDB38457	Dihydrocapsaicin
310.131061	N	C11H21N5O2S [M+Na]+	-	-
314.127455	N	C12H27NO2S3 [M+H]+	-	-
315.116219	N	C11H20N2O7 [M+Na]+	-	-
315.128937	N	C11H16N8O2 [M+Na]+	-	-
316.060428	N	C12H17N3OS3 [M+H]+	-	-
316.106021	N	C10H21NO8S [M+H]+	-	-
317.144404	N	C11H18N8O2 [M+Na]+	-	-
318.139399	N	C10H25N5OS2 [M+Na]+	-	-
319.079437	N	C7H16N6O5S [M+Na]+	-	-
319.136379	N	C12H24O8 [M+Na]+	-	-
319.190471	H / N	C19H26O4 [M+H]+	HMDB06709	Ubiquinone-2
319.190471	H / N	C19H26O4 [M+H]+	HMDB30064	Cohulupone
319.190471	H / N	C19H26O4 [M+H]+	HMDB31373	(1(10)E,4E,6a,9b)-9-(2-Methylpropanoyloxy)-1(10),4,11(13)-germacratrien-12,6-olide
319.190471	H / N	C19H26O4 [M+H]+	HMDB35500	Panaquinquecol 6
319.190471	H / N	C19H26O4 [M+H]+	HMDB39277	[8]-Dehydrogingerdione
320.183166	N	C16H27NO4 [M+Na]+	-	-
320.219621	N	C17H31NO3 [M+Na]+	-	-
321.094730	H / N	C14H18O7 [M+Na]+	HMDB10350	2-Phenylethanol glucuronide
321.149392	N	C16H26O3S [M+Na]+	-	-
322.087283	N	C17H17NO2S [M+Na]+	-	-
322.198729	N	C16H29NO4 [M+Na]+	-	-
322.271684	H / N	C18H37NO2 [M+Na]+	HMDB00252	Sphingosine
322.271684	H / N	C18H37NO2 [M+Na]+	HMDB01480	3-Dehydrosphinganine
322.271684	H / N	C18H37NO2 [M+Na]+	HMDB02100	Palmitoylethanolamide
324.326140	H / N	C21H41NO [M+H]+	HMDB34373	N-(14-Methylhexadecanoyl)pyrrolidine
325.077252	N	C12H20O6S2 [M+H]+	-	-
325.154678	H / N	C19H20N2O3 [M+H]+	HMDB14895	Dolasetron
325.237321	H / N	C19H32O4 [M+H]+	HMDB31007	1-Acetoxy-2-hydroxy-16-heptadecyn-4-one
328.227222	H / N	C21H29NO2 [M+H]+	HMDB14749	Butorphanol
328.227222	H / N	C21H29NO2 [M+H]+	HMDB15658	Norelgestromin
328.248244	N	C18H33NO4 [M+H]+	-	-
329.247409	H / N	C22H32O2 [M+H]+	HMDB02183	Docosahexaenoic acid
329.247409	H / N	C22H32O2 [M+H]+	HMDB30053	Neogrifolin
329.247409	H / N	C22H32O2 [M+H]+	HMDB30446	Grifolin

329.247409	H / N	C22H32O2 [M+H]+	HMDB35185	Retinol acetate
329.247409	H / N	C22H32O2 [M+H]+	HMDB38908	(Z,Z)-2-Methyl-5-(8,11,14-pentadecatrienyl)-1,3-benzenediol
330.140622	N	C12H19N5O6 [M+H]+	-	-
330.175679	N	C12H29N5S2 [M+Na]+	-	-
330.315524	N	C23H39N [M+H]+	-	-
331.263197	H / N	C22H34O2 [M+H]+	HMDB01976	Docosapentaenoic acid (22n-6)
331.263197	H / N	C22H34O2 [M+H]+	HMDB06528	Docosapentaenoic acid
331.263197	H / N	C22H34O2 [M+H]+	HMDB32257	Ethyl abietate
331.263197	H / N	C22H34O2 [M+H]+	HMDB35024	ent-16-Kauren-19-ol acetate
331.263197	H / N	C22H34O2 [M+H]+	HMDB35581	1-Phenyl-1,3-hexadecanedione
331.263197	H / N	C22H34O2 [M+H]+	HMDB38909	2-Methyl-5-(8,11-pentadecadienyl)-1,3-benzenediol
331.263197	H / N	C22H34O2 [M+H]+	HMDB39133	4,8,12,15,19-Docosapentaenoic acid
331.263197	H / N	C22H34O2 [M+H]+	HMDB39530	Ethyl icosapentate
331.263197	H / N	C22H34O2 [M+H]+	HMDB60113	Docosa-4,7,10,13,16-pentaenoic acid
332.162297	H / N	C20H23NO2 [M+Na]+	HMDB30304	Atherosperminine
332.162297	H / N	C20H23NO2 [M+Na]+	HMDB40368	Zanthosimuline
332.170336	N	C15H25NO7 [M+H]+	-	-
335.214941	N	C19H30N2OS [M+H]+	-	-
335.279191	N	C18H38O5 [M+H]+	-	-
338.192476	N	C13H27N3O7 [M+H]+	-	-
339.087265	N	C14H20O6S [M+Na]+	-	-
341.180657	N	C14H28O9 [M+H]+	-	-
343.139612	N	C17H26O3S2 [M+H]+	-	-
343.166582	N	C22H24O2 [M+Na]+	-	-
344.140521	H / N	C16H23N3O2S [M+Na]+	HMDB61011	N-desmethylalmotriptan
344.222106	H / N	C21H29NO3 [M+H]+	HMDB30340	Piperolein B
344.222106	H / N	C21H29NO3 [M+H]+	HMDB33959	Isopiperolein B
345.237624	N	C16H30N6O [M+Na]+	-	-
345.253684	H / N	C21H32N2O2 [M+H]+	HMDB03166	16b-Hydroxystanozolol
345.253684	H / N	C21H32N2O2 [M+H]+	HMDB03318	4b-Hydroxystanozolol
345.253684	H / N	C21H32N2O2 [M+H]+	HMDB06001	3'-Hydroxystanozolol
346.070924	N	C13H19N3O2S3 [M+H]+	-	-
347.133501	H / N	C15H22O9 [M+H]+	HMDB32742	Di-O-methylcrenatin
347.133501	H / N	C15H22O9 [M+H]+	HMDB35057	1-(3-Hydroxy-4-Methoxyphenyl)-1,2-ethanediol 3'-O-b-D-glucoside
347.133501	H / N	C15H22O9 [M+H]+	HMDB36562	Aucubin
347.133501	H / N	C15H22O9 [M+H]+	HMDB40601	(1xi,2xi)-1-(4-Hydroxyphenyl)-1,2,3-propanetriol 2-O-beta-D-glucopyranoside
347.133501	H / N	C15H22O9 [M+H]+	HMDB40602	(1xi,2xi)-1-(4-Hydroxyphenyl)-1,2,3-propanetriol 3-O-beta-D-Glucopyranoside
347.133501	H / N	C15H22O9 [M+H]+	HMDB41189	3,4,5-Trimethoxyphenyl glucoside
347.232960	N	C20H30N2O3 [M+H]+	-	-
347.269311	N	C21H34N2O2 [M+H]+	-	-
349.175877	H / N	C18H24N2O5 [M+H]+	HMDB41886	Enalaprilat
350.156374	N	C14H27N3O3S2 [M+H]+	-	-
350.180956	N	C15H27NO8 [M+H]+	-	-
351.187196	N	C13H26N4O7 [M+H]+	-	-
351.200167	N	C15H28N4O4 [M+Na]+	-	-
351.289369	H / N	C22H38O3 [M+H]+	HMDB31126	3,4-Dimethyl-5-pentyl-2-furanundecanoic acid
352.232901	N	C16H33NO7 [M+H]+	-	-
352.245936	H / N	C18H35NO4 [M+Na]+	HMDB06202	4,8 Dimethylnonanoyl carnitine
352.245936	H / N	C18H35NO4 [M+Na]+	HMDB13321	Undecanoylcarnitine
354.116471	N	C13H19N7OS2 [M+H]+	-	-
355.112296	N	C14H24N2O3S2 [M+Na]+	-	-
355.251954	N	C18H34N4OS [M+H]+	-	-
357.235666	N	C16H34N2O5 [M+Na]+	-	-
357.318360	N	C22H44OS [M+H]+	-	-
358.295168	N	C20H39NO4 [M+H]+	-	-
360.223889	N	C15H29N5O5 [M+H]+	-	-
362.129114	N	C11H25N5O3S2 [M+Na]+	-	-
362.191188	N	C14H25N7O3 [M+Na]+	-	-
362.302975	N	C21H41NO2 [M+Na]+	-	-
362.339339	H / N	C22H45NO [M+Na]+	HMDB00583	Docosanamide
363.162546	N	C14H28O9 [M+Na]+	-	-
363.187172	N	C14H26N4O7 [M+H]+	-	-
363.194042	N	C15H28N6OS [M+Na]+	-	-
365.106280	N	C13H26O6S2 [M+Na]+	-	-
365.339027	N	C22H46O2 [M+Na]+	-	-
366.105822	N	C9H21N5O7S [M+Na]+	-	-
367.127536	N	C11H20N8O3S [M+Na]+	-	-
367.331917	N	C22H42N2O2 [M+H]+	-	-
367.393431	H / N	C25H50O [M+H]+	HMDB40907	7-Pentacosanone
368.132152	N	C14H21N7OS2 [M+H]+	-	-
368.191421	N	C15H29NO9 [M+H]+	-	-
370.246796	N	C20H33N3O2 [M+Na]+	-	-

373.213264	N	C16H34N2O4S [M+Na]+	-	-
374.258679	N	C17H35N5O2S [M+H]+	-	-
374.268981	N	C23H35NO3 [M+H]+	-	-
375.259167	N	C16H32N8O [M+Na]+	-	-
376.188597	N	C22H27NO3 [M+Na]+	-	-
378.224822	N	C17H27N7O3 [M+H]+	-	-
378.279257	N	C26H35NO [M+H]+	-	-
379.220855	N	C11H32N8O3S [M+Na]+	-	-
379.251913	N	C20H42S3 [M+H]+	-	-
379.354634	H / N	C23H48O2 [M+Na]+	HMDB41070	erythro-6,8-Tricosanediol
380.202905	N	C15H29N3O8 [M+H]+	-	-
380.206902	N	C20H29NO6 [M+H]+	-	-
381.154362	H / N	C19H24O8 [M+H]+	HMDB36893	Gibberellin A75
381.154362	H / N	C19H24O8 [M+H]+	HMDB37056	8-Oxodiacetoxyscirpenol
381.154362	H / N	C19H24O8 [M+H]+	HMDB38328	(S)-Bitalin A 12-glucoside
381.154362	H / N	C19H24O8 [M+H]+	HMDB38450	Gibberellin A86
381.154362	H / N	C19H24O8 [M+H]+	HMDB40899	Methyl helianthenoate A glucoside
381.210135	N	C14H32N6O2S2 [M+H]+	-	-
382.147779	N	C15H23N7OS2 [M+H]+	-	-
382.265795	N	C15H35N5O6 [M+H]+	-	-
383.281221	N	C18H40N4OS [M+Na]+	-	-
384.204261	N	C15H31N5O3S [M+Na]+	-	-
385.033447	N	C14H12N2O9S [M+H]+	-	-
385.219702	N	C18H34O7 [M+Na]+	-	-
385.279985	N	C18H34N8 [M+Na]+	-	-
386.248927	N	C22H37NOS [M+Na]+	-	-
387.073735	N	C15H16N4O5S [M+Na]+	-	-
387.253297	H / N	C24H34O4 [M+H]+	HMDB00385	12a-Hydroxy-3-oxocholadienic acid
387.253297	H / N	C24H34O4 [M+H]+	HMDB12867	9'-Carboxy-alpha-tocotrienol
388.267835	N	C17H29N11 [M+H]+	-	-
389.109586	N	C10H24N6O4S3 [M+H]+	-	-
389.167674	N	C16H28N4O3S2 [M+H]+	-	-
389.228333	N	C18H32N2O7 [M+H]+	-	-
389.259541	N	C21H38N2OS [M+Na]+	-	-
389.375387	H / N	C25H50O [M+Na]+	HMDB40907	7-Pentacosanone
391.069577	N	C15H18O10S [M+H]+	-	-
391.270591	N	C21H34N4O3 [M+H]+	-	-
392.198550	N	C21H30NO4P [M+H]+	-	-
393.370290	H / N	C24H50O2 [M+Na]+	HMDB30885	1,24-Tetracosanediol
395.226409	N	C17H32N4O5 [M+Na]+	-	-
397.066144	N	C11H16N4O10S [M+H]+	-	-
398.274698	N	C18H39NO8 [M+H]+	-	-
399.186172	N	C16H30O11 [M+H]+	-	-
402.269701	N	C17H41N5S2 [M+Na]+	-	-
402.283752	N	C20H37N5O2 [M+Na]+	-	-
402.290103	N	C27H35N3 [M+H]+	-	-
403.232664	H / N	C20H34O8 [M+H]+	HMDB34159	Acetyl tributyl citrate
406.217460	N	C16H29N7O4 [M+Na]+	-	-
406.248249	N	C17H35N5O4S [M+H]+	-	-
407.188753	N	C16H32O10 [M+Na]+	-	-
407.220923	H / N	C18H34N2O6S [M+H]+	HMDB15564	Lincomycin
407.255493	H / N	C25H36O3 [M+Na]+	HMDB34952	Persicaxanthin
407.255493	H / N	C25H36O3 [M+Na]+	HMDB36425	Persicachrome
408.220225	N	C22H33NO4S [M+H]+	-	-
408.274469	N	C23H37NO5 [M+H]+	-	-
408.308418	N	C22H43NO4 [M+Na]+	-	-
410.229586	N	C21H35N3OS2 [M+H]+	-	-
412.238647	N	C27H29N3O [M+H]+	-	-
412.276577	N	C16H37N5O7 [M+H]+	-	-
413.109594	N	C12H24N6O4S3 [M+H]+	-	-
413.293863	N	C21H40N4O2S [M+H]+	-	-
414.266172	N	C21H37N5S [M+Na]+	-	-
415.045089	N	C12H17N4O7PS [M+Na]+	-	-
415.105034	N	C17H20N4O5S [M+Na]+	-	-
416.259474	N	C23H39NO2S [M+Na]+	-	-
417.239579	N	C18H38N2O5S [M+Na]+	-	-
417.249308	N	C22H40O3S2 [M+H]+	-	-
417.406667	N	C27H54O [M+Na]+	-	-
419.137222	N	C18H26O9S [M+H]+	-	-
421.167987	N	C16H30O11 [M+Na]+	-	-
422.277642	N	C24H37N3O2 [M+Na]+	-	-
422.287645	N	C22H41NO5 [M+Na]+	-	-

422.326523	H / N	C25H43NO4 [M+H]+	HMDB06318	Gamma-linolenyl carnitine
422.326523	H / N	C25H43NO4 [M+H]+	HMDB06319	Alpha-linolenyl carnitine
424.258143	N	C16H35N9OS [M+Na]+	-	-
425.311264	N	C21H38N8 [M+Na]+	-	-
426.013036	N	C9H11N7O9S2 [M+H]+	-	-
428.230495	N	C17H35N5O4S [M+Na]+	-	-
429.235485	N	C20H28N8O3 [M+H]+	-	-
430.275153	N	C24H41NO2S [M+Na]+	-	-
431.236820	N	C17H34N8OS2 [M+H]+	-	-
432.381373	N	C26H51NO2 [M+Na]+	-	-
433.115586	N	C17H22N4O6S [M+Na]+	-	-
433.299899	N	C18H42N4O6 [M+Na]+	-	-
435.380947	N	C26H52O3 [M+Na]+	-	-
436.241147	N	C18H37N5O3S2 [M+H]+	-	-
436.339711	H / N	C24H47NO4 [M+Na]+	HMDB06210	Heptadecanoyl carnitine
437.111812	N	C18H28O6S3 [M+H]+	-	-
439.252620	N	C19H36N4O6 [M+Na]+	-	-
439.263174	N	C16H38N8O2S2 [M+H]+	-	-
439.331933	N	C28H42N2O2 [M+H]+	-	-
440.482619	N	C29H61NO [M+H]+	-	-
441.156991	N	C20H26N4O4S [M+Na]+	-	-
442.240376	N	C18H39N3O5S2 [M+H]+	-	-
442.267494	N	C23H37N3O4 [M+Na]+	-	-
443.076393	N	C14H21N4O7PS [M+Na]+	-	-
443.240567	H / N	C24H36O6 [M+Na]+	HMDB32099	Dimethyl 3-methoxy-4-oxo-5-(8,11,14-pentadecatrienyl)-2-hexenedioate
443.263927	N	C23H38O8 [M+H]+	-	-
445.326559	N	C22H42N6O2 [M+Na]+	-	-
446.258859	N	C17H37N5O7 [M+Na]+	-	-
447.016306	N	C15H14N2O10S2 [M+H]+	-	-
448.227979	N	C18H31N7O5 [M+Na]+	-	-
450.243670	N	C18H33N7O5 [M+Na]+	-	-
451.298777	N	C25H42N2O3S [M+H]+	-	-
451.327118	N	C24H50O3S2 [M+H]+	-	-
452.290084	N	C19H41N5O5S [M+H]+	-	-
453.249589	N	C25H32N4O4 [M+H]+	-	-
456.302779	N	C18H41N5O8 [M+H]+	-	-
458.198443	N	C16H25N11O4 [M+Na]+	-	-
459.243449	N	C19H40N4O3S2 [M+Na]+	-	-
460.279937	H / N	C21H44NO6P [M+Na]+	HMDB11152	PE(P-16:0e/0:0)
461.265768	N	C20H42N2O6S [M+Na]+	-	-
461.309704	N	C23H42N4O4 [M+Na]+	-	-
462.296961	N	C20H45N3O5S [M+Na]+	-	-
465.293105	N	C21H36N8O4 [M+H]+	-	-
466.283330	N	C22H43NO7S [M+H]+	-	-
466.291975	N	C25H43N3OS2 [M+H]+	-	-
466.317937	N	C27H39N5O2 [M+H]+	-	-
468.200250	N	C17H31N7O5S [M+Na]+	-	-
468.235188	N	C23H29N7O4 [M+H]+	-	-
470.272447	N	C22H41NO8 [M+Na]+	-	-
471.167532	N	C21H28N4O5S [M+Na]+	-	-
471.331710	N	C26H46O7 [M+H]+	-	-
472.256597	N	C19H39N5O5S [M+Na]+	-	-
472.287813	N	C20H37N7O6 [M+H]+	-	-
473.259678	N	C20H34N8O4 [M+Na]+	-	-
473.469279	H / N	C31H62O [M+Na]+	HMDB29996	9-Hentriacontanone
473.469279	H / N	C31H62O [M+Na]+	HMDB31036	Palmitone
473.469279	H / N	C31H62O [M+Na]+	HMDB40886	25-Methyl-10-triacontanone
475.153619	N	C17H28N2O12 [M+Na]+	-	-
475.243149	N	C21H41O8P [M+Na]+	-	-
475.448546	H / N	C30H60O2 [M+Na]+	HMDB29987	(+)-11-Hydroxy-9-triacontanone
475.448546	H / N	C30H60O2 [M+Na]+	HMDB30925	Melissic acid A
477.326244	N	C34H40N2 [M+H]+	-	-
479.140282	N	C20H30O9S2 [M+H]+	-	-
479.173395	N	C18H32O13 [M+Na]+	-	-
482.308863	N	C24H45NO7 [M+Na]+	-	-
483.266170	N	C19H38N4O10 [M+H]+	-	-
483.278833	N	C21H40N4O7 [M+Na]+	-	-
483.344709	H / N	C29H48O4 [M+Na]+	HMDB12555	13'-Carboxy-alpha-tocopherol
483.344709	H / N	C29H48O4 [M+Na]+	HMDB33634	(3beta,5alpha,6beta,9alpha,22E,24R)-23-Methylergosta-7,22-diene-3,5,6,9-tetrol
486.254310	N	C20H41N5O3S2 [M+Na]+	-	-
487.191616	N	C20H28N6O7 [M+Na]+	-	-
487.194264	N	C17H32N6O7S [M+Na]+	-	-

487.267699	N	C27H36N4O3 [M+Na]+	-	-
487.291601	N	C26H38N4O5 [M+H]+	-	-
487.309316	N	C27H50OS3 [M+H]+	-	-
487.375877	N	C29H52O4 [M+Na]+	-	-
488.279356	N	C31H37NO4 [M+H]+	-	-
488.293365	N	C23H48NO4PS [M+Na]+	-	-
489.105385	N	C19H22N4O8S [M+Na]+	-	-
489.178100	N	C21H30N4O6S [M+Na]+	-	-
491.258637	N	C21H36N6O6 [M+Na]+	-	-
491.443466	N	C30H60O3 [M+Na]+	-	-
494.269668	N	C20H37N7O6 [M+Na]+	-	-
495.241141	N	C20H40O12 [M+Na]+	-	-
495.323584	H / N	C33H44O2 [M+Na]+	HMDB31381	Methyl (7Z,9Z,9'Z)-6'-apo-y-caroten-6'-oate
495.323584	H / N	C33H44O2 [M+Na]+	HMDB36882	Reticulataxanthin
500.328963	N	C20H45N5O9 [M+H]+	-	-
501.010928	N	C20H16O10P2 [M+Na]+	-	-
503.355490	N	C25H52O8 [M+Na]+	-	-
505.292077	N	C30H42O5 [M+Na]+	-	-
507.147364	H / N	C22H28O12 [M+Na]+	HMDB34909	7-Methyl-1,4,5-naphthalenetriol 4-[xylosyl-(1->6)-glucoside]
507.190184	N	C23H38O6S3 [M+H]+	-	-
507.292798	H / N	C26H44O8 [M+Na]+	HMDB38539	Goshonoside F1
507.292798	H / N	C26H44O8 [M+Na]+	HMDB38540	Goshonoside F2
507.376813	N	C27H52N2O5 [M+Na]+	-	-
508.311758	N	C24H45NO10 [M+H]+	-	-
509.278478	N	C25H48O4S3 [M+H]+	-	-
514.290334	N	C24H46NO7P [M+Na]+	-	-
515.192199	N	C22H36O10S [M+Na]+	-	-
516.282892	N	C21H43N5O6S [M+Na]+	-	-
516.313523	N	C22H49N3O6S2 [M+H]+	-	-
517.065982	N	C18H27N2O6PS3 [M+Na]+	-	-
520.285883	N	C30H43NO3S [M+Na]+	-	-
521.118080	N	C18H32O11S3 [M+H]+	-	-
521.200247	N	C17H34N6O9S [M+Na]+	-	-
522.196624	N	C17H35N3O13S [M+H]+	-	-
526.335455	N	C25H47N7OS2 [M+H]+	-	-
527.288289	N	C31H40N2O4 [M+Na]+	-	-
527.304560	N	C21H46N6O5S2 [M+H]+	-	-
527.355290	N	C27H52O8 [M+Na]+	-	-
528.182886	N	C19H32N5O9P [M+Na]+	-	-
530.280633	N	C22H45N5O4S2 [M+Na]+	-	-
530.353472	N	C24H51NO11 [M+H]+	-	-
531.253161	N	C23H44N2O6S2 [M+Na]+	-	-
535.278874	N	C22H40N8O4S [M+Na]+	-	-
536.270148	N	C24H41NO12 [M+H]+	-	-
536.371157	N	C32H51NO4 [M+Na]+	-	-
538.295979	N	C30H45NO4S [M+Na]+	-	-
539.267397	N	C22H44O13 [M+Na]+	-	-
540.391504	N	C26H55N5O3S [M+Na]+	-	-
541.225599	H / N	C24H38O12 [M+Na]+	HMDB29773	6S,9R-Dihydroxy-4,7E-megastigmadien-3-one 9-[apiosyl-(1->6)-glucoside]
541.225599	H / N	C24H38O12 [M+Na]+	HMDB35520	Vomifoliol 9-[xylosyl-(1->6)-glucoside]
541.225599	H / N	C24H38O12 [M+Na]+	HMDB38923	Cinnamoside
543.225183	N	C25H36N4O6S [M+Na]+	-	-
544.267455	N	C24H39N7O4S [M+Na]+	-	-
545.405143	N	C30H50N8 [M+Na]+	-	-
549.455617	N	C32H60N4OS [M+H]+	-	-
551.169862	N	C18H30N8O8S2 [M+H]+	-	-
552.379698	N	C33H49N3O4 [M+H]+	-	-
553.283191	N	C23H46O13 [M+Na]+	-	-
557.224958	N	C22H38N4O9S [M+Na]+	-	-
560.312103	N	C33H41N3O5 [M+H]+	-	-
569.248063	N	C21H38N8O7S [M+Na]+	-	-
569.249510	N	C23H44N4O6S3 [M+H]+	-	-
569.251928	N	C26H38N6O5S [M+Na]+	-	-
569.256946	H / N	C26H42O12 [M+Na]+	HMDB36317	Canavalioside
569.264836	H / N	C34H36N2O6 [M+H]+	HMDB31751	y-Morphine
569.372866	N	C29H52N4O5S [M+H]+	-	-
570.280203	N	C26H46NO9P [M+Na]+	-	-
571.469355	H / N	C35H64O4 [M+Na]+	HMDB31168	Cohibin A
571.469355	H / N	C35H64O4 [M+Na]+	HMDB31169	Cohibin B
572.267039	N	C23H45N3O9S2 [M+H]+	-	-
574.258978	N	C24H45N3O7S2 [M+Na]+	-	-
575.214942	N	C25H36N4O8S [M+Na]+	-	-

577.198570	N	C32H33O8P [M+H]+	-	-
577.392278	N	C28H58O10 [M+Na]+	-	-
578.245993	N	C27H47NO4S4 [M+H]+	-	-
579.393763	N	C31H54N4O4S [M+H]+	-	-
583.262295	N	C29H40N2O9 [M+Na]+	-	-
583.293650	N	C24H48O14 [M+Na]+	-	-
584.276028	N	C34H37N3O6 [M+H]+	-	-
584.488519	N	C34H65NO6 [M+H]+	-	-
587.215554	N	C19H36N10O6S2 [M+Na]+	-	-
587.343190	N	C27H53N2O8P [M+Na]+	-	-
594.340169	N	C33H49NO7 [M+Na]+	-	-
596.264493	N	C36H37NO7 [M+H]+	-	-
597.176810	N	C29H34O10S [M+Na]+	-	-
598.305278	N	C31H51NO4S3 [M+H]+	-	-
599.286816	H / N	C34H38N4O6 [M+H]+	HMDB00668	Hematoporphyrin IX
601.486592	N	C36H72S3 [M+H]+	-	-
602.397292	N	C25H49N13O3 [M+Na]+	-	-
604.302404	N	C29H47N3O7S [M+Na]+	-	-
606.229453	N	C28H35N3O12 [M+H]+	-	-
607.201970	N	C21H32N10O8S [M+Na]+	-	-
607.360935	N	C28H52N6O5S [M+Na]+	-	-
607.409053	N	C28H56N8O3S [M+Na]+	-	-
609.278891	N	C24H42N8O7S [M+Na]+	-	-
609.373171	N	C31H50N6O5 [M+Na]+	-	-
611.022456	N	C14H25N2O17PS2 [M+Na]+	-	-
611.066704	N	C17H25N4O15PS [M+Na]+	-	-
621.205373	N	C22H38N4O13S [M+Na]+	-	-
627.468080	N	C32H66O11 [M+H]+	-	-
628.393306	N	C33H55N3O7 [M+Na]+	-	-
628.435442	N	C33H61N3O6S [M+H]+	-	-
638.279677	N	C30H41N5O9 [M+Na]+	-	-
640.439715	N	C33H63NO9 [M+Na]+	-	-
641.335654	N	C27H54O15 [M+Na]+	-	-
644.329924	N	C27H51N5O9S [M+Na]+	-	-
646.351652	N	C26H55N5O9S2 [M+H]+	-	-
647.358455	N	C32H50N6O6S [M+H]+	-	-
648.235001	N	C27H42N3O11PS [M+H]+	-	-
648.413317	N	C32H59N5O5S [M+Na]+	-	-
649.289904	N	C31H44N4O9S [M+H]+	-	-
653.213472	N	C29H40N4O7S3 [M+H]+	-	-
653.278305	N	C30H46O14 [M+Na]+	-	-
656.351534	N	C33H51N3O9 [M+Na]+	-	-
658.422220	N	C35H61N3O5S [M+Na]+	-	-
659.263199	N	C22H49N6O9PS2 [M+Na]+	-	-
661.456585	N	C33H64N4O7S [M+H]+	-	-
668.470771	N	C35H67NO9 [M+Na]+	-	-
670.428201	N	C35H63N3O5S2 [M+H]+	-	-
671.346012	N	C28H56O16 [M+Na]+	-	-
671.468241	N	C39H68O5S [M+Na]+	-	-
673.520328	N	C46H64N4 [M+H]+	-	-
675.227391	N	C25H44N6O8S3 [M+Na]+	-	-
677.451498	N	C33H64N4O8S [M+H]+	-	-
677.502833	N	C38H68N4O4S [M+H]+	-	-
687.329896	N	C27H44N12O8 [M+Na]+	-	-
689.267653	N	C33H44N4O8S2 [M+H]+	-	-
692.479144	N	C45H61N3O3 [M+H]+	-	-
695.185669	N	C25H41N2O15PS [M+Na]+	-	-
697.295807	N	C32H51O13P [M+Na]+	-	-
699.523112	N	C40H74O7S [M+H]+	-	-
701.393224	N	C30H62O16 [M+Na]+	-	-
702.345412	N	C33H55N3O9S2 [M+H]+	-	-
702.396306	N	C37H55N3O10 [M+H]+	-	-
703.563787	N	C45H76O4 [M+Na]+	-	-
713.334578	N	C38H50N4O6S [M+Na]+	-	-
713.408324	N	C35H62O13 [M+Na]+	-	-
715.315046	H / N	C32H52O16 [M+Na]+	HMDB37125	Pisumoside B
718.350352	N	C31H59NO13S2 [M+H]+	-	-
718.495028	N	C34H71NO14 [M+H]+	-	-
721.477290	N	C34H66N8O5S [M+Na]+	-	-
725.530735	N	C40H72N2O9 [M+H]+	-	-
727.387268	N	C35H60O14 [M+Na]+	-	-
728.292201	N	C32H51NO14S [M+Na]+	-	-

735.493014	N	C35H68N8O5S [M+Na]+	-	-
737.305817	N	C34H56O11S3 [M+H]+	-	-
739.387326	N	C36H60O14 [M+Na]+	-	-
741.299367	N	C34H49N2O14P [M+H]+	-	-
752.455782	N	C38H67NO12 [M+Na]+	-	-
757.239604	N	C25H49N4O16PS2 [M+H]+	-	-
762.520848	N	C36H75NO15 [M+H]+	-	-
773.315448	N	C34H50N6O11S [M+Na]+	-	-
776.536512	N	C50H69N3O4 [M+H]+	-	-
776.559022	N	C50H75NO4 [M+Na]+	-	-
778.422259	N	C37H57N9O8 [M+Na]+	-	-
778.617267	H / N	C44H85NO8 [M+Na]+	HMDB04973	Glucosylceramide (d18:1/20:0)
778.617267	H / N	C44H85NO8 [M+Na]+	HMDB10710	Galactosylceramide (d18:1/20:0)
787.273582	N	C37H44N6O10S [M+Na]+	-	-
792.531991	N	C45H75N3O5S [M+Na]+	-	-
795.495127	N	C44H72N2O7S [M+Na]+	-	-
809.372025	N	C42H58O14 [M+Na]+	-	-
810.557419	N	C41H79NO14 [M+H]+	-	-
814.484951	N	C44H67N3O11 [M+H]+	-	-
815.393807	N	C40H60N2O14 [M+Na]+	-	-
821.338056	N	C37H60N2O12S3 [M+H]+	-	-
822.542170	N	C38H79NO17 [M+H]+	-	-
824.372353	N	C36H59N5O13S [M+Na]+	-	-
833.546930	N	C40H80O17 [M+H]+	-	-
845.315054	N	C37H59O16PS [M+Na]+	-	-
855.525292	N	C41H72N10O6S [M+Na]+	-	-
858.388218	N	C42H61NO16 [M+Na]+	-	-
876.485464	N	C45H69N3O14 [M+H]+	-	-
878.460115	N	C39H69N9O8S2 [M+Na]+	-	-
878.617192	N	C42H83N7O12 [M+H]+	-	-
906.531190	N	C46H73N7O10 [M+Na]+	-	-
911.542268	N	C41H82O21 [M+H]+	-	-
975.411763	N	C43H60N12O11S [M+Na]+	-	-

Abbreviations: H – annotated with HMDB, N – annotated with NetCalc.

Table S17. Features selected by ML-PLS-DA (followed by filtering out variables most likely influenced by time) in case of data represented by OTU counts.

id	Phylym	Order	Class	Family	Genus
Features selected for the BR group					
OTU-23	Firmicutes	Clostridia	Clostridiales	Lachnospiraceae	Blautia
OTU-24	Firmicutes	Clostridia	Clostridiales	Lachnospiraceae	Ruminococcus2
OTU-42	Bacteroidetes	Bacteroidia	Bacteroidales	Bacteroidaceae	Bacteroides
OTU-44	Firmicutes	Erysipelotrichia	Erysipelotrichales	Erysipelotrichaceae	Coprobacillus
OTU-48	Firmicutes	Bacilli	Lactobacillales	Streptococcaceae	Lactococcus
OTU-56	Firmicutes	Clostridia	Clostridiales	Ruminococcaceae	Clostridium IV
OTU-70	Bacteroidetes	Bacteroidia	Bacteroidales	Bacteroidaceae	Bacteroides
OTU-94	Bacteroidetes	Bacteroidia	Bacteroidales	Rikenellaceae	Alistipes
OTU-95	Firmicutes	Erysipelotrichia	Erysipelotrichales	Erysipelotrichaceae	Turicibacter
OTU-105	Firmicutes	Clostridia	Clostridiales	Ruminococcaceae	Butyricicoccus
OTU-112	Firmicutes	Clostridia	Clostridiales	Peptostreptococcaceae	Clostridium XI
OTU-114	Firmicutes	Clostridia	Clostridiales	Ruminococcaceae	unclassified
OTU-114	Firmicutes	unclassified	-	-	-
OTU-114	unclassified	-	-	-	-
OTU-139	Firmicutes	Clostridia	Clostridiales	Ruminococcaceae	unclassified
OTU-139	Firmicutes	unclassified	-	-	-
OTU-139	unclassified	-	-	-	-
OTU-140	Firmicutes	Clostridia	Clostridiales	Lachnospiraceae	Coprococcus
OTU-151	Firmicutes	Clostridia	Clostridiales	Ruminococcaceae	Clostridium IV
OTU-151	Firmicutes	Clostridia	Clostridiales	Ruminococcaceae	unclassified
OTU-152	Firmicutes	Clostridia	Clostridiales	Ruminococcaceae	Acetanaerobacterium
OTU-152	Firmicutes	Clostridia	Clostridiales	Ruminococcaceae	Hydrogenoanaerobacterium
OTU-152	Firmicutes	Clostridia	Clostridiales	Ruminococcaceae	unclassified
OTU-175	Firmicutes	Clostridia	Clostridiales	Eubacteriaceae	Eubacterium
OTU-175	Firmicutes	Clostridia	Clostridiales	Ruminococcaceae	Clostridium IV
OTU-175	Firmicutes	Clostridia	Clostridiales	Ruminococcaceae	unclassified
OTU-182	Firmicutes	Erysipelotrichia	Erysipelotrichales	Erysipelotrichaceae	Coprobacillus
OTU-182	Firmicutes	Erysipelotrichia	Erysipelotrichales	Erysipelotrichaceae	unclassified
OTU-190	Firmicutes	Clostridia	Clostridiales	Lachnospiraceae	Clostridium XlVa
OTU-190	Firmicutes	Clostridia	Clostridiales	Lachnospiraceae	unclassified
OTU-193	Firmicutes	Clostridia	Clostridiales	Lachnospiraceae	Clostridium XlVa
OTU-193	Firmicutes	Clostridia	Clostridiales	Lachnospiraceae	Lachnospiracea_incertae_sedis
OTU-198	Firmicutes	Clostridia	Clostridiales	Clostridiales_Incertae Sedis XIII	Anaerovorax
OTU-198	Firmicutes	Clostridia	Clostridiales	unclassified	-
OTU-213	Firmicutes	Clostridia	Clostridiales	Ruminococcaceae	Clostridium IV
OTU-213	Firmicutes	Clostridia	Clostridiales	Ruminococcaceae	Oscillibacter
OTU-213	Firmicutes	Clostridia	Clostridiales	Ruminococcaceae	unclassified
OTU-215	Bacteroidetes	Bacteroidia	Bacteroidales	Bacteroidaceae	Bacteroides
OTU-225	Firmicutes	Clostridia	Clostridiales	Ruminococcaceae	Gemmiger
OTU-225	Firmicutes	Clostridia	Clostridiales	Ruminococcaceae	Subdoligranulum
OTU-225	Firmicutes	Clostridia	Clostridiales	Ruminococcaceae	unclassified
OTU-232	Firmicutes	Clostridia	Clostridiales	Lachnospiraceae	Blautia
OTU-232	Firmicutes	Clostridia	Clostridiales	Lachnospiraceae	Clostridium XlVa
OTU-232	Firmicutes	Clostridia	Clostridiales	Lachnospiraceae	Lachnospiracea_incertae_sedis
OTU-232	Firmicutes	Clostridia	Clostridiales	Lachnospiraceae	Ruminococcus2
OTU-239	Firmicutes	Clostridia	Clostridiales	Lachnospiraceae	Blautia
OTU-245	Firmicutes	Clostridia	Clostridiales	unclassified	-
OTU-247	Firmicutes	Clostridia	Clostridiales	Clostridiales_Incertae Sedis XIII	Anaerovorax
OTU-247	Firmicutes	Clostridia	Clostridiales	Eubacteriaceae	Eubacterium
OTU-247	Firmicutes	Clostridia	Clostridiales	unclassified	-
OTU-257	Bacteroidetes	Bacteroidia	Bacteroidales	Bacteroidaceae	Bacteroides
OTU-265	Firmicutes	Clostridia	Clostridiales	Ruminococcaceae	Clostridium IV
OTU-267	Firmicutes	Clostridia	Clostridiales	Lachnospiraceae	Lachnospiracea_incertae_sedis
OTU-277	Bacteroidetes	Bacteroidia	Bacteroidales	Bacteroidaceae	Anaerorhabdus
OTU-277	Firmicutes	Erysipelotrichia	Erysipelotrichales	Erysipelotrichaceae	Holdemania
OTU-277	unclassified	-	-	-	-
OTU-281	Firmicutes	Clostridia	Clostridiales	Ruminococcaceae	Clostridium IV
OTU-290	Firmicutes	Clostridia	Clostridiales	Lachnospiraceae	Roseburia
OTU-295	Bacteroidetes	Bacteroidia	Bacteroidales	Bacteroidaceae	Bacteroides
OTU-309	Firmicutes	Clostridia	Clostridiales	Clostridiaceae 1	Clostridium sensu stricto
OTU-424	Firmicutes	Clostridia	Clostridiales	Ruminococcaceae	Oscillibacter
OTU-547	Firmicutes	Clostridia	Clostridiales	Peptostreptococcaceae	Clostridium XI
OTU-572	Firmicutes	Clostridia	Clostridiales	Lachnospiraceae	Lachnospiracea_incertae_sedis
OTU-572	Firmicutes	Clostridia	Clostridiales	Lachnospiraceae	unclassified
OTU-574	Firmicutes	Clostridia	Clostridiales	Lachnospiraceae	Blautia
OTU-589	Firmicutes	Clostridia	Clostridiales	Lachnospiraceae	Roseburia

OTU-600	Firmicutes	Clostridia	Clostridiales	Lachnospiraceae	Lachnospiracea_incertae_sedis
OTU-678	Firmicutes	Clostridia	Clostridiales	Ruminococcaceae	Faecalibacterium
OTU-679	Firmicutes	Clostridia	Clostridiales	Lachnospiraceae	Ruminococcus2
OTU-686	Firmicutes	Clostridia	Clostridiales	Ruminococcaceae	Faecalibacterium
OTU-715	Firmicutes	Clostridia	Clostridiales	Lachnospiraceae	Lachnospiracea_incertae_sedis
OTU-752	Firmicutes	Clostridia	Clostridiales	Lachnospiraceae	Lachnospiracea_incertae_sedis
OTU-781	Firmicutes	Clostridia	Clostridiales	Lachnospiraceae	Blautia
OTU-781	Firmicutes	Clostridia	Clostridiales	Lachnospiraceae	unclassified
OTU-822	Firmicutes	Clostridia	Clostridiales	Lachnospiraceae	Clostridium XlVa
OTU-822	Firmicutes	Clostridia	Clostridiales	Lachnospiraceae	Ruminococcus2
OTU-822	Firmicutes	Clostridia	Clostridiales	Lachnospiraceae	unclassified
OTU-836	Firmicutes	Clostridia	Clostridiales	Lachnospiraceae	Blautia
Features selected for the WGB group					
OTU-1	Firmicutes	Clostridia	Clostridiales	Lachnospiraceae	Lachnospiracea_incertae_sedis
OTU-16	Verrucomicrobia	Verrucomicrobiae	Verrucomicrobiales	Verrucomicrobiaceae	Akkermansia
OTU-16	Verrucomicrobia	Verrucomicrobiae	Verrucomicrobiales	Verrucomicrobiaceae	Prosthecobacter
OTU-20	Firmicutes	Clostridia	Clostridiales	Lachnospiraceae	Clostridium XlVa
OTU-21	Actinobacteria	Actinobacteria	Actinobacteridae	Bifidobacteriales	Bifidobacteriaceae
OTU-22	Firmicutes	Negativicutes	Selenomonadales	Veillonellaceae	Dialister
OTU-24	Firmicutes	Clostridia	Clostridiales	Lachnospiraceae	Ruminococcus2
OTU-34	Bacteroidetes	Bacteroidia	Bacteroidales	Bacteroidaceae	Bacteroides
OTU-38	Bacteroidetes	Bacteroidia	Bacteroidales	Bacteroidaceae	Bacteroides
OTU-50	Firmicutes	Clostridia	Clostridiales	Lachnospiraceae	Roseburia
OTU-56	Firmicutes	Clostridia	Clostridiales	Ruminococcaceae	Clostridium IV
OTU-77	Firmicutes	Clostridia	Clostridiales	Ruminococcaceae	Clostridium IV
OTU-77	Firmicutes	Clostridia	Clostridiales	Ruminococcaceae	unclassified
OTU-84	Firmicutes	Clostridia	Clostridiales	Peptostreptococcaceae	Clostridium XI
OTU-86	Firmicutes	Clostridia	Clostridiales	Lachnospiraceae	Clostridium XlVa
OTU-86	Firmicutes	Clostridia	Clostridiales	Lachnospiraceae	unclassified
OTU-87	Bacteroidetes	Bacteroidia	Bacteroidales	Porphyromonadaceae	Parabacteroides
OTU-96	Firmicutes	Clostridia	Clostridiales	Lachnospiraceae	Clostridium XlVb
OTU-114	Firmicutes	Clostridia	Clostridiales	Ruminococcaceae	unclassified
OTU-114	Firmicutes	unclassified	-	-	-
OTU-114	unclassified	-	-	-	-
OTU-116	Firmicutes	Clostridia	Clostridiales	Lachnospiraceae	Ruminococcus2
OTU-116	Firmicutes	Clostridia	Clostridiales	Lachnospiraceae	unclassified
OTU-120	Firmicutes	Clostridia	Clostridiales	Lachnospiraceae	Clostridium XlVa
OTU-120	Firmicutes	Clostridia	Clostridiales	Lachnospiraceae	Ruminococcus2
OTU-120	Firmicutes	Clostridia	Clostridiales	Lachnospiraceae	unclassified
OTU-146	Bacteroidetes	Bacteroidia	Bacteroidales	Porphyromonadaceae	Odoribacter
OTU-169	Firmicutes	Clostridia	Clostridiales	Ruminococcaceae	Oscillibacter
OTU-169	Firmicutes	Clostridia	Clostridiales	Ruminococcaceae	unclassified
OTU-190	Firmicutes	Clostridia	Clostridiales	Lachnospiraceae	Clostridium XlVa
OTU-190	Firmicutes	Clostridia	Clostridiales	Lachnospiraceae	unclassified
OTU-195	Firmicutes	Clostridia	Clostridiales	Ruminococcaceae	Clostridium III
OTU-195	Firmicutes	Clostridia	Clostridiales	Ruminococcaceae	unclassified
OTU-215	Bacteroidetes	Bacteroidia	Bacteroidales	Bacteroidaceae	Bacteroides
OTU-224	Firmicutes	Clostridia	Clostridiales	Ruminococcaceae	Oscillibacter
OTU-236	Firmicutes	Clostridia	Clostridiales	Ruminococcaceae	Pseudoflavonifractor
OTU-236	Firmicutes	Clostridia	Clostridiales	Ruminococcaceae	unclassified
OTU-256	Firmicutes	Clostridia	Clostridiales	Ruminococcaceae	Clostridium IV
OTU-261	Actinobacteria	Actinobacteria	Coriobacteridae	Coriobacteriales	Coriobacterineae
OTU-267	Firmicutes	Clostridia	Clostridiales	Lachnospiraceae	Lachnospiracea_incertae_sedis
OTU-291	Firmicutes	Clostridia	Clostridiales	Ruminococcaceae	Pseudoflavonifractor
OTU-291	Firmicutes	Clostridia	Clostridiales	Ruminococcaceae	unclassified
OTU-294	Firmicutes	Bacilli	Lactobacillales	Streptococcaceae	Streptococcus
OTU-300	Firmicutes	Clostridia	Clostridiales	Ruminococcaceae	Butyricicoccus
OTU-305	Firmicutes	Clostridia	Clostridiales	Lachnospiraceae	Lachnospiracea_incertae_sedis
OTU-313	Firmicutes	Clostridia	Clostridiales	Lachnospiraceae	Ruminococcus2
OTU-313	Firmicutes	Clostridia	Clostridiales	Lachnospiraceae	unclassified
OTU-334	Firmicutes	Clostridia	Clostridiales	Lachnospiraceae	Coprococcus
OTU-351	Firmicutes	Clostridia	Clostridiales	Lachnospiraceae	Clostridium XlVa
OTU-351	Firmicutes	Clostridia	Clostridiales	Lachnospiraceae	Ruminococcus2
OTU-362	Bacteroidetes	Bacteroidia	Bacteroidales	Bacteroidaceae	Bacteroides
OTU-378	Firmicutes	Clostridia	Clostridiales	Ruminococcaceae	Clostridium IV
OTU-378	Firmicutes	Clostridia	Clostridiales	Ruminococcaceae	Oscillibacter
OTU-380	Firmicutes	Clostridia	Clostridiales	Ruminococcaceae	Anaerotruncus
OTU-494	Firmicutes	Clostridia	Clostridiales	Lachnospiraceae	Lachnospiracea_incertae_sedis
OTU-569	Firmicutes	Clostridia	Clostridiales	Lachnospiraceae	Lachnospiracea_incertae_sedis
OTU-596	Firmicutes	Clostridia	Clostridiales	Ruminococcaceae	Gemmiger
OTU-596	Firmicutes	Clostridia	Clostridiales	Ruminococcaceae	Subdoligranulum
OTU-596	Firmicutes	Clostridia	Clostridiales	Ruminococcaceae	unclassified

OTU-607	Firmicutes	Clostridia	Clostridiales	Lachnospiraceae	Lachnospiracea_incertae_sedis
OTU-694	Firmicutes	Clostridia	Clostridiales	Lachnospiraceae	Lachnospiracea_incertae_sedis
OTU-734	Firmicutes	Clostridia	Clostridiales	Lachnospiraceae	Lachnospiracea_incertae_sedis
OTU-738	Firmicutes	Clostridia	Clostridiales	Lachnospiraceae	Lachnospiracea_incertae_sedis
OTU-741	Firmicutes	Clostridia	Clostridiales	Lachnospiraceae	Lachnospiracea_incertae_sedis
OTU-781	Firmicutes	Clostridia	Clostridiales	Lachnospiraceae	Blautia
OTU-781	Firmicutes	Clostridia	Clostridiales	Lachnospiraceae	unclassified
OTU-783	Firmicutes	Clostridia	Clostridiales	Ruminococcaceae	Gemmiger
OTU-783	Firmicutes	Clostridia	Clostridiales	Ruminococcaceae	Subdoligranulum
OTU-783	Firmicutes	Clostridia	Clostridiales	Ruminococcaceae	unclassified
OTU-822	Firmicutes	Clostridia	Clostridiales	Lachnospiraceae	Clostridium XlVa
OTU-822	Firmicutes	Clostridia	Clostridiales	Lachnospiraceae	Ruminococcus2
OTU-822	Firmicutes	Clostridia	Clostridiales	Lachnospiraceae	unclassified
OTU-853	Bacteroidetes	Bacteroidia	Bacteroidales	Bacteroidaceae	Bacteroides
Features selected for the COMB group					
OTU-1	Firmicutes	Clostridia	Clostridiales	Lachnospiraceae	Lachnospiracea_incertae_sedis
OTU-2	Firmicutes	Clostridia	Clostridiales	Lachnospiraceae	Clostridium XlVa
OTU-2	Firmicutes	Clostridia	Clostridiales	Lachnospiraceae	unclassified
OTU-4	Bacteroidetes	Bacteroidia	Bacteroidales	Bacteroidaceae	Bacteroides
OTU-19	Firmicutes	Clostridia	Clostridiales	Ruminococcaceae	Ruminococcus
OTU-30	Firmicutes	Negativicutes	Selenomonadales	Acidaminococcaceae	Phascolarctobacterium
OTU-32	Firmicutes	Erysipelotrichia	Erysipelotrichales	Erysipelotrichaceae	Erysipelotrichaceae_incertae_sedis
OTU-59	Bacteroidetes	Bacteroidia	Bacteroidales	Bacteroidaceae	Bacteroides
OTU-71	Firmicutes	Erysipelotrichia	Erysipelotrichales	Erysipelotrichaceae	Clostridium XVIII
OTU-87	Bacteroidetes	Bacteroidia	Bacteroidales	Porphyromonadaceae	Parabacteroides
OTU-89	Firmicutes	Clostridia	Clostridiales	Ruminococcaceae	Oscillibacter
OTU-93	Bacteroidetes	Bacteroidia	Bacteroidales	Rikenellaceae	Alistipes
OTU-96	Firmicutes	Clostridia	Clostridiales	Lachnospiraceae	Clostridium XlVb
OTU-101	Firmicutes	Clostridia	Clostridiales	Ruminococcaceae	Clostridium IV
OTU-101	Firmicutes	Clostridia	Clostridiales	Ruminococcaceae	Oscillibacter
OTU-101	Firmicutes	Clostridia	Clostridiales	Ruminococcaceae	unclassified
OTU-106	Firmicutes	Clostridia	Clostridiales	Lachnospiraceae	Clostridium XlVa
OTU-106	Firmicutes	Clostridia	Clostridiales	Lachnospiraceae	unclassified
OTU-117	Firmicutes	Clostridia	Clostridiales	Lachnospiraceae	Lachnospiracea_incertae_sedis
OTU-126	Firmicutes	Clostridia	Clostridiales	Lachnospiraceae	Clostridium XlVa
OTU-126	Firmicutes	Clostridia	Clostridiales	Lachnospiraceae	unclassified
OTU-127	Firmicutes	Clostridia	Clostridiales	Lachnospiraceae	Lachnospiracea_incertae_sedis
OTU-130	Firmicutes	Negativicutes	Selenomonadales	Acidaminococcaceae	Phascolarctobacterium
OTU-140	Firmicutes	Clostridia	Clostridiales	Lachnospiraceae	Coprococcus
OTU-143	Bacteroidetes	Bacteroidia	Bacteroidales	Bacteroidaceae	Bacteroides
OTU-146	Bacteroidetes	Bacteroidia	Bacteroidales	Porphyromonadaceae	Odoribacter
OTU-173	Bacteroidetes	Bacteroidia	Bacteroidales	Porphyromonadaceae	Barnesiella
OTU-175	Firmicutes	Clostridia	Clostridiales	Eubacteriaceae	Eubacterium
OTU-175	Firmicutes	Clostridia	Clostridiales	Ruminococcaceae	Clostridium IV
OTU-175	Firmicutes	Clostridia	Clostridiales	Ruminococcaceae	unclassified
OTU-178	Firmicutes	Clostridia	Clostridiales	Lachnospiraceae	Clostridium XlVa
OTU-178	Firmicutes	Clostridia	Clostridiales	Lachnospiraceae	Lachnospiracea_incertae_sedis
OTU-178	Firmicutes	Clostridia	Clostridiales	Lachnospiraceae	unclassified
OTU-197	Firmicutes	Clostridia	Clostridiales	Lachnospiraceae	Blautia
OTU-218	Firmicutes	Erysipelotrichia	Erysipelotrichales	Erysipelotrichaceae	Coprobacillus
OTU-218	Firmicutes	Erysipelotrichia	Erysipelotrichales	Erysipelotrichaceae	unclassified
OTU-225	Firmicutes	Clostridia	Clostridiales	Ruminococcaceae	Gemmiger
OTU-225	Firmicutes	Clostridia	Clostridiales	Ruminococcaceae	Subdoligranulum
OTU-225	Firmicutes	Clostridia	Clostridiales	Ruminococcaceae	unclassified
OTU-245	Firmicutes	Clostridia	Clostridiales	unclassified	-
OTU-255	Firmicutes	Clostridia	Clostridiales	Lachnospiraceae	Anaerostipes
OTU-255	Firmicutes	Clostridia	Clostridiales	Lachnospiraceae	Clostridium XlVa
OTU-278	Firmicutes	Clostridia	Clostridiales	Lachnospiraceae	Clostridium XlVa
OTU-278	Firmicutes	Clostridia	Clostridiales	Lachnospiraceae	Lachnospira
OTU-278	Firmicutes	Clostridia	Clostridiales	Lachnospiraceae	unclassified
OTU-282	Firmicutes	Clostridia	Clostridiales	Ruminococcaceae	Clostridium IV
OTU-282	Firmicutes	Clostridia	Clostridiales	Ruminococcaceae	Ethanoligenens
OTU-294	Firmicutes	Bacilli	Lactobacillales	Streptococcaceae	Streptococcus
OTU-295	Bacteroidetes	Bacteroidia	Bacteroidales	Bacteroidaceae	Bacteroides
OTU-300	Firmicutes	Clostridia	Clostridiales	Ruminococcaceae	Butyricicoccus
OTU-318	Firmicutes	Bacilli	Lactobacillales	Streptococcaceae	Streptococcus
OTU-334	Firmicutes	Clostridia	Clostridiales	Lachnospiraceae	Coprococcus
OTU-336	Firmicutes	Clostridia	Clostridiales	Lachnospiraceae	Clostridium XlVa
OTU-336	Firmicutes	Clostridia	Clostridiales	Lachnospiraceae	unclassified
OTU-365	Bacteroidetes	Bacteroidia	Bacteroidales	Porphyromonadaceae	Butyricimonas
OTU-374	Bacteroidetes	Bacteroidia	Bacteroidales	Bacteroidaceae	Bacteroides
OTU-399	Firmicutes	Clostridia	Clostridiales	Lachnospiraceae	Clostridium XlVa

OTU-399	Firmicutes	Clostridia	Clostridiales	Lachnospiraceae	Ruminococcus2
OTU-526	Firmicutes	Clostridia	Clostridiales	Ruminococcaceae	Faecalibacterium
OTU-600	Firmicutes	Clostridia	Clostridiales	Lachnospiraceae	Lachnospiracea_incertae_sedis
OTU-623	Firmicutes	Clostridia	Clostridiales	Lachnospiraceae	Roseburia
OTU-636	Firmicutes	Clostridia	Clostridiales	Lachnospiraceae	Clostridium XlVa
OTU-636	Firmicutes	Clostridia	Clostridiales	Lachnospiraceae	unclassified
OTU-651	Bacteroidetes	Bacteroidia	Bacteroidales	Bacteroidaceae	Bacteroides
OTU-731	Firmicutes	Clostridia	Clostridiales	Lachnospiraceae	Clostridium XlVa
OTU-731	Firmicutes	Clostridia	Clostridiales	Lachnospiraceae	Coprococcus
OTU-731	Firmicutes	Clostridia	Clostridiales	Lachnospiraceae	Lachnospiracea_incertae_sedis
OTU-731	Firmicutes	Clostridia	Clostridiales	Lachnospiraceae	Pseudobutyrivibrio
OTU-752	Firmicutes	Clostridia	Clostridiales	Lachnospiraceae	Lachnospiracea_incertae_sedis
OTU-766	Bacteroidetes	Bacteroidia	Bacteroidales	Bacteroidaceae	Bacteroides
OTU-822	Firmicutes	Clostridia	Clostridiales	Lachnospiraceae	Clostridium XlVa
OTU-822	Firmicutes	Clostridia	Clostridiales	Lachnospiraceae	Ruminococcus2
OTU-822	Firmicutes	Clostridia	Clostridiales	Lachnospiraceae	unclassified
OTU-853	Bacteroidetes	Bacteroidia	Bacteroidales	Bacteroidaceae	Bacteroides

8. Acknowledgments

I would like to thank my supervisor, Prof. Philippe Schmitt-Kopplin, for the provided opportunity to do research in an exciting and friendly environment occupied with brilliant minds and faces. I am grateful for the chance of understading myself better and to get to know my wishes and desires for further self-development and improvements. Also, huge thanks to Prof. Jens Walter from the University of Alberta for providing the biological samples necessary for conducting an incredibly interesting research. Moreover, I would like to thank my family that they supported my intention to work and study abroad. I can imagine how hard for them is the understanding that their child is growing as well as the fact of incredibly rare meetings. Moreover, I am thankful to my old and new friends, without who I would definitely not enjoy the new experience and taste of German beer in a bar. And of course, I thank my love who did not stop believing in me even during the hardest moments.

Thank you all!

9. Bibliography

Abdi, H., 2010. Partial least squares regression and projection on latent structure regression (PLS Regression). Wiley Interdisciplinary Reviews: Computational Statistics 2, 97-106.

Adams, S.H., Hoppel, C.L., Lok, K.H., Zhao, L., Wong, S.W., Minkler, P.E., Hwang, D.H., Newman, J.W., Garvey, W.T., 2009. Plasma acylcarnitine profiles suggest incomplete long-chain fatty acid beta-oxidation and altered tricarboxylic acid cycle activity in type 2 diabetic African-American women. The Journal of Nutrition 139, 1073-1081.

Alvaro, A., Sola, R., Rosales, R., Ribalta, J., Anguera, A., Masana, L., Vallve, J.C., 2008. Gene expression analysis of a human enterocyte cell line reveals downregulation of cholesterol biosynthesis in response to short-chain fatty acids. IUBMB Life 60, 757-764.

Assfalg, M., Bertini, I., Colangiuli, D., Luchinat, C., Schafer, H., Schutz, B., Spraul, M., 2008. Evidence of different metabolic phenotypes in humans. Proceedings of the National Academy of Sciences of the United States of America 105, 1420-1424.

Astarita, G., Langridge, J., 2013. An emerging role for metabolomics in nutrition science. Journal of Nutrigenetics and Nutrigenomics 6, 181-200.

Ballereau, S., Glaab, E., Kolodkin, A., Chaiboonchoe, A., Biryukov, M., Vlassis, N., Ahmed, H., Pellet, J., Baliga, N., Hood, L., Schneider, R., Balling, R., Auffray, C., 2013. Functional genomics, proteomics, metabolomics and bioinformatics for systems biology. 3-41.

Banerjee, S., Mazumdar, S., 2012. Electrospray ionization mass spectrometry: a technique to access the information beyond the molecular weight of the analyte. International Journal of Analytical Chemistry 2012, 282574.

Becker, C.H., Kumar, P., Jones, T., Lin, H., 2007. Nonparametric mass calibration using hundreds of internal calibrants. Analytical Chemistry 79, 1702-1707.

Blachier, F., Boutry, C., Bos, C., Tome, D., 2009. Metabolism and functions of L-glutamate in the epithelial cells of the small and large intestines. The American Journal of Clinical Nutrition 90, 814S-821S.

Breitling, R., Ritchie, S., Goodenowe, D., Stewart, M.L., Barrett, M.P., 2006. prediction of metabolic networks using Fourier transform mass spectrometry data. Metabolomics 2, 155-164.

Brenton, A.G., Godfrey, A.R., 2010. Accurate mass measurement: terminology and treatment of data. Journal of the American Society for Mass Spectrometry 21, 1821-1835.

Brown, S.C., Kruppa, G., Dasseux, J.L., 2005. Metabolomics applications of FT-ICR mass spectrometry. Mass Spectrometry Reviews 24, 223-231.

Cani, P.D., Plovier, H., Van Hul, M., Geurts, L., Delzenne, N.M., Druart, C., Everard, A., 2016. Endocannabinoids - at the crossroads between the gut microbiota and host metabolism. Nature Reviews. Endocrinology 12, 133-143.

Cassol, E., Misra, V., Holman, A., Kamat, A., Morgello, S., Gabuzda, D., 2013. Plasma metabolomics identifies lipid abnormalities linked to markers of inflammation, microbial translocation, and hepatic function in HIV patients receiving protease inhibitors. BMC Infectious Diseases 13, 203.

Chen, Z., Guo, L., Zhang, Y., Walzem, R.L., Pendergast, J.S., Printz, R.L., Morris, L.C., Matafonova, E., Stien, X., Kang, L., Coulon, D., McGuinness, O.P., Niswender, K.D., Davies, S.S., 2014. Incorporation of therapeutically modified bacteria into gut microbiota inhibits obesity. The Journal of Clinical Investigation 124, 3391-3406.

Christians, U., Klawitter, J., Hornberger, A., Klawitter, J., 2011. How unbiased is non-targeted metabolomics and is targeted pathway screening the solution? Current Pharmaceutical Biotechnology 12, 1053-1066.

Cinar, R., Godlewski, G., Liu, J., Tam, J., Jourdan, T., Mukhopadhyay, B., Harvey-White, J., Kunos, G., 2014. Hepatic cannabinoid-1 receptors mediate diet-induced insulin resistance by increasing de novo synthesis of long-chain ceramides. Hepatology 59, 143-153.

Cooper, D., Martin, R., Keim, N., 2015. Does whole grain consumption alter gut microbiota and satiety? Healthcare 3, 364-392.

De Angelis, M., Montemurno, E., Vannini, L., Cosola, C., Cavallo, N., Gozzi, G., Maranzano, V., Di Cagno, R., Gobbetti, M., Gesualdo, L., 2015. Effect of whole-grain barley on the human fecal microbiota and metabolome. Applied and Environmental Microbiology 81, 7945-7956.

De Livera, A.M., Olshansky, M., Speed, T.P., 2013. Statistical analysis of metabolomics data. Methods in Molecular Biology 1055, 291-307.

Dhanjal, C., Clemencon, S., 2014. On recent advances in supervised ranking for metabolite profiling.

Dorrestein, P.C., Mazmanian, S.K., Knight, R., 2014. Finding the missing links among metabolites, microbes, and the host. Immunity 40, 824-832.

Draper, J., Lloyd, A.J., Goodacre, R., Beckmann, M., 2012. Flow infusion electrospray ionisation mass spectrometry for high throughput, non-targeted metabolite fingerprinting: a review. Metabolomics 9, 4-29.

Ferre, F.S., 2016. Worldwide occurrence of mycotoxins in rice. Food Control 62, 291-298.

Fezza, F., Bari, M., Florio, R., Talamonti, E., Feole, M., Maccarrone, M., 2014. Endocannabinoids, related compounds and their metabolic routes. Molecules 19, 17078-17106.

Forcisi, S., Moritz, F., Kanawati, B., Tziotis, D., Lehmann, R., Schmitt-Kopplin, P., 2013. Liquid chromatography-mass spectrometry in metabolomics research: mass analyzers in ultra high pressure liquid chromatography coupling. Journal of Chromatography A 1292, 51-65.

Forcisi, S., Moritz, F., Lucio, M., Lehmann, R., Stefan, N., Schmitt-Kopplin, P., 2015. Solutions for low and high accuracy mass spectrometric data matching: a data-driven annotation strategy in nontargeted metabolomics. Analytical Chemistry 87, 8917-8924.

Fuhrer, T., Zamboni, N., 2015. High-throughput discovery metabolomics. Current Opinion in Biotechnology 31, 73-78.

Ghaste, M., Mistrik, R., Shulaev, V., 2016. Applications of Fourier transform ion cyclotron resonance (FT-ICR) and Orbitrap based high resolution mass spectrometry in metabolomics and lipidomics. International Journal of Molecular Sciences 17.

Gibson, D.G., Glass, J.I., Lartigue, C., Noskov, V.N., Chuang, R.Y., Algire, M.A., Benders, G.A., Montague, M.G., Ma, L., Moodie, M.M., Merryman, C., Vashee, S., Krishnakumar, R., Assad-Garcia, N., Andrews-Pfannkoch, C., Denisova, E.A., Young, L., Qi, Z.Q., Segall-Shapiro, T.H., Calvey, C.H., Parmar, P.P., Hutchison, C.A., Smith, H.O., Venter, J.C., 2010. Creation of a bacterial cell controlled by a chemically synthesized genome. Science 329, 52-56.

Hanhineva, K., Lankinen, M.A., Pedret, A., Schwab, U., Kolehmainen, M., Paananen, J., de Mello, V., Sola, R., Lehtonen, M., Poutanen, K., Uusitupa, M., Mykkanen, H., 2015. Nontargeted metabolite profiling discriminates diet-specific biomarkers for consumption of whole grains, fatty fish, and bilberries in a randomized controlled trial. The Journal of Nutrition 145, 7-17.

Heinken, A., Thiele, I., 2015. Systems biology of host-microbe metabolomics. Wiley Interdisciplinary Reviews. Systems Biology and Medicine 7, 195-219.

Ho, C.S., Lam, C.W., Chan, M.H., Cheung, R.C., Law, L.K., Lit, L.C., Ng, K.F., Suen, M.W., Tai, H.L., 2003. Electrospray ionisation mass spectrometry: principles and clinical applications. The Clinical Biochemist. Reviews 24, 3-12.

Holmes, E., Li, J.V., Athanasiou, T., Ashrafian, H., Nicholson, J.K., 2011. Understanding the role of gut microbiome-host metabolic signal disruption in health and disease. Trends in Microbiology 19, 349-359.

Hrydziuszko, O., Viant, M.R., 2012. Missing values in mass spectrometry based metabolomics: an undervalued step in the data processing pipeline. Metabolomics 8, S161-S174.

Jansen, J.J., Hoefsloot, H.C.J., van der Greef, J., Timmerman, M.E., Smilde, A.K., 2005. Multilevel component analysis of time-resolved metabolic fingerprinting data. Analytica Chimica Acta 530, 173-183.

Johnson, C.H., Ivanisevic, J., Siuzdak, G., 2016. Metabolomics: beyond biomarkers and towards mechanisms. Nature Reviews. Molecular cell biology 17, 451-459.

Jones, D.P., Park, Y., Ziegler, T.R., 2012. Nutritional metabolomics: progress in addressing complexity in diet and health. Annual Review of Nutrition 32, 183-202.

Junot, C., Fenaille, F., Colsch, B., Becher, F., 2014. High resolution mass spectrometry based techniques at the crossroads of metabolic pathways. Mass Spectrometry Reviews 33, 471-500.

Kell, D.B., 2006. Systems biology, metabolic modelling and metabolomics in drug discovery and development. Drug Discovery Today 11, 1085-1092.

Kell, D.B., Oliver, S.G., 2016. The metabolome 18 years on: a concept comes of age. Metabolomics 12, 148.

Kesic, S., 2016. Systems biology, emergence and antireductionism. Saudi Journal of Biological Sciences 23, 584-591.

Kimura, M., Tokai, T., Takahashi-Ando, N., Ohsato, S., Fujimura, M., 2014. Molecular and genetic studies of *Fusarium* trichothecene biosynthesis: pathways, genes, and evolution. Bioscience, Biotechnology, and Biochemistry 71, 2105-2123.

Kind, T., Fiehn, O., 2007. Seven Golden Rules for heuristic filtering of molecular formulas obtained by accurate mass spectrometry. BMC Bioinformatics 8, 1-20.

Kitano, H., 2002. Systems biology: a brief overview. Science 295, 1662-1664.

Kozhinov, A.N., Zhurov, K.O., Tsybin, Y.O., 2013. Iterative method for mass spectra recalibration via empirical estimation of the mass calibration function for Fourier transform mass spectrometry-based petroleomics. Analytical Chemistry 85, 6437-6445.

Lankinen, M., Schwab, U., Kolehmainen, M., Paananen, J., Poutanen, K., Mykkanen, H., Seppanen-Laakso, T., Gylling, H., Uusitupa, M., Oresic, M., 2011a. Whole grain products, fish and bilberries alter glucose and lipid metabolism in a randomized, controlled trial: the Sysdimet study. PLoS One 6, e22646.

Lankinen, M., Schwab, U., Seppanen-Laakso, T., Mattila, I., Juntunen, K., Mykkanen, H., Poutanen, K., Gylling, H., Oresic, M., 2011b. Metabolomic analysis of plasma metabolites that may mediate effects of rye bread on satiety and weight maintenance in postmenopausal women. The Journal of Nutrition 141, 31-36.

Lehmann, R., Zhao, X., Weigert, C., Simon, P., Fehrenbach, E., Fritsche, J., Machann, J., Schick, F., Wang, J., Hoene, M., Schleicher, E.D., Haring, H.U., Xu, G., Niess, A.M., 2010. Medium chain acylcarnitines dominate the metabolite pattern in humans under moderate intensity exercise and support lipid oxidation. PLoS One 5, e11519.

Likic, V.A., McConville, M.J., Lithgow, T., Bacic, A., 2010. Systems biology: the next frontier for bioinformatics. Advances in Bioinformatics, 268925.

Marion-Letellier, R., Savoye, G., Ghosh, S., 2016. Fatty acids, eicosanoids and PPAR gamma. European Journal of Pharmacology 785, 44-49.

Marshall, A.G., Comisarow, M.B., Parisod, G., 1979. Relaxation and spectral line shape in Fourier transform ion resonance spectroscopy. The Journal of Chemical Physics 71, 4434-4444.

Marshall, A.G., Hendrickson, C.L., 2002. Fourier transform ion cyclotron resonance detection: principles and experimental configurations. International Journal of Mass Spectrometry 215, 59-75.

Marshall, A.G., Hendrickson, C.L., Jackson, G.S., 1998. Fourier transform ion cyclotron resonance mass spectrometry: a primer. Mass Spectrometry Reviews 17, 1-35.

Martinez, I., Kim, J., Duffy, P.R., Schlegel, V.L., Walter, J., 2010. Resistant starches types 2 and 4 have differential effects on the composition of the fecal microbiota in human subjects. PLoS One 5, e15046.

Martinez, I., Lattimer, J.M., Hubach, K.L., Case, J.A., Yang, J.Y., Weber, C.G., Louk, J.A., Rose, D.J., Kyureghian, G., Peterson, D.A., Haub, M.D., Walter, J., 2013. Gut microbiome composition is linked to whole grain-induced immunological improvements. The ISME Journal 7, 269-280.

McNiven, E.M., German, J.B., Slupsky, C.M., 2011. Analytical metabolomics: nutritional opportunities for personalized health. The Journal of Nutritional Biochemistry 22, 995-1002.

Mihalik, S.J., Goodpaster, B.H., Kelley, D.E., Chace, D.H., Vockley, J., Toledo, F.G., DeLany, J.P., 2010. Increased levels of plasma acylcarnitines in obesity and type 2 diabetes and identification of a marker of glucolipotoxicity. Obesity 18, 1695-1700.

Miller, A., Engel, K.H., 2006. Content of gamma-oryzanol and composition of steryl ferulates in brown rice (*Oryza sativa L.*) of European origin. Journal of Agricultural and Food Chemistry 54, 8127-8133.

Moazzami, A.A., Bondia-Pons, I., Hanhineva, K., Juntunen, K., Antl, N., Poutanen, K., Mykkanen, H., 2012. Metabolomics reveals the metabolic shifts following an intervention with rye bread in postmenopausal women - a randomized control trial. Nutrition Journal 11, 88.

Moazzami, A.A., Zhang, J.X., Kamal-Eldin, A., Aman, P., Hallmans, G., Johansson, J.E., Andersson, S.O., 2011. Nuclear magnetic resonance-based metabolomics enable detection of the effects of a whole grain rye and rye bran diet on the metabolic profile of plasma in prostate cancer patients. The Journal of Nutrition 141, 2126-2132.

Moco, S., Ross, A.B., 2015. Can we use metabolomics to understand changes to gut microbiota populations and function? A Nutritional Perspective. 83-108.

Moongngarm, A., Daomukda, N., Khumpika, S., 2012. Chemical compositions, phytochemicals, and antioxidant capacity of rice bran, rice bran layer, and rice germ. APCBEE Procedia 2, 73-79.

Moritz, F., Kaling, M., Schnitzler, J.P., Schmitt-Kopplin, P., 2016. Characterization of poplar metabotypes via mass difference enrichment analysis. Plant, Cell & Environment 40, 1057-1073.

Mosblech, A., Feussner, I., Heilmann, I., 2009. Oxylipins: structurally diverse metabolites from fatty acid oxidation. Plant Physiology and Biochemistry 47, 511-517.

Naz, S., Vallejo, M., Garcia, A., Barbas, C., 2014. Method validation strategies involved in non-targeted metabolomics. Journal of Chromatography A 1353, 99-105.

Nicholson, G., Rantalainen, M., Maher, A.D., Li, J.V., Malmodin, D., Ahmadi, K.R., Faber, J.H., Hallgrimsdottir, I.B., Barrett, A., Toft, H., Krestyaninova, M., Viksna, J., Neogi, S.G., Dumas, M.E., Sarkans, U., The Molpage, C., Silverman, B.W., Donnelly, P., Nicholson, J.K., Allen, M., Zondervan, K.T., Lindon, J.C., Spector, T.D., McCarthy, M.I., Holmes, E., Baunsgaard, D., Holmes, C.C., 2011. Human metabolic profiles are stably controlled by genetic and environmental variation. Molecular Systems Biology 7, 525.

Nicholson, J.K., Lindon, J.C., 2008. Systems biology: metabonomics. Nature 455, 1054-1056.

Ohta, D., Kanaya, S., Suzuki, H., 2010. Application of Fourier-transform ion cyclotron resonance mass spectrometry to metabolic profiling and metabolite identification. Current Opinion in Biotechnology 21, 35-44.

Pajari, A.-M., Oikarinen, S., Grasten, S., Mutanen, M., 2000. Diets enriched with cereal brans or inulin modulate protein kinase C activity and isozyme expression in rat colonic mucosa. British Journal of Nutrition 84, 635-643.

Petyuk, V.A., Jaitly, N., Moore, R.J., Ding, J., Metz, T.O., Tang, K., Monroe, M.E., Tolmachev, A.V., Adkins, J.N., Belov, M.E., Dabney, A.R., Qian, W.J., Camp, D.G., 2nd, Smith, R.D., 2008. Elimination of systematic mass measurement errors in liquid chromatography-mass spectrometry based proteomics using regression models and a priori partial knowledge of the sample content. Analytical Chemistry 80, 693-706.

Pleil, J.D., Isaacs, K.K., 2016. High-resolution mass spectrometry: basic principles for using exact mass and mass defect for discovery analysis of organic molecules in blood, breath, urine and environmental media. Journal of Breath Research 10, 012001.

Poli, R., Kennedy, J., Blackwell, T., 2007. Particle swarm optimization. Swarm Intelligence 1, 33-57.

Portune, K.J., Beaumont, M., Davila, A.-M., Tomé, D., Blachier, F., Sanz, Y., 2016. Gut microbiota role in dietary protein metabolism and health-related outcomes: the two sides of the coin. Trends in Food Science & Technology 57, 213-232.

Qi, Y., O'Connor, P.B., 2014. Data processing in Fourier transform ion cyclotron resonance mass spectrometry. Mass Spectrometry Reviews 33, 333-352.

Rathahao-Paris, E., Alves, S., Junot, C., Tabet, J.-C., 2015. High resolution mass spectrometry for structural identification of metabolites in metabolomics. Metabolomics 12.

Ren, S., Hinzman, A.A., Kang, E.L., Szczesniak, R.D., Lu, L.J., 2015. Computational and statistical analysis of metabolomics data. Metabolomics 11, 1492-1513.

Reuter, S.E., Evans, A.M., Faull, R.J., Chace, D.H., Fornasini, G., 2005. Impact of haemodialysis on individual endogenous plasma acylcarnitine concentrations in end-stage renal disease. Annals of Clinical Biochemistry 42, 387-393.

Rinaldo, P., Matern, D., Bennett, M.J., 2002. Fatty acid oxidation disorders. Annual Review of Physiology 64, 477-502.

Roberts, A., Renwick, A.G., Sims, J., Snodin, D.J., 2000. Sucralose metabolism and pharmacokinetics in man. Food and Chemical Toxicology 38, 31-41.

Rochfort, S., 2005. Metabolomics reviewed: a new "omics" platform technology for systems biology and implications for natural products research. Journal of Natural Products 68, 1813-1820.

Ross, A.B., 2015. Whole grains beyond fibre: what can metabolomics tell us about mechanisms? The Proceedings of the Nutrition Society 74, 320-327.

Ross, A.B., Pere-Trepat, E., Montoliu, I., Martin, F.P., Collino, S., Moco, S., Godin, J.P., Cleroux, M., Guy, P.A., Breton, I., Bibiloni, R., Thorimbert, A., Tavazzi, I., Tornier, L., Bebuis, A., Bruce, S.J., Beaumont, M., Fay, L.B., Kochhar, S., 2013. A whole-grain-rich diet reduces urinary excretion of markers of protein catabolism and gut microbiota metabolism in healthy men after one week. The Journal of Nutrition 143, 766-773.

Saccenti, E., Hoefsloot, H.C.J., Smilde, A.K., Westerhuis, J.A., Hendriks, M.M.W.B., 2013. Reflections on univariate and multivariate analysis of metabolomics data. Metabolomics 10.

Sakia, R.M., 1992. The Box-Cox transformation technique: a review. The Statistician 41, 169.

Scott, D.W., Sain, S.R., 2005. Multidimensional density estimation. 24, 229-261.

Serrano, A.B., Font, G., Ruiz, M.J., Ferrer, E., 2012. Co-occurrence and risk assessment of mycotoxins in food and diet from Mediterranean area. Food Chemistry 135, 423-429.

Shulaev, V., 2006. Metabolomics technology and bioinformatics. Briefings in Bioinformatics 7, 128-139.

Smilde, A.K., Jansen, J.J., Hoefsloot, H.C., Lamers, R.J., van der Greef, J., Timmerman, M.E., 2005. ANOVA-simultaneous component analysis (ASCA): a new tool for analyzing designed metabolomics data. Bioinformatics 21, 3043-3048.

Smirnov, K.S., Maier, T.V., Walker, A., Heinzmann, S.S., Forcisi, S., Martinez, I., Walter, J., Schmitt-Kopplin, P., 2016. Challenges of metabolomics in human gut microbiota research. International Journal of Medical Microbiology 306, 266-279.

Sonnenburg, J.L., Backhed, F., 2016. Diet-microbiota interactions as moderators of human metabolism. Nature 535, 56-64.

Sumner, L.W., Amberg, A., Barrett, D., Beale, M.H., Beger, R., Daykin, C.A., Fan, T.W., Fiehn, O., Goodacre, R., Griffin, J.L., Hankemeier, T., Hardy, N., Harnly, J., Higashi, R., Kopka, J., Lane, A.N., Lindon, J.C., Marriott, P., Nicholls, A.W., Reily, M.D., Thaden, J.J., Viant, M.R., 2007. Proposed minimum reporting standards for chemical analysis Chemical Analysis Working Group (CAWG) Metabolomics Standards Initiative (MSI). Metabolomics 3, 211-221.

Sun, J., Chang, E.B., 2014. Exploring gut microbes in human health and disease: pushing the envelope. Genes & Diseases 1, 132-139.

Tanaka, K., Kobayashi, H., Nagata, T., Manabe, M., 2004. Natural occurrence of trichothecenes on lodged and water-damaged domestic rice in Japan. Journal of the Food Hygienic Society of Japan (Shokuhin Eiseigaku Zasshi) 45, 63-66.

Trewavas, A., 2006. A brief history of systems biology. The Plant Cell 18, 2420-2430.

Tziotis, D., Hertkorn, N., Schmitt-Kopplin, P., 2011. Kendrick-analogous network visualisation of ion cyclotron resonance Fourier transform mass spectra: improved options for the assignment of elemental compositions and the classification of organic molecular complexity. European Journal of Mass Spectrometry 17, 415-421.

van der Greef, J., Davidov, E., Verheij, E., Vogels, J., van der Heijden, R., Adourian, A.S., Oresic, M., Marple, E.W., Naylor, S., 2003. The role of metabolomics in systems biology. Topics in Current Genetics 18, 1-10.

Van Regenmortel, M.H., 2004. Reductionism and complexity in molecular biology. EMBO Reports 5, 1016-1020.

van Velzen, E.J., Westerhuis, J.A., van Duynhoven, J.P., van Dorsten, F.A., Hoefsloot, H.C., Jacobs, D.M., Smit, S., Draijer, R., Kroner, C.I., Smilde, A.K., 2008. Multilevel data analysis of a crossover designed human nutritional intervention study. Journal of Proteome Research 7, 4483-4491.

Velasco, G., Galve-Roperh, I., Sanchez, C., Blazquez, C., Haro, A., Guzman, M., 2005. Cannabinoids and ceramide: two lipids acting hand-by-hand. Life Sciences 77, 1723-1731.

Vernocchi, P., Del Chierico, F., Putignani, L., 2016. Gut microbiota profiling: metabolomics based approach to unravel compounds affecting human health. Frontiers in Microbiology 7, 1144.

Vulevic, J., McCartney, A.L., Gee, J.M., Johnson, I.T., Gibson, G.R., 2004. Microbial species involved in production of 1,2-sn-diacylglycerol and effects of phosphatidylcholine on human fecal microbiota. Applied and Environmental Microbiology 70, 5659-5666.

Waagsbo, B., Svardal, A., Ueland, T., Landro, L., Oktedalen, O., Berge, R.K., Flo, T.H., Aukrust, P., Damas, J.K., 2016. Low levels of short- and medium-chain acylcarnitines in HIV-infected patients. European Journal of Clinical Investigation 46, 408-417.

Walker, A., Pfitzner, B., Neschen, S., Kahle, M., Harir, M., Lucio, M., Moritz, F., Tziotis, D., Witting, M., Rothballer, M., Engel, M., Schmid, M., Endesfelder, D., Klingenspor, M., Rattei, T., Castell, W.Z., de Angelis, M.H., Hartmann, A., Schmitt-Kopplin, P., 2014. Distinct signatures of host-microbial meta-metabolome and gut microbiome in two C57BL/6 strains under high-fat diet. The ISME Journal 8, 2380-2396.

Wang, R.S., Maron, B.A., Loscalzo, J., 2015. Systems medicine: evolution of systems biology from bench to bedside. Wiley Interdisciplinary Reviews. Systems Biology and Medicine 7, 141-161.

Westerhoff, H.V., Palsson, B.O., 2004. The evolution of molecular biology into systems biology. Nature Biotechnology 22, 1249-1252.

Westerhuis, J.A., van Velzen, E.J., Hoefsloot, H.C., Smilde, A.K., 2010. Multivariate paired data analysis: multilevel PLSDA versus OPLSDA. Metabolomics 6, 119-128.

Witten, D.M., Tibshirani, R., 2010. A framework for feature selection in clustering. Journal of the American Statistical Association 105, 713-726.

Xie, G., Zhang, S., Zheng, X., Jia, W., 2013. Metabolomics approaches for characterizing metabolic interactions between host and its commensal microbes. Electrophoresis 34, 2787-2798.

Zeisel, S.H., Freake, H.C., Bauman, D.E., Bier, D.M., Burrin, D.G., German, J.B., Klein, S., Marquis, G.S., Milner, J.A., Pelto, G.H., Rasmussen, K.M., 2005. The nutritional phenotype in the age of metabolomics. The Journal of Nutrition 135, 1613-1616.

Zhang, A., Sun, H., Wang, P., Han, Y., Wang, X., 2012. Modern analytical techniques in metabolomics analysis. The Analyst 137, 293-300.

Zhurov, K.O., Kozhinov, A.N., Fornelli, L., Tsybin, Y.O., 2014. Distinguishing analyte from noise components in mass spectra of complex samples: where to cut the noise? Analytical Chemistry 86, 3308-3316.

Zwanenburg, G., Hoefsloot, H.C.J., Westerhuis, J.A., Jansen, J.J., Smilde, A.K., 2011. ANOVA-principal component analysis and ANOVA-simultaneous component analysis: a comparison. Journal of Chemometrics 25, 561-567.

10. Curriculum vitae

Kirill Smirnov

Full name:	Kirill S Smirnov (rus. Смирнов Кирилл Сергеевич)
Date and place of birth:	26.10.1988, Leningrad (pres. St. Petersburg), USSR
Nationality:	Russian
Marital status:	not married
Current address	Graf-Konrad-Str. 3, 80809 Munich
Phone number:	+49 (0) 157 32742721
E-mail:	kirill.smirnov.mail@gmail.com
Languages:	Russian (native) English (fluent) German (intermediate) Italian (basics)

Education and work experience

Since 06.2017: Jambit GmbH

Software Architect

10.2012 – 05.2017: Ph. D. fellowship

Technical University Munich, TUM School of Life Sciences Weihenstephan,
Research Department of Nutrition and Food Sciences,
Analytical Food Chemistry

Helmholtz Center Munich, Department of Environmental Sciences,
Research Unit Analytical BioGeoChemistry

- Various laboratory routines concerning metabolites
- Algorithm development for signal processing
- Development of user-oriented software
- Multidimensional data analysis

09.2011 – 06.2012: M. Sc. in physics

Saint-Petersburg State Polytechnic University,
Department of Physics and Mechanics, Unit of Biophysics

Petersburg Nuclear Physics Institute,
Department of Molecular and Radiation Biophysics

- Various laboratory routines concerning proteins
- Image data processing and analysis

09.2008 – 06.2010: B. Sc. In physics

Saint-Petersburg State Polytechnic University,
Department of Physics and Mechanics, Unit of Biophysics

Institute of Cytology of the Russian Academy of Sciences,
Interlaboratory Sector of Biomedical Technologies

- Various laboratory routines concerning DNA
- Data analysis

Skills and related experience

Working in the laboratory:

Handling biological samples
- DNA, protein, metabolite extraction

Dealing with sophisticated instruments and equipment
- Mass spectrometry (HPLC-MS, FT-ICR-MS)

Participating in scientific talks and conferences

Retrieving data from biological databases

Data processing and analysis:

Univariate statistics
(*e.g.* t-test, ANOVA, linear models, mixed effect models, correlation analysis)

Multivariate statistics
(*e.g.* Hotelling T^2, multivariate linear models, principal component analysis)

Machine learning
(*e.g.* logistic regression, random forests, naïve Bayes, neural networks)

Clustering methods
(*e.g.* hierarchical cluster analysis, K-means clustering)

Graph theory
(*e.g.* network analysis, community detection)

Programming languages:

MATLAB (very advanced)
- application of variety of toolboxes concerning analysis of data
- development of algorithms for feature selection and signal processing
- programming user-oriented graphical user interfaces

R (advanced)
- data visualisation with ggplot2 and other packages, *e.g.* corrplot
- application of machine learning packages, *e.g.* pcamethods

Python (advanced)
- application of common toolboxes for linear algebra and data processing (*e.g.* numpy, pandas, scipy, scikit-learn)
- web scraping using regular expressions
- development of user-oriented command line based interfaces

Java (advanced)
- design of user-oriented graphical user interfaces using swing package
- backend development

C (ground knowledge)

Databases:

MySQL (ground knowledge):
- creating and supporting biology-related databases on a department server

Interests

Work-related interests:	Univariate and multivariate data analysis Algorithm development for finding solution to challenging tasks Machine learning for descriptive or predictive model construction
Personal interests:	Mathematics (including logical and table games) Cycling, travelling, hiking Music instruments (guitar, piano, trumpet)

Workshops

06.06.2016:	ANOVA-SCA (ASCA) and Multilevel-SCA (MSCA), XVI Chemometrics in Analytical Chemistry, Barcelona, Spain
12.11 – 13.11.2015:	SysVasc WP3 modelling and analysis workshop, Swiss Institute of Bioinformatics, Lausanne, Switzerland
29.06. – 01.07.2015:	Introduction to statistics, Helmholtz Zentrum Munich, Munich, Germany
26.02. – 27.02.2014:	Introduction to statistics with R Tutorial, Helmholtz Zentrum Munich, Munich, Germany
Winter semester, 2014:	Machine learning, Technical University Munich, Munich, Germany
22.03. – 26.03.2014:	14th Bioinformatics Spring School, Bertinoro, Italy

Scholarships

Since 10.2012:	HELENA grant Helmholtz Center Munich, the International Helmholtz Graduate School Environmental Health

Conferences

06.06. – 10.06.2016:	XVI Chemometrics in Analytical Chemistry, Barcelona, Spain (Poster presentation)
10.07. – 12.07.2015:	8th Seeon Conference and Science Camp “From sequencing to functions”, Seeon, Germany (Poster presentation)
01.07. – 04.07.2013:	9th Annual Conference of the Metabolomics Society, Glasgow, Great Britain (Poster presentation)

Scientific publications

How representative are dissolved organic matter (DOM) extracts? A comprehensive study of sorbent selectivity for DOM isolation // Yan Li*, Mourad Harir, Jenny Uhl, Basem Kanawati, Marianna Lucio, **Kirill S Smirnov**, Boris P Koch, Philippe Schmitt-Kopplin, Norbert Hertkorn // Water Research, 2017 // doi: 10.1016/j.watres.2017.03.038

Proposed guidelines for solid phase extraction of Suwannee River dissolved organic matter // Yan Li*, Mourad Harir, Marianna Lucio, Basem Kanawati, **Kirill S Smirnov**, Ruth Flerus, Boris P Koch, Philippe Schmitt-Kopplin, Norbert Hertkorn // Analytical Chemistry, 2016 // doi: 10.1021/acs.analchem.5b04501

Challenges of metabolomics in human gut microbiota research // **Kirill S Smirnov***, Tanja V Maier*, Alesia Walker*, Silke S Heinzmann*, Sara Forcisi, Ines Martinez, Jens Walter, Philippe Schmitt-Kopplin // International Journal of Medical Microbiology, 2016 // doi: 10.1016/j.ijmm.2016.03.00

Oral versus intravenous iron replacement therapy distinctly alters the gut microbiota and metabolome in patients with inflammatory bowel diseases // Thomas Lee*, Thomas Clavel*, **Kirill S Smirnov***, Annemarie Schmidt, Ilias Lagkouvardos, Alesia Walker, Marianna Lucio, Bernhard Michalke, Philippe Schmitt-Kopplin, Richard Fedorak, Dirk Haller // Gut, 2016 // doi: 10.1136/gutjnl-2015-309940

MetICA: Independent component analysis of high-resolution mass-spectrometry based non-targeted metabolomics // Youzhong Liu*, **Kirill S Smirnov**, Marianna Lucio, Régis Geougeon, Hervé Alexandre, Philippe Schmitt-Kopplin // BMC Bioinformatics, 2016 // doi: 10.1186/s12859-016-0970-4